Stem Cells International

Interaction between Stem Cells and the Microenvironment for Musculoskeletal Repair

Lead Guest Editor: Yongcan Huang
Guest Editors: Zhen Li, Jun Li, and Fengjuan Lv

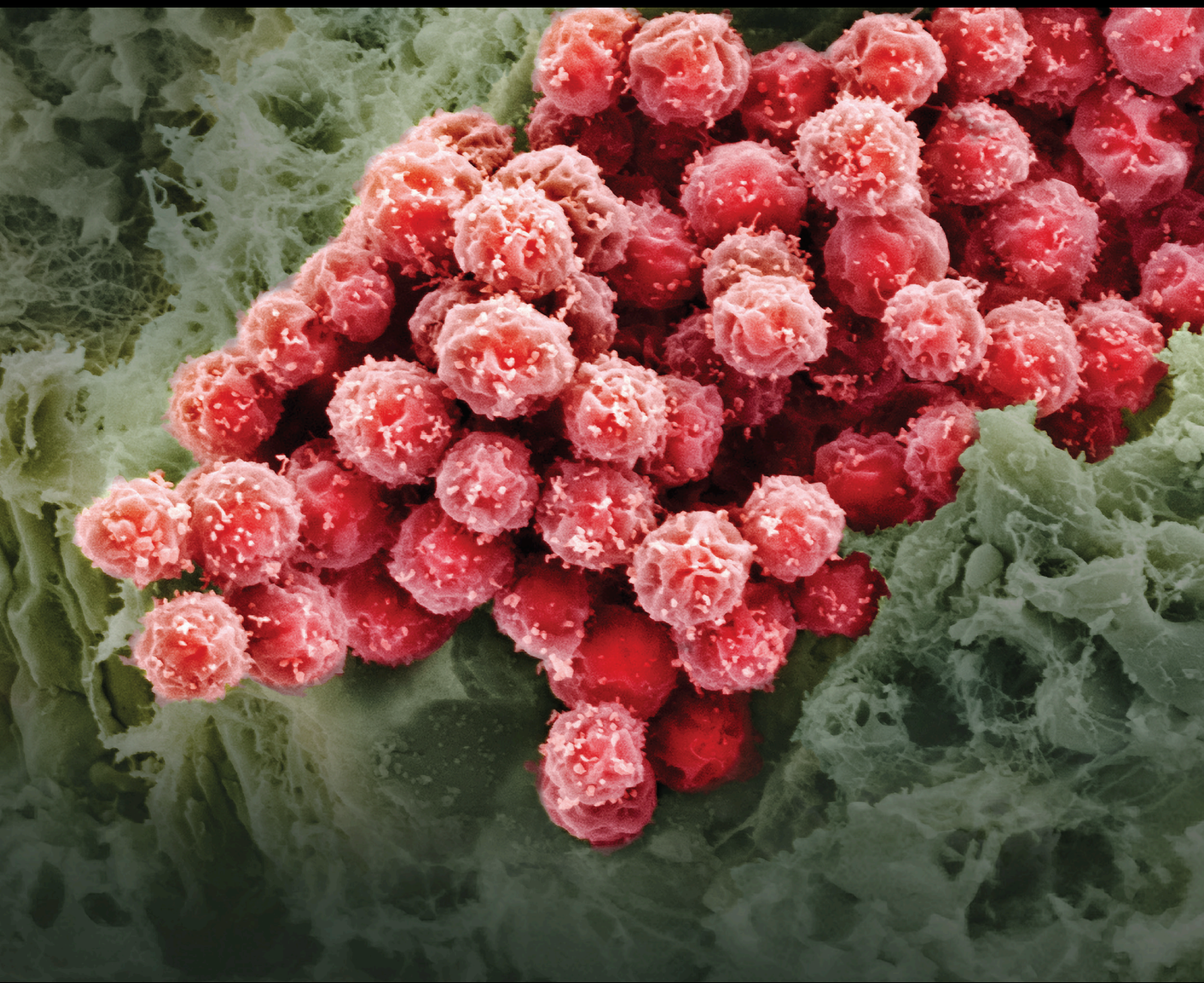

Interaction between Stem Cells and the Microenvironment for Musculoskeletal Repair

Stem Cells International

Interaction between Stem Cells and the Microenvironment for Musculoskeletal Repair

Lead Guest Editor: Yongcan Huang
Guest Editors: Zhen Li, Jun Li, and Fengjuan Lv

Contents

Hindawi
Stem Cells International
Volume 2020, Article ID 7587428, 3 pages
https://doi.org/10.1155/2020/7587428

Editorial

Interaction between Stem Cells and the Microenvironment for Musculoskeletal Repair

Yong-Can Huang,[1,2] **Zhen Li**,[3] **Jun Li**,[4] **and Feng-Juan Lyu**[5]

[1]*Shenzhen Engineering Laboratory of Orthopaedic Regenerative Technologies, Department of Spine Surgery, Peking University Shenzhen Hospital, Shenzhen 518036, China*
[2]*National & Local Joint Engineering Research Center of Orthopaedic Biomaterials, Peking University Shenzhen Hospital, Shenzhen 518036, China*
[3]*AO Research Institute Davos, Davos, Switzerland*
[4]*Department of Orthopedic Surgery, Rush University Medical Center, Chicago, IL 60612, USA*
[5]*Guangdong General Hospital (Guangdong Academy of Medical Sciences), South China University of Technology-the University of Western Australia Joint Center for Regenerative Medicine Research, School of Medicine, South China University of Technology, Guangzhou, China*

Correspondence should be addressed to Yong-Can Huang; y.c.huang@connect.hku.hk, Zhen Li; zhen.li@aofoundation.org, Jun Li; jun_v_li@rush.edu, and Feng-Juan Lyu; lufj0@scut.edu.cn

Received 11 December 2019; Accepted 12 December 2019; Published 20 March 2020

Manipulation of the tissue microenvironment has become a promising method to enhance the regenerative abilities of stem cells/progenitors for musculoskeletal repair. The composition of the microenvironment is determined by the resident cells, extracellular matrix, cytokines, and chemokines as well as the biomechanical property and nutrient status. The microenvironment is altered by the homeostasis and degenerative stage of the native tissue. All the alterations of the surrounding host microenvironment will definitely change the biology of the implanted stem cells/progenitors. Thus, a thorough understanding of the stem cell-microenvironment communication would therefore accelerate the success of musculoskeletal repair. In this special issue with the theme "Interaction between stem cells and the microenvironment for musculoskeletal repair," we are very pleased to present the 11 accepted papers (7 research articles and 4 review articles) in which how the microenvironment affects the stem cells/progenitors was well investigated.

Bone marrow mesenchymal stem cells (BM-MSCs) play a central role during the process of bone modeling and remodeling; yet, their biology is regulated by the cytokines, biomechanical stimuli, and other types of cells. Increased B lymphopoiesis was found in mouse with osteoporosis [1], which constitutes a microenvironmental factor for BM-MSCs. The study of Pan et al. checked the involvement of activated B lymphocytes in osteoporosis by first establishing two rat models of osteoporosis by ovariectomy or splenectomized variectomy. Examination at 3 months postsurgery showed that both models exhibited signs of osteoporosis, represented by loss of bone volume and quality, as well as the activation of B lymphocytes, represented as increased proportion of CD3-CD45RA dual positivity in bone marrow cells, while SPX alone induced activation of B lymphocytes but did not induce osteoporosis. Further cell study revealed that lipopolysaccharide pretreated B lymphocytes suppressed the mineral deposition and alkaline phosphatase activities of BM-MSCs under osteogenic inductive condition, suggesting impaired osteogenesis, while untreated normal B lymphocytes had no such effect. On the other hand, the suppression of osteogenesis of BM-MSCs could be relieved by the addition of a dexamethasone or Notch inhibitor. These results suggest that bone loss after menopause may have resulted from activated B lymphocytes which have a negative impact on the osteogenesis of BM-MSCs and that the dexamethasone or Notch inhibitor could

reduce bone loss through suppressing B lymphocytes. Glutamine provides the energy demand for the cells and serves as a secondary metabolic regulator in bone homeostasis. Dr. Zhou and coauthors contributed a review paper in this issue to majorly summarize the recent evidences regarding how glutamine metabolism mediates the bioenergy of BM-MSCs and how glutamine influences proliferation, differentiation, and mineralization. The authors suggested that extensively basic and clinical investigations are needed to deeply understand the importance of glutamine metabolism in bone homeostasis and to develop new therapeutic strategies. To facilitate the osteogenesis of rat BM-MSCs *in vitro*, Dr. Ni's group used 20 IU/ml erythropoietin combined with the cyclic mechanical stretch (1 Hz sinusoidal curve set at 10% elongation); the underlying mechanism may be associated with the activation of ERK1/2 signaling pathway. Dr. Huang's group found that 10 mM strontium (a trace element in the bone tissue) was able to promote the osteogenic gene expression and mineralization of human BM-MSCs and placenta-derived MSCs. Interestingly, using the exosomes derived from the osteogenically differentiated adipose-derived stem cells (ADSCs), obvious enhancements in the osteogenic differentiation of ADSCs were recorded. Dr. Yang and colleagues further determined that this enhancement was related to the upregulated (201) and downregulated (33) exosomal miRNAs derived from the osteogenically differentiated ADSCs. Hence, beyond the resident cells, the bioactive compounds, and the biomechanical stimuli, exosomal miRNAs probably became a new target to enhance the osteogenesis of endogenous and exogenous stem cells/progenitors.

During the cause of intervertebral disc (IVD) degeneration, gradual changes in the disc morphology, matrix composition, and microenvironment have been observed [2, 3]. In the review paper contributed by Dr. Vadalà and coauthors, the updated knowledge regarding the microenvironment in the healthy and the degenerated IVD was described and how the components of IVD microenvironment regulated the MSC viability and biological potential was summarized. The authors further emphasized the consideration of IVD microenvironment before developing MSC-based and biomaterial-based therapies. The IVD microenvironment is also affected by the phenotype of native resident cells, which can change during aging. Cheng et al. isolated nucleus pulposus (NP) cells from the caudal IVD of young (2 months) and old (24 months) SD rats; the NP cells from old rats showed a senescent phenotype, as well as declined cell proliferation and migration capacity. The transcriptomes of the young and senescent NP cells were analyzed by microarray. A total of 1038 differentially expressed genes were reported between the young and senescent NP cells, with the upregulated genes mainly enriched in the TNF signaling pathway and downregulated genes enriched in the extracellular matrix receptor interaction. The results revealed the underlying genes and pathways of senescent NP cells that were supposed to increase with aging. The reported findings provide a rich transcriptomic dataset for young *vs.* senescent NP cells, which may assist the development of novel biological methods to treat degenerative disc diseases.

The tendon is to transmit muscular forces to the bone, permitting joint motion and subsequent body movement [4]. It was thought that the tendon only consists of tenocytes; nevertheless, the recent studies demonstrated that human and mouse tendons contain stem cells, namely, tendon stem/progenitor cells (TSPCs) [5]. In the review contributed by Dr. Zhang and colleagues, the recent advances in the identification and characterization of TSPCs and their interactions with extracellular matrix and mechanical loading were summarized; meanwhile, the authors outlined the challenges in understanding TSPC biology and function *in vivo* due to the heterogeneity and lack of specific markers and suggested that the mechanobiology of TSPCs and its role in tendon development, growth, repair, and pathology need to be better clarified.

The interaction between stem cells and local microenvironment goes in both directions. Not only the microenvironment can impose on the fate of stem cells, but also stem cells can positively affect the local microenvironment of injured tissues. In Fang's study using a rat peripheral nerve injury model, except from generating neurons, transplanted embryonic spinal cord cells were found to have a regulatory effect on local Schwann cells in the distal nerve and induced them to produce proximal axons to facilitate nerve regeneration. Amyotrophic lateral sclerosis (ALS) is a progressive disease that affects nerve cells in the brain and spinal cord, causing loss of muscle control. Due to the low bioavailability and short half-life *in vivo*, in clinics, the expected outcomes of the intrathecal administration of neurotrophic factors alone was hard to achieve. Pawlukowska et al. performed a clinical study using the autologous lineage negative (Lin^-) stem cells to treat ALS. The authors thought Lin^- stem cell-based therapy would be a reasonable and promising alternative for classic ALS treatments because the Lin^- stem cells could produce the trophic support for the host's neurons, stimulate the secretion of neurotrophins (NTs), and differentiate into oligodendrocyte progenitor cells or neurons. In this article, the authors completed a clinical trial to assess the impact of intrathecal administration of bone marrow Lin^- stem cells in 32 patients suffering from ALS on articulation; it was demonstrated that 6 patients achieved the improvement of articulation after 28 days, 23 patients remained stable, and 3 deteriorated. Although some valuable findings were observed, several limitations should be acknowledged such as the small number of patients, the lack of control group, and a short observation period.

During muscle regeneration, as reviewed by Dort et al., the spatial recruitment of proinflammatory and anti-inflammatory macrophages is different in addition to their temporal recruitment; proinflammatory macrophages are located close to proliferating satellite cells, while anti-inflammatory macrophages are found close to the regenerating area containing differentiated myoblasts. Depletion of proinflammatory macrophages resulted in impaired muscle regeneration in animal models. The suppression of the switch of macrophage from proinflammatory phenotype to anti-inflammatory phenotype reduced muscle fiber growth but did not affect the clearance of necrotic tissues. At the cellular level, proinflammatory macrophages

promote myoblast proliferation and inhibit differentiation, while anti-inflammatory macrophages inhibit myoblast proliferation and stimulate their differentiation and myofiber growth. Direct coculture of macrophages also promoted proliferation and inhibited apoptosis of myogenic cells. Altogether, these findings suggest that different subsets of macrophages have complementary roles in the regulation of satellite cell/myoblast function, myogenesis progression, and optimal muscle regeneration.

In summary, the published articles in this special issue add new perspectives to the understanding regarding the interaction between stem cells/progenitors and the microenvironment for the bone, intervertebral disc, tendon, muscle, and nerve regeneration. We hope that all these basic and clinical studies will be helpful for the development of stem cell-based therapies for musculoskeletal repair. Finally, we would like to express our gratitude to all the authors, the reviewers, and the editorial board members of this journal for their contribution and assistance to make this special issue successful.

Conflicts of Interest

The editors declare no conflict of interest.

Acknowledgments

This work was supported by the AO Foundation, AOSpine International, the National Natural Science Foundation of China (grant numbers 81702171, 81772333, 51873069, and 81702191), the Fundamental Research Funds for the Central Universities, South China University of Technology (2018MS70), the Shenzhen Double Chain Project for Innovation and Development Industry supported by the Bureau of Industry and Information Technology of Shenzhen (No. 201806081018272960), and the Guangdong Provincial Science and Technology Program from Department of Science and Technology of Guangdong Province (No. 2017A010105026).

Yong-Can Huang
Zhen Li
Jun Li
Feng-Juan Lyu

References

[1] T. Masuzawa, C. Miyaura, Y. Onoe et al., "Estrogen deficiency stimulates B lymphopoiesis in mouse bone marrow," *The Journal of Clinical Investigation*, vol. 94, no. 3, pp. 1090–1097, 1994.

[2] Y.-C. Huang, V. Y. L. Leung, W. W. Lu, and K. D. K. Luk, "The effects of microenvironment in mesenchymal stem cell-based regeneration of intervertebral disc," *The Spine Journal*, vol. 13, no. 3, pp. 352–362, 2013.

[3] Y.-C. Huang, J. P. G. Urban, and K. D. K. Luk, "Intervertebral disc regeneration: do nutrients lead the way?," *Nature Reviews Rheumatology*, vol. 10, no. 9, pp. 561–566, 2014.

[4] J. Zhang and J. H.-C. Wang, "Characterization of differential properties of rabbit tendon stem cells and tenocytes," *BMC Musculoskeletal Disorders*, vol. 11, no. 1, p. 10, 2010.

[5] G. C. Dai, Y. J. Li, M. H. Chen, P. P. Lu, and Y. F. Rui, "Tendon stem/progenitor cell ageing: modulation and rejuvenation," *World Journal of Stem Cells*, vol. 11, no. 9, pp. 677–692, 2019.

Hindawi
Stem Cells International
Volume 2019, Article ID 7378594, 15 pages
https://doi.org/10.1155/2019/7378594

Research Article

Reactivation of Denervated Schwann Cells by Embryonic Spinal Cord Neurons to Promote Axon Regeneration and Remyelination

Xinyu Fang, Chaofan Zhang, Chongjing Zhang, Yuanqing Cai, Zibo Yu, Zida Huang, Wenbo Li, and Wenming Zhang

Department of Orthopedic Surgery, First Affiliated Hospital of Fujian Medical University, Fuzhou, Fujian, China

Correspondence should be addressed to Wenming Zhang; zhangwm0591@163.com

Received 16 June 2019; Accepted 6 September 2019; Published 2 December 2019

Guest Editor: Fengjuan Lyu

In peripheral nerve injuries (PNIs) in which proximal axons do not regenerate quickly enough, significant chronic degeneration of Schwann cells (SCs) can occur at the distal stump of the injured nerve and obstruct regeneration. Cell transplantation can delay the degeneration of SCs, but transplanted cells fail to generate voluntary electrical impulses without downstream signal stimulation from the central nervous system. In this study, we combined cell transplantation and nerve transfer strategies to investigate whether the transplantation of embryonic spinal cord cells could benefit the microenvironment of the distal stump of the injured nerve. The experiment consisted of two stages. In the first-stage surgery, common peroneal nerves were transected, and embryonic day 14 (E14) cells or cell culture medium was transplanted into the distal stump of the CPs. Six months after the first-stage surgery, the transplanted cells were removed, and the nerve segment distal to the transplanted site was used to bridge freshly cut tibial nerves to detect whether the cell-treated graft promoted axon growth. The phenotypic changes and the neurotrophic factor expression pattern of SCs distal to the transplanted site were detected at several time points after cell transplantation and excision. The results showed that at different times after transplantation, the cells could survive and generate neurons. Thus, the neurons play the role of proximal axons to prevent chronic degeneration and fibrosis of SCs. After excision of the transplanted cells, the SCs returned to their dedifferentiated phenotype and upregulated growth-associated gene expression. The ability of SCs to be activated again allowed a favorable microenvironment to be created and enhanced the regeneration and remyelination of proximal axons. Muscle reinnervation was also elevated. This transplantation strategy could provide a treatment option for complex neurological injuries in the clinic.

1. Introduction

There are many serious traumas in the clinic that often lead to long segmental defects of the peripheral nerves without direct tension-free anastomosis repair methods. Autografts, acellular nerves, and allografts (ANAs) are alternative options [1, 2]. There are also cases limited by soft tissue conditions that require delayed repair [3]. However, these cases often have poor outcomes because the slow-growing proximal axons do not reach the distal nerve fast enough, and chronic degeneration of distal nerves and muscles hinders the potential for reinnervation [4, 5].

Currently, the most widely accepted clinical option to alleviate chronic degeneration is transferring an adjacent nerve to protect the distal nerve and muscles, known as the "babysit" procedure [6–9]. When the temporary neuroanastomosis is terminated months later and the original proximal end of the injured nerve stump (or including graft) is sutured back, the regenerated axons within can regrow into the distal stump [10]. However, these methods are characterized by the disadvantage of causing additional injury to the donor nerve, and sometimes, the source of the donor nerve is insufficient. Cell transplantation (including neural stem cells, embryonic spinal neurons, or in vitro-induced motor neurons) to the distal stump of peripheral nerve damage has been shown to delay chronic degeneration of the distal nerve and muscle [11]. However, transplanted cells fail to generate voluntary electrical impulses without downstream signal stimulation

from the central nervous system [12]. In a previous study, we combined the "cell transplantation" and "nerve transfer" strategies to address this problem. We transplanted E14 neurons to the distal stump of transected nerves and showed that, 3 months after transplantation, after resection of the transplanted site, the ability of the distal nerve and muscle to support proximal axon regeneration was enhanced compared with the control group [13]. However, it remains unclear whether this improvement was induced by effects on the distal nerves, muscles, or both.

After peripheral nerve injury, Schwann cells (SCs) at the distal stump dedifferentiate and secrete growth-associated neurotrophic factors to induce proximal axonal regeneration [14]. However, this state is only temporary. If the regenerative axons are unable to contact the distal SCs within a certain time window, the SCs will enter a quiescent state, reducing the secretion of neurotrophic factors. Even if the proximal axon is in contact during this period, the distal SCs are unable to support elongation and remyelination. Sulaiman and Gordon confirmed that this time window was 6 months in rats [15]. In contrast, recent research believed that even if a rat has been denervated for more than 1 year, the muscle still has the ability to regenerate, which corresponds to better tolerance than nerves [16, 17]. Therefore, this study is aimed at determining the effect of transplanted embryonic neurons on SCs in distal nerve stumps in a rat peripheral nerve injury (PNI) model. We hypothesized that transplanted cells interact with SCs to maintain the microenvironment of the distal nerve stump in an axon-innervated condition. When these cells are removed, the nerves distal to the cells undergo another process that is equivalent to the denervation process, and the expression of GAGs rises again, creating a better environment for proximal axon regeneration. To verify this hypothesis, we designed the following experiment.

Briefly, the procedure consisted of two stages. In the first-stage (1^{st}) surgery, the right common peroneal nerves (CPs) were transected, and embryonic day 14 (E14) cells or cell culture medium was transplanted into the distal stump of the CPs. The phenotype changes and neurotrophic factor expression of SCs distal to the transplanted site were measured at multiple time points after transplantation. Six months after the 1^{st} surgery, the transplanted cells were removed (second-stage surgery-I), and the phenotypic changes and neurotrophic factor expression pattern of SCs distal to the transplanted site were compared with the state after the 1^{st} surgery. Then, the nerve segment distal to the transplanted site was used to bridge the freshly cut tibial nerves (TIBs) to detect whether the nerve segment has the effect of promoting axon growth (second-stage surgery-II).

2. Materials and Methods

All surgical interventions and subsequent care and treatment were approved by the Ethics Committee for the Use of Animals at Fujian Medical University (No. SYXK-min-2016-0006). Animals were provided by the Laboratory Animal Unit at Fujian Medical University. We followed the methodology of our previously published work [13, 18, 19].

2.1. Cell Preparation. The Sprague-Dawley transgenic rats expressing green fluorescent protein (GFP; "green rat" CZ-004; SLC, Shizuoka, Japan) were used. The ventral spinal cord cells from embryonic day 14 (E14) rats were prepared with reference to a modified published protocol [20]. Briefly, under sterile conditions, the spinal cord was separated and the surrounding tissues were removed. The ventral horn of cord was collected and transferred to DMEM-F12 culture medium (Gibco, Grand Island, NY, USA). Trypsin (0.15%, Invitrogen, 25200-072, USA) was supplemented to the medium and digested for 7 minutes and then neutralized with trypsin inhibitor (Invitrogen, 17075-029, USA). Next, the spinal cord was dissociated into single-cell suspension by mechanical trituration and further filtered through a 40 μm cell strainer (BD Falcon, San Jose, CA, USA). After centrifugation, the suspension was resuspended in DMEM-F12 culture medium at a density of 1.0×10^5 cells/μl and kept on ice for transplantation.

2.2. Staging Animal Surgery. Sixty female Sprague-Dawley rats (250-300 g) were used in this study. Animals were anesthetized with an intraperitoneal injection of ketamine (80 mg/kg) and xylazine (8 mg/kg) and placed in prone position. The surgeries were performed in two stages (Figure 1). In the first-stage (1^{st}) surgery (nerve denervation and cell/vehicle injection), the animals were randomly divided into 2 groups. (i) Cell injection group: the CP was transected at a distance of 5 mm from the bifurcation of the sciatic nerve, and 3 μl of cell suspension was slowly injected into the distal stump of the CP. The transplanted cells were confined to a limited area of the distal nerve to facilitate the second-stage resection of the transplanted area, and the proximal and distal stumps were ligated and imbedded into the muscle to prevent regeneration (Figures 1(a), 1(h), 1(i), 1(j), and 1(k)). (ii) Vehicle injection group: the same surgical procedure was performed, and 3 μl of cell culture medium was injected (Figures 1(a), 1(h), 1(i), 1(j), and 1(k)). At different time points after the first surgery (1 month, 3 months, and 6 months), one-sixth of the rats in each group ($n = 5$) were killed, and 20 mm distal nerve segments including the transplanted site were collected for immunohistochemistry staining (IHC) and quantitative reverse transcription-PCR (qRT-PCR) analysis (Figure 1(b)).

Six months after the 1st surgery, the remaining rats underwent the second-stage (2nd) surgery (I-cell excision or II-cell excision plus distal nerve grafting). For the cell excision rats ($n = 5$), a 5 mm nerve segment including the transplanted cells was excised (2nd surgery-I, Figures 1(c) and 1(l)). The rats were maintained for an additional 2 weeks for the qRT-PCR analysis and IHC (Figure 1(e)). For the cell excision plus distal nerve grafting rats ($n = 10$), after the cells were excised, a 10 mm segment was cut from the distal stump of the transplanted site, and then, the TIB was transected. The distal and proximal stumps of the TIB were bridged by this segment with 10-0 sutures (2nd surgery-II, Figures 1(d) and 1(m)). The animals were kept for an additional 3 months, after which electrophysiology, fluorogold (FG) retrograde axonal

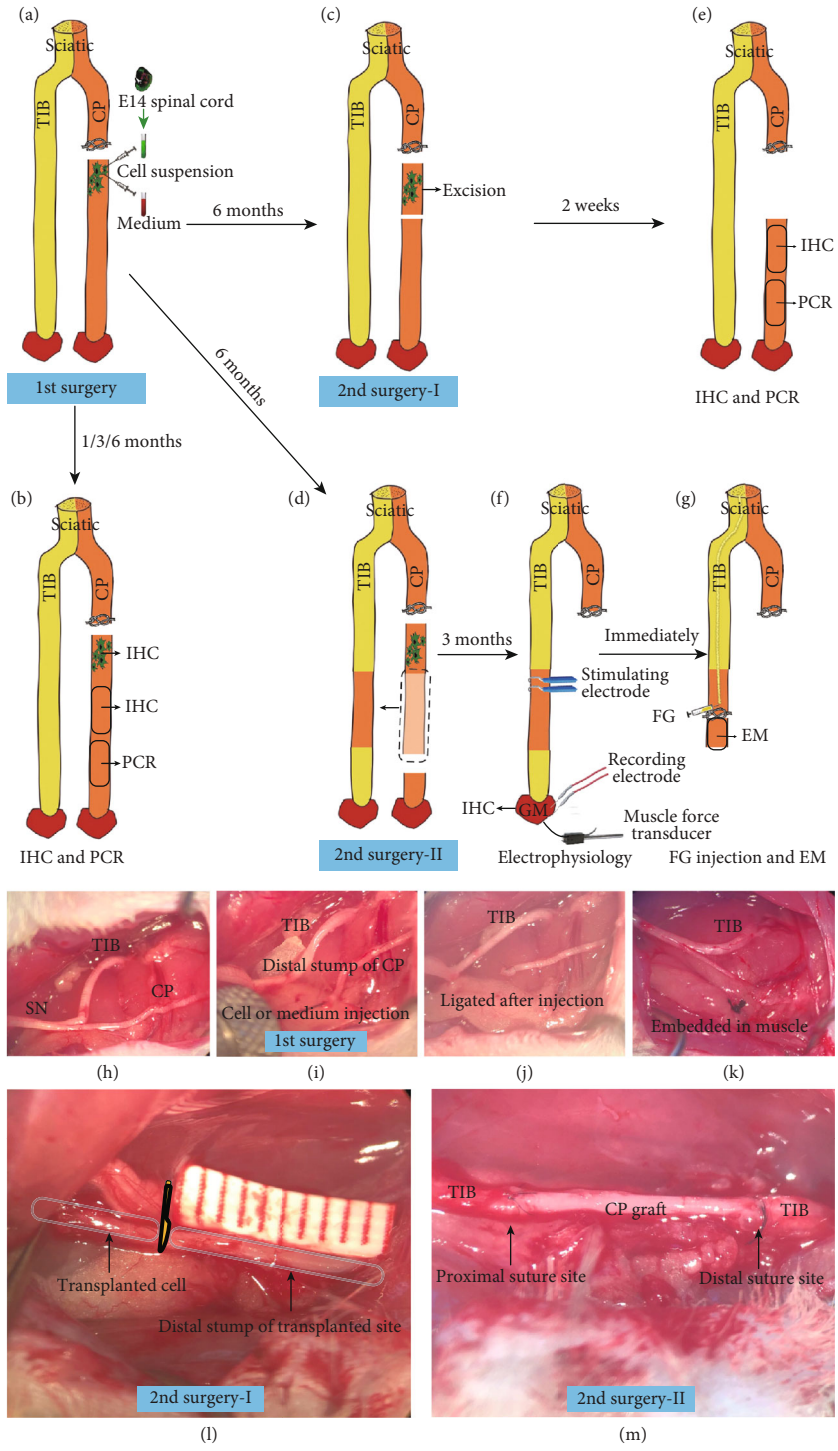

Figure 1: Schematic diagram of the stages of the surgery procedures. (a) In the first-stage surgery, the right CP was transected, and the proximal stump was ligated. Embryonic (E14) ventral spinal cord cells or an equivalent volume of cell culture medium was injected into the distal stump of the CP. (b) At different times (1, 3, or 6 months) after transplantation, IHC and PCR were performed using the nerve segments marked in the figure. (c) Six months after transplantation, the transplanted site was excised. (e) Two weeks later, the marked sites were processed for IHC and PCR. (d) Six months after transplantation, the transplanted site was excised, the marked segment was cut from the distal stump of the transplanted site, and then, the TIB was transected. The distal and proximal stumps of the TIB were bridged by this segment. (f) Three months after bridging surgery, electrophysiological examination was performed, and the GM was dissected for further IHC. (g) Immediately after electrophysiology, FG retrograde axonal tracing and EM analyses were performed. TIB: tibial nerve; GM: gastrocnemius muscle; IHC: immunohistochemical staining; EM: electron microscope; CP: common peroneal nerve; FG: fluorogold; EM: electron microscope.

tracing, and electron microscopy (EM) analyses were performed. The rats were maintained for an additional 3 days in favor of FG transportation (Figure 1(f)). Nerve segments of the same length were cut in the vehicle group ($n = 10$) during the second-stage surgery, and the subsequent procedures remained the same.

2.3. Immunohistochemistry Staining (IHC). At every detection time point after the 1st and 2nd surgery-I, rats were euthanized and perfused with 4% paraformaldehyde (PFA). A 5 mm segment of CP containing the transplanted cells and a 10 mm adjacent segment were cut and collected (Figures 1(b) and 1(e)). The nerves were postfixed in 4% PFA at 4°C overnight and then dehydrated in 30% sucrose (dissolved in 0.1 M PB) at 4°C for 48 hours. Serial longitudinal cryosections (20 μm thick) of the nerve segments were prepared. Every third section was used for IHC with reference to the published protocol [20] (5 rats per group per time point). For segments containing cells, staining of neuronal nuclei (NeuN) was performed. For adjacent distal segments, staining of neurofilament 200 (NF200, axon marker), myelin basic protein (MBP, myelin sheath marker), S100 (cytoplasmic marker of SCs), and P75 (dedifferentiated SCs marker) was performed. Briefly, after washed with 0.01 M phosphate-buffered saline (PBS), sections were blocked in 10% goat serum for 30 min and incubated with the primary antibodies at 4°C overnight (mouse anti-NeuN, 1 : 500, MAB377, EMD Millipore; mouse anti-NF200, 1 : 500, N0142, Sigma; rabbit anti-MBP, 1 : 200, M3821, Sigma; rabbit anti-S100, 1 : 200, Z0311, DAKO; rabbit anti-P75, 1 : 200, G3231, PROMEGA). After washed with 0.01 M PBS, sections were incubated with species-specific fluorescence-conjugated secondary antibodies at 20°C for 2 h (goat anti-mouse Alexa Fluor 586/488, 1 : 500, A11031/A11029, Invitrogen; donkey anti-rabbit Alexa Fluor 586/488, 1 : 500, A10042/A21206, Invitrogen). Sections were subsequently counterstained with 4′,6-diamidino-2-phenylindole (DAPI) to stain the nuclei and then coverslipped with antifade mounting medium (FluorSave, Calbiochem, San Diego, CA, USA).

The number of NeuN-positive cells was counted manually following a systematic random sampling technique [21]. Briefly, for all the measurements, one in 3 sections with a total of 6 sections was assessed. The counting was carried out in GFP-positive fields at ×40 magnification under a fluorescence microscope (Axioplan, Carl Zeiss, Germany). Cells that met all of the following criteria were counted: (1) cells that were present in the GFP-positive region and stained with NeuN and (2) cells that had a large cytoplasm and nucleus and contained at least one large nucleolus. The result is multiplied by 3 to yield the final count. The fluorescence intensity of NF200, MBP, S100, and P75 was evaluated in ImageJ software (National Institutes of Health, Bethesda, Maryland), which was presented as the mean gray values of the regions of interest (ROIs). In each sample evaluated, the mean gray value of ROI was normalized to the intensity of the uninjured CP and averaged over triplicate measurements from 1 rat for each time point [9].

At 3 months after the 2nd surgery-II, after the electrophysiological examination has been performed, the gastrocnemius muscle (GM) was dissected. The wet weight of GM was measured. And then the serial longitudinal cryostat sections (20 μm) were prepared using a freezing microtome (Leica CM 1900). The sections were blocked in 5% normal donkey serum for 1 hour and incubated with primary antibodies at 4°C overnight (rabbit anti-neurofilament 200, 1 : 500, N4142, Sigma-Aldrich), followed by secondary antibodies at 37°C (Alexa Fluor 594, 1 : 500, A30008, Invitrogen). Finally, alpha-bungarotoxin conjugated to Alexa Fluor 488 (a-BTX, 1 : 500, B13422, Invitrogen) was applied to label acetylcholine receptors (AchRs). Every fifth section of the GM was used to count the neuromuscular junctions (NMJs) (10 sections per animal). The AchR clusters were captured, and 100 randomly selected NMJs were studied in each animal (10 animals in each group). The NMJs were categorized into reinnervated and denervated based on previously described methods with modifications [22]. The reinnervation rate was calculated as the number of reinnervated NMJs divided by the total number of NMJs.

2.4. Quantitative Real Time-PCR (qRT-PCR). At every detection time point after the 1st and 2nd surgery-I, the expression levels of growth-associated genes (GAGs) in distal nerve, which has been previously shown to be significantly differentially expressed after denervation in vivo, were analyzed by qRT-PCR, including glial cell-derived neurotrophic factor (GDNF), brain-derived neurotrophic factor (BDNF), and nerve growth factor (NGF) [14]. The myelin-related gene myelin protein zero (MPZ) was also analyzed [23]. Additional contralateral intact CPs were used for normalization of the mRNA expression levels (i.e., day 0). Total RNA was extracted from the 5 mm CP segment using TRIzol reagent (Invitrogen, USA) following the manufacturer's protocol. The extracted RNA was further purified using DNase-I to eliminate residual genomic DNA. A total of 1 g of total RNA was reverse-transcribed using random primers and reverse transcriptase (M-MLV-RT, Takara, Japan) following the manufacturer's instructions. qRT-PCR was performed according to standard protocols using SYBR Green Kit (Takara, Japan) in the iCycler iQTM (Bio-Rad) system. Briefly, 1 μl of cDNA was added to a 19 μl reaction mixture containing 0.5 μM primer sets and 0.5X SYBR Green mixture. The primers were designed and synthesized by Integrated DNA Technologies (Shatin, N. T., Hong Kong, China): NGF: forward 5′ACCTCTTCGGACACTCTGGA3′ and reverse 5′GTCCGTGGCTGTGGTCTTAT3′; BDNF: forward 5′GAACAGGACGGAAACAGAACG3′ and reverse 5′GAACAGGACGGAAACAGAACG3′; GDNF: forward 5′GCGGTTCCTGTGAAGCGGCCGA3′ and reverse 5′TAGATACATCCACACCGTTTAGCGG3′; MPZ: forward 5′GGTGGTGCTGTTGCTGCTG3′ and reverse 5′TTGGTGCTTCGGCTGTGGTC3′; and β-actin: forward 5′-TCATGAAGTGTGACGTGGACATC-3′ and reverse 5′TGTTGCATTTGCGGG GACGATG-3′.

The PCR was run in the following cycling conditions: 95°C for 5 min and 35 cycles of 95°C for 30 s, 60°C for 30 s, and 72°C for 40 s. The expression level of each growth factor

gene in the distal nerve was calculated as the fold change compared with that in the contralateral intact nerve (normalized to 1 arbitrary unit) using the 2-$\Delta\Delta$Ct method, where ΔCt represents the difference between the Ct values of each gene and β-actin and $\Delta\Delta$Ct represents the difference in ΔCt between the transected nerve and the intact nerve after normalization to β-actin. All PCRs were performed in triplicate and repeated for 3 times.

2.5. Electrophysiological Analysis. Three months after the 2nd surgery-II, the functional recovery of the GM was evaluated by electrophysiological analysis via a standard nerve-evoked potential recording system (RM6240BD, Chengdu, China) in 10 animals per group. The procedure was performed as previously described and illustrated in Figure 1(f) [11, 13]. In brief, animals were anesthetized and placed in a prone position. The resutured TIB nerve and the right GM muscle were exposed. The bipolar stimulating electrode was placed underneath the nerve and kept contacted. The GM tendon was fixed to the transducer with a 4-0 suture to record muscle contraction force. For compound muscle action potential (CMAP) recording, the stainless-steel monopolar recording electrodes were inserted into the muscle belly, and the grounding electrode was inserted into the subcutaneous tissue. Initial electrical stimulus (0.1 mA; 1 ms duration; 1 Hz frequency; square wave) was applied and gradually increased by 0.1 mA until a supramaximal response was reached. The maximum muscle contraction force and the evoked CMAP were recorded for 5 times with a 2-minute interval. The same procedure was repeated on the contralateral side (L) which was set as the reference value. The results were presented as the ratio of the value on the surgical side (R) to that on the contralateral side (L) (R/L). After electrophysiological analysis, the GM muscle and distal nerve was collected. Subsequent retrograde axonal tracing was performed.

2.6. Electron Microscopy (EM) Analysis. At 3 months after the 2nd surgery-II, after electrophysiology analysis, a 2 mm nerve segment from the distal part of the nerve graft was excised (10 animals per group) (Figure 1(f)). Nerves were postfixed in EM fixative (2.5% glutaraldehyde and 2% PFA in 0.1 M PB, pH 7.4) and 2% osmic acid and then dehydrated in gradient alcohol (30%–95%). Next, nerves were infiltrated and embedded in pure Epon at 60°C for 3 days. Semithin sections (1 μm) were cut with glass knife in microtome and were then stained with 0.5% toluidine blue.

Sections were seen under microscopy and photos were taken. The number of myelinated axons was calculated using ImageJ. A total of 6 fields ($0.5 * 0.5\,\text{mm}^2$) from each animal (10 animals per group) were randomly selected. The G-ratio, which was calculated by dividing the inner diameter of the axon (without myelin) by the outer diameter of the entire fiber (including the myelin), was calculated to evaluate the myelination of regenerating axons. At least 100 myelinated axons were randomly selected in each animal.

2.7. Retrograde Axonal Tracing and FG Counting. At 3 months after the 2nd surgery-II, the regeneration of spinal cord motor neurons into the graft was examined by retrograde axonal tracing with FG (10 animals per group) [24]. In short, after the segment was excised for EM analysis (Figure 1(f)), 0.5 μl of 2% (w/v) FG solution was injected proximally. The injection was slow and lasted for 10 seconds, after which the injection site was clamped with microforceps for 10 seconds and sutured to prevent leakage. The rats were sacrificed 3 days later to examine FG transportation. The L3-6 spinal cord was harvested, used, and processed for frozen section. Longitudinal sections (30 μm thick) were evaluated under a fluorescence microscope (Axioplan, Carl Zeiss, Germany), and the FG-labeled neurons were counted. Two examiners independently counted the neurons with reference to the published protocol [24].

2.8. Statistical Analysis. Imaging analyses were evaluated in a blinded manner. Sections were randomly assigned identification numbers, and two experienced investigators (X Fang and C Zhang), respectively, assessed the slides. The values were averaged before further analysis. All the data are presented as the mean ± SEM. Two-way ANOVA followed by a post hoc Dunnett's test for multiple comparisons was carried out in the SPSS 13.0 software (Chicago, IL). A P value less than 0.05 was considered significant.

3. Results

3.1. Transplanted Neurons Survived in the Distal Stump of CPs at Different Time Points after Injection. At different detection time points after the 1st surgery, IHC was performed to confirm that the transplanted cells survived and differentiated to neurons at the injection sites. One month, three months, and six months after transplantation, many GFP-positive transplanted cells were observed at the distal stump of CPs (Figures 2(a), 2(d), and 2(g)). NeuN-positive neurons were abundant in the transplanted area (Figures 2(b), 2(e), and 2(h)). Cell counts revealed that the number of NeuN-positive cells gradually decreased over time, but there was no significant difference in the number of neurons among the three time points ($P > 0.05$). In the vehicle group, no GFP-positive area was found, and there were no NeuN-positive cells (Figures 2(j)–2(l)). Interestingly, we also noted that the intensity of GFP in NeuN-positive cells was somehow much weaker than that in NeuN-negative cells, similar to a previous report [20].

3.2. The Presence and Absence of Neurons Induced a Transition between the Denervated and Innervated States in the Distal Nerve. Due to the intensity of GFP attenuation in transplanted cells as mentioned above, we used NF200 to label regenerated axons and MBP to label myelin sheath. The immunoreactivity of NF200-positive axons and MBP-positive myelin sheath in the vehicle group decreased gradually as time progressed and was almost undetectable 6 months after the 1st surgery, indicating long-term denervation and fibrosis status (Figures 3(a), 3(b), 3(e), 3(f), 3(i), 3(j), and 3(u)). The regeneration of NF200-positive axons coincided with the expression of MBP-positive myelin sheath, and both were gradually increased in the cell group (Figures 3(c), 3(d), 3(g), 3(h),3(k), 3(l), and 3(u)). Two weeks

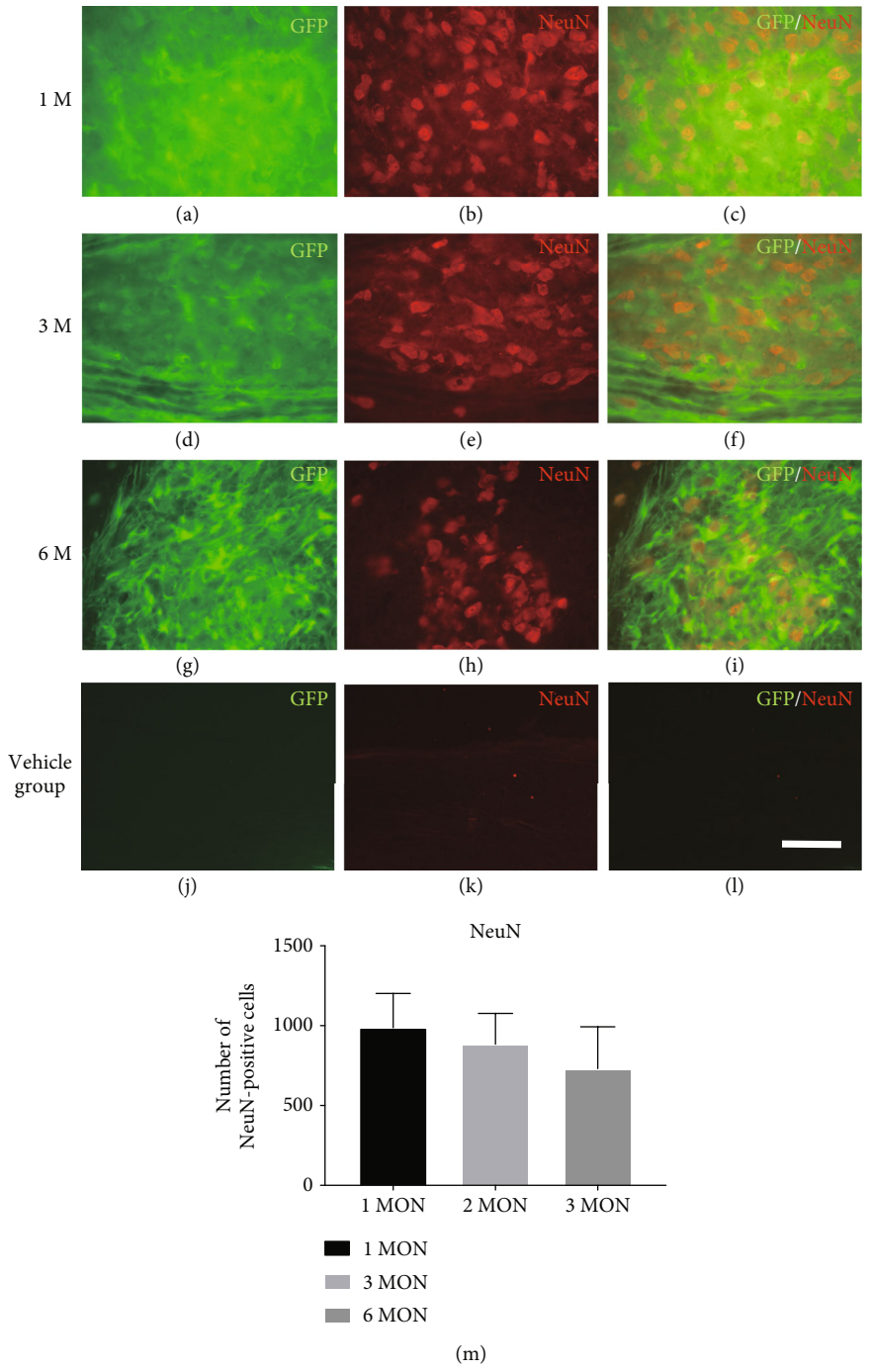

Figure 2: Neuronal survival at different time points after transplantation. A longitudinal section of the transplanted site with NeuN staining showed that many GFP-positive transplanted embryonic cells differentiated into NeuN-positive neurons at different time points. (a–c) One month after transplantation; (d–f) three months after transplantation; (g–i) six months after transplantation. (m) Comparing the mean numbers of NeuN-positive cells per time point revealed no significant differences. Scale bar = 50 μm.

after the 2nd surgery-I, the NF200-positive and MBP-positive signals in the cell group became discontinuous, indicating that Wallerian degeneration reemerges in axons and the myelin sheath (Figures 3(o) and 3(p)); there was no immunoreactivity in the vehicle group (Figures 3(m) and 3(n)). The fluorescent intensity of each section was normalized to the intensity of the contralateral intact CP (Figures 3(q)–3(t)). The time course of axons from transplanted cells grown into denervated CP nerve stumps in the cell group and the process of axonal gradual degeneration in the vehicle group are shown in the histograms in Figure 4(f). The expression of MBP showed the same trend as the expression of NF200.

3.3. The Presence and Absence of Transplanted Neurons Affected the SC Quantity and Phenotype Change in the Distal Nerve. The expression of P75 neurotrophic factor,

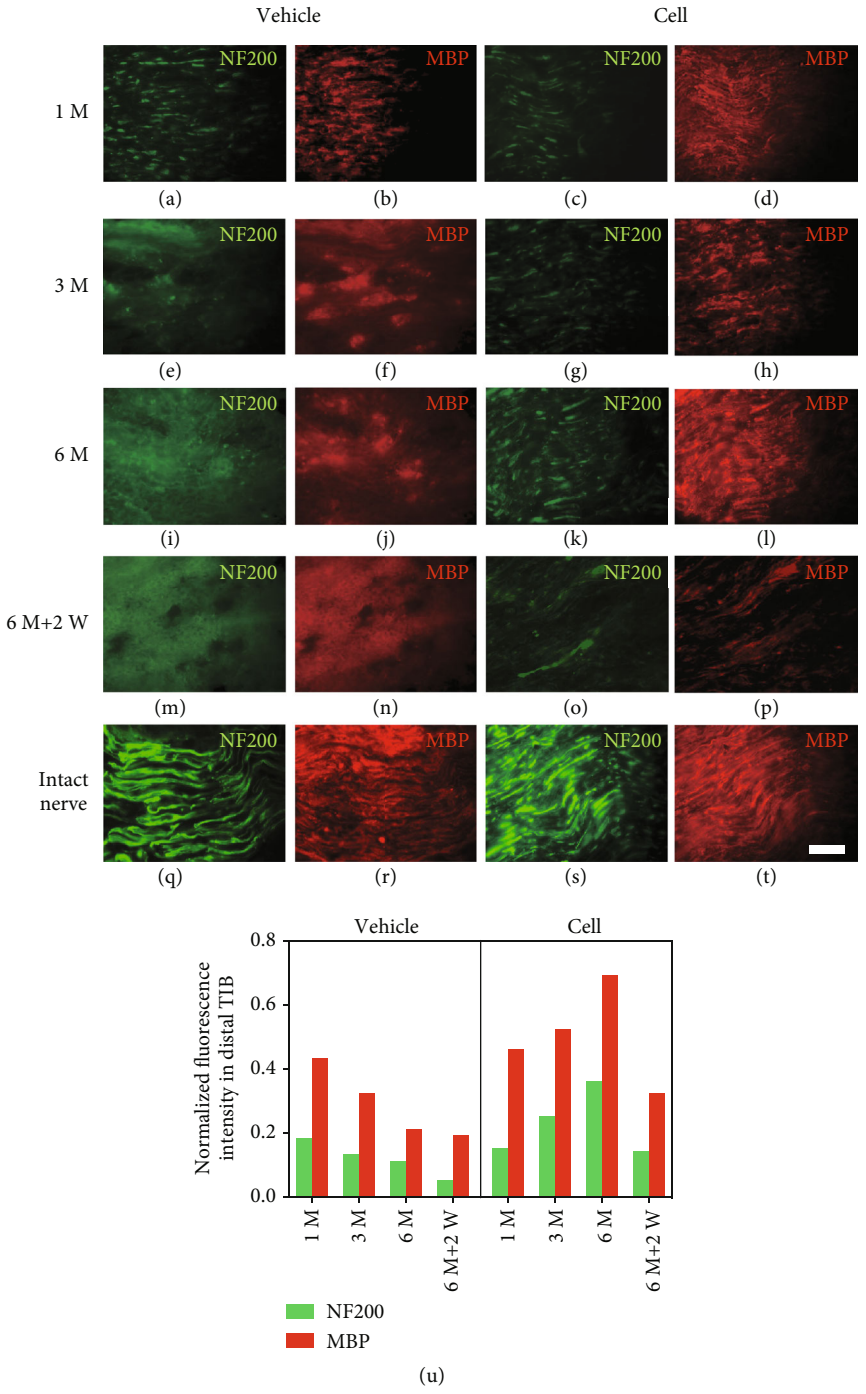

Figure 3: Axonal and myelin sheath status in the distal nerve stump after the 1st and 2nd surgery-I. Longitudinal sections of the distal part of the transplanted site were stained with NF200 (an axon marker) and MBP (a myelin sheath marker). (a–d) One month after the 1st surgery, there were small amounts of myelin debris and axons in the distal stump in the vehicle group. Meanwhile, NF200-positive axons appeared in the cell group and were partially wrapped by the MBP-positive myelin sheath. (e–h) Three months and (i–l) six months after the 1st surgery, the axonal and myelin debris had been gradually eliminated in the vehicle group, and abundant NF200-positive axons and MBP-positive myelin sheath were observed in the cell group. (m–p) Two weeks after the 2nd surgery-I, the vehicle group showed no positive staining. Meanwhile, the distal stump in the cell group reentered a denervated status, exhibiting discontinuous axons and myelin sheath debris. (u) The normalized intensities were determined in triplicate in sections taken from 1 rat. The trend in the expression intensity of NF200-positive axons was consistent with the MBP-positive myelin sheath in both groups. A sharp decline was observed in the expression of both markers after cell excision in the cell group. Scale bar = 100 μm.

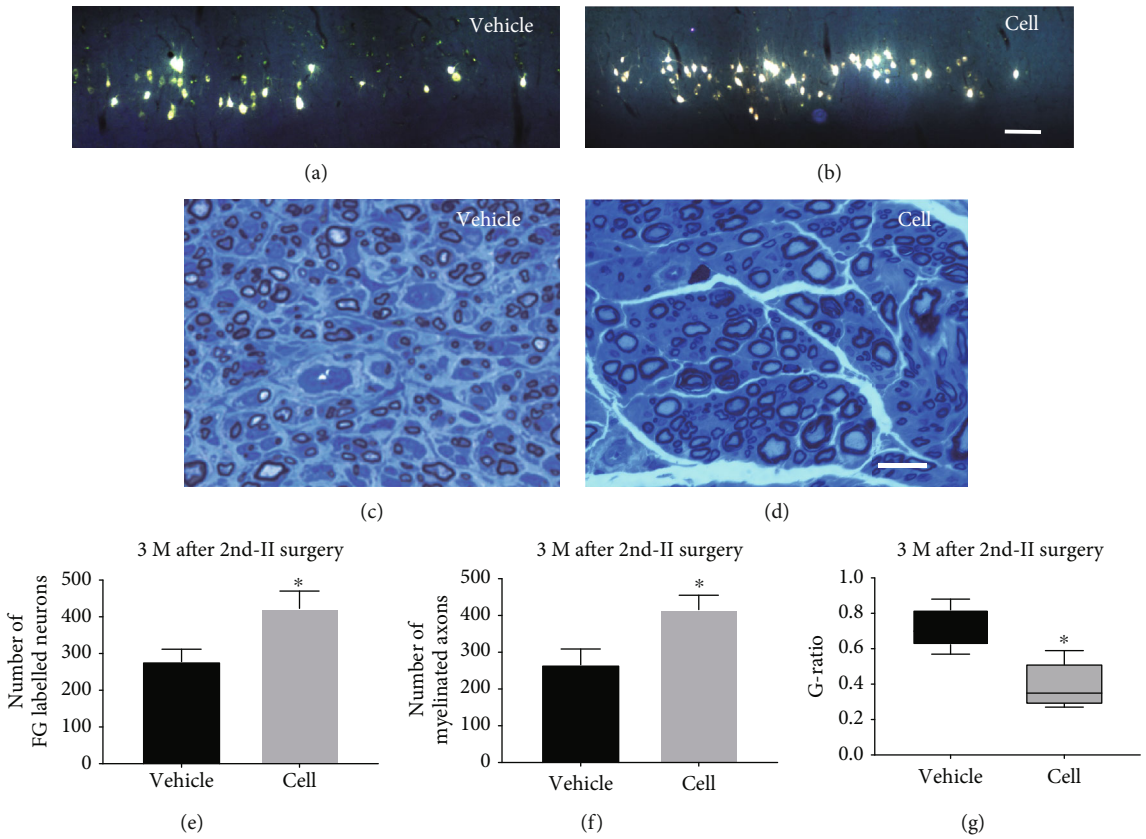

Figure 4: FG labeling of neurons and EM analysis of the distal TIB 3 months after the 2nd surgery-II. (a, b) More FG-labeled neurons were found in the cell group than in the vehicle group. Scale bar = 100 μm. (c, d) More myelinated axons were observed in the cell transplantation group than in the vehicle group. Scale bar = 25 μm. (e) Statistical analysis showed significantly more regenerating neurons in the cell group than in the vehicle group ($^*P < 0.05$, compared with the vehicle group). (f) Statistical analysis showed significantly more myelinated axons in the cell group than in the control group ($^*P < 0.05$, compared with the vehicle group). (g) The G-ratio was significantly lower in the cell group than in the vehicle group ($^*P < 0.05$, compared with the vehicle group).

which is a marker of dedifferentiated SCs, was significantly elevated in the vehicle group 1 month after the 1st surgery (Figure 5(a)). Meanwhile, the expression of P75 in the cell group was weaker than that in the vehicle group (Figure 5(c)). As time progressed, the expression of P75 gradually decreased in both groups, and the expression of P75 in the cell group decreased faster than that in the vehicle group (Figures 5(e) and 5(g)). Six months after the first-stage surgery, the P75 immunoreactivity in the cell group returned to the baseline of myelinating SCs, while a small degree of expression remained in the vehicle group (Figures 5(i) and 5(k)). Two weeks after the second-stage surgery-I, the expression of P75 in the cell group increased again (Figure 5(o)), indicating that the SCs in the cell group underwent another process of dedifferentiation. This process was not observed in the vehicle group, which maintained a low level of expression (Figure 5(m)).

S100, the characteristic cytoplasmic marker of SCs, was used to label the quantity of SCs. One month after the 1st surgery, the intensity of S100 in both groups was slightly lower than that in intact nerves (Figures 5(b) and 5(d)). Three months after the 1st surgery, the intensity of S100 in the vehicle group gradually decreased, and there was only occasional visible fluorescence at 6 months after the 1st surgery (Figures 5(f) and 5(j)). In the cell group, S100 was maintained at a high level at both 3 and 6 months after the 1st surgery (Figures 5(h) and 5(l)). Two weeks after the 2nd stage-I surgery, the expression of S100 in the vehicle group was still low (Figure 5(n)), and the expression of S100 in the cell group declined (Figure 5(p)), indicating that the number of SCs begins to decline after denervation. The fluorescent intensity of each section was normalized to the intensity of the contralateral intact CP (Figures 5(q)–5(t)).

3.4. The Presence and Absence of Transplanted Neurons Affected the Expression of GAGs and a Myelin-Related Gene in the Distal Nerve. Current evidence suggests that SCs in denervated nerves resume a more primitive, nonmyelinating phenotype, upregulate GAGs, and downregulate myelin-related genes to attract proximal axons [25]. The expression of GDNF, BDNF, NGF, and MPZ was measured by qRT-PCR at different time points, and the expression levels in the contralateral intact nerve were normalized to 1 as an arbitrary unit (Figure 6).

One month after the 1st surgery, GDNF expression in the vehicle group was upregulated (by 11-fold compared with intact nerve). In the cell group, GDNF expression was also

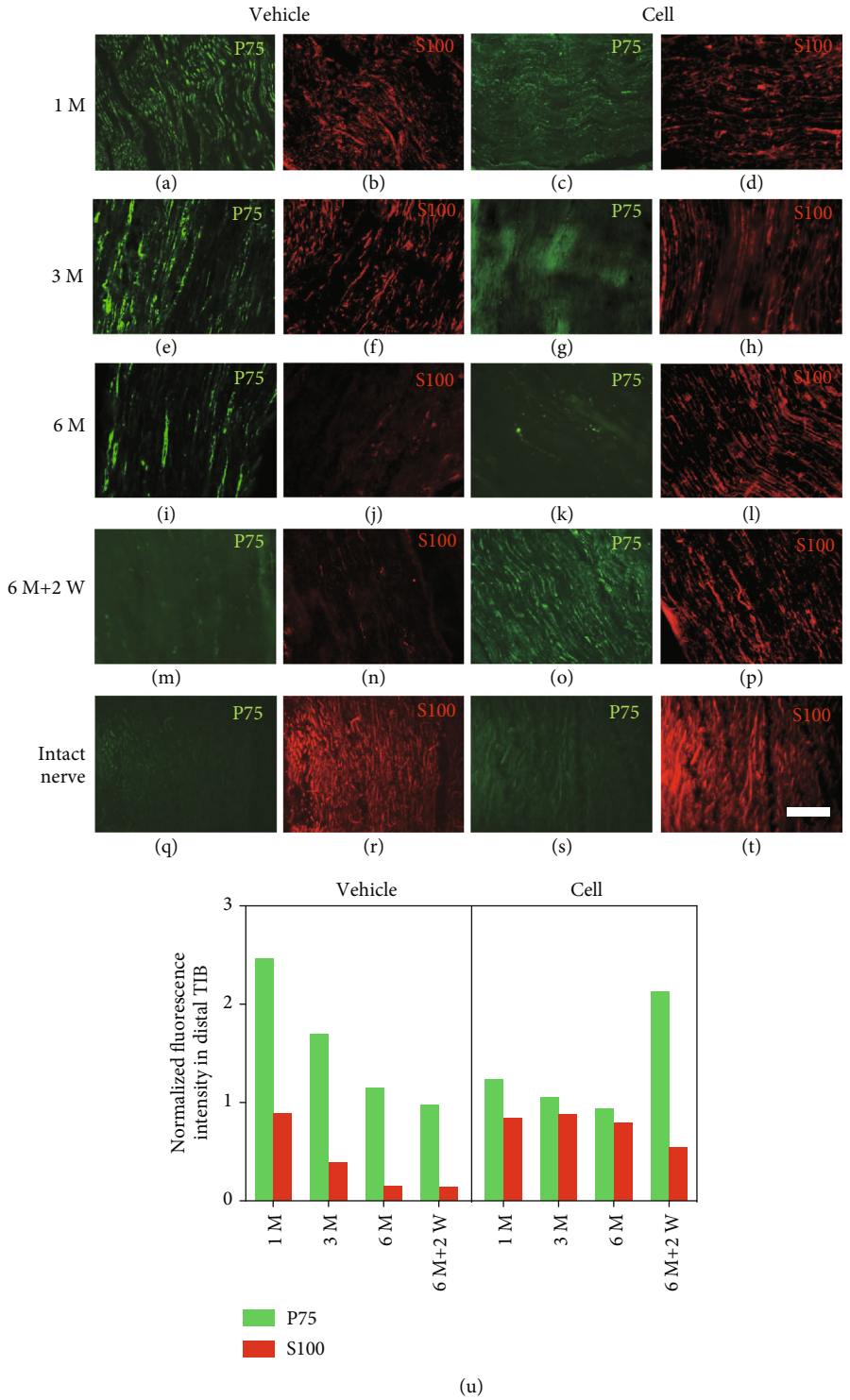

Figure 5: SC quantity and phenotype change in distal nerve stump after the 1st and 2nd surgery-I. Longitudinal sections of the distal part of the transplanted site were stained with S100 (an SC cytoplasmic marker) and P75 (a dedifferentiated SC marker). (a–d) In the vehicle group, one month after the 1st surgery, the intensity of P75 was significantly higher and the intensity of S100 was lower on the transected side than on the intact side. In the cell group, the increase in P75 expression and the decrease in S100 expression were not obvious compared with the vehicle group. (e–l) At 3 and 6 months after the 1st surgery, the expression of both markers had gradually decreased to a low level in the vehicle group. In the cell group, P75 was maintained at a low level while S100 expression was maintained at a high level, and their levels did not significantly fluctuate. (m–p) Two weeks after the 2nd surgery-I, the expression of P75 in the cell group increased, while the expression of S100 decreased; the vehicle group did not exhibit these changes. (u) The expression intensity of P75 and S100 in the vehicle group declined over time. In the cell group, a reversal in the expression of P75 (low to high) and S100 (high to low) was observed after excision of the transplanted cells. Scale bar = 100 μm.

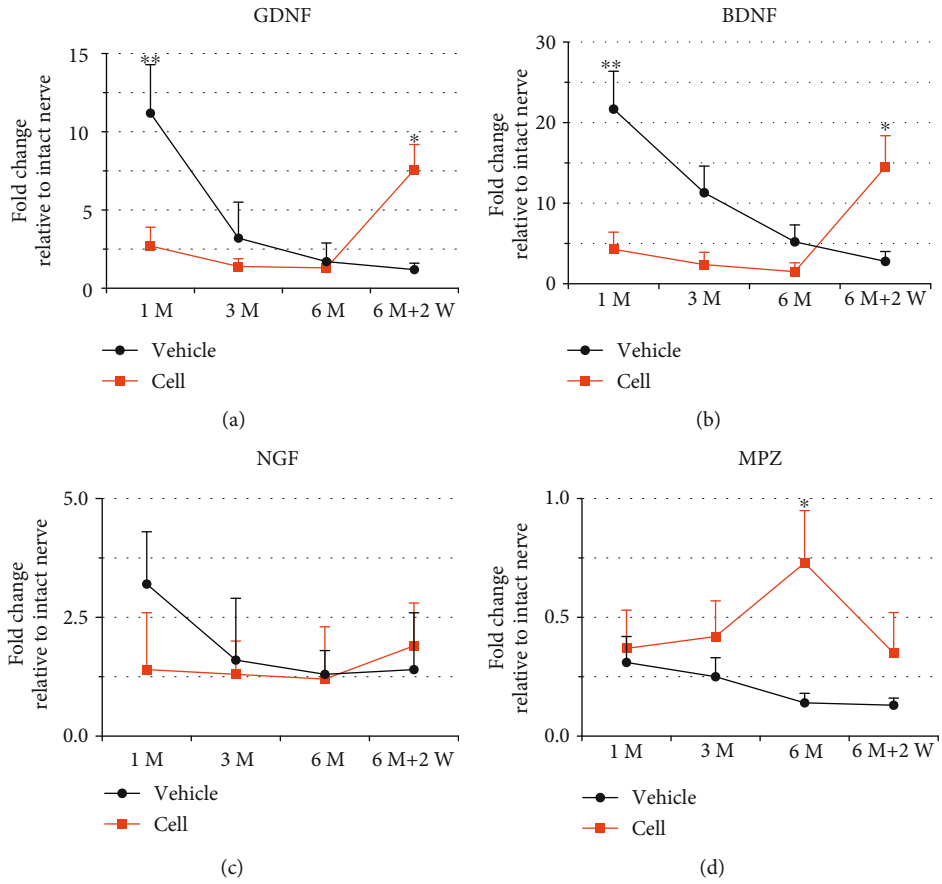

Figure 6: Temporal mRNA expression of growth factors in the distal nerve stump after the 1st and 2nd surgery-I. The transplanted neurons downregulated the expression of GAGs (a, GDNF; b, BDNF; c, NGF) and upregulated the expression of a myelin-related gene (d, MPZ). Two weeks after the 2nd surgery-I, the excision of transplanted neurons upregulated the expression of GAGs and downregulated the expression of a myelin-related gene. The expression level for each gene in the distal nerve was calculated as the fold change compared with that in the contralateral intact nerve (normalized to 1 as an arbitrary unit). Asterisks placed above the standard error bars indicate a significant difference between the cell injection and vehicle injection groups at a given time point ($^{**}P < 0.01$ compared with the vehicle injection group, $^{*}P < 0.05$ compared with the vehicle injection group). Error bars represent SEM.

upregulated (by 3-fold compared with intact nerve) but was significantly lower than that in the vehicle injection group (Figure 6(a), $^{**}P < 0.01$ compared with the vehicle injection group). Three and six months after the 1st surgery, the expression levels of GDNF in the vehicle injection and cell injection groups both declined and were not significantly different (Figure 6(a), $P > 0.05$). Two weeks after the 2nd surgery-I, the expression of GDNF in the cell injection group was significantly elevated, reaching 8-fold the level in the intact nerve, and was significantly higher than that in the vehicle injection group, which declined to 1.2-fold the level in the intact nerve (Figure 6(a), $^{*}P < 0.05$ compared with the vehicle injection group). BDNF expression exhibited similar changes. One month after the 1st surgery, BDNF expression was increased by 22-fold and 4-fold in the vehicle injection and cell injection groups, respectively, and the difference was significant (Figure 6(b), $^{**}P < 0.01$ compared with the vehicle injection group). Three and six months after the 1st surgery, the expression level of BDNF in the vehicle group declined over time; although it was still higher than the expression in the cell group, there was no significant difference between the groups (Figure 6(b), $P > 0.05$). Two weeks after the 2nd surgery-I, the expression level of BDNF in the cell injection group was significantly elevated, reaching 14-fold the level in the intact nerve, and was significantly higher than that in the vehicle injection group, which declined to 2.8-fold the level in the intact nerve (Figure 6(b), $^{*}P < 0.05$ compared with the vehicle injection group). NGF exhibited a different expression pattern from the former two factors. At one month after the 1st surgery, NGF expression increased in the vehicle group (by 3.2-fold compared with the intact nerve) but gradually fell to the baseline level at a later time point. The cell group remained at a low level of NGF expression at all time points. There was no significant difference in the expression between the two groups at any time point (Figure 6(c), $P > 0.05$).

The expression of MPZ in the two groups showed the opposite trend compared with the BDNF and GDNF. The cell group showed a gradually increasing trend at 1 month, 3 months, and 6 months after the 1st surgery and a decreasing trend 2 weeks after the 2nd surgery. The vehicle group showed a gradual downward trend after the 1st surgery. The

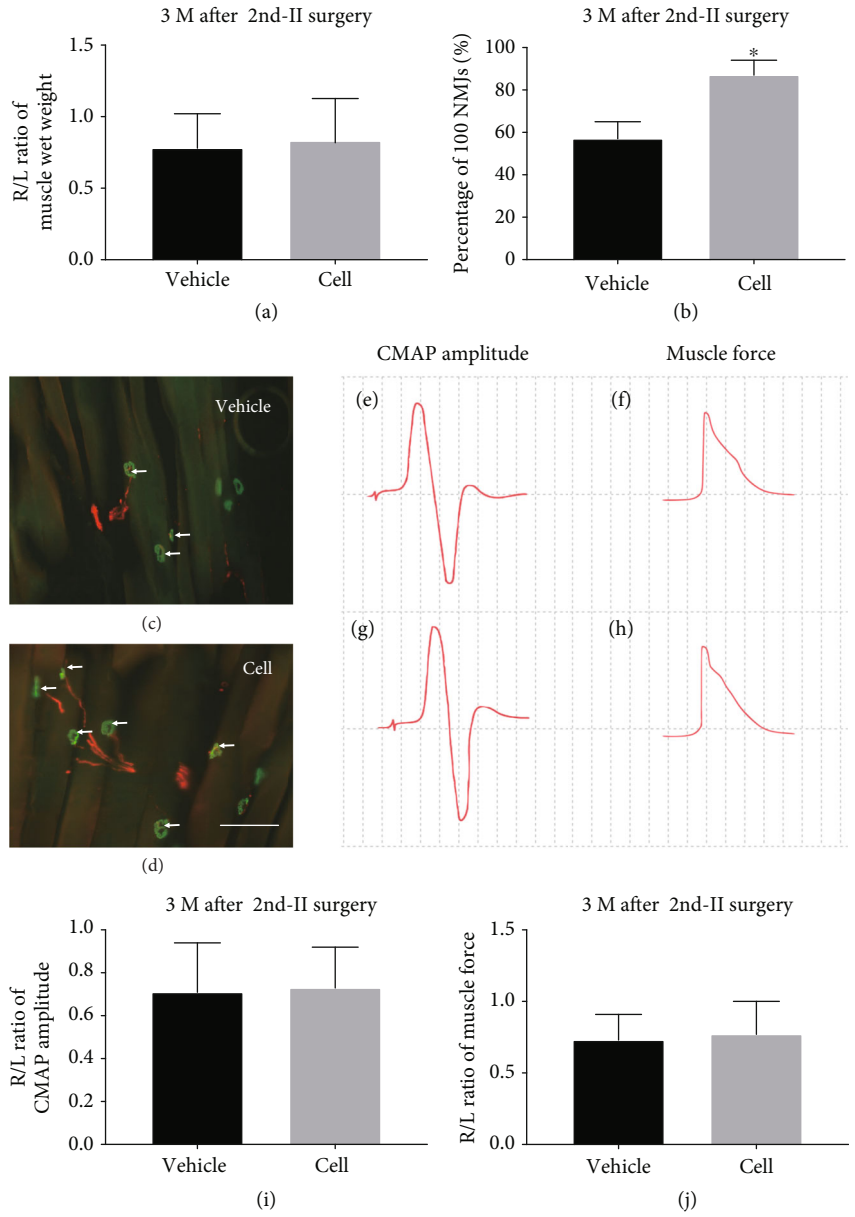

FIGURE 7: IHC and electrophysiological analysis of the GM 3 months after the 2nd surgery-II. (a) There was no significant difference in the R/L wet weight ratio between the two groups ($P > 0.05$). (b–d) IHC staining of NMJs showed more reestablished NMJs (arrows) in the cell group than in the vehicle group. Statistical analysis showed a higher reinnervation rate in the cell group ($^*P < 0.05$, compared with the vehicle injection group). (e–h) Typical CMAP amplitude and muscle force. (i, j) The R/L ratio of CMAP amplitude and muscle force in the cell group showed no significant differences compared with the vehicle group ($P > 0.05$).

expression of MPZ in the cell group at each time point was higher than that in the vehicle group, and the difference between the two groups at 6 months after the 1st surgery was significant (Figure 6(d), $^*P < 0.05$ compared with the vehicle injection group).

3.5. Reactivation of SCs in Grafts Promoted Axon Regeneration and Remyelination after 2nd Surgery-II. After the segment including the grafted cells was removed and a 10 mm segment of the distal stump was transplanted to bridge the freshly cut TIB nerve, the axon from the proximal TIB nerve was able to regenerate into the graft. Three months later, retrograde FG labeling and EM analysis were performed to evaluate regeneration and remyelination in the transplanted nerve. The number of labeled motor neurons in the cell group was significantly higher than that in the vehicle group (278.1 ± 34.3 vs. 423.4 ± 47.8, $P < 0.05$; Figures 4(a), 4(b), and 4(e)). Consistent with the finding of FG labeling, the number of myelinated axons in the vehicle group was more abundant in the cell group (266.2 ± 43.7 vs. 416.3 ± 49.5, $P < 0.05$; Figures 4(c), 4(d), and 4(f)). Moreover, the G-ratio (axonal diameter/total length of the myelin sheath) in the cell group was significantly higher than that in the PC group (0.71 ± 0.04 vs. $0.39 \pm$

0.05, $P < 0.05$; Figure 4(g)), indicating that the myelin sheath of the myelinated nerve fibers in the cell group was thicker than that in the vehicle group.

3.6. Reactivation of SCs in Grafts Promoted Reinnervation of the Muscle after the 2nd Surgery-II. Three months after the 2nd surgery-II, the muscles of each group were significantly atrophied compared with those on the contralateral side. The wet weight R/L ratios of the quadriceps muscles in the vehicle group and cell group were 0.77 ± 0.17 and 0.61 ± 0.12, respectively, which did not significantly differ (Figure 7(a), $P > 0.05$). We further analyzed the reinnervation of the denervated motor endplates by IHC staining of axon terminals and AchRs (Figures 7(c) and 7(d)). We found both denervated and reinnervated motor endplates in both groups, and the reinnervation rate was significantly higher in the cell group than in the vehicle group 3 months after the 2nd surgery-II ($P < 0.05$, Figure 7(b)). Electrophysiological analysis showed that the average CMAP and muscle contractility force were slightly higher in the cell group than in the vehicle group (Figures 7(e)–7(h)), but there were no statistically significant differences (Figures 7(i) and 7(j), $P > 0.05$).

4. Discussion

In this study, we combined cell transplantation and nerve transfer strategies to investigate whether the transplantation of embryonic spinal cord cells could benefit the microenvironment of the distal stump of the injured nerve. A two-stage surgery model was used, and we showed that at different times after transplantation, the transplanted embryonic spinal cord cells could survive and generate neurons. Thus, the neurons play the role of proximal axons to prevent chronic degeneration and fibrosis of SCs. After excision of the transplanted cells, the SCs returned to their dedifferentiated phenotype and upregulated growth-associated gene expression. The ability of SCs to be activated again allowed a favorable microenvironment to be created and enhanced the regeneration and remyelination of proximal axons. Muscle reinnervation was also elevated. This transplantation strategy could provide a treatment option for complex neurological injuries in the clinic.

4.1. The Principle Underlying the Design of the Experiment. As early as 1993, Erb et al. transplanted embryonic spinal cord cells into the distal stump of an injured peripheral nerve and found that neurons could survive and regenerate axons, dominating distal muscles [26]. To promote the efficacy of transplantation, later studies introduced several methods to transform the cells by inducing differentiation, applying electrical stimulation, increasing trophic factor expression, and transfecting with light-sensitive proteins [27–30]. However, the main purpose of these studies was neuronal replacement, and it remains difficult to use the abovementioned cells to replace autologous neurons in clinical practice. Because the distal nerve stump may be less tolerating than muscle, a more practical strategy to improve regeneration is to maintain the distal nerve in an "available" state to accept the proximal axons [17]. A previous study used mesenchymal stem cell transplantation to activate denervated SCs in predegenerated nerves, but because the denervation time of the distal stump is short, the true utility of this approach is uncertain [31]. The current "side-to-side," "side-to-end," "end-to-side," and "supercharge end-to-side" surgical methods in clinical practice are used to "babysit" distal nerves while waiting for the arrival of proximal regenerating axons [10, 32, 33]. Inspired by the clinical "babysit" concept, after transplanting cells to protect the distal nerve for a period of time, we cut off the cells and terminated the protection. The role of transplanted cells is "mobile power charging" without relying on surrounding donor nerves. The purpose of this study is to demonstrate that the presence and absence of transplanted cells have a regulatory effect on SCs in the distal nerve and this regulation can improve the ability of SCs to induce proximal axons.

In our previous studies, it was also proven that the reexcision of transplanted cells promoted the regeneration of axons after secondary replantation, although the degeneration time of the distal nerves in the experimental model was only 3 months [13]. Gordon et al. found that the proliferation and phenotypic changes of SCs in the distal nerves after peripheral nerve transection were maintained until one month after surgery. With prolonged denervation time, the number of SCs and the expression of GAGs in the distal nerves gradually decrease. Six months after transection, SCs are significantly atrophied, and the reversion of growth factor expression to baseline levels makes axonal regeneration difficult to induce [15]. Therefore, the time of chronic neurodegeneration was extended to 6 months in this study. Moreover, our previous research used a cross-suture model, which was unable to distinguish cells from promoting regeneration through the action of distal nerves or muscles. The mechanism underlying the phenomenon was not clearly explained. This study used a cell-treated graft to bridge fresh nerve axotomy, thus excluding the effects of muscle factors on the results, demonstrating that cell-treated grafts do improve the regeneration of proximal axons. Changes in the SC phenotype and GAG expression were also detected at different time points after cell transplantation and after excision of the transplanted cells to explore the interaction between transplanted cells and peripheral nerve SCs.

4.2. Innervation by Transplanted Neurons Maintained the Quantity and Myelinated Phenotype of SCs. During peripheral nerve regeneration, SC proliferation was enhanced by growth-associated proteins (GAPs), such as neuregulin and GAP-43, which are secreted by proximal axons. When SCs do not receive a proximal signal for a long period of time, they gradually degenerate and decrease in number [34]. In the present study, during the 6-month period of survival of transplanted cells, S100 IHC staining suggested that the number of SCs in the distal nerves was maintained at a high level, while the SCs in the vehicle group gradually degenerated, exhibited fibrosis, and decreased in number. Thus, transplanted cells may replace proximal axons and play a role in maintaining the number of SCs, laying the foundation for promoting regeneration after the 2nd surgery.

In addition to proliferation, dedifferentiated SCs transform the myelin-formation phenotype into a growth-supportive phenotype. The expression of myelin-related genes decreased, and the expression of dedifferentiated SC marker P75 and GAGs such as GDNF, BDNF, and NGF was upregulated [35]. Consistent with previous research, one month after the 1st surgery, P75 and the trophic factors GDNF and BDNF were highly expressed in the vehicle group. It was noted from our study that NGF was not statistically different at all time points. This may be due to the fact that NGF is a traditional sensory neurotrophins, the expression of which will be upregulated in denervated sensory nerve (cutaneous-derived SCs), but its degree of upregulation was significantly weaker than that of another sensory neurotrophins "BDNF." Moreover, the CP was a mixed nerve and predominated was motor axons, after denervation, the motor-derived SCs may not upregulate the expression of NGF. Together, these two factors lead to the upregulation of NGF in the vehicle group not as significant as BDNF and GDNF in the denervated CP. This is consistent with a previous report that the expression of NGF was not significantly different in the denervated nerve and immediately repaired nerve [14].

When proximal axonal growth occurs, SCs gradually change from a dedifferentiated phenotype to a mature phenotype when they form myelin to surround axons to support nerve impulse conduction, and therefore, the expression of P75 and GAGs declines [14, 35, 36]. Based on the IHC results, we confirmed that after the 1st surgery, in the cell group, neurons gradually emitted axons to innervate the distal nerves, while SCs gradually formed myelin sheaths to surround axons over time. The distal nerve switched from a denervated state to an innervated state. The expression of P75 was significantly lower in the cell group than in the vehicle group at 1 month after the 1st surgery, suggesting a decrease in dedifferentiated SCs. Similarly, the expression of regeneration-related factors was also significantly lower in the cell group than in the vehicle group. When more SCs were converted to mature phenotypes, the expression of P75 and regeneration-related factors in the cell group decreased slowly. SCs in the vehicle group decreased their P75 and trophic factor expression levels at a faster rate over time, which were similar to the levels in the cell group at 6 months after the 1st surgery. The growth-supportive phenotype cannot be maintained for a long period of time without proximal axons, and thus, SCs eventually enter a chronic degenerative and fibrotic state [14, 34, 37].

4.3. Reactivation of SCs by Transplanted Neuron Excision Promoted Axon Regeneration and Remyelination. Six months after the 1st surgery, minimal positive staining for P75 was found in the distal nerve in both groups. The expression of GAGs in the two groups was also at a low level close to baseline. However, the expression of the myelin gene was still active distal to the cell transplanted site in the cell group, indicating that remyelination was ongoing. MBP staining also confirmed gradual formation of the myelin sheath over time in the cell group. These phenomena were absent in the vehicle group.

Two weeks after the 2nd surgery-I, the expression of P75 in the distal cells of the cell group again increased. The levels of neurotrophic factors GDNF and BDNF were significantly higher than the baseline levels before excision, while the expression of the myelin gene was significantly lower than before excision. The vehicle group did not exhibit this effect, suggesting that resecting the cell transplanted site is equivalent to cutting off the proximal axon again. The SCs in the distal stump of the cell transplantation site undergo a "fresh degeneration" process and convert to a dedifferentiated phenotype. The function of SCs shifts from forming myelin to guiding axon regeneration. In the vehicle group, SCs undergo long-term degeneration for 6 months and become atrophic and fibrotic, and even if the proximal nerve segment is removed, a state of dedifferentiation cannot be reinitiated. These results also indirectly suggest an interaction between the transplanted cells and the distal segment of SCs, and the effect provides an ideal environment for axonal regeneration.

In the 2nd surgery-II, the redegeneration distal CP nerve was used as a graft to bridge the freshly cut TIB nerve end. The results also demonstrated that the cell-protected nerve segment promoted the regeneration of proximal axons, which verified our hypothesis. The EM analysis also revealed that the remyelination of regenerated axons was significantly improved, indicating that the SCs in the graft did not lose their ability to form myelin after redegeneration, but rather, this ability was enhanced. Furthermore, we examined the recovery of muscle after the 2nd surgery-II and found that the reinnervation rate of the GM in the cell group was increased, although there were no significant differences in muscle atrophy and EMG function. In a study by Gordon et al., the degree of muscle atrophy and contraction force after bridging surgery was similar between the chronic denervation graft group and the fresh graft group, which is consistent with our results [4]. A possible explanation is that although the number of axons through the chronic denervation graft is insufficient, the limited number of formed motor units can compensate for the loss of quantity by the increased function of a single motor unit, thereby achieving functional recovery and alleviating atrophy. In our previous study, the model protected both the distal nerves and muscles, and a difference in muscle atrophy and function was found after the second-stage repair. The findings proved that transplanted cells have a separate protective effect on muscles, although the mechanism requires further study [13]. These data prove our original argument that the activation of chronic SC denervation but not chronic denervation of muscles by our strategy improves axon regeneration and reinnervation independently.

There are several limitations of this study. First, our study lacked a noninjected control group containing animals that did not receive an injection. It is possible that the second surgery itself may have an effect on the distal stump even without the implantation of cells. Furthermore, the embryonic spinal cord cells were a mixture of neurons and neural progenitor cells [38]. We lacked a group of other cells (such as glial cells) and cannot rule out the possible effects of factors secreted by glial cells on the results; a more pure neuron source, such as

induced pluripotent cells, would be ideal. Moreover, the mechanisms underlying the protection of the denervated muscle from atrophy remain to be elucidated, and further studies from a molecular perspective are required.

5. Conclusions

Neurons transplanted into the distal stump of the injured nerve can interact with SCs, playing the role to some extent of proximal axons and preventing chronic degeneration and fibrosis of SCs. The ability of SCs to be activated again after resection of the neurons allows a favorable microenvironment to be created for promoting the growth of proximal axons. This transplant strategy could provide a treatment option for complex neurological injuries in the clinic.

Data Availability

The data used to support the findings of this study are included within the article.

Conflicts of Interest

The authors declare no conflicts of interest.

Authors' Contributions

Xinyu Fang and Chaofan Zhang contributed equally to this work.

Acknowledgments

This research was funded in part by the following: the National Science Foundation for Young Scientists of China (Grant No. 81702168), the Fujian Youth Development Programme of NHC (Grant No. 2018-ZQN-31), and the Fujian Science Foundation Youth Innovation Project (Grant No. 2018J05138).

References

[1] M. Siemionow and E. Sonmez, "Nerve allograft transplantation: a review," *Journal of Reconstructive Microsurgery*, vol. 23, no. 8, pp. 511–520, 2007.

[2] R. Deumens, A. Bozkurt, M. F. Meek et al., "Repairing injured peripheral nerves: bridging the gap," *Progress in Neurobiology*, vol. 92, no. 3, pp. 245–276, 2010.

[3] T. Gordon, P. Eva, and G. H. Borschel, "Delayed peripheral nerve repair: methods, including surgical "cross-bridging" to promote nerve regeneration," *Neural Regeneration Research*, vol. 10, no. 10, pp. 1540–1544, 2015.

[4] T. Gordon, N. Tyreman, and M. A. Raji, "The basis for diminished functional recovery after delayed peripheral nerve repair," *The Journal of Neuroscience*, vol. 31, no. 14, pp. 5325–5334, 2011.

[5] S. Jonsson, R. Wiberg, A. M. McGrath et al., "Effect of Delayed Peripheral Nerve Repair on Nerve Regeneration, Schwann Cell Function and Target Muscle Recovery," *PLoS ONE*, vol. 8, no. 2, article e56484, 2013.

[6] J. R. Bain, Y. Hason, K. Veltri, M. Fahnestock, and C. Quartly, "Clinical application of sensory protection of denervated muscle," *Journal of Neurosurgery*, vol. 109, no. 5, pp. 955–961, 2008.

[7] J. Barbour, A. Yee, L. C. Kahn, and S. E. Mackinnon, "Supercharged end-to-side anterior interosseous to ulnar motor nerve transfer for intrinsic musculature reinnervation," *The Journal of Hand Surgery*, vol. 37, no. 10, pp. 2150–2159, 2012.

[8] S. J. Farber, S. W. Glaus, A. M. Moore, D. A. Hunter, S. E. Mackinnon, and P. J. Johnson, "Supercharge nerve transfer to enhance motor recovery: a laboratory study," *The Journal of Hand Surgery*, vol. 38, no. 3, pp. 466–477, 2013.

[9] J. M. Hendry, M. C. Alvarez-Veronesi, A. Snyder-Warwick, T. Gordon, and G. H. Borschel, "Side-to-side nerve bridges support donor axon regeneration into chronically denervated nerves and are associated with characteristic changes in schwann cell phenotype," *Neurosurgery*, vol. 77, no. 5, pp. 803–813, 2015.

[10] J. K. Terzis and K. Tzafetta, "The "babysitter" procedure: minihypoglossal to facial nerve transfer and cross-facial nerve grafting," *Plastic and Reconstructive Surgery*, vol. 123, no. 3, pp. 865–876, 2009.

[11] Y. Liu, R. M. Grumbles, and C. K. Thomas, "Electrical stimulation of embryonic neurons for 1 hour improves axon regeneration and the number of reinnervated muscles that function," *Journal of Neuropathology and Experimental Neurology*, vol. 72, no. 7, pp. 697–707, 2013.

[12] N. G. Fairbairn, A. M. Meppelink, J. Ng-Glazier, M. A. Randolph, and J. M. Winograd, "Augmenting peripheral nerve regeneration using stem cells: a review of current opinion," *World Journal of Stem Cells*, vol. 7, no. 1, pp. 11–26, 2015.

[13] W. Zhang, X. Fang, C. Zhang et al., "Transplantation of embryonic spinal cord neurons to the injured distal nerve promotes axonal regeneration after delayed nerve repair," *The European Journal of Neuroscience*, vol. 45, no. 6, pp. 750–762, 2017.

[14] B. Michalski, J. R. Bain, and M. Fahnestock, "Long-term changes in neurotrophic factor expression in distal nerve stump following denervation and reinnervation with motor or sensory nerve," *Journal of Neurochemistry*, vol. 105, no. 4, pp. 1244–1252, 2008.

[15] O. A. R. Sulaiman and T. Gordon, "Role of chronic Schwann cell denervation in poor functional recovery after nerve injuries and experimental strategies to combat it," *Neurosurgery*, vol. 65, Supplement 4, pp. A105–A114, 2009.

[16] R. Lapalombella, H. Kern, N. Adami et al., "Persistence of regenerative myogenesis in spite of down-regulation of activity-dependent genes in long-term denervated rat muscle," *Neurological Research*, vol. 30, no. 2, pp. 197–206, 2008.

[17] U. Carraro, S. Boncompagni, V. Gobbo et al., "Persistent muscle fiber regeneration in long term denervation. Past, present, future," *European Journal of Translational Myology*, vol. 25, no. 2, p. 77, 2015.

[18] X.-Y. Fang, W.-M. Zhang, C.-F. Zhang et al., "Lithium accelerates functional motor recovery by improving remyelination of regenerating axons following ventral root avulsion and reimplantation," *Neuroscience*, vol. 329, pp. 213–225, 2016.

[19] X. Fang, C. Zhang, Z. Yu, W. Li, Z. Huang, and W. Zhang, "GDNF pretreatment overcomes Schwann cell phenotype mismatch to promote motor axon regeneration via sensory graft," *Experimental Neurology*, vol. 318, pp. 258–266, 2019.

[20] H. Su, W. Zhang, X. Yang et al., "Neural progenitor cells generate motoneuron-like cells to form functional connections

with target muscles after transplantation into the musculocutaneous nerve," *Cell Transplantation*, vol. 21, no. 12, pp. 2651–2663, 2012.

[21] R. W. Oppenheim, T. Cole, and D. Prevette, "Early regional variations in motoneuron numbers arise by differential proliferation in the chick embryo spinal cord," *Developmental Biology*, vol. 133, no. 2, pp. 468–474, 1989.

[22] C. Huzé, S. Bauché, P. Richard et al., "Identification of an agrin mutation that causes congenital myasthenia and affects synapse function," *American Journal of Human Genetics*, vol. 85, no. 2, pp. 155–167, 2009.

[23] S. G. Slutsky, A. K. Kamaraju, A. M. Levy, J. Chebath, and M. Revel, "Activation of myelin genes during transdifferentiation from melanoma to glial cell phenotype," *The Journal of Biological Chemistry*, vol. 278, no. 11, pp. 8960–8968, 2003.

[24] H.-Y. Gu, H. Chai, J.-Y. Zhang et al., "Survival, regeneration and functional recovery of motoneurons after delayed reimplantation of avulsed spinal root in adult rat," *Experimental Neurology*, vol. 192, no. 1, pp. 89–99, 2005.

[25] T. M. Brushart, M. Aspalter, J. W. Griffin et al., "Schwann cell phenotype is regulated by axon modality and central-peripheral location, and persists in vitro," *Experimental Neurology*, vol. 247, pp. 272–281, 2013.

[26] D. E. Erb, R. J. Mora, and R. P. Bunge, "Reinnervation of adult rat gastrocnemius muscle by embryonic motoneurons transplanted into the axotomized tibial nerve," *Experimental Neurology*, vol. 124, no. 2, pp. 372–376, 1993.

[27] G. T. Casella, V. W. Almeida, R. M. Grumbles, Y. Liu, and C. K. Thomas, "Neurotrophic factors improve muscle reinnervation from embryonic neurons," *Muscle & Nerve*, vol. 42, no. 5, pp. 788–797, 2010.

[28] D. C. Yohn, G. B. Miles, V. F. Rafuse, and R. M. Brownstone, "Transplanted mouse embryonic stem-cell-derived motoneurons form functional motor units and reduce muscle atrophy," *The Journal of Neuroscience*, vol. 28, no. 47, pp. 12409–12418, 2008.

[29] Y. Liu, R. M. Grumbles, and C. K. Thomas, "Electrical stimulation of transplanted motoneurons improves motor unit formation," *Journal of Neurophysiology*, vol. 112, no. 3, pp. 660–670, 2014.

[30] J. B. Bryson, C. B. Machado, M. Crossley et al., "Optical control of muscle function by transplantation of stem cell–derived motor neurons in mice," *Science*, vol. 344, no. 6179, pp. 94–97, 2014.

[31] Y. Zheng, C. Huang, F. Liu et al., "Reactivation of denervated Schwann cells by neurons induced from bone marrow- derived mesenchymal stem cells," *Brain Research Bulletin*, vol. 139, pp. 211–223, 2018.

[32] A. Ladak, P. Schembri, J. Olson, E. Udina, N. Tyreman, and T. Gordon, "Side-to-side nerve grafts sustain chronically denervated peripheral nerve pathways during axon regeneration and result in improved functional reinnervation," *Neurosurgery*, vol. 68, no. 6, pp. 1654–1666, 2011.

[33] J. Isaacs, "Supercharged end-to-side nerve transfer: too soon for "prime time"?," *The Journal of Hand Surgery*, vol. 38, no. 3, pp. 617-618, 2013.

[34] K. M. Chan, T. Gordon, D. W. Zochodne, and H. A. Power, "Improving peripheral nerve regeneration: from molecular mechanisms to potential therapeutic targets," *Experimental Neurology*, vol. 261, pp. 826–835, 2014.

[35] U. Namgung, "The role of Schwann cell-axon interaction in peripheral nerve regeneration," *Cells, Tissues, Organs*, vol. 200, no. 1, pp. 6–12, 2015.

[36] W. Sulaiman and T. Gordon, "Neurobiology of peripheral nerve injury, regeneration, and functional recovery: from bench top research to bedside application," *The Ochsner Journal*, vol. 13, no. 1, pp. 100–108, 2013.

[37] G. Ronchi, M. Cillino, G. Gambarotta et al., "Irreversible changes occurring in long-term denervated Schwann cells affect delayed nerve repair," *Journal of Neurosurgery*, vol. 127, no. 4, pp. 843–856, 2017.

[38] Z. Ren, Y. Wang, J. Peng, Q. Zhao, and S. Lu, "Role of stem cells in the regeneration and repair of peripheral nerves," *Reviews in the Neurosciences*, vol. 23, no. 2, pp. 135–143, 2012.

Hindawi
Stem Cells International
Volume 2019, Article ID 4242178, 11 pages
https://doi.org/10.1155/2019/4242178

Research Article

Strontium Promotes the Proliferation and Osteogenic Differentiation of Human Placental Decidual Basalis- and Bone Marrow-Derived MSCs in a Dose-Dependent Manner

Yi-Zhou Huang,[1,2] Cheng-Guang Wu,[1] Hui-Qi Xie,[1] Zhao-Yang Li,[3] Antonietta Silini,[4] Ornella Parolini,[4,5] Yi Wu,[6] Li Deng,[1] and Yong-Can Huang[7,8,9]

[1]*Laboratory of Stem Cell and Tissue Engineering, State Key Laboratory of Biotherapy and Cancer Center, West China Hospital, Sichuan University and Collaborative Innovation Center of Biotherapy, Chengdu, Sichuan 610041, China*
[2]*Department of Orthopaedics, West China Hospital, Sichuan University, Chengdu, Sichuan 610041, China*
[3]*School of Materials Science and Engineering, Tianjin University, Tianjin 300072, China*
[4]*Centro di Ricerca E. Menni, Fondazione Poliambulanza-Istituto Ospedaliero, Brescia 25124, Italy*
[5]*Istituto di Anatomia Umana e Biologia Cellulare, Università Cattolica del Sacro Cuore Facoltà di Medicina e Chirurgia, Roma 00168, Italy*
[6]*Medical College, Jinggangshan University, Ji'an, Jiangxi 343009, China*
[7]*Shenzhen Engineering Laboratory of Orthopaedic Regenerative Technologies, Orthopaedic Research Center, Peking University Shenzhen Hospital, Shenzhen, Guangdong 518036, China*
[8]*Shenzhen Key Laboratory of Spine Surgery, Department of Spine Surgery, Peking University Shenzhen Hospital, Shenzhen, Guangdong 518036, China*
[9]*National & Local Joint Engineering Research Center of Orthopaedic Biomaterials, Peking University Shenzhen Hospital, Shenzhen, Guangdong 518036, China*

Correspondence should be addressed to Li Deng; dengli2000@gmail.com and Yong-Can Huang; y.c.huang@connect.hku.hk

Received 28 April 2019; Revised 28 July 2019; Accepted 22 August 2019; Published 22 November 2019

Academic Editor: Laura Lasagni

The osteogenic potential of mesenchymal stromal cells (MSCs) varies among different tissue sources. Strontium enhances the osteogenic differentiation of bone marrow-derived MSCs (BM-MSCs), but whether it exerts similar effects on placental decidual basalis-derived MSCs (PDB-MSCs) remains unknown. Here, we compared the influence of strontium on the proliferation and osteogenic differentiation of human PDB- and BM-MSCs *in vitro*. We found that 1 mM and 10 mM strontium, but not 0.1 mM strontium, evidently promoted the proliferation of human PDB- and BM-MSCs. These doses of strontium showed a comparable alkaline phosphatase activity in both cell types, but their osteogenic gene expressions were promoted in a dose-dependent manner. Strontium at doses of 0.1 mM and 1 mM elevated several osteogenic gene expressions of PDB-MSCs, but not those of BM-MSCs at an early stage. Nevertheless, they failed to enhance the mineralization of either cell type. By contrast, 10 mM strontium facilitated the osteogenic gene expression as well as the mineralization of human PDB- and BM-MSCs. Collectively, this study demonstrated that human PDB- and BM-MSCs shared a great similarity in response to strontium, which promoted their proliferation and osteogenic differentiation in a dose-dependent manner.

1. Introduction

Large bone defects, resulting from trauma, infection, and congenital diseases, remain a great challenge in the clinic. Mesenchymal stromal cells (MSCs) are fibroblast-like adherent cells with a self-renewal ability and multipotency. They are considered as promising seed cells for bone regeneration, mainly due to their osteogenic potential and paracrine effects [1, 2]. Currently, bone marrow represents the main source of MSCs for clinical studies. A great

number of animal studies and several clinical trials have shown that bone marrow-derived MSCs (BM-MSCs) improved bone regeneration [2, 3]. However, several drawbacks hinder wide clinical application. For example, the isolation of BM-MSCs requires an invasive procedure, and the proliferation and differentiation capability of BM-MSCs decrease with donor age [4, 5]. Therefore, many researches tried to explore other sources of MSCs for bone regeneration.

The human placenta is an attractive source of MSCs because of the noninvasive tissue collection, the lack of ethical concerns, the high cell harvest rate, and the robust cell proliferation ability [6]. MSCs have been isolated from different parts of the placenta, including the chorionic villi, amnion membrane, and decidual basalis [7–10]. They can undergo osteogenic differentiation when cultured in the traditional osteogenic medium or stimulated by the osteogenic growth factors (e.g., bone morphogenic proteins) *in vitro* [11]. When grafted in combination with osteoinductive scaffolds, they are able to form bone tissue at the ectopic sites [12, 13]. Noticeably, they also enhanced bone regeneration after transplantation at the bone defects [14, 15]. Nevertheless, several studies have revealed that the osteogenic potential of placenta-derived MSCs was inferior to that of the BM-MSCs [16–18], highlighting the need of developing efficient strategies to improve the osteogenic commitment of cells.

Strontium is a trace element in natural bone tissue that has dual effects on bone metabolism. It enhances the proliferation of osteoprogenitor cells, while inhibiting the terminal differentiation of osteoclasts [19]. Considering the chemical stability and low cost of strontium, many efforts have been made in developing strontium-modified scaffolds to enhance bone repair in combination with MSCs [20, 21]. It is well-known that strontium promotes the osteogenic differentiation of osteoblast and BM-MSCs derived from rodent species [22–28]. However, much fewer studies have determined the effect of strontium on MSCs derived from human tissues [29–32], especially those derived from perinatal tissues. Yang et al. has reported the enhanced osteogenic response of human umbilical cord-derived MSCs to strontium stimulation [32], but the influence of strontium on MSCs derived from other human perinatal tissues, such as the decidual basalis, has not been investigated yet.

Since tissue origin profoundly influences the biological properties of MSCs, including their proliferation ability and differentiation potential [16–18, 33], it is reasonable to assume that human BM-MSCs and placental decidual basalis-derived MSCs (PDB-MSCs) might respond differently to strontium stimulation. In this study, we first determined the proper treatment doses of strontium for both cell types and then compared the effect of strontium on their osteogenic differentiation *in vitro*, with the aim of providing valuable information for potential applications of strontium for MSC-based bone regeneration.

2. Materials and Methods

2.1. Cell Isolation. This study was approved by the ethics committee of West China Hospital, Sichuan University. Human placentas were obtained from four healthy donors (age ranging from 25 to 33) with informed consent. PDB-MSCs were isolated as described in our previous report [7]. Briefly, decidua basalis was dissected from placentas, washed in phosphate-buffered saline (PBS), minced into small pieces of tissue, and digested with 0.25% Trypsin (Gibco, USA) and 0.1% Collagenase IV (Invitrogen, USA). After centrifugation, the nucleated cells were resuspended and cultured in the growth medium containing Dulbecco's modified Eagle's medium-high glucose (Gibco, USA), 10% fetal bovine serum (HyClone, USA), and 1% penicillin/streptomycin (Gibco, USA). The growth medium was changed every 3 days. When the cells reached 70-80% confluence, they were collected by 0.25% trypsin/ethylene diamine tetraacetic acid (EDTA; Sigma-Aldrich, USA) treatment and passaged at a dilution of 1 : 3. Cells from the 4th passage of each donor were pooled together, and the mixed cells were cultured for an additional 1 to 3 passages for further use in the subsequent studies.

Human bone marrow samples were obtained from one healthy female donor (25 years old) and three patients with scoliosis (one female donor and two male donors, age ranging from 15 to 18) with informed consent. BM-MSCs were isolated according to our previous description [34]. Briefly, bone marrow aspirates were diluted with PBS, layered over Ficoll solution (TBD Science, China), and centrifuged at 500 g for 30 mins to collect mononuclear cells from the gradient interface. Then, the mononuclear cells were cultured in the growth medium, which was changed to remove the nonadherent cells after 72 hours of culture. When the cells reached 70-80% confluence, they were passaged at a ratio of 1 : 3. The cells at passage 4 from each donor were pooled together, and the mixed cells were subcultured for additional passages. Cells at the 5th to 7th passage were used in the following experiments.

2.2. Cell Characterization. The multilineage differentiation potential of human BM-MSCs and PDB-MSCs was investigated according to our previous reports [7, 34]. Briefly, the cells were seeded at a density of 1×10^4 cells/cm^2. For osteogenic differentiation, the cells were cultured in the osteogenic medium containing the growth medium, 50 mg/L L-ascorbic acid-2-phosphate (Sigma-Aldrich, USA), 10^{-7} M dexamethasone (Sigma-Aldrich, USA), and 10 mM β-glycerophosphate (Sigma-Aldrich, USA). The osteogenic medium was changed every 3 days. After induction for 21 days, the samples were fixed in 75% ethanol and stained with 1% alizarin red solution (Sigma-Aldrich, USA) for 30 mins at 37°C.

For adipogenic differentiation, the cells were cultured in the adipogenic medium containing the growth medium, 0.25 μM dexamethasone (Sigma-Aldrich, USA), 10 μM insulin (Sigma-Aldrich, USA), 0.5 μM isobutyl-methylxanthine (Sigma-Aldrich, USA), and 50 μM indomethacin (Sigma-Aldrich, USA). The adipogenic medium was changed every 3 days. After induction for 15 days, the samples were fixed with 10% formalin and stained with oil red O solution (Sigma-Aldrich, USA) for 45 mins to detect lipid droplets in the cytoplasm.

For chondrogenic differentiation, the cells were cultured in the chondrogenic medium containing the growth

medium, 100 mg/L sodium pyruvate (Sigma-Aldrich, USA), 10 μg/L transforming growth factor-β1 (R&D Systems, USA), 100 mg/L ascorbate-2-phosphate (Sigma-Aldrich, USA), 1% insulin-transferrin-selenium (Gibco, USA), and 0.1 μM dexamethasone (Sigma-Aldrich, USA). The chondrogenic medium was changed every 3 days. After induction for 14 days, the samples were stained with Alcian Blue 8GX (Cyagen Biosciences, China) for 30 mins to observe the deposition of glycosaminoglycans. After histological staining, all of the samples were observed and photographed by a phase-contrast microscope (Olympus Corporation, Japan).

2.3. Cell Proliferation. Both BM- and PDB-MSCs were cultured in the growth medium or the growth medium supplemented with different concentrations of $SrCl_2{\cdot}6H_2O$ (Kelong, China), respectively. The cells cultured in the growth medium served as the control group. Briefly, the cells were seeded at a density of 3000 cells/well in 96-well plates. Cell proliferation was continually monitored using an alamarBlue® Cell Viability Reagent (Invitrogen, USA) on days 1, 3, and 7. At each timepoint, the cells were rinsed with PBS and then incubated with 100 μL working solution prepared according to the manufacturer's instructions for 4 h at 37°C. Finally, the absorbance was recorded using a plate reader (Molecular Devices, USA) at 570 nm, using 600 nm as a reference wavelength.

2.4. Live/Dead Staining. Human BM-MSCs were seeded at a density of 5,000 cells/cm^2 in 12-well plates and cultured in the growth medium or the growth medium supplemented with strontium at doses of 0.1 mM, 1 mM, and 10 mM, respectively. On days 1, 3, and 7, a Live/Dead® Cell Viability Assay Kit (Invitrogen, USA) was used to monitor cell viability. The samples ($n = 3$ for each group) were gently washed with PBS for two times and then incubated in the working solution for 30 mins at 37°C. Cell viability was observed by an inverted fluorescence microscope (Olympus Corporation, Japan).

2.5. Cell Apoptosis Analysis. Human BM-MSCs were seeded at a density of 5,000 cells/cm^2 in 25 cm^2 culture flasks and cultured in the growth medium or the growth medium supplemented with different doses of strontium (0.1 mM, 1 mM, and 10 mM) for 3 days, respectively. The cells cultured in the growth medium served as the control group. After cell culture, the cells were harvested for apoptosis detection (Annexin V-FITC Apoptosis Detection Kit, Beyotime Institute of Biotechnology, China) according to the manufacturer's instructions, and the samples were analysed using flow cytometry (FACSAria II, BD Biosciences, USA).

2.6. Alkaline Phosphatase (ALP) Activity Assay. Human BM- and PDB-MSCs were seeded at a density of 5000 cells/cm^2 and cultured in the growth medium or the osteogenic medium added with different doses of strontium (0.1 mM, 1 mM, and 10 mM), respectively. The cells cultured in the growth medium or the osteogenic medium served as the control group, respectively. After 7 days of culture, the ALP activity of cells ($n = 4$ for each group) was measured using an ALP assay kit (Nanjin Jiancheng Bioengineering Institute, China). Briefly, the cells were detached by 0.25% trypsin/EDTA, resuspended in deionized H_2O (100 μL/sample), and lysed by three freeze-thaw cycles. Then, the ALP activity of cell lysates was determined according to the manufacturer's instructions. The absorbance at 405 nm was read by a plate reader (Molecular Devices, USA). The ALP activity results were normalized to the amount of total protein, which was quantified using a BCA protein assay kit (Bio-Rad, USA).

2.7. ALP Staining. Human BM- and PDB-MSCs were seeded at a density of 5000 cells/cm^2 and cultured with different doses of strontium (0.1 mM, 1 mM, and 10 mM) supplemented in the growth medium or the osteogenic medium, respectively. The cells cultured in the growth medium or the osteogenic medium served as the control group, respectively. After 7 days of culture, the ALP activity of cells ($n = 3$ for each group) was observed using an ALP staining kit (Sigma-Aldrich, USA). Briefly, the cells were fixed in 4% phosphate-buffered paraformaldehyde for 30 mins at room temperature, washed with running water, stained with an ALP staining kit according to the manufacturer's instructions, and finally observed using microscopy (Olympus Corporation, Japan).

2.8. Real-Time Polymerase Chain Reaction (RT-PCR). Human BM- and PDB-MSCs were seeded at a density of 5000 cells/cm^2 and cultured with different doses of $SrCl_2{\cdot}6H_2O$ (0.1 mM, 1 mM, and 10 mM) supplemented in the growth medium or the osteogenic medium, respectively. The cells cultured in the growth medium or the osteogenic medium served as the control group, respectively. After culture for 3, 7, and 14 days, total RNA ($n = 4$ for each group) was extracted using a RNAiso Plus reagent (Takara Bio, Japan) and then reverse-transcribed into cDNA using a PrimeScript RT Reagent Kit (Takara Bio, Japan). Gene expression was quantified using a SYBR Premix Ex Taq II Kit (Takara Bio, Japan) in an iQ5 real-time system (Bio-Rad, USA). The primers for the osteogenic genes and the housekeeping gene, including *runt-related transcription factor 2* (*Runx2*), *osteocalcin* (*OC*), *osteoprotegerin* (*OPG*), *osteopontin* (*OPN*), and *glyceraldehyde-3-phosphate dehydrogenase* (*GADPH*), are listed as follows: *Runx 2*: forward primer—CCCAGTATGAGAGTAGGTGTCC, reverse primer—GGGTAAGACTGGTCATAGGACC; *OC*: forward primer—GAGGGCAGCGAGGTAGTGAA, reverse primer—TCCTGAAAGCCGATGTGGTC; *OPN*: forward primer—TGACCAGAGTGCTGAAACCCA, reverse primer—CCTGACTATCAATCACATCGGAAT; *OPG*: forward primer—GGTCTCCTGCTAACTCAGAAAGG, reverse primer—CAGCAAACCTGAAGAATGCCTCC; and *GAPDH*: forward primer—CTTTGGTATCGTGGAAGGACTC, reverse primer—GTAGAGGCAGGGATGATGTTCT. *GADPH* served as the housekeeping gene. Target gene expression was analyzed by the $2^{-\triangle\triangle Ct}$ method. Results were expressed relative to the gene expression level of the control group.

2.9. Mineralization Assay. Human BM- and PDB-MSCs were seeded at a density of 5000 cells/cm^2 in 6-well plates and were cultured in the osteogenic medium supplemented

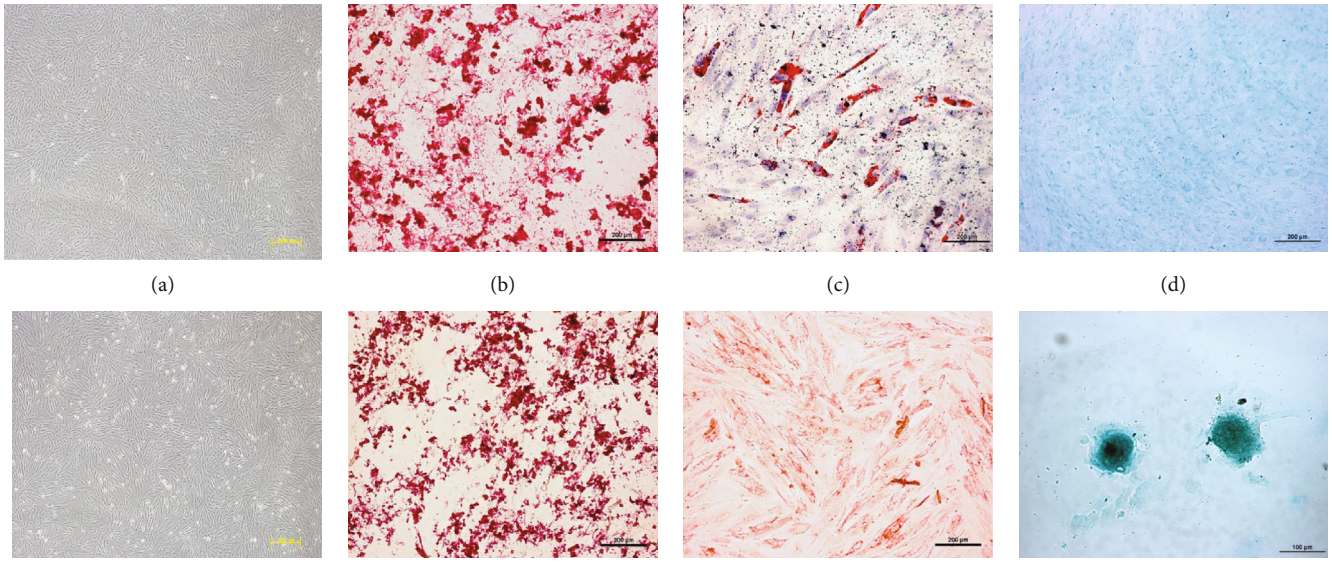

Figure 1: Characterization of human BM- and PDB-MSCs. Morphology of (a) BM-MSCs and (e) PDB-MSCs; scale bar: 200 μm. Alizarin red staining of (b) BM-MSCs and (f) PDB-MSCs after osteogenic induction; scale bar: 200 μm. Oil red O staining of (c) BM-MSCs and (g) PDB-MSCs after adipogenic induction; scale bar: 200 μm. Alcian blue staining of (d) BM-MSCs and (h) PDB-MSCs after chondrogenic induction; scale bar: 200 μm for (d) and 100 μm for (h).

with different doses of strontium (0.1 mM, 1 mM, and 10 mM) for 21 days, respectively. The cells cultured in the osteogenic medium served as the control group. After induction, the samples ($n = 3$ for each group) were stained with alizarin red as described above and were grossly visualized.

2.10. Statistical Analysis. Data were expressed as the mean ± standard deviation (SD). A one-way ANOVA followed by Dennett's Multiple Comparison Test was performed for statistical testing using GraphPad Prism software (GraphPad Software Inc., USA), and $p < 0.05$ was considered significant.

3. Results

3.1. Strontium Enhanced the Proliferation of BM- and PDB-MSCs. Human BM- and PDB-MSCs were characterized before investigating their responses to strontium stimulation. Similar to our previous reports [7, 34], both cells showed a fibroblastic-like morphology and possessed the osteogenic, adipogenic, and chondrogenic differentiation potential *in vitro* (Figure 1). Interestingly, after chondrogenic induction, both BM- and PDB-MSCs were positive for Alcian blue staining, but there was an obvious difference between them: a multilayered cell sheet was observed in BM-MSCs, while PDB-MSCs formed cellular nodules. This result indicates a tissue origin-dependent variation in the chondrogenic potential of MSCs, which has been reported by other research groups [35].

To determine the proper doses of strontium, both cell types were cultured with different concentrations of strontium (0.01 mM, 0.1 mM, 0.5 mM, 1 mM, 5 mM, 10 mM, and 20 mM). The cell proliferation was evaluated on days 1, 3, and 7. As shown in Figure 2(a), strontium, at doses of 0.01 mM, 0.5 mM, 1 mM, 5 mM, and 10 mM, facilitated the growth of BM-MSCs, while 20 mM strontium inhibited the replication. For PDB-MSCs, the growth rate of cells treated with 0.01 mM, 0.1 mM, and 0.5 mM strontium was comparable to the GM group at all timepoints. 1 mM, 5 mM, and 10 mM strontium promoted the proliferation of PDB-MSCs on day 7, while 20 mM strontium showed an evident inhibition on days 3 and 7 (Figure 2(b)).

To further confirm the cytotoxic effects of strontium on human BM-MSCs, live/dead staining and cell apoptosis analysis were performed. As shown in Figure 3(a), the cells showed good viability (green fluorescence) on days 1, 3, and 7, and few dead cells (red fluorescence) were observed in each group. Similarly, the result of an apoptosis assay revealed a comparable cell viability in the 0.1 mM, 1 mM, and 10 mM strontium groups when comparing with the GM group (Figure 3(b)).

Considering the fact that the average strontium concentration in the serum of postmenopausal women taking 2 g/day strontium ranelate orally is 0.117 mM [36], and combining this information with the above results, we therefore chose 0.1 mM, 1 mM, and 10 mM strontium in the subsequent experiments to investigate the osteogenic effects of strontium on BM- and PDB-MSCs.

3.2. Strontium Promoted the Osteogenic Differentiation of BM- and PDB-MSCs in the Growth Medium. To determine whether strontium promoted the osteogenic differentiation of human BM- and PDB-MSCs without any other soluble osteogenic factors, both cells were cultured in the growth medium supplemented with different doses of strontium. Then, the osteogenic differentiation of cells was measured, including the ALP activity and the osteogenic gene expression.

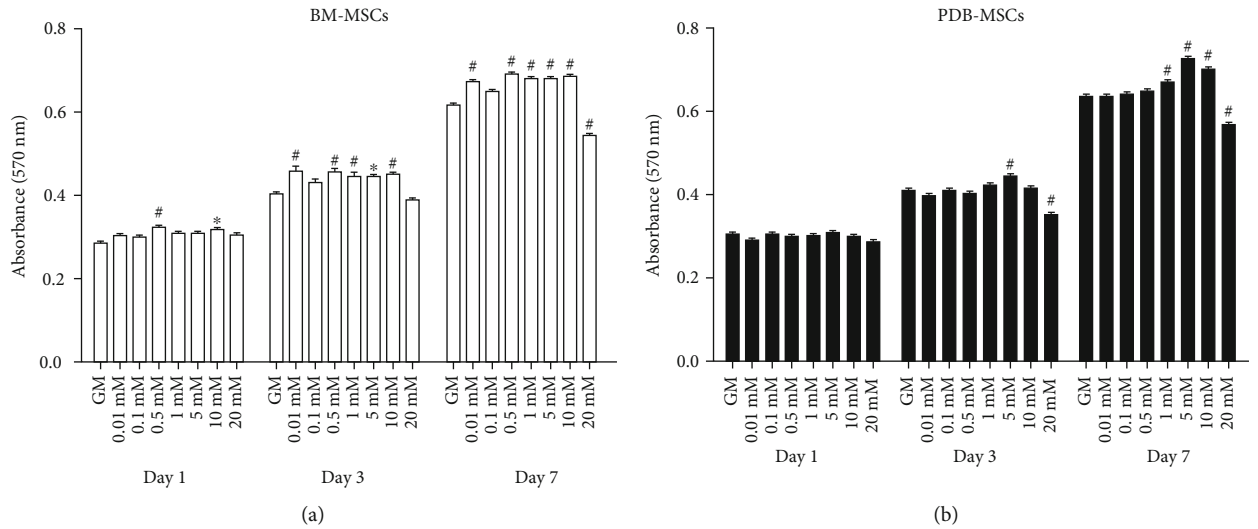

Figure 2: Proliferation of BM- and PDB-MSCs cultured with different doses of strontium supplemented in the growth medium. (a) BM-MSCs. (b) PDB-MSCs. $^{*}P < 0.05$ when compared with the GM group; $^{\#}P < 0.01$ when compared with the GM group. GM: growth medium. All of these results are representative of three independent experiments.

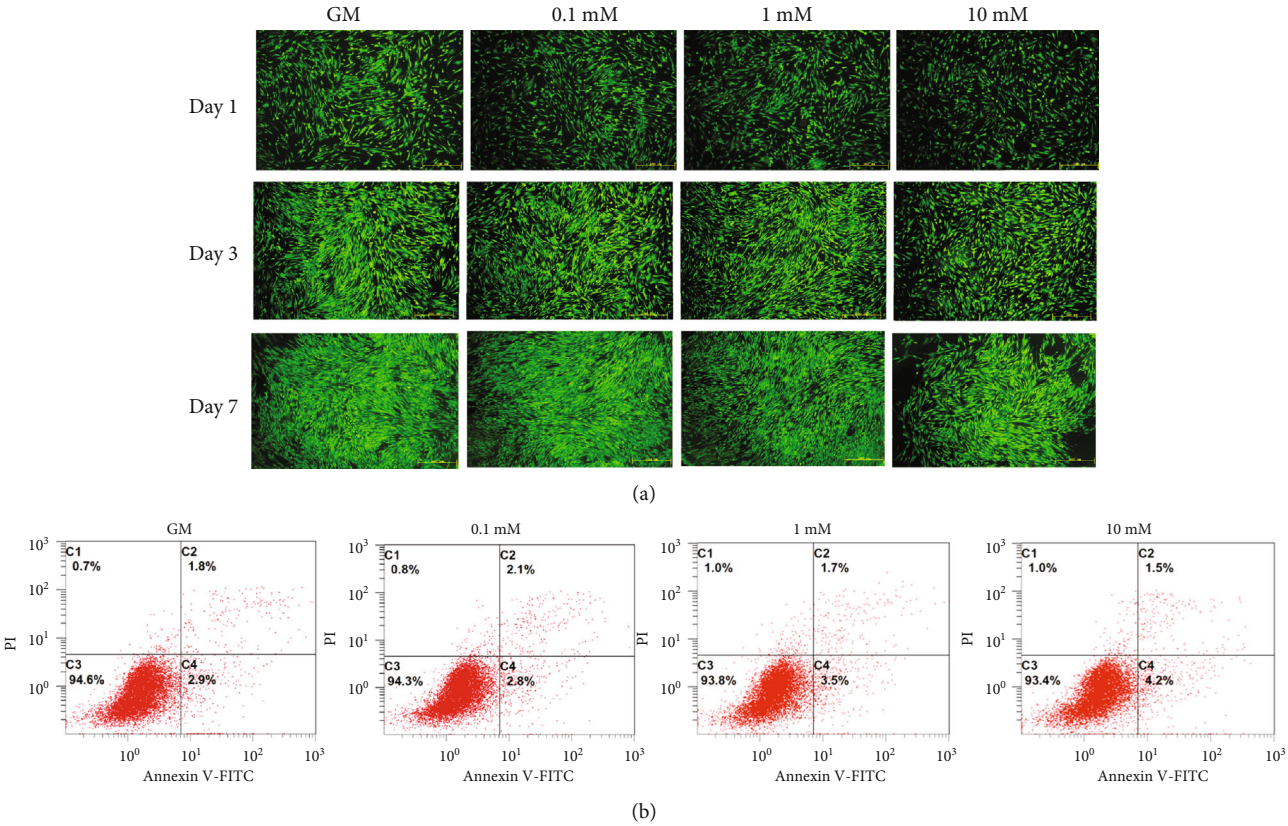

Figure 3: Cytotoxic effects of strontium on human BM-MSCs. (a) Live/dead staining of human BM-MSCs cultured with different concentrations of strontium; green fluorescence: live cells; red fluorescence: dead cells; scale bar: 500 μm. (b) Cell apoptosis analysis of human BM-MSCs. The percentages of the following cell populations are indicated on the respective density plots: necrotic cells (Annexin V-negative and PI-positive) are located in the upper left (C1), late apoptotic cells (Annexin V-positive and PI-positive) in the upper right (C2), viable cells (Annexin V-negative and PI-negative) in the lower left (C3), and early apoptotic cells (Annexin V-positive and PI-negative) in the lower right (C4) quadrants, respectively. GM: growth medium. All of these results are representative of three independent experiments.

As shown in Figure 4(a), only a few cells were positive for the ALP staining in both cell types after 7 days of culture, and there was no obvious difference among all groups in each cell type. Accordingly, the ALP activity of strontium groups (0.1 mM, 1 mM, and 10 mM) was comparable to that of the GM group ($P > 0.05$, Figure 4(b)). However, when comparing with the ALP staining of BM-MSCs, a much weaker staining result was found after PDB-MSCs were treated with the same concentration of strontium (Figure 4(a)).

The osteogenic gene expression of cells on days 3, 7, and 14, including the expression of *Runx2*, *OC*, *OPN*, and *OPG*, is shown in Figure 4(c). For BM-MSCs, 0.1 mM and 1 mM strontium demonstrated a similar gene expression level when compared with the GM group, while 10 mM strontium significantly enhanced the expression of *OC*, *OPN*, and *OPG* on days 3, 7, and 14, and the expression of *Runx2* on day 3. For PDB-MSCs, 0.1 mM and 1 mM strontium elevated the expression of *Runx2* on day 3, as well as the expression of *OC* on day 7. Furthermore, 10 mM strontium enhanced the expression of *OPN* and *OPG* on day 14.

Altogether, these results revealed that, even without any other soluble osteogenic factors, strontium promoted the osteogenic differentiation of both cells in a dose-dependent manner.

3.3. Strontium Promoted the Osteogenic Differentiation of BM- and PDB-MSCs in the Osteogenic Medium. We next determined whether strontium enhanced the osteogenic differentiation of BM- and PDB-MSCs in an osteogenic microenvironment *in vitro*. Both cells were cultured in the osteogenic medium supplemented with different doses of strontium. The osteogenic differentiation of cells was measured by the ALP activity on day 7, the expression of osteogenic genes on days 3, 7, and 14, and finally the mineralization of extracellular matrix on day 21.

As shown in Figure 5(a), both cells were positive for ALP staining after osteogenic induction, but there was no obvious difference among all groups in each cell type. Similarly, ALP activity of the strontium groups (0.1 mM, 1 mM, and 10 mM) was comparable to that of the osteogenic medium (OST) group on day 7 ($P > 0.05$, Figure 5(b)). Interestingly, BM-MSCs showed stronger staining results when comparing with that of PDB-MSCs after treated with the same concentration of strontium (Figure 5(a)).

As shown in Figure 5(c), strontium promoted the osteogenic gene expression of both cell types in a dose-dependent manner. For BM-MSCs, 0.1 mM and 1 mM strontium showed a comparable osteogenic gene expression level to that of the OST group, while 10 mM strontium enhanced the expression of *Runx2* on day 7, the expression of *OC* on days 3, 7, and 14, the expression of *OPN* on days 3 and 7, and the expression of *OPG* on days 7 and 14.

For PDB-MSCs, 0.1 mM strontium elevated the expression of *OPN* on days 7 and 14; 1 mM strontium enhanced the expression of *OC* on day 7; and notably, 10 mM strontium enhanced more osteogenic gene expressions than the 0.1 mM and 1 mM groups, facilitating the expression of *OC* on days 7 and 14, the expression of *OPN* on day 7, and the expression of *OPG* on days 3, 7, and 14 (Figure 5(c)).

The mineralization of cells was observed by the Alizarin red staining (Figure 5(d)). Compared with the OST group, 0.1 mM and 1 mM strontium showed a similar mineralization in both cell types, while 10 mM strontium obviously enhanced their mineralization.

Taken together, the above results clearly demonstrated that strontium can effectively promote the osteogenic differentiation of both BM- and PDB-MSCs under traditional osteogenic induction *in vitro*.

4. Discussion

PDB-MSCs are multipotent and readily available and, thus, present a potential cell source for bone repair. Nevertheless, the osteogenic potential of MSCs derived from the placenta tissues has been shown to be inferior to that of BM-MSCs [16–18], suggesting a need for effective osteogenic induction. As a trace element in natural human bone tissue, strontium pronouncedly enhances bone regeneration, mainly through stimulating the osteogenic differentiation of BM-MSCs while inhibiting the differentiation of osteoclasts [19]. In this study, we found that strontium facilitated the proliferation and osteogenic differentiation of PDB-MSCs, which shared a great similarity to the response of BM-MSCs. As far as we know, this is the first study to investigate the effect of strontium on the proliferation and osteogenic differentiation of PDB-MSCs *in vitro*.

According to our results, strontium exerted a dose-dependent effect on the proliferation of human PDB-MSCs, which was also observed in human BM-MSCs. Similarly, in other MSC cultures, such as rat BM-MSCs [26] and human adipose tissue-derived MSCs [37], strontium also exerted a dose-dependent effect on their proliferation. In this study, we found that 20 mM strontium inhibited the replication of both PDB- and BM-MSCs, while 1 mM, 5 mM, and 10 mM strontium promoted their proliferation. In the literature, different results have been reported regarding the cytotoxic effect of strontium on human BM-MSCs [29–31] and osteoblasts [38, 39]. For instance, it was found that strontium at concentrations of 1 mM and above drastically decreased the viability of human BM-MSCs [30]. However, 1 mM strontium was also reported to enhance the proliferation of human BM-MSCs by another research group [31]; additionally, it was determined that 210.7 μg/mL strontium (i.e., 2.4 mM) did not inhibit the proliferation of human BM-MSCs [29]. These discrepancies associated with strontium cytotoxicity may be partially due to the following reasons: First, human BM-MSCs derived from different donors respond differently to strontium stimulation [31]. Second, the experiment conditions, including cell culture medium, cell passage, and methods used to test cytotoxicity, varied greatly among studies [29–31]. Considering this, it is difficult to compare them directly; instead, the discrepancies described above highlight the need to determine proper concentrations for experiment cells.

Unlike a proproliferation effect of the high concentrations of strontium (1 mM, 5 mM, and 10 mM) on both BM- and PDB-MSCs, they responded differently to some lower concentrations of strontium. For instance, 0.01 mM and

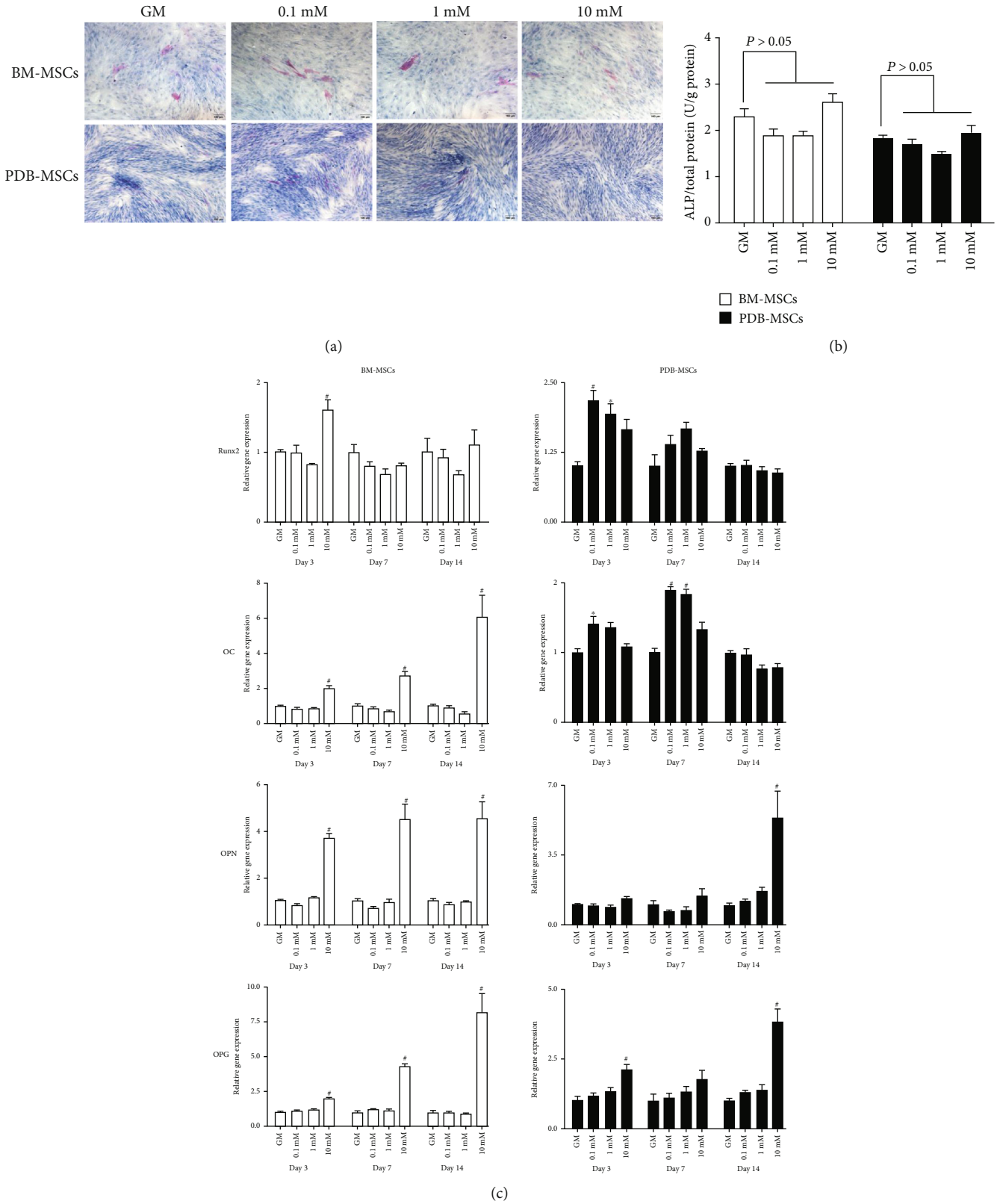

FIGURE 4: Effect of strontium on the osteogenic differentiation of BM- and PDB-MSCs cultured in the growth medium. (a) Results of the ALP staining of BM- and PDB-MSCs cultured with strontium for 7 days. Red indicates positive staining. Scale bar: 100 μm. (b) The ALP activity of BM- and PDB-MSCs treated with strontium for 7 days, $n = 4$ for each group. (c) The osteogenic gene expression of BM- and PDB-MSCs on days 3, 7, and 14, $n = 4$ for each group. All of these results are representative of three independent experiments. $^{*}P < 0.05$ when compared with the GM group; $^{\#}P < 0.01$ when compared with the GM group. GM: growth medium.

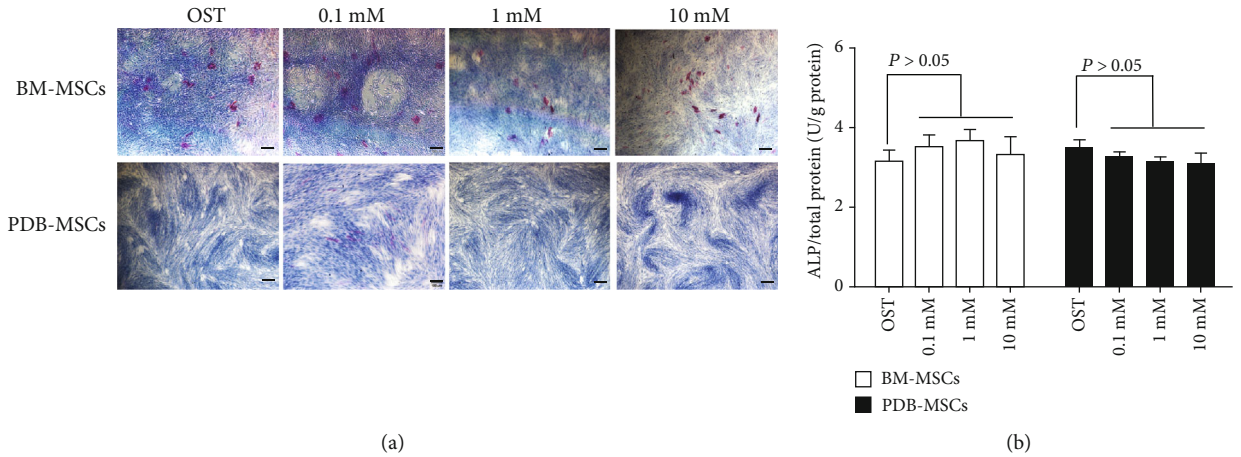

(a) (b)

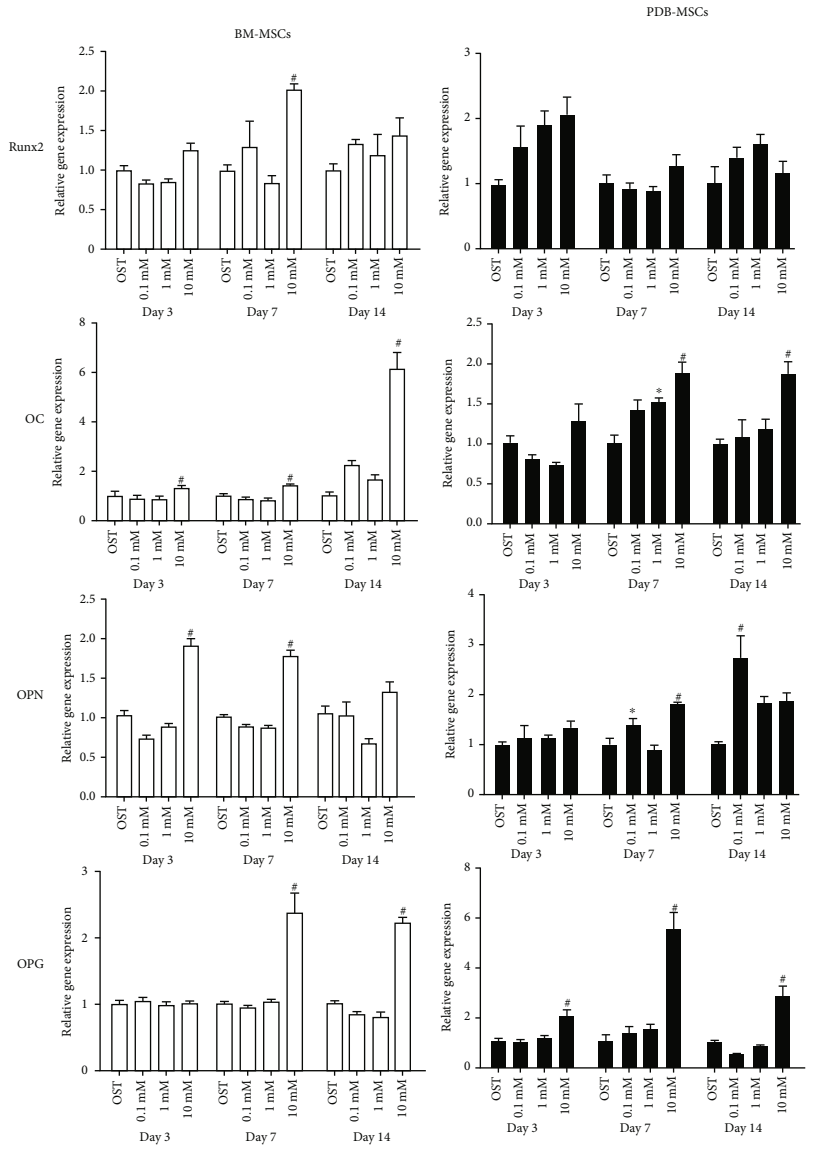

(c)

Figure 5: Continued.

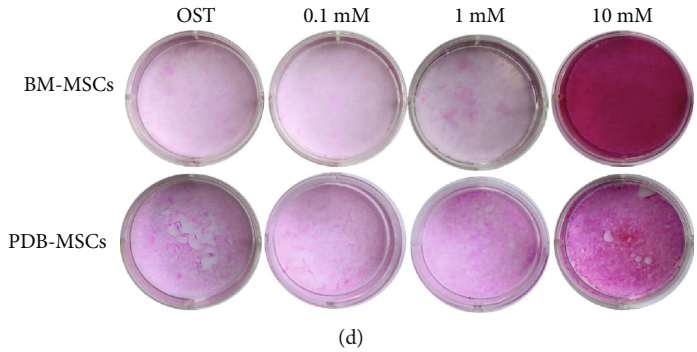

Figure 5: Effect of strontium on the osteogenic differentiation of BM- and PDB-MSCs cultured in the osteogenic medium. (a) ALP staining of BM- and PDB-MSCs cultured with strontium for 7 days. Red indicates positive staining. Scale bar: 100 μm. (b) ALP activity of BM- and PDB-MSCs treated with strontium for 7 days. $n = 4$ for each group. (c) Osteogenic gene expression of BM- and PDB-MSCs on days 3, 7, and 14. $n = 4$ for each group. (d) Alizarin red staining of BM- and PDB-MSCs after 21 days of culture. Red indicates the mineralization of the extracellular matrix. All of these results are representative of three independent experiments. $^{*}P < 0.05$ when compared with the OST group; $^{\#}P < 0.01$ when compared with the OST group. OST: osteogenic medium.

0.5 mM strontium increased the growth kinetics of human BM-MSCs but not that of PDB-MSCs. This cell-type-specific effect of strontium on the replication of somatic cells was also observed by other researchers [40], yet the mechanism underlying different cell responses remains largely unknown and needs further studies.

Regarding the osteogenic effects of strontium on MSCs, it has been reported that proper concentrations of strontium facilitated the osteogenic differentiation of rodent BM-MSCs [26–28], as well as MSCs derived from human tissues, such as bone marrow [29–31], umbilical cord [32], and adipose tissue [41]. In this study, we investigated, for the first time, the osteogenic effects of strontium on human PDB-MSCs, and found that 10 mM strontium, but not 0.1 mM or 1 mM strontium, promoted their osteogenic differentiation, which will provide a simple approach to stimulate the osteogenic potential of PDB-MSCs for bone regeneration.

Nevertheless, we should acknowledge that there are some limitations in this work. First, a pool of MSCs derived from four donors, but not cell replicates from each donor, was used in the experiments. Although this makes the comparison of MSCs derived from two different tissues simple and straightforward, it fails to uncover the donor-dependent variation in the responses of each cell type, which is important for future clinical applications. Second, the cells used in this study were at the middle passages. It is well-known that MSC-based therapies need a large number of cells, and that MSCs at passage 3-7 are usually used as graft cells in clinics [42]; therefore, we used both cell types at passage 5-7 in this study, which were relevant to the clinics. However, it should be noted that the differentiation potential of human MSCs declines with increasing passage number [43], and consequently, further studies are suggested to determine the proper cell passage for strontium stimulation. Last but not least, the mechanism underlining the osteogenic effects of strontium on human PDB-MSCs remains unknown. It has been reported that strontium enhanced the osteogenic differentiation of MSCs through different cell signaling pathways, such as the Ras/MAPK pathway [28], the Wnt/β-catenin pathway [32], and the MAPK/ERK pathway [44]. However, it is still unknown whether these signaling pathways are involved in the osteogenic differentiation of PDB-MSCs treated with strontium, and thus further studies are required to understand the target pathway.

Based on the above studies, it is clearly demonstrated that 10 mM strontium, rather than 0.1 mM and 1 mM strontium, obviously facilitated the proliferation and osteogenic lineage commitment of human PDB- and BM-MSCs. Considering the dose-dependent effect of strontium on the proliferation and differentiation of human MSCs, it is noteworthy to determine the proper ion release profile of strontium-containing bone scaffolds when using these MSCs to fabricate tissue engineered bone grafts.

5. Conclusions

In conclusion, strontium promoted the proliferation and osteogenic differentiation of human PDB- and BM-MSCs in a dose-dependent manner. At low doses of strontium (0.1 mM and 1 mM), the osteogenic gene expression of PDB-MSCs was slightly different from that of BM-MSCs, but the mineralization of both cell types was not enhanced. By contrast, they shared a great similarity in the response to a relative high dose of strontium (10 mM), which promoted their proliferation and osteogenic differentiation. This dose-dependent effect of strontium should be taken into consideration when combining strontium and human MSCs for bone regeneration.

Abbreviations

ALP: Alkaline phosphatase
BM-MSCs: Bone marrow-derived mesenchymal stromal cells
GADPH: Glyceraldehyde-3-phosphate dehydrogenase
GM: Growth medium
OC: Osteocalcin
OST: Osteogenic medium
OPG: Osteoprotegerin
OPN: Osteopontin

PDB-MSCs: Placental decidual basalis-derived mesenchymal stromal cells
Runx2: Runt-related transcription factor 2.

Data Availability

The data used to support the findings of this study are included within the article.

Conflicts of Interest

The authors declare no conflicts of interest.

Acknowledgments

This work was financially supported by the National Natural Science Foundation of China (Grant Nos. 31570970, 31600792, and 81702171), the Tianjin Research Program of Application Foundation and Advanced Technology (Grant No. 14JCQNJC03100), the Shenzhen Double Chain Project for Innovation and Development Industry supported by the Bureau of Industry and Information Technology of Shenzhen (Grant No. 201806081018272960), the 1.3.5 Project for Disciplines of Excellence, West China Hospital, Sichuan University (Grant No. ZYJC18002), and the Scientific Research Starting Foundation for Doctor from Jinggangshan University (Grant No. JZB15013).

References

[1] F. Granero-Molto, J. A. Weis, L. Longobardi, and A. Spagnoli, "Role of mesenchymal stem cells in regenerative medicine: application to bone and cartilage repair," *Expert Opinion on Biological Therapy*, vol. 8, no. 3, pp. 255–268, 2008.

[2] L. Watson, S. J. Elliman, and C. M. Coleman, "From isolation to implantation: a concise review of mesenchymal stem cell therapy in bone fracture repair," *Stem Cell Research & Therapy*, vol. 5, no. 2, p. 51, 2014.

[3] S. P. Bruder, N. Jaiswal, N. S. Ricalton, J. D. Mosca, K. H. Kraus, and S. Kadiyala, "Mesenchymal stem cells in osteobiology and applied bone regeneration," *Clinical Orthopaedics and Related Research*, vol. 355, pp. S247–S256, 1998.

[4] J. D. Kretlow, Y. Q. Jin, W. Liu et al., "Donor age and cell passage affects differentiation potential of murine bone marrow-derived stem cells," *BMC Cell Biology*, vol. 9, no. 1, p. 60, 2008.

[5] S. Zhou, J. S. Greenberger, M. W. Epperly et al., "Age-related intrinsic changes in human bone-marrow-derived mesenchymal stem cells and their differentiation to osteoblasts," *Aging Cell*, vol. 7, no. 3, pp. 335–343, 2008.

[6] S. Barlow, G. Brooke, K. Chatterjee et al., "Comparison of human placenta- and bone marrow-derived multipotent mesenchymal stem cells," *Stem Cells and Development*, vol. 17, no. 6, pp. 1095–1107, 2008.

[7] Y. C. Huang, Z. M. Yang, X. H. Chen et al., "Isolation of mesenchymal stem cells from human placental decidua basalis and resistance to hypoxia and serum deprivation," *Stem Cell Reviews and Reports*, vol. 5, pp. 247–255, 2009.

[8] C. M. Raynaud, M. Maleki, R. Lis et al., "Comprehensive characterization of mesenchymal stem cells from human placenta and fetal membrane and their response to osteoactivin stimulation," *Stem Cells International*, vol. 2012, Article ID 658356, 13 pages, 2012.

[9] M. H. Abumaree, M. A. A. I. Jumah, B. Kalionis et al., "Phenotypic and functional characterization of mesenchymal stem cells from chorionic villi of human term placenta," *Stem Cell Reviews and Reports*, vol. 9, no. 1, pp. 16–31, 2013.

[10] A. B. Araújo, G. D. Salton, J. M. Furlan et al., "Comparison of human mesenchymal stromal cells from four neonatal tissues: amniotic membrane, chorionic membrane, placental decidua and umbilical cord," *Cytotherapy*, vol. 19, no. 5, pp. 577–585, 2017.

[11] S. Manochantr, K. Marupanthorn, C. Tantrawatpan, P. Kheolamai, D. Tantikanlayaporn, and P. Sanguanjit, "The effects of BMP-2, miR-31, miR-106a, and miR-148a on osteogenic differentiation of MSCs derived from amnion in comparison with MSCs derived from the bone marrow," *Stem Cells International*, vol. 2017, Article ID 7257628, 14 pages, 2017.

[12] G. D. Kusuma, D. Menicanin, S. Gronthos et al., "Ectopic bone formation by mesenchymal stem cells derived from human term placenta and the decidua," *PLoS One*, vol. 10, no. 10, article e0141246, 2015.

[13] X. Fu, H. Yang, H. Zhang et al., "Improved osteogenesis and upregulated immunogenicity in human placenta-derived mesenchymal stem cells primed with osteogenic induction medium," *Stem Cell Research & Therapy*, vol. 7, no. 1, p. 138, 2016.

[14] X. Li, W. Ling, A. Pennisi et al., "Human placenta-derived adherent cells prevent bone loss, stimulate bone formation, and suppress growth of multiple myeloma in bone," *Stem Cells*, vol. 29, pp. 263–273, 2011.

[15] Z. X. Fan, Y. Lu, L. Deng et al., "Placenta- versus bone-marrow-derived mesenchymal cells for the repair of segmental bone defects in a rabbit model," *FEBS Journal*, vol. 279, no. 13, pp. 2455–2465, 2012.

[16] C. Cavallo, C. Cuomo, S. Fantini et al., "Comparison of alternative mesenchymal stem cell sources for cell banking and musculoskeletal advanced therapies," *Journal of Cellular Biochemistry*, vol. 112, no. 5, pp. 1418–1430, 2011.

[17] Z. Y. Zhang, S. H. Teoh, M. S. Chong et al., "Superior osteogenic capacity for bone tissue engineering of fetal compared with perinatal and adult mesenchymal stem cells," *Stem Cells*, vol. 27, no. 1, pp. 126–137, 2009.

[18] J. S. Heo, Y. Choi, H. S. Kim, and H. O. Kim, "Comparison of molecular profiles of human mesenchymal stem cells derived from bone marrow, umbilical cord blood, placenta and adipose tissue," *International Journal of Molecular Medicine*, vol. 37, no. 1, pp. 115–125, 2016.

[19] Z. Saidak and P. J. Marie, "Strontium signaling: molecular mechanisms and therapeutic implications in osteoporosis," *Pharmacology & Therapeutics*, vol. 136, no. 2, pp. 216–226, 2012.

[20] S. Chandran, S. J. Shenoy, S. Suresh Babu, R. P. Nair, H. K. Varma, and A. John, "Strontium hydroxyapatite scaffolds engineered with stem cells aid osteointegration and osteogenesis in osteoporotic sheep model," *Colloids and Surfaces B: Biointerfaces*, vol. 163, pp. 346–354, 2017.

[21] Y. Z. Huang, J. J. Wang, Y. C. Huang et al., "Organic composite-mediated surface coating of human acellular bone matrix with strontium," *Materials Science and Engineering: C*, vol. 84, pp. 12–20, 2018.

[22] M. M. Almeida, E. P. Nani, L. N. Teixeira et al., "Strontium ranelate increases osteoblast activity," *Tissue and Cell*, vol. 48, pp. 183–188, 2016.

[23] S. Choudhary, P. Halbout, C. Alander, L. Raisz, and C. Pilbeam, "Strontium ranelate promotes osteoblastic differentiation and mineralization of murine bone marrow stromal cells: involvement of prostaglandins," *Journal of Bone and Mineral Research*, vol. 22, no. 7, pp. 1002–1010, 2007.

[24] S. Peng, X. S. Liu, S. Huang et al., "The cross-talk between osteoclasts and osteoblasts in response to strontium treatment: involvement of osteoprotegerin," *Bone*, vol. 49, no. 6, pp. 1290–1298, 2011.

[25] G. A. B. Silva, B. M. Bertassoli, C. A. Sousa, J. D. Albergaria, R. S. de Paula, and E. C. Jorge, "Effects of strontium ranelate treatment on osteoblasts cultivated onto scaffolds of trabeculae bovine bone," *Journal of Bone and Mineral Metabolism*, vol. 36, no. 1, pp. 73–86, 2018.

[26] X. Guo, S. Wei, M. Lu et al., "Dose-dependent effects of strontium ranelate on ovariectomy rat bone marrow mesenchymal stem cells and human umbilical vein endothelial cells," *International Journal of Biological Sciences*, vol. 12, no. 12, pp. 1511–1522, 2016.

[27] Y. Li, J. Li, S. Zhu et al., "Effects of strontium on proliferation and differentiation of rat bone marrow mesenchymal stem cells," *Biochemical and Biophysical Research Communications*, vol. 418, no. 4, pp. 725–730, 2012.

[28] S. Peng, G. Zhou, K. D. Luk et al., "Strontium promotes osteogenic differentiation of mesenchymal stem cells through the Ras/MAPK signaling pathway," *Cellular Physiology and Biochemistry*, vol. 23, no. 1-3, pp. 165–174, 2009.

[29] M. Sila-Asna, A. Bunyaratvej, S. Maeda, H. Kitaguchi, and N. Bunyaratavej, "Osteoblast differentiation and bone formation gene expression in strontium-inducing bone marrow mesenchymal stem cell," *Kobe Journal of Medical Sciences*, vol. 53, pp. 25–35, 2007.

[30] M. Schumacher, A. Lode, A. Helth, and M. Gelinsky, "A novel strontium(II)-modified calcium phosphate bone cement stimulates human-bone-marrow-derived mesenchymal stem cell proliferation and osteogenic differentiation *in vitro*," *Acta Biomaterialia*, vol. 9, no. 12, pp. 9547–9557, 2013.

[31] Z. T. Birgani, A. Malhotra, C. A. van Blitterswijk, and P. Habibovic, "Human mesenchymal stromal cells response to biomimetic octacalcium phosphate containing strontium," *Journal of Biomedical Materials Research Part A*, vol. 104, no. 8, pp. 1946–1960, 2016.

[32] F. Yang, D. Yang, J. Tu, Q. Zheng, L. Cai, and L. Wang, "Strontium enhances osteogenic differentiation of mesenchymal stem cells and in vivo bone formation by activating Wnt/catenin signaling," *Stem Cells*, vol. 29, no. 6, pp. 981–991, 2011.

[33] Y. Z. Huang, H. Q. Xie, A. Silini et al., "Mesenchymal stem/progenitor cells derived from articular cartilage, synovial membrane and synovial fluid for cartilage regeneration: current status and future perspectives," *Stem Cell Reviews and Reports*, vol. 13, no. 5, pp. 575–586, 2017.

[34] Y. Z. Huang, J. Q. Cai, F. J. Lv et al., "Species variation in the spontaneous calcification of bone marrow-derived mesenchymal stem cells," *Cytotherapy*, vol. 15, no. 3, pp. 323–329, 2013.

[35] D. Kanematsu, T. Shofuda, A. Yamamoto et al., "Isolation and cellular properties of mesenchymal cells derived from the decidua of human term placenta," *Differentiation*, vol. 82, no. 2, pp. 77–88, 2011.

[36] P. J. Meunier, C. Roux, E. Seeman et al., "The effects of strontium ranelate on the risk of vertebral fracture in women with postmenopausal osteoporosis," *New England Journal of Medicine*, vol. 350, no. 5, pp. 459–468, 2004.

[37] V. Nardone, R. Zonefrati, C. Mavilia et al., "In vitro effects of strontium on proliferation and osteoinduction of human preadipocytes," *Stem Cells International*, vol. 2015, Article ID 871863, 12 pages, 2015.

[38] J. Braux, F. Velard, C. Guillaume et al., "A new insight into the dissociating effect of strontium on bone resorption and formation," *Acta Biomaterialia*, vol. 7, no. 6, pp. 2593–2603, 2011.

[39] G. J. Atkins, K. J. Welldon, P. Halbout, and D. M. Findlay, "Strontium ranelate treatment of human primary osteoblasts promotes an osteocyte-like phenotype while eliciting an osteoprotegerin response," *Osteoporosis International*, vol. 20, no. 4, pp. 653–664, 2009.

[40] J. Caverzasio, "Strontium ranelate promotes osteoblastic cell replication through at least two different mechanisms," *Bone*, vol. 42, no. 6, pp. 1131–1136, 2008.

[41] A. Aimaiti, A. Maimaitiyiming, X. Boyong, K. Aji, C. Li, and L. Cui, "Low-dose strontium stimulates osteogenesis but high-dose doses cause apoptosis in human adipose-derived stem cells via regulation of the ERK1/2 signaling pathway," *Stem Cell Research & Therapy*, vol. 8, no. 1, p. 282, 2017.

[42] N. Sareen, G. L. Sequiera, R. Chaudhary et al., "Early passaging of mesenchymal stem cells does not instigate significant modifications in their immunological behavior," *Stem Cell Research & Therapy*, vol. 9, no. 1, p. 121, 2018.

[43] H. J. Sun, Y. Y. Bahk, Y. R. Choi, J. H. Shim, S. H. Han, and J. W. Lee, "A proteomic analysis during serial subculture and osteogenic differentiation of human mesenchymal stem cell," *Journal of Orthopaedic Research*, vol. 24, no. 11, pp. 2059–2071, 2006.

[44] M. Huang, R. G. Hill, and S. C. Rawlinson, "Strontium (Sr) elicits odontogenic differentiation of human dental pulp stem cells (hDPSCs): a therapeutic role for Sr in dentine repair?," *Acta Biomaterialia*, vol. 38, pp. 201–211, 2016.

Hindawi
Stem Cells International
Volume 2019, Article ID 3674647, 10 pages
https://doi.org/10.1155/2019/3674647

Review Article

Tendon Stem/Progenitor Cells and Their Interactions with Extracellular Matrix and Mechanical Loading

Chuanxin Zhang,[1] Jun Zhu,[1] Yiqin Zhou,[1] Bhavani P. Thampatty,[2] and James H-C. Wang[2]

[1]*Joint Surgery and Sports Medicine Department, Shanghai Changzheng Hospital, Second Military Medical University, Shanghai, China*
[2]*MechanoBiology Laboratory, Departments of Orthopaedic Surgery, Bioengineering, and Physical Medicine and Rehabilitation, University of Pittsburgh, Pittsburgh, Pennsylvania, USA*

Correspondence should be addressed to James H-C. Wang; wanghc@pitt.edu

Received 21 May 2019; Revised 4 August 2019; Accepted 17 August 2019; Published 13 October 2019

Guest Editor: Jun Li

Tendons are unique connective tissues in the sense that their biological properties are largely determined by their tendon-specific stem cells, extracellular matrix (ECM) surrounding the stem cells, mechanical loading conditions placed on the tendon, and the complex interactions among them. This review is aimed at providing an overview of recent advances in the identification and characterization of tendon stem/progenitor cells (TSPCs) and their interactions with ECM and mechanical loading. In addition, the effects of such interactions on the maintenance of tendon homeostasis and the initiation of tendon pathological conditions are discussed. Moreover, the challenges in further investigations of TSPC mechanobiology *in vitro* and *in vivo* are outlined. Finally, future research efforts are suggested, which include using specific gene knockout models and single-cell transcription profiling to enable a broad and deep understanding of the physiology and pathophysiology of tendons.

1. Introduction

Tendons are specialized tissues that enable joint movements by transmitting muscular forces from muscle to bone. They are relatively hypocellular tissues that are composed of an extracellular matrix (ECM), predominantly of collagen [1, 2], which is organized in a hierarchical manner. The collagen molecules assemble into fibrils that form fibers, fibers form fascicles, and bundles of fascicles form the fascicular matrix (FM). Endotenon, also known as the interfascicular matrix (IFM), occupies the space between fascicle bundles and is covered by epitenon and another layer of paratenon forming the whole tendon unit [1, 3]. Additionally, tendon contains two major types of cells, tenocytes and tendon stem/progenitor cells (TSPCs). Under normal conditions, tenocytes are responsible for maintaining tendon homeostasis, whereas TSPCs replenish tendon cells by undergoing self-renewal and differentiation [4, 5]. Tendon also contains other cell types such as endothelial cells, synovial cells of the tendon sheaths, and chondrocytes at the pressure and insertion sites in smaller amounts [3, 6].

The first study that isolated and characterized TSPCs indicates that these cell populations reside within the tendon proper (midsubstance) that comprises FM and IFM [4]. These cells are not strictly classified as "stem" cells, since they display heterogeneity in their biological properties. Instead, they were classified as "stem/progenitor" cells considering the possibility of inclusion of progenitor cells, which are destined to undergo differentiation towards a specific lineage. Indeed, while TSPCs possess multidifferentiation potential, they may contain progenitors that may specifically differentiate into tenocytes. Although TSPCs have been isolated and identified more than a decade ago, the lack of specific markers poses a challenge to study them further. In addition, distinctive populations of TSPCs have been identified from locations other than the tendon proper

such as peritenon [7–9], but their functions are yet to be defined.

The hierarchical tendon structure is well optimized for its specific functions. Mechanical loads placed on the tendons are transformed into biochemical signals to tendon cells, which respond appropriately to regulate the metabolism of tendon and its structural properties [10, 11]. However, mechanical overloading may cause tendon injury, which is a common clinical problem affecting the quality of life for millions [12, 13]. Once tendon injury occurs, a successive natural healing process is thought to take place in three phases: inflammation (infiltration of inflammatory cells), proliferation (formation of new cells), and remodeling of ECM (change in the structure and form of tendon matrix) [14].

There are two categories of tendon injury: acute and chronic. Acute tendon injury, either partial or complete tear, results from a sudden tendon rupture that may be spontaneous or caused by direct trauma. Chronic tendon injury, commonly referred to as tendinopathy, is generally thought to result from repetitive mechanical overloading on the tendon, genetic predisposition, and age-related degeneration [15–17]. While pain and disability are the clinical indicators, the pathological features of tendinopathy include changes in the extracellular matrix (ECM) with collagen disorganization, proteoglycan deposition, neovascularization, and calcification [18, 19]. Several mechanisms have been proposed for the pathogenesis of tendinopathy that include with or without inflammation-mediated changes in tendon [20–22].

Due to the hypocellularity and hypovascularity of the tendon, the natural healing ability of tendons is rather limited [23, 24]. Moreover, tendon healing results in the formation of scar tissues, manifested by disorganized collagen matrix, increased proteoglycan and glycosaminoglycan content, and increased noncollagenous ECM [25–27]. Despite years of research, restoration of damaged tendon tissues to normal structure and function remains a great challenge in sports medicine and orthopaedic surgery. In particular, tendinopathic tendons respond poorly to current treatments including NSAIDS, corticosteroid and PRP injections, exercise-based physical therapy, and surgery [28]. Although heavy slow resistance (HSR) training reduces pain and improves collagen fibril morphology in a small number of patients [29], the efficacy of HSR training remains to be verified with large randomized controlled trials. By and large, current therapeutic strategies are palliative due to the limited understanding of the cellular and molecular mechanisms of tendinopathy. The development of new effective treatment options needs an in-depth understanding of basic tendon biology and, in particular, the function of tendon cells and their interactions with ECM in tendon.

Moreover, tendon is a mechanoresponsive tissue. Therefore, tendon homeostasis is maintained not only by the cells and ECM, but also by the mechanical loads placed on the tendon. TSPCs are responsive to mechanical loading, and some findings suggest that TSPCs are likely responsible for the development of degenerative tendinopathy by virtue of their multidifferentiation potential to nontenocyte phenotypes under excessive mechanical loading conditions [30–33]. Considering the emerging role of TSPCs in tendon homeostasis and in the development of tendon's pathological conditions, and their potential applications in tissue engineering of injured tendons, a deeper understanding of the interactions between TSPCs, ECM, and mechanical loading is essential. In this review, we discuss the efforts to identify and characterize TSPCs with regard to their locations in tendon. We also provide an overview of the interactions between TSPCs, ECM, and mechanical loading that may be important advances in tendon biology and pathology. Finally, we discuss the challenges in understanding TSPC biology and provide our perspectives on future research directions.

2. Tendon Cells

The cell populations in tendon are heterogeneous, and they are identified based on their anatomical locations such as FM, IFM, and paratenon, as well as the perivascular area close to paratenon in and around the tendon [34]. Still, there is little understanding of the phenotypical differences between these cell populations and specific markers to discriminate between them. The primary cell type in tendon is tenocytes, which are elongated fibroblast-like cells with spindle-shaped nuclei that are found mainly in FM [35]. Commonly used markers for tenocytes are collagen types I and III and tenomodulin (TNMD) [36]. It should be noted, however, that the term tenocyte in literature can be somewhat "arbitrary," meaning that some so-called tenocytes are likely stem/progenitor cells.

Until the discovery of TSPCs, tenocytes were thought to be the only major cell type in tendon. The quest for the presence of adult stem cells in tendons began with two previous observations: (a) human and mouse tendons develop fibrocartilage and ossification in response to injury and (b) tendon-derived immortalized cell lines and human tendon-derived "fibroblasts" possess multidifferentiation capabilities *in vitro* [24, 37, 38]. Before long, TSPCs were first identified in humans and mice in 2007 [4]. The TSPCs isolated from the tendon proper with stem cell characteristics of clonogenicity, multipotency, and self-renewal could regenerate tendon-like tissues after *in vitro* expansion and *in vivo* transplantation [4]. In addition, an ECM-rich niche composed of biglycan and fibromodulin controls the self-renewal and differentiation of TSPCs [4]. Shortly, two other groups isolated and identified this unique stem cell population from tendons of rabbits and rats and characterized them extensively [5, 39]. In these studies, TSPC colonies exhibit large variations in cell proliferation and differentiation possibly due to differences in species, tissue origin, and initial seeding density in culture. The shape of TSPCs also varies between species, tissue origin, cell passages, and confluence of the culture [40]. Additionally, the success of obtaining a large pool of TSPCs depends on the age of the animal/individual; aged tendon tissues are depleted of at least 70% TSPCs, they proliferate much slower than young TSPCs, and they have much lower expression of stem cell markers [41].

TSPCs possess distinct properties compared to resident tenocytes. They differ from tenocytes in many aspects such as shape, proliferation and differentiation potential, and expression of stem cell-specific markers [5]. Rabbit TSPCs are more cobblestone-shaped with large nuclei, while

tenocytes are more elongated, fibroblast-like with small nuclei in culture. Overall, TSPCs also proliferate much faster than tenocytes in culture [5]. Moreover, the capacity of multidifferentiation potency allows TSPCs to differentiate into tenocytes as well as nontenocytes, including adipocytes, chondrocytes, and osteocytes [4, 5, 39]. While both express common tendon-related markers including collagen type I, collagen type III, tenascin C, and TNMD, TSPCs *in vitro* express stem cell markers such as Oct-4, SSEA-1/4 and nucleostemin, while tenocytes exhibit a minimal expression of these markers [5].

TSPCs and bone marrow mesenchymal stem cells (BMSCs) share many of the same markers, yet the expression pattern is not identical between humans, mice, and rats [4, 41]. For example, human and mouse TSPCs lack CD18, but it is expressed in human BMSCs, and human and rat TSPCs do not express CD106, while it is expressed in human and mouse BMSCs [4, 39, 42, 43]. Also, over 60% of mouse TSPCs express CD90.2 whereas mouse BMSCs lack the expression [4]. Compared to mouse BMSCs, mouse TSPCs express higher mRNA levels of scleraxis (Scx), Comp, SOX-9, and Runx2. Human TSPCs also express higher levels of TNMD than human BMSCs [4]. Moreover, rat TSPCs have higher mRNA expression of tenogenic, adipogenic, and osteogenic markers compared to rat BMSCs at basal level [44]. These differences between species could suggest that TSPCs and BMSCs represent different developmental stages of a common MSC predecessor. Finally, since TSPCs tend to differentiate into tendon-specific cells (tenocytes) compared to BMSCs, whereas BMSCs tend to differentiate towards osteogenic lineage [4, 45], TSPCs may be ideal cells for tissue engineering of injured tendons.

3. Locations of TSPCs

The exact location of TSPCs in tendon is unclear. The IFM is a suggested location based on several observations. First of all, in the pioneering studies, TSPCs were isolated and characterized from the tendon proper after stripping off the tendon sheath and surrounding paratenon possibly to exclude vascular cells from the peritenon region [4, 5, 39], indicating IFM as a potential source of TSPCs. This speculation is strengthened by the observation that there are morphological and metabolic differences between IFM and FM. The IFM region is highly cellular and more vascular and has a fast turnover of noncollagenous matrix compared to FM, and the cells within IFM are round in shape compared to elongated tenocytes in FM (Figure 1) [46, 47]. However, tendon healing is thought to result from cells originating from multiple locations [48]. Therefore, it is possible that TSPCs may exist within each region in tendon and they may differ from one region to another, in terms of origins of progenitors, numbers of progenitor cells, and differentiation potentials. In fact, TSPCs have been isolated from peritenon/perivascular sources and their stem cell properties, such as clonogenicity, multipotency, and surface marker expression, have been determined and compared with TSPCs from the tendon proper (Table 1).

The perivascular area is an important source of stem/progenitor cells in tendon. Cells in intact human supraspinatus tendon biopsies and perivascular cells isolated from the microvessels of the same biopsies have been characterized. The results suggest that the perivascular region is a source of tendon precursor cells [7]. These cells express classical stem cell markers musashi-1, nestin, prominin-1/CD133, CD29, and CD44 as well as tendon-specific markers Scx and Smad 8. They also retain stem cell characteristics in culture. Later on, another study characterized TSPCs from the peritenon and tendon proper of mouse Achilles tendons [8]. Cells derived from the peritenon form less stem/progenitor cell colonies relative to those from the tendon proper. Analysis of surface markers for TSPCs from both regions indicated that they are $Sca1^+$ (stem cell marker), $CD90^+$, and $CD44^+$ (fibroblast markers) (Table 1).

Progenitors from both the tendon proper and the peritenon demonstrate a low percentage of cells positive for leukocytic, hematopoietic, and perivascular markers CD18, CD34, and CD133, indicative of subpopulations of progenitor cells with stem cell properties, fibroblast features, and little contribution from leukocytic, hematopoietic, or perivascular sources. The marker profile of TSPCs isolated from the tendon proper is consistent with that described by Bi et al. [4]. Tendon proper stem/progenitor cells express high levels of TNMD and Scx, indicative of enrichment of stem/progenitor cells of a tendon origin. In contrast, cells of the peritenon demonstrate relative increases in the expression of vascular (endomucin) and pericyte (CD133) markers relative to cells from the tendon proper. However, cells from both regions were able to form primitive tendon constructs when seeded within a fibrin gel. These tendon constructs displayed tendon-like characteristics such as the expression of collagen type I and TNMD and formation of collagen fibril and fiber along the long axis. One particular distinction noted between the progenitors from the two sources was that when these cells were grown in osteogenic media, only progenitors from the tendon proper deposited calcium within the cell layer. This feature may provide an explanation for the calcification and ossification, which is a typical feature of tendinopathy in the tendon proper. Recently, transcriptome profiles of isolated murine Achilles tendon proper- and peritenon-derived progenitor cells were carried out [49]. It was found that progenitor cells from the tendon proper differ from peritenon progenitor cells in the differential expression of genes, including Scx, Mohawk, Thbs4, and Wnt10α. The distinct types of TSPCs within the tendon proper and the peritenon may differentially contribute to intrinsic (tendon proper) and extrinsic (epitenon and paratenon) tendon repair mechanisms. The intrinsic repair may require those progenitor cells that predominantly express tendon markers, while extrinsic repair may involve those stem cells recruited from the perivascular area.

To understand the location of tendon stem/progenitor cells in tendons and their role in tendon repair, *in vivo* identity of TSPCs and their role in tendon healing have been investigated in rats using the IdU label-retaining method [9]. The results showed that label-retaining cells (LRCs) could be identified at the tendon proper, peritenon, and

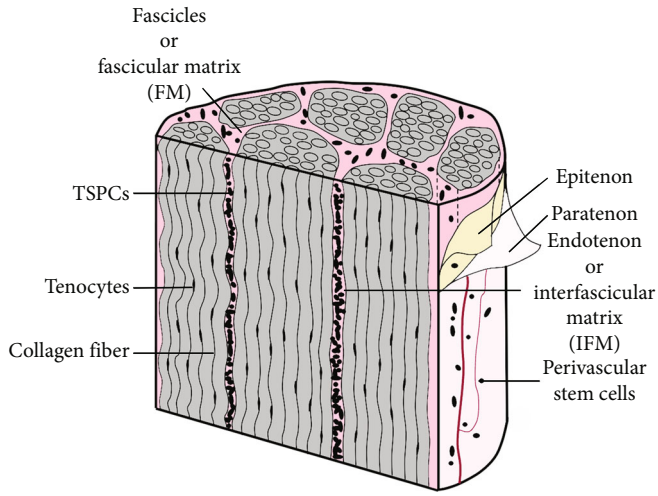

Figure 1: A simplified model of tendon structure adapted from Speisz et al. [47] showing fascicular matrix (FM), interfascicular matrix (IFM), and paratenon. The elongated tenocytes are located in FM in between fibers. The TSPCs from the tendon proper are presumably located in IFM; its exact location is yet to be determined, however.

Table 1: Sources and properties of TSPCs.

Sources	Properties	Markers	Reference
Tendon proper/midsubstance	(i) Typical stem cell characteristics (ii) Multipotent (iii) Distinct from BMSCs	Scleraxis, TNMD, collagen type I, tenascin, Sca1, CD90.2, CD44, CD146, Oct-4, SSEA-4, nucleostemin	Bi et al., 2007 [4]; Zhang and Wang, 2010 [5]; Rui et al., 2010 [39]
	(i) Typical stem cell characteristics (ii) Form tendon constructs that express collagen type I and TNMD (iii) Deposit calcium in osteogenic medium (iv) Potential nonvascular origin	Sca1, CD90, CD44, CD19, CD34, CD13, musashi-1, TNMD, scleraxis	Mienaltowski et al., 2013 [8]
	(i) Typical stem cell characteristics (ii) Potential nonvascular origin	CD146, Oct-4, nanog, SOX-2, nucleostemin	Tan et al., 2013 [9]
	(i) Typical stem cell characteristics (ii) Higher self-renewal and tenogenesis capacity, larger collagen fibril diameter compared to nestin-negative TSPCs	Nestin, CD146, CD90, CD44, CD105, CD51	Yin et al., 2016 [52]
Peritenon	(i) Express classical stem cell markers (ii) Retain stem cell characteristics in culture (iii) Potential vascular origin	Musashi-1, nestin, prominin-1/CD133, nestin, collagen types I and III, Smad8, CD29, CD44, scleraxis	Tempfer et al., 2009 [7]
	(i) Typical stem cell characteristics (ii) Display TSPC surface profile (iii) Form tendon constructs that express collagen type I and TNMD (iv) Potential vascular origin	Sca1, CD90, CD44, CD19, CD34, CD13, musashi-1	Mienaltowski et al., 2013 [8]
	(v) Both vascular and nonvascular sources	CD146, Oct-4, Nanog, SOX-2, nucleostemin	Tan et al., 2013 [9]
	(i) Typical stem cell characteristics (ii) Neural crest-like stem cells (iii) Potential vascular origin (iv) Involved in tendon repair	CD29, CD90, P75, vimentin, Snail, SOX-10	Xu et al., 2015 [50]

tendon-bone junction. Most of the TSPCs isolated from the tendon proper were LRCs suggesting that LRCs were likely to be TSPCs isolated from tendon tissue. Most of the LRCs were found to be embedded between parallel collagen fibers; however, some LRCs were also found at the perivascular region at the peritenon, and these LRCs expressed CD146. Isolated TSPCs also expressed CD146 initially, but lost its expression during the *in vitro* expansion, although they still expressed Nanog, Oct-4, SOX-2, and nucleostemin. In the tendon injury model with a window defect, the LRCs migrated,

proliferated, and activated for tenogenesis in the wound [9]. In another study, a subpopulation of cells exhibiting stem characteristics of clonogenicity, multipotency, and self-renewal capacity putatively of perivascular origin that reside within rat peritenon has been identified [50]. These cells expressed markers P75 (neurotrophin receptor), vimentin, SOX-10, and Snail consistent with neural crest stem cells (NCSCs). In the event of tendon injury, these perivascular cells may migrate from the vessels to interstitial space, and produce collagenous and noncollagenous proteins to repair damaged ECM [51].

The molecular profiling of individual cells derived from tendon identified a distinct subpopulation of nestin$^+$ cells that express stem cell markers (CD146, CD105, etc.) and tenolineage markers (Col I, tenascin C, etc.) that are likely to be TSPCs [52]. Nestin is a type IV filament protein expressed in a variety of adult stem/progenitor cell populations that is required for the proper self-renewal [53–55]. Analysis of phenotypic differences between nestin$^+$ TSPCs isolated *in vitro* from the tendon proper of human Achilles tendon shows a better tenogenic potential and self-renewing capacity and larger collagen fibril diameter than nestin$^-$ TSPCs (Table 1). The nestin expression seems to be essential for the tenogenesis of TSPCs since the expression of nestin led to a strong induction of Scx and Mkx and tendon-related marker genes elastin and collagen type I and XIV. However, both nestin$^+$ and nestin$^-$ TSPCs display a similar propensity to differentiate into osteocytes, adipocytes, and chondrocytes and have similar proliferation potential. Nestin knockdown significantly reduces colony forming capacity and causes the loss of the typical shape of TSPCs. Nestin knockdown also impairs tendon repair and regeneration in a rat model of patellar tendon defect. Collectively, these data show that nestin could function as a marker for TSPCs. This is further strengthened by a previous study showing high levels of nestin expression in TSPCs isolated from human Achilles tendon [56]. Taken together, these studies identify sources for TSPCs including the tendon proper (midsubstance) and peritenon that may contribute towards tendon tissue maintenance, healing, or repair.

4. Interactions of TSPCs with ECM and Mechanical Loading

Stem cells cannot function without the signals from their niche. The various niche factors for stem cells include ECM and mechanical stress, as well as oxygen tension, growth factors, and cytokines [4, 40, 57, 58]. Considering the surrounding rich ECM, the main niche signals that TSPCs receive may be from those ECM components such as biglycan and fibromodulin [4]. The ECM microenvironment likely plays an important role in TSPC fate that ultimately affects tendon maintenance and repair when injury occurs to the tendon [4]. Alteration of the ECM may lead to tendon pathological conditions, but whether this altered composition of ECM will directly affect the fate of TSPCs remains rather unexplored.

In addition to rich collagen, tendon ECM contains small amounts of proteoglycans (PGs) [2, 35]. Small leucine-rich proteins (SLRPs) are the most abundant PGs present in tendon and act as the crucial components of ECM, as well as function as an organizer for collagen fibril assembly and regulators of ECM turnover [59, 60]. Decorin and biglycan are the main SLRPs in tendon. SLRPs such as fibromodulin and lumican are also present in tendon. The tendons of decorin/biglycan/fibromodulin-deficient animals are mechanically inferior to normal tendons of wild-type mice [61, 62], and the collagen fibers within the tendon become disorganized in the absence of biglycan and fibromodulin [4]. Tendon integrity is impaired in lumican and fibromodulin-deficient mice [63]. Alteration of the ECM composition changes the structure of the TSPC niche consequently affecting the fate of TSPCs, which leads to tendon malformation and ossification [4]. Biglycan and fibromodulin are two critical SLRPs that control the fate of TSPCs. This may be mediated in part by modulating bone morphogenic protein (BMP) activity. TSPCs from biglycan and fibromodulin double-knockout mice proliferate faster, form larger colonies, and form bone-like tissues in addition to tendon-like tissues compared to those from wild type (WT) mice which form only tendon-like tissues [4]. The increased sensitivity of TSPCs to BMP-2 in the absence of biglycan and fibromodulin could be a mechanism for altering the fate of TSPCs. The expression of tendon markers Scx and collagen type I is decreased in TSPCs from these knockout mice compared to cells from WT mice. Therefore, the integrity of ECM is important in maintaining the stemness of TSPCs, and the precise regulation of the tenogenic differentiation of TSPCs is essential for the positive outcome of stem cell-based therapy for injured tendons.

In tendon, cell-ECM interactions maintain tissue homeostasis by generating cell signals that affect cell proliferation, differentiation, migration, and adhesion [35]. On the other hand, the ECM plays an important role in disease progression. The tendon ECM is enriched in growth factors and cytokines, and the ECM plays a major role in regulating the local availability of growth factors at a cellular level [64]. The changes of the structure and composition of ECM may disturb the local release of growth factors and cytokines as well as the modulation of cell shape and signaling cascade affecting the cell fate. Aberrant ECM changes including calcification, ossification, and lipid and proteoglycan accumulation are evident in human tendinopathy samples [65, 66]. The aberrant differentiation of TSPCs to nontenocytes (adipocytes, chondrocytes, and osteoblasts), which produce non-tendinous tissues, is suggested as a possible mechanism in the development of tendinopathy due to mechanical overloading placed on the tendon [30, 32, 33].

An engineered tendon matrix (ETM) from decellularized tendon tissues stimulates rabbit TSPC proliferation and better preserves stemness compared to plastic culture surfaces commonly used in culture, and implantation of ETM-TSPC composite promotes tendon-like tissue formation [67]. The ECM components and/or growth factors may contribute these properties to TSPCs, which are important in tissue engineering applications of such composites in injured tendon repair. A similar study using decellularized collagenous matrix from three different tissues (tendon, bone, and dermis) showed that tendon-derived decellularized matrix

promotes the tendinous phenotype in human TSPCs and inhibits their osteogenesis, even under osteogenic induction conditions, although all the three matrices support cell adhesion and proliferation [68]. The bone-derived decellularized matrix robustly induces osteogenic differentiation of TSPCs, whereas the dermal skin-derived collagen matrix induces only an intermediate level of osteogenesis. The differential cellular response could be attributed to the differences in the structure and topography but otherwise similar bioactivity of the matrices. The cell shape and alignment also differed in the three matrices; cells adopt an elongated shape and align on the tendon matrix, but not on the dermis matrix. This shows that besides the composition, ECM topographical cues are important in regulating the stem cell fate. This is supported by yet another study, which indicated that the culture of human TSPCs in an aligned nanofiber scaffold promotes tenogenic commitment, but in a random scaffold enhances osteogenic differentiation [42]. Compared to embryonic stem cell-mesenchymal stromal cells, TSPCs combined with the decellularized matrix also show more improvement in the structural and biomechanical properties of regenerated tendons *in vivo* [69]. In short, ECM components provide niche signals to TSPCs and play a significant role in deciding their fate depending on the changes in ECM composition and topographical cues.

The precise function of TSPCs *in vivo* is not well defined yet, and comparison studies with tenocytes are rare. Tendons have poor regenerative capacity as demonstrated by the inferior quality of tissues following injury or chronic degeneration [70, 71]. Therefore, it is conceivable that TSPCs alone may not be able to functionally restore the damaged tissues, although TSPCs promote functional repair of tendon tissues [72–77].

It is well known that mechanical loads play a major role in tendon development, homeostasis, pathology, and injury healing. These forces are translated into biochemical signals by molecules possessing mechanotransduction capabilities which activate and control key cellular processes of tendon [11, 78]. Normal mechanical loads are essential for appropriate tendon development and maintenance, because such loads like moderate loading patterns induce cellular anabolic adaptation of tendon [78–80]. On the other hand, abnormal mechanical loads cause pathological conditions (e.g. tendinopathy) in tendon by inducing dominant catabolic responses in tendon cells [14, 81–85]. Tendon cells respond to mechanical loads and modulate ECM via various mechanisms/pathways which have been extensively investigated using both *in vitro* and *in vivo* loading models (e.g., [86–88]).

TSPCs are capable of altering the tendon ECM in response to modifications of the loading environments. Also, the multidifferentiation potential of TSPCs allow them to differentially respond to altering mechanical loads. For example, an *in vitro* study showed that a uniaxial cyclic mechanical stretching of patellar and Achilles TSPCs from mice at moderate levels (4% elongation, 0.5 Hz for 12 hrs) increases proliferation and collagen type I gene expression without affecting the gene expressions of PPARγ (a marker for adipocytes), collagen type II, SOX-9 (markers for chondrocytes), and Runx2 (a marker osteocytes) [30]. Similarly, mechanical loading in the form of moderate treadmill running in mice increases the proliferation of TSPCs and TSPC-related cellular production of collagen [57].

However, mechanical stretching of mouse TSPCs at an excessive level (8% elongation) increases the gene expression of PPARγ, collagen type II, SOX-9, and Runx2 [30]. A further study showed that a 4% stretching of TSPCs increases the expression of tenocyte-related genes (collagen I and TNMD) while 8% stretching increased the expression of both tenocyte and non-tenocyte-related genes (LPL, SOX-9, and Runx2) in TSPCs but not in tenocytes [33]. The increase in both tenocyte and nontenocyte-related gene expression under 8% stretching may be due to the fact that the TSPC population is heterogeneous, meaning that individual TSPC may have different levels of threshold in response to mechanical loading and as a result, they respond differently in their gene expression. Similar results were obtained when the study was performed *in vivo* using moderate and intensive treadmill running to apply low and excess mechanical loading, respectively [33]. Although the results from cellular and tissue levels are presented only at gene expression levels, it may indicate that mechanical overloading may prime TSPCs to undergo nontenocyte differentiation. Further studies are warranted to link the nontenogenic differentiation of TSPCs and degenerative changes in tendinopathy.

Also, in another study, mechanical stretching at 4% and 8% (0.5 Hz for 4 hrs) increased BMP-2 expression at gene and protein levels in rat TSPCs [31]. BMP-2 increased osteogenic differentiation of TSPCs as indicated by ALP activity and calcium nodule formation. The observation of osteogenic differentiation at 4% is in contrast with the previous findings [30, 33], possibly due to the differences in the stretching regimen, species difference, and culture conditions. Involvement of BMP-2 in the pathogenesis of tendinopathy has been suggested previously based on the reported observations that chondrocyte phenotype and ectopic ossification are present in calcifying tendinopathy and based on the expression of BMP-2 protein at those sites [89–92]. Moreover, the addition of BMP-2 to human TSPCs in culture decreased cell proliferation and induced osteogenic differentiation [93]. Higher BMP-2 receptor expression and BMP-2-induced osteogenic differentiation of rat TSPCs compared to BMSCs have been reported [94]. Taken together, these studies indicate that the activation of BMP-2 expression in TSPCs during tendon overuse might provide a possible explanation for ectopic calcification in calcifying tendinopathy. Overall, the data indicate that moderate mechanical loads are beneficial for maintaining tendon homeostasis, but mechanical overloading may contribute to degenerative changes in tendon, with TSPCs playing a major role.

5. Conclusion

TSPCs have been identified in both the tendon proper and peritenon in tendon that may have both vascular and nonvascular origins. However, how TSPCs from different locations contribute to tendon maintenance, repair, and

tendinopathy remains to be better understood. This is indeed a challenging task now considering the lack of definitive genetic lineage tracing and specific markers for TSPC identity, functions, and biological characterization. To this end, advanced studies using state-of-the-art novel approaches, including genetic models, genetic lineage tracing, and single-cell transcription profiling to identify the heterogeneity of TSPCs, need to be conducted.

TSPCs reside in tendons and are constantly subjected to mechanical loading due to the fact that tendons like Achilles and patellar are load-bearing tissues. Consequently, the function of TSPCs is regulated by ECM composition, organization, and mechanical loads. Therefore, further investigations are necessary to understand the crosstalk among TSPCs, ECM, and mechanical loads, and also those signaling pathways involved, so that tendon physiology and pathophysiology can be better understood. The findings from these investigations will surely aid in devising new yet effective tissue engineering approaches to regenerate injured tendons and also developing novel treatment strategies to manage tendinopathy, a prevalent tendon disorder commonly seen in both athletic and general populations.

Abbreviations

ALP: Alkaline phosphatase
BMP-2: Bone morphogenetic protein-2
BMSCs: Bone marrow mesenchymal stem cells
Col I: Collagen type I
Comp: Collagen oligomeric matrix protein
ECM: Extracellular matrix
ETM: Engineered tendon matrix
FM: Fascicular matrix
GAG: Glycosaminoglycans
HSR: Heavy slow resistance
IFM: Interfascicular matrix
LPL: Lipoprotein lipase
LRC: Label-retaining cells
NSAIDs: Nonsteroidal anti-inflammatory drugs
NCSCs: Neuronal crest stem cells
Oct-4: Octamer-binding transcription factor 4
PGs: Proteoglycans
PPARγ: Peroxisome proliferator-activated receptor γ
PRP: Platelet-rich plasma
Runx2: Runt-related transcription factor 2
Scx: Scleraxis
SLRPs: Small leucine-rich proteins
Smad8: Mothers against decapentaplegic homolog 8
SOX-9: Sex-determining region SRY
SSEA-1/4: Stage-specific embryonic antigen 1/4
Thbs4: Thrombospondin 4
TNMD: Tenomodulin
TSPCs: Tendon stem/progenitor cells.

Conflicts of Interest

The authors declare that there are no conflicts of interest regarding the publication of this paper.

Authors' Contributions

Chuanxin Zhang and Jun Zhu contributed equally to this review.

Acknowledgments

This work was supported by grants from the National Natural Science Foundation of China (8170090144) and the National Institutes of Health, USA (AR065949). The authors thank Dr. Juntao Ji for preparing the illustration (Figure 1).

References

[1] G. Nourissat, F. Berenbaum, and D. Duprez, "Tendon injury: from biology to tendon repair," *Nature Reviews Rheumatology*, vol. 11, no. 4, pp. 223–233, 2015.

[2] C. T. Thorpe and H. R. C. Screen, "Tendon structure and composition," in *Metabolic Influences on Risk for Tendon Disorders*, P. Ackermann and D. Hart, Eds., vol. 920 of Advances in Experimental Medicine and Biology, pp. 3–10, Springer, Cham, 2016.

[3] P. Kannus, "Structure of the tendon connective tissue," *Scandinavian Journal of Medicine & Science in Sports*, vol. 10, no. 6, pp. 312–320, 2000.

[4] Y. Bi, D. Ehirchiou, T. M. Kilts et al., "Identification of tendon stem/progenitor cells and the role of the extracellular matrix in their niche," *Nature Medicine*, vol. 13, no. 10, pp. 1219–1227, 2007.

[5] J. Zhang and J. H. C. Wang, "Characterization of differential properties of rabbit tendon stem cells and tenocytes," *BMC Musculoskeletal Disorders*, vol. 11, no. 1, p. 10, 2010.

[6] E. Zelzer, E. Blitz, M. L. Killian, and S. Thomopoulos, "Tendon-to-bone attachment: from development to maturity," *Birth Defects Research Part C: Embryo Today: Reviews*, vol. 102, no. 1, pp. 101–112, 2014.

[7] H. Tempfer, A. Wagner, R. Gehwolf et al., "Perivascular cells of the supraspinatus tendon express both tendon- and stem cell-related markers," *Histochemistry and Cell Biology*, vol. 131, no. 6, pp. 733–741, 2009.

[8] M. J. Mienaltowski, S. M. Adams, and D. E. Birk, "Regional differences in stem cell/progenitor cell populations from the mouse Achilles tendon," *Tissue Engineering Part A*, vol. 19, no. 1-2, pp. 199–210, 2013.

[9] Q. Tan, P. P. Y. Lui, and Y. W. Lee, "In vivo identity of tendon stem cells and the roles of stem cells in tendon healing," *Stem Cells and Development*, vol. 22, no. 23, pp. 3128–3140, 2013.

[10] J. H. C. Wang, Q. Guo, and B. Li, "Tendon biomechanics and mechanobiology—a minireview of basic concepts and recent advancements," *Journal of Hand Therapy*, vol. 25, no. 2, pp. 133–141, 2012.

[11] M. Lavagnino, M. E. Wall, D. Little, A. J. Banes, F. Guilak, and S. P. Arnoczky, "Tendon mechanobiology: current knowledge and future research opportunities," *Journal of Orthopaedic Research*, vol. 33, no. 6, pp. 813–822, 2015.

[12] C. N. Maganaris, M. V. Narici, L. C. Almekinders, and N. Maffulli, "Biomechanics and pathophysiology of overuse tendon injuries: ideas on insertional tendinopathy," *Sports Medicine*, vol. 34, no. 14, pp. 1005–1017, 2004.

[13] M. Kjaer, "Role of extracellular matrix in adaptation of tendon and skeletal muscle to mechanical loading," *Physiological Reviews*, vol. 84, no. 2, pp. 649–698, 2004.

[14] D. Docheva, S. A. Müller, M. Majewski, and C. H. Evans, "Biologics for tendon repair," *Advanced Drug Delivery Reviews*, vol. 84, pp. 222–239, 2015.

[15] J. F. Kaux, B. Forthomme, C. L. Goff, J. M. Crielaard, and J. L. Croisier, "Current opinions on tendinopathy," *Journal of Sports Science and Medicine*, vol. 10, no. 2, pp. 238–253, 2011.

[16] J. C. Patterson-Kane and T. Rich, "Achilles tendon injuries in elite athletes: lessons in pathophysiology from their equine counterparts," *ILAR Journal*, vol. 55, no. 1, pp. 86–99, 2014.

[17] B. J. F. Dean, S. G. Dakin, N. L. Millar, and A. J. Carr, "Review: emerging concepts in the pathogenesis of tendinopathy," *The Surgeon*, vol. 15, no. 6, pp. 349–354, 2017.

[18] J. L. Y. Leung and J. F. Griffith, "Sonography of chronic Achilles tendinopathy: a case-control study," *Journal of Clinical Ultrasound*, vol. 36, no. 1, pp. 27–32, 2008.

[19] U. G. Longo, M. Ronga, and N. Maffulli, "Achilles tendinopathy," *Sports Medicine and Arthroscopy Review*, vol. 17, no. 2, pp. 112–126, 2009.

[20] J. L. Cook and C. R. Purdam, "Is tendon pathology a continuum? A pathology model to explain the clinical presentation of load-induced tendinopathy," *British Journal of Sports Medicine*, vol. 43, no. 6, pp. 409–416, 2009.

[21] J. L. Cook, E. Rio, C. R. Purdam, and S. I. Docking, "Revisiting the continuum model of tendon pathology: what is its merit in clinical practice and research?," *British Journal of Sports Medicine*, vol. 50, no. 19, pp. 1187–1191, 2016.

[22] N. L. Millar, G. A. C. Murrell, and I. B. McInnes, "Inflammatory mechanisms in tendinopathy—towards translation," *Nature Reviews Rheumatology*, vol. 13, no. 2, pp. 110–122, 2017.

[23] M. Benjamin and J. R. Ralphs, "The cell and developmental biology of tendons and ligaments," *International Review of Cytology*, vol. 196, pp. 85–130, 2000.

[24] S. A. Fenwick, B. L. Hazleman, and G. P. Riley, "The vasculature and its role in the damaged and healing tendon," *Arthritis Research*, vol. 4, no. 4, pp. 252–260, 2002.

[25] G. Riley, "The pathogenesis of tendinopathy. A molecular perspective," *Rheumatology*, vol. 43, no. 2, pp. 131–142, 2004.

[26] Y. Xu and G. A. C. Murrell, "The basic science of tendinopathy," *Clinical Orthopaedics and Related Research*, vol. 466, no. 7, pp. 1528–1538, 2008.

[27] G. Riley, "Tendinopathy—from basic science to treatment," *Nature Clinical Practice Rheumatology*, vol. 4, no. 2, pp. 82–89, 2008.

[28] N. Maffulli, U. G. Longo, and V. Denaro, "Novel approaches for the management of tendinopathy," *The Journal of Bone and Joint Surgery*, vol. 92, no. 15, pp. 2604–2613, 2010.

[29] M. Kongsgaard, K. Qvortrup, J. Larsen et al., "Fibril morphology and tendon mechanical properties in patellar tendinopathy: effects of heavy slow resistance training," *The American Journal of Sports Medicine*, vol. 38, no. 4, pp. 749–756, 2010.

[30] J. Zhang and J. H. C. Wang, "Mechanobiological response of tendon stem cells: implications of tendon homeostasis and pathogenesis of tendinopathy," *Journal of Orthopaedic Research*, vol. 28, no. 5, pp. 639–643, 2010.

[31] Y. F. Rui, P. P. Y. Lui, M. Ni, L. S. Chan, Y. W. Lee, and K. M. Chan, "Mechanical loading increased BMP-2 expression which promoted osteogenic differentiation of tendon-derived stem cells," *Journal of Orthopaedic Research*, vol. 29, no. 3, pp. 390–396, 2011.

[32] Y. F. Rui, P. P. Lui, L. S. Chan, K. M. Chan, S. C. Fu, and G. Li, "Does erroneous differentiation of tendon-derived stem cells contribute to the pathogenesis of calcifying tendinopathy?," *Chinese Medical Journal*, vol. 124, no. 4, pp. 606–610, 2011.

[33] J. Zhang and J. H. C. Wang, "The effects of mechanical loading on tendons—an *in vivo* and *in vitro* model study," *PLoS One*, vol. 8, no. 8, article e71740, 2013.

[34] N. A. Dyment and J. L. Galloway, "Regenerative biology of tendon: mechanisms for renewal and repair," *Current Molecular Biology Reports*, vol. 1, no. 3, pp. 124–131, 2015.

[35] H. R. C. Screen, D. E. Berk, K. E. Kadler, F. Ramirez, and M. F. Young, "Tendon functional extracellular matrix," *Journal of Orthopaedic Research*, vol. 33, no. 6, pp. 793–799, 2015.

[36] D. Docheva, E. B. Hunziker, R. Fassler, and O. Brandau, "Tenomodulin is necessary for tenocyte proliferation and tendon maturation," *Molecular and Cellular Biology*, vol. 25, no. 2, pp. 699–705, 2005.

[37] R. Salingcarnboriboon, H. Yoshitake, K. Tsuji et al., "Establishment of tendon-derived cell lines exhibiting pluripotent mesenchymal stem cell-like property," *Experimental Cell Research*, vol. 287, no. 2, pp. 289–300, 2003.

[38] M. de Mos, W. J. L. M. Koevoet, H. Jahr et al., "Intrinsic differentiation potential of adolescent human tendon tissue: an in-vitro cell differentiation study," *BMC Musculoskeletal Disorders*, vol. 8, no. 1, p. 16, 2007.

[39] Y. F. Rui, P. P. Y. Lui, G. Li, S. C. Fu, Y. W. Lee, and K. M. Chan, "Isolation and characterization of multipotent rat tendon-derived stem cells," *Tissue Engineering Part A*, vol. 16, no. 5, pp. 1549–1558, 2010.

[40] P. P. Y. Lui, "Identity of tendon stem cells — how much do we know?," *Journal of Cellular and Molecular Medicine*, vol. 17, no. 1, pp. 55–64, 2013.

[41] P. P. Y. Lui and K. M. Chan, "Tendon-derived stem cells (TDSCs): from basic science to potential roles in tendon pathology and tissue engineering applications," *Stem Cell Reviews and Reports*, vol. 7, no. 4, pp. 883–897, 2011.

[42] Z. Yin, X. Chen, J. L. Chen et al., "The regulation of tendon stem cell differentiation by the alignment of nanofibers," *Biomaterials*, vol. 31, no. 8, pp. 2163–2175, 2010.

[43] Z. Zhou, T. Akinbiyi, L. Xu et al., "Tendon-derived stem/progenitor cell aging: defective self-renewal and altered fate," *Aging Cell*, vol. 9, no. 5, pp. 911–915, 2010.

[44] P. P. Lui, Y. F. Rui, and M. Ni, "Comparison of potentials of stem cells isolated from tendon and bone marrow for musculoskeletal tissue engineering," in *57th Annual Meeting of the Orthopaedic Research Society*, Long Beach, CA, 2011.

[45] M. T. Harris, D. L. Butler, G. P. Boivin, J. B. Florer, E. J. Schantz, and R. J. Wenstrup, "Mesenchymal stem cells used for rabbit tendon repair can form ectopic bone and express alkaline phosphatase activity in constructs," *Journal of Orthopaedic Research*, vol. 22, no. 5, pp. 998–1003, 2004.

[46] C. T. Thorpe, P. D. Clegg, and H. L. Birch, "A review of tendon injury: why is the equine superficial digital flexor tendon most at risk?," *Equine Veterinary Journal*, vol. 42, no. 2, pp. 174–180, 2010.

[47] E. M. Spiesz, C. T. Thorpe, S. Chaudhry et al., "Tendon extracellular matrix damage, degradation and inflammation in response to in vitro overload exercise," *Journal of Orthopaedic Research*, vol. 33, no. 6, pp. 889–897, 2015.

[48] G. Yang, B. B. Rothrauff, and R. S. Tuan, "Tendon and ligament regeneration and repair: clinical relevance and developmental paradigm," *Birth Defects Research Part C: Embryo Today*, vol. 99, no. 3, pp. 203–222, 2013.

[49] M. J. Mienaltowski, A. Cánovas, V. A. Fates et al., "Transcriptome profiles of isolated murine Achilles tendon proper- and peritenon-derived progenitor cells," *Journal of Orthopaedic Research*, vol. 37, no. 6, pp. 1409–1418, 2019.

[50] W. Xu, Y. Sun, J. Zhang et al., "Perivascular-derived stem cells with neural crest characteristics are involved in tendon repair," *Stem Cells and Development*, vol. 24, no. 7, pp. 857–868, 2015.

[51] N. A. Dyment, Y. Hagiwara, B. G. Matthews, Y. Li, I. Kalajzic, and D. W. Rowe, "Lineage tracing of resident tendon progenitor cells during growth and natural healing," *PLoS One*, vol. 9, no. 4, article e96113, 2014.

[52] Z. Yin, J. J. Hu, L. Yang et al., "Single-cell analysis reveals a nestin^{+} tendon stem/progenitor cell population with strong tenogenic potentiality," *Science Advances*, vol. 2, no. 11, article e1600874, 2016.

[53] C. Wiese, A. Rolletschek, G. Kania et al., "Nestin expression—a property of multi-lineage progenitor cells?," *Cellular and Molecular Life Sciences*, vol. 61, no. 19-20, pp. 2510–2522, 2004.

[54] K. Rizzoti, "Adult pituitary progenitors/stem cells: from *in vitro* characterization to *in vivo* function," *The European Journal of Neuroscience*, vol. 32, no. 12, pp. 2053–2062, 2010.

[55] D. Park, A. P. Xiang, F. F. Mao et al., "Nestin is required for the proper self-renewal of neural stem cells," *Stem Cells*, vol. 28, no. 12, pp. 2162–2171, 2010.

[56] C. Popov, M. Burggraf, L. Kreja, A. Ignatius, M. Schieker, and D. Docheva, "Mechanical stimulation of human tendon stem/progenitor cells results in upregulation of matrix proteins, integrins and MMPs, and activation of p38 and ERK1/2 kinases," *BMC Molecular Biology*, vol. 16, no. 1, p. 6, 2015.

[57] J. Zhang, T. Pan, Y. Liu, and J. H. C. Wang, "Mouse treadmill running enhances tendons by expanding the pool of tendon stem cells (TSCs) and TSC-related cellular production of collagen," *Journal of Orthopaedic Research*, vol. 28, no. 9, pp. 1178–1183, 2010.

[58] W. Y. W. Lee, P. P. Y. Lui, and Y. F. Rui, "Hypoxia-mediated efficient expansion of human tendon-derived stem cells *in vitro*," *Tissue Engineering Part A*, vol. 18, no. 5-6, pp. 484–498, 2012.

[59] J. H. Yoon and J. Halper, "Tendon proteoglycans: biochemistry and function," *Journal of Musculoskeletal & Neuronal Interactions*, vol. 5, no. 1, pp. 22–34, 2005.

[60] C. T. Thorpe, H. L. Birch, P. D. Clegg, and H. R. C. Screen, "The role of the non-collagenous matrix in tendon function," *International Journal of Experimental Pathology*, vol. 94, no. 4, pp. 248–259, 2013.

[61] M. F. Young, Y. Bi, L. Ameye, and X. D. Chen, "Biglycan knockout mice: new models for musculoskeletal diseases," *Glycoconjugate Journal*, vol. 19, no. 4/5, pp. 257–262, 2002.

[62] L. M. Dourte, L. Pathmanathan, A. F. Jawad et al., "Influence of decorin on the mechanical, compositional, and structural properties of the mouse patellar tendon," *Journal of Biomechanical Engineering*, vol. 134, no. 3, article 031005, 2012.

[63] K. J. Jepsen, F. Wu, J. H. Peragallo et al., "A syndrome of joint laxity and impaired tendon integrity in lumican- and fibromodulin-deficient mice," *The Journal of Biological Chemistry*, vol. 277, no. 38, pp. 35532–35540, 2002.

[64] G. S. Schultz and A. Wysocki, "Interactions between extracellular matrix and growth factors in wound healing," *Wound Repair and Regeneration*, vol. 17, no. 2, pp. 153–162, 2009.

[65] P. Kannus and L. Jozsa, "Histopathological changes preceding spontaneous rupture of a tendon. A controlled study of 891 patients," *The Journal of Bone and Joint Surgery*, vol. 73, no. 10, pp. 1507–1525, 1991.

[66] S. C. Fu, K. M. Chan, and C. G. Rolf, "Increased deposition of sulfated glycosaminoglycans in human patellar tendinopathy," *Clinical Journal of Sport Medicine*, vol. 17, no. 2, pp. 129–134, 2007.

[67] J. Zhang, B. Li, and J. H. C. Wang, "The role of engineered tendon matrix in the stemness of tendon stem cells *in vitro* and the promotion of tendon-like tissue formation *in vivo*," *Biomaterials*, vol. 32, no. 29, pp. 6972–6981, 2011.

[68] Z. Yin, X. Chen, T. Zhu et al., "The effect of decellularized matrices on human tendon stem/progenitor cell differentiation and tendon repair," *Acta Biomaterialia*, vol. 9, no. 12, pp. 9317–9329, 2013.

[69] H. Song, Z. Yin, T. Wu et al., "Enhanced effect of tendon stem/progenitor cells combined with tendon-derived decellularized extracellular matrix on tendon regeneration," *Cell Transplantation*, vol. 27, no. 11, pp. 1634–1643, 2018.

[70] H. Miyashita, M. Ochi, and Y. Ikuta, "Histological and biomechanical observations of the rabbit patellar tendon after removal of its central one-third," *Archives of Orthopaedic and Trauma Surgery*, vol. 116, no. 8, pp. 454–462, 1997.

[71] M. Järvinen, L. Józsa, P. Kannus, T. L. N. Järvinen, M. Kvist, and W. Leadbetter, "Histopathological findings in chronic tendon disorders," *Scandinavian Journal of Medicine & Science in Sports*, vol. 7, no. 2, pp. 86–95, 1997.

[72] M. Ni, P. P. Y. Lui, Y. F. Rui et al., "Tendon-derived stem cells (TDSCs) promote tendon repair in a rat patellar tendon window defect model," *Journal of Orthopaedic Research*, vol. 30, no. 4, pp. 613–619, 2012.

[73] C. Tan, P. P. Y. Lui, Y. W. Lee, and Y. M. Wong, "Scx-transduced tendon-derived stem cells (tdscs) promoted better tendon repair compared to mock-transduced cells in a rat patellar tendon window injury model," *PLoS One*, vol. 9, no. 5, article e97453, 2014.

[74] L. Chen, J. P. Liu, K. L. Tang et al., "Tendon derived stem cells promote platelet-rich plasma healing in collagenase-induced rat Achilles tendinopathy," *Cellular Physiology and Biochemistry*, vol. 34, no. 6, pp. 2153–2168, 2014.

[75] D. Jiang, B. Xu, M. Yang, Z. Zhao, Y. Zhang, and Z. Li, "Efficacy of tendon stem cells in fibroblast-derived matrix for tendon tissue engineering," *Cytotherapy*, vol. 16, no. 5, pp. 662–673, 2014.

[76] P. P. Y. Lui, O. T. Wong, and Y. W. Lee, "Transplantation of tendon-derived stem cells pre-treated with connective tissue growth factor and ascorbic acid *in vitro* promoted better tendon repair in a patellar tendon window injury rat model," *Cytotherapy*, vol. 18, no. 1, pp. 99–112, 2016.

[77] I. Komatsu, J. H. C. Wang, K. Iwasaki, T. Shimizu, and T. Okano, "The effect of tendon stem/progenitor cell (TSC) sheet on the early tendon healing in a rat Achilles tendon injury model," *Acta Biomaterialia*, vol. 42, pp. 136–146, 2016.

[78] M. T. Galloway, A. L. Lalley, and J. T. Shearn, "The role of mechanical loading in tendon development, maintenance, injury, and repair," *The Journal of Bone and Joint Surgery*, vol. 95, no. 17, pp. 1620–1628, 2013.

[79] K. M. Heinemeier and M. Kjaer, "*In vivo* investigation of tendon responses to mechanical loading," *Journal of Musculoskeletal & Neuronal Interactions*, vol. 11, no. 2, pp. 115–123, 2011.

[80] K. M. Heinemeier, D. Skovgaard, M. L. Bayer et al., "Uphill running improves rat Achilles tendon tissue mechanical properties and alters gene expression without inducing pathological changes," *Journal of Applied Physiology (Bethesda, MD: 1985)*, vol. 113, no. 5, pp. 827–836, 2012.

[81] J. G. Snedeker and J. Foolen, "Tendon injury and repair—a perspective on the basic mechanisms of tendon disease and future clinical therapy," *Acta Biomaterialia*, vol. 63, pp. 18–36, 2017.

[82] L. J. Soslowsky, S. Thomopoulos, S. Tun et al., "Neer Award 1999. Overuse activity injures the supraspinatus tendon in an animal model: a histologic and biomechanical study," *Journal of Shoulder and Elbow Surgery*, vol. 9, no. 2, pp. 79–84, 2000.

[83] J. H. C. Wang, "Mechanobiology of tendon," *Journal of Biomechanics*, vol. 39, no. 9, pp. 1563–1582, 2006.

[84] M. Attia, A. Scott, A. Duchesnay et al., "Alterations of overused supraspinatus tendon: a possible role of glycosaminoglycans and HARP/pleiotrophin in early tendon pathology," *Journal of Orthopaedic Research*, vol. 30, no. 1, pp. 61–71, 2012.

[85] T. W. Herod and S. P. Veres, "Development of overuse tendinopathy: a new descriptive model for the initiation of tendon damage during cyclic loading," *Journal of Orthopaedic Research*, vol. 36, no. 1, pp. 467–476, 2018.

[86] R. C. Dirks and S. J. Warden, "Models for the study of tendinopathy," *Journal of Musculoskeletal & Neuronal Interactions*, vol. 11, no. 2, pp. 141–149, 2011.

[87] T. Wang, P. Chen, M. Zheng et al., "In vitro loading models for tendon mechanobiology," *Journal of Orthopaedic Research*, vol. 36, no. 2, pp. 566–575, 2018.

[88] B. P. Thampatty and J. H. C. Wang, "Mechanobiology of young and aging tendons: in vivo studies with treadmill running," *Journal of Orthopaedic Research*, vol. 36, no. 2, pp. 557–565, 2018.

[89] S. Fenwick, R. Harrall, R. Hackney et al., "Endochondral ossification in Achilles and patella tendinopathy," *Rheumatology*, vol. 41, no. 4, pp. 474–476, 2002.

[90] N. Maffulli, J. Reaper, S. W. B. Ewen, S. W. Waterston, and V. Barrass, "Chondral metaplasia in calcific insertional tendinopathy of the Achilles tendon," *Clinical Journal of Sport Medicine*, vol. 16, no. 4, pp. 329–334, 2006.

[91] P. P. Y. Lui, S. C. Fu, L. S. Chan, L. K. Hung, and K. M. Chan, "Chondrocyte phenotype and ectopic ossification in collagenase-induced tendon degeneration," *Journal of Histochemistry & Cytochemistry*, vol. 57, no. 2, pp. 91–100, 2009.

[92] P. P. Y. Lui, L. S. Chan, Y. C. Cheuk, Y. W. Lee, and K. M. Chan, "Expression of bone morphogenetic protein-2 in the chondrogenic and ossifying sites of calcific tendinopathy and traumatic tendon injury rat models," *Journal of Orthopaedic Surgery and Research*, vol. 4, no. 1, p. 27, 2009.

[93] J. Zhang and J. H. C. Wang, "BMP-2 mediates PGE_2-induced reduction of proliferation and osteogenic differentiation of human tendon stem cells," *Journal of Orthopaedic Research*, vol. 30, no. 1, pp. 47–52, 2012.

[94] Y. F. Rui, P. P. Y. Lui, Y. W. Lee, and K. M. Chan, "Higher BMP receptor expression and BMP-2-induced osteogenic differentiation in tendon-derived stem cells compared with bone-marrow-derived mesenchymal stem cells," *International Orthopaedics*, vol. 36, no. 5, pp. 1099–1107, 2012.

Hindawi
Stem Cells International
Volume 2019, Article ID 8928934, 13 pages
https://doi.org/10.1155/2019/8928934

Review Article

Glutamine Metabolism Is Essential for Stemness of Bone Marrow Mesenchymal Stem Cells and Bone Homeostasis

Tao Zhou, Yuqing Yang, Qianming Chen, and Liang Xie

State Key Laboratory of Oral Diseases, National Clinical Research Center for Oral Diseases, Chinese Academy of Medical Sciences Research Unit of Oral Carcinogenesis and Management, West China Hospital of Stomatology, Sichuan University, 610041 Chengdu, Sichuan, China

Correspondence should be addressed to Liang Xie; lxie@scu.edu.cn

Received 2 May 2019; Accepted 23 August 2019; Published 12 September 2019

Guest Editor: Jun Li

Skeleton has emerged as an endocrine organ which is both capable of regulating energy metabolism and being a target for it. Glutamine is the most bountiful and flexible amino acid in the body which provides adenosine 5′-triphosphate (ATP) demands for cells. Emerging evidences support that glutamine which acts as the second metabolic regulator after glucose exerts crucial roles in bone homeostasis at cellular level, including the lineage allocation and proliferation of bone mesenchymal stem cells (BMSCs), the matrix mineralization of osteoblasts, and the biosynthesis in chondrocytes. The integrated mechanism consisting of WNT, mammalian target of rapamycin (mTOR), and reactive oxygen species (ROS) signaling pathway in a glutamine-dependent pattern is responsible to regulate the complex intrinsic biological process, despite more extensive molecules are deserved to be elucidated in glutamine metabolism further. Indeed, dysfunctional glutamine metabolism enhances the development of degenerative bone diseases, such as osteoporosis and osteoarthritis, and glutamine or glutamine progenitor supplementation can partially restore bone defects which may promote treatment of bone diseases, although the mechanisms are not quite clear. In this review, we will summarize and update the latest research findings and clinical trials on the crucial regulatory roles of glutamine metabolism in BMSCs and BMSC-derived bone cells, also followed with the osteoclasts which are important in bone resorption.

1. Introduction

Bone is a relatively dynamic organ which provides stiffness, shape, support, and locomotion for body structures [1]. It undergoes modeling and constant remodeling throughout life, exhibiting structure and shape changes. Bone modeling occurs from birth to adulthood and is responsible for gaining mass and changing the skeletal structure, as exemplified by the increases in bone length and diameter. Bone remodeling, tightly coupling bone resorption and formation, behaves the substitute for old tissues by new bones, thereby maintaining the mineral homeostasis and strength [2]. Osteoblasts for bone formation and osteoclasts for bone resorption are the main cells involved in bone remodeling; meanwhile, osteocytes derived from osteoprogenitors are also crucial in this biological process [3–6]. Recently, emerging evidences support that bone is an endocrine organ and manifests active metabolism, where cell bioenergetics plays an essential role in regulating intermediary metabolism [1, 7]. Collaboratively signaling networks contribute to an efficient transition in organisms between anabolic and catabolic states; thus, bone cells are capable to survive and grow in environments in which nutrient availability differs.

Virtually, biosynthesis requires amounts of exogenous fuel uptake, which can be converted to hydrolysis of adenosine 5′-triphosphate (ATP) inside the body to drive all cellular processes later [8]. The fuel sources containing glucose, free fatty acids, and the amino acids are excellent substrates for generating ATP in both cytoplasm and mitochondria through oxidative phosphorylation [9–11]. Their consumption and catabolism are adjusted automatically in order to match the distinctive energy demands in different stages covering proliferation, differentiation, and apoptosis, in which intracellular signaling molecules serve as checkpoints

for fuel selection, storage, transport, and utilization [12]. In addition, extrinsic factors like glucocorticoids also change the fuel metabolism and biological behavior of bone cells in result [13].

Previous studies supported that glutamine metabolism as a regulatory node participated in many biological processes, including vessel formation, cancer progress, and immune regulation [14–16]. Recently, glutamine in bone homeostasis gained increasing concentration in mediating the proliferation, osteoblast, and adipocyte differentiation, immunological features of cell BMSCs [17]. Alternatively, the bioenergetics of osteoblasts, osteocytes, and even the adipocytes were also regulated directly or indirectly by glutamine metabolism, which were tightly related to the degenerative diseases such as osteoporosis. Mechanistically, it was elucidated that WNT/β-catenin signaling, mammalian target of rapamycin signaling (mTOR), hypoxia-inducible transcription factors (HIFs), and some other signaling pathways were involved in bone cell metabolic activities [18–20]. In this paper, we reviewed and updated the crucial regulatory roles of glutamine metabolism in BMSCs, BMSC-derived bone cells, and osteoclasts which expected to provide a novel therapeutic perspective for bone destructive disorders.

2. Glutamine Metabolism

Glutamine, a nonessential amino acid (NEAA) composed of carbon (41.09%), hydrogen (6.90%), oxygen (32.84%), and nitrogen (19.17%), is mainly synthesized by the enzyme glutamine synthetase (GS) using glutamate and ammonia (NH_3) as a source. As the most bountiful and flexible amino acid in the body, it represents about 20% of the total free amino acids pool in the blood and 40% to 60% of the total amino acid pool in certain tissues [21–23]. Glutamine is hydrolyzed by glutaminase (GLS) to ammonium-ion (NH_4) and glutamate, the latter is subsequently transformed to α-ketoglutarate (α-KG) occurring as a transamination or a deamination [24]. Then, α-KG enters the tricarboxylic acid cycle (TCA cycle) to generate ATP through the production of nicotinamide adenine dinucleotide (NADH) and flavin adenine dinucleotide ($FADH_2$) [25]. Rather than being a substitute fuel source in TCA cycle, glutamine is also used as substrate for constructing proteins and nucleotides [26]. The nitrogen from glutamine through the practice of aminotransferases maintains the degrees of numerous amino acid pools in the cell, as exemplified by more than 50% of NEAAs originated from glutamine are used in protein synthesis in cancer cells *in vitro* [27]. It is indicated that, in cancer cells, mutations in TCA cycle enzymes, fumarate hydratase (FH) and succinate dehydrogenase (SDH), or complexes of the electron transfer chain (ETC), such as complex I and complex III, could promote glutamine utilization. In other words, TCA cycle, FH, SDH, and ETC are involved in its participation of nonessential amino acid production. For example, taken in by the cell through a transporter, glutamine is deaminated to glutamate by cytoplasmic GLS1, transferred by SLC25A11 into the mitochondrial matrix, and converted into α-KG. Then, α-KG follows TCA cycle steps until oxaloacetic acid, which is then converted into aspartate by aspartate transaminase (GOT2) and exported into the cytoplasm, which is critical to both purine and pyrimidine biosynthesis. After that, Asparate may be transformed into asparagine and arginine. In addition, glutamate in cytoplasm could be converted into arginine and proline [28–30]. Besides, glutamine also powers fatty acid synthesis through reductive carboxylation [31].

Glutamine metabolism was first put forward in 1935 by Hans Krebs, who reported that the brain cortex and retina of vertebrates and the kidney of rabbits and Guinea pigs could synthesize glutamate into glutamine and hydrolyze glutamine to ammonium glutamate [32]. Developing over time, much is known about the importance of glutamine metabolism in pathological conditions. Some tumor cells utilized glutamine to provide both nicotinamide adenine dinucleotide phosphate (NADPH) and carbon for lipid and glutathione biosynthesis as well as nitrogen for nucleotide biosynthesis, which was essential in controlling oxidative stress and supporting proliferation [33, 34]. Moreover, glutamine metabolism is also critical for liver-to-pancreas transdifferentiation, mature adipocyte inflammatory responses, and immunological cell functions [35–37]. And glutamine metabolism impacted epigenetic states as well as genome organization via α-KG, eventually altered cellular differentiation decisions [38]. More than 30 years ago, Biltz et al. firstly reported an active consumption and metabolism of glutamine in isolated calvaria and long bones [39]; subsequently, the role of glutamine in bone has drawn increasing attention.

3. Glutamine Metabolism in BMSCs

BMSCs, known as nonhemopoietic multipotent mesenchymal cells, are traditionally capable to differentiate into osteoblasts, adipocytes, and chondrocytes, thereby regulating bone homeostasis [40–42]. Recently, the energy metabolisms including glucose metabolism, glutamine metabolism, and fatty acids in MSCs in various contexts are reported constantly [43–45]. Glucose is a major energy and carbon source for mammalian cells and has been known as a major nutrient for osteoblasts since the early 1960s [46]. Instead of energy supplement, aerobic glycolysis in osteoblasts may be linked with the citrate secretion, which plays a critical role in the formation of apatite nanocrystals in bone [47, 48]. Therapeutic strategies that target glucose metabolism tend to apply to patients diagnosed with systemic diseases such as type 2 diabetes mellitus and chronic kidney disease [49, 50]. Moreover, Thrailkill et al. suggested that treatment with insulin alone only partially corrected both hyperglycemia and diabetic bone phenotype in twelve-week-old diabetic mice, which means the therapy targets in other metabolism are required [51]. Fatty acids, generated from stored triacylglycerides or fat depots and released into the circulation, are degraded in the mitochondria for the generation of ATP in bone cells, while the amount that is utilized for ATP production is currently unknown [52]. Similar to fatty acids, the extent that amino acids contributes to oxidative phosphorylation remains unclear at present; however, there are increasing numbers of researches on glutamine. Glutamine as the

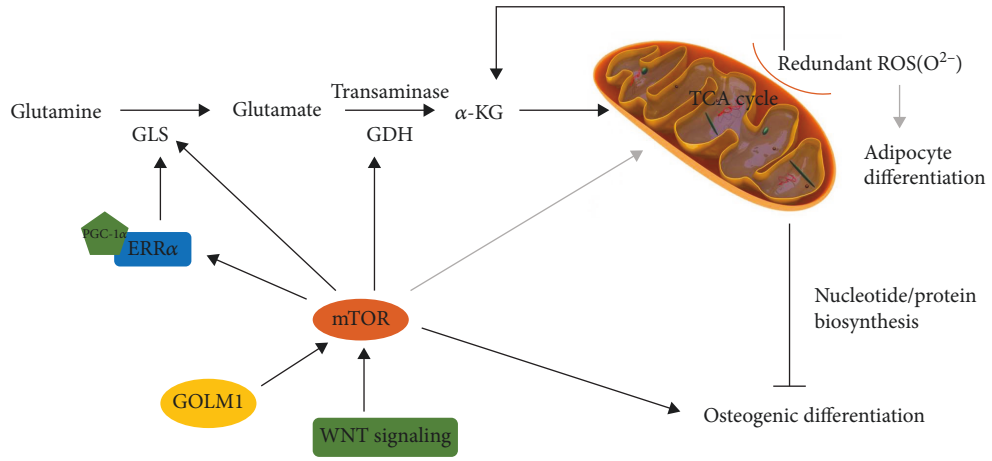

Figure 1: Glutamine-dependent regulation of BMSC osteogenic and adipocyte differentiation. The black arrows represent the signaling pathway in osteogenic differentiation regulated by glutamine; meanwhile, the gray arrows represent the signaling pathway in adipogenic differentiation.

second critical regulator after glucose exerts an essential modulation in BMSC proliferation, lineage allocation, osteoblast specification, and even the immunomodulatory properties.

3.1. Glutamine Metabolism in BMSC Proliferation. With regard to the proliferation of cells, Eagle et al. initially described the importance of glutamine in cell proliferation *in vitro* and meticulously essential for MSC proliferation [53]. In synchronized HeLa cells, glutamine, as well as glucose, is required for progression through the restriction point in mid-to-late G1. And glutamine is the only essential substrate for the progression through S phase into cell division, which was also indicated by combining pulse-chase LC-MS-based isotope tracing with computational deconvolution and metabolic flux modeling in synchronized cell populations [54, 55]. Mechanistically, glutamine has been reported to progress through the restriction point in mid-to-late G1 as well as exit S phase that was efficient for cell division beginning [54]. It is indicated that glutamine could enhance the expression of cyclin D1 and D3 and regulate cyclin-dependent kinase (CDKs) that were able to promote the passage into S phase and downregulate p21 expression, a key regulator for the cycle checkpoint of G1/S [56]. And this phenomenon may be associated with GLS, since glutamine increased the activity of GLS and glutamate dehydrogenase (GDH) through the mTOR/S6 and MAPK pathways in a dose-dependent manner, which finally promoted the cell proliferation [57]. However, the concrete mechanism remains unclear currently. In addition, it is commonly accepted that glutamine provided precursors for downstream synthetic steps, such as the DNA replication in S phase and lipid synthesis in G2 phase. And the majority of TCA carbons and nitrogen of some NEAAs derived from degraded glutamine in endothelial cells [15, 58]. Glucose is a major energy and carbon source for mammalian cells and has been known as a major nutrient for osteoblasts since the early 1960s. What is more, glutamine also provides a small amount of energy, since the glutamine-consuming enzymes are found largely in mitochondria and far from the primary need for ATP. Additionally, Karner's group found that BMSC proliferation and colony expansion were largely correlated with amino acid transaminase-dependent α-KG production, which could partially explain the negative impact of reduced GLS activity on BMSC proliferation [17]. However, the contribution of other amino acid biosynthesis derived from glutamine metabolism to BMSC proliferation has not been clear yet [33, 59]. For tumor cells in other tissues, glutamine satisfies biosynthetic and bioenergetic demands of these cells via anaplerotic entry to the TCA cycle and reductive carboxylation, thus regulating cell survival and proliferation [60, 61]. In contrast, the proliferation rates of skeletal progenitor cells seemed less important connection with glutamine-dependent reductive carboxylation or TCA cycle anaplerosis, which suggested distinctive roles of glutamine metabolism in different types of cells [19].

3.2. Glutamine Metabolism in BMSC Differentiation. Osteogenic and adipocyte differentiations are the pivotal linage commitments of BMSCs in skeletal development. BMSCs consume and metabolize a significant amount of glutamine as they undergo differentiation into the osteoblast but not the adipocyte lineage. As BMSCs differentiated toward osteoblasts, glutamine metabolism provided ATP through the TCA cycle with a declined contribution to citrate [17]. Furthermore, an integrated mechanism in a glutamine-dependent pattern was involved to meet energetic and synthetic demands during BMSC differentiation (see Figure 1).

3.2.1. GLS. Mitochondria is a pivotal place covering many complex metabolic reactions [62]. GLS catabolizes glutamine into glutamate, then α-KG, which replenishes anaplerosis of TCA intermediates to maintain mitochondrial activity and supply metabolic intermediates for active biosynthesis in osteogenesis [63]. Experimental evidence suggested GLS as the targeted enzyme of glutamine metabolism which influenced the differentiation of BMSCs. Genetically inhibiting glutamine metabolism via deletion of *Gls* in BMSCs resulted in reduction of overall osteoblast numbers and capability of

bone information, consequently causing decreased bone mass relative to wild-type littermates [17]. Alternatively, miRNA as an important regulator was able to establish a complex circuit in bone homeostasis by interacting with different genes [64]. Recent evidences reported that miRNA-206 participated BMSC bioenergy by directly bounding to the 3′-untranslated region (3′-UTR) of GLS mRNA, which resulted in the suppression of GLS expression and glutamine metabolism and eventually inhibited the osteogenic differentiation of BMSCs [65].

3.2.2. mTOR. mTOR is a sensor of growth factors whose activation increases bone width and mass as a result of hyperproliferated MSCs but declines bone length and mineral contents due to defective MSC differentiation [66]. Mechanistically, mTOR is a central target of intrinsic control in bone cells which integrates various molecules associated with glutamine metabolism in BMSC differentiation. Previous studies indicated WNT signaling influenced osteoblasts biological behaviors by enhancing both cell numbers and protein synthesis activity [67]. Importantly, to meet the increased energetic and synthetic need, the anabolic mechanism directly responded to WNT signaling to impact osteoblast differentiation of BMSCs. WNT signaling targeted the mammalian target of rapamycin complex1 (mTORC1) to stimulate glutamine entry to the TCA cycle, subsequently it lowered intracellular glutamine levels. Then, the general control nonderepressible 2-mediated (GCN2-mediated) with integrated stress response (ISR) pathway was triggered due to the WNT-induced reduction of glutamine, which stimulated the expression of genes that responsible for amino acid transport, tRNA aminoacylation, and protein folding [68]. Previous studies also suggested that mTORC1 activation stimulated glutamate to α-KG conversion by activating GDH, thus promoting cancer cell proliferation [69]. The activation of mTOR signaling pathway stimulated by Golgi membrane protein 1 (GOLM1) overexpression in BMSCs was in sympathy with that in cancer cells, behaving inhibited osteogenic differentiation of BMSCs due to increased GDH activity and glutamine to α-KG conversion. [20].

3.2.3. ERRα. Estrogen-related receptor α (ERRα), an orphan nuclear hormone receptor, is capable of regulating the transcription of related genes. Previous studies reported that ERRα positively regulated adipocytic and chondrocytic differentiation of MSCs while behaved a dual effect on osteoblast differentiation in Runx2- and/or WNT-target manner [70]. Recently, the age-related restriction of BMSCs has been reported as an essential factor in bone degenerative progress because of declined osteogenic capacity and unbalanced lineage allocation [71, 72]. And the dynamic expression patterns of ERRα with ages were tightly associated with BMSC osteoblast differentiation. A study displayed that ERRα expression was obviously reduced in elder rats, which was consistent with the deteriorated osteogenic capacity with ages [73]. Besides, ERRα was dysregulated in age-prevalent diseases like osteoarthritis and rheumatoid arthritis [74, 75]. As for cell level, ERRα reached peak protein expression levels at early phase of osteoblast differentiation and declined at mineralization stage while mRNA levels remained stable. It indeed supported the view that ERRα was inactivated after the onset of osteoblast maturation and it regulated osteoblast differentiation in a time-specific manner [76]. However, precise molecular mechanism remains unclear. Dysregulation of mitochondrial function is a common feature of aging, and coactivation of ERRα with proliferator-activated receptor gamma coactivator 1-α (PGC-1α) regulated mitochondrial biogenesis through fatty acid oxidation and energy expenditure related to ROS [77, 78]. Through binding to its promoter, ERRα directly regulated GLS expression, leading mitochondrial Gln-dependent anaplerosis critical to TCA cycle and biosynthesis of nucleotides and proteins. Aging negatively impacted on this ERRα/GLS signaling pathway, and repaired ERRα and GLS expression could partially restore osteogenic capacity of MSCs to resist bone loss [73]. In addition, the synthesis master regulator mTOR modulated ERRα/GLS signaling via affecting ERRα transcriptional activity, which may be a targeted therapy for aging-related bone loss [73].

3.2.4. ROS. Reactive oxygen species (ROS) originate from the oxidation of metabolic intermediates of ETC and are usually produced in the form of superoxide in the mitochondria [79]. The complexes of the respiratory chain in mitochondria are the main ROS production sites, especially complexes I and III. Besides, many other proteins such as pyruvate dehydrogenase (PDH) and electron transfer flavoprotein (ETF) are also ROS producers [80]. ROS are not only a consequence of differentiation but also are critical components of pathways regulating stem cell differentiation [81]. They are precisely regulated to prevent oxidative damage of cells in normal circumstances; elevated ROS in BMSCs with ages were reported to destruct the lineage allocation, displaying promoted adipogenesis and blocked osteogenesis [82, 83]. A potential mechanism may be the toxic accumulation of α-KG under excessive oxidative metabolism. Increased activity of PDH and loss of mitochondrial membrane potential (MMP) with a transformation to TCA cycle most likely enhanced pyruvate entry into mitochondria, thus accumulating toxic metabolites [84]. Then, it resulted in nucleocytoplasmic vacuolation and chromatin condensation which obviously prevented osteogenic and adipocyte differentiation. Simultaneously, the accompanying DNA damage, inhibition of histone H3 (Lys27) of acetylation, and increased HIF-1α degradation contributed to the death of BMSCs [84]. Moreover, another study reported that increased glutathione content from glutamine was important to offset the detrimental effect of ROS to the osteoblast fate [17]. Alternatively, compared with the positive role of ROS, glutamine was less chief in adipocyte differentiation of BMSCs. The mitochondrial-generated ROS enhanced adipocyte differentiation in a mTORC1-dependent pattern, which could explain the phenomenon that neither glutamine consumption nor GLS activity altered during adipocyte differentiation relative to undifferentiated BMSCs [85, 86].

3.3. Glutamine Metabolism of BMSCs in Osteoimmunology. Apart from the self-renewal and multilineage differentiation features, MSCs are known to exert an immunosuppressed modulation by expressing adhesion molecules and secreting effectual factors like cytokines, chemokines, and growth factors [87–89]. Researches about glutamine metabolism in immune system in recent decades also prompted the recognition of its regulatory role in adaptive immunity and innate immunity, covering lymphocytes, neutrophils, and macrophages as well as a series of cytokines [90–92]. In BMSCs, the concentration of glutamine was relevant to their immunology properties. High dose of glutamine displayed an enhancement for immunosuppressive properties of BMSCs via affecting inflammatory cytokines, displaying decreased levels of proinflammatory cytokines like interleukin-1β (IL-1β) and IL-6 and increased levels of anti-inflammatory cytokines IL-10, and transforming growth factor-β (TGF-β) [93]. Mechanistically, varied production of proinflammatory cytokines may relate to the reduced expression of phosphorylated nuclear factor kappa-B (NF-κB) and high level of signal transducer and activator (STAT-3) in BMSCs as they control cytokine production [94]. Additionally, IL-10 was critical in immune responses in glutamine concentration as they inhibited activation of NF-κB, thus modulating the cytokine production. Meanwhile, both IL-10 and STAT-3 increased in BMSCs with glutamine, which could be explained that the anti-inflammatory effects of IL-10 were mediated by STAT-3, and in turn, IL-10 was also reported to promote STAT-3 to reduce amounts of proinflammatory cytokines [95, 96]. Additionally, the proliferation of lymphocytes and macrophages was inhibited when cocultured with BMSCs in glutamine medium, both followed with an increased production of IL-10 [97]. The increased IL-10 may be attributed to the transformation of macrophages to an anti-inflammatory M2 phenotype with the induction of MSCs [98], whereas the precise mechanism of immunomodulation in BMSC-mediated glutamine is unclear.

4. Glutamine Metabolism in Osteoblasts

Characterized as the chief bone-making cells, osteoblasts take charge of producing large amounts of both collagen I-rich bone matrix and ectoenzymes controlling matrix mineralization. They follow timely programmed steps and express specific genes under the control of proosteogenic pathways. WNT signaling pathway is pivotal to promote the commitment towards an osteo/chondroprogenitor of BMSCs, especially in the early steps in osteoblast differentiation [99]. It is suggested that WNT signaling directly reprograms cellular metabolism in osteoblast lineage cells by stimulating aerobic glycolysis, glutamine catabolism, and fatty acid oxidation [67]. Additionally, glutamine catabolism has been identified as a crucial regulatory step in satisfying both energetic and synthetic requirements which is connected with WNT-induced bone anabolism in immature osteoblasts.

Karner et al. reported that glutamine was both an energy source and a protein-translation rheostat which was responsive to osteoblast differentiation [68], and impaired osteoblast differentiation with ages in BMSCs may be linked with declined glutamine consumption [73]. Meanwhile, Brown et al. supported that glutamine significantly improved osteoblast viability and enhanced the utilization of glucose in both human osteoblast-like cell lines and mouse calvarial osteoblasts, and higher levels of osteocalcin expression were beneficial for matrix mineralization [100]. Furthermore, considering that glutamine directly stimulated collagen type1a1 transcription in fibroblasts, the practice of glutamine on mineralization in osteoblast cultures might be owing to an influence on collagen expression [101]. However, it remains unknown whether glutamine anaplerosis is required for physiological osteoblasts activity in bone formation due to the lack of systematic analyses in osteoblasts with *Gls* depletion [102].

5. Glutamine Metabolism in Chondrocytes

The commitment of BMSCs to the chondrogenic lineage is a significant event to initiate the endochondral ossification that BMSCs firstly give rise to immature chondrocytes and cartilage primordia. Integrated signaling among growth factors and components of the extracellular matrix containing collagens, proteoglycans, glycosaminoglycans (GAGs), and proteases regulate chondrocytes collaboratively to facilitate progressive changes in endochondral ossification and bone formation [103]. Glutamine was initially shown to sustain glycosaminoglycan and protein synthesis as a carbon and nitrogen provider in extracellular matrix metabolism in chondrocytes [104]. In view of the special avascular environment of cartilage, it was widely assumed that cells within cartilage were hypoxic and hypoxia regulated the energetic state of maturing cells [105]. However, an excessive hypoxic environment was harmful for chondrocytes, and it was usually followed with a reduced utilization of glutamine and declined content of glutathione, which was possibly attributed to the downregulated mitochondria1 function and inhibited oxidative deamination [105]. HIF-1α is a protein expressing in hypoxic microenvironment, and higher expression of HIF-1α under hypoxic condition is of great necessity for chondrocytes survival in an intrinsic mechanism [106, 107]. As HIF-1α mediated an upregulated expression of GLS1, the flux of glutamine to α-KG was enhanced to favor α-KG-dependent proline and lysine hydroxylation of collagen, and it was beneficial to increase bone mass by endowing the resistance of the cartilaginous matrix to protease-mediated degradation [108]. In some pathological situations, glutamine also exhibited a protective effect on chondrocytes. For instance, glutamine upregulated glutathione concentration in chondrocytes to protect cells from injury in surgery or infectious conditions [109, 110]. In stress conditions, glutamine exerted chondroprotective effect by enhancing the expression of heat shock protein 70 (HSP70), which reduced chondrocytes apoptosis to prevent the progress of cartilage degeneration [111]. Importantly, two energy-dependent anabolic processes collaboratively regulated the biological behavior in chondrocytes. The imbalance of glucose-mediated reduced collagen synthesis and glutamine-mediated increased bone mass in chondrocytes will lead to the skeletal dysplasia [108].

6. Glutamine Metabolism in Osteoclasts

To maintain skeletal architecture and strength, a homeostatic balance between new bone formation and old or damaged bone resorption is required. Osteoclasts derived from the hematopoietic lineage mainly degrade bone matrix and liberate the calcium and phosphate, eventually exhibiting regulation on bone mass as well as quality [112]. It was suggested that L-glutamine had a significant impact on early phase of osteoclast differentiation and maturation stage [113]. Following the uptake through SLC1A5, a Na^+-dependent transporter of L-glutamine [114–116], osteoclasts converted glutamine to glutamate and then to α-KG, which was important as an anaplerotic substrate in osteoclast differentiation [117]. Additionally, glutamine was an essential fuel for the acquisition of bone-resorbing activity in mature, multinucleated osteoclasts [113]. Morten et al. reported that hypoxia stimulated glutamine consumption in osteoclasts, which was similar to SK–N–SH neuroblastoma and A549 lung adenocarcinoma cells [118, 119]. The increased glutamine uptake may mainly contribute to biosynthesis as glutamine withdrawal had no effect on either ATP production [61].

7. Therapeutic Potential of Glutamine in Bone Disorder Treatment

Energetic metabolism has gained improving attentions in the past decades for the regulation in the delivery and utilization of nutrients throughout the body, and the metabolic inflexibility is associated with various pathological process [120]. In updated clinical trials, amounts of researches have been arisen to elucidate the influence of glutamine in the improvement of adverse reactions induced by treatments and the potential applications in diagnosis (see Table 1). Additionally, glutamine is pivotal for both energy production and redox homeostasis in bone homeostasis, which can be a potential strategy in bone diseases such as osteoporosis and osteoarthritis.

7.1. Osteoporosis. Osteoporosis, mainly occurring in postmenopausal women and elder group, is characterized by low bone mass and deterioration of the bone microarchitecture which eventually behaves increased fracture susceptibility [151]. Previous researches reported aging-related changes of glutamine metabolism in osteoporosis could break the balance between osteogenic and adipocyte differentiation of BMSCs through key enzyme destruction in glutamine metabolism or mitochondria metabolic deterioration [73, 84]. Early anabolic therapies associated with glutamine may be a good way to treat osteoporosis from the perspective of etiology. Glutamine supplement (L-glutamine/L-alanyl solution (2.0 ml/kg) through the tail veins in the first 7 d was noted to obtain quicker and more regular primary callus and cartilaginous callus through attainments of positive nitrogen balance in standardized albino rats, which was instrumental in the healing of fractured osteoporosis patients [152]. However, the effect was tiny on enhancing the quality of fracture healing under conditions of stress, only exhibiting some influence on the speed of healing [152]. Virtually, glutamine precursor has been explored to apply in the treatment of osteoporosis in animal model. 2-Oxoglutarate (2-Ox), a precursor of glutamine, has been identified to promote the thickness of cancellous bone, growth plate, and articular cartilage in fundectomy-induced osteopenic bone [153]. It was also applied in osteoporosis induced by glucocorticoid treatment in premature infants with inflammatory and autoimmune disorders, which improved levels of growth hormone and osteocalcin concentration and preserved microarchitecture of trabecular bone [154].

7.2. Osteoarthritis. Osteoarthritis, characterized by degeneration of the articular cartilage and subchondral bone pathologically, is often diagnosed by the symptoms of pain, joint stiffness, and disability [155]. In osteoarthritis patients, inflammatory cytokines and ROS are induced by nonphysiological mechanical loading and heat stress facilitated by deviant joint movements, eventually contribute to the pathological progression. The treatment of chondrocytes with glutamine protected cells from heat stress and NO-induced apoptosis, thereby preventing osteoarthritis [111]. Fujita et al. indicated that heat stimulation and glutamine could stimulate the expression of HSP70 in rat articular cartilage *in vivo*, which may be involved in the suppression of osteoarthritis progression [156]. As stem cell-based therapy is a potential approach for osteoarthritis, researches about cellular metabolism in stem cells contribute to the application of cell-based treatment in general. Stegen et al. suggested that HIF-1α-mediated conversion of glutamine to glutathione synthesis was beneficial to maintain redox homeostasis under oxidative or nutrient stress, consequently exerting beneficial impact on cell survival [19]. The transplantation of adipose-derived mesenchymal stem cells (Ad-MSCs) in 1 ml of Dulbecco's modified Eagle's medium (DMEM) was injected into articular defect area of the osteoarthritis rabbits, and the overall healing score of experimental knees was superior when compared to the control group just received 1 ml of DMEM, in which 2 mM L-glutamine was included [157]. In addition, when it comes to osteoarthritis patients who received TKA, supplementation with a combination of β-hydroxy-β-methyl butyrate, L-arginine, and L-glutamine (HMB/Arg/Gln) during the postoperative recovery could suppress the loss of muscle strength [150].

8. Conclusion

Recent evidences indicated that glutamine is a critical regulator in bone homeostasis via supporting energy as a substitute carbon source through TCA cycle and providing precursors for protein and nucleic acid synthesis. At cellular level, glutamine metabolism mediate the bioenergy of bone cells including BMSCs, osteoblasts, chondrocytes, and osteoclasts, thus influencing their capabilities of the proliferation, differentiation, and mineralization. Abnormal glutamine metabolism is associated with clinical disorders such as osteoporosis and osteoarthritis and expected to provide novel guideline for treatments. In bone tissues, an integrated regulatory network where glutamine acting as the target participate BMSC differentiation, whereas researches of

Table 1: The application of glutamine in clinical trials.

	Disorders/treatment/diagnosis	Detailed effect
Digestive system disease	Postinfectious irritable bowel syndrome	Restore tight junction proteins, increase claudin-1 expression, and improve permeability [121]
	Crohn's disease	Increase the insoluble fraction of claudin-1 and occludin proteins, prevent the tight junction proteins, and maintain the intercellular junction [122]
	Short bowel syndrome	Provide energy for enterocytes, enhance the transport of sodium and water in the ileum, and upregulate intracellular protein synthesis [123–125]
	Acute pancreatitis	Improve lymphocyte proliferation, reduce proinflammatory cytokine, release C-reactive protein, and improve the nutritional status [126, 127]
	Cirrhotic	Increase blood ammonia [128]
Circulation system disease	Sickle cell disease	Raise the NAD redox ratio within sickle cells and synthesize NAD and decrease endothelial cell adhesion in sickled red cells [129, 130]
	Heart failure	Maintain a positive nitrogen balance and activate the suppressed oxidative metabolism [131]
Locomotor system disease	Duchenne muscular dystrophy	Inhibit whole-body protein degradation and stimulate insulin secretion [132, 133]
Systemic disorders	Critically ill patients	Maintain high level of HSP70 [134]
	Sepsis	Increase immune response, donate nitrogen for many anabolic processes, and promote wound healing [135]
	Type 2 diabetes mellitus	Delay gastric emptying to lower glycemia, stimulate GLP-1 concentration, and increase circulating insulin
	Low birthweight infants	Aid in maturation of the intestinal tract enhances growth, development, and function of the immunologic system [136, 137]
Imaging diagnosis	PET assay of tumor	A potential tumor biomarker for targeted radiotracer imaging [138]
Regulatory effect on certain treatments	Radiotherapy-induced toxicities	Protective effects of diarrhea minimized dermatitis [139, 140]
	Chemotherapy-induced toxicities	Treat neuropathy induced by vincristine and decrease mucositis severity [141–144]
	Peripheral blood stem cell transplantation	Improve $CD3^+$ and $CD4^+$lymphocyte recovery [145, 146]
	Liver transplantation	Synthesize glutathione and protect the liver graft against lipid peroxidation [147]
	Cardiac surgery	Enhance cell survival, attenuate the systemic inflammatory response, and prevent intracellular lactate accumulation [148, 149]
	Total knee replacement (TKA)	Suppress the loss of muscle strength after TKA [150]

downstream effectors of glutamine metabolism are seldom studied currently. Therefore, the mechanism of glutamine in bone homeostasis is likely multifaceted and additional basic investigation is needed beyond doubt. Glutamine metabolism has diversified influences on other cells or tissues, for example, it impacted the cellular differentiation through the epigenetic regulation in embryonic stem cells [158]; nevertheless, it has not been elucidated in bone cells. Alternatively, glutamine supplement has been applied in some systemic disease treatment and is expected to restore the impairment of osteoporosis and osteoarthritis. Virtually, the targets of glutamine in bone disease therapy are little known. Therefore, more fundamental and clinical studies are needed to deeply investigate the role of glutamine metabolism in regulating bone homeostasis and provide a new strategy for the clinical treatment of bone diseases.

Conflicts of Interest

The authors declare that there is no conflict of interest regarding the publication of this paper.

Authors' Contributions

Tao Zhou and Yuqing Yang contributed equally.

Acknowledgments

This work was supported by grants from the National Natural Science Foundation of China (NSFC, 81600842, 81621062, and 81520108009) and the Innovative Spark Program of Sichuan University (2018SCUH0056).

References

[1] H. K. Datta, W. F. Ng, J. A. Walker, S. P. Tuck, and S. S. Varanasi, "The cell biology of bone metabolism," *Journal of Clinical Pathology*, vol. 61, no. 5, pp. 577–587, 2008.

[2] P. Katsimbri, "The biology of normal bone remodelling," *European Journal of Cancer Care*, vol. 26, no. 6, 2017.

[3] G. Karsenty, H. M. Kronenberg, and C. Settembre, "Genetic control of bone formation," *Annual Review of Cell and Developmental Biology*, vol. 25, no. 1, pp. 629–648, 2009.

[4] T. A. P. Fernandes, L. M. L. Gonçalves, and J. A. A. Brito, "Relationships between bone turnover and energy metabolism," *Journal of Diabetes Research*, vol. 2017, 11 pages, 2017.

[5] M. Prideaux, D. M. Findlay, and G. J. Atkins, "Osteocytes: the master cells in bone remodelling," *Current Opinion in Pharmacology*, vol. 28, pp. 24–30, 2016.

[6] K. Fukasawa, G. Park, T. Iezaki et al., "ATF3 controls proliferation of osteoclast precursor and bone remodeling," *Scientific Reports*, vol. 6, no. 1, 2016.

[7] K. J. Suchacki, F. Roberts, A. Lovdel et al., "Skeletal energy homeostasis: a paradigm of endocrine discovery," *The Journal of Endocrinology*, vol. 234, no. 1, pp. R67–r79, 2017.

[8] D. F. Rolfe and G. C. Brown, "Cellular energy utilization and molecular origin of standard metabolic rate in mammals," *Physiological Reviews*, vol. 77, no. 3, pp. 731–758, 1997.

[9] S. Hui, J. M. Ghergurovich, R. J. Morscher et al., "Glucose feeds the TCA cycle via circulating lactate," *Nature*, vol. 551, no. 7678, pp. 115–118, 2017.

[10] P. E. Porporato, V. L. Payen, B. Baselet, and P. Sonveaux, "Metabolic changes associated with tumor metastasis, part 2: mitochondria, lipid and amino acid metabolism," *Cellular and Molecular Life Sciences*, vol. 73, no. 7, pp. 1349–1363, 2016.

[11] P. Kumar and K. K. Dubey, "Modulation of fatty acid metabolism and tricarboxylic acid cycle to enhance the lipstatin production through medium engineering in Streptomyces toxytricini," *Bioresource Technology*, vol. 213, pp. 64–68, 2016.

[12] R. C. Riddle and T. L. Clemens, "Bone cell bioenergetics and skeletal energy homeostasis," *Physiological Reviews*, vol. 97, no. 2, pp. 667–698, 2017.

[13] M. S. Cooper, M. J. Seibel, and H. Zhou, "Glucocorticoids, bone and energy metabolism," *Bone*, vol. 82, pp. 64–68, 2016.

[14] D. E. Biancur, J. A. Paulo, B. Małachowska et al., "Compensatory metabolic networks in pancreatic cancers upon perturbation of glutamine metabolism," *Nature Communications*, vol. 8, no. 1, 2017.

[15] H. Huang, S. Vandekeere, J. Kalucka et al., "Role of glutamine and interlinked asparagine metabolism in vessel formation," *The EMBO Journal*, vol. 36, no. 16, pp. 2334–2352, 2017.

[16] S. Yao, C. Li, M. Beckley, and D. Liu, "Expression of odontogenic ameloblast-associated protein in the dental follicle and its role in osteogenic differentiation of dental follicle stem cells," *Archives of Oral Biology*, vol. 78, pp. 6–12, 2017.

[17] Y. Yu, H. Newman, L. Shen et al., "Glutamine metabolism regulates proliferation and lineage allocation in skeletal stem cells," *Cell Metabolism*, vol. 29, no. 4, pp. 966–978.e4, 2019.

[18] A. Olkku and A. Mahonen, "Wnt and steroid pathways control glutamate signalling by regulating glutamine synthetase activity in osteoblastic cells," *Bone*, vol. 43, no. 3, pp. 483–493, 2008.

[19] S. Stegen, N. van Gastel, G. Eelen et al., "HIF-1α Promotes Glutamine-Mediated Redox Homeostasis and Glycogen-Dependent Bioenergetics to Support Postimplantation Bone Cell Survival," *Cell Metabolism*, vol. 23, no. 2, pp. 265–279, 2016.

[20] G. Shen, H. Zhang, P. Jia et al., "GOLM1 stimulation of glutamine metabolism promotes osteoporosis via inhibiting osteogenic differentiation of BMSCs," *Cellular Physiology and Biochemistry*, vol. 50, no. 5, pp. 1916–1928, 2018.

[21] J. R. Mayers and M. G. Vander Heiden, "Famine versus feast: understanding the metabolism of tumors in vivo," *Trends in Biochemical Sciences*, vol. 40, no. 3, pp. 130–140, 2015.

[22] J. Bergstrom, P. Furst, L. O. Noree, and E. Vinnars, "Intracellular free amino acid concentration in human muscle tissue," *Journal of Applied Physiology*, vol. 36, no. 6, pp. 693–697, 1974.

[23] B. I. Labow, W. W. Souba, and S. F. Abcouwer, "Mechanisms governing the expression of the enzymes of glutamine metabolism–glutaminase and glutamine synthetase," *The Journal of Nutrition*, vol. 131, no. 9, pp. 2467S–2474S, 2001.

[24] J. Neu, V. Shenoy, and R. Chakrabarti, "Glutamine nutrition and metabolism: where do we go from here?," *FASEB Journal*, vol. 10, no. 8, pp. 829–837, 1996.

[25] R. W. Moreadith and A. L. Lehninger, "The pathways of glutamate and glutamine oxidation by tumor cell mitochondria. Role of mitochondrial NAD(P)+-dependent malic enzyme," *The Journal of Biological Chemistry*, vol. 259, no. 10, pp. 6215–6221, 1984.

[26] A. M. Hosios, V. C. Hecht, L. V. Danai et al., "Amino acids rather than glucose account for the majority of cell mass in proliferating mammalian cells," *Developmental Cell*, vol. 36, no. 5, pp. 540–549, 2016.

[27] L. Alberghina and D. Gaglio, "Redox control of glutamine utilization in cancer," *Cell Death & Disease*, vol. 5, no. 12, p. e1561, 2014.

[28] D. Patel, D. Menon, E. Bernfeld et al., "Aspartate rescues S-phase arrest caused by suppression of glutamine utilization in KRas-driven cancer cells," *The Journal of Biological Chemistry*, vol. 291, no. 17, pp. 9322–9329, 2016.

[29] K. Birsoy, T. Wang, W. W. Chen, E. Freinkman, M. Abu-Remaileh, and D. M. Sabatini, "An essential role of the mitochondrial electron transport chain in cell proliferation is to enable aspartate synthesis," *Cell*, vol. 162, no. 3, pp. 540–551, 2015.

[30] L. B. Sullivan, D. Y. Gui, A. M. Hosios, L. N. Bush, E. Freinkman, and M. G. Vander Heiden, "Supporting aspartate biosynthesis is an essential function of respiration in proliferating cells," *Cell*, vol. 162, no. 3, pp. 552–563, 2015.

[31] P. S. Ward, J. Patel, D. R. Wise et al., "The Common Feature of Leukemia-Associated IDH1 and IDH2 Mutations Is a Neomorphic Enzyme Activity Converting α-Ketoglutarate to 2-Hydroxyglutarate," *Cancer Cell*, vol. 17, no. 3, pp. 225–234, 2010.

[32] E. R. Still and M. O. Yuneva, "Hopefully devoted to Q: targeting glutamine addiction in cancer," *British Journal of Cancer*, vol. 116, no. 11, pp. 1375–1381, 2017.

[33] A. Le, A. N. Lane, M. Hamaker et al., "Glucose-Independent Glutamine Metabolism via TCA Cycling for Proliferation and Survival in B Cells," *Cell Metabolism*, vol. 15, no. 1, pp. 110–121, 2012.

[34] R. J. DeBerardinis, A. Mancuso, E. Daikhin et al., "Beyond aerobic glycolysis: transformed cells can engage in glutamine metabolism that exceeds the requirement for protein and nucleotide synthesis," *Proceedings of the National Academy of Sciences of the United States of America*, vol. 104, no. 49, pp. 19345–19350, 2007.

[35] H. Cohen, H. Barash, I. Meivar-Levy et al., "The Wnt/β-catenin pathway determines the predisposition and efficiency of liver-to-pancreas reprogramming," *Hepatology*, vol. 68, no. 4, pp. 1589–1603, 2018.

[36] V. Cruzat, M. Macedo Rogero, K. Noel Keane, R. Curi, and P. Newsholme, "Glutamine: metabolism and immune function, supplementation and clinical translation," *Nutrients*, vol. 10, no. 11, p. 1564, 2018.

[37] E. M. Palmieri, I. Spera, A. Menga, V. Infantino, V. Iacobazzi, and A. Castegna, "Glutamine synthetase desensitizes differentiated adipocytes to proinflammatory stimuli by raising intracellular glutamine levels," *FEBS Letters*, vol. 588, no. 24, pp. 4807–4814, 2014.

[38] D. A. Chisolm and A. S. Weinmann, "Metabolites, genome organization, and cellular differentiation gene programs," *Current Opinion in Immunology*, vol. 51, pp. 62–67, 2018.

[39] R. M. Biltz, J. M. Letteri, E. D. Pellegrino, A. Palekar, and L. M. Pinkus, "Glutamine metabolism in bone," *Mineral and Electrolyte Metabolism*, vol. 9, no. 3, pp. 125–131, 1983.

[40] P. Bianco and P. G. Robey, "Skeletal stem cells," *Development*, vol. 142, no. 6, pp. 1023–1027, 2015.

[41] J. Wu, W. Zhang, Q. Ran et al., "The differentiation balance of bone marrow mesenchymal stem cells is crucial to hematopoiesis," *Stem Cells International*, vol. 2018, 13 pages, 2018.

[42] L. Xie, X. Zeng, J. Hu, and Q. Chen, "Characterization of nestin, a selective marker for bone marrow derived mesenchymal stem cells," *Stem Cells International*, vol. 2015, 9 pages, 2015.

[43] A. Nuschke, M. Rodrigues, A. W. Wells, K. Sylakowski, and A. Wells, "Mesenchymal stem cells/multipotent stromal cells (MSCs) are glycolytic and thus glucose is a limiting factor of in vitro models of MSC starvation," *Stem Cell Research & Therapy*, vol. 7, no. 1, p. 179, 2016.

[44] S. Tohyama, J. Fujita, T. Hishiki et al., "Glutamine oxidation is indispensable for survival of human pluripotent stem cells," *Cell Metabolism*, vol. 23, no. 4, pp. 663–674, 2016.

[45] N. Fillmore, A. Huqi, J. S. Jaswal et al., "Effect of fatty acids on human bone marrow mesenchymal stem cell energy metabolism and survival," *PLoS One*, vol. 10, no. 3, 2015.

[46] A. B. Borle, N. Nichols, and G. Nichols, "Metabolic studies of bone in vitro. I. Normal bone," *The Journal of Biological Chemistry*, vol. 235, no. 4, pp. 1206–1210, 1960.

[47] T. F. Dixon and H. R. Perkins, "Citric acid and bone metabolism," *The Biochemical Journal*, vol. 52, no. 2, pp. 260–265, 1952.

[48] L. C. Costello, R. B. Franklin, M. A. Reynolds, and M. Chellaiah, "The important role of osteoblasts and citrate production in bone formation: "osteoblast citration" as a new concept for an old relationship,," *The Open Bone Journal*, vol. 4, no. 1, pp. 27–34, 2012.

[49] A. Covic, M. Vervloet, Z. A. Massy et al., "Bone and mineral disorders in chronic kidney disease: implications for cardiovascular health and ageing in the general population," *The Lancet Diabetes & Endocrinology*, vol. 6, no. 4, pp. 319–331, 2018.

[50] N. Bonnet, "Bone-derived factors: a new gateway to regulate glycemia," *Calcified Tissue International*, vol. 100, no. 2, pp. 174–183, 2017.

[51] K. M. Thrailkill, J. S. Nyman, R. C. Bunn et al., "The impact of SGLT2 inhibitors, compared with insulin, on diabetic bone disease in a mouse model of type 1 diabetes," *Bone*, vol. 94, pp. 141–151, 2017.

[52] W. C. Lee, A. R. Guntur, F. Long, and C. J. Rosen, "Energy metabolism of the osteoblast: implications for osteoporosis," *Endocrine Reviews*, vol. 38, no. 3, pp. 255–266, 2017.

[53] H. Eagle, V. I. Oyama, M. F. Levy, C. E. Horton, and R. Fleischman, "The growth response of mammalian cells in tissue culture to L-glutamine and L-glutamic acid," *The Journal of Biological Chemistry*, vol. 218, no. 2, pp. 607–616, 1956.

[54] S. L. Colombo, M. Palacios-Callender, N. Frakich et al., "Molecular basis for the differential use of glucose and glutamine in cell proliferation as revealed by synchronized HeLa cells," *Proceedings of the National Academy of Sciences of the United States of America*, vol. 108, no. 52, pp. 21069–21074, 2011.

[55] E. Ahn, P. Kumar, D. Mukha, A. Tzur, and T. Shlomi, "Temporal fluxomics reveals oscillations in TCA cycle flux throughout the mammalian cell cycle," *Molecular Systems Biology*, vol. 13, no. 11, p. 953, 2017.

[56] P. Lenz, R. Pfeiffer, D. Baris et al., "Cell-cycle control in urothelial carcinoma: large-scale tissue array analysis of tumor tissue from Maine and Vermont," *Cancer Epidemiology, Biomarkers & Prevention*, vol. 21, no. 9, pp. 1555–1564, 2012.

[57] L. Yuan, X. Sheng, A. K. Willson et al., "Glutamine promotes ovarian cancer cell proliferation through the mTOR/S6 pathway," *Endocrine-Related Cancer*, vol. 22, no. 4, pp. 577–591, 2015.

[58] B. Kim, J. Li, C. Jang, and Z. Arany, "Glutamine fuels proliferation but not migration of endothelial cells," *The EMBO Journal*, vol. 36, no. 16, pp. 2321–2333, 2017.

[59] D. R. Wise, P. S. Ward, J. E. S. Shay et al., "Hypoxia promotes isocitrate dehydrogenase-dependent carboxylation of -ketoglutarate to citrate to support cell growth and viability," *Proceedings of the National Academy of Sciences of the United States of America*, vol. 108, no. 49, pp. 19611–19616, 2011.

[60] P. A. Gameiro, J. Yang, A. M. Metelo et al., "In vivo HIF-mediated reductive carboxylation is regulated by citrate levels and sensitizes VHL-deficient cells to glutamine deprivation," *Cell Metabolism*, vol. 17, no. 3, pp. 372–385, 2013.

[61] C. M. Metallo, P. A. Gameiro, E. L. Bell et al., "Reductive glutamine metabolism by IDH1 mediates lipogenesis under hypoxia," *Nature*, vol. 481, no. 7381, pp. 380–384, 2012.

[62] C. T. Chen, S. H. Hsu, and Y. H. Wei, "Mitochondrial bioenergetic function and metabolic plasticity in stem cell differentiation and cellular reprogramming," *Biochimica et Biophysica Acta*, vol. 1820, no. 5, pp. 571–576, 2012.

[63] T. M. Skerry, "The role of glutamate in the regulation of bone mass and architecture," *Journal of Musculoskeletal & Neuronal Interactions*, vol. 8, no. 2, pp. 166–173, 2008.

[64] L. Deng, H. Hong, X. Zhang et al., "Down-regulated lncRNA MEG3 promotes osteogenic differentiation of human dental follicle stem cells by epigenetically regulating Wnt pathway," *Biochemical and Biophysical Research Communications*, vol. 503, no. 3, pp. 2061–2067, 2018.

[65] Y. Chen, Y. R. Yang, X. L. Fan et al., "miR-206 inhibits osteogenic differentiation of bone marrow mesenchymal stem cells by targetting glutaminase," *Bioscience Reports*, vol. 39, no. 3, p. BSR20181108, 2019.

[66] H. Wu, Z. Wu, P. Li et al., "Bone size and quality regulation: concerted actions of mTOR in mesenchymal stromal cells and osteoclasts," *Stem Cell Reports*, vol. 8, no. 6, pp. 1600–1616, 2017.

[67] C. M. Karner and F. Long, "Wnt signaling and cellular metabolism in osteoblasts," *Cellular and Molecular Life Sciences*, vol. 74, no. 9, pp. 1649–1657, 2017.

[68] C. M. Karner, E. Esen, A. L. Okunade, B. W. Patterson, and F. Long, "Increased glutamine catabolism mediates bone anabolism in response to WNT signaling," *The Journal of Clinical Investigation*, vol. 125, no. 2, pp. 551–562, 2015.

[69] A. Csibi, S. M. Fendt, C. Li et al., "The mTORC1 pathway stimulates glutamine metabolism and cell proliferation by repressing SIRT4," *Cell*, vol. 153, no. 4, pp. 840–854, 2013.

[70] J. Carnesecchi and J. M. Vanacker, "Estrogen-related receptors and the control of bone cell fate," *Molecular and Cellular Endocrinology*, vol. 432, pp. 37–43, 2016.

[71] X. D. Chen, S. Shi, T. Xu, P. G. Robey, and M. F. Young, "Age-related osteoporosis in biglycan-deficient mice is related to defects in bone marrow stromal cells," *Journal of Bone and Mineral Research*, vol. 17, no. 2, pp. 331–340, 2002.

[72] T. Wang, H. He, S. Liu et al., "Autophagy: a promising target for age-related osteoporosis," *Current Drug Targets*, vol. 20, no. 3, pp. 354–365, 2019.

[73] T. Huang, R. Liu, X. Fu et al., "Aging reduces an ERRalpha-directed mitochondrial glutaminase expression suppressing glutamine anaplerosis and osteogenic differentiation of mesenchymal stem cells," *Stem Cells*, vol. 35, no. 2, pp. 411–424, 2017.

[74] E. Bonnelye, P. Reboul, N. Duval, M. Cardelli, and J. E. Aubin, "Estrogen receptor-related receptor α regulation by interleukin-1β in prostaglandin E2- and cAMP-dependent pathways in osteoarthritic chondrocytes," *Arthritis and Rheumatism*, vol. 63, no. 8, pp. 2374–2384, 2011.

[75] E. Bonnelye, N. Laurin, P. Jurdic, D. A. Hart, and J. E. Aubin, "Estrogen receptor-related receptor-α (ERR-α) is dysregulated in inflammatory arthritis," *Rheumatology*, vol. 47, no. 12, pp. 1785–1791, 2008.

[76] M. Gallet, S. Saïdi, E. Haÿ et al., "Repression of Osteoblast Maturation by ERRα Accounts for Bone Loss Induced by Estrogen Deficiency," *PLoS One*, vol. 8, no. 1, p. e54837, 2013.

[77] C. Luo, E. Balsa, A. Thomas et al., "ERRα Maintains Mitochondrial Oxidative Metabolism and Constitutes an Actionable Target in PGC1α-Elevated Melanomas," *Molecular Cancer Research*, vol. 15, no. 10, pp. 1366–1375, 2017.

[78] E. Bonnelye and J. E. Aubin, "An energetic orphan in an endocrine tissue: a revised perspective of the function of estrogen receptor-related receptor alpha in bone and cartilage," *Journal of Bone and Mineral Research*, vol. 28, no. 2, pp. 225–233, 2013.

[79] S. S. Sabharwal and P. T. Schumacker, "Mitochondrial ROS in cancer: initiators, amplifiers or an Achilles' heel?," *Nature Reviews. Cancer*, vol. 14, no. 11, pp. 709–721, 2014.

[80] E. Holzerova and H. Prokisch, "Mitochondria: much ado about nothing? How dangerous is reactive oxygen species production?," *The International Journal of Biochemistry & Cell Biology*, vol. 63, pp. 16–20, 2015.

[81] W. Geng, H. Shi, X. Zhang, W. Tan, Y. Cao, and R. Mei, "Substance P enhances BMSC osteogenic differentiation via autophagic activation," *Molecular Medicine Reports*, vol. 20, no. 1, pp. 664–670, 2019.

[82] N. Shyh-Chang, G. Q. Daley, and L. C. Cantley, "Stem cell metabolism in tissue development and aging," *Development*, vol. 140, no. 12, pp. 2535–2547, 2013.

[83] D. A. Callaway and J. X. Jiang, "Reactive oxygen species and oxidative stress in osteoclastogenesis, skeletal aging and bone diseases," *Journal of Bone and Mineral Metabolism*, vol. 33, no. 4, pp. 359–370, 2015.

[84] K. Singh, L. Krug, A. Basu et al., "Alpha-ketoglutarate curbs differentiation and induces cell death in mesenchymal stromal precursors with mitochondrial dysfunction," *Stem Cells*, vol. 35, no. 7, pp. 1704–1718, 2017.

[85] K. V. Tormos, E. Anso, R. B. Hamanaka et al., "Mitochondrial complex III ROS regulate adipocyte differentiation," *Cell Metabolism*, vol. 14, no. 4, pp. 537–544, 2011.

[86] W. Wang, Y. Zhang, W. Lu, and K. Liu, "Mitochondrial reactive oxygen species regulate adipocyte differentiation of mesenchymal stem cells in hematopoietic stress induced by arabinosylcytosine," *PLoS One*, vol. 10, no. 3, p. e0120629, 2015.

[87] M. E. Bernardo and W. E. Fibbe, "Mesenchymal stromal cells and hematopoietic stem cell transplantation," *Immunology Letters*, vol. 168, no. 2, pp. 215–221, 2015.

[88] M. W. Lee, S. Ryu, D. S. Kim, K. W. Sung, H. H. Koo, and K. H. Yoo, "Strategies to improve the immunosuppressive properties of human mesenchymal stem cells," *Stem Cell Research & Therapy*, vol. 6, no. 1, 2015.

[89] M. Wang, Q. Yuan, and L. Xie, "Mesenchymal stem cell-based immunomodulation: properties and clinical application," *Stem Cells International*, vol. 2018, 12 pages, 2018.

[90] E. Sasaki, T. Umeda, I. Takahashi et al., "Effect of glutamine supplementation on neutrophil function in male judoists," *Luminescence*, vol. 28, no. 4, pp. 442–449, 2013.

[91] T. Sartori, G. Galvão dos Santos, A. Nogueira-Pedro et al., "Effects of glutamine, taurine and their association on inflammatory pathway markers in macrophages," *Inflammopharmacology*, vol. 26, no. 3, pp. 829–838, 2018.

[92] F. Wasinski, M. F. Gregnani, F. H. Ornellas et al., "Lymphocyte glucose and glutamine metabolism as targets of the anti-inflammatory and immunomodulatory effects of exercise," *Mediators of Inflammation*, vol. 2014, 10 pages, 2014.

[93] D. Qian, G. Wei, C. Xu et al., "Bone marrow-derived mesenchymal stem cells (BMSCs) repair acute necrotized pancreatitis by secreting microRNA-9 to target the NF-κB1/p50 gene in rats," *Scientific Reports*, vol. 7, no. 1, p. 581, 2017.

[94] R. Ganesan and M. Rasool, "Interleukin 17 regulates SHP-2 and IL-17RA/STAT-3 dependent Cyr61, IL-23 and GM-CSF expression and RANKL mediated osteoclastogenesis by fibroblast-like synoviocytes in rheumatoid arthritis," *Molecular Immunology*, vol. 91, pp. 134–144, 2017.

[95] Y. Sun, J. Ma, D. Li et al., "Interleukin-10 inhibits interleukin-1β production and inflammasome activation of microglia in epileptic seizures," *Journal of Neuroinflammation*, vol. 16, no. 1, p. 66, 2019.

[96] D. E. Levy and C. K. Lee, "What does Stat3 do?," *The Journal of Clinical Investigation*, vol. 109, no. 9, pp. 1143–1148, 2002.

[97] G. G. Dos Santos, A. A. Hastreiter, T. Sartori, P. Borelli, and R. A. Fock, "L-Glutamine in vitro modulates some immunomodulatory properties of bone marrow mesenchymal stem cells," *Stem Cell Reviews and Reports*, vol. 13, no. 4, pp. 482–490, 2017.

[98] P. Sukho, J. W. Hesselink, N. Kops, J. Kirpensteijn, F. Verseijden, and Y. M. Bastiaansen-Jenniskens, "Human mesenchymal stromal cell sheets induce macrophages predominantly to an anti-inflammatory phenotype," *Stem Cells and Development*, vol. 27, no. 13, pp. 922–934, 2018.

[99] M. Capulli, R. Paone, and N. Rucci, "Osteoblast and osteocyte: games without frontiers," *Archives of Biochemistry and Biophysics*, vol. 561, pp. 3–12, 2014.

[100] P. M. Brown, J. D. Hutchison, and J. C. Crockett, "Absence of glutamine supplementation prevents differentiation of murine calvarial osteoblasts to a mineralizing phenotype," *Calcified Tissue International*, vol. 89, no. 6, pp. 472–482, 2011.

[101] G. Bellon, B. Chaqour, Y. Wegrowski, J. C. Monboisse, and J. P. Borel, "Glutamine increases collagen gene transcription in cultured human fibroblasts," *Biochimica et Biophysica Acta*, vol. 1268, no. 3, pp. 311–323, 1995.

[102] J. Masson, M. Darmon, A. Conjard et al., "Mice lacking brain/kidney phosphate-activated glutaminase have impaired glutamatergic synaptic transmission, altered breathing, disorganized goal-directed behavior and die shortly after birth," *The Journal of Neuroscience*, vol. 26, no. 17, pp. 4660–4671, 2006.

[103] J. Melrose, C. Shu, J. M. Whitelock, and M. S. Lord, "The cartilage extracellular matrix as a transient developmental scaffold for growth plate maturation," *Matrix Biology*, vol. 52-54, pp. 363–383, 2016.

[104] C. J. Handley, G. Speight, K. M. Leyden, and D. A. Lowther, "Extracellular matrix metabolism by chondrocytes 7. Evidence that L-glutamine is an essential amino acid for chondrocytes and other connective tissue cells," *Biochimica et Biophysica Acta*, vol. 627, no. 3, pp. 324–331, 1980.

[105] R. Rajpurohit, C. J. Koch, Z. Tao, C. M. Teixeira, and I. M. Shapiro, "Adaptation of chondrocytes to low oxygen tension: relationship between hypoxia and cellular metabolism," *Journal of Cellular Physiology*, vol. 168, no. 2, pp. 424–432, 1996.

[106] C. Maes, E. Araldi, K. Haigh et al., "VEGF-independent cell-autonomous functions of HIF-1α regulating oxygen consumption in fetal cartilage are critical for chondrocyte survival," *Journal of Bone and Mineral Research*, vol. 27, no. 3, pp. 596–609, 2012.

[107] J. Yu, F. Liang, H. Huang, P. Pirttiniemi, and D. Yu, "Effects of loading on chondrocyte hypoxia, HIF-1α and VEGF in the mandibular condylar cartilage of young rats," *Orthodontics & Craniofacial Research*, vol. 21, no. 1, pp. 41–47, 2018.

[108] S. Stegen, K. Laperre, G. Eelen et al., "HIF-1α metabolically controls collagen synthesis and modification in chondrocytes," *Nature*, vol. 565, no. 7740, pp. 511–515, 2019.

[109] J. N. Gouze, K. Bordji, S. Gulberti et al., "Interleukin-1β down-regulates the expression of glucuronosyltransferase I, a key enzyme priming glycosaminoglycan biosynthesis: Influence of glucosamine on interleukin-1β–mediated effects in rat chondrocytes," *Arthritis and Rheumatism*, vol. 44, no. 2, pp. 351–360, 2001.

[110] R. Issa, M. Boeving, M. Kinter, and T. M. Griffin, "Effect of biomechanical stress on endogenous antioxidant networks in bovine articular cartilage," *Journal of Orthopaedic Research*, vol. 36, no. 2, pp. 760–769, 2018.

[111] H. Tonomura, K. A. Takahashi, O. Mazda et al., "Glutamine protects articular chondrocytes from heat stress and NO-induced apoptosis with HSP70 expression," *Osteoarthritis and Cartilage*, vol. 14, no. 6, pp. 545–553, 2006.

[112] J. H. Kim, K. Kim, I. Kim, S. Seong, K. B. Lee, and N. Kim, "BCAP promotes osteoclast differentiation through regulation of the p38-dependent CREB signaling pathway," *Bone*, vol. 107, pp. 188–195, 2018.

[113] Y. Indo, S. Takeshita, K. A. Ishii et al., "Metabolic regulation of osteoclast differentiation and function," *Journal of Bone and Mineral Research*, vol. 28, no. 11, pp. 2392–2399, 2013.

[114] N. Utsunomiya-Tate, H. Endou, and Y. Kanai, "Cloning and functional characterization of a system ASC-like Na+-dependent neutral amino acid transporter," *The Journal of Biological Chemistry*, vol. 271, no. 25, pp. 14883–14890, 1996.

[115] P. Nicklin, P. Bergman, B. Zhang et al., "Bidirectional transport of amino acids regulates mTOR and autophagy," *Cell*, vol. 136, no. 3, pp. 521–534, 2009.

[116] G. Cooney, R. Curi, A. Mitchelson, P. Newsholme, M. Simpson, and E. A. Newsholme, "Activities of some key enzymes of carbohydrate, ketone body, adenosine and glutamine metabolism in liver, and brown and white adipose tissues of the rat," *Biochemical and Biophysical Research Communications*, vol. 138, no. 2, pp. 687–692, 1986.

[117] R. J. DeBerardinis, J. J. Lum, G. Hatzivassiliou, and C. B. Thompson, "The biology of cancer: metabolic reprogramming fuels cell growth and proliferation," *Cell Metabolism*, vol. 7, no. 1, pp. 11–20, 2008.

[118] H. Soh, M. Wasa, and M. Fukuzawa, "Hypoxia upregulates amino acid transport in a human neuroblastoma cell line," *Journal of Pediatric Surgery*, vol. 42, no. 4, pp. 608–612, 2007.

[119] K. J. Morten, L. Badder, and H. J. Knowles, "Differential regulation of HIF-mediated pathways increases mitochondrial metabolism and ATP production in hypoxic osteoclasts," *The Journal of Pathology*, vol. 229, no. 5, pp. 755–764, 2013.

[120] T. M. Griffin, K. M. Humphries, M. Kinter, H. Y. Lim, and L. I. Szweda, "Nutrient sensing and utilization: getting to the heart of metabolic flexibility," *Biochimie*, vol. 124, pp. 74–83, 2016.

[121] Q. Zhou, M. L. Verne, J. Z. Fields et al., "Randomised placebo-controlled trial of dietary glutamine supplements for postinfectious irritable bowel syndrome," *Gut*, vol. 68, no. 6, pp. 996–1002, 2018.

[122] J. Benjamin, G. Makharia, V. Ahuja et al., "Glutamine and whey protein improve intestinal permeability and morphology in patients with Crohn's disease: a randomized controlled trial," *Digestive Diseases and Sciences*, vol. 57, no. 4, pp. 1000–1012, 2012.

[123] T. A. Byrne, D. W. Wilmore, K. Iyer et al., "Growth hormone, glutamine, and an optimal diet reduces parenteral nutrition in patients with short bowel syndrome: a prospective, randomized, placebo-controlled, double-blind clinical trial," *Annals of Surgery*, vol. 242, no. 5, pp. 655–661, 2005.

[124] G. H. Wu, Z. H. Wu, and Z. G. Wu, "Effects of bowel rehabilitation and combined trophic therapy on intestinal adaptation in short bowel patients," *World Journal of Gastroenterology*, vol. 9, no. 11, pp. 2601–2604, 2003.

[125] M. Guo, Y. Li, and J. Li, "Effect of growth hormone, glutamine, and enteral nutrition on intestinal adaptation in

patients with short bowel syndrome," *The Turkish Journal of Gastroenterology*, vol. 24, no. 6, pp. 463–468, 2013.

[126] X. Liu, X. F. Sun, and Q. X. Ge, "The role of glutamine supplemented total parenteral nutrition (TPN) in severe acute pancreatitis," *European Review for Medical and Pharmacological Science*, vol. 20, no. 19, pp. 4176–4180, 2016.

[127] A. C. de Beaux, M. G. O'Riordain, J. A. Ross, L. Jodozi, D. C. Carter, and K. C. H. Fearon, "Glutamine-supplemented total parenteral nutrition reduces blood mononuclear cell interleukin-8 release in severe acute pancreatitis," *Nutrition*, vol. 14, no. 3, pp. 261–265, 1998.

[128] A. Masini, C. Efrati, M. Merli et al., "Effect of blood ammonia elevation following oral glutamine load on the psychometric performance of cirrhotic patients," *Metabolic Brain Disease*, vol. 18, no. 1, pp. 27–35, 2003.

[129] Y. Niihara, S. T. Miller, J. Kanter et al., "A Phase 3 Trial of l-Glutamine in Sickle Cell Disease," *The New England Journal of Medicine*, vol. 379, no. 3, pp. 226–235, 2018.

[130] D. W. Wilmore, "Food and Drug Administration approval of glutamine for sickle cell disease: success and precautions in glutamine research," *Journal of Parenteral and Enteral Nutrition*, vol. 41, no. 6, pp. 912–917, 2017.

[131] C. Wu, T. S. Kato, R. Ji et al., "Supplementation ofl-Alanyl-l-Glutamine and Fish Oil Improves Body Composition and Quality of Life in Patients With Chronic Heart Failure," *Circulation. Heart Failure*, vol. 8, no. 6, pp. 1077–1087, 2015.

[132] E. Mok, C. E. D. Violante, C. Daubrosse et al., "Oral glutamine and amino acid supplementation inhibit whole-body protein degradation in children with Duchenne muscular dystrophy," *The American Journal of Clinical Nutrition*, vol. 83, no. 4, pp. 823–828, 2006.

[133] G. Letellier, E. Mok, C. Alberti et al., "Effect of glutamine on glucose metabolism in children with Duchenne muscular dystrophy," *Clinical Nutrition*, vol. 32, no. 3, pp. 386–390, 2013.

[134] I. Jordan, M. Balaguer, M. E. Esteban et al., "Glutamine effects on heat shock protein 70 and interleukines 6 and 10: randomized trial of glutamine supplementation versus standard parenteral nutrition in critically ill children," *Clinical Nutrition*, vol. 35, no. 1, pp. 34–40, 2016.

[135] G. M. Koksal, E. Erbabacan, Y. Tunali, G. Karaoren, S. Vehid, and H. Oz, "The effects of intravenous, enteral and combined administration of glutamine on malnutrition in sepsis: a randomized clinical trial," *Asia Pacific Journal of Clinical Nutrition*, vol. 23, no. 1, pp. 34–40, 2014.

[136] J. M. Lacey, J. B. Crouch, K. Benfell et al., "The effects of glutamine-supplemented parenteral nutrition in premature infants," *Journal of Parenteral and Enteral Nutrition*, vol. 20, no. 1, pp. 74–80, 1996.

[137] R. A. Ehrenkranz, A. Das, L. A. Wrage et al., "Early nutrition mediates the influence of severity of illness on extremely LBW infants," *Pediatric Research*, vol. 69, no. 6, pp. 522–529, 2011.

[138] M. P. S. Dunphy, J. J. Harding, S. Venneti et al., "In Vivo PET Assay of Tumor Glutamine Flux and Metabolism: In-Human Trial of18F-(2S,4R)-4-Fluoroglutamine," *Radiology*, vol. 287, no. 2, pp. 667–675, 2018.

[139] K. Eda, K. Uzer, T. Murat, and U. Cenk, "The effects of enteral glutamine on radiotherapy induced dermatitis in breast cancer," *Clinical Nutrition*, vol. 35, no. 2, pp. 436–439, 2016.

[140] E. Kucuktulu, A. Guner, I. Kahraman, M. Topbas, and U. Kucuktulu, "The protective effects of glutamine on radiation-induced diarrhea," *Supportive Care in Cancer*, vol. 21, no. 4, pp. 1071–1075, 2013.

[141] T. A. K. A. E. TSUJIMOTO, Y. YAMAMOTO, M. WASA et al., "L-glutamine decreases the severity of mucositis induced by chemoradiotherapy in patients with locally advanced head and neck cancer: A double-blind, randomized, placebo-controlled trial," *Oncology Reports*, vol. 33, no. 1, pp. 33–39, 2015.

[142] Y. Tanaka, T. Takahashi, K. Yamaguchi, S. Osada, T. Shimokawa, and K. Yoshida, "Elemental diet plus glutamine for the prevention of mucositis in esophageal cancer patients receiving chemotherapy: a feasibility study," *Supportive Care in Cancer*, vol. 24, no. 2, pp. 933–941, 2016.

[143] S. C. Chang, Y. C. Lai, J. C. Hung, and C. Y. Chang, "Oral glutamine supplements reduce concurrent chemoradiotherapy-induced esophagitis in patients with advanced non-small cell lung cancer," *Medicine (Baltimore)*, vol. 98, no. 8, p. e14463, 2019.

[144] S. Sands, E. J. Ladas, K. M. Kelly et al., "Glutamine for the treatment of vincristine-induced neuropathy in children and adolescents with cancer," *Supportive Care in Cancer*, vol. 25, no. 3, pp. 701–708, 2017.

[145] N. Piccirillo, S. de Matteis, L. Laurenti et al., "Glutamine-enriched parenteral nutrition after autologous peripheral blood stem cell transplantation: effects on immune reconstitution and mucositis," *Haematologica*, vol. 88, no. 2, pp. 192–200, 2003.

[146] R. Pytlik, E. Gregora, P. Benes, and T. Kozak, "Effect of parenteral glutamine on restoration of lymphocyte subpopulations after high-dose chemotherapy and autologous hematopoietic cell transplantation: data from a double-blind randomized study," *Epidemiologie, Mikrobiologie, Imunologie*, vol. 51, no. 4, pp. 152–155, 2002.

[147] M. A. P. Barros, P. R. L. Vasconcelos, C. M. Souza et al., "L-Alanyl-glutamine attenuates oxidative stress in liver transplantation patients," *Transplantation Proceedings*, vol. 47, no. 8, pp. 2478–2482, 2015.

[148] M. N. Hissa, R. C. . Vasconcelos, S. B. Guimarães, R. P. Silva, J. H. P. Garcia, and P. R. L. . Vasconcelos, "Preoperative glutamine infusion improves glycemia in heart surgery patients," *Acta Cirurgica Brasileira*, vol. 26, Suppl 1, pp. 77–81, 2011.

[149] M. Chávez-Tostado, F. Carrillo-Llamas, P. E. Martínez-Gutiérrez et al., "Oral glutamine reduces myocardial damage after coronary revascularization under cardiopulmonary bypass. A randomized clinical trial," *Nutrición Hospitalaria*, vol. 34, no. 2, pp. 277–283, 2017.

[150] K. Nishizaki, H. Ikegami, Y. Tanaka, R. Imai, and H. Matsumura, "Effects of supplementation with a combination of β-hydroxy-β-methyl butyrate, L-arginine, and L-glutamine on postoperative recovery of quadriceps muscle strength after total knee arthroplasty," *Asia Pacific Journal of Clinical Nutrition*, vol. 24, no. 3, pp. 412–420, 2015.

[151] J. A. Eisman, E. R. Bogoch, R. Dell et al., "Making the first fracture the last fracture: ASBMR task force report on secondary fracture prevention," *Journal of Bone and Mineral Research*, vol. 27, no. 10, pp. 2039–2046, 2012.

[152] O. Polat, S. S. Kilicoglu, and E. Erdemli, "A controlled trial of glutamine effects on bone healing," *Advances in Therapy*, vol. 24, no. 1, pp. 154–160, 2007.

[153] E. TOMASZEWSKA, P. DOBROWOLSKI, Ł. PROST, M. HUŁAS-STASIAK, S. MUSZYŃSKI, and T. BLICHARSKI, "The effect of supplementation of a glutamine precursor on the growth plate, articular cartilage and cancellous bone in fundectomy-induced osteopenic bone," *The Journal of Veterinary Medical Science*, vol. 78, no. 4, pp. 563–571, 2016.

[154] P. Dobrowolski, E. Tomaszewska, S. Muszynski, T. Blicharski, and S. G. Pierzynowski, "Dietary 2-oxoglutarate prevents bone loss caused by neonatal treatment with maximal dexamethasone dose," *Experimental Biology and Medicine*, vol. 242, no. 7, pp. 671–682, 2017.

[155] A. C. Thomas, T. Hubbard-Turner, E. A. Wikstrom, and R. M. Palmieri-Smith, "Epidemiology of posttraumatic osteoarthritis," *Journal of Athletic Training*, vol. 52, no. 6, pp. 491–496, 2017.

[156] S. Fujita, Y. Arai, S. Nakagawa et al., "Combined microwave irradiation and intraarticular glutamine administration-induced HSP70 expression therapy prevents cartilage degradation in a rat osteoarthritis model," *Journal of Orthopaedic Research*, vol. 30, no. 3, pp. 401–407, 2012.

[157] D. Mehrabani, M. Babazadeh, N. Tanideh et al., "The healing effect of adipose-derived mesenchymal stem cells in full-thickness femoral articular cartilage defects of rabbit," *International Journal of Organ Transplantation Medicine*, vol. 6, no. 4, pp. 165–175, 2015.

[158] B. W. Carey, L. W. S. Finley, J. R. Cross, C. D. Allis, and C. B. Thompson, "Intracellular α-ketoglutarate maintains the pluripotency of embryonic stem cells," *Nature*, vol. 518, no. 7539, pp. 413–416, 2015.

Hindawi
Stem Cells International
Volume 2019, Article ID 2376172, 15 pages
https://doi.org/10.1155/2019/2376172

Review Article

Interaction between Mesenchymal Stem Cells and Intervertebral Disc Microenvironment: From Cell Therapy to Tissue Engineering

Gianluca Vadalà, Luca Ambrosio, Fabrizio Russo, Rocco Papalia, and Vincenzo Denaro

Department of Orthopaedic and Trauma Surgery, Campus Bio-Medico University of Rome, Via Alvaro del Portillo 200, 00128 Rome, Italy

Correspondence should be addressed to Luca Ambrosio; luc.ambros@gmail.com

Received 4 May 2019; Revised 20 July 2019; Accepted 19 August 2019; Published 10 September 2019

Guest Editor: Yong-Can Huang

Low back pain (LBP) in one of the most disabling symptoms affecting nearly 80% of the population worldwide. Its primary cause seems to be intervertebral disc degeneration (IDD): a chronic and progressive process characterized by loss of viable cells and extracellular matrix (ECM) breakdown within the intervertebral disc (IVD) especially in its inner region, the nucleus pulposus (NP). Over the last decades, innovative biological treatments have been investigated in order to restore the original healthy IVD environment and achieve disc regeneration. Mesenchymal stem cells (MSCs) have been widely exploited in regenerative medicine for their capacity to be easily harvested and be able to differentiate along the osteogenic, chondrogenic, and adipogenic lineages and to secrete a wide range of trophic factors that promote tissue homeostasis along with immunomodulation and anti-inflammation. Several *in vitro* and preclinical studies have demonstrated that MSCs are able to acquire a NP cell-like phenotype and to synthesize structural components of the ECM as well as trophic and anti-inflammatory mediators that may support resident cell activity. However, due to its unique anatomical location and function, the IVD presents distinctive features: avascularity, hypoxia, low glucose concentration, low pH, hyperosmolarity, and mechanical loading. Such conditions establish a hostile microenvironment for both resident and exogenously administered cells, which limited the efficacy of intradiscal cell therapy in diverse investigations. This review is aimed at describing the characteristics of the healthy and degenerated IVD microenvironment and how such features influence both resident cells and MSC viability and biological activity. Furthermore, we focused on how recent research has tried to overcome the obstacles coming from the IVD microenvironment by developing innovative cell therapies and functionalized bioscaffolds.

1. Introduction

Low back pain (LBP) is one of the most common musculoskeletal symptoms; it is estimated that up to 84% of adults will experience LBP at least once in their life, while more than 25% report to have suffered from an episode of LBP in the previous three months [1]. The peak prevalence of LBP occurs between 45 and 64 of age and is slightly more frequent in women, who usually complain of a higher rate of recurrence [2]. In addition, LBP is a major cause of disability and loss of working capacity worldwide [3], resulting in an enormous socioeconomic burden that significantly impacts on patients' quality of life as well as on healthcare expenditure. Indeed, it has been estimated that LBP is the second most common cause of loss of productive time among adult workers, especially if female, older than 60 years of age, and exposed to hostile and unsafe working conditions [4].

Although being triggered by several different causes, LBP is mainly provoked by intervertebral disc degeneration (IDD) [5]. The intervertebral disc (IVD) is a complex structure located between the vertebrae which provides the spine with bending capacity and shock-absorbing properties while helping in distributing mechanical loads across vertebral segments [6]. With the onset of IDD, the IVD especially its inner portion, namely, the nucleus pulposus

(NP), undergoes a progressive dehydration due to proteolytic cleavage of aggrecan together with a substantial reduction of resident cell viability [7]. This ultimately impairs IVD biomechanical properties subsequently leading to structural alterations and development of discogenic LBP, as well as more severe sequelae, including disc herniation, spinal instability, and stenosis with serious neurological consequences [8]. To date, there is no treatment—neither conservative nor surgical—able to arrest or at least slow down the degenerative process. For this reason, several efforts are being made in order to develop innovative approaches to repair or ideally regenerate IVD original morphofunctional features.

One of the most appealing and promising strategies is disc regeneration through the supplementation of the degenerated IVD with exogenous mesenchymal stem cells (MSCs) [9, 10]. MSCs are multipotent adult stem cells provided with the capacity to self-renew and to differentiate into several tissues, including bone, cartilage, muscle, and fat. In the last decades, MSCs have been widely employed in different areas of regenerative medicine with promising results, especially in the musculoskeletal field and also in IDD. A major advantage of MSC-based treatments is their high accessibility as they can be easily and safely isolated from the bone marrow and the adipose tissue [9]. MSCs are identified upon three criteria proposed by the International Society for Cellular Therapy: (1) adherence to plastic, (2) marker expression ($CD105^+$, $CD73^+$, $CD90^+$, $CD45^-$, $CD34^-$, $CD14^-$ or $CD11b^-$, $CD79a^-$ or $CD19^-$, and HLA-DR^-), and (3) the capacity to differentiate along the chondrogenic, osteogenic, and adipogenic lineages [11]. The underlying concept is to induce the differentiation of MSCs towards a NP cell phenotype and/or to stimulate resident NP cells *via* released growth factors. This may increase the synthesis of extracellular matrix (ECM) main components, so as to regenerate the IVD [12, 13]. In the last 20 years, several preclinical and clinical studies have been conducted to confirm such proof of concept. Despite the incredible heterogeneity among these investigations (different animal models, cell sources and number, injection routes, and association with biomaterials), overall results showed a substantial improvement of LBP and IVD structure, even if no *restitutio ad integrum* was ever documented [12]. In addition, several studies demonstrated that injected MSCs rapidly become undetectable due to premature death soon after implantation [14, 15], while studies associating MSCs with bioscaffolds resulted in higher cell viability and improved differentiation, possibly by providing exogenous MSCs with a proper microenvironment [16, 17]. This has generated the hypothesis that the hostile environment of the degenerated IVD may critically impact on MSC survival, metabolism, and differentiation thus limiting or even abolishing their regenerative effect [18]. In order to tackle such limitations, innovative tissue engineering approaches have been investigated so as to mimic the original IVD healthy microenvironment by combining cell therapy, bioscaffolds, and soluble factors.

This review is aimed at describing the characteristics of the IVD microenvironment in both physiological and degenerative conditions and how they affect both endogenous and exogenous cell viabilities, functionalities, and phenotypes. Furthermore, this paper will discuss how recent research efforts have developed innovative cell therapies and biomaterials to overcome such harsh asperities and to encourage disc regeneration.

2. The Intervertebral Disc in Physiological Conditions

The IVD consists of three specialized tissues: the cartilaginous end plate (CEP), connecting the disc with the adjacent vertebral bodies, the annulus fibrosus (AF) and the NP [19].

The CEP is about 0.6 mm thick in humans and resembles hyaline articular cartilage in structure [20]. It is fundamental for the nourishment of the AF and NP; indeed, nutrients to the IVD pass through the bone marrow cavities of the vertebral bodies and then to the capillaries branching through the CEP, so that they can diffuse to the inner AF and NP which are definitely avascular [21].

The AF constitutes the external part of the IVD and surrounds the NP. It is composed of 15-25 concentric lamellae mainly made of type I collagen fibers directed radially and perpendicularly [22] with an interlamellar matrix containing noncollagenous proteins (*e.g.*, elastin), proteoglycans, and fibroblast-like cells [23].

The NP is a gelatinous tissue mainly constituted by type II collagen and proteoglycans, especially aggrecan, which establishes a high level of hydration and swelling pressure due to the large number of sulfated glycosaminoglycans (GAGs) present in the ECM, providing the NP with its unique biomechanical properties [24]. Additional proteoglycans contained in the NP include versican, decorin, biglycan, and fibromodulin, as well as significant amounts of elastin, laminin, and fibronectin [25]. Within the NP, chondrocyte-like round cells, also known as nucleopulpocytes (NPCy) [12], can be found; such cells are characterized by specific markers, including hypoxia-inducible factor (HIF) 1α, glypican 3 (GPC3), keratin (KRT) 8, 18, and 19, paired box 1 and forkhead box 1, Noto, Brachyury, and glioma-associated oncogene (Gli) 1 and 3 [26, 27]. In the immature and young IVD, the NP also contains large vacuolated cells that are referred as notochordal cells, whose number gradually decreases with advancing age [28]. Considering the ratio between the cell number and the disc volume, the IVD is considered to be relatively acellular. Indeed, it presents an average cell density of 5.8×10^3 cells/mm^3 (with the NP containing 4×10^3 cells/mm^3 and the AF with 9×10^3 cells/mm^3); however, such values progressively decline with aging [29]. In the healthy IVD, cell anabolism and proliferation are orchestrated by numerous growth factors that are normally present in the disc. These include members of the transforming growth factor β (TGF-β) superfamily, insulin-like growth factor 1 (IGF-1), epidermal growth factor (EGF), connective tissue growth factor (CTGF), bone morphogenetic protein- (BMP-) 2, osteogenic protein-1 (OP-1), and growth and differentiation factor- (GDF-) 5 and 6 [30]. Several *in vitro* and *in vivo* studies have showed the capacity of such factors to enhance cell

proliferation, proteoglycan, and collagen synthesis while reducing the production of metalloproteinases and proinflammatory cytokines [30].

Recent studies have demonstrated the existence of a population of progenitor stem cells within the IVD. These cells have been isolated from the NP, AF, CEP, and niches located in the perichondrium outside of the epiphyseal plate [12]. Such cells exhibited plastic adherence capacity, multilineage differentiation *in vitro*, and expression of a characteristic surface marker pattern ($CD73^+$ $CD90^+$ $CD105^+$ $CD11b^-$ $CD14^-$ $CD19^-$ $CD34^-$ $CD79^-$ $HLADR^-$) and thus can be classified as NP-MSCs [31]. However, compared to bone marrow-derived MSCs (BM-MSCs), NP progenitor cells isolated from degenerated IVDs showed a reduced or even defective adipogenic differentiation [32]. In addition, NP-MSCs exhibited increased viability and proliferative capacity under hypoxic and acidic conditions compared to AD-MSCs *in vitro* [33, 34]. Furthermore, a specific subpopulation of clones derived from IVD progenitors expressing the tyrosine protein kinase receptor TIE2 and the disialoganglioside GD2 was recognized for its superior capacity to proliferate, form spheroid colonies, synthesize ECM components, self-renew, and differentiate into diverse lineages, both *in vitro* and *in vivo* [35]. More specifically, $TIE2^+$ $GD2^-$ cells are considered to be dormant precursors of $TIE2^+$ $GD2^+$ cells; this switch denotes the activation of NP progenitor cells and the irreversible and unidirectional differentiative process characterized by the loss of TIE2 and GD2 and the expression of CD24, eventually leading to the acquisition of the mature NP cell phenotype [31]. In this context, angiopoietin-1 (ANG-1), a ligand of the TIE2 receptor, has been shown to stimulate the formation of NP progenitor cell colonies *in vitro*. This molecule may thus be a key regulating factor in the IVD stem cell niche [35].

Due to its unique anatomical location and function, the IVD displays intrinsic physicochemical features that collectively establish a harsh microenvironment for both resident cells and transplanted exogenous cells, whose viability and functionality may thus be significantly blunted [36]. Indeed, the IVD presents with an avascular, nutrient-deficient, hypoxic, acidic, hyperosmolar, and mechanically solicited environment [37]. Such conditions even worsen with the onset and progression of IDD [38]. Main IVD microenvironment characteristics are summarized in Table 1.

3. Intervertebral Disc Degeneration: A Great Challenge for Cell Survival

The pathophysiology of IDD is complex and still not completely understood. Major contributors include aging [38], smoking [52], mechanical overload [53], obesity [54], and diabetes [55]. The structural hallmark of IDD is the progressive dehydration of the NP mainly due to the gradual loss of proteoglycans within the ECM [19, 56]. The principal proteolytic enzymes involved include the matrix metalloproteinases (MMPs) and a disintegrin and metalloproteinase with thrombospondin motifs (ADAMTS) [57] which are upregulated together with proinflammatory cytokines, including tumor necrosis factor α (TNF-α), interleukin- (IL-) 6, IL-1, IL-17, and interferon γ (IFN-γ) [51], while anabolic factors, such as IGF-1 [58] and TGF-β [59], appear to be downregulated. Tissue inflammation [51], increased oxidative stress [60], mechanical overload [61], and the prevalence of catabolic events notably impact on NPCy viability by boosting cell senescence [62] and apoptosis [55, 63].

Cell senescence is defined as the irreversible arrest of the cell cycle with loss of proliferative capacity, reduced anabolic activity, and aberrant production of metalloproteinases, proinflammatory cytokines, and chemokines [64]. During IDD, cell senescence is triggered by several stimuli, including oxidative stress, acidity, nutrient depletion, mechanical overloading, and tissue inflammation [65]. These lead to DNA damage and the activation of the p53-p21-Rb, p38-p16-Rb, and Wnt/β-catenin pathways, which ultimately cause the acquisition of the senescent phenotype [66]. As IDD progresses, the number of senescence-associated β galactosidase- (SA-β-Gal-) positive cells increases and positively correlates with the Thompson and Pfirrmann degeneration grade of degenerated IVDs [64].

The reduced number of functional cells progressively results in the incapacity of NPCy to counteract degenerative changes by producing an adequate amount of ECM to maintain IVD structural integrity [67]. Furthermore, the enhanced secretion of proinflammatory and catabolic factors by senescent cells may favour the senescence of neighbouring healthy cells thus precipitating a sort of degenerative domino effect. The strong relationships among IDD, cell senescence, and inflammation have been recently described as "inflammaging," a process with distinctive biological and proteomic features typical of aging and degenerating IVDs [68].

Eventually, NP dehydration leads to a decrease of disc height and shock-absorbing properties of the NP itself, thus causing circumferential forces to be transmitted to the AF which eventually result in the formation of cracks and fissures, providing a basis for the development of discogenic LBP, disc herniations, and segmental instability [69].

3.1. Avascularity and Nutrient Deficiency. As stated above, the nourishment of IVD tissues strictly depends on the diffusion of nutrients from the capillaries running through the CEP [21]. Therefore, the IVD itself is inherently avascular. The diffusion process may be further hampered because of end plate calcification and subsequent capillary obliteration, which is common in IDD due to IVD aging and mechanical overstress [39]. The lack of blood flow consequently establishes a hypoxic microenvironment with higher O_2 concentrations at the AF surface (19.5%) that then drop towards the center of the NP (0.65%), where cell survival is fully maintained even when oxygen tension falls below 5% [40]. Resulting oxygen concentration is determined by the balance among O_2 transportation across the CEP, cell density, and metabolism [70]. As a consequence of avascularity, IVD tissue are exposed to low glucose concentrations that vary from approximately 5 mM at the periphery to circa 0.8 mM in the center of the IVD [42]. To maintain their viability, IVD cells adjust their metabolic requirements to the hypoxic low glucose environment by mainly relying on anaerobic glycolysis, which allows generating energy while consuming less O_2 and producing less reactive oxygen species (ROS) [71].

Table 1: Main IVD microenvironment features under physiological and degenerative conditions.

	Healthy IVD	IDD
Avascularity	Vessels from the vertebral bodies branch into capillaries terminating in the CEP [21]	CEP calcification may hinder nutrient diffusion [39]
Hypoxia	Oxygen concentration decreases from AF surfaces (19.5%) to the inner portion of the NP (0.65%) [40]	Oxygen concentration falls due to reduced blood supply and shift of NP cell metabolism towards oxidative phosphorylation [41]
Low glucose concentration	Glucose concentration is higher at IVD boundaries while it falls towards the center of the NP [42]	Glucose levels diminish together with blood supply and increased consumption by degenerative cells [43]
Acidity	Due to anaerobic glycolysis and lactic acid production, average pH is 7.0-7.2 [38]	pH may decrease to 6.5 in mild IDD and 5.6 in severe IDD due to nutrient depletion and increase lactic acid production [38]
Hyperosmolarity	The high GAG content within the NP determines a high osmolarity which varies upon mechanical load (430-500 mOsm/L) [44]	The loss of proteoglycans due to matrix breakdown reduces IVD osmolarity [45]
Mechanical loading	Mechanical stimuli (flexion, torsion, shear, and compression) regulate IVD cell activity and metabolism within a physiological range (0.1-2.5 MPa) [46, 47]	Disruption of IVD structure alters loading transmission across the IVD and the vertebral segments, resulting in tissue damage and cellular overstress [48]
Inflammation	Proinflammatory cytokines and chemokines may have a role in IVD development and recruitment of local progenitor cells [49, 50]	The excess of proinflammatory cytokines increases cell apoptosis, senescence, autophagy, matrix breakdown, and discogenic LBP [51]

CEP = cartilaginous end plate; AF = annulus fibrosus; NP = nucleus pulposus; IVD = intervertebral disc; IDD = intervertebral disc degeneration; GAG = glycosaminoglycan; LBP = low back pain.

Such degree of adaptation has been confirmed by the fact that NPCy are able to survive in hypoxic conditions by HIF-1 and -2 expression, which positively regulate cell proliferation, energy metabolism, type 2 collagen production, oxidative stress, and cell autophagy and apoptosis. These mechanisms may hold a fundamental role in the adaptation of NPCy to even lower levels of oxygen and nutrients as it occurs during IDD [72]. Similarly, BM-MSCs and adipose-derived stem cells (ADSCs) have been demonstrated to increase cell viability and synthesis of ECM components in hypoxic (1-5% O_2) and low glucose conditions *in vitro* [36, 73]. BM-MSCs have shown a greater development of colony-forming units (CFU) [74], a decrease of osteogenic differentiation [75], and an attenuation of the inhibitory effect of IL-1β towards chondrogenic differentiation when exposed to a hypoxic environment [76]. Moreover, hypoxia has demonstrated to inhibit MSC senescence and to maintain cell stemness through stimulation of telomerase activity via the HIF1α-Twist-mediated downregulation of the E2A-p21 pathway [77]. Collectively, these adaptive strategies may favour MSC survival in the hostile IVD microenvironment after implantation. However, it has been shown that the prolonged exposure to severe hypoxia (oxygen tension < 1%) together with serum deprivation eventually resulted in complete cell death [78].

MSC viability and differentiation into a NPCy-like phenotype may be further enhanced by the supplementation of growth factors, namely, TGF-β, IGF-1, growth differentiation factor- (GDF-) 5, GDF-6, platelet-derived growth factor (PDGF), and basic fibroblast-like growth factor (bFGF). Such molecules are normally expressed by IVD resident cells, but as cell density decreases, nutrient diffusion hinders and ECM becomes disrupted; their anabolic effect gets almost completely blunted. For this reason, preexposing MSCs *in vitro* to such growth factors before implantation or embedding them in MSC-loaded bioscaffolds could maintain their biological activity and boost cell proliferation, differentiation, and synthetic potential [37]. Several *in vitro* and preclinical studies have been conducted in this regard [79–83].

3.2. Acidity. Due to the extensive recourse to anaerobic glycolysis by disc cells, lactic acid is produced and accumulated within IVD tissues (average concentration between 2 mM and 6 mM), whose average pH is slightly acidic (7.0-7.2) in physiological conditions. However, in mild degenerative conditions, the pH may drop to 6.5 and even to 5.6 in severely degenerated IVDs, with a significant effect on NP cell viability and ECM composition resulting in a reduction of collagen and proteoglycan synthesis [38]. pH variations are recognized by IVD cells through acid-sensing ion channels (ASICs), which regulate Ca^{2+} transmembrane influx upon fluctuations of extracellular H^+ levels. Moreover, ASIC expression by both NPCy and AF cells is upregulated in IDD, thus suggesting the crucial role of these channels [84]. Human IVD cells express all ASIC isoforms (ASIC-1, ASIC-2, ASIC-3, and ASIC-4); ASIC-1a activation has been shown to increase Ca^{2+} cellular influx eventually resulting in apoptosis of CEP chondrocytes [85], while ASIC-3 has been involved in NPCy survival under acidic and hyperosmolar conditions *via* the nerve growth factor (NGF)/p75/extracellular signal-related kinases (ERK) pathway [86]. However, NGF is also renowned for its role in IDD as it promotes nerve ingrowth within the injured IVD and hence favours the development of discogenic LBP [87]. Based upon these observations, it has been questioned whether the survival of disc cells within the acidic environment may be enhanced by inhibiting ASIC1a and/or stimulating ASIC3, although the increased expression of the latter in dorsal root ganglions has been associated with

enhanced radicular pain [88]. Gilbert et al. elegantly showed that, when exposed to a pH of 6.8 *in vitro*, human NPCy viability remained high while proliferation stopped. At lower pH values, cells began to die and secrete significant amounts of proinflammatory cytokines (IL-1β and IL-6) and neurotrophic pain-related factors, including NGF and brain-derived neurotrophic factor (BDNF). Highly acidic culture conditions also resulted in a decrease of aggrecan content together with an upregulation of MMP-3, ADAMTS-4, and ASIC-3, while ASIC-1 and ASIC-2 levels remained unchanged. Interestingly, when ASIC-3 was selectively inhibited using APETx2, the increase of cytokines and neurotrophic factors was prevented, even if no positive effect was reported on cell viability nor on ECM breakdown in acidic conditions. However, this study pointed out again the importance of ASIC-3 in triggering the pH-dependent inflammatory and neurogenic response of NPCy [89].

Differently from IVD cells, MSC biosynthetic activity is largely impaired when exposed to acidic pH *in vitro*. A study from Wuertz et al. showed that rat BM-MSCs underwent a significant decrease of cell viability and proliferation together with the inhibition of aggrecan, type 1 collagen, and tissue inhibitor of metalloproteinases- (TIMP-) 3 even when exposed to a pH corresponding to a mild degenerative condition (6.8) [90]. More recently, Liu and colleagues reported that, with decreasing pH (from 7.4 to 6.2), human NP-MSCs displayed a reduction of cell proliferation, an increase of apoptosis, and a diminished gene expression of type 1 collagen, type II collagen, aggrecan, and SOX-9, as well as of stemness-related genes (Oct4, Nanog, Jagged, and Notch1) *in vitro*. Contrariwise, as pH decreased, ASIC-1, ASIC-2, ASIC-3, and ASIC-4 expression gradually increased. Blocking ASIC activity by using amiloride resulted in a significant improvement of cell viability and a normalization of ECM and stem cell-related gene expression, thus suggesting the importance of ASICs in the negative regulation of IVD cell metabolism within the acidic degenerative disc environment [91]. Similar results were previously documented by Han et al., who compared the effect of the acidic environment on AD-MSCs and NP-MSCs eventually reporting that the latter were less sensitive to the inhibitory and catabolic consequences of low pH, thus being more promising as candidates for IVD regeneration [34].

3.3. Hyperosmolarity. Due to the large amount of negatively charged GAG side chains of aggrecan molecules, the IVD and especially the NP are characterized by a high osmolarity, which is responsible for the notable imbibition and swelling pressure of the NP in physiological conditions. However, NP osmolarity (and thus water content) is not fixed but cyclically varies upon applied mechanical load; indeed, it diminishes by 20-25% during diurnal activities while it is restored at rest, with values ranging between 430 and 500 mOsm/L *in vivo* [44]. Due to the progressive loss of proteoglycans with IDD, IVD osmolarity declines as the degenerative process goes on [45].

NPCy are able to sense changes of osmolarity by regulating the expression of tonicity enhancer-binding protein (TonEBP), which is activated in hypertonic conditions and binds to the tonicity-responsive enhancer element (TonE) motif, eventually resulting in the upregulation of downstream genes, namely, heat shock protein 70, betaine/γ-aminobutyric acid transporter, sodium myo-inositol transporter, taurine transporter, and aquaporin-2, which are fundamental to control intracellular osmotic stress [92, 93]. However, hyperosmolarity was not found to induce autophagy in NPCy as it occurs with other cell types [94]. Moreover, TonEBP activation may positively regulate the production of ECM components by directly increasing the expression of both aggrecan and galactose-β1,3-glucuronosyltransferase-I (GlcAT-I), which is a key enzyme for the synthesis of GAG side chains [95]. Notwithstanding, a recent *in vitro* study showed that although hyperosmolarity upregulated ECM gene expression, no notable increase was noted at the protein level [96]. TonEBP is also involved in the upregulation of proinflammatory cytokines under hypertonic stress, including C-C motif chemokine ligand (CCL), nitric oxide synthase 2 (NOS-2), IL-6, and TNFα [97].

An excessive hypertonic stress has been documented to induce DNA damage and subsequent arrest of the cell cycle in bovine NPCy, though cells exhibited the capacity to repair DNA after the genotoxic insult [98]. An interesting study conducted by Li and colleagues using a whole organ-cultured porcine IVD model assessed the effect of hypoosmolarity (330 mOsm/L), isoosmolarity (430 mOsm/L), hyperosmolarity (550 mOsm/L), and cyclic osmolarity (430 mOsm/L for 8 h and then 550 mOsm/L for 16 h) on NPCy viability and ECM synthesis. They found that hypo- and hyperosmolarity significantly increased NPCy apoptosis compared to isoosmolarity and cyclic osmolarity; the process was even more pronounced after the inhibition of ERK 1/2, which may physiologically protect NPCy against osmotic stress-induced apoptosis [99]. Similarly, expression and protein synthesis of SOX9, aggrecan, and type 2 collagen as well as GAG content were notably higher in isoosmolarity and cyclic osmolarity cultures [100].

Mizuno et al. investigated the effect of different combinations of hydrostatic and osmotic pressures on bovine NPCy *in vitro* and demonstrated that the association of a cyclic hydrostatic stress (0.5 MPa, 0.5 Hz) with a high osmolarity (450 mOsm/L) mimicking daily spinal stress resulted in an upregulation of aggrecan, type II collagen, and other anabolic markers [101].

Differently from mature NPCy, notochordal cells can better adapt to fluctuations in osmolarity. In case of a hypotonic stress, notochordal cells have shown to release a low osmotic solution from intracellular vacuoles so as to dilute the cytoplasm and maintain an osmotic equilibrium across the membrane thus preventing excessive cell swelling and death [102]. Conversely, hyperosmolarity has demonstrated to induce notochordal cell differentiation towards a mature NP cell phenotype characterized by upregulation of aquaporin-3 and downregulation of N-cadherin [103].

Less is known about the effect of hyperosmolarity on MSCs. A previous study has shown that hypertonic culture conditions reduced BM-MSC proliferation, anabolic marker expression, and chondrogenic differentiation [73]; similarly, AD-MSC viability and proliferation together with aggrecan and type 1 collagen expression were abated [36]. In a recent

study, Li et al. showed that exposing NP-MSCs to osmotic pressures mimicking the healthy IVD environment (430-500 mOsm/L) resulted in a decrease of cell proliferation and chondrogenic differentiation *via* activation of the ERK pathway, while the relative hypoosmotic condition of mild IDD proved to increase NP-MSC proliferation and chondrogenic potential. Based on this study, a degenerative microenvironment, due to lower osmotic pressures, may be less hostile to NP-MSCs, providing an interesting insight for future regenerative strategies [104].

3.4. Mechanical Loading. IVDs, especially in the cervical and lumbar regions, are naturally exposed to complex biomechanical stimuli, including flexion, torsion, shear, and compression. Diverse load intensity, duration, frequency, and direction profoundly influence IVD cell activity and ECM dynamic composition [46]. Normally, intradiscal pressure (L4-L5) is approximately 0.1-0.24 MPa in supine position and may increase up to 2.0 MPa when carrying a 20 kg weight with the flexed back [47]. It has been previously shown that, at physiological pressures, MMP-3 production is reduced while TIMP-1 synthesis is increased, thus exerting a net anabolic effect on the ECM. Conversely, as intradiscal pressure drops during IDD due to NP dehydration, the MMP-3/TIMP-1 ratio is inverted and catabolic events predominate. In addition, IVD cells harvested from degenerated discs seem to exhibit a less anabolic response at a physiological intradiscal pressure [46]. When exposed to increasing mechanical loads, NPCy get overstressed due to mitochondrial damage and excessive ROS production. Under a certain threshold, NPCy can counteract such stress by activating autophagy and removing damaged mitochondria so as to reduce the generation of ROS [105]. However, with prolonged loading, NPCy irreversibly undergo apoptosis through caspase-dependent mitochondrial pathways. In addition, a specific form of programmed cell death with necrosis-like features, namely, necroptosis, seems to be involved in the compression-induced death of NPCy [106].

The effect of different loading modalities on IVD cells has been extensively investigated by several studies. In most investigations, static compressive loading has been associated with increased cell death and matrix catabolism due to diminished expression of collagen and aggrecan while metalloproteases were produced in higher amounts. Conversely, dynamic compressive loading has been described to often elicit an anabolic response and to enhance transportation of nutrients and especially high molecular weight molecules, such as growth factors (IGF-1, TGF-β, FGF, and PDGF), within the NP [48]. The type, degree, and duration of metabolic responses of IVD cells to loading strictly depend upon experimental design, cell source, age of donor, and culturing conditions and have been reviewed elsewhere [46, 48].

Similarly to IVD cells, cyclic mechanical loading has been shown to stimulate ECM production and chondrogenic differentiation of BM-MSCs [26] and NP-MSCs [37] *in vitro*. A study from Gan et al. demonstrated that the anabolic response of BM-MSCs to low-magnitude compression was triggered by the activation of the mechanotransducer transient receptor potential vanilloid 4 (TRPV-4) on the cell surface [107]. While mechanical loading may be a convenient resource to predifferentiate MSCs in view of a subsequent cell therapy, it could be speculated that the enhanced chondrogenic commitment of NP progenitors upon prolonged mechanical stimulation may contribute to the exhaustion of the resident stem cell compartment during IDD. This has been also demonstrated by previous studies showing an increased NP-like differentiation upon dynamic loading of AD-MSCs [108] and the acquisition of an AF-like phenotype by BM-MSCs when exposed to radial compressive stimulation [109]. Differently from dynamic loading, static prolonged loading (1 MPa, >24 h) significantly diminished NP-MSC viability, migration, differentiation, CFU formation, and stemness-related gene expression, suggesting that biomechanical overload might be a cause of endogenous repair failure for IVD regeneration [110]. However, in a coculture experiment involving AD-MSCs and NPCy undergoing high prolonged loading (3 MPa for 48 h), the presence of AD-MSCs resulted in a reduction on NPCy apoptosis *via* the inhibition of activated caspase-9 and 3 as well as in an upregulation of ECM genes with diminished expression of metalloproteinases and proinflammatory cytokines (IL-1β, IL-6, and TNF-α) [111].

3.5. Inflammation. IDD is thought to be sustained in part by the abnormal secretion of proinflammatory cytokines by AF cells, NPCy as well as by T cells, neutrophils, and macrophages located within the IVD. A wide array of inflammatory mediators is involved in the process, including interleukins (IL-1, IL-2, IL-4, IL-6, IL-8, IL-10, and IL-17), TNF-α, IFN-γ, chemokines, and prostaglandin E_2 (PGE_2). These molecules are able to induce cell apoptosis, senescence, and autophagy, to favour the development of discogenic LBP and to upregulate the synthesis of MMPs (-1, -3, -7, -9, and -13) and ADAMTS (-1, -4, -5, -9, and -15) by NPCy, thus leading to ECM breakdown [51].

IL-1β is considered a key molecule in the IDD-driven inflammatory response. Indeed, IL-1β expression is positively associated with the severity of IDD and promotes ECM catabolism both by upregulating proteolytic enzymes and inhibiting aggrecan expression and synthesis [112]. In addition, it has been shown that IL-1β can reduce aggrecan and SOX9 expression by rat NP-MSCs and improve their neurogenic potential, which may eventually result in IVD neoinnervation and generation of LBP [49]. However, it has been noted that IL-1β is expressed even in healthy IVDs since birth, thence possibly presenting an unknown physiological function. Interestingly, a recent study from Gorth et al. reported that, compared to controls, IL-1α/β knockout mice unexpectedly showed bone morphology alterations and higher degrees of IDD mainly involving the AF, while NP structure remained mostly unaffected [50].

Together with IL-1β, TNF-α holds a fundamental role in IVD inflammation as the two cytokines are present at high levels in degenerated and herniated disc as well as in the epidural space [51]. Furthermore, TNF-α is able to amplify the inflammatory response by stimulating IVD cells to synthesize additional cytokines, including IL-6, IL-8, IL-17, IL-1β,

and substance P (SP), and numerous chemokines. Among the latter, CCL-5 has been shown to attract eosinophils and macrophages towards the inflamed IVD and to correlate with both discogenic LBP and the severity of IDD [113].

A previous study has reported that MSCs are able to secrete anti-inflammatory mediators (IL-1 receptor antagonist, IL-10, IL-13, and tumor necrosis factor-inducible gene 6 protein), anticatabolic factors (TIMPs), and growth factors (TGF-β, GDF-5) when cultured in IDD-like conditions, thus exerting an immunomodulatory effect on surrounding cells [114]. In a recent study, Teixeira and colleagues evaluated the biological responses of human BM-MSCs using an *ex vivo* bovine model of IDD (needle puncture with IL-1β supplementation). While not presenting a tangible effect on ECM production, BM-MSCs showed an increased production of IL-6, IL-8, PGE_2, and monocyte chemoattractant protein 1 (MCP-1) and a downregulation of the expression of IL-6, IL-8, and TNF-α by bovine IVD cells [79]. Moreover, MSC migration to inflamed IVD tissues was enhanced probably due to the presence of IL-1β, which has renowned chemoattractant properties towards MSCs [115]. Indeed, many of the proinflammatory mediators that have been previously cited exhibit chemotactic features which may be crucial in the recruitment of MSCs (both endogenous and exogenous) into the degenerating IVD by resident NP cells [106]. On the other hand, MSCs have been described to secrete cytokines and factors that support NP cell viability and functionality under stress. For example, TGF-β and IGF-1 have shown to inhibit NP cell senescence [116], while IGF-1 and bone morphogenetic protein 7 protected NPCy against apoptosis [91] and together with TGF-β reduced ECM degradation and inflammation [117].

4. Intervertebral Disc Regeneration: The Need to Learn from the Disc Microenvironment

As IDD is mainly sustained by progressive NPCy depletion, several research efforts have been conducted to develop biological treatments that may replenish the NP with active and functional cells. In the last decades, numerous attempts to regenerate the IVD by introducing viable stem cells into the degenerating disc have been made, using different cell sources, animal models, injection routes, and bioengineered scaffolds [12, 118]. Among the diverse cell utilized in the studies within the field, MSCs have been widely adopted for their prompt availability (as they can be easily and safely harvested from the bone marrow and the adipose tissue) and the capacity to differentiate along the chondrogenic pathway [9]. In addition, MSCs acquire a NPCy-like phenotype when exposed to specific growth factors *in vitro* [119] and have been shown to increase ECM production and even to improve radiographically assessed disc height and IVD hydration at T2-weighed magnetic resonance imaging (MRI) in different preclinical studies [31, 120]. The rationale behind intradiscal cell therapy is to increase NP cellularity due to the differentiation of MSCs into functional NPCy and to support residual NPCy activity through the secretion of growth factors, anti-inflammatory cytokines, and anticatabolic mediators, thus eventually resulting in ECM restoration and regeneration of the IVD [106]. Furthermore, the recent individuation of endogenous IVD stem/progenitor cells has raised the possibility that this mechanism may naturally occur during IDD upon release of specific cues by resident IVD cells that could recruit local progenitors from stem cell niches to regenerate the tissues. However, as IDD advances, both progenitor cell number and ability to migrate (and hence their intrinsic regenerative capacity) decline because of the hostility of the degenerating IVD microenvironment [106]. The lack of a full regenerative response and, in some studies, the absence of significant changes compared to the controls, apart from methodological issues, have been imputed to the unlikely capacity of transplanted cells to survive in the degenerating IVD harsh microenvironment, which is profoundly different from stem cell niches [37]. While hypoxia [76] and mechanical loading [26] have been described to enhance MSC differentiation, proliferation, and anabolism, acidic pH [90, 91] and hyperosmolarity [73] drastically impair cell viability and phenotype (Figure 1).

In addition, the cell response to the degenerating microenvironment may significantly vary when comparing NP-MSCs, BM-MSCs, and ADSCs (Table 2). Among the three cell types, NP-MSCs tend to exhibit a higher chondrogenic differentiation capacity, considering that MSCs isolated from a specific tissue are more prone to acquire the residing cell phenotype [121]. However, the role of NP-MSCs in IDD cell therapy may be significantly limited by the low number of available cells, by the reduced regenerative potential due to the degree of IDD at the time of cell harvest and by the need of an invasive approach to the IVD for NP-MSC retrieval [33]. Conversely, BM-MSCs have been demonstrated to be promptly available, easy, and safe to harvest and able to maintain a significantly high viability and CFU capacity even in adverse conditions. This cell type is the most extensively investigated with regard to IVD regeneration and thus constitute the most convenient source for intradiscal cell therapy at the present time [9]. ADSCs have also shown to hold potential for regenerating the IVD. Even with a lower ability to differentiate along the chondrogenic line and a reduced capacity to tolerate the acidic and hyperosmolar microenvironment compared to NP- and BM-MSCs, the use of ADSCs may be favoured by their high proliferation rate and the little donor site morbidity [36].

In the last years, the growing body of preclinical research has confirmed the safety, feasibility, and efficacy of MSC-based intradiscal cell therapy, thus funding the basis for clinical application. Orozco et al. conducted a pilot study on 10 patients affected by LBP unresponsive to conservative treatment. Patients were injected with autologous expanded BM-MSCs into the NP area; pain and disability (measured with the Visual Analogue Scale (VAS) and Oswestry Disability Index (ODI), respectively) were significantly reduced at 3, 6, and 12 after injection. In addition, although disc height was not restored, MRI demonstrated a significant elevation of NP water content at 12 months [122]. Similar results were described by Pettine et al., who reported that 8 of 20 treated patients showed a reduction of one modified Pfirrmann

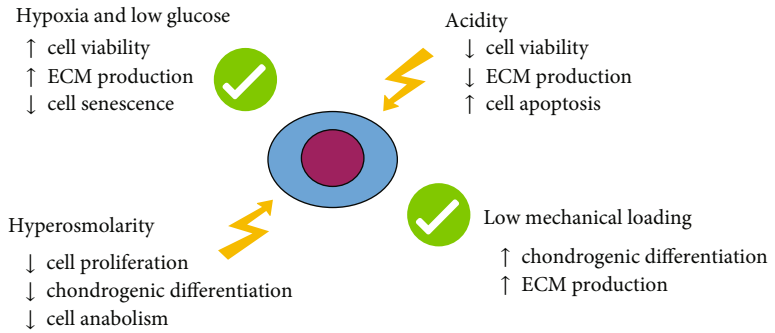

Figure 1: Schematic representation of the major effect of the IVD microenvironment on MSCs based upon actual evidences. ECM = extracellular matrix.

Table 2: Different responses of NPCy, NP-MSCs, BM-MSCs, and ADSCs to the degenerative microenvironment.

	NPCy	NP-MSCs	BM-MSCs	ADSCs
Hypoxia and low glucose concentration	NPCy survive by relying on anaerobic glycolysis [71]. Low O_2 concentration increases the expression of HIF-1 and 2, which upregulate cell proliferation and matrix production [72].	Low O_2 concentration is associated with a higher viability and proliferative capacity of NP-MSCs compared to ADSCs [33, 34].	Hypoxia increases BM-MSCs CFU, reduces cell senescence and maintains cell stemness [74–77].	Low glucose slightly increases cell apoptosis and inhibits cell proliferation while enhancing aggrecan production [36, 73].
Acidity	NPCy survival at low pH is mediated by ASICs [84–86], even if critically acidic pH has been associated with decreased cell viability and upregulation of metalloproteinases and proinflammatory cytokines [87–89].	Low pH leads to reduced cell proliferation, enhanced apoptosis, and diminished expression of stemness-related and ECM genes [91]. However, overall performance was better than BM-MSCs and ADSCs [34].	Acidic pH significantly decreases cell proliferation, aggrecan, and type I collagen production [90].	Low pH promoted cell necrosis, reduced the proliferation rate, and diminished aggrecan production, while increasing type I collagen synthesis [36].
Hyperosmolarity	NPCy respond to hyperosmolarity through TonEBP activation [92, 93], which increases ECM gene expression [96]. However, excessive hyperosmolarity results in upregulation of proinflammatory cytokines and cell apoptosis [97–100].	Hyperosmolarity has been demonstrated to induce progenitor cell differentiation towards a mature NP phenotype [104].	Hypertonic conditions reduced BM-MSC proliferation, anabolism, and chondrogenic differentiation [73].	IVD-like hyperosmolarity significantly reduced ADSC viability and proliferative capacity and abated aggrecan and type I collagen synthesis [36].
Mechanical loading	Physiological loadings promote cell anabolism while abnormal mechanical stimuli cause ECM breakdown and reduced cell viability [46, 105].	Cyclic mechanical loading favours the differentiation of NP-MSCs towards mature NPCy [37], while static prolonged loading diminished cell viability, migration, differentiation, and stemness [110].	Cyclic mechanical loading enhances BM-MSC chondrogenic differentiation and cell anabolism [26].	ADCs may protect NPCy from apoptosis and promote the synthesis of ECM genes under prolonged loading [111].
Inflammation	Proinflammatory cytokines induce NPCy apoptosis, senescence, and autophagy and upregulate the synthesis of metalloproteinases, thus resulting in ECM breakdown [51, 112].	IL-1β may reduce aggrecan and SOX expression by NP-MSCs while improving their neurogenic differentiation, which may have a role in IVD neoinnervation [49].	BM-MSCs may support resident cells by secreting anti-inflammatory cytokines, anticatabolic, and growth factors [79, 114].	Under inflammatory conditions, ADSCs have been shown to increase proliferation, proinflammatory cytokine production, and osteogenic differentiation [125].

NPCy = nucleopulpocytes; NP-MSCs = nucleus pulposus-derived mesenchymal stem cells; BM-MSCs = bone marrow-derived mesenchymal stem cells; ADSCs = adipose tissue-derived mesenchymal stem cells; HIF = hypoxia-inducible factor; CFU = colony-forming units; ASIC = acid-sensing ion channels; ECM = extracellular matrix; TonEBP = tonicity enhancer-binding protein; NP = nucleus pulposus; IVD = intervertebral disc; IL = interleukin.

grade at 12 months. Furthermore, improvement of pain and disability was faster in patient receiving a higher dose of BM-MSCs but reduced in patients >40 years of age, suggesting that MSC regenerative capacity may depend on both cell concentration and patients' characteristics [123]. The study by Centeno et al. was conducted on 33 patients affected by LBP and radiculopathy and injected with autologous BM-MSCs. The follow-up period was extended until 6 years; pain was significantly reduced at 3, 36, 48, 60, and 72 months after injection, as well as reported functionality (functional rating index, FRI), which was improved at each time point excluding 12 months. In addition, 17 patients showed a reduction of the disc herniation volume (average reduction of 23% in size) [124]. The first, small randomized controlled trial has been conducted by Noriega et al., who randomized 24 patients with degenerative LBP treated with either sham infiltration or allogeneic BM-MSCs from healthy donors.

40% of the patients in the experimental group showed a rapid improvement of pain and functionality as well as Pfirrmann grading, which instead worsened in the control group [126].

The only clinical evidence of an intradiscal therapy involving ADSCs has been provided by Kumar et al., who performed a phase I clinical trial on 10 patients affected by chronic LBP. Patients were injected with a combination of hyaluronic acid (HA) and ADSCs and followed up to 1 year. 60% of individuals displayed a significant improvement of pain, disability, and quality of life, with 3 patients additionally showing increased water content as demonstrated by MRI [127].

Overall, intradiscal cell therapy has demonstrated to be safe in all previous reports; no major adverse events were observed, while minor event basically consisted in local pain treated with analgesics [128].

Another strategy that is being widely investigated in the field is tissue engineering, whose principal aim is to mimic the natural IVD microenvironment through the combination of biomaterials, soluble factors, and functional cells so as to reproduce IVD original biological and biomechanical properties. Regarding IDD, three main bioengineering approaches have been developed: repair of the AF, NP regeneration or replacement, and NP/AF combined repair [25].

AF fissures and tears usually occur with IDD due to higher tensile and compressive stresses transmitted to the AF as a consequence of NP dehydration and loss of disc height. At the latest stages, AF disruption may lead to NP displacement thus causing IVD herniation [129]. In this regard, a strategy to repair the AF may result in the restoration of IVD function and prevention of reherniation. Different suturing devices and polymeric meshes have been employed to close the annular defect; such approaches have demonstrated to be efficacious and safe in numerous *in vitro* studies [130] and in some clinical applications, although the complexity of the techniques and their consistent costs have limited their diffusion [25]. Alternatively, diverse biomaterials have been exploited as void fillers of the AF damage in the form of hydrogels and sponges (polylactic acid, polyglycolic acid, GAGs, poly(s-caprolactone), silk, etc.) with or without a cellular component. Indeed, BM-MSCs engrafted within a poly(trimethylene carbonate) scaffold and covered by a poly(ester-urethane) membrane were tested in a bovine organ culture annulotomy model. After 14 days under dynamic load, disc height was restored and no reherniation occurred. Moreover, MSCs displayed an increased expression of anabolic genes and markers of the AF phenotype [131].

Tissue engineering attempts to regenerate the NP ideally aimed at reproducing the nucleus functions so as to restore disc height and spinal biomechanics. Hydrating synthetic polymers were firstly investigated for their potential ability to mimic the water retention capacity of GAGs lost during IDD thus leading to increased IVD height and pressure. However, the *in vivo* application of such materials often resulted in excessive swelling with consequent development of segmental stiffness, end plate fractures, and device failure [25]. A similar strategy that is gaining growing interest is the design of synthetic polymers that undergo a transition from an easily injectable form to a gel-like form when exposed to particular pH levels or when combined with cross-linking molecules [132]. Biomaterials that have been tested in this field include HA, GAG-containing scaffolds, and collagen. Again, this approach mainly focuses on biomechanical goals and the integration and interaction of the implants with resident cells have been neglected in most studies [25]. The most appealing solution to regenerate the NP at the present time seems to be the design of proper scaffolds that could provide transplanted MSCs with an adequate three-dimensional microenvironment. The ideal scaffold should be biocompatible and easy to manipulate, while biomechanically stable and respectful to cell morphology and functionality [133]. To date, various biomaterials including HA, collagen, fibrin, alginate, gelatin, and silk have been investigated as scaffolds for cell engraftment and IVD regeneration [12]. Although there is no definitive evidence for preferring a carrier than another, hydrogels are being more thoroughly evaluated due to the high-water content (90-95%) similar to the healthy NP ECM and their easy handling and tunability. Hydrogels are composed of natural or synthetic macromolecules that can be assembled to be either "mechanically competent" or "biologically competent" [134]. The former are constituted by highly cross-linked molecular networks that are able to increase disc height and withstand biomechanical stimuli, while not allowing for an adequate matrix hydration and cell encapsulation. On the other hand, "biologically competent" hydrogels present a less cross-linking degree which permits embedded cells to proliferate, differentiate, and produce ECM components whereas they lack adequate biomechanical characteristics [135]. Major drawbacks of these biomaterials have recently been overcome by the development of double network hydrogels, which combine a highly cross-linked network (providing the scaffold with mechanical competence) with a less dense network that may consent cell survival and matrix deposition, and thus hold a promising role in IVD regeneration [136]. Recent studies have reported that the macromolecules employed to build hydrogels for IVD regeneration may modulate the harsh degenerative microenvironment by naturally presenting anti-inflammatory properties or by being combined with other active molecules. Indeed, Teixeira et al. have showed that the injection of chitosan/diclofenac/γ-polyglycolic acid nanoparticles was able to reduce the production of IL-6, IL-

8, and PGE_2 in an organ model of IDD [137]. HA is a high molecular weight-nonsulfated GAG which is normally expressed within the healthy IVD matrix. Such molecule is fundamental in multiple biological processes, including cell migration, survival, apoptosis, and morphogenesis as well as tumorigenesis and tissue inflammation [138]. For these reasons, HA is being widely investigated as a bioscaffold in IVD regeneration in various formulations. A recent *in vivo* study demonstrated that the intradiscal injection of HA in a rat model of IDD resulted in a strong analgesic effect with the reduction of hyperalgesia, allodynia, and sensory hyperinnervation, while decreasing the expression of IL-1β and IL-6 and the deposition of fibrous tissue within the ECM [139].

In addition, biomaterials can be further implemented with biological cues that may boost differentiation and anabolism of the cells embedded in the scaffold. For example, the combination of TGF-β with a MSC-embedded polymerized fibrin scaffold implanted in a rat model demonstrated to inhibit MSC apoptosis and led to an increased disc height when compared to the scaffold alone [16]. Similarly, in another study, BM-MSCs were cultured with collagen microcarriers functionalized with either TGF-β or bFGF; while the former was significantly upregulated MSC chondrogenic differentiation and production of aggrecan, collagen, and proteoglycan, bFGF notably increased cell proliferation [140].

An additional innovative solution involves the use of self-assembling peptides that are able to form stable nanofiber hydrogels which can be further enriched with specific motifs that have been shown to improve cell migration, adhesion, proliferation, and differentiation [141].

5. Conclusions

The IVD is a complex organ with unique physicochemical characteristics; the absence of vasculature, hypoxia, low glucose concentration, acidity, hyperosmolarity, and continuous mechanical stimulation contribute to establish a hostile microenvironment for cell survival and endogenous tissue repair. With the progression of IDD, such asperities become harsher and are further worsened by the local inflammatory response, eventually leading to excessive resident cell death, ECM breakdown, and loss of IVD original features. Intradiscal cell therapy has raised the possibility to regenerate the IVD by restoring the functional cell compartment and reversing the degenerative changes of IDD. However, the design of an efficacious and long-lasting therapeutical approach must carefully consider the deleterious effects of the IVD microenvironment on implanted cells. In this regard, more efforts are needed to better identify the most suitable cell source and an adequate scaffold that may provide an immediate mechanical support while allowing for cell nourishment, proliferation, differentiation, and synthesis of anti-inflammatory and trophic factors. As our understanding of IDD is still limited, it is essential to conduct further studies to better comprehend how the IVD microenvironment orchestrates local biology and how it impacts on exogenously delivered cells when far from their original niche.

Conflicts of Interest

The authors declare that there is no conflict of interest regarding the publication of this paper.

Acknowledgments

The financial support by the Research Grant of INAIL and the Italian National Institute for Insurance against Accidents at Work (BRiC-2018 ID3) is gratefully acknowledged.

References

[1] B. F. Walker, "The prevalence of low back pain: a systematic review of the literature from 1966 to 1998," *Journal of Spinal Disorders*, vol. 13, no. 3, pp. 205–217, 2000.

[2] D. Hoy, C. Bain, G. Williams et al., "A systematic review of the global prevalence of low back pain," *Arthritis and Rheumatism*, vol. 64, no. 6, pp. 2028–2037, 2012.

[3] W. F. Stewart, J. A. Ricci, E. Chee, D. Morganstein, and R. Lipton, "Lost productive time and cost due to common pain conditions in the US workforce," *Journal of the American Medical Association*, vol. 290, no. 18, pp. 2443–2454, 2003.

[4] B. I. Martin, R. A. Deyo, S. K. Mirza et al., "Expenditures and health status among adults with back and neck problems," *Journal of the American Medical Association*, vol. 299, no. 6, pp. 656–664, 2008.

[5] G. Fontana, E. See, and A. Pandit, "Current trends in biologics delivery to restore intervertebral disc anabolism," *Advanced Drug Delivery Reviews*, vol. 84, pp. 146–158, 2015.

[6] J. Takatalo, J. Karppinen, J. Niinimäki et al., "Does lumbar disc degeneration on magnetic resonance imaging associate with low back symptom severity in young Finnish adults?," *Spine*, vol. 36, no. 25, pp. 2180–2189, 2011.

[7] J. A. Buckwalter, "Aging and degeneration of the human intervertebral disc," *Spine*, vol. 20, no. 11, pp. 1307–1314, 1995.

[8] S. Roberts, H. Evans, J. Trivedi, and J. Menage, "Histology and pathology of the human intervertebral disc," *The Journal of Bone and Joint Surgery. American Volume*, vol. 88, Supplement 2, pp. 10–14, 2006.

[9] G. Vadalà, F. Russo, L. Ambrosio, M. Loppini, and V. Denaro, "Stem cells sources for intervertebral disc regeneration," *World Journal of Stem Cells*, vol. 8, no. 5, pp. 185–201, 2016.

[10] M. Loibl, K. Wuertz-Kozak, G. Vadalà, S. Lang, J. Fairbank, and J. P. Urban, "Controversies in regenerative medicine: should intervertebral disc degeneration be treated with mesenchymal stem cells?," *JOR Spine*, vol. 2, no. 1, article e1043, 2019.

[11] M. Ruiz, S. Cosenza, M. Maumus, C. Jorgensen, and D. Noel, "Therapeutic application of mesenchymal stem cells in osteoarthritis," *Expert Opinion on Biological Therapy*, vol. 16, no. 1, pp. 33–42, 2016.

[12] J. Clouet, M. Fusellier, A. Camus, C. Le Visage, and J. Guicheux, "Intervertebral disc regeneration: from cell therapy to the development of novel bioinspired endogenous repair strategies," *Advanced Drug Delivery Reviews*, 2018.

[13] G. Vadala, F. Russo, L. Ambrosio, R. Papalia, and V. Denaro, "Mesenchymal stem cells for intervertebral disc regeneration," *Journal of Biological Regulators and Homeostatic Agents*, vol. 30, 4, Supplement 1, pp. 173–179, 2016.

[14] G. Vadala, G. Sowa, M. Hubert, L. G. Gilbertson, V. Denaro, and J. D. Kang, "Mesenchymal stem cells injection in

degenerated intervertebral disc: cell leakage may induce osteophyte formation," *Journal of Tissue Engineering and Regenerative Medicine*, vol. 6, no. 5, pp. 348–355, 2012.

[15] F. L. Acosta Jr., L. Metz, H. D. Adkisson IV et al., "Porcine intervertebral disc repair using allogeneic juvenile articular chondrocytes or mesenchymal stem cells," *Tissue Engineering. Part A*, vol. 17, no. 23-24, pp. 3045–3055, 2011.

[16] H. Yang, J. Wu, J. Liu et al., "Transplanted mesenchymal stem cells with pure fibrinous gelatin-transforming growth factor-beta1 decrease rabbit intervertebral disc degeneration," *The Spine Journal*, vol. 10, no. 9, pp. 802–810, 2010.

[17] D. Sakai, J. Mochida, T. Iwashina et al., "Regenerative effects of transplanting mesenchymal stem cells embedded in atelocollagen to the degenerated intervertebral disc," *Biomaterials*, vol. 27, no. 3, pp. 335–345, 2006.

[18] S. M. Naqvi and C. T. Buckley, "Extracellular matrix production by nucleus pulposus and bone marrow stem cells in response to altered oxygen and glucose microenvironments," *Journal of Anatomy*, vol. 227, no. 6, pp. 757–766, 2015.

[19] G. Vadala, F. Russo, A. Di Martino, and V. Denaro, "Intervertebral disc regeneration: from the degenerative cascade to molecular therapy and tissue engineering," *Journal of Tissue Engineering and Regenerative Medicine*, vol. 9, no. 6, pp. 679–690, 2015.

[20] S. Roberts, J. Menage, and J. P. Urban, "Biochemical and structural properties of the cartilage end-plate and its relation to the intervertebral disc," *Spine*, vol. 14, no. 2, pp. 166–174, 1989.

[21] T. Grunhagen, A. Shirazi-Adl, J. C. T. Fairbank, and J. P. G. Urban, "Intervertebral disk nutrition: a review of factors influencing concentrations of nutrients and metabolites," *The Orthopedic Clinics of North America*, vol. 42, no. 4, pp. 465–477, 2011.

[22] J. J. Cassidy, A. Hiltner, and E. Baer, "Hierarchical structure of the intervertebral disc," *Connective Tissue Research*, vol. 23, no. 1, pp. 75–88, 2009.

[23] S. B. Bruehlmann, J. B. Rattner, J. R. Matyas, and N. A. Duncan, "Regional variations in the cellular matrix of the annulus fibrosus of the intervertebral disc," *Journal of Anatomy*, vol. 201, no. 2, pp. 159–171, 2002.

[24] J. P. Urban and J. F. McMullin, "Swelling pressure of the intervertebral disc: influence of proteoglycan and collagen contents," *Biorheology*, vol. 22, no. 2, pp. 145–157, 1985.

[25] R. D. Bowles and L. A. Setton, "Biomaterials for intervertebral disc regeneration and repair," *Biomaterials*, vol. 129, pp. 54–67, 2017.

[26] Y. C. Huang, V. Y. L. Leung, W. W. Lu, and K. D. K. Luk, "The effects of microenvironment in mesenchymal stem cell-based regeneration of intervertebral disc," *The Spine Journal*, vol. 13, no. 3, pp. 352–362, 2013.

[27] K. Li, D. Kapper, B. Youngs et al., "Potential biomarkers of the mature intervertebral disc identified at the single cell level," *Journal of Anatomy*, vol. 234, no. 1, pp. 16–32, 2017.

[28] B. M. Minogue, S. M. Richardson, L. A. H. Zeef, A. J. Freemont, and J. A. Hoyland, "Transcriptional profiling of bovine intervertebral disc cells: implications for identification of normal and degenerate human intervertebral disc cell phenotypes," *Arthritis Research & Therapy*, vol. 12, no. 1, p. R22, 2010.

[29] T. Liebscher, M. Haefeli, K. Wuertz, A. G. Nerlich, and N. Boos, "Age-related variation in cell density of human lumbar intervertebral disc," *Spine*, vol. 36, no. 2, pp. 153–159, 2011.

[30] S. M. Richardson, A. J. Freemont, and J. A. Hoyland, "Pathogenesis of intervertebral disc degeneration," in *The Intervertebral Disc*, I. M. Shapiro and M. R. Risbud, Eds., pp. 177–200, Springer-Verlag, Wien, 2014.

[31] D. Sakai and G. B. Andersson, "Stem cell therapy for intervertebral disc regeneration: obstacles and solutions," *Nature Reviews Rheumatology*, vol. 11, no. 4, pp. 243–256, 2015.

[32] J. F. Blanco, I. F. Graciani, F. M. Sanchez-Guijo et al., "Isolation and characterization of mesenchymal stromal cells from human degenerated nucleus pulposus: comparison with bone marrow mesenchymal stromal cells from the same subjects," *Spine*, vol. 35, no. 26, pp. 2259–2265, 2010.

[33] X. C. Li, Y. Tang, J. H. Wu, P. S. Yang, D. L. Wang, and D. K. Ruan, "Characteristics and potentials of stem cells derived from human degenerated nucleus pulposus: potential for regeneration of the intervertebral disc," *BMC Musculoskeletal Disorders*, vol. 18, no. 1, p. 242, 2017.

[34] B. Han, H. C. Wang, H. Li et al., "Nucleus pulposus mesenchymal stem cells in acidic conditions mimicking degenerative intervertebral discs give better performance than adipose tissue-derived mesenchymal stem cells," *Cells, Tissues, Organs*, vol. 199, no. 5-6, pp. 342–352, 2015.

[35] D. Sakai, Y. Nakamura, T. Nakai et al., "Exhaustion of nucleus pulposus progenitor cells with ageing and degeneration of the intervertebral disc," *Nature Communications*, vol. 3, no. 1, article 1264, 2012.

[36] C. Liang, H. Li, Y. Tao et al., "Responses of human adipose-derived mesenchymal stem cells to chemical microenvironment of the intervertebral disc," *Journal of Translational Medicine*, vol. 10, no. 1, p. 49, 2012.

[37] F. Wang, R. Shi, F. Cai, Y. T. Wang, and X. T. Wu, "Stem cell approaches to intervertebral disc regeneration: obstacles from the disc microenvironment," *Stem Cells and Development*, vol. 24, no. 21, pp. 2479–2495, 2015.

[38] N. V. Vo, R. A. Hartman, P. R. Patil et al., "Molecular mechanisms of biological aging in intervertebral discs," *Journal of Orthopaedic Research*, vol. 34, no. 8, pp. 1289–1306, 2016.

[39] S. Rajasekaran, S. Vidyadhara, M. Subbiah et al., "ISSLS prize winner: a study of effects of in vivo mechanical forces on human lumbar discs with scoliotic disc as a biological model: results from serial postcontrast diffusion studies, histopathology and biochemical analysis of twenty-one human lumbar scoliotic discs," *Spine*, vol. 35, no. 21, pp. 1930–1943, 2010.

[40] E. M. Bartels, J. C. T. Fairbank, C. P. Winlove, and J. P. G. Urban, "Oxygen and lactate concentrations measured in vivo in the intervertebral discs of patients with scoliosis and back pain," *Spine*, vol. 23, no. 1, pp. 1–7, 1998.

[41] S. E. Cisewski, Y. Wu, B. J. Damon, B. L. Sachs, M. J. Kern, and H. Yao, "Comparison of oxygen consumption rates of nondegenerate and degenerate human intervertebral disc cells," *Spine*, vol. 43, no. 2, pp. E60–E67, 2018.

[42] É. Sélard, A. Shirazi-Adl, and J. P. G. Urban, "Finite element study of nutrient diffusion in the human intervertebral disc," *Spine*, vol. 28, no. 17, pp. 1945–1953, 2003.

[43] A. R. Jackson, C. Y. C. Huang, M. D. Brown, and W. Yong Gu, "3D finite element analysis of nutrient distributions and cell viability in the intervertebral disc: effects of deformation and degeneration," *Journal of Biomechanical Engineering*, vol. 133, no. 9, article 91006, 2011.

[44] J. P. Urban, "The role of the physicochemical environment in determining disc cell behaviour," *Biochemical Society Transactions*, vol. 30, no. 6, pp. 858–863, 2002.

[45] B. van Dijk, E. Potier, and K. Ito, "Culturing bovine nucleus pulposus explants by balancing medium osmolarity," *Tissue Engineering. Part C, Methods*, vol. 17, no. 11, pp. 1089–1096, 2011.

[46] P.-P. A. Vergroesen, I. Kingma, K. S. Emanuel et al., "Mechanics and biology in intervertebral disc degeneration: a vicious circle," *Osteoarthritis and Cartilage*, vol. 23, no. 7, pp. 1057–1070, 2015.

[47] H.–. J. Wilke, P. Neef, M. Caimi, T. Hoogland, and L. E. Claes, "New in vivo measurements of pressures in the intervertebral disc in daily life," *Spine*, vol. 24, no. 8, pp. 755–762, 1999.

[48] B. V. Fearing, P. A. Hernandez, L. A. Setton, and N. O. Chahine, "Mechanotransduction and cell biomechanics of the intervertebral disc," *JOR Spine*, vol. 1, no. 3, 2018.

[49] F. J. Lyu, K. M. Cheung, Z. Zheng, H. Wang, D. Sakai, and V. Y. Leung, "IVD progenitor cells: a new horizon for understanding disc homeostasis and repair," *Nature Reviews Rheumatology*, vol. 15, no. 2, pp. 102–112, 2019.

[50] D. J. Gorth, I. M. Shapiro, and M. V. Risbud, "A new understanding of the role of IL-1 in age-related intervertebral disc degeneration in a murine model," *Journal of Bone and Mineral Research*, vol. 34, no. 8, pp. 1531–1542, 2019.

[51] M. V. Risbud and I. M. Shapiro, "Role of cytokines in intervertebral disc degeneration: pain and disc content," *Nature Reviews Rheumatology*, vol. 10, no. 1, pp. 44–56, 2014.

[52] L. A. Nasto, K. Ngo, A. S. Leme et al., "Investigating the role of DNA damage in tobacco smoking-induced spine degeneration," *The Spine Journal*, vol. 14, no. 3, pp. 416–423, 2014.

[53] G. Vadala', F. Russo, L. Ambrosio, A. di Martino, R. Papalia, and V. Denaro, "Biotechnologies and biomaterials in spine surgery," *Journal of Biological Regulators and Homeostatic Agents*, vol. 29, Supplement 4, pp. 137–147, 2015.

[54] F. Russo, R. A. Hartman, K. M. Bell et al., "Biomechanical evaluation of transpedicular nucleotomy with intact annulus fibrosus," *Spine*, vol. 42, no. 4, pp. E193–E201, 2017.

[55] F. Russo, L. Ambrosio, K. Ngo et al., "The role of type I diabetes in intervertebral disc degeneration," *Spine*, vol. 44, no. 17, pp. 1177–1185, 2019.

[56] G. Vadalà, F. Russo, F. de Strobel et al., "Novel stepwise model of intervertebral disc degeneration with intact annulus fibrosus to test regeneration strategies," *Journal of Orthopaedic Research*, vol. 36, no. 9, pp. 2460–2468, 2018.

[57] C. L. Le Maitre, A. Pockert, D. J. Buttle, A. J. Freemont, and J. A. Hoyland, "Matrix synthesis and degradation in human intervertebral disc degeneration," *Biochemical Society Transactions*, vol. 35, Part 4, pp. 652–655, 2007.

[58] S. Okuda, A. Myoui, K. Ariga, T. Nakase, K. Yonenobu, and H. Yoshikawa, "Mechanisms of age-related decline in insulin-like growth factor-I dependent proteoglycan synthesis in rat intervertebral disc cells," *Spine*, vol. 26, no. 22, pp. 2421–2426, 2001.

[59] S. Matsunaga, S. Nagano, T. Onishi, N. Morimoto, S. Suzuki, and S. Komiya, "Age-related changes in expression of transforming growth factor-beta and receptors in cells of intervertebral discs," *Journal of Neurosurgery*, vol. 98, Supplement 1, pp. 63–67, 2003.

[60] L. A. Nasto, A. R. Robinson, K. Ngo et al., "Mitochondrial-derived reactive oxygen species (ROS) play a causal role in aging-related intervertebral disc degeneration," *Journal of Orthopaedic Research*, vol. 31, no. 7, pp. 1150–1157, 2013.

[61] D. Purmessur, C. C. Guterl, S. K. Cho et al., "Dynamic pressurization induces transition of notochordal cells to a mature phenotype while retaining production of important patterning ligands from development," *Arthritis Research & Therapy*, vol. 15, no. 5, p. R122, 2013.

[62] C. L. Le Maitre, A. J. Freemont, and J. A. Hoyland, "Accelerated cellular senescence in degenerate intervertebral discs: a possible role in the pathogenesis of intervertebral disc degeneration," *Arthritis Research & Therapy*, vol. 9, no. 3, p. R45, 2007.

[63] C. Q. Zhao, L. S. Jiang, and L. Y. Dai, "Programmed cell death in intervertebral disc degeneration," *Apoptosis*, vol. 11, no. 12, pp. 2079–2088, 2006.

[64] C. Feng, H. Liu, M. Yang, Y. Zhang, B. Huang, and Y. Zhou, "Disc cell senescence in intervertebral disc degeneration: causes and molecular pathways," *Cell Cycle*, vol. 15, no. 13, pp. 1674–1684, 2016.

[65] J. M. van Deursen, "The role of senescent cells in ageing," *Nature*, vol. 509, no. 7501, pp. 439–446, 2014.

[66] M. Muller, "Cellular senescence: molecular mechanisms, in vivo significance, and redox considerations," *Antioxidants & Redox Signaling*, vol. 11, no. 1, pp. 59–98, 2009.

[67] H. E. Gruber and E. N. Hanley Jr., "Analysis of aging and degeneration of the human intervertebral disc. Comparison of surgical specimens with normal controls," *Spine*, vol. 23, no. 7, pp. 751–757, 1998.

[68] S. Rajasekaran, C. Tangavel, K. S. Sri Vijay Anand et al., "Inflammaging determines health and disease in lumbar discs-evidence from differing proteomic signatures of healthy, aging, and degenerating discs," *The Spine Journal*, 2019.

[69] E. R. Acaroglu, J. C. Latridis, L. A. Setton, R. J. Foster, V. C. Mow, and M. Weidenbaum, "Degeneration and aging affect the tensile behavior of human lumbar anulus fibrosus," *Spine*, vol. 20, no. 24, pp. 2690–2701, 1995.

[70] C. T. Buckley, J. A. Hoyland, K. Fujii, A. Pandit, J. C. Iatridis, and S. Grad, "Critical aspects and challenges for intervertebral disc repair and regeneration-harnessing advances in tissue engineering," *JOR Spine*, vol. 1, no. 3, article e1029, 2018.

[71] D. C. Lee, C. S. Adams, T. J. Albert, I. M. Shapiro, S. M. Evans, and C. J. Koch, "In situ oxygen utilization in the rat intervertebral disc," *Journal of Anatomy*, vol. 210, no. 3, pp. 294–303, 2007.

[72] M. V. Risbud, E. Schipani, and I. M. Shapiro, "Hypoxic regulation of nucleus pulposus cell survival: from niche to notch," *The American Journal of Pathology*, vol. 176, no. 4, pp. 1577–1583, 2010.

[73] K. Wuertz, K. Godburn, C. Neidlinger-Wilke, J. Urban, and J. C. Iatridis, "Behavior of mesenchymal stem cells in the chemical microenvironment of the intervertebral disc," *Spine*, vol. 33, no. 17, pp. 1843–1849, 2008.

[74] W. L. Grayson, F. Zhao, R. Izadpanah, B. Bunnell, and T. Ma, "Effects of hypoxia on human mesenchymal stem cell expansion and plasticity in 3D constructs," *Journal of Cellular Physiology*, vol. 207, no. 2, pp. 331–339, 2006.

[75] E. Potier, E. Ferreira, R. Andriamanalijaona et al., "Hypoxia affects mesenchymal stromal cell osteogenic differentiation

and angiogenic factor expression," *Bone*, vol. 40, no. 4, pp. 1078–1087, 2007.

[76] T. Felka, R. Schafer, B. Schewe, K. Benz, and W. K. Aicher, "Hypoxia reduces the inhibitory effect of IL-1β on chondrogenic differentiation of FCS-free expanded MSC," *Osteoarthritis and Cartilage*, vol. 17, no. 10, pp. 1368–1376, 2009.

[77] C. C. Tsai, Y. J. Chen, T. L. Yew et al., "Hypoxia inhibits senescence and maintains mesenchymal stem cell properties through down-regulation of E2A-p21 by HIF-TWIST," *Blood*, vol. 117, no. 2, pp. 459–469, 2011.

[78] E. Potier, E. Ferreira, A. Meunier, L. Sedel, D. Logeart-Avramoglou, and H. Petite, "Prolonged hypoxia concomitant with serum deprivation induces massive human mesenchymal stem cell death," *Tissue Engineering*, vol. 13, no. 6, pp. 1325–1331, 2007.

[79] G. Q. Teixeira, C. L. Pereira, J. R. Ferreira et al., "Immunomodulation of human mesenchymal stem/stromal cells in intervertebral disc degeneration: insights from a proinflammatory/degenerative ex vivo model," *Spine*, vol. 43, no. 12, pp. E673–E682, 2018.

[80] D. A. Frauchiger, S. R. Heeb, R. D. May, M. Woltje, L. M. Benneker, and B. Gantenbein, "Differentiation of MSC and annulus fibrosus cells on genetically engineered silk fleece-membrane-composites enriched for GDF-6 or TGF-β3," *Journal of Orthopaedic Research*, vol. 36, no. 5, pp. 1324–1333, 2018.

[81] A. Tekari, R. D. May, D. A. Frauchiger, S. C. Chan, L. M. Benneker, and B. Gantenbein, "The BMP2 variant L51P restores the osteogenic differentiation of human mesenchymal stromal cells in the presence of intervertebral disc cells," *European Cells & Materials*, vol. 33, pp. 197–210, 2017.

[82] C. L. Pereira, R. M. Gonçalves, M. Peroglio et al., "The effect of hyaluronan-based delivery of stromal cell-derived factor-1 on the recruitment of MSCs in degenerating intervertebral discs," *Biomaterials*, vol. 35, no. 28, pp. 8144–8153, 2014.

[83] Y. Tao, X. Zhou, C. Liang et al., "TGF-β3 and IGF-1 synergy ameliorates nucleus pulposus mesenchymal stem cell differentiation towards the nucleus pulposus cell type through MAPK/ERK signaling," *Growth Factors*, vol. 33, no. 5-6, pp. 326–336, 2015.

[84] A. Cuesta, M. E. del Valle, O. García-Suárez et al., "Acid-sensing ion channels in healthy and degenerated human intervertebral disc," *Connective Tissue Research*, vol. 55, no. 3, pp. 197–204, 2014.

[85] X. Li, F. R. Wu, R. S. Xu et al., "Acid-sensing ion channel 1a-mediated calcium influx regulates apoptosis of endplate chondrocytes in intervertebral discs," *Expert Opinion on Therapeutic Targets*, vol. 18, no. 1, pp. 1–14, 2014.

[86] Y. Uchiyama, C. C. Cheng, K. G. Danielson et al., "Expression of acid-sensing ion channel 3 (ASIC3) in nucleus pulposus cells of the intervertebral disc is regulated by p75NTR and ERK signaling," *Journal of Bone and Mineral Research*, vol. 22, no. 12, pp. 1996–2006, 2007.

[87] A. la Binch, A. A. Cole, L. M. Breakwell et al., "Expression and regulation of neurotrophic and angiogenic factors during human intervertebral disc degeneration," *Arthritis Research & Therapy*, vol. 16, no. 4, p. 416, 2014.

[88] S. Ohtori, G. Inoue, T. Koshi et al., "Up-regulation of acid-sensing ion channel 3 in dorsal root ganglion neurons following application of nucleus pulposus on nerve root in rats," *Spine*, vol. 31, no. 18, pp. 2048–2052, 2006.

[89] H. T. J. Gilbert, N. Hodson, P. Baird, S. M. Richardson, and J. A. Hoyland, "Acidic pH promotes intervertebral disc degeneration: acid-sensing ion channel -3 as a potential therapeutic target," *Scientific Reports*, vol. 6, no. 1, article 37360, 2016.

[90] K. Wuertz, K. Godburn, and J. C. Iatridis, "MSC response to pH levels found in degenerating intervertebral discs," *Biochemical and Biophysical Research Communications*, vol. 379, no. 4, pp. 824–829, 2009.

[91] J. Liu, H. Tao, H. Wang et al., "Biological behavior of human nucleus pulposus mesenchymal stem cells in response to changes in the acidic environment during intervertebral disc degeneration," *Stem Cells and Development*, vol. 26, no. 12, pp. 901–911, 2017.

[92] T. T. Tsai, K. G. Danielson, A. Guttapalli et al., "TonEBP/OREBP is a regulator of nucleus pulposus cell function and survival in the intervertebral disc," *The Journal of Biological Chemistry*, vol. 281, no. 35, pp. 25416–25424, 2006.

[93] S. Gajghate, A. Hiyama, M. Shah et al., "Osmolarity and intracellular calcium regulate aquaporin2 expression through TonEBP in nucleus pulposus cells of the intervertebral disc," *Journal of Bone and Mineral Research*, vol. 24, no. 6, pp. 992–1001, 2009.

[94] C. Liu, H. Choi, Z. I. Johnson, J. Tian, I. M. Shapiro, and M. V. Risbud, "Lack of evidence for involvement of TonEBP and hyperosmotic stimulus in induction of autophagy in the nucleus pulposus," *Scientific Reports*, vol. 7, no. 1, p. 4543, 2017.

[95] A. Hiyama, S. Gajghate, D. Sakai, J. Mochida, I. M. Shapiro, and M. V. Risbud, "Activation of TonEBP by calcium controls β1,3-glucuronosyltransferase-I expression, a key regulator of glycosaminoglycan synthesis in cells of the intervertebral disc," *The Journal of Biological Chemistry*, vol. 284, no. 15, pp. 9824–9834, 2009.

[96] A. Krouwels, J. Popov-Celeketic, S. G. M. Plomp et al., "No effects of hyperosmolar culture medium on tissue regeneration by human degenerated nucleus pulposus cells despite upregulation extracellular matrix genes," *Spine*, vol. 43, no. 5, pp. 307–315, 2018.

[97] Z. I. Johnson, I. M. Shapiro, and M. V. Risbud, "RNA sequencing reveals a role of TonEBP transcription factor in regulation of pro-inflammatory genes in response to hyperosmolarity in healthy nucleus pulposus cells: a homeostatic response?," *The Journal of Biological Chemistry*, vol. 291, no. 52, pp. 26686–26697, 2016.

[98] E. Mavrogonatou and D. Kletsas, "High osmolality activates the G1 and G2 cell cycle checkpoints and affects the DNA integrity of nucleus pulposus intervertebral disc cells triggering an enhanced DNA repair response," *DNA Repair*, vol. 8, no. 8, pp. 930–943, 2009.

[99] P. Li, Y. Gan, H. Wang et al., "Role of the ERK1/2 pathway in osmolarity effects on nucleus pulposus cell apoptosis in a disc perfusion culture," *Journal of Orthopaedic Research*, vol. 35, no. 1, pp. 86–92, 2017.

[100] P. Li, Y. Gan, Y. Xu et al., "Osmolarity affects matrix synthesis in the nucleus pulposus associated with the involvement of MAPK pathways: a study of ex vivo disc organ culture system," *Journal of Orthopaedic Research*, vol. 34, no. 6, pp. 1092–1100, 2016.

[101] S. Mizuno, K. Kashiwa, and J. D. Kang, "Molecular and histological characteristics of bovine caudal nucleus pulposus by combined changes in hydrostatic and osmotic pressures

in vitro," *Journal of Orthopaedic Research*, vol. 37, no. 2, pp. 466–476, 2019.

[102] C. J. Hunter, S. Bianchi, P. Cheng, and K. Muldrew, "Osmoregulatory function of large vacuoles found in notochordal cells of the intervertebral disc running title: an osmoregulatory vacuole," *Molecular & Cellular Biomechanics*, vol. 4, no. 4, pp. 227–237, 2007.

[103] P. E. Palacio-Mancheno, T. W. Evashwick-Rogler, D. M. Laudier, D. Purmessur, and J. C. Iatridis, "Hyperosmolarity induces notochordal cell differentiation with aquaporin3 upregulation and reduced N-cadherin expression," *Journal of Orthopaedic Research*, vol. 36, no. 2, pp. 788–798, 2018.

[104] H. Li, J. Wang, F. Li, G. Chen, and Q. Chen, "The influence of hyperosmolarity in the intervertebral disc on the proliferation and chondrogenic differentiation of nucleus pulposus-derived mesenchymal stem cells," *Cells, Tissues, Organs*, vol. 205, no. 3, pp. 178–188, 2018.

[105] K. G. Ma, Z. W. Shao, S. H. Yang et al., "Autophagy is activated in compression-induced cell degeneration and is mediated by reactive oxygen species in nucleus pulposus cells exposed to compression," *Osteoarthritis and Cartilage*, vol. 21, no. 12, pp. 2030–2038, 2013.

[106] K. Ma, S. Chen, Z. Li et al., "Mechanisms of endogenous repair failure during intervertebral disc degeneration," *Osteoarthritis and Cartilage*, vol. 27, no. 1, pp. 41–48, 2019.

[107] Y. Gan, B. Tu, P. Li et al., "Low magnitude of compression enhances biosynthesis of mesenchymal stem cells towards nucleus pulposus cells via the TRPV4-dependent pathway," *Stem Cells International*, vol. 2018, Article ID 7061898, 12 pages, 2018.

[108] J. Dai, H. Wang, G. Liu, Z. Xu, F. Li, and H. Fang, "Dynamic compression and co-culture with nucleus pulposus cells promotes proliferation and differentiation of adipose-derived mesenchymal stem cells," *Journal of Biomechanics*, vol. 47, no. 5, pp. 966–972, 2014.

[109] E. Y.-S. See, S. L. Toh, and J. C.-H. Goh, "Effects of radial compression on a novel simulated intervertebral disc-like assembly using bone marrow-derived mesenchymal stem cell cell-sheets for annulus fibrosus regeneration," *Spine*, vol. 36, no. 21, pp. 1744–1751, 2011.

[110] H. Liang, S. Chen, D. Huang, X. Deng, K. Ma, and Z. Shao, "Effect of compression loading on human nucleus pulposus-derived mesenchymal stem cells," *Stem Cells International*, vol. 2018, Article ID 1481243, 10 pages, 2018.

[111] Z. Sun, B. Luo, Z. H. Liu et al., "Adipose-derived stromal cells protect intervertebral disc cells in compression: implications for stem cell regenerative disc therapy," *International Journal of Biological Sciences*, vol. 11, no. 2, pp. 133–143, 2015.

[112] C. L. Le Maitre, A. J. Freemont, and J. A. Hoyland, "The role of interleukin-1 in the pathogenesis of human intervertebral disc degeneration," *Arthritis Research & Therapy*, vol. 7, no. 4, pp. R732–R745, 2005.

[113] C. Wang, X. Yu, Y. Yan et al., "Tumor necrosis factor-α: a key contributor to intervertebral disc degeneration," *Acta Biochimica et Biophysica Sinica*, vol. 49, no. 1, pp. 1–13, 2017.

[114] S. M. Richardson, G. Kalamegam, P. N. Pushparaj et al., "Mesenchymal stem cells in regenerative medicine: focus on articular cartilage and intervertebral disc regeneration," *Methods*, vol. 99, pp. 69–80, 2016.

[115] C. L. Le Maitre, J. A. Hoyland, and A. J. Freemont, "Interleukin-1 receptor antagonist delivered directly and by gene therapy inhibits matrix degradation in the intact degenerate human intervertebral disc: an in situ zymographic and gene therapy study," *Arthritis Research & Therapy*, vol. 9, no. 4, p. R83, 2007.

[116] F. Wang, F. Cai, R. Shi, X. H. Wang, and X. T. Wu, "Aging and age related stresses: a senescence mechanism of intervertebral disc degeneration," *Osteoarthritis and Cartilage*, vol. 24, no. 3, pp. 398–408, 2016.

[117] H. Yang, C. Cao, C. Wu et al., "TGF-βl suppresses inflammation in cell therapy for intervertebral disc degeneration," *Scientific Reports*, vol. 5, no. 1, article 13254, 2015.

[118] G. Vadalà, F. Russo, G. Pattappa et al., "A nucleotomy model with intact annulus fibrosus to test intervertebral disc regeneration strategies," *Tissue Engineering. Part C, Methods*, vol. 21, no. 11, pp. 1117–1124, 2015.

[119] J. V. Stoyanov, B. Gantenbein-Ritter, A. Bertolo et al., "Role of hypoxia and growth and differentiation factor-5 on differentiation of human mesenchymal stem cells towards intervertebral nucleus pulposus-like cells," *European Cells & Materials*, vol. 21, pp. 533–547, 2011.

[120] Z. Wang, C. M. Perez-Terzic, J. Smith et al., "Efficacy of intervertebral disc regeneration with stem cells - a systematic review and meta-analysis of animal controlled trials," *Gene*, vol. 564, no. 1, pp. 1–8, 2015.

[121] B. Fang, N. Li, Y. Song, Q. Lin, and R. C. Zhao, "Comparison of human post-embryonic, multipotent stem cells derived from various tissues," *Biotechnology Letters*, vol. 31, no. 7, pp. 929–938, 2009.

[122] L. Orozco, R. Soler, C. Morera, M. Alberca, A. Sanchez, and J. Garcia-Sancho, "Intervertebral disc repair by autologous mesenchymal bone marrow cells: a pilot study," *Transplantation*, vol. 92, no. 7, pp. 822–828, 2011.

[123] K. A. Pettine, M. B. Murphy, R. K. Suzuki, and T. T. Sand, "Percutaneous injection of autologous bone marrow concentrate cells significantly reduces lumbar discogenic pain through 12 months," *Stem Cells*, vol. 33, no. 1, pp. 146–156, 2015.

[124] C. Centeno, J. Markle, E. Dodson et al., "Treatment of lumbar degenerative disc disease-associated radicular pain with culture-expanded autologous mesenchymal stem cells: a pilot study on safety and efficacy," *Journal of Translational Medicine*, vol. 15, no. 1, p. 197, 2017.

[125] R. Borem, A. Madeline, M. Bowman, S. Gill, J. Tokish, and J. Mercuri, "Differential effector response of amnion- and adipose-derived mesenchymal stem cells to inflammation; implications for intradiscal therapy," *Journal of Orthopaedic Research*, 2019.

[126] D. C. Noriega, F. Ardura, R. Hernández-Ramajo et al., "Intervertebral disc repair by allogeneic mesenchymal bone marrow cells: a randomized controlled trial," *Transplantation*, vol. 101, no. 8, pp. 1945–1951, 2017.

[127] H. Kumar, D. H. Ha, E. J. Lee et al., "Safety and tolerability of intradiscal implantation of combined autologous adipose-derived mesenchymal stem cells and hyaluronic acid in patients with chronic discogenic low back pain: 1-year follow-up of a phase I study," *Stem Cell Research & Therapy*, vol. 8, no. 1, p. 262, 2017.

[128] H. J. Meisel, N. Agarwal, P. C. Hsieh et al., "Cell therapy for treatment of intervertebral disc degeneration: a systematic review," *Global Spine Journal*, vol. 9, Supplement 1, pp. 39S–52S, 2019.

[129] C. C. Guterl, E. Y. See, S. B. Blanquer et al., "Challenges and strategies in the repair of ruptured annulus fibrosus," *European Cells & Materials*, vol. 25, pp. 1–21, 2013.

[130] J. L. Bron, M. N. Helder, H. J. Meisel, B. J. Van Royen, and T. H. Smit, "Repair, regenerative and supportive therapies of the annulus fibrosus: achievements and challenges," *European Spine Journal*, vol. 18, no. 3, pp. 301–313, 2009.

[131] T. Pirvu, S. B. G. Blanquer, L. M. Benneker et al., "A combined biomaterial and cellular approach for annulus fibrosus rupture repair," *Biomaterials*, vol. 42, pp. 11–19, 2015.

[132] D. R. Pereira, J. Silva-Correia, J. M. Oliveira, and R. L. Reis, "Hydrogels in acellular and cellular strategies for intervertebral disc regeneration," *Journal of Tissue Engineering and Regenerative Medicine*, vol. 7, no. 2, pp. 85–98, 2013.

[133] J. Fernandez-Moure, C. A. Moore, K. Kim et al., "Novel therapeutic strategies for degenerative disc disease: review of cell biology and intervertebral disc cell therapy," *SAGE Open Medicine*, vol. 6, 2018.

[134] G. Vadalà, F. Russo, M. Musumeci et al., "Clinically relevant hydrogel-based on hyaluronic acid and platelet rich plasma as a carrier for mesenchymal stem cells: rheological and biological characterization," *Journal of Orthopaedic Research*, vol. 35, no. 10, pp. 2109–2116, 2017.

[135] M. D'Este, D. Eglin, and M. Alini, "Lessons to be learned and future directions for intervertebral disc biomaterials," *Acta Biomaterialia*, vol. 78, pp. 13–22, 2018.

[136] T. Nonoyama and J. P. Gong, "Double-network hydrogel and its potential biomedical application: a review," *Proceedings of the Institution of Mechanical Engineers. Part H*, vol. 229, no. 12, pp. 853–863, 2015.

[137] G. Q. Teixeira, C. Leite Pereira, F. Castro et al., "Anti-inflammatory chitosan/poly-γ-glutamic acid nanoparticles control inflammation while remodeling extracellular matrix in degenerated intervertebral disc," *Acta Biomaterialia*, vol. 42, pp. 168–179, 2016.

[138] Y. Choi, M. H. Park, and K. Lee, "Tissue engineering strategies for intervertebral disc treatment using functional polymers," *Polymers*, vol. 11, no. 5, p. 872, 2019.

[139] I. L. Mohd Isa, S. A. Abbah, M. Kilcoyne et al., "Implantation of hyaluronic acid hydrogel prevents the pain phenotype in a rat model of intervertebral disc injury," *Science Advances*, vol. 4, no. 4, article eaaq0597, 2018.

[140] A. Bertolo, F. Arcolino, S. Capossela et al., "Growth factors cross-linked to collagen microcarriers promote expansion and chondrogenic differentiation of human mesenchymal stem cells," *Tissue Engineering. Part A*, vol. 21, no. 19-20, pp. 2618–2628, 2015.

[141] H. Tao, Y. Wu, H. Li et al., "BMP7-based functionalized self-assembling peptides for nucleus pulposus tissue engineering," *ACS Applied Materials & Interfaces*, vol. 7, no. 31, pp. 17076–17087, 2015.

Hindawi
Stem Cells International
Volume 2019, Article ID 4761427, 20 pages
https://doi.org/10.1155/2019/4761427

Review Article

Macrophages Are Key Regulators of Stem Cells during Skeletal Muscle Regeneration and Diseases

Junio Dort,[1,2] **Paul Fabre**,[1,3] **Thomas Molina**,[1,3] **and Nicolas A. Dumont**[1,2]

[1]*CHU Sainte-Justine Research Center, Montreal, QC, Canada*
[2]*School of Rehabilitation, Faculty of Medicine, Université de Montréal, Montreal, QC, Canada*
[3]*Department of Pharmacology and Physiology, Faculty of Medicine, Université de Montréal, Montreal, QC, Canada*

Correspondence should be addressed to Nicolas A. Dumont; nicolas.dumont.1@umontreal.ca

Received 3 April 2019; Accepted 9 June 2019; Published 14 July 2019

Guest Editor: Fengjuan Lyu

Muscle regeneration is a closely regulated process that involves a variety of cell types such as satellite cells, myofibers, fibroadipogenic progenitors, endothelial cells, and inflammatory cells. Among these different cell types, macrophages emerged as a central actor coordinating the different cellular interactions and biological processes. Particularly, the transition of macrophages from their proinflammatory to their anti-inflammatory phenotype was shown to regulate inflammation, myogenesis, fibrosis, vascularization, and return to homeostasis. On the other hand, deregulation of macrophage accumulation or polarization in chronic degenerative muscle disorders was shown to impair muscle regeneration. Considering the key roles of macrophages in skeletal muscle, they represent an attractive target for new therapeutic approaches aiming at mitigating various muscle disorders. This review aims at summarizing the novel insights into macrophage heterogeneity, plasticity, and functions in skeletal muscle homeostasis, regeneration, and disease.

1. Introduction

Skeletal muscle injury can be caused by a variety of conditions such as direct trauma, disuse, ischemia, exercise, toxins, and genetic diseases. To face these challenges, skeletal muscle has developed a remarkable regenerative capacity, which relies on muscle stem cells, named satellite cells. Skeletal muscle regeneration is a tightly regulated process during which quiescent satellite cells are activated and become proliferating myoblasts, which will differentiate and fuse to form multinucleated myotubes (newly formed muscle fiber) [1]. The coordination of the myogenesis process (formation of new muscle tissue) involves the cooperation of numerous other cellular and molecular components [2]. Particularly, the onset, development, and the resolution of the inflammatory response play an instrumental role in the regulation of myogenesis.

Monocytes and macrophages are predominant myeloid cells that chronologically accumulate in skeletal muscle at the onset of injury-induced inflammation [3]. There are numerous evidences indicating that macrophages are key regulators of different biological processes involved during skeletal muscle regeneration, such as myogenesis, fibrosis, inflammation, and revascularization [3–9]. On the other hand, in chronic degenerative conditions, the excessive and disorganized influx of macrophages stimulates muscle necrosis, fibrosis, and defective muscle repair. Therefore, the spatiotemporal regulation of inflammation is vital for an effective regeneration of skeletal muscle.

In recent years, novel discoveries revealed that the plasticity, heterogeneity, and the roles played by macrophages in skeletal muscles are much more complex than anticipated. This review will discuss these novel insights into the role of macrophages in muscle homeostasis, regeneration, and diseases with a particular focus on Duchenne muscular dystrophy (DMD). Promising strategies targeting macrophage polarization in physiopathological conditions will also be discussed.

2. Origin and Recruitment of Monocyte and Macrophages

Numerous tissues contain long-lived resident macrophages that originate from the yolk sac during development [10]. In steady state, these tissue-resident macrophages self-renew through in situ proliferation or are replenished by blood monocytes [11–13]. Resident macrophages are observed in healthy skeletal muscles where they regulate tissue homeostasis. In rats, resident macrophages are identified by the marker ED2, while infiltrating monocytes/macrophages are defined by the expression of the marker ED1. In humans, resident macrophages were shown to largely coexpress CD11b and CD206 [14]. Contrary to infiltrating macrophages, $ED2^+$ resident macrophages do not contribute to phagocytosis [15]; instead, it is suggested that they act as sentinels that are readily activated by damage-associated molecular patterns (DAMPs) secreted during muscle injury to facilitate the invasion of circulating leukocytes. However, the literature on these resident cells is limited, and further research is needed to clearly comprehend their roles in healthy and regenerating skeletal muscle.

After an injury, activated monocytes originating from the bone marrow adhere to the blood vessels, roll, and migrate to damaged sites, where they start differentiating into macrophages. In mice, two main monocyte subsets have been described according to their mechanism of extravasation and their level of expression of the protein Ly6C [16, 17]. The proinflammatory $Ly6C^{hi}$ population recruited via the C-C motif chemokine receptor 2 axis (CCR2/CCL2) preferentially accumulates during the acute phase of inflammation, while the CX3C chemokine receptor-1- (CX3CR1-) dependent $Ly6C^{lo}$ subset appears later and exhibits anti-inflammatory properties. Similar monocyte subsets have also been identified in humans using the markers CD14 and CD16. Monocytes $CD14^{hi}CD16^{lo}$ correspond to the $Ly6C^{hi}$ monocytes in mice, while $CD14^{lo}CD16^{hi}$ relate to the $Ly6C^{lo}$ monocyte profile [16].

The mechanism of monocyte recruitment appears to be specific to the tissue and the nature of the insult. For instance, both $Ly6C^{hi}$ and $Ly6C^{lo}$ were shown to sequentially invade the injured tissue after myocardial infarction using their CCR2 or CX3CR1 receptor, respectively [18]. On the other hand, it has been shown that only the $Ly6C^{hi}$ subtype is recruited during sterile skeletal muscle injury, which thereafter switch to the $Ly6C^{lo}$ phenotype [17]. The phagocytosis of apoptotic neutrophils by macrophages was shown to partially contribute to this switch [17]; however, it is likely that many other cellular and chemical interactions present in the dynamic regenerative microenvironment also contribute to this process. In addition to their transition from $Ly6C^{hi}$ monocytes/macrophages, the $Ly6C^{lo}$ cells also accumulate from local proliferation [19]. This finding was also observed in rats where the accumulation of $ED1^+$ and $ED2^+$ macrophages was shown to be partially mediated by local proliferation, especially when invasion of circulating monocytes is reduced by injection of liposome-encapsulated clodronate [20]. Notably, while the different subsets of macrophages were suggested to accumulate sequentially in the injured tissue, it is important to notice that both subsets of macrophages could be simultaneously present in acute regenerating muscles [21], a phenomenon which is exacerbated in chronic degenerative muscle diseases such as DMD [22].

3. Macrophage Subsets and Polarization

A general classification suggests that macrophages can be immunologically classified into two main subsets according to their specific functions: the "classically activated" M1 macrophages, which are present in the inflammatory period and associated with phagocytosis, and the "alternatively activated" M2 macrophages, accumulating at the site of injury once necrotic tissue has been removed and participating in the regeneration and remodelling process. *In vitro*, the M2 phenotype has been further classified into three main subsets—M2a, M2b, and M2c—each of which requires specific polarization cues [23, 24]. The alternatively activated M2a macrophages arise from exposure to interleukin-4 (IL-4) and IL-13, the M2b subtype is polarized by IL-1 receptor ligands, and the M2c phenotype is promoted by IL-10 and glucocorticoids [25, 26]. In mice, the M2 macrophages are identified by the expression of the pan-macrophage marker F4/80 and the alternative activation markers such as Fizz-1 and Ym1 [27]. Of note, Arginase-1 was considered as a specific marker for M2 macrophages; however, it is also expressed in the spectrum of M1 macrophage polarization [28]. In humans, M2 macrophages express the pan-macrophage marker CD68 and alternative activation markers such as CD163 and/or CD206 [27].

Recent insights suggest that this classification based on specific activating factors *in vitro* is an important underestimation of the different macrophage subsets. Accordingly, a study investigating the transcriptional program of macrophages showed that there is a wide spectrum of macrophage activation states [29]. The authors showed that while the bipolar activation state is maintained when the macrophages are stimulated with factors classically associated with M1 or M2 polarization (e.g., TNF-α vs. IL-4), it becomes much more complex when other factors such as fatty acids or a combination of molecules associated with chronic inflammation are used. From the 29 different conditions tested, the authors identified 10 major clusters of activation [29]. These different conditions *in vitro* only give a glimpse of the complexity of the microenvironment of macrophages during muscle regeneration *in vivo*. Indeed, macrophages are interacting with a fluctuating network of hundreds of different molecular, physical, and cellular components that affect their phenotype. For instance, after their extravasation into the injured tissue, monocytes will attach to the extracellular matrix (ECM), which continuously evolves during muscle regeneration. Notably, components of the ECM, such as collagen and fibrinogen, were shown to stimulate macrophage phagocytosis and expression of proinflammatory factors, respectively [30]. Alternatively, attachment of macrophages through their $\alpha 4\beta 1$ integrin receptor to ECM matrix components (fibronectin and vascular cell adhesion molecule-1 (VCAM-1)) stimulates their transition toward the anti-inflammatory phenotype by activating Rac2

signalling [31]. Moreover, macrophage polarization is also sensitive to mechanical stress. Low-frequency mechanical stretch pushes macrophages toward the anti-inflammatory phenotype, while high-frequency strains maintain macrophages in their proinflammatory state [32]. These results suggest that macrophage activation and polarization *in vivo* are processes that are much more complex than what has been described so far. Accordingly, recent analysis of macrophage transcriptional signature after an *in vivo* muscle injury induced by cardiotoxin showed that Ly6C^{hi} and Ly6C^{lo} macrophages only partially overlap with M1 and M2 gene expression patterns, respectively [19]. Instead, the authors showed that the time lapse was the prevalent driving force regulating macrophage gene expression profile, suggesting that a global and coordinated change in the microenvironment components is required to regulate macrophage polarization. The authors identified four key features that account for the changes in gene expression in macrophages during the course of muscle regeneration: firstly, an early expression of genes involved in acute inflammation (e.g., S100A8/9, lipocalin-2, haptoglobin, formyl peptide receptor-1, and leukotriene B4 receptor-1); secondly, a metabolic shift from glycolysis to glutamine and oxidative metabolism-associated genes (e.g., glutamate synthase-1, glycerol-3-phosphate dehydrogenase 2, and superoxide dismutase 2); thirdly, a transient increase in genes associated with cell proliferation (e.g., cyclin-D1 and -A2, many members of the minichromosome maintenance (mcm-2, -3, -4, -5, -6, and -7), DNA ligase-1, replication factor C subunit-1, and ribonucleotide reductase catalytic subunit-M1 and -M2); and fourthly, an increase in the expression of ECM genes (e.g., fibrillin-1, decorin, periostin, lumican, osteonectin, and biglycan). These different clusters of genes could be used to identify new markers to characterize macrophage heterogeneity in skeletal muscle regeneration.

Overall, the M1 and M2 macrophage nomenclature is oversimplistic to characterize macrophage polarization *in vivo*, which should rather be considered as a continuum of activation. Recent effort has been made to propose a common framework for the macrophage-activation nomenclature [28]. Here, for the sake of clarity, we propose to use a bipolar nomenclature (proinflammatory vs. anti-inflammatory) to describe the two opposite sides of the spectrum of macrophage activation; however, one should keep in mind that the actual activation state of macrophages is much more plastic, heterogeneous, and complex.

4. Macrophages Regulate the Different Biological Processes Implicated in Acute Skeletal Muscle Healing

4.1. Macrophages Interact with Other Leukocytes to Regulate Inflammation. The inflammatory process is constituted of different types of leukocytes such as mast cells, neutrophils, eosinophils, monocytes/macrophages, and lymphocytes, which have all been shown to act on skeletal muscle regeneration [6]. Particularly, monocytes/macrophages emerged as the key cellular component orchestrating leukocyte accumulation and function during the different phases of the inflammatory process, i.e., the onset, development, and resolution stages (Figure 1).

4.1.1. Onset. As described previously, resident macrophages are important to sense damage to the tissue and initiate the recruitment of circulating leukocytes. Once activated, resident macrophages secrete chemokines such as cytokine-induced neutrophil chemoattractant 1 (CINC-1) and monocyte chemoattractant protein-1 (MCP-1) that promote the recruitment of neutrophils and monocytes [6]. Moreover, it was also observed that a subset of Ly6C^{lo} circulating monocytes was "crawling" inside the blood vessels independently of the blood flow, with the help of their receptors CX3CR1 and lymphocyte function-associated antigen-1 (LFA-1) [33]. These patrolling monocytes sense tissue damage or infection and transiently invade the tissue as soon as 1 h after an insult (much faster than other circulating leukocytes). At this timepoint, patrolling monocytes are the principal source of TNF-α, which promotes the recruitment of other inflammatory cells. Moreover, patrolling monocytes were also shown to promote the recruitment of neutrophils through prolonged cell-cell contact in the microvasculature [34]. This direct physical interaction stimulates neutrophil retention and production of reactive oxygen species (ROS) at the site of the injury.

4.1.2. Development. Starting a few hours after the injury, the accumulation of neutrophils in the injured muscle remains elevated for a few days. Neutrophils stimulate host defense and the clearance of cell debris by phagocytosis and by the release of ROS and proteases [3]. Accordingly, depletion of neutrophils during acute muscle regeneration leads to persistence of necrotic tissue and delayed regeneration [35]. Moreover, a subset of neutrophils was also shown to promote angiogenesis [36]. Neutrophils also stimulate the development of the inflammatory process by expressing cytokines such as macrophage inflammatory protein 1 (MIP-1α) and MCP-1 that attract circulating monocytes at the damaged sites [37]. Ly6C^{hi} monocytes massively infiltrate in the injured muscle, where they play a key role in the development of inflammation by secreting proinflammatory cytokines such as TNF-α that further promote the recruitment of neutrophils and monocytes [17, 38]. This proinflammatory environment peaks around 48 h after the injury. Thereafter, Ly6C^{lo} monocytes become the predominant subsets in the regenerating muscle, in which they play a key role to dampen inflammation.

4.1.3. Resolution. The phase of resolution of inflammation is not a passive process caused by the decrease in proinflammatory signals; it is an active process that involves a variety of cell types and mediators [39]. Ly6C^{lo} antimacrophages are actively promoting the resolution of inflammation by expressing a wide array of anti-inflammatory cytokines (e.g., IL-4 and IL-13) and by switching their expression of proinflammatory lipids (e.g., prostaglandin-E_2 (PGE_2)) to proresolving lipids (e.g., 15Δ-PGJ2) [40]. These mediators do not only reduce proinflammatory signals and ROS

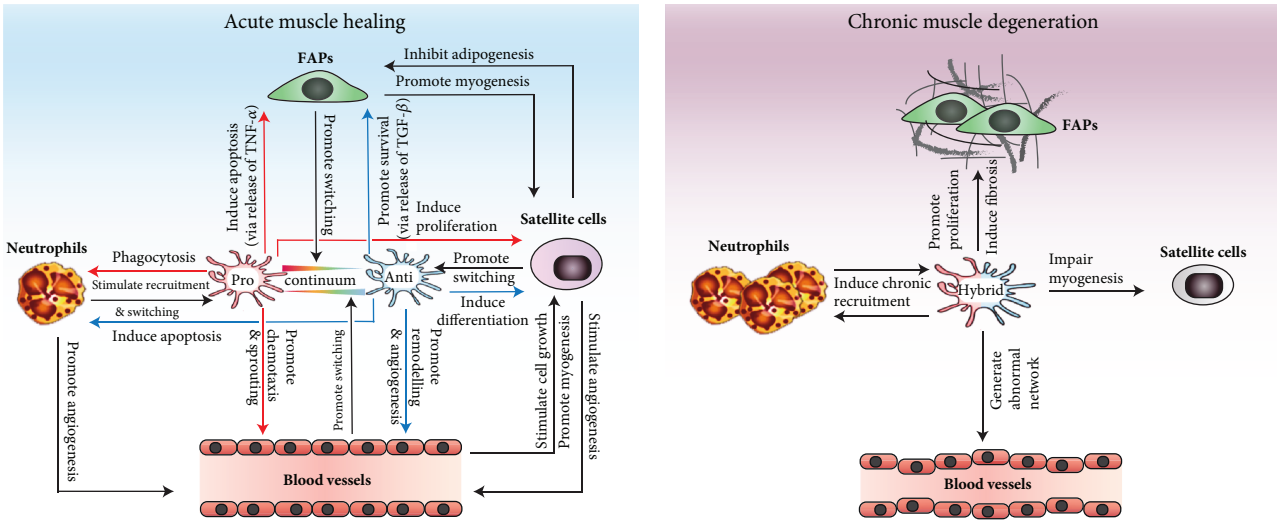

FIGURE 1: Macrophages are central regulators in skeletal muscle regeneration and diseases. In acute muscle injury (a), the inflammatory process is characterized by early accumulation of proinflammatory macrophages, which play a key role in various biological processes involved in muscle regeneration, by regulating fibrosis (FAP apoptosis), myogenesis (satellite cell proliferation), angiogenesis (sprouting), and inflammation (phagocytosis). Thereafter, macrophages switch toward the anti-inflammatory phenotype, which dampens inflammation, stimulates satellite cell/myoblast differentiation, and promotes tissue remodelling. This temporal and coordinated process is essential for optimal muscle healing. In a chronic degenerative muscle (b), the concurrent pro- and anti-inflammatory signals lead to the adoption of an abnormal hybrid phenotype by macrophages, which promote chronic inflammatory cell infiltration, excessive fibrosis, impaired myogenesis, and disorganized blood vessel network.

production, but they also actively stop the recruitment of neutrophils and promote their apoptosis and their non-phlogistic phagocytosis by macrophages [39]. Accordingly, the depletion of macrophages during muscle regeneration prolonged the presence of neutrophils in the injured muscle [41]. The importance of macrophages in the resolution of inflammation is crucial considering that the chronic presence of inflammatory cells has been associated with impaired tissue regeneration. At the late stages of muscle regeneration, macrophages ceased the expression of both pro- and anti-inflammatory cytokines and turned to a silenced mode, which precede the return to homeostasis [42]. Overall, monocytes/macrophages play a central role in the regulation of inflammation from the beginning to the end.

4.2. Macrophages Interact with Satellite Cells to Regulate Myogenesis. Proinflammatory macrophages are key regulators of the host defense, and they are typically associated with clearance of cell debris during skeletal muscle repair [3, 8]. Necrotic fibers may act either as atrophic factors to repress myoblast growth or as physical barriers to prevent myoblast contact, indicating that sufficient infiltration of macrophages might be required for proper regeneration. For instance, using a mouse model deficient in CCR2, which is essential for Ly6C^{hi} monocyte extravasation, it was shown that the drastic reduction of infiltrating monocytes following muscle injury induced by ischemia [43], notexin or cardiotoxin [17, 44], and barium chloride [45] is accompanied by altered muscle regeneration. This impaired regeneration was partially mediated by insufficient phagocytosis of necrotic fibers [45]. However, even after adequate phagocytosis, myofibers failed to efficiently recover when intramuscular macrophages are depleted in a model of notexin-induced injury in mice [17].

Macrophages have multiple beneficial roles during muscle regeneration in addition to their participation in the clearance of cell debris. Particularly, the importance of macrophages in the regulation satellite cells and myoblasts during the myogenesis process is now well defined (Figure 1). The hypothesis that macrophages promote myogenesis was first supported by experiments showing that macrophage-conditioned medium triggers myoblast proliferation *in vitro* and improves muscle regeneration *in vivo* [46, 47]. The crucial role of macrophages to stimulate myogenesis is further illustrated in a model of 3D muscle construct *in vitro*, in which the addition of macrophages is necessary to allow the tissue to self-repair after an injury [48]. Pioneer work from Chazaud's lab has shown that the release of proinflammatory cytokines by Ly6C^{hi} macrophages promotes myoblast proliferation and inhibits differentiation, while the release of anti-inflammatory cytokines by Ly6C^{lo} macrophages inhibits myoblast proliferation and stimulates their differentiation and fusion [17]. The exact cocktail of paracrine factors regulating satellite cell function has not been precisely characterized; however, many molecules secreted by macrophages have been shown to partially mediate these effects. For instance, cytokines highly expressed by proinflammatory macrophages such as interleukin-6 (IL-6) [49], TNF-α, and PGE_2 [50] were shown to stimulate satellite cell proliferation. Moreover, Ly6C^{hi} macrophages secrete the enzyme ADAMTS1 (A Disintegrin-Like And Metalloproteinase

With Thrombospondin Type 1 Motif) that reduces the Notch signalling pathway, leading to increased satellite cell activation and muscle regeneration [51]. On the other hand, cytokines and growth factors highly expressed by anti-inflammatory macrophages such as interleukin-4 (IL-4) [52] and insulin-like growth factor-1 (IGF-1) [41] were shown to stimulate myoblast differentiation/fusion and myofiber growth. In addition to paracrine factors, the direct physical contact of myogenic cells with macrophages is important to regulate their cell function and fate decision. Accordingly, *in vitro* coculture of macrophages and myogenic cells showed that macrophages have a proproliferative effect through the release of paracrine factors and an antiapoptotic effect by direct physical contact through a set of different adhesion molecules (VCAM1, intercellular adhesion molecule-1 (ICAM-1), platelet endothelial cell adhesion molecule-1 (PECAM-1), and CX3CR1) [53, 54].

The critical role of the different subsets of macrophages was also confirmed *in vivo*. It was first observed that in regenerating muscle, proinflammatory macrophages are in close proximity to proliferating satellite cells, while anti-inflammatory macrophages are near to the regenerating area containing differentiated myoblasts [21]. Depletion experiments were used to further characterize the role of the different subsets of macrophages *in vivo*. For instance, the depletion of infiltrating Ly6C^{hi} monocytes using genetic models or pharmacological compounds, prolonged the presence of necrotic cells, promoted the accumulation of muscle fat and fibrosis, and impaired the overall muscle regeneration [17, 41, 55, 56]. On the other hand, the suppression of the ability of macrophages to switch to their anti-inflammatory phenotype, induced by loss-of-function mutations in AMP-activated protein kinase-1 (AMPKα1) [57], IGF-1 [58], CCAAT/enhancer binding protein-β (CEBPB) [59], or peroxisome proliferator-activated receptor-γ (PPAR-γ) [60], was shown to reduce muscle fiber growth, without affecting the removal of necrotic tissue. In turn, models of satellite cell deletion also showed to have delayed macrophage transition to their anti-inflammatory phenotype, suggesting that there is a regulatory feedback by which myogenic cells contribute to the phenotypic switch of macrophages [61]. Altogether, these *in vitro* and *in vivo* experiments demonstrate that the different subsets of macrophages have complementary roles in the regulation of satellite cell/myoblast function, myogenesis progression, and optimal muscle regeneration. Furthermore, these findings also suggest that the temporal and spatial recruitment of macrophages is crucial to regulate the progression of satellite cells through the myogenesis process. Therefore, disorganized macrophage accumulation could send aberrant signals to satellite cells and impair their myogenesis capacity, which will be further discussed later in this manuscript.

4.3. Macrophages Interact with FAPs to Regulate Muscle Fibrosis. Another stem cell type, the fibroadipogenic progenitors (FAPs), plays a crucial role in skeletal muscle regeneration. These tissue-resident stem cells can differentiate into fibroblasts or adipocytes. In acute skeletal muscle injury, FAPs support satellite cell activation and differentiation and, retroactively, satellite cells inhibit FAP differentiation into adipocytes [62–64]. However, in chronic muscle disorders, FAPs can turn into direct contributors of ectopic fat deposition and formation of fibrotic scars that fail to support satellite cell activity [65]. Therefore, FAP activity and accumulation need to be closely regulated. It was shown that FAPs quickly and massively accumulate in the early phase of acute muscle injury, while their number quickly decreases after a few days [5]. Interestingly, this decrease in FAP accumulation correlates with the peak of macrophage accumulation [2]. It was demonstrated that the infiltration of proinflammatory macrophages is essential to control the accumulation of FAPs, via their secretion of TNF-α that directly stimulates FAP apoptosis [5]. Nitric oxide is another factor abundantly produced by proinflammatory macrophages that was shown to inhibit FAP differentiation toward adipocytes *in vitro* and to reduce the deposition of intramuscular fat and connective tissue *in vivo* [66]. The absence of monocyte recruitment to the site of injury in CCR2$^{-/-}$ mice or following diphtheria toxin injection to ITGAM-DTR mice impairs FAP clearance and prolongs their presence in the injured muscle leading to abnormal collagen deposition [5, 67]. On the other hand, anti-inflammatory macrophages release transforming growth factor-β (TGF-β) that promotes FAP survival, which could be important for tissue remodelling during late muscle healing phases. Coculture of fibroblasts with the different subsets of macrophages confirmed that anti-inflammatory macrophages promote fibroblast proliferation and collagen synthesis, while proinflammatory macrophages reduce collagen synthesis and secrete enzymes such as MMP-1 and MMP-3 that degrade ECM [68, 69]. In turn, evidence suggests that a subset of FAPs could also contribute to the phenotypic switch of macrophages [67].

Overall, macrophages play a crucial role to control fibrogenic cell accumulation and activity and to regulate muscle fibrosis. Particularly, the sequential accumulation of the different macrophage subsets is decisive in this process to find the delicate balance that not only limits the excessive activity of fibrotic cells and fibrosis deposition but also allows tissue remodelling needed for the return to homeostasis (Figure 1).

4.4. Macrophages Interact with Endothelial Cells to Regulate Neovascularization. In steady state, satellite cells reside in close proximity to the blood vessels [70]. There is a regulatory cross talk by which satellite cells secrete VEGFA to recruit endothelial cells, which in turn maintain satellite cell quiescence through the notch ligand Dll4 (Delta-like 4) [70]. Similarly, the interaction between angiopoietin-1 secreted by the smooth muscle cells and the Tie-2 receptor of the satellite cells was also demonstrated to promote quiescence [71]. Following an injury, cells from the blood vessels interact with satellite cells to promote revascularization, which is critical for muscle recovery. Particularly, endothelial cells directly regulate satellite cell growth by secreting various growth factors (IGF-1, hepatocyte growth factor (HGF), basic fibroblast growth factor (bFGF), platelet-derived growth factor (PDGF), and vascular endothelial growth

factor (VEGF)), and through a retroactive loop, differentiated myoblasts stimulate angiogenesis [72]. Similarly, pericytes, which are juxtaposed to capillary endothelial cells, were shown to have myogenic capacities *in vitro* and to stimulate myoblast function and muscle regeneration *in vivo* [73].

Macrophages play a central role during muscle regeneration to regulate the function of endothelial cells, which in turn promote the polarization of macrophages to their anti-inflammatory phenotype (Figure 1) [74]. For instance, the depletion of infiltrating monocytes in $CCR2^{-/-}$ mice impairs collateral arteriogenesis after ischemic hindlimb occlusion [75]. However, the role of the different subsets of macrophages on vascularization is still debated. The proangiogenic role of tumour-associated macrophages, a distinct subset of anti-inflammatory macrophages [76], is well defined; however, the role of the different macrophage subsets in a nontumourigenic environment is variable and dependent on various factors. An *in vitro* study indicated that anti-inflammatory macrophages promote the formation of new blood vessels to a higher level than proinflammatory macrophages [77]. Another *in vitro* model showed that proinflammatory macrophages (stimulated with lipopolysaccharide (LPS) + interferon-γ (IFN-γ)) increase the length and number of blood vessel sprouts to a higher level than anti-inflammatory M2a macrophages (induced by IL-4 + IL-13), but to a lower level than anti-inflammatory M2c macrophages (induced by IL-10) [78]. Notably, the anti-inflammatory M2a macrophage subset in these experiments produced higher levels of paracrine factors recruiting pericytes [78]. A model of *in vitro* coculture between endothelial cells, myogenic progenitor cells, and macrophages stimulated with IL-4 or IL-10 showed that anti-inflammatory macrophages coordinate angiogenesis and myogenesis in part by the secretion of oncostatin M [79]. Overall, the subsets of macrophages play several roles that contribute to the different phases of angiogenesis. Accordingly, it was shown that the subsequent incubation of endothelial cells with proinflammatory followed by anti-inflammatory M2a macrophages *in vitro* (to mimic the macrophage phenotype switch observed *in vivo*) enhances the blood vessel network formation [78].

Neovascularization was studied *in vivo* with different models of biomaterial implementation. Similar to *in vitro* experiments, the conclusion regarding the roles of the different subsets of macrophages on angiogenesis is variable depending on the experimental design and the outcomes measured. While some studies indicated that anti-inflammatory macrophages are primarily responsible for microvascular network growth and remodelling [80], others showed that the vascularization is related to a higher ratio of proinflammatory : anti-inflammatory macrophages [81]. This discrepancy might be related to the diversity of macrophage phenotypes *in vivo* and to the complex regulatory network between these subsets of macrophages and the numerous cell types involved in angiogenesis. Overall, macrophages play a crucial role in the regulation of muscle revascularization after an injury; however, further studies are needed to delineate the specific impacts of the different subsets of macrophages.

5. Macrophages in Chronic Muscle Disorders

To mediate their beneficial effects on the different cellular processes involved in skeletal muscle regeneration, the accumulation of the different subsets of macrophages needs to be controlled, transient, and sequential. Disorganization or excessive macrophage activity is a common feature of many chronic conditions, which contributes to tissue degeneration. For instance, iron overloading caused by the excessive engulfment of erythrocytes by anti-inflammatory macrophages induces their switch to an unrestrained proinflammatory phenotype, which stimulates chronic inflammation and impairs wound healing [82]. Asynchronous muscle injuries (induced by two consecutive traumatic injuries separated by a few days) also perturb the proper course of inflammation leading to the concurrent (nonsequential) accumulation of proinflammatory and anti-inflammatory macrophages in the injured area that increases muscle fibrosis [83].

Many muscular diseases are associated with chronic inflammation and impaired muscle regeneration. For instance, skeletal muscles from patients with Pompe disease, which is caused by acid-alpha glucosidase deficiency resulting in lysosomal glycogen accumulation, are subjected to an excessive invasion of proinflammatory macrophages that is correlated with impaired satellite cell differentiation [84]. Similarly, dysferlinopathy, another type of progressive myopathy caused by a mutation in the dysferlin gene, is associated with chronic accumulation of macrophages. These macrophages are maintained in a cytodestructive proinflammatory state that promotes myogenic cell apoptosis/necrosis [85].

The most studied form of muscular disorders is DMD, a frequent and severe debilitating disease characterized by progressive muscle weakness resulting in loss of ambulation, respiratory dysfunctions, and premature death. DMD is caused by a mutation in the gene that encodes for dystrophin, a protein important for muscle fiber stability and for satellite cell function [86]. Therefore, in the absence of dystrophin the muscles are subjected to repetitive and overlapping cycles of degeneration and regeneration. The microenvironment in these dystrophic muscles is characterized by the overactivation of inflammatory pathways such as NF-κB [87], increased cell membrane permeability, and abnormal intracellular calcium influx, as well as a deregulated nitric oxide signalling [88]. These abnormalities provoke changes in gene expression toward a chronic inflammatory molecular signature characterized by the high expression of molecules associated with cytokine and chemokine signalling, vascular adhesion and permeability, and lymphoid and myeloid markers [89]. Particularly, osteopontin is one of the most highly upregulated genes in muscles from mdx mice (mouse model of DMD) and in DMD patients [89, 90]. Osteopontin is an immunomodulator protein involved in immune cell migration and survival, and its ablation in dystrophic mdx mice was shown to promote the transition of proinflammatory macrophages toward their anti-inflammatory phenotype leading to reduced fibrosis and improved muscle function [91]. The chronic inflammatory environment in dystrophic

muscles promotes the long-lasting recruitment of neutrophils and monocytes/macrophages, which instead of contributing to tissue clearance through phagocytosis of cell debris, rather stimulate muscle cell lysis [92] through their high levels of expression of cytotoxic molecules such as ROS. Accordingly, the depletion of neutrophils [93] or monocytes [92] reduces the number of necrotic fibers in mdx mice. Interestingly, the ablation of CCR2 in mdx mice not only reduces the number of infiltrating macrophages but also restores the macrophage polarization balance by skewing macrophages to their anti-inflammatory phenotype, which decreases muscle histopathology and increases muscle force [94]. This beneficial effect was not sustained at long term, potentially due to the local proliferation of resident macrophages that compensate for the lack of infiltrating monocytes [94, 95].

In contrast to the self-limited inflammation following acute sterile muscle injury, the conflicting signals sent simultaneously by degenerative and regenerative environments in chronic or excessive muscle injuries impair macrophage polarization. For instance, following a massive injury induced by muscle laceration, macrophages adopt an intermediary phenotype, which was associated with impaired muscle regeneration and persistent collagen deposition [96]. Interestingly, in this model, the exogenous transplantation of proinflammatory macrophages in the injured muscle reestablished the polarization state, which resulted in decreased fibrosis and improved muscle healing. Likewise, macrophages expressing high levels of both the proinflammatory macrophage marker iNOS (inducible nitric oxide synthase) and the anti-inflammatory macrophage marker CD206 have been observed in mdx mice [94]. In dystrophic muscles, hybrid macrophages expressing high levels of both proinflammatory cytokines (TNF-α) and anti-inflammatory cytokines (TGF-β) showed their inability to reduce the accumulation of FAPs in the injured muscle [5]. Similarly, it was shown that the binding of macrophages to excessive fibrinogen deposition in dystrophic muscle stimulates the production of the proinflammatory cytokine IL-1β together with TGF-β [97]. These hybrid macrophages, particularly Ly6C^{hi} macrophages expressing high levels of LTBP4 (latent TGF-β binding protein), promote the overexpression of the ECM component by FAPs and fibroblasts, leading to aberrant muscle fibrosis [98]. Interestingly, therapeutic strategies promoting the switch of macrophages toward the proinflammatory or anti-inflammatory phenotype were demonstrated to reduce fibrosis in dystrophic mice. For instance, blocking TGF-β-induced p38 kinase activation with the tyrosine kinase inhibitor Nilotinib restores the ability of proinflammatory macrophages to induce FAP apoptosis and promote the resolution of fibrosis in mdx mice [5]. On the other hand, skewing macrophages toward their anti-inflammatory phenotype by AMPK activation blocks their production of latent-TGF-b1 and reduces fibrosis deposition [98]. Overall, the chronic and deregulated macrophage accumulation and polarization observed in dystrophic muscles perturb the inflammatory process, enhance myofiber degeneration, impair myogenesis, and stimulate fibrosis deposition, which contribute to accelerate the progression of the disease (Figure 1).

6. Macrophages in Muscle Aging

Aging is associated with progressive degeneration that affects multiple tissues, including skeletal muscles. Progressive loss of muscle mass of approximately 1% to 2% per year is observed beyond the age of 50 [99]. In some conditions, aging is also associated with sarcopenia, a phenomenon characterized by progressive and generalized loss of muscle mass and force/function leading to physical disability, poor quality of life, and death. Genome-wide transcription analysis revealed that the expression of inflammatory- and immunology-related genes is particularly affected in skeletal muscle during aging [100]. Evidence suggests that altered macrophages during aging impair satellite cell function and muscle regeneration. An *in vitro* model showed that conditioned medium collected from old bone marrow-derived macrophages (BMDM) decreased the number of Ki67$^+$ myoblasts compared to conditioned medium generated from young BMDM, suggesting a reduction in the ability of macrophages to secrete proproliferative factors during aging [101]. In resting muscles of aged mice, an increase in M2a macrophages (CD68$^+$CD163$^+$) has been observed, which correlates with an increase in skeletal muscle fibrosis [102]. Furthermore, the transplantation of bone marrow cells isolated from young mice into aged mice prevented the increase of M2a macrophages and the accumulation of connective tissues in these muscles. In humans, one study comparing young (21-33 years) to elderly subjects (70-81 years) showed that total macrophage density (CD68$^+$) is not different between the two groups, but that the gene expression of CD206 is higher in the elderly group, suggesting an increase in the proportion of anti-inflammatory macrophages in aging human skeletal muscle, similar to what has been observed in mice [103]. However, another study showed that in elderly subjects (average 71.4 years), there is a decrease in the number of both proinflammatory macrophages (CD11b$^+$ cells) and anti-inflammatory macrophages (CD163$^+$ cells) when compared to young individuals (average 31.9 years) [104]. Notably, both subpopulations of macrophages increase following acute resistance exercise in young adults but not in the elderly, indicating an impaired ability of aged muscle to develop a coordinated inflammatory response. Moreover, another study investigating the effect of aging on skeletal muscle macrophages in different conditions (healthy, bed rest, and rehabilitation exercise) showed that elderly individuals (average 66 years old) have less proinflammatory macrophages (CD11b$^+$CD68$^+$) and a similar number of anti-inflammatory macrophages (CD68$^+$CD163$^+$) than young individuals (average 23 years old) in each condition [105]. These studies indicate that the effect of aging on skeletal muscle macrophages in humans is variable depending on the marker used, the population examined, and the condition studied. Overall, we can conclude that the function of macrophages in skeletal muscle homeostasis and regeneration seems to be perturbed during aging; however, further high-quality research is needed to better define

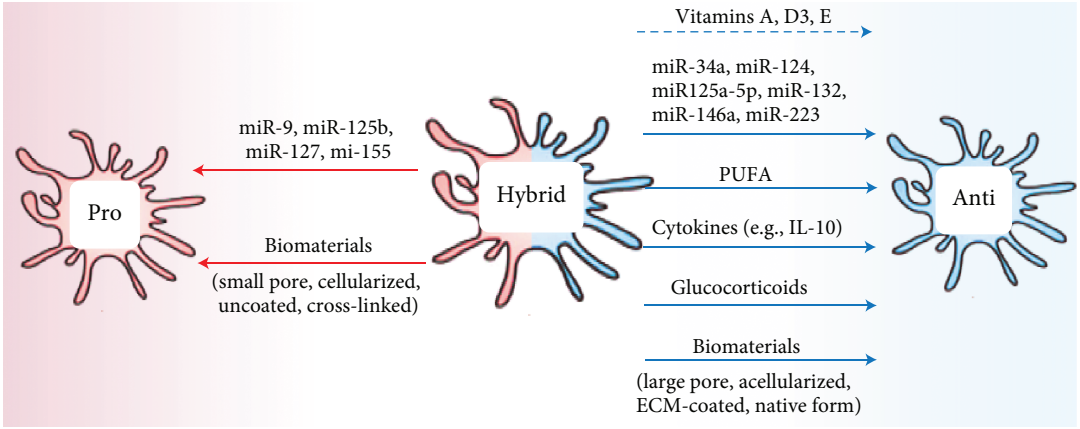

Figure 2: Macrophage-centered therapeutic approaches. Different strategies were developed to restore a balance in macrophage polarization in chronic degenerative muscle disorders. These strategies include cytokines (e.g., IL-10), nutritional compounds (e.g., PUFA and vitamins), RNA silencing (e.g., miRNA), pharmacological drugs (e.g., glucocorticoids), and biomaterials (synthetic, biological, or mixed). These strategies could be used to skew macrophage polarization toward their pro- or anti-inflammatory phenotype depending on the desired therapeutic effect.

these dysfunctions and comprehend the physiopathological mechanisms.

7. Promoting Muscle Regeneration by Modulating the Macrophage Phenotype

Considering the detrimental effect of inflammation in dystrophic muscles, anti-inflammatory drugs are a standard therapeutic approach for many muscle diseases. Accordingly, glucocorticoids are the only drugs that consistently demonstrated efficacy on the preservation of muscle force and ambulatory function in DMD patients [106]. Glucocorticoid treatment reduces macrophage accumulation and promotes their switch toward the anti-inflammatory phenotype, which is correlated with reduction of muscle necrosis and preservation of muscle force and function in DMD [107, 108]. However, glucocorticoids are nonspecific and have many detrimental side effects. Particularly, they stimulate signalling pathways involved in muscle catabolism and indirectly contribute to muscle wasting [109]. Therefore, novel therapeutic approaches specifically targeting macrophages in order to restore their polarization are a promising avenue for the treatment of DMD (Figure 2) [110].

7.1. Anti-Inflammatory Cytokines and Growth Factors

7.1.1. Interleukin-10. IL-10 has been used as an immune-based intervention because of its potential to deactivate proinflammatory macrophages and induce the anti-inflammatory phenotype *in vitro* [111–116]. To determine the role of IL-10 *in vivo*, the regenerative capacity of IL-10-null mice was investigated after hind limb muscle unloading and reloading [117]. The authors showed that IL-10 mutant mice exhibit high levels of proinflammatory markers (IL-6 and CCL2), persistent signs of muscle damage, and reduced accumulation of anti-inflammatory macrophages (expressing CD163 and arginase-1), leading to altered muscle regeneration [117]. Similarly, ablation of IL-10 expression in 12-week-old dystrophic mice reduces anti-inflammatory M2c macrophage polarization and muscle strength [118]. *In vitro* coculture assays revealed that IL-10 does not affect directly myoblast proliferation or differentiation, but rather affects myogenesis indirectly by promoting the transition of macrophages toward their anti-inflammatory M2c phenotype, which favours myoblast differentiation [117, 118]. Therefore, IL-10 has been considered as a therapeutic target to improve muscle regeneration; however, administration of IL-10 early in the regenerative process leads to the premature differentiation of myoblasts which reduces fiber size at 7 days postcardiotoxin injury [42] and may promote tissue fibrosis [118, 119].

7.1.2. Insulin Growth Factor-1. IGF-1 is a key growth factor involved in numerous biological processes. During muscle regeneration, IGF-1 was shown to mediate myogenic cell proliferation, differentiation, and survival, and it also plays a crucial role in shaping the macrophage activation state [58, 120]. During muscle regeneration, IGF-1 is secreted by various cell types, including pro- and anti-inflammatory macrophages, which show a similar level of expression of this growth factor [58]. Conditional deletion of the IGF-1 gene in myeloid cells promotes the accumulation of the $Ly6C^{hi}$ proinflammatory monocyte/macrophage phenotype and reduces $CD206^{+}$ anti-inflammatory macrophages during muscle regeneration, leading to increased fat deposition and reduced fiber size at 10 days after cardiotoxin injury [58]. Analysis of the transcriptional profile showed that IGF-1 deletion skewed macrophages toward their proinflammatory profile, which indicates that IGF-1 is an autocrine factor regulating macrophage polarization [58]. Moreover, IGF-1 is necessary for IL-4-induced transition of macrophages toward their anti-inflammatory phenotype [121]. The therapeutic efficacy of IGF-1 injection has been observed by increased fiber size after sterile muscle injury in transgenic mice [45, 122] and improved muscle strength in old adult mice [123]. However, because myeloid cell-derived IGF-1

peaks by 3 days postinjury and then decline to baseline [45], the long-term beneficial effect of IGF-1 remains uncertain. Particularly, since IGF-1 is involved in a variety of cellular processes, its exogenous administration could have detrimental side effects. For instance, IGF-1 suppresses circulating insulin and growth hormone levels, causing hypoglycemia in humans [124] and stimulates human osteogenic sarcomas [125].

Overall, anti-inflammatory cytokines and growth factors have a great potential to skew macrophages toward their anti-inflammatory profile, which would be beneficial in chronic degenerative muscle diseases; however, the mitigation of their potential side effects is technically challenging and remains a concern for the development of successful therapeutic approaches (Table 1).

7.2. RNA Silencing

7.2.1. Small Interfering RNA. The potential of small interfering RNA (siRNA) has been investigated in many studies to silence proinflammatory markers and adhesion molecules such as TNF-α, VCAM-1, and P-selectins during inflammatory diseases [126, 127]. The ability of siRNA to promote macrophage skewing toward their anti-inflammatory phenotype has been evaluated in different conditions. For instance, the delivery of siRNA targeting collapsin response mediator protein-2 (CRMP2) through lipidoid nanoparticles resulted in a drastic switch toward the anti-inflammatory macrophage phenotype which decreased inflammation, fibrosis, and heart failure postmyocardial infarction [128]. Similarly, silencing of TIMP-1 in proinflammatory macrophages was shown to promote their proangiogenesis capacity at a similar level than the anti-inflammatory phenotype [77]. Receptors such as toll-like receptor-4 (TLR4) and CCR2 are also potential targets in inflammatory diseases and healthy muscle regeneration. The ablation of these receptors blunts the total macrophage accumulation, which results in reduced inflammation in acute injury and dystrophic mdx mice [45, 129, 130]. Genetic or pharmacologic blockage of TLR4, TLR2, or CCR2 in chronic degenerative muscles of mdx mice reduced total macrophage numbers and skewed them toward an anti-inflammatory profile ($iNOS^{-}CD206^{+}$), leading to enhanced histopathology and muscle force generation [94, 129, 131]. On the other hand, loss-of-function of TLR2 or CCR2 decreases total monocytes/macrophages during acute muscle injury but fails to polarize macrophages toward an anti-inflammatory phenotype and causes abnormal persistence of necrotic fibers and impaired regeneration [44, 45, 131]. Therefore, the therapeutic strategies aiming at reprograming the macrophage phenotype must be carefully selected for the treatment of chronic degenerative conditions, since the controlled and coordinated accumulation of both pro- and anti-inflammatory phenotypes is essential for optimal muscle healing after an acute injury.

7.2.2. Small Noncoding RNA Molecules. MicroRNA (miRNAs) are small noncoding RNA molecules containing about 22 nucleotides, which function as posttranscriptional regulators of many genes and cellular processes in an autocrine or paracrine manner. Multiple miRNAs were shown to be involved in macrophage polarization. For instance, miR-9, miR-127, miR-155, and miR-125b were classified as proinflammatory inducers, while miR-124, miR-223, miR-34a, let-7c, miR-132, miR-146a, and miR-125a-5p skewed macrophages toward an anti-inflammatory phenotype [132]. The way that miRNAs regulate proinflammatory macrophage phenotypes includes silencing of specific targets such PPAR-δ, B-cell lymphoma 6 (Bcl6), dual-specificity protein phosphatase 1 (Dusp1), signal transducer and activator of transcription-6 (STAT6), C/EBP, suppressors of cytokine signalling-1 (SOCS1), and interferon regulatory factor 4 (IRF4) and stimulating the c-Jun N-terminal kinase (JNK) pathway [133–135]. miRNAs that promote anti-inflammatory polarization mechanistically inhibit Notch1, signal-regulatory protein beta-1 (SIRPb1), STAT3, C/EBP-δ, and interleukin 1 receptor-associated kinase-1/tumour-necrosis-factor-receptor-associated factor-6 (IRAK1-TRAF6) [136–138]. Transfection of either miR-34a, miR-146a, or miR-132 reduces the levels of proinflammatory-associated markers (iNOS, IL-12) upon LPS challenge [136, 137] and enhances anti-inflammatory markers [137]. Knockout gene strategies of either let-7c or miR-124 also showed an increase in proinflammatory markers (CD86, iNOS, TNF-α, and IL-12), in parallel with a decrease in anti-inflammatory-associated markers (FR-b, CD206, and Ym1) [136, 139]. Delivering a mixture of miR-1, -133, and -206 after laceration of rat tibialis anterior muscle enhances muscle regeneration and prevents fibrosis formation [140]. Although the effect of these myomiRNAs is likely to be mediated through a direct muscle-specific effect, rather than by acting on inflammation, it illustrates the potential of this therapeutic strategy for muscle disorders. However, the use of miRNA as a therapeutic approach is challenging because of inappropriate biodistribution, poor *in vivo* stability, and untoward side effects (Table 1) [141].

7.3. NF-κB Inhibitors. NF-κB is a key transcription factor in macrophages that is required for the expression of numerous proinflammatory genes [142]. In DMD, the NF-κB pathway is persistently overexpressed in immune cells and skeletal muscle cells [143]. Inhibition of this pathway specifically in myeloid cells of dystrophic mdx mice reduced inflammation and muscle necrosis, while its specific deletion in muscle progenitor cells increased myogenesis [143]. Pharmacological inhibition of this pathway mitigated the disease and improved muscle function in dystrophic mdx mice and golden retriever muscular dystrophy dog model [143, 144]. Therefore, it is a promising therapeutic target for chronic muscle diseases.

However, while the NF-κB pathway has been initially described as an inflammatory pathway, accumulating evidence indicate that its effect on inflammation is more complex than anticipated [145]. A pioneer study showed that the inhibition of NF-κB during the onset of inflammation reduces the inflammatory response, while its inhibition during the resolution of inflammation results in the prolongation of the inflammatory response [146]. *In vitro* models have also shown that inhibition of NF-κB impairs the

Table 1: Table showing the pros and cons of the different therapeutic approaches targeting macrophages to improve muscle regeneration and/or mitigate muscle diseases.

Therapeutic approaches	Advantages	Challenges	References
Anti-inflammatory cytokines (e.g., IL-10)	Endogenous molecules; deactivate proinflammatory macrophages and induce the anti-inflammatory phenotype	Short-term effect; nonspecific (could directly impair other cellular processes in skeletal muscle regeneration)	[115, 117]
Growth factors (e.g., IGF-1)	Endogenous molecules; promote macrophage transition to their anti-inflammatory phenotype; promote muscle growth	Short-term effect; systemic side effects	[121, 124, 125]
RNA silencing (e.g., miRNA, siRNA)	Specifically target genes implicated in chronic inflammation; skewed macrophages toward pro- or anti-inflammatory phenotype	Poor stability; inappropriate distribution; off-target side effects; delivery	[126, 127, 136, 138, 200]
NF-κB inhibitors	Dampen inflammation; easy to deliver; good stability	Nonspecific (could directly impair other cellular processes in skeletal muscle regeneration)	[143]
Nutritional compounds (proteins, amino acids, PUFA, vitamins, and antioxidants)	Promote macrophage transition; potentiate the effect of other therapies; inexpensive; easy to administer	Mild therapeutic effect	[166, 171, 172]
Biomaterials	Skewed macrophages toward pro- or anti-inflammatory phenotype; local effects; long-term effects; combination with other therapies	Invasive; biocompatibility; risk of contamination; degradation of the biomaterial	[201]
Macrophage transplantation	Specifically deliver the desired macrophage subset; increase the success rate of satellite cell transplantation	Invasive; systemic side effects; expensive; time consuming	[193–195]

maturation of human monocytes into both pro- and anti-inflammatory macrophages [147]. Other models have shown that the effect of the NF-κB pathway varies depending on different factors such as the type of cell and insult. For instance, in a model of bacterial infection, the specific knockout of IKKβ (factor involved in the NF-κB pathway) in airway epithelial cells inhibited inflammation; however, its inhibition in myeloid cells promoted the inflammation response [148]. IKKβ-deficient macrophages showed increased markers of inflammation and an impaired ability to skew to their anti-inflammatory phenotype, which suggests an important role of NF-κB in the macrophage phenotype switch [148]. Overall, while NF-κB inhibitors are attractive compounds for the treatment of chronic muscle disorders, the broad and complex roles of this pathway make it a difficult target for the development of a macrophage-centered therapeutic approach (Table 1) [145].

7.4. Nutritional Compounds

7.4.1. Proteins and Amino Acids. Many nutritional compounds were shown to regulate the inflammatory process, which represent a simple therapeutic approach for the treatment of chronic muscle disorders. Cod and shrimp proteins were shown to decrease the density of neutrophils and proinflammatory macrophages, while increasing the anti-inflammatory subset in rat muscles following acute sterile injury [149–151]. The beneficial effects of cod protein on the resolution of inflammation and muscle regeneration after injury were attributable to its high content of arginine, glycine, taurine, and lysine [150]. These amino acids have been shown to decrease muscle cell damage in various rodent models of inflammation including endotoxin- and exercise-induced muscle damage by inhibiting the secretion of inflammatory markers, such as TNF-α, IL-1β, IL-6, and PGE_2, and by reducing COX-2 expression and ROS generation [152–158]. The protective effects of L-arginine on muscle cell membrane integrity in mdx mice was reported to be mediated through a decrease in TNF-α, IL-1β, and IL-6 expression levels [153]. Therefore, dietary fish protein rich in arginine, glycine, and taurine represents a safe, inexpensive, and efficient approach for the treatment of inflammatory musculoskeletal diseases (Table 1).

7.4.2. Long-Chain Polyunsaturated Fatty Acids. Omega-3 polyunsaturated fatty acids (PUFA) were shown to have a variety of anti-inflammatory effects such as decreasing adhesion molecules and leukocyte chemotaxis in a variety of inflammatory conditions [159–161]. This effect is partly mediated by their ability to inhibit NF-κB-dependent inflammatory genes and blunt the production of eicosanoids, such as prostaglandins and leukotrienes [162]. In addition to reducing leukocyte accumulation, PUFA directly target macrophages to inhibit their activation and promote their switch toward their anti-inflammatory phenotype [163]. In skeletal muscle, the long-term therapy of omega-3 supplementation to mdx mice reduced proinflammatory markers (TNF-α and NF-κB levels) and improved muscle regeneration [164]. Similarly, a diet supplemented with fish oil diminished the signs of inflammation and reduced fibrosis in the diaphragm muscle of old mdx mice [165]. Therefore, a diet rich in PUFA represents a simple strategy for the treatment of chronic muscle disorders.

7.4.3. Vitamins and Antioxidants. Different studies looked at the role of vitamins to regulate inflammation and macrophage phenotype. So far, retinoic acid (active form of vitamin A), vitamin D3, and vitamin E have been shown to play a role in the functional polarization of macrophages. Using a microarray to scan over 40,000 genes in peritoneal macrophages, it was shown that retinoic acid acts through GATA-6 signalling to change the profile of macrophages, which acquire some markers of the anti-inflammatory profile (e.g., Arg1) but not others (e.g., CD206) [166]. These findings show that retinoic acid promotes an anti-inflammatory-oriented profile that is located in a broad spectrum of macrophage polarization states. Retinoic acid was also shown to potentiate the ability of IL-4 to skew macrophages toward their anti-inflammatory phenotype, indicating that macrophage polarization is a result of the complex interaction of various molecular components [167]. Skeletal muscle regeneration was delayed in mice deficient in retinoic acid receptor-γ, while the treatment of injured wild-type mice with a retinoic acid receptor-γ agonist reduced fibrotic/adipose tissue and improved muscle repair [168]. However, the exact contribution of macrophages in the positive effect of retinoic acid on skeletal muscle repair remains to be determined.

Vitamin D3 has an inhibitory role in a plethora of cellular immune processes, including in T cells, by reducing the inclination of Th0 toward Th1 cells, along with a selective reduction of Th1-related cytokines [169, 170]. Moreover, vitamin D3 was shown to promote Treg development, which plays an important role in driving the M2 macrophage phenotype [171]. Vitamin D3 deficiency was shown to impair the maturation of monocytes to macrophages, while vitamin D3 addition increases the expression of macrophage-specific surface antigens. Macrophages treated with vitamin D3 adopt an intermediary phenotype located on the broad spectrum of macrophage polarization, which is characterized by a controlled increase in oxidative burst, chemotaxis, and phagocytosis, together with a decrease in the expression of TLR2/4 and a reduced level of the proinflammatory cytokines TNF-α, IL-1, and IL-6 [172].

As the most abundant lipid soluble chain-breaking antioxidant in cell membranes, vitamin E has been shown to prevent mitochondrial oxidative damages and entrap peroxyl radicals and oxygen species, all of which are putative factors in several human diseases [173]. Besides its well-known antioxidant properties, accumulating evidences support the immunostimulating effects of vitamin E in pathogen-infected subjects through different mechanisms that enhance the Th1-like pattern immune response [174]. In conditions with a low-grade inflammation (e.g., obesity and aortic lesions), vitamin E appears to suppress infiltrating macrophage accumulation and related cytokines [175, 176]. Indeed, γ-tocopherol, one of the active forms of vitamin E, substantially reduced the recruitment of adipose tissue macrophages in high-fat-fed mice. Moreover, LPS-mediated

proinflammatory macrophage polarization was reduced in γ-tocopherol-treated human adipose tissue with minimal influence on alternative polarization into anti-inflammatory macrophages [175].

Altogether, these findings indicate that vitamins are not classical inducers of the anti-inflammatory phenotype, but they rather promote an intermediary phenotype located in the continuum of macrophage polarization. Thus, the contribution of vitamins to the promotion of the pro- or anti-inflammatory phenotype of macrophages is dependent on their combinatory effect with other molecular and cellular components.

7.5. Biomaterials. The advancement in bioengineering led to the development of new implantable medical devices that can be used in regenerative medicine to modulate macrophage response in different tissues, such as skeletal muscles [177]. The interface between the biomaterial surface and the tissue initiates cellular events that activate a subsequent signalling cascade of paracrine and autocrine factors in the host tissue. These biomaterials can be either synthetic (biodegradable or nonbiodegradable) or biologic [178, 179].

7.5.1. Biologic Materials. These biomaterials include human and porcine skin substitutes, porcine small intestine submucosa, dermal, and other natural substitutes (e.g., collagen, chitosan, silk, and keratin) [178, 180]. The nature and the age of the source animal have a significant impact on the effect of the transplanted biomaterial. For instance, porcine small intestine submucosa harvested from pigs at different ages revealed that a scaffold isolated from younger animals promote a dominant anti-inflammatory macrophage response and better muscle regeneration than a scaffold derived from older animals [181]. The macrophage response is also affected depending on whether the scaffold is implanted in its native form or its cross-linked form (which increases the protein cross-links to improve stability and durability), the former enhancing the anti-inflammatory phenotype, while the latter promoting the proinflammatory phenotype of macrophages [182, 183].

7.5.2. Synthetic Biomaterials. Synthetic biomaterials such as polyethylene, polyethylene terephthalate, polyacrylamide, perfluoropolyether, and polydioxanone elicit an anti-inflammatory response in macrophages *in vitro* [178]. Macrophage response to biomaterials is dependent on many factors including their composition, characteristics (dimension, pore size, and topography), and the quality of the sterilisation [178]. The pore size is a critical regulator of macrophage polarization, with a smaller pore size inducing the proinflammatory phenotype of macrophages cultured on perfluoropolyether [184], while larger pores induce an anti-inflammatory response [185]. In addition to pore size, other factors such as the nature of the material play a significant role in polarizing macrophages, since macrophages cultured on expanded polytetrafluoroethylene and chitosan with large pores show a proinflammatory cytokine profile [186, 187].

7.5.3. Hybrid Biomaterials. These biomaterials are derived from both synthetic and biologic materials. For instance, the coating of polypropylene mesh with ECM components (isolated from decellularized porcine skin) was shown to increase the ratio of anti-inflammatory macrophages compared to uncoated polypropylene mesh [188]. Moreover, these biomaterials could be used as a carrier for biochemical cues (e.g., cytokines and growth factors) or pharmacological compounds. Therefore, biomaterials could be used as a mixed therapy with other anti-inflammatory-stimulating factors described previously. Moreover, biomaterials can also be used as a carrier in cellular transplantation experiments (e.g., for macrophages, satellite cells, or other stem cells). For instance, a tissue engineering strategy showed that a compound containing mesenchymal stem cells and a decellularized ECM scaffold synergistically promoted macrophage polarization toward the M2 phenotype and improved skeletal muscle regeneration in rats [189]. Biomaterials were also shown to improve the success of myoblast transplantation; however, the contribution of macrophage polarization in the beneficial impact of these biomaterials is still elusive [190].

Biomaterials were also used as a scaffold to increase muscle regeneration. Acellular biological scaffolds were shown to elicit an anti-inflammatory macrophage response resulting in constructive remodelling, while scaffolds containing cellular components were associated with a proinflammatory macrophage response resulting in fibrosis and failed regeneration [191]. Biomaterials were also tested as a strategy to improve innervation, vascularization, and myofiber contractility in skeletal muscles [192]; however, the potential of biomaterials as a macrophage-centered approach for the treatment of DMD remains to be investigated. Nonetheless, the recent advances in bioengineering open an exciting new therapeutic avenue that could be used in combination with other factors regulating macrophage polarization for the treatment of chronic degenerative muscle disorders (Table 1).

7.6. Macrophage Transplantation. Transplantation of M2 macrophages is considered as a new cell-based therapy for many diseases including Alzheimer, diabetes, and peripheral arterial disease [193–195]. In a rat model of Alzheimer, M2 macrophage transplantation greatly attenuated inflammation and cognitive impairment by skewing endogenous microglial cells toward the M2 phenotype [193]. Moreover, systemic administration of peritoneal M2 macrophages enhanced glucose tolerance, prevented rejection, and prolonged the survival time of islet allografts in diabetic mice [194]. With regard to skeletal muscle regeneration, it was shown that transplantation of M1-polarized macrophages (LPS/IFN-γ) following ischemia-induced muscle injury enhanced the recovery of muscle function, while the administration of nonpolarized macrophages did not [196]. Similar results were observed in another model of muscle injury (laceration) [96]. Another study demonstrated that early administration of M1-polarized macrophages (IFN-γ) reduced fibrosis and improved myofiber size and muscle function, while early administration of M2-polarized macrophages (IL-4/IL-13) improved myofiber

size but not muscle force and fibrosis [195]. These results indicate that the transplantation of macrophages needs to be timely coordinated to improve skeletal muscle regeneration. Notably, the safety and efficacy of macrophage transplantation have already been tested in two clinical studies, showing a significant improvement of motor and cognitive activities in patients with stroke and neurological affectations [197, 198].

Satellite cell transplantation is also a promising therapeutic avenue to treat different muscle diseases; however, it faces many technical challenges such as poor cell survival, lack of self-renewal, and long-term engraftment. Macrophages represent an attractive approach to improve the success rate of satellite cell transplantation. For instance, coinjection of myoblasts with proinflammatory macrophages supported myoblast engraftment by extending their proliferative phase and delaying their differentiation, while coinjection with anti-inflammatory macrophages did not improve myoblast engraftment [199]. Altogether, these findings suggest that macrophages are an interesting therapeutic approach, either as a direct therapy or as a cofactor for the transplantation of other cell types. However, macrophage polarization needs to be tightly regulated to optimize muscle regeneration.

8. Conclusion

Muscle regeneration relies on different stem cell types, especially satellite cells and FAPs. While these cells are the ultimate executors of muscle repair, their activity is regulated and coordinated by neighbouring cells. Particularly, macrophage polarization toward their proinflammatory or anti-inflammatory phenotype has been shown to play key roles in myogenesis and skeletal muscle healing. The novel insights into the field of inflammation have revealed that macrophages span a continuum of polarization states, which evolves depending on intrinsic and extrinsic factors. In chronic degenerative muscle disorders, the abnormal phenotype adopted by macrophages was shown to contribute to this detrimental process. Therefore, new therapeutics targeting macrophage polarization such as cytokines and growth factors, nutritional compounds, RNA silencing, pharmacological drugs, and biomaterials are tested to improve skeletal muscle regeneration. Depending on the type of muscle injury and on the desired therapeutic effect, these strategies could be used to skew macrophage polarization toward the proinflammatory phenotype (e.g., to decrease excessive fibrosis) or toward the anti-inflammatory phenotype (e.g., to dampen inflammation and promote myogenesis). Despite some technical challenges, these new strategies have a strong therapeutic potential to mitigate different muscle disorders such as DMD. The recent technological advances combined with our improved comprehension of the role of macrophages in skeletal muscle regeneration and diseases will synergize to develop this promising field of research.

Conflicts of Interest

The authors declare that they have no conflict of interest.

Acknowledgments

J.D., T.M., and P.F. are supported by the CHU Sainte-Justine Foundation. N.A.D. is supported by the Canadian Institutes of Health Research, Natural Sciences and Engineering Research Council (NSERC), CHU Sainte-Justine Foundation, Fonds de Recherche Québec-Santé, and Grand Défi Pierre Lavoie Foundation. N.A.D. acknowledges the support of the ThéCell network and the Stem Cell Network.

References

[1] N. A. Dumont, C. F. Bentzinger, M. C. Sincennes, and M. A. Rudnicki, "Satellite cells and skeletal muscle regeneration," *Comprehensive Physiology*, vol. 5, no. 3, pp. 1027–1059, 2015.

[2] C. F. Bentzinger, Y. X. Wang, N. A. Dumont, and M. A. Rudnicki, "Cellular dynamics in the muscle satellite cell niche," *EMBO Reports*, vol. 14, no. 12, pp. 1062–1072, 2013.

[3] J. G. Tidball, "Mechanisms of muscle injury, repair, and regeneration," *Comprehensive Physiology*, vol. 1, no. 4, pp. 2029–2062, 2011.

[4] P. Muñoz-Cánoves and A. L. Serrano, "Macrophages decide between regeneration and fibrosis in muscle," *Trends in Endocrinology & Metabolism*, vol. 26, no. 9, pp. 449-450, 2015.

[5] D. R. Lemos, F. Babaeijandaghi, M. Low et al., "Nilotinib reduces muscle fibrosis in chronic muscle injury by promoting TNF-mediated apoptosis of fibro/adipogenic progenitors," *Nature Medicine*, vol. 21, no. 7, pp. 786–794, 2015.

[6] S. S. Dufresne, J. Frenette, and N. A. Dumont, "Inflammation and muscle regeneration, a double-edged sword," *Medicine Sciences*, vol. 32, no. 6-7, pp. 591–597, 2016.

[7] J. G. Tidball, "Inflammatory processes in muscle injury and repair," *American Journal of Physiology-Regulatory, Integrative and Comparative Physiology*, vol. 288, no. 2, pp. R345–R353, 2005.

[8] J. G. Tidball and S. A. Villalta, "Regulatory interactions between muscle and the immune system during muscle regeneration," *American Journal of Physiology-Regulatory, Integrative and Comparative Physiology*, vol. 298, no. 5, pp. R1173–R1187, 2010.

[9] C. Smith, M. J. Kruger, R. M. Smith, and K. H. Myburgh, "The inflammatory response to skeletal muscle injury: illuminating complexities," *Sports Medicine*, vol. 38, no. 11, pp. 947–969, 2008.

[10] C. Schulz, E. G. Perdiguero, L. Chorro et al., "A lineage of myeloid cells independent of Myb and hematopoietic stem cells," *Science*, vol. 336, no. 6077, pp. 86–90, 2012.

[11] L. C. Davies, M. Rosas, P. J. Smith, D. J. Fraser, S. A. Jones, and P. R. Taylor, "A quantifiable proliferative burst of tissue macrophages restores homeostatic macrophage populations after acute inflammation," *European Journal of Immunology*, vol. 41, no. 8, pp. 2155–2164, 2011.

[12] D. Hashimoto, A. Chow, C. Noizat et al., "Tissue-resident macrophages self-maintain locally throughout adult life with minimal contribution from circulating monocytes," *Immunity*, vol. 38, no. 4, pp. 792–804, 2013.

[13] S. Gordon and A. Plüddemann, "Tissue macrophages: heterogeneity and functions," *BMC Biology*, vol. 15, no. 1, p. 53, 2017.

[14] K. Kosmac, B. Peck, R. Walton et al., "Immunohistochemical identification of human skeletal muscle macrophages," *Bio-protocol*, vol. 8, no. 12, 2018.

[15] I. S. McLennan, "Resident macrophages (ED2- and ED3-positive) do not phagocytose degenerating rat skeletal muscle fibres," *Cell and Tissue Research*, vol. 272, no. 1, pp. 193–196, 1993.

[16] F. Geissmann, S. Jung, and D. R. Littman, "Blood monocytes consist of two principal subsets with distinct migratory properties," *Immunity*, vol. 19, no. 1, pp. 71–82, 2003.

[17] L. Arnold, A. Henry, F. Poron et al., "Inflammatory monocytes recruited after skeletal muscle injury switch into antiinflammatory macrophages to support myogenesis," *The Journal of Experimental Medicine*, vol. 204, no. 5, pp. 1057–1069, 2007.

[18] M. Nahrendorf, F. K. Swirski, E. Aikawa et al., "The healing myocardium sequentially mobilizes two monocyte subsets with divergent and complementary functions," *The Journal of Experimental Medicine*, vol. 204, no. 12, pp. 3037–3047, 2007.

[19] T. Varga, R. Mounier, A. Horvath et al., "Highly dynamic transcriptional signature of distinct macrophage subsets during sterile inflammation, resolution, and tissue repair," *Journal of Immunology*, vol. 196, no. 11, pp. 4771–4782, 2016.

[20] C. H. Côté, P. Bouchard, N. van Rooijen, D. Marsolais, and E. Duchesne, "Monocyte depletion increases local proliferation of macrophage subsets after skeletal muscle injury," *BMC Musculoskeletal Disorders*, vol. 14, no. 1, p. 359, 2013.

[21] M. Saclier, H. Yacoub-Youssef, A. L. Mackey et al., "Differentially activated macrophages orchestrate myogenic precursor cell fate during human skeletal muscle regeneration," *Stem Cells*, vol. 31, no. 2, pp. 384–396, 2013.

[22] S. A. Villalta, H. X. Nguyen, B. Deng, T. Gotoh, and J. G. Tidball, "Shifts in macrophage phenotypes and macrophage competition for arginine metabolism affect the severity of muscle pathology in muscular dystrophy," *Human Molecular Genetics*, vol. 18, no. 3, pp. 482–496, 2009.

[23] A. Mantovani, S. Sozzani, M. Locati, P. Allavena, and A. Sica, "Macrophage polarization: tumor-associated macrophages as a paradigm for polarized M2 mononuclear phagocytes," *Trends in Immunology*, vol. 23, no. 11, pp. 549–555, 2002.

[24] A. Mantovani, A. Sica, S. Sozzani, P. Allavena, A. Vecchi, and M. Locati, "The chemokine system in diverse forms of macrophage activation and polarization," *Trends in Immunology*, vol. 25, no. 12, pp. 677–686, 2004.

[25] S. Gordon, "Alternative activation of macrophages," *Nature Reviews Immunology*, vol. 3, no. 1, pp. 23–35, 2003.

[26] F. O. Martinez and S. Gordon, "The M1 and M2 paradigm of macrophage activation: time for reassessment," *F1000Prime Reports*, vol. 6, 2014.

[27] L. Bosurgi, A. A. Manfredi, and P. Rovere-Querini, "Macrophages in injured skeletal muscle: a *perpetuum mobile* causing and limiting fibrosis, prompting or restricting resolution and regeneration," *Frontiers in Immunology*, vol. 2, p. 62, 2011.

[28] P. J. Murray, J. E. Allen, S. K. Biswas et al., "Macrophage activation and polarization: nomenclature and experimental guidelines," *Immunity*, vol. 41, no. 1, pp. 14–20, 2014.

[29] J. Xue, S. V. Schmidt, J. Sander et al., "Transcriptome-based network analysis reveals a spectrum model of human macrophage activation," *Immunity*, vol. 40, no. 2, pp. 274–288, 2014.

[30] F. Y. McWhorter, C. T. Davis, and W. F. Liu, "Physical and mechanical regulation of macrophage phenotype and function," *Cellular and Molecular Life Sciences*, vol. 72, no. 7, pp. 1303–1316, 2015.

[31] S. Joshi, A. R. Singh, M. Zulcic et al., "Rac2 controls tumor growth, metastasis and M1-M2 macrophage differentiation in vivo," *PLoS One*, vol. 9, no. 4, article e95893, 2014.

[32] V. Ballotta, A. Driessen-Mol, C. V. C. Bouten, and F. P. T. Baaijens, "Strain-dependent modulation of macrophage polarization within scaffolds," *Biomaterials*, vol. 35, no. 18, pp. 4919–4928, 2014.

[33] C. Auffray, D. Fogg, M. Garfa et al., "Monitoring of blood vessels and tissues by a population of monocytes with patrolling behavior," *Science*, vol. 317, no. 5838, pp. 666–670, 2007.

[34] M. Finsterbusch, P. Hall, A. Li et al., "Patrolling monocytes promote intravascular neutrophil activation and glomerular injury in the acutely inflamed glomerulus," *Proceedings of the National Academy of Sciences of the United States of America*, vol. 113, no. 35, pp. E5172–E5181, 2016.

[35] C. F. P. Teixeira, S. R. Zamunér, J. P. Zuliani et al., "Neutrophils do not contribute to local tissue damage, but play a key role in skeletal muscle regeneration, in mice injected with *Bothrops asper* snake venom," *Muscle & Nerve*, vol. 28, no. 4, pp. 449–459, 2003.

[36] E. Kolaczkowska and P. Kubes, "Angiogenic neutrophils: a novel subpopulation paradigm," *Blood*, vol. 120, no. 23, pp. 4455–4457, 2012.

[37] P. Scapini, J. A. Lapinet-Vera, S. Gasperini, F. Calzetti, F. Bazzoni, and M. A. Cassatella, "The neutrophil as a cellular source of chemokines," *Immunological Reviews*, vol. 177, no. 1, pp. 195–203, 2000.

[38] C. Shi and E. G. Pamer, "Monocyte recruitment during infection and inflammation," *Nature Reviews Immunology*, vol. 11, no. 11, pp. 762–774, 2011.

[39] C. N. Serhan and J. Savill, "Resolution of inflammation: the beginning programs the end," *Nature Immunology*, vol. 6, no. 12, pp. 1191–1197, 2005.

[40] J. U. Scher and M. H. Pillinger, "15d-PGJ 2: the anti-inflammatory prostaglandin?," *Clinical Immunology*, vol. 114, no. 2, pp. 100–109, 2005.

[41] N. Dumont and J. Frenette, "Macrophages protect against muscle atrophy and promote muscle recovery *in vivo* and *in vitro*: a mechanism partly dependent on the insulin-like growth factor-1 signaling molecule," *The American Journal of Pathology*, vol. 176, no. 5, pp. 2228–2235, 2010.

[42] E. Perdiguero, P. Sousa-Victor, V. Ruiz-Bonilla et al., "p38/MKP-1-regulated AKT coordinates macrophage transitions and resolution of inflammation during tissue repair," *The Journal of Cell Biology*, vol. 195, no. 2, pp. 307–322, 2011.

[43] V. Contreras-Shannon, O. Ochoa, S. M. Reyes-Reyna et al., "Fat accumulation with altered inflammation and regeneration in skeletal muscle of CCR2-/- mice following ischemic injury," *American Journal of Physiology-Cell Physiology*, vol. 292, no. 2, pp. C953–C967, 2007.

[44] D. Sun, C. O. Martinez, O. Ochoa et al., "Bone marrow-derived cell regulation of skeletal muscle regeneration," *The FASEB Journal*, vol. 23, no. 2, pp. 382–395, 2009.

[45] H. Lu, D. Huang, N. Saederup, I. F. Charo, R. M. Ransohoff, and L. Zhou, "Macrophages recruited via CCR2 produce

insulin-like growth factor-1 to repair acute skeletal muscle injury," *FASEB Journal*, vol. 25, no. 1, pp. 358–369, 2011.

[46] M. Cantini, E. Giurisato, C. Radu et al., "Macrophage-secreted myogenic factors: a promising tool for greatly enhancing the proliferative capacity of myoblasts in vitro and in vivo," *Neurological Sciences*, vol. 23, no. 4, pp. 189–194, 2002.

[47] M. Cantini, M. L. Massimino, A. Bruson, C. Catani, L. Dallalibera, and U. Carraro, "Macrophages regulate proliferation and differentiation of satellite cells," *Biochemical and Biophysical Research Communications*, vol. 202, no. 3, pp. 1688–1696, 1994.

[48] M. Juhas, N. Abutaleb, J. T. Wang et al., "Incorporation of macrophages into engineered skeletal muscle enables enhanced muscle regeneration," *Nature Biomedical Engineering*, vol. 2, no. 12, pp. 942–954, 2018.

[49] C. Zhang, Y. Li, Y. Wu, L. Wang, X. Wang, and J. du, "Interleukin-6/signal transducer and activator of transcription 3 (STAT3) pathway is essential for macrophage infiltration and myoblast proliferation during muscle regeneration," *Journal of Biological Chemistry*, vol. 288, no. 3, pp. 1489–1499, 2013.

[50] A. T. V. Ho, A. R. Palla, M. R. Blake et al., "Prostaglandin E2 is essential for efficacious skeletal muscle stem-cell function, augmenting regeneration and strength," *Proceedings of the National Academy of Sciences*, vol. 114, no. 26, pp. 6675–6684, 2017.

[51] H. du, C. H. Shih, M. N. Wosczyna et al., "Macrophage-released ADAMTS1 promotes muscle stem cell activation," *Nature Communications*, vol. 8, no. 1, p. 669, 2017.

[52] V. Horsley, K. M. Jansen, S. T. Mills, and G. K. Pavlath, "IL-4 acts as a myoblast recruitment factor during mammalian muscle growth," *Cell*, vol. 113, no. 4, pp. 483–494, 2003.

[53] B. Chazaud, C. Sonnet, P. Lafuste et al., "Satellite cells attract monocytes and use macrophages as a support to escape apoptosis and enhance muscle growth," *The Journal of Cell Biology*, vol. 163, no. 5, pp. 1133–1143, 2003.

[54] C. Sonnet, "Human macrophages rescue myoblasts and myotubes from apoptosis through a set of adhesion molecular systems," *Journal of Cell Science*, vol. 119, no. 12, pp. 2497–2507, 2006.

[55] C. O. Martinez, M. J. McHale, J. T. Wells et al., "Regulation of skeletal muscle regeneration by CCR2-activating chemokines is directly related to macrophage recruitment," *American Journal of Physiology-Regulatory, Integrative and Comparative Physiology*, vol. 299, no. 3, pp. R832–R842, 2010.

[56] M. Summan, G. L. Warren, R. R. Mercer et al., "Macrophages and skeletal muscle regeneration: a clodronate-containing liposome depletion study," *American Journal of Physiology-Regulatory, Integrative and Comparative Physiology*, vol. 290, no. 6, pp. R1488–R1495, 2006.

[57] R. Mounier, M. Théret, L. Arnold et al., "AMPKα1 regulates macrophage skewing at the time of resolution of inflammation during skeletal muscle regeneration," *Cell Metabolism*, vol. 18, no. 2, pp. 251–264, 2013.

[58] J. Tonkin, L. Temmerman, R. D. Sampson et al., "Monocyte/macrophage-derived IGF-1 orchestrates murine skeletal muscle regeneration and modulates autocrine polarization," *Molecular Therapy*, vol. 23, no. 7, pp. 1189–1200, 2015.

[59] D. Ruffell, F. Mourkioti, A. Gambardella et al., "A CREB-C/EBPβ cascade induces M2 macrophage-specific gene expression and promotes muscle injury repair," *Proceedings of the National Academy of Sciences*, vol. 106, no. 41, pp. 17475–17480, 2009.

[60] T. Varga, R. Mounier, A. Patsalos et al., "Macrophage PPARγ, a lipid activated transcription factor controls the growth factor GDF3 and skeletal muscle regeneration," *Immunity*, vol. 45, no. 5, pp. 1038–1051, 2016.

[61] A. Patsalos, A. Pap, T. Varga et al., "*In situ* macrophage phenotypic transition is affected by altered cellular composition prior to acute sterile muscle injury," *The Journal of Physiology*, vol. 595, no. 17, pp. 5815–5842, 2017.

[62] M. M. Murphy, J. A. Lawson, S. J. Mathew, D. A. Hutcheson, and G. Kardon, "Satellite cells, connective tissue fibroblasts and their interactions are crucial for muscle regeneration," *Development*, vol. 138, no. 17, pp. 3625–3637, 2011.

[63] A. W. B. Joe, L. Yi, A. Natarajan et al., "Muscle injury activates resident fibro/adipogenic progenitors that facilitate myogenesis," *Nature Cell Biology*, vol. 12, no. 2, pp. 153–163, 2010.

[64] A. Uezumi, S. I. Fukada, N. Yamamoto, S.'. Takeda, and K. Tsuchida, "Mesenchymal progenitors distinct from satellite cells contribute to ectopic fat cell formation in skeletal muscle," *Nature Cell Biology*, vol. 12, no. 2, pp. 143–152, 2010.

[65] C. Mozzetta, S. Consalvi, V. Saccone et al., "Fibroadipogenic progenitors mediate the ability of HDAC inhibitors to promote regeneration in dystrophic muscles of young, but not old Mdx mice," *EMBO Molecular Medicine*, vol. 5, no. 4, pp. 626–639, 2013.

[66] N. Cordani, V. Pisa, L. Pozzi, C. Sciorati, and E. Clementi, "Nitric oxide controls fat deposition in dystrophic skeletal muscle by regulating fibro-adipogenic precursor differentiation," *Stem Cells*, vol. 32, no. 4, pp. 874–885, 2014.

[67] B. Malecova, S. Gatto, U. Etxaniz et al., "Dynamics of cellular states of fibro-adipogenic progenitors during myogenesis and muscular dystrophy," *Nature Communications*, vol. 9, no. 1, p. 3670, 2018.

[68] E. Song, N. Ouyang, M. Hörbelt, B. Antus, M. Wang, and M. S. Exton, "Influence of alternatively and classically activated macrophages on fibrogenic activities of human fibroblasts," *Cellular Immunology*, vol. 204, no. 1, pp. 19–28, 2000.

[69] D. T. Ploeger, N. A. Hosper, M. Schipper, J. A. Koerts, S. de Rond, and R. A. Bank, "Cell plasticity in wound healing: paracrine factors of M1/M2 polarized macrophages influence the phenotypical state of dermal fibroblasts," *Cell Communication and Signaling*, vol. 11, no. 1, p. 29, 2013.

[70] M. Verma, Y. Asakura, B. S. R. Murakonda et al., "Muscle satellite cell cross-talk with a vascular niche maintains quiescence via VEGF and Notch signaling," *Cell Stem Cell*, vol. 23, no. 4, pp. 530–543.e9, 2018.

[71] R. Abou-Khalil, F. le Grand, G. Pallafacchina et al., "Autocrine and paracrine angiopoietin 1/Tie-2 signaling promotes muscle satellite cell self-renewal," *Cell Stem Cell*, vol. 5, no. 3, pp. 298–309, 2009.

[72] C. Christov, F. Chrétien, R. Abou-Khalil et al., "Muscle satellite cells and endothelial cells: close neighbors and privileged partners," *Molecular Biology of the Cell*, vol. 18, no. 4, pp. 1397–1409, 2007.

[73] A. Birbrair, T. Zhang, Z. M. Wang, M. L. Messi, A. Mintz, and O. Delbono, "Pericytes: Multitasking Cells in the

Regeneration of Injured, Diseased, and Aged Skeletal Muscle," *Frontiers in Aging Neuroscience*, vol. 6, 2014.

[74] H. He, J. Xu, C. M. Warren et al., "Endothelial cells provide an instructive niche for the differentiation and functional polarization of M2-like macrophages," *Blood*, vol. 120, no. 15, pp. 3152–3162, 2012.

[75] M. Heil, T. Ziegelhoeffer, S. Wagner et al., "Collateral artery growth (arteriogenesis) after experimental arterial occlusion is impaired in mice lacking CC-chemokine receptor-2," *Circulation Research*, vol. 94, no. 5, pp. 671–677, 2004.

[76] A. Sica, T. Schioppa, A. Mantovani, and P. Allavena, "Tumour-associated macrophages are a distinct M2 polarised population promoting tumour progression: potential targets of anti-cancer therapy," *European Journal of Cancer*, vol. 42, no. 6, pp. 717–727, 2006.

[77] E. Zajac, B. Schweighofer, T. A. Kupriyanova et al., "Angiogenic capacity of M1- and M2-polarized macrophages is determined by the levels of TIMP-1 complexed with their secreted proMMP-9," *Blood*, vol. 122, no. 25, pp. 4054–4067, 2013.

[78] K. L. Spiller, R. R. Anfang, K. J. Spiller et al., "The role of macrophage phenotype in vascularization of tissue engineering scaffolds," *Biomaterials*, vol. 35, no. 15, pp. 4477–4488, 2014.

[79] C. Latroche, M. Weiss-Gayet, L. Muller et al., "Coupling between myogenesis and angiogenesis during skeletal muscle regeneration is stimulated by restorative macrophages," *Stem Cell Reports*, vol. 9, no. 6, pp. 2018–2033, 2017.

[80] J. R. Krieger, M. E. Ogle, J. McFaline-Figueroa, C. E. Segar, J. S. Temenoff, and E. A. Botchwey, "Spatially localized recruitment of anti-inflammatory monocytes by SDF-1α-releasing hydrogels enhances microvascular network remodeling," *Biomaterials*, vol. 77, pp. 280–290, 2016.

[81] E. Tous, H. M. Weber, M. H. Lee et al., "Tunable hydrogel-microsphere composites that modulate local inflammation and collagen bulking," *Acta Biomaterialia*, vol. 8, no. 9, pp. 3218–3227, 2012.

[82] A. Sindrilaru, T. Peters, S. Wieschalka et al., "An unrestrained proinflammatory M1 macrophage population induced by iron impairs wound healing in humans and mice," *The Journal of Clinical Investigation*, vol. 121, no. 3, pp. 985–997, 2011.

[83] S. Dadgar, Z. Wang, H. Johnston et al., "Asynchronous remodeling is a driver of failed regeneration in Duchenne muscular dystrophy," *The Journal of Cell Biology*, vol. 207, no. 1, pp. 139–158, 2014.

[84] G. J. Schaaf, T. J. M. van Gestel, E. Brusse et al., "Lack of robust satellite cell activation and muscle regeneration during the progression of Pompe disease," *Acta Neuropathologica Communications*, vol. 3, no. 1, p. 65, 2015.

[85] J.-H. Baek, G. M. Many, F. J. Evesson, and V. R. Kelley, "Dysferlinopathy promotes an intramuscle expansion of macrophages with a cyto-destructive phenotype," *The American Journal of Pathology*, vol. 187, no. 6, pp. 1245–1257, 2017.

[86] N. A. Dumont, Y. X. Wang, J. von Maltzahn et al., "Dystrophin expression in muscle stem cells regulates their polarity and asymmetric division," *Nature Medicine*, vol. 21, no. 12, pp. 1455–1463, 2015.

[87] Y.-W. Chen, K. Nagaraju, M. Bakay et al., "Early onset of inflammation and later involvement of TGFβ in Duchenne muscular dystrophy," *Neurology*, vol. 65, no. 6, pp. 826–834, 2005.

[88] B. J. Petrof, "Molecular pathophysiology of myofiber injury in deficiencies of the dystrophin-glycoprotein complex," *American Journal of Physical Medicine & Rehabilitation*, vol. 81, pp. S162–S174, 2002.

[89] J. D. Porter, S. Khanna, H. J. Kaminski et al., "A chronic inflammatory response dominates the skeletal muscle molecular signature in dystrophin-deficient *mdx* mice," *Human Molecular Genetics*, vol. 11, no. 3, pp. 263–272, 2002.

[90] J. N. Haslett, D. Sanoudou, A. T. Kho et al., "Gene expression comparison of biopsies from Duchenne muscular dystrophy (DMD) and normal skeletal muscle," *Proceedings of the National Academy of Sciences of the United States of America*, vol. 99, no. 23, pp. 15000–15005, 2002.

[91] J. Capote, I. Kramerova, L. Martinez et al., "Osteopontin ablation ameliorates muscular dystrophy by shifting macrophages to a pro-regenerative phenotype," *The Journal of Cell Biology*, vol. 213, no. 2, pp. 275–288, 2016.

[92] M. Wehling, M. J. Spencer, and J. G. Tidball, "A nitric oxide synthase transgene ameliorates muscular dystrophy in mdx mice," *Journal of Cell Biology*, vol. 155, no. 1, pp. 123–132, 2001.

[93] S. Hodgetts, H. Radley, M. Davies, and M. D. Grounds, "Reduced necrosis of dystrophic muscle by depletion of host neutrophils, or blocking TNFα function with Etanercept in mdx mice," *Neuromuscular Disorders*, vol. 16, no. 9-10, pp. 591–602, 2006.

[94] K. Mojumdar, F. Liang, C. Giordano et al., "Inflammatory monocytes promote progression of Duchenne muscular dystrophy and can be therapeutically targeted via CCR2," *EMBO Molecular Medicine*, vol. 6, no. 11, pp. 1476–1492, 2014.

[95] W. Zhao, X. Wang, R. M. Ransohoff, and L. Zhou, "CCR2 deficiency does not provide sustained improvement of muscular dystrophy in *mdx*^{5cv} mice," *The FASEB Journal*, vol. 31, no. 1, pp. 35–46, 2017.

[96] M. L. Novak, E. M. Weinheimer-Haus, and T. J. Koh, "Macrophage activation and skeletal muscle healing following traumatic injury," *The Journal of Pathology*, vol. 232, no. 3, pp. 344–355, 2014.

[97] B. Vidal, A. L. Serrano, M. Tjwa et al., "Fibrinogen drives dystrophic muscle fibrosis via a TGFβ/alternative macrophage activation pathway," *Genes & Development*, vol. 22, no. 13, pp. 1747–1752, 2008.

[98] G. Juban, M. Saclier, H. Yacoub-Youssef et al., "AMPK activation regulates LTBP4-dependent TGF-β1 secretion by pro-inflammatory macrophages and controls fibrosis in Duchenne muscular dystrophy," *Cell Reports*, vol. 25, no. 8, pp. 2163–2176 e6, 2018.

[99] W. R. Frontera, V. A. Hughes, R. A. Fielding, M. A. Fiatarone, W. J. Evans, and R. Roubenoff, "Aging of skeletal muscle: a 12-yr longitudinal study," *Journal of Applied Physiology*, vol. 88, no. 4, pp. 1321–1326, 2000.

[100] I. H. Lin, J. L. Chang, K. Hua, W. C. Huang, M. T. Hsu, and Y. F. Chen, "Skeletal muscle in aged mice reveals extensive transformation of muscle gene expression," *BMC Genetics*, vol. 19, no. 1, p. 55, 2018.

[101] Y. Wang, M. Wehling-Henricks, S. S. Welc, A. L. Fisher, Q. Zuo, and J. G. Tidball, "Aging of the immune system causes reductions in muscle stem cell populations, promotes their shift to a fibrogenic phenotype, and modulates sarcopenia," *The FASEB Journal*, vol. 33, no. 1, pp. 1415–1427, 2018.

[102] Y. Wang, M. Wehling-Henricks, G. Samengo, and J. G. Tidball, "Increases of M2a macrophages and fibrosis in aging muscle are influenced by bone marrow aging and negatively regulated by muscle-derived nitric oxide," *Aging Cell*, vol. 14, no. 4, pp. 678–688, 2015.

[103] C. S. Tam, L. M. Sparks, D. L. Johannsen, J. D. Covington, T. S. Church, and E. Ravussin, "Low macrophage accumulation in skeletal muscle of obese type 2 diabetics and elderly subjects," *Obesity*, vol. 20, no. 7, pp. 1530–1533, 2012.

[104] B. Przybyla, C. Gurley, J. Harvey et al., "Aging alters macrophage properties in human skeletal muscle both at rest and in response to acute resistance exercise," *Experimental Gerontology*, vol. 41, no. 3, pp. 320–327, 2006.

[105] P. T. Reidy, C. C. Lindsay, A. I. McKenzie et al., "Aging-related effects of bed rest followed by eccentric exercise rehabilitation on skeletal muscle macrophages and insulin sensitivity," *Experimental Gerontology*, vol. 107, pp. 37–49, 2018.

[106] A. Y. Manzur, T. Kuntzer, M. Pike, and A. V. Swan, "Glucocorticoid corticosteroids for Duchenne muscular dystrophy," *Cochrane Database of Systematic Reviews*, vol. 2008, no. 1, article CD003725, 2008.

[107] M. R. Hussein, S. A. Hamed, M. G. Mostafa, E. E. Abu-Dief, N. F. Kamel, and M. R. Kandil, "The effects of glucocorticoid therapy on the inflammatory and dendritic cells in muscular dystrophies," *International Journal of Experimental Pathology*, vol. 87, no. 6, pp. 451–461, 2006.

[108] G. Zizzo, B. A. Hilliard, M. Monestier, and P. L. Cohen, "Efficient clearance of early apoptotic cells by human macrophages requires M2c polarization and MerTK induction," *The Journal of Immunology*, vol. 189, no. 7, pp. 3508–3520, 2012.

[109] O. Schakman, S. Kalista, C. Barbé, A. Loumaye, and J. P. Thissen, "Glucocorticoid-induced skeletal muscle atrophy," *The International Journal of Biochemistry & Cell Biology*, vol. 45, no. 10, pp. 2163–2172, 2013.

[110] B. N. Brown, B. M. Sicari, and S. F. Badylak, "Rethinking regenerative medicine: a macrophage-centered approach," *Frontiers in Immunology*, vol. 5, 2014.

[111] D. F. Fiorentino, M. W. Bond, and T. Mosmann, "Two types of mouse T helper cell. IV. Th2 clones secrete a factor that inhibits cytokine production by Th1 clones," *Journal of Experimental Medicine*, vol. 170, no. 6, pp. 2081–2095, 1989.

[112] D. F. Fiorentino, A. Zlotnik, T. R. Mosmann, M. Howard, and A. O'Garra, "IL-10 inhibits cytokine production by activated macrophages," *The Journal of Immunology*, vol. 147, no. 11, pp. 3815–3822, 1991.

[113] T. H. Sulahian, P. Högger, A. E. Wahner et al., "Human monocytes express CD163, which is upregulated by IL-10 and identical to p155," *Cytokine*, vol. 12, no. 9, pp. 1312–1321, 2000.

[114] P. J. Murray, "Understanding and exploiting the endogenous interleukin-10/STAT3-mediated anti-inflammatory response," *Current Opinion in Pharmacology*, vol. 6, no. 4, pp. 379–386, 2006.

[115] D. M. Mosser and X. Zhang, "Interleukin-10: new perspectives on an old cytokine," *Immunological Reviews*, vol. 226, no. 1, pp. 205–218, 2008.

[116] J. Hao, Y. Hu, Y. Li, Q. Zhou, and X. Lv, "Involvement of JNK signaling in IL4-induced M2 macrophage polarization," *Experimental Cell Research*, vol. 357, no. 2, pp. 155–162, 2017.

[117] B. Deng, M. Wehling-Henricks, S. A. Villalta, Y. Wang, and J. G. Tidball, "IL-10 triggers changes in macrophage phenotype that promote muscle growth and regeneration," *The Journal of Immunology*, vol. 189, no. 7, pp. 3669–3680, 2012.

[118] S. A. Villalta, C. Rinaldi, B. Deng, G. Liu, B. Fedor, and J. G. Tidball, "Interleukin-10 reduces the pathology of mdx muscular dystrophy by deactivating M1 macrophages and modulating macrophage phenotype," *Human Molecular Genetics*, vol. 20, no. 4, pp. 790–805, 2011.

[119] M. Wehling-Henricks, M. C. Jordan, T. Gotoh, W. W. Grody, K. P. Roos, and J. G. Tidball, "Arginine metabolism by macrophages promotes cardiac and muscle fibrosis in mdx muscular dystrophy," *PLoS One*, vol. 5, no. 5, article e10763, 2010.

[120] O. Spadaro, C. D. Camell, L. Bosurgi et al., "IGF1 shapes macrophage activation in response to immunometabolic challenge," *Cell Reports*, vol. 19, no. 2, pp. 225–234, 2017.

[121] J. P. Barrett, A. M. Minogue, A. Falvey, and M. A. Lynch, "Involvement of IGF-1 and Akt in M1/M2 activation state in bone marrow-derived macrophages," *Experimental Cell Research*, vol. 335, no. 2, pp. 258–268, 2015.

[122] H. Lu, D. Huang, R. M. Ransohoff, and L. Zhou, "Acute skeletal muscle injury: CCL2 expression by both monocytes and injured muscle is required for repair," *The FASEB Journal*, vol. 25, no. 10, pp. 3344–3355, 2011.

[123] E. R. Barton-Davis, D. I. Shoturma, A. Musaro, N. Rosenthal, and H. L. Sweeney, "Viral mediated expression of insulin-like growth factor I blocks the aging-related loss of skeletal muscle function," *Proceedings of the National Academy of Sciences of the United States of America*, vol. 95, no. 26, pp. 15603–15607, 1998.

[124] Z. Laron, B. Klinger, A. Silbergeld, R. Lewin, B. Erster, and I. Gil-Ad, "Intravenous administration of recombinant IGF-I lowers serum GHRH and TSH," *Acta Endocrinologica*, vol. 123, no. 3, pp. 378–382, 1990.

[125] M. N. Pollak, C. Polychronakos, and M. Richard, "Insulinlike growth factor I: a potent mitogen for human osteogenic sarcoma," *Journal of the National Cancer Institute*, vol. 82, no. 4, pp. 301–305, 1990.

[126] H. B. Sager, P. Dutta, J. E. Dahlman et al., "RNAi targeting multiple cell adhesion molecules reduces immune cell recruitment and vascular inflammation after myocardial infarction," *Science Translational Medicine*, vol. 8, no. 342, article 342ra80, 2016.

[127] P. M. Mountziaris, S. N. Tzouanas, D. C. Sing, P. R. Kramer, F. K. Kasper, and A. G. Mikos, "Intra-articular controlled release of anti-inflammatory siRNA with biodegradable polymer microparticles ameliorates temporomandibular joint inflammation," *Acta Biomaterialia*, vol. 8, no. 10, pp. 3552–3560, 2012.

[128] L.-S. Zhou, G. L. Zhao, Q. Liu, S. C. Jiang, Y. Wang, and D. M. Zhang, "Silencing collapsin response mediator protein-2 reprograms macrophage phenotype and improves infarct healing in experimental myocardial infarction model," *Journal of Inflammation*, vol. 12, no. 1, p. 11, 2015.

[129] C. Giordano, K. Mojumdar, F. Liang et al., "Toll-like receptor 4 ablation in mdx mice reveals innate immunity as a therapeutic target in Duchenne muscular dystrophy," *Human Molecular Genetics*, vol. 24, no. 8, pp. 2147–2162, 2014.

[130] G. Courties, M. Baron, J. Presumey et al., "Cytosolic phospholipase $A_2\alpha$ gene silencing in the myeloid lineage alters development of Th1 responses and reduces disease severity in collagen-induced arthritis," *Arthritis & Rheumatism*, vol. 63, no. 3, pp. 681–690, 2011.

[131] K. Mojumdar, C. Giordano, C. Lemaire et al., "Divergent impact of Toll-like receptor 2 deficiency on repair mechanisms in healthy muscle versus Duchenne muscular dystrophy," *The Journal of Pathology*, vol. 239, no. 1, pp. 10–22, 2016.

[132] K. Essandoh, Y. Li, J. Huo, and G. C. Fan, "MiRNA-mediated macrophage polarization and its potential role in the regulation of inflammatory response," *Shock*, vol. 46, no. 2, pp. 122–131, 2016.

[133] A. A. Chaudhuri, A. Y. L. So, N. Sinha et al., "MicroRNA-125b potentiates macrophage activation," *The Journal of Immunology*, vol. 187, no. 10, pp. 5062–5068, 2011.

[134] P. Thulin, T. Wei, O. Werngren et al., "MicroRNA-9 regulates the expression of peroxisome proliferator-activated receptor δ in human monocytes during the inflammatory response," *International Journal of Molecular Medicine*, vol. 31, no. 5, pp. 1003–1010, 2013.

[135] R. T. Martinez-Nunez, F. Louafi, and T. Sanchez-Elsner, "The interleukin 13 (IL-13) pathway in human macrophages is modulated by microRNA-155 via direct targeting of interleukin 13 receptor α1 (IL13Rα1)," *Journal of Biological Chemistry*, vol. 286, no. 3, pp. 1786–1794, 2011.

[136] S. Banerjee, N. Xie, H. Cui et al., "MicroRNA let-7c regulates macrophage polarization," *The Journal of Immunology*, vol. 190, no. 12, pp. 6542–6549, 2013.

[137] E. Vergadi, K. Vaporidi, E. E. Theodorakis et al., "Akt2 deficiency protects from acute lung injury via alternative macrophage activation and miR-146a induction in mice," *The Journal of Immunology*, vol. 192, no. 1, pp. 394–406, 2014.

[138] F. Liu, Y. Li, R. Jiang et al., "miR-132 inhibits lipopolysaccharide-induced inflammation in alveolar macrophages by the cholinergic anti-inflammatory pathway," *Experimental Lung Research*, vol. 41, no. 5, pp. 261–269, 2015.

[139] T. Veremeyko, S. Siddiqui, I. Sotnikov, A. Yung, and E. D. Ponomarev, "IL-4/IL-13-dependent and independent expression of miR-124 and its contribution to M2 phenotype of monocytic cells in normal conditions and during allergic inflammation," *PLoS One*, vol. 8, no. 12, article e81774, 2013.

[140] T. Nakasa, M. Ishikawa, M. Shi, H. Shibuya, N. Adachi, and M. Ochi, "Acceleration of muscle regeneration by local injection of muscle-specific microRNAs in rat skeletal muscle injury model," *Journal of Cellular and Molecular Medicine*, vol. 14, no. 10, pp. 2495–2505, 2010.

[141] Y. Zhang, Z. Wang, and R. A. Gemeinhart, "Progress in microRNA delivery," *Journal of Controlled Release*, vol. 172, no. 3, pp. 962–974, 2013.

[142] P. P. Tak and G. S. Firestein, "NF-kappaB: a key role in inflammatory diseases," *The Journal of Clinical Investigation*, vol. 107, no. 1, pp. 7–11, 2001.

[143] S. Acharyya, S. A. Villalta, N. Bakkar et al., "Interplay of IKK/NF-κB signaling in macrophages and myofibers promotes muscle degeneration in Duchenne muscular dystrophy," *The Journal of Clinical Investigation*, vol. 117, no. 4, pp. 889–901, 2007.

[144] D. W. Hammers, M. M. Sleeper, S. C. Forbes et al., "Disease-modifying effects of orally bioavailable NF-κB inhibitors in dystrophin-deficient muscle," *JCI Insight*, vol. 1, no. 21, article e90341, 2016.

[145] T. Lawrence, "The Nuclear Factor NF-κB Pathway in Inflammation," *Cold Spring Harbor Perspectives in Biology*, vol. 1, no. 6, article a001651, 2009.

[146] T. Lawrence, D. W. Gilroy, P. R. Colville-Nash, and D. A. Willoughby, "Possible new role for NF-κB in the resolution of inflammation," *Nature Medicine*, vol. 7, no. 12, pp. 1291–1297, 2001.

[147] D. Bayik, D. Tross, L. A. Haile, D. Verthelyi, and D. M. Klinman, "Regulation of the maturation of human monocytes into immunosuppressive macrophages," *Blood Advances*, vol. 1, no. 26, pp. 2510–2519, 2017.

[148] C. H. Y. Fong, M. Bebien, A. Didierlaurent et al., "An antiinflammatory role for IKKβ through the inhibition of "classical" macrophage activation," *Journal of Experimental Medicine*, vol. 205, no. 6, pp. 1269–1276, 2008.

[149] J. Dort, A. Sirois, N. Leblanc, C. H. Côté, and H. Jacques, "Beneficial effects of cod protein on skeletal muscle repair following injury," *Applied Physiology, Nutrition, and Metabolism*, vol. 37, no. 3, pp. 489–498, 2012.

[150] J. Dort, N. Leblanc, J. Maltais-Giguère, B. Liaset, C. H. Côté, and H. Jacques, "Beneficial effects of cod protein on inflammatory cell accumulation in rat skeletal muscle after injury are driven by its high levels of arginine, glycine, taurine and lysine," *PLoS One*, vol. 8, no. 10, article e77274, 2013.

[151] J. Dort, N. Leblanc, J. Maltais-Giguère, B. Liaset, C. H. Côté, and H. Jacques, "Shrimp protein hydrolysate modulates the timing of proinflammatory macrophages in bupivacaine-injured skeletal muscles in rats," *BioMed Research International*, vol. 2016, Article ID 5214561, 13 pages, 2016.

[152] F. Alarcon-Aguilar, J. Almanza-Perez, G. Blancas et al., "Glycine regulates the production of pro-inflammatory cytokines in lean and monosodium glutamate-obese mice," *European Journal of Pharmacology*, vol. 599, no. 1-3, pp. 152–158, 2008.

[153] K. Hnia, J. Gayraud, G. Hugon et al., "L-Arginine decreases inflammation and modulates the nuclear factor-κB/matrix metalloproteinase cascade in mdx muscle fibers," *The American Journal of Pathology*, vol. 172, no. 6, pp. 1509–1519, 2008.

[154] C. Kim and Y. N. Cha, "Production of reactive oxygen and nitrogen species in phagocytes is regulated by taurine chloramine," *Advances in Experimental Medicine and Biology*, vol. 643, pp. 463–472, 2009.

[155] N. Schaefer, K. Tahara, S. Schuchtrup et al., "Perioperative glycine treatment attenuates ischemia/reperfusion injury and ameliorates smooth muscle dysfunction in intestinal transplantation," *Transplantation*, vol. 85, no. 9, pp. 1300–1310, 2008.

[156] S. W. Schaffer, J. Azuma, and M. Mozaffari, "Role of antioxidant activity of taurine in diabetes," *Canadian Journal of Physiology and Pharmacology*, vol. 87, no. 2, pp. 91–99, 2009.

[157] G. B. Schuller-Levis and E. Park, "Taurine: new implications for an old amino acid," *FEMS Microbiology Letters*, vol. 226, no. 2, pp. 195–202, 2003.

[158] L. A. Silva, P. C. L. Silveira, M. M. Ronsani et al., "Taurine supplementation decreases oxidative stress in skeletal muscle

after eccentric exercise," *Cell Biochemistry & Function*, vol. 29, no. 1, pp. 43–49, 2011.

[159] S. Li, Y. Sun, C. P. Liang et al., "Defective phagocytosis of apoptotic cells by macrophages in atherosclerotic lesions of ob/ob mice and reversal by a fish oil diet," *Circulation Research*, vol. 105, no. 11, pp. 1072–1082, 2009.

[160] H. Tayyebi-Khosroshahi, J. Houshyar, R. Dehgan-Hesari et al., "Effect of treatment with omega-3 fatty acids on C-reactive protein and tumor necrosis factor-alfa in hemodialysis patients," *Saudi Journal of Kidney Diseases and Transplantation*, vol. 23, no. 3, pp. 500–506, 2012.

[161] P. C. Calder, "Omega-3 fatty acids and inflammatory processes," *Nutrients*, vol. 2, no. 3, pp. 355–374, 2010.

[162] P. C. Calder, "Omega-3 polyunsaturated fatty acids and inflammatory processes: nutrition or pharmacology?," *British Journal of Clinical Pharmacology*, vol. 75, no. 3, pp. 645–662, 2013.

[163] B. Xue, Z. Yang, X. Wang, and H. Shi, "Omega-3 polyunsaturated fatty acids antagonize macrophage inflammation via activation of AMPK/SIRT1 pathway," *PLoS One*, vol. 7, no. 10, article e45990, 2012.

[164] L. M. Apolinário, S. C. de Carvalho, H. Santo Neto, and M. J. Marques, "Long-term therapy with omega-3 ameliorates myonecrosis and benefits skeletal muscle regeneration in *mdx* mice," *The Anatomical Record*, vol. 298, no. 9, pp. 1589–1596, 2015.

[165] A. F. Mauricio, J. A. Pereira, H. S. Neto, and M. J. Marques, "Effects of fish oil containing eicosapentaenoic acid and docosahexaenoic acid on dystrophic mdx mice hearts at later stages of dystrophy," *Nutrition*, vol. 32, no. 7-8, pp. 855–862, 2016.

[166] Y. Okabe and R. Medzhitov, "Tissue-specific signals control reversible program of localization and functional polarization of macrophages," *Cell*, vol. 157, no. 4, pp. 832–844, 2014.

[167] H. D. Dawson, C. Chen, and J. F. Urban, "The regulatory actions of retinoic acid on M2a macrophage polarization of porcine and human myeloid-derived cells," *The Journal of Immunology*, vol. 198, Supplement 1, 2017.

[168] A. Di Rocco, K. Uchibe, C. Larmour et al., "Selective retinoic acid receptor γ agonists promote repair of injured skeletal muscle in mouse," *The American Journal of Pathology*, vol. 185, no. 9, pp. 2495–2504, 2015.

[169] K. Muller, N. Odum, and K. Bendtzen, "1,25-Dihydroxyvitamin D_3 selectively reduces interleukin-2 levels and proliferation of human T cell lines in vitro," *Immunology Letters*, vol. 35, no. 2, pp. 177–182, 1993.

[170] F. Mattner, S. Smiroldo, F. Galbiati et al., "Inhibition of Th1 development and treatment of chronic-relapsing experimental allergic encephalomyelitis by a non-hypercalcemic analogue of 1,25-dihydroxyvitamin D_3," *European Journal of Immunology*, vol. 30, no. 2, pp. 498–508, 2000.

[171] F. Baeke, T. Takiishi, H. Korf, C. Gysemans, and C. Mathieu, "Vitamin D: modulator of the immune system," *Current Opinion in Pharmacology*, vol. 10, no. 4, pp. 482–496, 2010.

[172] M. Di Rosa, M. Malaguarnera, F. Nicoletti, and L. Malaguarnera, "Vitamin D3: a helpful immuno-modulator," *Immunology*, vol. 134, no. 2, pp. 123–139, 2011.

[173] G. W. Burton and K. U. Ingold, "Vitamin E as an *in vitro* and *in vivo* antioxidant," *Annals of the New York Academy of Sciences*, vol. 570, pp. 7–22, 1989.

[174] O. H. Bellock, *New Topics in Vitamin E Research*, Nova Publishers, 2006.

[175] L. Zhao, I. Kang, X. Fang et al., "Gamma-tocotrienol attenuates high-fat diet-induced obesity and insulin resistance by inhibiting adipose inflammation and M1 macrophage recruitment," *International Journal of Obesity*, vol. 39, no. 3, pp. 438–446, 2015.

[176] T. Koga, P. Kwan, L. Zubik, C. Ameho, D. Smith, and M. Meydani, "Vitamin E supplementation suppresses macrophage accumulation and endothelial cell expression of adhesion molecules in the aorta of hypercholesterolemic rabbits," *Atherosclerosis*, vol. 176, no. 2, pp. 265–272, 2004.

[177] B. N. Brown, B. D. Ratner, S. B. Goodman, S. Amar, and S. F. Badylak, "Macrophage polarization: an opportunity for improved outcomes in biomaterials and regenerative medicine," *Biomaterials*, vol. 33, no. 15, pp. 3792–3802, 2012.

[178] G. S. A. Boersema, N. Grotenhuis, Y. Bayon, J. F. Lange, and Y. M. Bastiaansen-Jenniskens, "The effect of biomaterials used for tissue regeneration purposes on polarization of macrophages," *BioResearch Open Access*, vol. 5, no. 1, pp. 6–14, 2016.

[179] J. A. Hunt, R. Chen, D. Williams, and Y. Bayon, *Surgical materials*, Ullmann's Encyclopedia of Industrial Chemistry, 2012.

[180] A. S. Halim, T. L. Khoo, and J. M. Y. Shah, "Biologic and synthetic skin substitutes: an overview," *Indian Journal of Plastic Surgery*, vol. 43, pp. 23–28, 2010.

[181] B. M. Sicari, S. A. Johnson, B. F. Siu et al., "The effect of source animal age upon the in vivo remodeling characteristics of an extracellular matrix scaffold," *Biomaterials*, vol. 33, no. 22, pp. 5524–5533, 2012.

[182] S. B. Orenstein, Y. Qiao, U. Klueh, D. L. Kreutzer, and Y. W. Novitsky, "Activation of human mononuclear cells by porcine biologic meshes in vitro," *Hernia*, vol. 14, no. 4, pp. 401–407, 2010.

[183] S. F. Badylak, J. E. Valentin, A. K. Ravindra, G. P. McCabe, and A. M. Stewart-Akers, "Macrophage phenotype as a determinant of biologic scaffold remodeling," *Tissue Engineering Part A*, vol. 14, no. 11, pp. 1835–1842, 2008.

[184] M. Bartneck, V. A. Schulte, N. E. Paul, M. Diez, M. C. Lensen, and G. Zwadlo-Klarwasser, "Induction of specific macrophage subtypes by defined micro-patterned structures," *Acta Biomaterialia*, vol. 6, no. 10, pp. 3864–3872, 2010.

[185] K. Garg, N. A. Pullen, C. A. Oskeritzian, J. J. Ryan, and G. L. Bowlin, "Macrophage functional polarization (M1/M2) in response to varying fiber and pore dimensions of electrospun scaffolds," *Biomaterials*, vol. 34, no. 18, pp. 4439–4451, 2013.

[186] P. C. S. Bota, A. M. B. Collie, P. Puolakkainen et al., "Biomaterial topography alters healing *in vivo* and monocyte/macrophage activation *in vitro*," *Journal of Biomedical Materials Research Part A*, vol. 95A, no. 2, pp. 649–657, 2010.

[187] C. R. Almeida, T. Serra, M. I. Oliveira, J. A. Planell, M. A. Barbosa, and M. Navarro, "Impact of 3-D printed PLA- and chitosan-based scaffolds on human monocyte/macrophage responses: unraveling the effect of 3-D structures on inflammation," *Acta Biomaterialia*, vol. 10, no. 2, pp. 613–622, 2014.

[188] M. T. Wolf, C. L. Dearth, C. A. Ranallo et al., "Macrophage polarization in response to ECM coated polypropylene mesh," *Biomaterials*, vol. 35, no. 25, pp. 6838–6849, 2014.

[189] X. Qiu, S. Liu, H. Zhang et al., "Mesenchymal stem cells and extracellular matrix scaffold promote muscle regeneration by synergistically regulating macrophage polarization toward the M2 phenotype," *Stem Cell Research & Therapy*, vol. 9, no. 1, p. 88, 2018.

[190] C. A. Cezar and D. J. Mooney, "Biomaterial-based delivery for skeletal muscle repair," *Advanced Drug Delivery Reviews*, vol. 84, pp. 188–197, 2015.

[191] B. N. Brown, J. E. Valentin, A. M. Stewart-Akers, G. P. McCabe, and S. F. Badylak, "Macrophage phenotype and remodeling outcomes in response to biologic scaffolds with and without a cellular component," *Biomaterials*, vol. 30, no. 8, pp. 1482–1491, 2009.

[192] T. H. Qazi, D. J. Mooney, M. Pumberger, S. Geißler, and G. N. Duda, "Biomaterials based strategies for skeletal muscle tissue engineering: existing technologies and future trends," *Biomaterials*, vol. 53, pp. 502–521, 2015.

[193] D. Zhu, N. Yang, Y. Y. Liu, J. Zheng, C. Ji, and P. P. Zuo, "M2 macrophage transplantation ameliorates cognitive dysfunction in amyloid-β-treated rats through regulation of microglial polarization," *Journal of Alzheimer's Disease*, vol. 52, no. 2, pp. 483–495, 2016.

[194] Q. Liang, T. Liu, L. Feng, L. Deng, P. Rong, and W. Wang, "Effect of M2 macrophage against rejection on islet allografts in diabetic mice," *Zhong Nan Da Xue Xue Bao Yi Xue Ban*, vol. 42, no. 7, pp. 783–789, 2017.

[195] P. L. Hsieh, V. Rybalko, A. B. Baker, L. J. Suggs, and R. P. Farrar, "Recruitment and therapeutic application of macrophages in skeletal muscles after hind limb ischemia," *Journal of Vascular Surgery*, vol. 67, no. 6, pp. 1908–1920.e1, 2018.

[196] V. Rybalko, P. L. Hsieh, M. Merscham-Banda, L. J. Suggs, and R. P. Farrar, "The development of macrophage-mediated cell therapy to improve skeletal muscle function after injury," *PLoS One*, vol. 10, no. 12, article e0145550, 2015.

[197] E. R. Chernykh, E. Y. Shevela, N. M. Starostina et al., "Safety and therapeutic potential of M2 macrophages in stroke treatment," *Cell Transplantation*, vol. 25, no. 8, pp. 1461–1471, 2016.

[198] E. R. Chernykh, M. Y. Kafanova, E. Y. Shevela et al., "Clinical experience with autologous M2 macrophages in children with severe cerebral palsy," *Cell Transplantation*, vol. 23, Supplement 1, pp. 97–104, 2014.

[199] M. Bencze, E. Negroni, D. Vallese et al., "Proinflammatory macrophages enhance the regenerative capacity of human myoblasts by modifying their kinetics of proliferation and differentiation," *Molecular Therapy*, vol. 20, no. 11, pp. 2168–2179, 2012.

[200] K. Gavrilov and W. M. Saltzman, "Therapeutic siRNA: principles, challenges, and strategies," *Yale Journal of Biology and Medicine*, vol. 85, no. 2, p. 187, 2012.

[201] K. Bazaka and M. Jacob, "Implantable devices: issues and challenges," *Electronics*, vol. 2, no. 4, pp. 1–34, 2013.

Hindawi
Stem Cells International
Volume 2019, Article ID 2785207, 16 pages
https://doi.org/10.1155/2019/2785207

Research Article

Identification of Aberrantly Expressed Genes during Aging in Rat Nucleus Pulposus Cells

Shi Cheng,[1] **Xiaochuan Li**,[2,3] **Linghan Lin**,[4] **Zhiwei Jia**,[5] **Yachao Zhao**,[4] **Deli Wang**,[6,7] **Dike Ruan**,[4] **and Yu Zhang**[1]

[1]*Department of Orthopedics, Guangdong General Hospital, Guangdong Academy of Medical Science, South China University of Technology, Guangzhou 510080, China*
[2]*Department of Orthopedic Surgery, Gaozhou People's Hospital, Guangdong 525200, China*
[3]*Post-Doctoral Innovation Practice Base of Gaozhou People's Hospital, Guangdong 525200, China*
[4]*Department of Orthopaedics, The Sixth Medical Centre of PLA General Hospital, 100048 Beijing, China*
[5]*Department of Orthopaedics, The 306th Hospital of People's Liberation Army, Beijing, China*
[6]*Department of Bone & Joint Surgery, Peking University Shenzhen Hospital, Shenzhen, 518036 Guangdong, China*
[7]*National & Local Joint Engineering Research Center of Orthopaedic Biomaterials, Peking University Shenzhen Hospital, Shenzhen, 518036 Guangdong, China*

Correspondence should be addressed to Deli Wang; wangdelinavy@163.com, Dike Ruan; ruandikengh@163.com, and Yu Zhang; luck_2001@126.com

Received 2 March 2019; Revised 6 May 2019; Accepted 30 May 2019; Published 10 July 2019

Guest Editor: Zhen Li

Nucleus pulposus cells (NPCs) play a vital role in maintaining the homeostasis of the intervertebral disc (IVD). Previous studies have discovered that NPCs exhibited malfunction due to cellular senescence during disc aging and degeneration; this might be one of the key factors of IVD degeneration. Thus, we conducted this study in order to investigate the altered biofunction and the underlying genes and pathways of senescent NPCs. We isolated and identified NPCs from the tail discs of young (2 months) and old (24 months) SD rats and confirmed the senescent phenotype through SA-β-gal staining. CCK-8 assay, transwell assay, and cell scratch assay were adopted to detect the proliferous and migratory ability of two groups. Then, a rat Gene Chip Clariom™ S array was used to detect differentially expressed genes (DEGs). After rigorous bioinformatics analysis of the raw data, totally, 1038 differentially expressed genes with a fold change > 1.5 were identified out of 23189 probes. Among them, 617 were upregulated and 421 were downregulated. Furthermore, Gene Ontology (GO) and Kyoto Encyclopedia of Genes and Genomes (KEGG) pathway analysis were conducted and revealed numerous number of enriched GO terms and signaling pathways associated with senescence of NPCs. A protein-protein interaction (PPI) network of the DEGs was constructed using the Search Tool for the Retrieval of Interacting Genes (STRING) database and Cytoscape software. Module analysis was conducted for the PPI network using the MCODE plugin in Cytoscape. Hub genes were identified by the CytoHubba plugin in Cytoscape. Derived 5 hub genes and most significantly up- or downregulated genes were further verified by real-time PCR. The present study investigated underlying mechanisms in the senescence of NPCs on a genome-wide scale. The illumination of molecular mechanisms of NPCs senescence may assist the development of novel biological methods to treat degenerative disc diseases.

1. Introduction

Low back pain (LBP) is a major age-related disease, not only contributing to patients' suffering and disability but also causing large financial burden to society [1]. Intervertebral disc degeneration (IVDD) has been confirmed to be one of the most fundamental pathological changes of LBP [2]. Due to a largely unknown mechanism of IVDD, effective therapy methods still need investigation.

Traditional therapy strategies including surgery and conservative therapy are aimed at alleviating symptoms instead of regenerating the degenerated disc. Thus, biological approaches which mainly focus on restoring the structure and function of the IVD are considered more promising [3, 4]. The structure of the intervertebral disc could be divided into three different regions: nucleus pulposus (NP), annulus fibrosus (AF), and cartilaginous endplate (CEP) [5]. NP is a kind of gelatinous tissue containing extracellular matrix (ECM) comprising highly hydrated proteoglycan, collagen fibers, and aggrecan [6]. It plays a vital role in maintaining the physiological function of IVD because NP could absorb stress when the IVD is confronting diverse mechanical impact [7]. Nucleus pulposus cells (NPCs) are the organ-specific cells residing in the nucleus pulposus [8]. NPCs are responsible for the metabolism homeostasis of the ECM by producing collagen I, collagen II, and proteoglycan, which are the main components of the gelatinous structures of NP [9]. During aging and degeneration of IVD, the normal function of NPCs was disrupted, thus resulting in aberrant metabolism of ECM, which could accelerate the process of IVDD [10, 11]. Cytotherapy by reactivate degenerated NPCs has been proposed to be an ideal biological therapy method to treat IVDD [11]. However, the specific mechanism of NPC degeneration is still unknown, which hindered the development of cytotherapy.

Cell senescence is defined as a cellular program that leads to a stable growth arrest along with distinct phenotypic alterations and presentation of senescence-associated secretory phenotype (SASP) [12, 13]. Senescence of disc cells has been widely accepted as one of the major factors of IVD degeneration and aging [14, 15]. The number of viable cell in NP was decreased, and the cellular function of NPCs is being impaired with age, eventually leading to biomechanical failure and degeneration of IVD [15, 16]. There were two historically forms of senescence: one is replicative senescence which is related to shortened telomere length; the other is stress-induced premature senescence which is induced by a variety of environmental stimuli [17, 18]. Among them, time-dependent accumulation of cell replication and replicative senescence is considered to be more related with aging [19]. Accumulating researches focus on rejuvenating aged NPCs by preventing senescence [11]. However, little progress has been achieved due to the unclear potential regulators or mechanisms of senescence of NPCs. Therefore, elucidating the major regulators and mechanisms underlying NPCs senescence will help us better understand the pathogenesis of IVD aging and degeneration and may illustrate a new therapy target to rejuvenate aged IVD.

Gene microarray technology can simultaneously analyse differences in the expression level of thousands of genes from predefined groups of samples [20]. It also has the advantage of highly effective evaluation of whole genome-wide expression changes [21]. This technology gives researchers a novel point of view to investigate the mechanism of different diseases more deeply. Although the senescence of NPCs plays an important role during IVDD, yet there were limited number of studies that focus on the aberrantly expressed genes during NPC aging.

Thus, the aim of this study was to investigate the abnormally expressed mRNA and signaling pathways during NPC aging by the method of microarray analysis and bioinformatics analysis. We also compared the migration capability between young and old NPCs because decreased migration of IVD cells may be another important reason for the declining regenerative potential of IVD. These analyses may help to elucidate the senescence mechanism of NPCs, which will contribute in identifying the key factors necessary to rejuvenate NPCs in IVDD patients and promoting the effect of cytotherapy in IVDD.

2. Materials and Methods

2.1. Ethic Statement. All experimental procedures described blow were reviewed and approved by the Laboratory Animal Ethics Committee of The Sixth Medical Centre of PLA General Hospital, Beijing, China, and carried out in accordance with the relevant guidelines and regulations.

2.2. Isolation and Culture of NPCs. 12 Sprague-Dawley (SD) rats were involved in this experiment and were divided into two groups according to their age: the young group ($n = 6$, 2 months old) and old group ($n = 6$, 24 months old). 24-month-old rats were defined as the old group according to a previous study [22]. Then, they were sacrificed by intraperitoneal injection of 5 ml 10% chloral hydrate. After being soaked in 70% ethanol for 1 h, the coccygeal NP tissues (C3-C7) of each rat were collected by ophthalmic surgical instruments under a sterile dissecting microscope. After being washed with PBS for three times, the harvested NP tissues were mechanically minced and digested with 0.2% collagenase II (Sigma-Aldrich, St. Louis, MO, USA) in Dulbecco's modified Eagle's medium-low glucose (DMEM-LG, Solarbio Science & Technology Co. Ltd., Beijing, China) for 4 h. The suspension was centrifuged at 1000 rpm/min for 5 min. Then, the suspension solution was discarded, and the pellets were resuspended with standard culture medium containing DMEM-LG, 10% FBS (Gibco BRL, Grand Island, NY, USA), and 1% penicillin-streptomycin (Hyclone, USA). Finally, the cell pellets were cultured in 25 cm^2 cell culture flasks in a humidified incubator at 37°C and 5% CO_2. The culture medium was replaced every two days. When the cells reached 70-80% confluence, they were collected using 0.25% trypsin-EDTA (Gibco, USA) and subcultured at 1 : 3; cells at passage 2 were used for experiment.

2.3. Cell Phenotype Identification. To identify the cell phenotype of young and old NPCs, a series of surface markers were

detected. Both groups of NPCs at P2 were collected and resuspended in cold PBS to a concentration of 1×10^6 cells/ml. Then, 100 μl cell suspension was incubated with antibodies against CD34-PE, CD24-FITC, CD29-PE, CD45-FITC, and CD90-PerCP-Cy5.5 (Abcam, Cambridge, MA, USA) for 30 min at 4°C in the dark. Then, cells were washed twice and resuspended in 500 μl PBS. Finally, quantitative analyses for the expression of surface markers of each samples were performed using the FACSCalibur system (FACScan, BD, USA).

2.4. Senescence-Associated β-Galactosidase (SA-β-gal) Staining. When NPCs were cultured to 80%-90% confluence, SA-β-gal staining (Beyotime Institute of Biotechnology, China) was performed to analyse the rate of senescent cells in the young and old groups according to the manufacturers' protocol. Briefly, cells were washed by PBS for three times, then fixed with fixative solution for 15 minutes at RT, washed twice with PBS, and stained with X-Gal containing SA-β-gal working solution overnight at 37°C without CO_2. Quantification analysis was performed under fluorescence microscopy by determining the average percentage of total SA-β-gal-positive cells in 5 randomly selected fields of each well.

2.5. Cell Counting Kit-8 Proliferation Assay. To compare the proliferation ability of young and old NPCs, P2 cells were plated at a 96-well plate at 1000 cells/well and cultured in standard medium containing 10% FBS for 1, 3, 5, 7, and 9 days. At each time point, the medium was replaced by the mixture solution which contains 100 μl fresh medium and 10 μl CCK-8 reagent. After being incubated in the humidified incubator at 37°C and 5% CO_2 for 4 h, the absorbance of each sample was measured at 450 nm using a microplate reader (Model 680, Bio-Rad Laboratories K.K., Tokyo, Japan).

2.6. Cell Scratch Assay. Young and old NPCs were seeded in 6-well plates at a concentration of 1×10^5 cells/ml. After growing to 100% confluence, parallel scratches were made at the bottom of the 6-well plate with a 200 ml pipet tip. The suspended cells were washed off with serum-free medium, and the width of the scratches was observed and pictured at 0 h and 24 h under an Olympus photomicroscope. The migration of the cells was determined by measuring the distance between the wound edges using ImageJ software. Three different areas were measured for each group, and the average distance was calculated for analysis.

2.7. Transwell Assay. The migration capability of young and old NPCs was evaluated with transwell cell culture chambers (pore size 8 μm, Corning, USA), and these chambers were inserted into 24-well plates. The lower chamber was filled with 600 ml medium with 10% FBS, and the upper chamber contained 150 μl of DMEM along and 5×10^4 cells. After 24 h, the media in both chambers were removed and the non-migratory cells in the upper chamber were wiped off gently by a cotton swab. After being fixed with 4% paraformaldehyde, the migrated cells in the lower chamber were stained with 0.1% crystal violet at room temperature for 30 min. Then, cells traversing the membranes were counted in three randomly selected areas under a light microscope (Olympus Optical Co. Ltd., Tokyo, Japan) at 100x magnification.

2.8. RNA Extraction and Quality Control. After being grown to 90% confluence, NPCs of the young and old groups were treated with Trizol. Then, the total RNA was extracted and purified with an RNase Kit (Bio-Rad, CA, USA). The quality of derived mRNA was measured by a spectrophotometer (NanoDrop-1000, Thermo Scientific, MA, USA). The mRNA integrity and DNA contamination were detected by agarose-gel electrophoresis (results are shown in supplementary materials (available here)).

2.9. Microarray Analysis. Obtained RNA from young and old NPCs was hybridised to Rat GeneChip Clariom™ S Array from Affymetrix Corporation. The procedures of hybridization and scanning of the microarray were performed according to Whole Transcript (WT) Expression Arrays User Guide of Affymetrix Corporation. Briefly, after the process of probe set signal integration, background correction, and quantile normalisation, these files were transferred to the Affymetrix Transcriptome Analysis Console software to analyse the differentially expressed genes (DEGs). The threshold set for up- and downregulated genes was fold change ≥ 1.5 and $P < 0.05$. The data had been uploaded to the NCBI Gene Expression Omnibus (GEO) and can be accessed via GEO Series accession [GEO:GSE126883] (https://www.ncbi.nlm.nih.gov/geo/query/acc.cgi?acc=GSE126883).

2.10. GO Functional and KEGG Pathway Enrichment Analysis. The Database for Annotation, Visualization, and Integrated Discovery (DAVID, http://david.abcc.ncifcrf.gov/) is a gene functional classification implement that accommodates a set of functional annotation tools for investigators to analyse the biological roles of genes and to perform GO (Gene Ontology) and KEGG (Kyoto Encyclopedia of Genes and Genomes) pathway enrichment analysis of DEGs. The functions and pathway enrichment of up- and downregulated DEGs were analysed using the DAVID database. A count > 2 and EASE > 0.1 was considered as the cut-off criteria.

2.11. PPI Network Construction and Module Analysis. Functional PPI analysis was essential to interpret the molecular mechanisms of key cellular activities. The Search Tool for the Retrieval of Interacting Genes (STRING, https://string-db.org/) database was adopted to obtain the PPI relationships for DEGs. Briefly, DEGs were uploaded to the STRING database, and the result which interaction score is more than 0.7 (high confidence) was visualized in Cytoscape software. Furthermore, significant modules were detected through the MCODE (Molecular Complex Detection) plugin in Cytoscape based on the constructed PPI networks with the criteria of K score = 4, Degree cut − off = 2; node score cut − off = 0.2 , and maximum depth = 100. GO functional and KEGG pathway enrichment analyses of the highest score module were performed using DAVID.

2.12. Identification of Hub Genes. Cytoscape software was applied to analyse the hub genes, which are important nodes

Table 1: Primers used for real-time PCR.

Gene name	Forward sequence 5′-3′	Reverse sequence 5′-3′
Fos	CAAACCGACCTACTGTCCC	ACCAACAACCTTGTCGTCATAT
Egr1	GCAACACTTTGTGGCCTGAA	GAGTTGGGACTGGTAGGTGT
Cxcl1	AAATGGTGAAGGTCGGTGTGAAC	CAACAATCTCCACTTTGCCACTG
Igf1	GCACTCTGCTTGCTCACCTTTA	TCCGAATGCTGGAGCCATA
Ptgs2	TTCGGGAGCACAACAGAGTG	TGAAGTGGTAACCGCTCAGG
Kininogen 1	ATGGTCCCGACTGTGAAATGCCAAG	CTATCTCTGGGTAGTCTGCTTTACAC
Periostin	ACAAGCCAACAAAAGGGTTCA	ACGGCCTTCTCTTGATCGC
GAPDH	GGCATCCTGGGCTACACT	CCACCACCCTGTTGCTGT

with many interaction partners. We utilized the CytoHubba plugin in Cytoscape to find hub genes and employed six calculation methods: Degree, EPC, EcCentricity, MCC, BottleNeck, and MNC. The intersecting genes derived using these six algorithms represent key candidate genes with important biological regulatory functions. These hub genes were further performed by GO and KEGG pathway enrichment analyses using the DAVID database.

2.13. Real-Time PCR. To validate the microarray results, derived 5 hub genes and the most significantly up- or downregulated genes were selected for the real-time PCR validation. Briefly, complementary DNA (cDNA) was synthesized by the reverse transcript using the Quantscript RT Kit (TianGen Biotech, China) according to the manufacturer's protocol. Then, derived cDNAs were taken for quantitative real-time PCR (qPCR) using a SYBR Premix Ex Taq™ (Tli RnaseH Plus; TaKaRa Bio, Otsu, Japan) in a Peltier thermal cycler (Bio-Rad Laboratories K.K., Tokyo, Japan) at an ultimate reaction volume of 20 μl. The cDNA was amplified for 40 cycles. GAPDH was selected as the internal control to calculate the relative expression of target genes by the $2^{-\Delta\Delta CT}$ method. All reactions were performed in triplicate, and the sequences of the used primers are shown in Table 1.

2.14. Statistical Analysis. All the data were expressed as the means ± SD. The comparative analyses between the groups were made by independent sample *t*-tests to determine the significant difference through SPSS 20.0 software (Chicago IL, USA). A chi-square test was adopted for enumeration data. $P < 0.05$ was considered statistically significant.

3. Results

3.1. Immunophenotypes of Young and Old NPCs. NPCs were successfully isolated from rat nucleus pulposus tissues. The P2 generation of young NPCs exhibited a characteristic of small, spindle-like morphology, with an abundant cytoplasm containing large ovoid and prominent nucleoli. Old NPCs had a more relatively round shape with polygonal and flat morphology (Figure 1(a)).

A series of cell surface antigens were selected to detect the cell surface marker of young and old NPCs [23, 24]. Both groups of NPCs were highly positive for CD29 and CD90 and CD24 (Figures 1(b) and 1(c)). However, the expression of CD24 was significantly lower in the old group than that in the young group ($P < 0.05$). The positive rates in the young group were CD29 (99.15 ± 0.67%), CD90 (97.63 ± 0.62%), and CD24 (92.68 ± 0.88%). The positive rates in the old group were CD29 (97.3 ± 1.26%), CD90 (96.36 ± 0.54%), and CD24 (77.91 ± 2.49%). All NPCs were negative for the hematopoietic stem cell markers CD34 (1.1 ± 0.4% in the young group and 3.98 ± 0.22% in the old group) and CD45 (3.98 ± 0.22% in the young group and 1.9 ± 0.16% in the old group) (Figures 1(b) and 1(c)).

3.2. β-Galactosidase (SA-β-gal) Staining and Aging-Related Decline in Proliferation and Migration Ability. β-Galactosidase (SA-β-gal) staining is a sensitive measurement to detect senescent cells, the results showed a higher positive staining cell percentage in the old group (45.32 ± 6.87%) than that in the young group (10.84 ± 1.41%) ($P < 0.05$) (Figures 2(a) and 2(b)). To assess the proliferation of young and old NPCs, CCK-8 assay was performed. Results showed old NPCs went into early plateau phase approx. 7 days after initially culture and young NPCs did not enter a growth plateau until 9 days of culture (Figure 2(c)). The migration ability was assessed through transwell assay and cell scratch assay. Results of transwell assay showed a decreased migration cell number in the old group (56.33 ± 8.327) compared with the young group cells (169.3 ± 16.44) ($P < 0.05$) (Figures 2(e) and 2(f)). Quantification of the migration area percent after 24 h of the young group (41.02 ± 6.13%) is higher than that of the old group (14.9 ± 3.15%) ($P < 0.05$), indicating a decreased migration speed of old NPCs (Figures 2(d) and 2(g)). Thus, our results clearly demonstrate a dramatic decrease in the proliferous and migratory capacity of NPCs during aging.

3.3. Identification of Differentially Expressed Genes. To detect molecular factors involved in NPC aging, we performed microchip hybridization with RNA from NPCs of the young and old groups. A total of 1038 differentially expressed genes (DEGs) were detected, including 617 upregulated genes and 421 downregulated genes. The upregulated genes refer to those increase expressed in old NPCs. Volcano plot was plotted to show the DEGs of two groups according to the gene expression values (Figure 3). The hierarchical clustering heat map is shown in the supplementary materials. The greatest upregulated gene is kininogen 1 (fold change = 25.06), followed by lipocalin 2, upregulated, and EGF-containing fibulin-like extracellular matrix protein 1, upregulated. The greatest downregulated gene is periostin (fold change = −24.05),

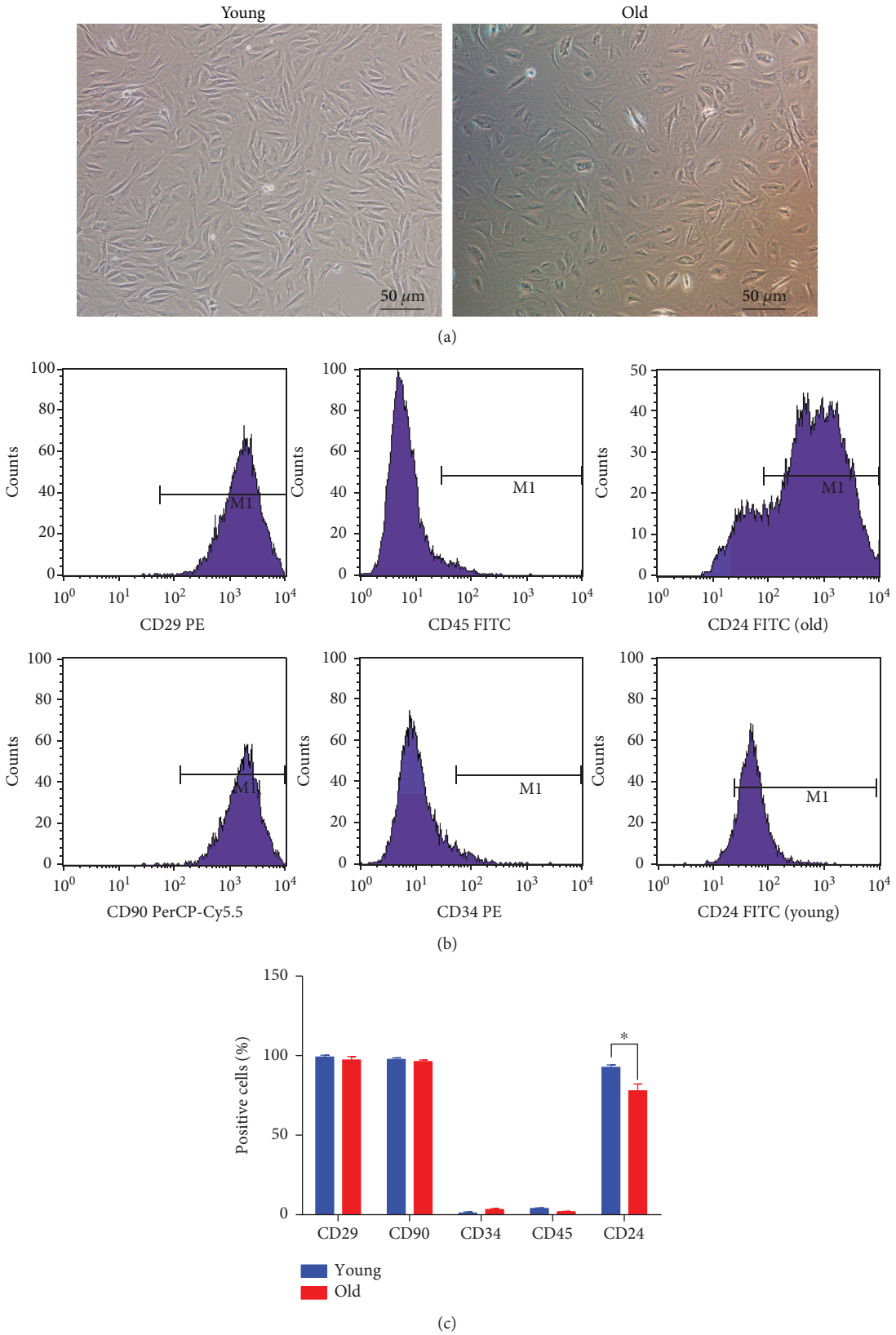

Figure 1: The cell morphology and immunophenotype identification of young and old NPCs. (a) Cell morphology of P2 young and old NPCs. (b, c) Both young and old NPCs exhibited high expression of CD29 and CD90 (>95%) and low expression of CD34 and CD45 (<5%). The expression of CD24 in the young group was 92.68 ± 0.88% and in the old group was 77.91 ± 2.49%. The difference of CD24 expression between young and old NPCs was significant ($P < 0.05$). $^{*}P < 0.05$ compared with the young group.

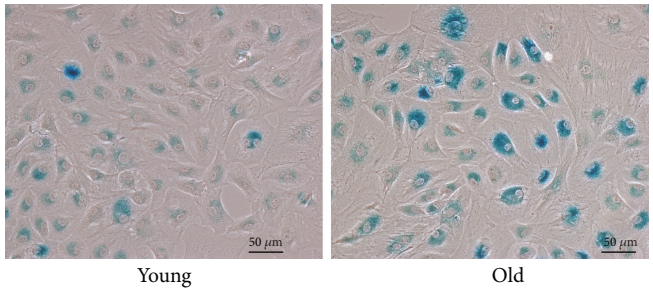

(a)

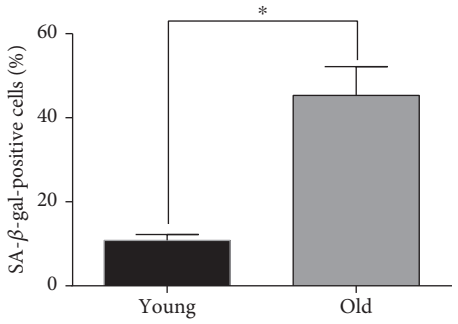

(b)

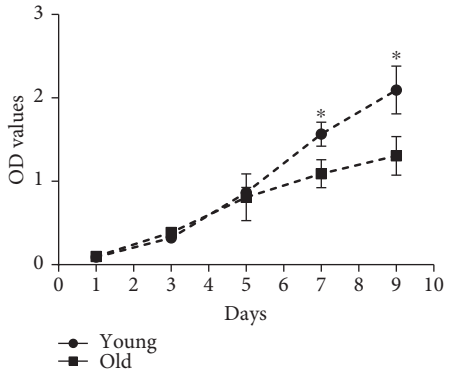

(c)

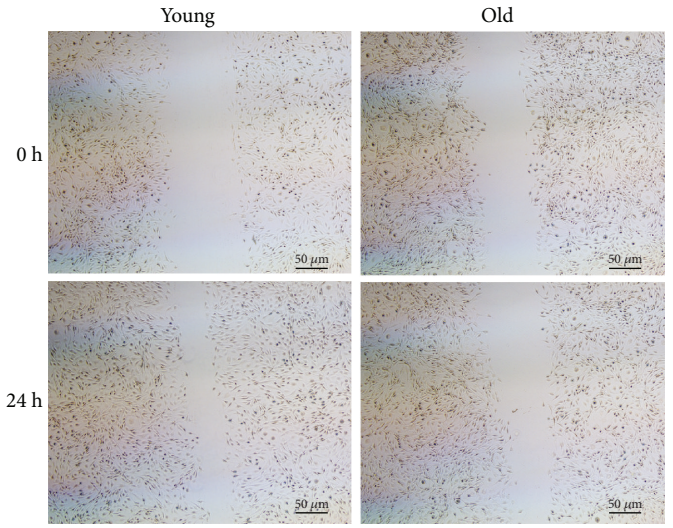

(d)

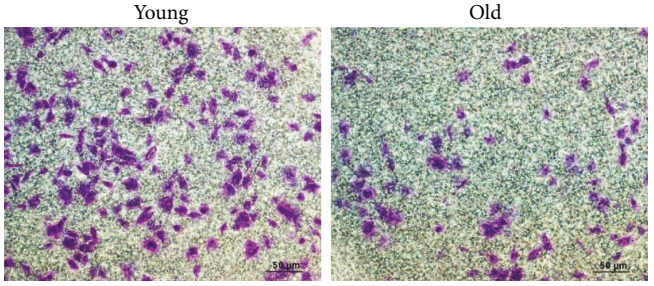

(e)

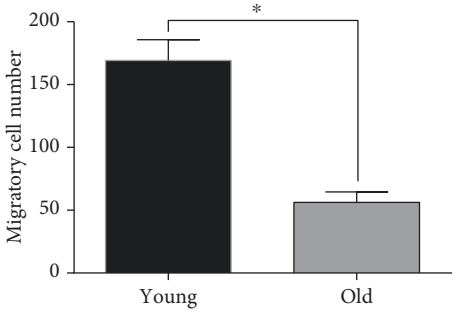

(f)

Figure 2: Continued.

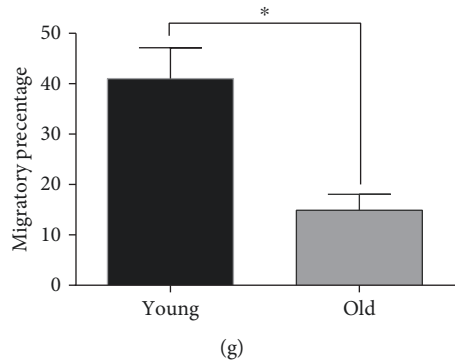

Figure 2: The aging phenotype and migration capacity of young and old NPCs. (a, b) Representative images of SA-β-gal staining for the detection of senescent NPCs from the young and old groups. Quantitative analysis showed that the senescent cell number in the old group was higher than that in the young group. (c) Cell proliferation curve detected by CCK-8 assay. The OD value is higher in the young group after 7 days culture, indicating a higher proliferation capability of young NPCs. (d, g) Cell scratch assay showed declined migrated percentage in old NPCs after 12 h. (e, f) Transwell assay showed a declined migrated cell number in the old group. All samples examined in triplicate. Data are presented as the mean ± SD. $^*P < 0.05$.

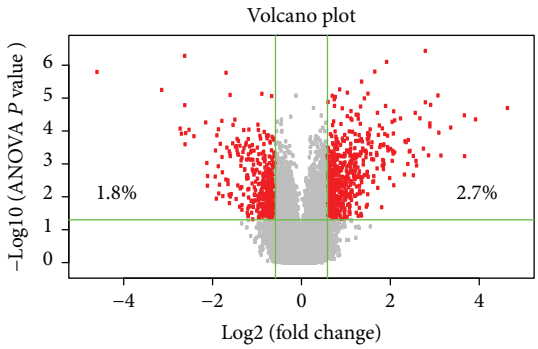

Figure 3: Volcano plot showed differentially expressed genes between the young and old groups. Volcano plot of differentially expressed genes in young and old group. Left: significantly downregulated genes, which account for 1.8% of total detected probes. Middle: nondifferentially expressed genes. Right: significantly upregulated genes, which account for 2.7% of total detected probes (based on |log2 FC| > 2 and $P < 0.05$). Heat map and hierarchical clustering of DEG profile comparison between the young and old NPCs are included in the supplementary materials.

followed by neuronal regeneration-related protein, downregulated, and dermatopontin, downregulated. The top 10 up- and downregulated genes are shown in Tables 2 and 3.

3.4. GO Functional and KEGG Pathway Enrichment Analysis of DEGs. The functions of up and downregulated DEGs were evaluated at DAVID. The GO analysis showed that, in terms of biological processes (BP), the upregulated genes were mainly enriched in response to lipopolysaccharide and response to organic cyclic compound and negative regulation of cell proliferation (Table 4 and Figure 4). The downregulated genes were mainly enriched in cell adhesion, endodermal cell differentiation, and ossification (Table 5 and Figure 5). In terms of cellular components (CC), upregulated genes were mainly enriched in the extracellular space and extracellular exosome (Table 4 and Figure 4). Downregulated genes were mainly enriched in the extracellular matrix and basement membrane (Table 5 and Figure 5). In terms of molecular function (MF), upregulated genes were mainly enriched in endopeptidase inhibitor activity and transcriptional activator activity (Table 4 and Figure 4), while

Table 2: The top 10 upregulated genes.

Gene names	Fold change	*P* value
Kininogen 1	25.06	2.00117*E*-05
Lipocalin 2	15.25	4.43512*E*-05
EGF-containing fibulin-like extracellular matrix protein 1	12.85	0.000583062
Collagen 14a1	12.81	3.332*E*-05
Phospholipase A2	10.35	7.85477*E*-05
Interferon-induced transmembrane protein 1	8.89	0.000557976
LOC100125362	8.48	8.31466*E*-06
Carboxypeptidase X	7.57	1.60859*E*-05
Complement component 6	7.48	5.87991*E*-05
Inhibitor of DNA binding 1	7.48	0.000073019

Filter criteria for significant difference gene: |fold change| > 1.5, *P* value < 0.05.

Table 3: The top 10 downregulated genes.

Gene names	Fold change	*P* value
Periostin	-24.05	1.60411*E*-06
Neuronal regeneration-related protein	-8.77	5.64411*E*-06
Dermatopontin	-6.57	8.44669*E*-05
Integrin alpha 4	-6.44	0.000120932
Syntaxin-binding protein 5-like	-6.12	5.20189*E*-07
Fibulin 2	-6.11	1.64021*E*-05
Dihydropyrimidinase-like 3	-6.09	0.000253521
Calponin 1	-6.03	0.000115957
Sphingosine-1-phosphate receptor 3	-5.72	9.20555*E*-05
Gliomedin	-5.30	0.000144277

Filter criteria for significant difference gene: |fold change| > 1.5, *P* value < 0.05.

Table 4: List of top 5 terms of upregulated genes enriched by GO and KEGG analysis.

Terms	Count	-log10 (P value)
KEGG:rno04668:TNFsignaling pathway	15	4.863619311
KEGG:rno04151:PI3K-Aktsignaling pathway	27	4.249211392
KEGG:rno05200:Pathways in cancer	29	3.912805981
KEGG:rno04630:Jak-STAT signaling pathway	14	3.272521081
KEGG:rno04512:ECM-receptor interaction	10	2.566175661
GO BP:0032496~response to lipopolysaccharide	29	7.485884419
GO BP:0014070~response to organic cyclic compound	28	7.172760304
GO BP:0008285~negative regulation of cell proliferation	33	6.863888026
GO BP:0001666~response to hypoxia	27	6.668325051
GO BP:0050680~negative regulation of epithelial cell proliferation	13	5.878814283
GO MF:0004866~endopeptidase inhibitor activity	9	5.741812795
GO MF:0001077~transcriptional activator activity, RNA polymerase II core promoter proximal region sequence-specific binding	24	5.695518301
GO MF:0005509~calcium ion binding	39	3.672674033
GO MF:0008134~transcription factor binding	23	3.591418924
GO MF:0043565~sequence-specific DNA binding	33	3.418128712
GO CC:0005615~extracellular space	99	16.94638876
GO CC:0070062~extracellular exosome	135	9.756235253
GO CC:0009986~cell surface	48	8.51199254
GO CC:0005578~proteinaceous extracellular matrix	25	6.200499673
GO CC:0031012~extracellular matrix	25	6.169491531

downregulated genes were mainly enriched in extracellular matrix structural constituent and calcium ion binding (Table 5 and Figure 5).

The KEGG pathway analysis showed that the upregulated genes were enriched in 36 pathways; the most significant pathway was the TNF signaling pathway, and the top 5 significant pathways are shown in Table 4 and Figure 4. The downregulated genes were enriched in 19 pathways; among them, the most significant pathway is ECM-receptor interaction, and the top 5 significant pathways are shown in Table 5 and Figure 5.

3.5. PPI Analysis and Hub Gene Screening. Based on information from the STRING database, a PPI network comprising 311 nodes and 696 edges with parameters including a minimum required interaction score > 0.7 (high confidence) was constructed using the Cytoscape software (Figure 6(a)). Then, the networks were analysed by plugin MCODE with the criteria of node score > 4 and number of nodes > 4. Finally, 3 significant modules were selected (Figures 6(b)–6(d)). The KEGG pathways enriched of the genes in the highest scored modules (score 6.276) were the TNF signaling pathway, PI3K-Akt signaling pathway, and cytokine-cytokine receptor interaction; the GO biological processes were chiefly enriched in cellular response to organic substance, skeletal muscle cell differentiation, and inflammatory response (Table 6). Then, we detected the hub genes in the network. After running the CytoHubba plugin, there were 5 hub genes identified by the 6 calculation methods (Degree, EPC, EcCentricity, BottleNeck, MCC, and MNC). Results are listed in Table 7. The 6 most significant genes were chemokine (C-X-C motif), ligand 1 (Cxcl1), early growth response 1 (Egr1), FBJ osteosarcoma oncogene (Fos), insulin-like growth factor 1 (Igf1), and prostaglandin-endoperoxide synthase 2 (Ptgs2). Furthermore, we performed GO and KEGG enrichment analysis of hub genes in DAVID. These hub genes were mainly enriched in the TNF signaling pathway and pathways in cancer (Table 8). The chief GO biological processes were in response to lipopolysaccharide and response to glucocorticoid (Table 8).

3.6. Validation of Hub Gene by Real-Time PCR. To validate the results of microarray date, we selected the 5 hub genes and the most significantly up- or downregulated genes for real-time PCR analysis. Results were showed consistent with the microarray data. The gene chip analysis demonstrated these mRNAs were upregulated up to 2.643-fold (CXCL1), 5.429-fold (Fos), 2.386-fold (Igf1), 2.369-fold (Egf1), and 3.748-fold (Ptgs2). The RT-PCR results exhibit the expression of CXCL1 ($P < 0.05$), Fos ($P < 0.05$), Igf1 ($P < 0.05$), Egf1 ($P < 0.05$), and Ptgs2 ($P < 0.05$) in the old group which were significantly increased up to 3.8-fold, 4.36-fold, 2.39-fold, 3.04-fold, and 3.27-fold, respectively. The expression of periostin ($P < 0.05$) in the old group was -12.7-fold compared with that in the young group, and the expression of kininogen 1 ($P < 0.05$) in the old group was 12.4-fold compared with that in the young group. Results of RT-PCR were consistent with the results of microarray data. The results are shown in Figure 7.

4. Discussion

Cellular senescence serves as an important disease-causing determinant [12, 17]. Senescence of NPCs with age is closely related to the change of IVD aging and degeneration [7, 10, 11]. In this study, we compared the biological functions and analysed the differentially expressed gene in young and old NPCs to uncover the potential therapeutic target during NPC senescence. This study has a significant value in clinic therapy of IVDD because the key regulated genes during the NPC senescence could be manipulated to reactivate the senescent NPCs. It would be unnecessary to isolate NPCs from the tissue by invasive operation, patients may just need to receive molecules to rejuvenate NPCs, and then, the self-repair procedure could be started.

To identify the surface phenotypes of isolated young and old NPCs, a variety of surface markers were adopted for

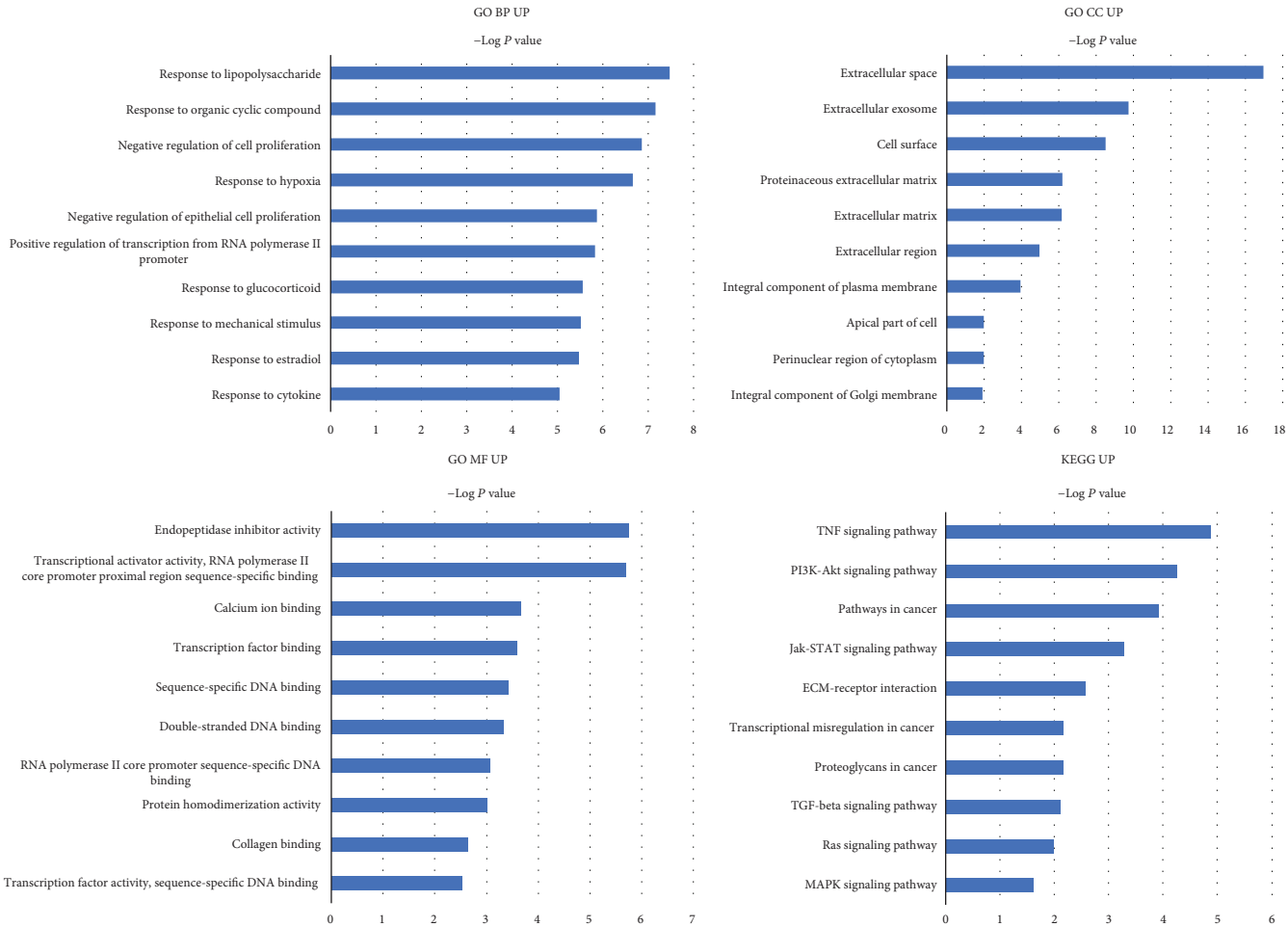

Figure 4: Go function and KEGG pathway enrichment analysis of upregulated genes. Top 5 most significantly enriched GO terms and KEGG pathways of upregulated genes. The length of the bars on the x-axis represents the negative logarithm of the P value (-log10 P) of each pathway; higher (-log10 P) values indicate a higher significance, and lower (-log10 P) values indicate a lower significance. The GO terms and KEGG pathway names are shown on the y-axis. GO MF UP, GO CC UP, and GO BP UP refer to GO terms enriched by upregulated genes. KEGG UP refers to the KEGG terms enriched by upregulated genes.

detection according to previous studies [23–25]. CD24 is a glycosylphosphatidylinositol-anchored cell surface protein, which has been defined as a marker of healthy NPCs by Risbud et al. [23]. Tang et al. found a strong expression of CD24 in juvenile human NP tissue, and its expression would decline with age [26]. Although the species in this study was different with previous studies, we also found the expression of CD24 in old NPCs decreased significantly than that in young NPCs. This result indicated that CD24 may serve as a marker of NPC senescence. We further detected the expression of CD90, which is a cell-surface-anchored glycoprotein found in many kinds of stem/progenitor cells [27]. In the present study, CD90 was highly expressed in both young and old NPCs. However, Tang et al. found that CD90 is only expressed in AF cells and may serve as a non-NP marker in rats [14]. We considered that this may be due to the different isolation method used in their study. Previous study of Molinos et al. found that NPCs highly express CD29 and Brachyury with a low expression of CD34, CD45, and CD146 [24]. In our study, the expression of CD34 and CD45 was lower than 5% in both the young and old groups, which indicated no contamination of hematopoietic-lineage cells. Both young and old NPCs could highly express CD29 (>95%), and its expression discovered no difference in young and old NPCs, which was consistent with the previous study [24].

Then, we compared the proliferation and migration capabilities of young and old NPCs. An age-related decline in the growth kinetics was reported for NPCs before. Jeong et al. found that human NPCs from young patients have a higher proliferation ability and less SA-β-gal staining percentage than old ones [28]. In line with the above-mentioned research, our study also showed a diminished proliferation capacity of old NPCs. We further investigate the migration capability between young and old NPCs, and results showed a declined migration ability in old NPCs than young NPCs. Thus, based on the combined above results, we propose that the declined proliferous and migratory capabilities of NPCs are two key processes of IVD aging.

In the present study, we further revealed the DEGs between young and old NPCs. Among the downregulated genes, periostin was the most significantly altered gene. Previous studies have shown that periostin could regulate the

Table 5: List of top 5 terms of down regulated genes enriched by GO and KEGG analysis.

Terms	Count	-log10 (P value)
KEGG:rno04512:ECM-receptor interaction	12	6.305467082
KEGG:rno04510:Focal adhesion	16	5.283730936
KEGG:rno04151:PI3K-Akt signaling pathway	18	3.918980827
KEGG:rno04974:Protein digestion and absorption	8	2.964674869
KEGG:rno04024:cAMP signaling pathway	11	2.565239027
GO BP:0007155~cell adhesion	19	5.677119186
GO BP:0035987~endodermal cell differentiation	6	3.820807813
GO BP:0001503~ossification	9	3.307311242
GO BP:0007160~cell-matrix adhesion	8	3.272206365
GO BP:0010628~positive regulation of gene expression	17	2.767181699
GO MF:0005201~extracellular matrix structural constituent	7	3.709602001
GO MF:0005509~calcium ion binding	28	3.596212048
GO MF:0003735~structural constituent of ribosome	18	2.633105261
GO MF:0044325~ion channel binding	9	2.592276912
GO MF:0005178~integrin binding	8	2.584636716
GO CC:0031012~extracellular matrix	28	12.71649934
GO CC:0005604~basement membrane	16	9.863156842
GO CC:0005615~extracellular space	53	6.939058168
GO CC:0005578~proteinaceous extracellular matrix	20	6.645158563
GO CC:0005925~focal adhesion	25	6.484468766

proliferation and differentiation of many kinds of cells such as periodontal ligament mesenchymal stem cells [29, 30], skeletal stem cells [31], and adipose-derived stem cell [32, 33]. Furthermore, periostin could interact with structural collagens, thereby influencing the mechanical structure of the ECM in a local tissue [34]. Egbert et al. found that periostin contributes to proper collagen function and is downregulated during skin aging, indicating an important role of periostin in the regulation of collagen function [35]. Previous research found that periostin is also being expressed in the human and rat IVD and has relevance to the IVDD because it binds to several ECM components such as fibronectin, tenascin, and collagen V and is related to the expression of several inflammatory cytokines such as IL-4 and TNF-α [36]. However, Tsai et.al reported an increased expression of periostin in IVD cells during IVDD, which was contradicting with our results [37]. We consider that it is because their model represents rapid injury of IVD, thus stimulating periostin expression to regulate the structure of ECM. The reaction of cells to the change of environment might be declined with age, thus showing a downregulation of periostin of NPCs. Consistent with our hypothesis, Graja et.al reported that loss of periostin occurs in aging adipose tissue is closely associated with the age-related alterations of the adipose tissue extracellular matrix [32]. Moreover, Duchamp de Lageneste et.al discovered that the bone regenerative potential of skeletal stem cells in periosteum is determined by periostin [31]. Thus, methods that upregulate the expression of periostin might reverse the malfunction of NPCs during aging. Among the high expression genes, kininogen 1 was the highest one. Kininogen 1 has been detected in numerous pathophysiological conditions, such as arthritis [38] and inflammatory bowel disease [39]. Although there is no literature that reported the association of kininogen 1 with IVD aging, the relationship of kininogen 1 with aging in other tissues has been recognized [40, 41]. Besides, Dai et.al reported that cleaved kininogen could accelerate the onset of endothelial progenitor cell senescence by activating the ROS-p38 kinase-p16INK4a signaling cascade [42]. Therefore, kininogen 1 might have a similar effect on NPC senescence.

Functional annotation of upregulated genes was conducted by GO and KEGG pathway analysis. Interestingly, the top 5 enrichments of GO BP included response to lipopolysaccharide (GO BP:003249), negative regulation of cell proliferation (GO BP:0008285), and response to hypoxia (GO BP:0001666). Lots of literatures reported that lipopolysaccharide could induce inflammatory response of IVD; thus, the biological processes in response to lipopolysaccharide indicated an important role of inflammation in NPC senescence [43]. Besides, hypoxia and inflammation are two important characteristics of the environment of degenerated IVD [44]; thus, these results highlighted a vital role of a local environment in NPC senescence. Additionally, the most significant signaling pathways of upregulated genes included the TNF signaling pathway (KEGG:rno04668), PI3K-Akt signaling pathway (KEGG:rno04151), and pathways in cancer (KEGG:rno05200). The TNF signaling pathway has been widely recognized as a vital regulator of the inflammatory cascade during IVDD [45, 46]. Thus, our results showed that the biological function of old NPCs might been influenced by the harsh conditions existing in the microenvironment of IVD. Among the downregulated genes, GO functional enrichment of BP is mainly enriched at cell adhesion (GO BP:0007155), cell-matrix adhesion (GO BP:0007160), and endodermal cell differentiation (GO BP:0035987). Pathway enrichment analysis is mainly at ECM-receptor interaction (KEGG:rno04512) and focal adhesion (KEGG:rno04510). Interestingly, these results were consistent with our cellular experiment results which showed a declined migratory capability of old NPCs. Therefore, these results indicated a decreased migratory capability of old NPCs.

We further analysed the hub genes in the PPI network by 6 calculation methods. All derived 5 hub genes (Cxcl1, Egr1, Ptgs2, Fos, and Igf1) were upregulated in the old group. We further conducted real-time PCR to verify the results of microarray. Results showed a consistent expression trend with microarray. Cxcl1, Egr1, and Ptgs2 have been reported to be existing in IVD tissues and revealed a close relationship with the immune response and inflammation. [47–49] Fos is a well-studied oncogene. It was reported that Fos existed in the herniated disc tissue instead of the healthy disc [50]. Besides, a recent study had shown that Fos could regulate the transcription of Sox9 and that the cfos-Sox9 axis is critical

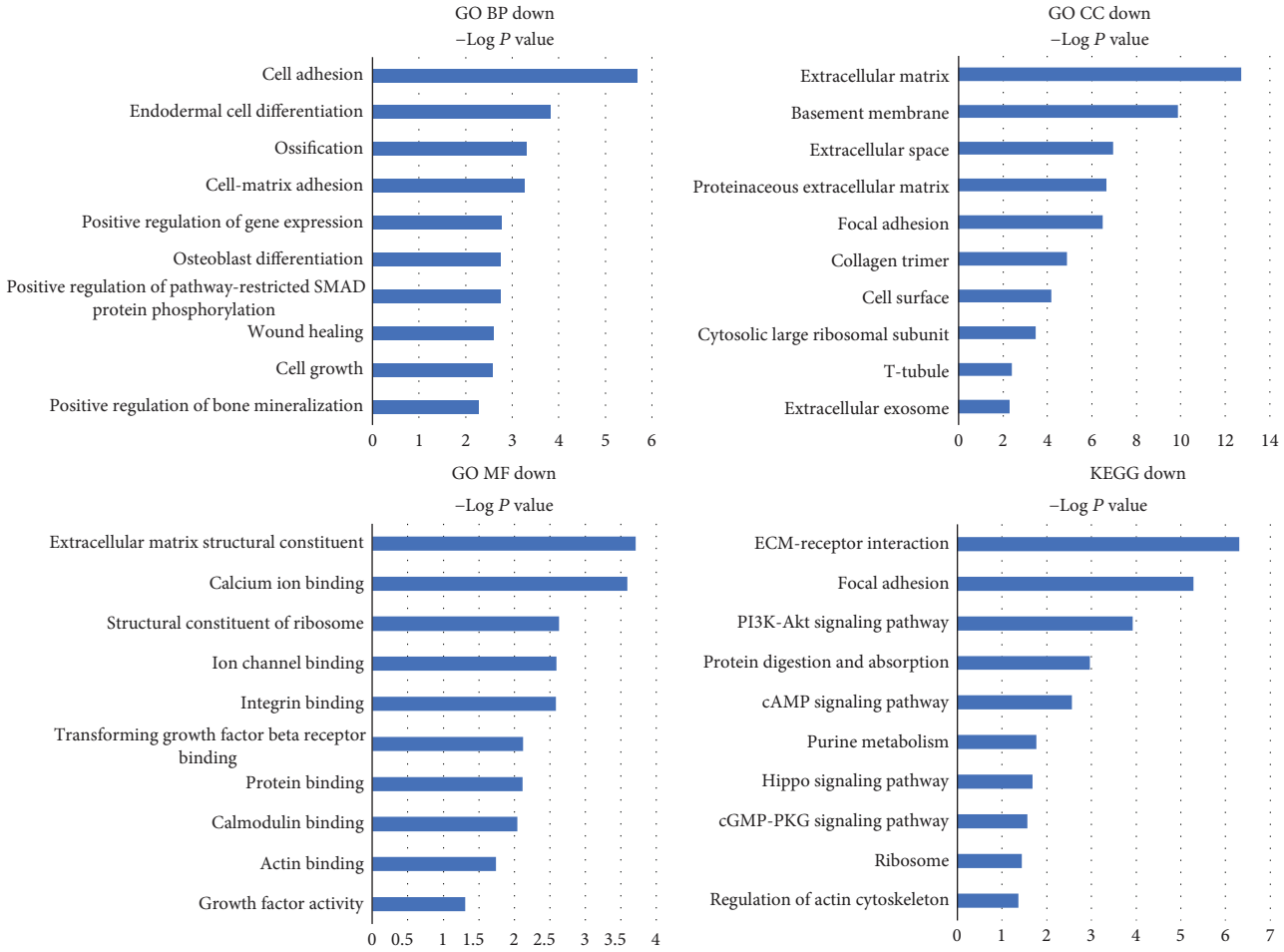

Figure 5: Go functional and KEGG pathway enrichment analysis of downregulated genes. Top 5 most significantly enriched GO terms and KEGG pathways of downregulated genes. The length of the bars on the x-axis represents the negative logarithm of the P value (-log10 P) of each pathway; higher (-log10 P) values indicate a higher significance, and lower (-log10 P) values indicate a lower significance. The GO terms and KEGG pathway names are shown on the y-axis. GO MF DOWN, GO CC DOWN, and GO BP DOWN refer to GO terms enriched by downregulated genes. KEGG DOWN refers to the KEGG terms enriched by downregulated genes.

for the role of cfos in the induction of chondroblastic Osteosarcoma [51]. Considering that SOX-9 is also an important marker of nucleus pulposus cells, the role of cfos in the regulation of NPCs during aging is needed to be deeply investigated. Igf1 is a growth factor known to activate matrix metabolism. Igf1 has also been found to have a close relationship with IVDD [52]. A previous study has described that the responsiveness of chondrocytes to IGF-I decreased with age [53]. Okuda et.al found that the increased expression of IGF-I binding proteins (IGFBPs) and downregulation of IGF-I receptor might be the two key mechanisms for the aging-related nonresponsiveness to IGF-1 [54]. Therefore, we hypothesized the upregulated expression of IGF-1 might be the compensation feedback in old NPCs. We also performed the GO and KEGG analysis of derived hub genes. Results showed that the TNF signaling pathways in response to lipopolysaccharide were enriched, which is consistent with the GO and KEGG results of upregulated genes.

The three most significant submodules of DEGs were extracted from the PPI network with MCODE scores of ≥4. After GO functional and KEGG pathway enrichment analyses of the DEGs in the highest scored modules, the genes in this module were mainly associated with the cellular response to organic substance (GO:0071310), skeletal muscle cell differentiation (GO:0035914), and inflammatory response (GO:0006954). The pathways were enriched in the TNF signaling pathway (rno04668), and PI3K-Akt signaling pathway (rno04151), which further illustrated the importance of these two pathways during NPC aging.

There were several limitations in this study. First, numerous RNA probes were detected in the microarray analysis and this limited the validation of the gene chip results. Therefore, we only interpreted the results based on previous studies and our interests. It was reported that NP consists of a mixture of small chondrocyte-like mesenchymal cells and larger notochordal-derived cells [26]. In mature NP tissues, notochordal cells gradually disappeared, replaced by smaller fibrochondrocyte-like cells [8]. However, the harvested cells in this study were mainly fibrochondrocyte-like cells in both the young and old groups, which was different with the

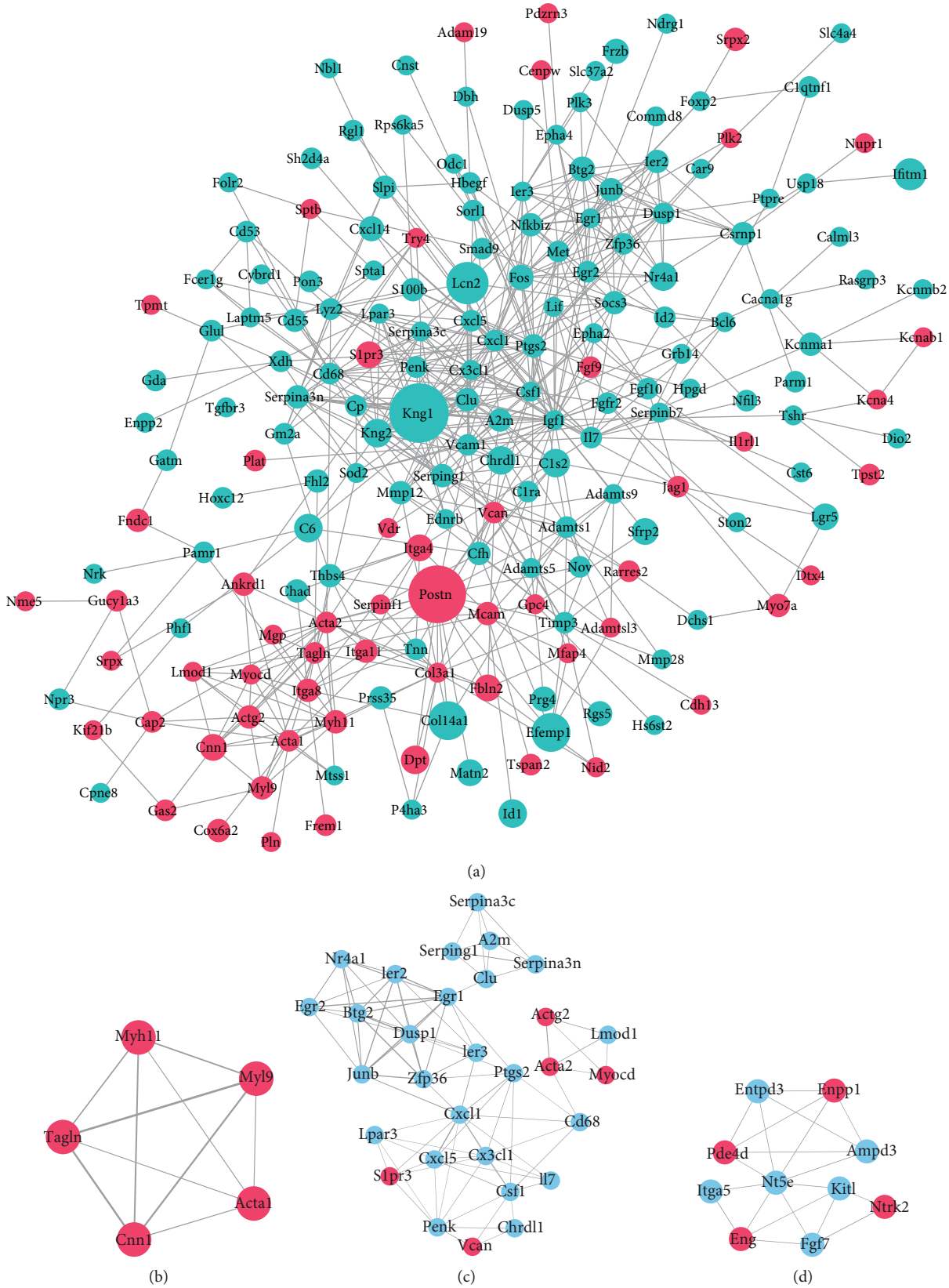

Figure 6: Protein-protein interaction network and significant modules of differentially expressed genes. (a) Red: significantly downregulated genes; green and light blue: significantly upregulated genes. Node size is positively related to fold change; edge width is positively related to the combined score. (b, c, d) Significant modules in the protein-protein interaction (PPI) network with a MCODE score ≥ 4: (b) module 1 (score = 5); (c) module 2 (score = 6.276); and (d) module 3 (score = 4.444).

Table 6: KEGG and GO analysis of the highest scored module genes.

Terms	-log10 (P value)	Count
GO BP:0071310~cellular response to organic substance	4.428041285	4
GO BP:0035914~skeletal muscle cell differentiation	4.06731104	4
GO BP:0006954~inflammatory response	4.016795968	6
GO BP:0009611~response to wounding	3.559234434	4
GO BP:0032496~response to lipopolysaccharide	3.016316347	5
KEGG:rno04668:TNF signaling pathway	3.913584453	5
KEGG:rno04151:PI3K-Akt signaling pathway	1.320427527	4
KEGG: rno04060:Cytokine-cytokine receptor interaction	1.074017917	3

Table 7: The hub genes were analysed by different topological algorithms in the protein-protein interaction network.

Topological algorithm	Top 20 genes were ranked by score
Maximal Clique Centrality (MCC)	Btg2, Clu, Csf1, Cx3cl1, Cxcl1, Cxcl5, Dusp1, Egr1, Egr2, Fos, Ier2, Igf1, Junb, Kng1, Kng2, Nfkbiz, Penk, Ptgs2, Serping1, Zfp36
Degree	A2m, Acta2, Clu, Col3a1, Csf1, Cxcl1, Cxcl5, Dusp1, Egr1, Fos, Igf1, Il7, Kitl, Kng1, Kng2, Postn, Ptgs2, Socs3, Vcam1, Vcan
Edge Percolated Component	Cd68, Clu, Cp, Csf1, Cx3cl1, Cxcl1, Cxcl5, Egr1, Fos, Igf1, Il7, Kitl, Kng1, Kng2, Nfkbiz, Penk, Ptgs2, Serpina3n, Socs3, Vcam1
Maximum Neighborhood Component	Acta2, Clu, Col3a1, Csf1, Cx3cl1, Cxcl1, Cxcl5, Dusp1, Egr1, Fos, Igf1, Il7, Kitl, Kng1, Kng2, Nfkbiz, Postn, Ptgs2, Serpina3n, Vcam1
BottleNeck	A2m, Acta1, Cd68, Cfh, Cxcl1, Dusp1, Egr1, Eng, Folr2, Fos, Igf1, Il7, Jag1, Kitl, Mcam, Negr1, Postn, Ptgs2, Timp3, Vcam1
EcCentricity	Acta2, Cd68, Csf1, Cx3cl1, Cxcl1, Egr1, Eng, Fgf10, Fgf9, Fgfr2, Fos, Igf1, Junb, Lyz2, Mmp12, Myh11, Ptgs2, Serping1, Smad9, Vcam1
Common genes of 6 topological algorithms	Cxcl1, Egr1, Fos, Igf1, Ptgs2

cellular morphology of notochordal cells (characterized by lots of vacuoles). The culture method in this study was a monolayer with normoxic condition, which may be difficult to preserve the phenotype of notochordal cells due to the phenotype of notochordal cells that would quickly disappear after in vitro culture. Since the optimal culture condition for notochordal cell phenotype maintenance is still under investigation, our study may only represent a part of the mechanism of NPC senescence. Another limitation exists in the normoxic culture condition. Hypoxia is one of characteristics of IVD. Previous studies shown that the gene expression of NPCs may be altered due to the normoxic culture condition [55]. Thus, hypoxia and 3 dimensional cultures may be more suitable to maintain the phenotype of NPCs.

Table 8: KEGG and GO analysis of hub gene.

Terms	-log10 (P value)	Count
KEGG:rno04668:TNF signaling pathway	2.937464369	3
KEGG:rno05200:Pathways in cancer	1.8358872	3
KEGG:rno04913:Ovarian steroidogenesis	1.543625084	2
KEGG:rno05140:Leishmaniasis	1.435827789	2
KEGG:rno05132:Salmonella infection	1.375008637	2
GO BP:0032496~response to lipopolysaccharide	4.797953003	4
GO BP:0051384~response to glucocorticoid	3.469546007	3
GO BP:0042127~regulation of cell proliferation	2.980755828	3
GO BP:0014070~response to organic cyclic compound	2.85105501	3
GO BP:0042493~response to drug	2.282716935	3

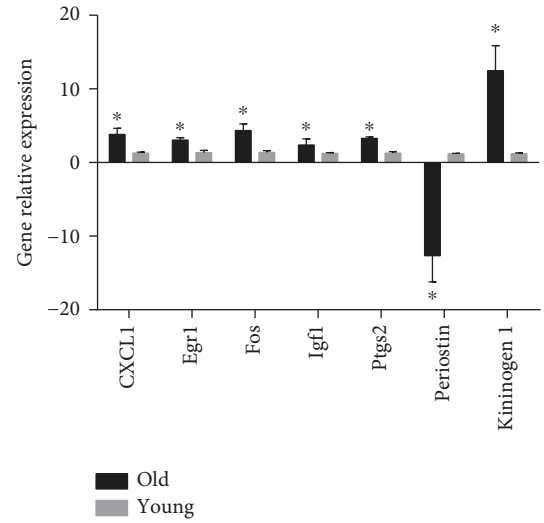

Figure 7: Validation of microarray results by RT-PCR. Five hub genes (Cxcl1, Egr1, Fos, Igf1, and Ptgs2) and the most significantly upregulated (kininogen 1) and downregulated (periostin) genes were selected for the real-time PCR validation. GAPDH was selected as the internal control. Data are presented as the mean ± SD. $^*P < 0.05$ compared with the young group.

5. Conclusions

Taken together, we discovered that the old NPCs showed declined proliferation and migration abilities. Furthermore, we identified a series of molecular pathways that contribute to NPC aging and degeneration through microarray analysis. Further studies will be needed to elucidate downstream mechanisms of potential targets. An understanding of the

mechanisms underlying these aging processes may lead to a novel breakthrough in the prevention and treatment of disc aging and aging-related degeneration.

Abbreviations

NP: Nucleus pulposus
IVD: Intervertebral disc
RT-PCR: Real-time polymerase chain reaction
SA-β-gal: Senescence-associated β-galactosidase
FITC: Fluorescein isothiocyanate
PE: Phycoerythrin
EPC: Edge Percolated Component
MCC: Maximal Clique Centrality
MNC: Maximum Neighborhood Component.

Data Availability

The data used to support the findings of this study are included within the article and the supplementary materials. The gene microarray datasets had been uploaded to the NCBI Gene Expression Omnibus (GEO) and can be accessed via GEO Series accession [GEO:GSE126883] (https://www.ncbi.nlm.nih.gov/geo/query/acc.cgi?acc=GSE126883). Other related data generated and/or analysed during the current study are available from the corresponding authors upon reasonable request.

Conflicts of Interest

The authors declare no conflicts of interest.

Authors' Contributions

Shi Cheng and Xiaochuan Li conceived and designed the experiment. Shi Cheng, Zhiwei Jia, and Yachao Zhao performed experiments, analysed the data, and wrote the manuscript. Linghan Lin provided experimental help and advice. Deli Wang and Dike Ruan supervised the whole process of the research for its accuracy and compliance with institutional regulations. Yu Zhang revised the manuscript. All authors discussed the results and commented on the manuscript. All authors read and approved the final manuscript.

Acknowledgments

This work was supported by grants from the National Natural Science Foundation of China (81470102 and 81802130) and Research Funding of Peking University Shenzhen Hospital (JCYJ2019003RC).

Supplementary Materials

Heat map and hierarchical clustering of DEG profile comparison between the young and old NPCs. Red colour indicates high expression, and green colour indicates low expression. Every column represents a tissue sample, and every row represents an mRNA probe. Z641, Z643, and Z642 were samples in the old group; Z644, Z645, and Z646 were samples in the young group. *(Supplementary Materials)*

References

[1] J. N. Katz, "Lumbar disc disorders and low-back pain: socioeconomic factors and consequences," *The Journal of Bone and Joint Surgery(American)*, vol. 88, Supplement_2, pp. 21–24, 2006.

[2] M. A. Adams and P. J. Roughley, "What is intervertebral disc degeneration, and what causes it?," *Spine*, vol. 31, no. 18, pp. 2151–2161, 2006.

[3] D. S. Mern, A. Beierfuss, C. Thome, and A. A. Hegewald, "Enhancing human nucleus pulposus cells for biological treatment approaches of degenerative intervertebral disc diseases: a systematic review," *Journal of Tissue Engineering and Regenerative Medicine*, vol. 8, no. 12, pp. 925–936, 2014.

[4] S. Huang, V. Tam, K. M. C. Cheung et al., "Stem cell-based approaches for intervertebral disc regeneration," *Current Stem Cell Research & Therapy*, vol. 6, no. 4, pp. 317–326, 2011.

[5] Y. C. Huang, J. P. G. Urban, and K. D. K. Luk, "Intervertebral disc regeneration: do nutrients lead the way?," *Nature reviews Rheumatology*, vol. 10, no. 9, pp. 561–566, 2014.

[6] J. Silva-Correia, S. I. Correia, J. M. Oliveira, and R. L. Reis, "Tissue engineering strategies applied in the regeneration of the human intervertebral disk," *Biotechnology Advances*, vol. 31, no. 8, pp. 1514–1531, 2013.

[7] D. Chen, D. Xia, Z. Pan et al., "Metformin protects against apoptosis and senescence in nucleus pulposus cells and ameliorates disc degeneration in vivo," *Cell Death & Disease*, vol. 7, no. 10, article e2441, 2016.

[8] J. J. Trout, J. A. Buckwalter, and K. C. Moore, "Ultrastructure of the human intervertebral disc: II. Cells of the nucleus pulposus," *The Anatomical Record*, vol. 204, no. 4, pp. 307–314, 1982.

[9] L. Zheng, Y. Cao, S. Ni et al., "Ciliary parathyroid hormone signaling activates transforming growth factor-β to maintain intervertebral disc homeostasis during aging," *Bone Research*, vol. 6, no. 1, article 21, 2018.

[10] F. Wang, F. Cai, R. Shi, X. H. Wang, and X. T. Wu, "Aging and age related stresses: a senescence mechanism of intervertebral disc degeneration," *Osteoarthritis and Cartilage*, vol. 24, no. 3, pp. 398–408, 2016.

[11] P. Priyadarshani, Y. Li, and L. Yao, "Advances in biological therapy for nucleus pulposus regeneration," *Osteoarthritis and Cartilage*, vol. 24, no. 2, pp. 206–212, 2016.

[12] D. McHugh and J. Gil, "Senescence and aging: causes, consequences, and therapeutic avenues," *The Journal of Cell Biology*, vol. 217, no. 1, pp. 65–77, 2018.

[13] J.-S. Lee, "Cellular senescence, aging, and age-related disease: special issue of BMB reports in 2019," *BMB Reports*, vol. 52, no. 1, pp. 1-2, 2019.

[14] X. Tang, L. Jing, and J. Chen, "Changes in the molecular phenotype of nucleus pulposus cells with intervertebral disc aging," *PLoS One*, vol. 7, no. 12, article e52020, 2012.

[15] C. Q. Zhao, L. M. Wang, L. S. Jiang, and L. Y. Dai, "The cell biology of intervertebral disc aging and degeneration," *Ageing Research Reviews*, vol. 6, no. 3, pp. 247–261, 2007.

[16] K. W. Kim, H. N. Chung, K. Y. Ha, J. S. Lee, and Y. Y. Kim, "Senescence mechanisms of nucleus pulposus chondrocytes in human intervertebral discs," *The Spine Journal*, vol. 9, no. 8, pp. 658–666, 2009.

[17] J. Campisi and F. d'Adda di Fagagna, "Cellular senescence: when bad things happen to good cells," *Nature Reviews Molecular Cell Biology*, vol. 8, no. 9, pp. 729–740, 2007.

[18] O. Toussaint, E. E. Medrano, and T. von Zglinicki, "Cellular and molecular mechanisms of stress-induced premature senescence (SIPS) of human diploid fibroblasts and melanocytes," *Experimental Gerontology*, vol. 35, no. 8, pp. 927–945, 2000.

[19] M. Shawi and C. Autexier, "Telomerase, senescence and ageing," *Mechanisms of Ageing and Development*, vol. 129, no. 1-2, pp. 3–10, 2008.

[20] A. L. Tarca, R. Romero, and S. Draghici, "Analysis of microarray experiments of gene expression profiling," *American Journal of Obstetrics and Gynecology*, vol. 195, no. 2, pp. 373–388, 2006.

[21] D. K. Slonim and I. Yanai, "Getting started in gene expression microarray analysis," *PLoS Computational Biology*, vol. 5, no. 10, article e1000543, 2009.

[22] Y. G. Zhang, Z. M. Sun, J. T. Liu, S. J. Wang, F. L. Ren, and X. Guo, "Features of intervertebral disc degeneration in rat's aging process," *Journal of Zhejiang University Science B*, vol. 10, no. 7, pp. 522–527, 2009.

[23] M. V. Risbud, Z. R. Schoepflin, F. Mwale et al., "Defining the phenotype of young healthy nucleus pulposus cells: recommendations of the Spine Research Interest Group at the 2014 annual ORS meeting," *Journal of Orthopaedic Research*, vol. 33, no. 3, pp. 283–293, 2015.

[24] M. Molinos, C. R. Almeida, R. M. Goncalves, and M. A. Barbosa, "Improvement of bovine nucleus pulposus cells isolation leads to identification of three phenotypically distinct cell subpopulations," *Tissue Engineering Part A*, vol. 21, no. 15-16, pp. 2216–2227, 2015.

[25] N. Fujita, T. Miyamoto, J. Imai et al., "CD24 is expressed specifically in the nucleus pulposus of intervertebral discs," *Biochemical and Biophysical Research Communications*, vol. 338, no. 4, pp. 1890–1896, 2005.

[26] X. Tang, L. Jing, W. J. Richardson et al., "Identifying molecular phenotype of nucleus pulposus cells in human intervertebral disc with aging and degeneration," *Journal of Orthopaedic Research*, vol. 34, no. 8, pp. 1316–1326, 2016.

[27] Y. Nakamura, Y. Muguruma, T. Yahata et al., "Expression of CD90 on keratinocyte stem/progenitor cells," *The British Journal of Dermatology*, vol. 154, no. 6, pp. 1062–1070, 2006.

[28] S. W. Jeong, J. S. Lee, and K. W. Kim, "In vitro lifespan and senescence mechanisms of human nucleus pulposus chondrocytes," *The Spine Journal*, vol. 14, no. 3, pp. 499–504, 2014.

[29] P. Panchamanon, P. Pavasant, and C. Leethanakul, "Periostin plays role in force-induced stem cell potential by periodontal ligament stem cells," *Cell Biology International*, vol. 43, no. 5, pp. 506–515, 2019.

[30] Z. Wu, W. Dai, P. Wang et al., "Periostin promotes migration, proliferation, and differentiation of human periodontal ligament mesenchymal stem cells," *Connective Tissue Research*, vol. 59, no. 2, pp. 108–119, 2018.

[31] O. Duchamp de Lageneste, A. Julien, R. Abou-Khalil et al., "Periosteum contains skeletal stem cells with high bone regenerative potential controlled by periostin," *Nature Communications*, vol. 9, no. 1, article 773, 2018.

[32] A. Graja, F. Garcia-Carrizo, A.-M. Jank et al., "Loss of periostin occurs in aging adipose tissue of mice and its genetic ablation impairs adipose tissue lipid metabolism," *Aging Cell*, vol. 17, no. 5, article e12810, 2018.

[33] T. Chow and I. M. Rogers, "Periostin is critical for improving the therapeutic properties of adipocyte-derived stem cells," *Stem Cell Research & Therapy*, vol. 6, no. 1, article 214, 2015.

[34] A. Kudo, "Periostin in fibrillogenesis for tissue regeneration: periostin actions inside and outside the cell," *Cellular and Molecular Life Sciences*, vol. 68, no. 19, pp. 3201–3207, 2011.

[35] M. Egbert, M. Ruetze, M. Sattler et al., "The matricellular protein periostin contributes to proper collagen function and is downregulated during skin aging," *Journal of Dermatological Science*, vol. 73, no. 1, pp. 40–48, 2014.

[36] H. E. Gruber, R. A. Norris, M. J. Kern et al., "Periostin is expressed by cells of the human and sand rat intervertebral discs," *Biotechnic & Histochemistry*, vol. 86, no. 3, pp. 199–206, 2011.

[37] T. T. Tsai, P. L. Lai, J. C. Liao et al., "Increased periostin gene expression in degenerative intervertebral disc cells," *The Spine Journal*, vol. 13, no. 3, pp. 289–298, 2013.

[38] I. M. Sainz, I. Isordia-Salas, J. L. Castaneda et al., "Modulation of inflammation by kininogen deficiency in a rat model of inflammatory arthritis," *Arthritis and Rheumatism*, vol. 52, no. 8, pp. 2549–2552, 2005.

[39] I. Isordia-Salas, R. A. Pixley, I. M. Sainz, C. Martinez-Murillo, and R. W. Colman, "The role of plasma high molecular weight kininogen in experimental intestinal and systemic inflammation," *Archives of Medical Research*, vol. 36, no. 1, pp. 87–95, 2005.

[40] C. H. Lin, C. C. Liao, C. H. Huang et al., "Proteomics analysis to identify and characterize the biomarkers and physical activities of non-frail and frail older adults," *International Journal of Medical Sciences*, vol. 14, no. 3, pp. 231–239, 2017.

[41] Y. W. Lam, N. N. C. Tam, J. E. Evans, K. M. Green, X. Zhang, and S. M. Ho, "Differential proteomics in the aging Noble rat ventral prostate," *Proteomics*, vol. 8, no. 13, pp. 2750–2763, 2008.

[42] J. Dai, X. Zhu, M. C. Yoder, Y. Wu, and R. W. Colman, "Cleaved high-molecular-weight kininogen accelerates the onset of endothelial progenitor cell senescence by induction of reactive oxygen species," *Arteriosclerosis, Thrombosis, and Vascular Biology*, vol. 31, no. 4, pp. 883–889, 2011.

[43] K. Li, Y. Li, B. Xu, L. Mao, and J. Zhao, "Sesamin inhibits lipopolysaccharide-induced inflammation and extracellular matrix catabolism in rat intervertebral disc," *Connective Tissue Research*, vol. 57, no. 5, pp. 347–359, 2016.

[44] T. Kadow, G. Sowa, N. Vo, and J. D. Kang, "Molecular basis of intervertebral disc degeneration and herniations: what are the important translational questions?," *Clinical Orthopaedics and Related Research*, vol. 473, no. 6, pp. 1903–1912, 2015.

[45] S. Wang, J. Wei, Y. Fan et al., "Progranulin is positively associated with intervertebral disc degeneration by interaction with IL-10 and IL-17 through TNF pathways," *Inflammation*, vol. 41, no. 5, pp. 1852–1863, 2018.

[46] Z. I. Johnson, Z. R. Schoepflin, H. Choi, I. M. Shapiro, and M. V. Risbud, "Disc in flames: roles of TNF-α and IL-1β in intervertebral disc degeneration," *European Cells and Materials*, vol. 30, pp. 104–117, 2015.

[47] Z. Tian, X. Ma, M. Yasen et al., "Intervertebral disc degeneration in a percutaneous mouse tail injury model," *American Journal of Physical Medicine & Rehabilitation*, vol. 97, no. 3, pp. 170–177, 2018.

[48] C. A. Seguin, R. M. Pilliar, J. A. Madri, and R. A. Kandel, "TNF-alpha induces MMP2 gelatinase activity and MT1-MMP expression in an in vitro model of nucleus pulposus tissue degeneration," *Spine*, vol. 33, no. 4, pp. 356–365, 2008.

[49] T. Yoshida, J. S. Park, K. Yokosuka et al., "Effect of a non-protein bioactive agent on the reduction of cyclooxygenase-2 and tumor necrosis factor–α in human intervertebral disc cells in vitro," *Journal of Neurosurgery: Spine*, vol. 9, no. 5, pp. 411–418, 2008.

[50] J. Tolonen, M. Grönblad, J. Virri, S. Seitsalo, T. Rytömaa, and E. Karaharju, "Oncoprotein c-Fos and c-Jun immunopositive cells and cell clusters in herniated intervertebral disc tissue," *European Spine Journal*, vol. 11, no. 5, pp. 452–458, 2002.

[51] Y. He, W. Zhu, M. H. Shin et al., "cFOS-SOX9 axis reprograms bone marrow-derived mesenchymal stem cells into chondroblastic osteosarcoma," *Stem Cell Reports*, vol. 8, no. 6, pp. 1630–1644, 2017.

[52] A. Tsarouhas, G. Soufla, K. Tsarouhas et al., "Molecular profile of major growth factors in lumbar intervertebral disc herniation: correlation with patient clinical and epidemiological characteristics," *Molecular Medicine Reports*, vol. 15, no. 4, pp. 2195–2203, 2017.

[53] R. F. Loeser, G. Shanker, C. S. Carlson, J. F. Gardin, B. J. Shelton, and W. E. Sonntag, "Reduction in the chondrocyte response to insulin-like growth factor 1 in aging and osteoarthritis: studies in a non-human primate model of naturally occurring disease," *Arthritis and Rheumatism*, vol. 43, no. 9, pp. 2110–2120, 2000.

[54] S. Okuda, A. Myoui, K. Ariga, T. Nakase, K. Yonenobu, and H. Yoshikawa, "Mechanisms of age-related decline in insulin-like growth factor-I dependent proteoglycan synthesis in rat intervertebral disc cells," *Spine*, vol. 26, no. 22, pp. 2421–2426, 2001.

[55] S. H. Yang, M. H. Hu, W. Y. Lo, Y. H. Sun, C. C. Wu, and K. C. Yang, "The influence of oxygen concentration on the extracellular matrix production of human nucleus pulposus cells during isolation-expansion process," *Journal of Biomedical Materials Research Part A*, vol. 105, no. 6, pp. 1575–1582, 2017.

Hindawi
Stem Cells International
Volume 2019, Article ID 1839627, 12 pages
https://doi.org/10.1155/2019/1839627

Research Article

Mechanical Stretch Promotes the Osteogenic Differentiation of Bone Mesenchymal Stem Cells Induced by Erythropoietin

Yong-Bin He,[1,2] Sheng-Yao Liu,[3] Song-Yun Deng,[4] Li-Peng Kuang,[2] Shao-Yong Xu,[4] Zhe Li,[5] Lei Xu,[4] Wei Liu,[6] and Guo-Xin Ni[1]

[1]*School of Sport Medicine and Rehabilitation, Beijing Sport University, China*
[2]*Department of Orthopedics, The Fifth Affiliated Hospital of Zunyi Medical University, China*
[3]*Department of Orthopedics, The Second Affiliated Hospital of Guangzhou Medical University, China*
[4]*Department of Orthopeadics and Traumatology, Nanfang Hospital, Southern Medical University, China*
[5]*Department of Orthopaedics and Traumatology, Zhengzhou Orthopaedics Hospital, Zhengzhou, China*
[6]*Department of Orthopedics, The People's Hospital of Gaoming District of Foshan City, China*

Correspondence should be addressed to Guo-Xin Ni; fjrehab@163.com

Received 19 March 2019; Revised 18 May 2019; Accepted 29 May 2019; Published 7 July 2019

Guest Editor: Yongcan Huang

Introduction. The effects of erythropoietin (EPO) on the behaviors of bone marrow mesenchymal stem cells (BMSCs) subjected to mechanical stretch remain unclear. This study was therefore aimed at establishing the dose-response effect of EPO stimulation on rat BMSCs and investigating the effects of mechanical stretch combined with EPO on the proliferation and osteogenic differentiation of BMSCs. *Material and Methods*. The proliferation and osteogenic differentiation of rat BMSCs were examined and compared using EPO with different concentrations. Thereafter, BMSCs were subjected to 10% elongation using a Flexcell strain unit, combined with 20 IU/ml EPO. The proliferation of BMSCs was detected by Cell Counting Kit-8, colony formation assay, and cell cycle assay; meanwhile, the mRNA expression levels of Ets-1, C-myc, Ccnd1, and C-fos were detected by reverse transcription and real-time quantitative PCR (qPCR). The osteogenic differentiation of BMSCs was detected by alkaline phosphatase (ALP) staining, and the mRNA expression levels of ALP, OCN, COL, and Runx2 were detected by qPCR. The role of the extracellular signal-regulated kinases 1/2 (ERK1/2) in the osteogenesis of BMSCs stimulated by mechanical stretch combined with 20 IU/ml EPO was examined by Western blot. *Results*. Our results showed that effects of EPO on BMSCs included a dose-response relationship, with the 20 IU/ml EPO yielding the largest. Mechanical stretch combined with 20 IU/ml EPO promoted proliferation and osteogenic differentiation of BMSCs. The increase in ALP, mineral deposition, and osteoblastic genes induced by the mechanical stretch–EPO combination was inhibited by U0126, an ERK1/2 inhibitor. *Conclusion*. EPO was able to promote the proliferation and osteogenic differentiation of BMSCs, and these effects were enhanced when combined with mechanical stretch. The underlying mechanism may be related to the activation of the ERK1/2 signaling pathway.

1. Introduction

Large bone defects resulting from trauma, congenital defects, neoplasm, failed arthroplasty, and infection are quite common [1, 2], and the incidences of nonunion and delayed union are very high [3]. It remains a great challenge for orthopedic surgeons to achieve osseous reconstruction for nonunion and bone defects. Distraction osteogenesis (DO) is regarded as one of the most effective therapeutic strategies for posttraumatic complex nonunion [4–7]; but the overall therapeutic process lasts for a relatively long period, and a variety of complications may arise, such as pin loss, infection around the transmucosal pin, bone fracture, and restriction in joint motion [8]. Various approaches have been tested to promote bone formation in order to shorten the DO period. Among them, bone morphogenic proteins (BMPs) are thought to be the most potent osteoinductive factors and play a key role in the process of bone formation during DO. However, the high cost and the short half-life *in vivo* restrict usage of their applications [9–12]. It is therefore necessary to seek

alternatives with good therapeutic outcomes for use in the DO technique.

Erythropoietin is a glycoprotein hormone that stimulates red blood cell (RBC) production in bone marrow via binding to the cell-surface receptor on hematopoietic progenitor cells, and it has been widely used for treating anemia [13]. In addition to its classical role in the regulation of RBC proliferation, EPO has been shown to exert protective and regenerative capabilities in a variety of nonhematopoietic tissues [14]. Notably, it promotes the osteogenic differentiation of bone mesenchymal stem cells (BMSCs) [15–17]. Furthermore, mechanical stretch may induce the differentiation of BMSCs into mature osteoblasts and enhance the deposition of the bone matrix [18–20]. Nevertheless, the effects of EPO remain unknown on the behaviors of BMSCs subjected to mechanical stretch, which is an *in vitro* condition simulated to an *in vivo* DO procedure.

This study was therefore aimed at addressing three key issues: First, is there a dose-dependent effect of EPO on the proliferation and osteogenic differentiation of BMSCs? And which is the optimal concentration if so? Second, what is the effect of EPO at its optimal concentration on the proliferation and osteogenic differentiation of BMSCs subjected to mechanical stretch? Third, is the ERK1/2 signaling pathway involved in the promotion of the osteogenic differentiation of EPO combined with mechanical stretch on BMSCs?

2. Material and Methods

2.1. BMSC Isolation, Identification, and Culture. This study was approved by the Animal Ethics Committee of Nanfang Hospital, Southern Medical University. The BMSCs were isolated from 4-week-old male Sprague-Dawley rats using a method described previously [21]. The morphology of the cells was observed by optic and inverted phase contrast microscope. After identification by flow cytometry, the third generation (P3) cells were selected for further study. L-DMEM containing 10% fetal bovine serum (FBS) was used as the culture medium.

Flow cytometry analysis and cell cycle assay were conducted using a method described in our previous study [21]. Briefly, the isolated cells were collected and incubated with antibodies of CD11b, CD45, CD79, and CD90 according to the manufacturer's instructions. After being incubated for 30 minutes at 4°C, the cells were analyzed by flow cytometry (BD Biosciences, USA). The isolated cells were then collected and fixed in 70% precooling ethanol overnight at 4°C. After being stained with propidium iodide (PI)/RNase buffer at room temperature in the dark for 30 minutes, the isolated cells were analyzed for cell cycle by flow cytometry.

2.2. Experimental Design. After incubation for 24 hours, the cells were treated with EPO with different concentrations of rhEPO (5 IU/ml, 10 IU/ml, 20 IU/ml, and 40 IU/ml). Cells untreated with rhEPO were defined as the control group. After 7 days of being cultured, the cells were examined for their proliferation and osteogenic differentiation. Thereafter, the optimal concentration of rhEPO was chosen for further investigations.

After being incubated for 24 hours, the cells were treated with EPO and/or mechanical stretch and divided into the following 4 groups: the control (CON) group, EPO group, stretch (STR) group, and EPO+STR group. In terms of mechanical stretch, a cyclic mechanical stretch with a 1 Hz sinusoidal curve set at 10% elongation was applied for 4 hours twice a day using the FX-5000TM Flexcell Tension Plus™ unit (Flexcell International Corporation, NC, USA). After treatment for 7 days, CCK-8 was applied to the cells to detect proliferation. The colony formations and the cell cycles were examined by colony formation assay (CFA) and flow cytometry, respectively. The osteogenic differentiation of the cells was detected by ALP staining and ALP activity. Reverse transcription and real-time qPCR were used to examine the gene expressions of Ets-1, C-myc, Ccnd1, C-fos, ALP, OCN, COL, and Runx2.

The cells were divided into 4 groups based on treatment methods: CON, EPO, STR, and EPO+STR. After 7 days of treatment, the expression levels of t-ERK1/2 and p-ERK1/2 were detected by Western blot. In addition, the P3 cells were further divided into 4 groups based on treatment methods: CON, STR+EPO, CON+blocking, STR+EPO+blocking. An osteogenic-induced medium was used to induce cell osteogenesis, whereas U0126 (10 μM) was used as an ERK1/2 blocker. After 7 days of treatment, the osteogenic differentiation of the cells was detected by ALP activity.

2.3. Cell Proliferation. Cell Counting Kit-8 (CCK-8) assay was used to assess cell proliferation. In brief, all cells were harvested and incubated with CCK-8 solution according to the manufacturer's instructions. After being incubated for 2 hours at 37°C, the optical density (OD) value of the cells was measured at 450 nm with a microplate reader (SpectraMax M5, Molecular Devices, USA).

2.4. CFA Assessment. Approximately 1×10^3 cells from each group were seeded in 3 wells of a 6-well culture plate and incubated under the same conditions noted above for 14 days. After incubation, the medium was removed by aspiration and the colonies were washed with PBS. The colonies were fixed with 4.0% (w/v) paraformaldehyde for 20 minutes, then stained with 0.1% crystal violet for 1 hour at room temperature. After washing excess crystal violet with ddH_2O, the plates were left to dry in normal air at room temperature overnight.

2.5. ALP Activity and Staining Measurement. ALP activity and staining was performed according to a previous protocol [22]. For the ALP activity assay, cells from each group were rinsed twice with PBS, then lysed with 10 mM Tris–HCl containing 2 mM $MgCl_2$ and 0.05% Triton X-100 (pH 8.2) at 4°C. Sonicated cell lysates were subsequently centrifuged at 12000g for 10 min at 4°C, then the supernatants were used for the assays. Lysates were incubated in an ALP detection buffer for 30 min at 37°C. The reaction was stopped by adding 0.1 M NaOH and then monitored at 405 nm. Total protein was measured spectrophotometrically using a Micro BCA Protein Assay Kit (Pierce) and read at 562 nm. The enzymatic activity of ALP was normalized to the total protein

Table 1: Primer sequences for qPCR.

Gene	Primer	Primer sequence (5′-3′)	Product (bp)
C-fos	Forward	TGCATGAATTCCCCAGCCGACTC	618
	Reverse	TGCATAAGCTTCAGCTCCCTCCT	
Ets-1	Forward	GAGTTCAGCCTGAAGGGTGTT	153
	Reverse	CACATCCTCTTTCTGCAGGATCT	
C-myc	Forward	AATTCCAGCGAGAGACAGAG	434
	Reverse	CAAAGCCCTTCTCACTCCA	
Ccnd1	Forward	CGTACCCTGACACCAATCTC	434
	Reverse	TGAAGTAAGAAACGGAGGGC	
ALP	Forward	TATGTCTGGAACCGCACTGAAC	90
	Reverse	CACTAGCAAGAAGAAGCCTTTGG	
OCN	Forward	GCCCTGACTGCATTCTGCCTCT	192
	Reverse	TCACCACCTTACTGCCCTCCTG	
COL	Forward	CAGGCTGGTGTGATGGGATT	278
	Reverse	CCAAGGTCTCCAGGAACACC	
Runx2	Forward	ATCCAGCCACCTTCACTTACACC	199
	Reverse	GGGACCATTGGGAACTGATAGG	
GAPDH	Forward	TGCCACTCAGAAGACTGTGG	129
	Reverse	TTCAGCTCTGGGATGCCTT	

content of the sample (405/562 nm). For the ALP staining assay, cells from each group were fixed with 4% paraformaldehyde for 15 min, stained with ALP detection solution for 30 min at 37°C, and washed with PBS to remove excess staining.

2.6. qPCR. Total RNA was extracted from cells both in the experiment group and in the control group using RNAiso Plus (Takara Bio Inc., Dalian, China). RNA purity and concentration were quantified spectrophotometrically using a NanoDrop ND-1000 (NanoDrop Technologies, USA). The cDNA (10 μl final volume) was synthesized from the total RNA using the Bestar qPCR RT Kit (DBI Bioscience, Germany) according to the manufacturer protocol. The qPCR reactions (20 μl final volume) were conducted using the Bestar SybrGreen qPCR Mastermix (DBI Bioscience, Germany). The primer sequences for these experiments are listed in Table 1.

The cDNA was amplified in triplicate at 95°C for 2 minutes, followed by 40 denaturation cycles at 95°C for 10 seconds, annealing and extension at 60°C for 30 seconds, and 40 more denaturation cycles at 72°C for 30 seconds. A dissociation curve was constructed to confirm that there was no nonspecific amplification. Glyceraldehyde-3-phosphate dehydrogenase (GAPDH) was quantified as an endogenous reference, and each sample was normalized to its GAPDH content. Dissociation curve analysis was used to determine the specificity of qPCR. The data from qPCR experiments was analyzed using the comparative CT method as described in the manual for the LightCycler® 480 System (Roche Life Science, Canada) to determine relative quantitative gene expression.

2.7. Western Blot Analysis. After 7 days of treatment, the cells from 4 groups were washed with ice-cold PBS and digested immediately. The proteins were extracted using a cell lysis buffer. After electrophoretic separation by 8% SDS-polyacrylamide gel electrophoresis, the proteins were electrotransferred onto polyvinylidene fluoride (PVDF) membranes (Millipore, Billerica, MA, USA). The membranes were then blocked with Tris-buffered saline containing 0.1% Tween-20 (TBST) and 5% skim milk for 1 hour at room temperature. t-ERK1/2 rabbit mAb, phospho-ERK1/2 (p-ERK1/2) rabbit mAb (Cell Signaling Technology, Danvers, MA, USA), and GAPDH rabbit mAb (4A Biotech, Beijing, China) were used according to the manufacturers' protocols, and the membranes were incubated overnight with these antibodies at 4°C with slight shaking. Thereafter, the membranes were washed 3 times in TBST and further incubated with an HRP-conjugated antibody (goat anti-rabbit IgG, Sigma-Aldrich, Saint Louis, MO, USA) for 1 hour at room temperature. Finally, the membranes were washed 3 times in TBST, and the signals were developed using an enhanced chemiluminescence kit (KeyGen Biotech, Nanjing, China). A semiquantitative evaluation of the bands was performed by densitometry (VersaDoc, Bio-Rad, Hercules, CA, USA). The levels of t-ERK1/2 and p-ERK1/2 proteins were determined through their normalization to the protein level of GAPDH.

For inhibition of ERK1/2 activation, BMSCs were incubated with U0126 (10 μM, Sigma-Aldrich, Saint Louis, MO, USA) for 30 minutes at 37°C before they were subjected to cyclic mechanical stretch combined with 20 IU/ml EPO.

2.8. Statistical Analysis. Data was statistically analyzed using SPSS 19.0 software. All experimental data were expressed as the means ± standard deviation. Differences between 2

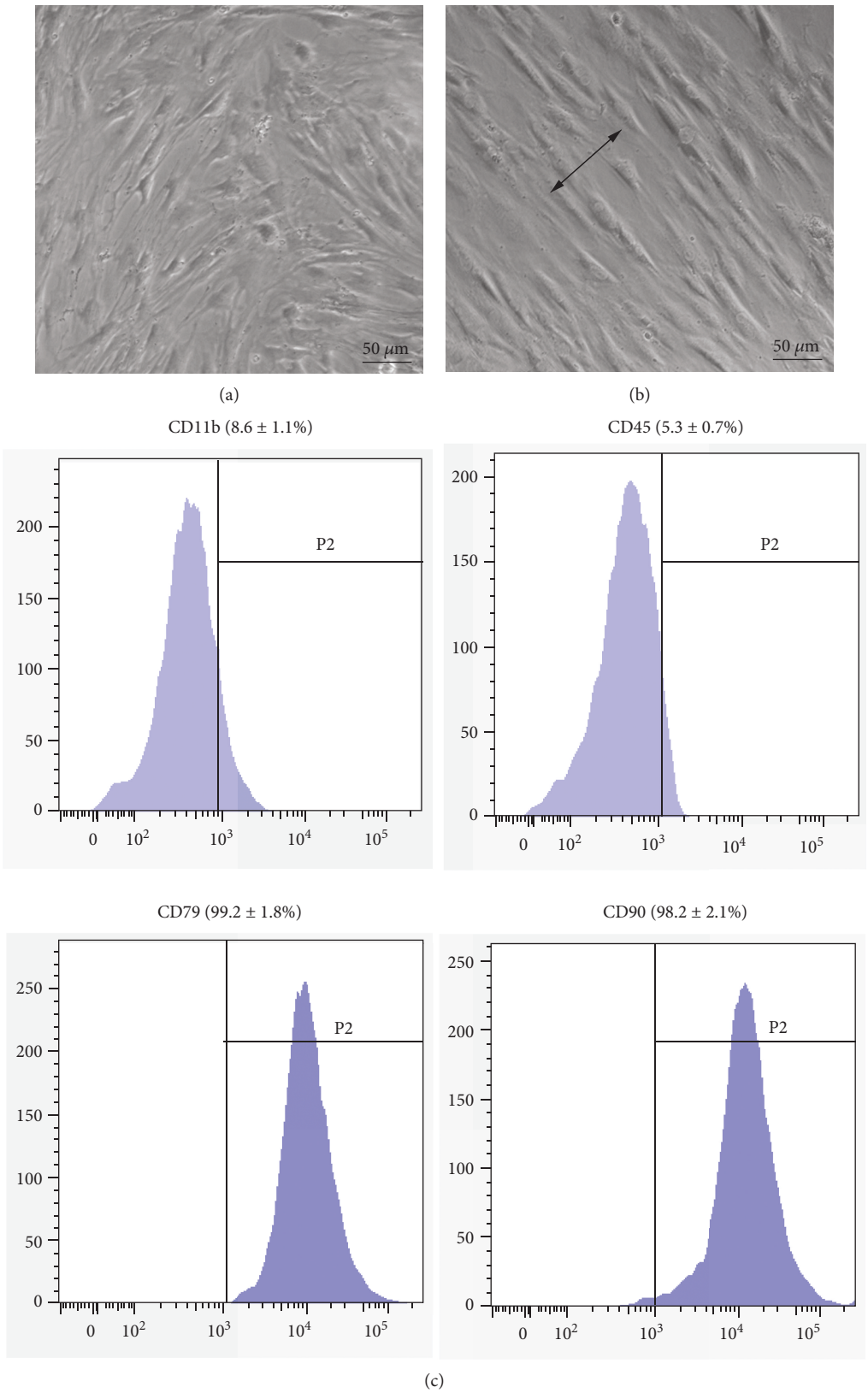

Figure 1: Representative images of BMSCs before and after mechanical stretch. Before mechanical stretch, the obtained cells were fibroblast-like, spindle-shaped, and randomly oriented (a). After mechanical stretch, the BMSCs were still fibroblast-like and spindle-shaped but became much thinner compared to the nonstretch cells. The cells were oriented perpendicularly to the axis of the external strain (b). In addition, immunophenotypic characterization was analyzed by flow cytometry, indicating that the obtained cells were BMSCs (c). The arrow indicates direction of stretch field. Bar = 50 μm.

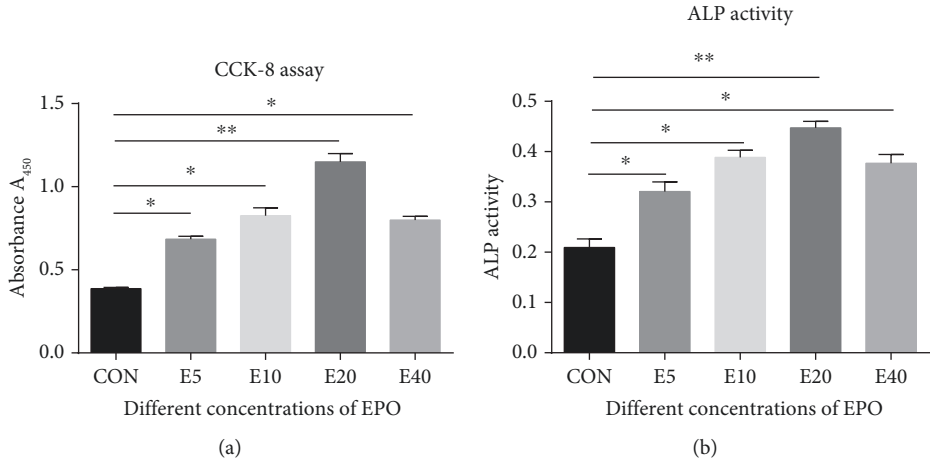

Figure 2: The proliferation and ALP staining of BMSCs under the stimulus of different concentrations of EPO. A dose-response relationship was evident among the experiment groups, and the group of 20 IU/ml EPO showed the maximum value, with the cell proliferation significantly increased about 3-fold compared to the control (a). On the other hand, the staining of the cells treated with EPO is much more obvious than that in the control. Furthermore, the EPO dosage of 20 IU/ml yielded the largest effect relative to the control (b). $^{*}p < 0.05$ and $^{**}p < 0.001$ compared with the control group.

groups were determined statistically by Student's t-test, and the variance was analyzed. One-way ANOVA with post hoc LSD was performed, and p values < 0.05 were considered statistically significant.

3. Results

3.1. Cell Characterization. The obtained cells were fibroblast-like and spindle-shaped (Figure 1(a)). The BMSCs were still fibroblast-like and spindle-shaped after mechanical stretch but were much thinner compared to the nonstretch cells. The cells were oriented perpendicularly to the axis of the external strain, whether in the absence or the presence of applied EPO (Figure 1(b)). In order to evaluate the character of the cells, CD11b, CD45, CD79, and CD90 expressions were analyzed using flow cytometry. The results showed that all cells were positive for cell surface markers CD79 and CD90 with percentages of 99.2 ± 1.8 and 98.2 ± 2.1, respectively; all cells were negative for CD11b and CD45 with percentages of 8.6 ± 1.1 and 5.3 ± 0.7, respectively (Figure 1(c)). These results indicate that the obtained cells were BMSCs.

3.2. EPO Promoted the Proliferation of BMSCs. CCK-8 assay was used to examine the proliferation of the cells. As shown in Figure 2(a), under the stimulus of different concentrations of EPO, a dose-response relationship was evident among the experiment groups, and the group of 20 IU/ml EPO showed the maximum value, with the cell proliferation significantly increased about 3-fold compared to the control ($p < 0.001$). These results indicated that EPO promoted proliferation of BMSCs; meanwhile, the EPO concentration of 20 IU/ml yielded the largest effect.

3.3. EPO Promoted the Osteogenic Differentiation of BMSCs. The osteogenic potential of BMSCs was detected using ALP activity. As shown in Figure 2(b), ALP activity of the cells treated with EPO is much higher than in the control. Furthermore, the EPO dosage of 20 IU/ml yielded the largest effect relative to the control. These results indicated that EPO promoted osteogenic differentiation of BMSCs.

3.4. Mechanical Stretch Combined with 20 IU/ml EPO Promoted the Proliferation of BMSCs. CCK-8 assay was used to examine the proliferation of the cells, both stretched and nonstretched. As shown in Figure 3(a), under the stimulus of stretch whether combined with EPO or not, the cell proliferation increased significantly compared to the control ($p < 0.01$). Among the experiment groups, the STR+EPO group showed the maximum value, with the cell proliferation significantly increased about 4.5-fold compared to the control ($p < 0.001$). These results indicated that mechanical stretch combined with 20 IU/ml EPO promoted proliferation of BMSCs.

To further show the proliferation of BMSCs under the intervention of mechanical stretch whether combined with EPO or not, we investigated the colony-forming characteristic of the cells by evaluating the number of cell colonies that developed after 14 days of being cultured (Figure 3(b)). The number of cell colonies that developed was evidently higher under the intervention of mechanical stretch combined with 20 IU/ml EPO compared to the other groups.

In order to further clarify the role of mechanical stretch combined with 20 IU/ml EPO in regulating the proliferation of BMSCs, qPCR was used to analyze the proliferation genes. As seen in Figure 3(c), BMSCs subjected to mechanical stretch with or without EPO clearly show a change in the mRNA expression levels of Ets-1, C-myc, Ccnd1, and C-fos compared to the control ($p < 0.01$). The mRNA expression of Ets-1 in the group subjected to mechanical stretch combined with 20 IU/ml EPO showed the maximum value, with the expression significantly increased about 5.32-fold compared to the control ($p < 0.001$), as shown in Figure 3(c). The mRNA expressions of C-myc, Ccnd1, and C-fos in the group subjected to mechanical stretch combined with

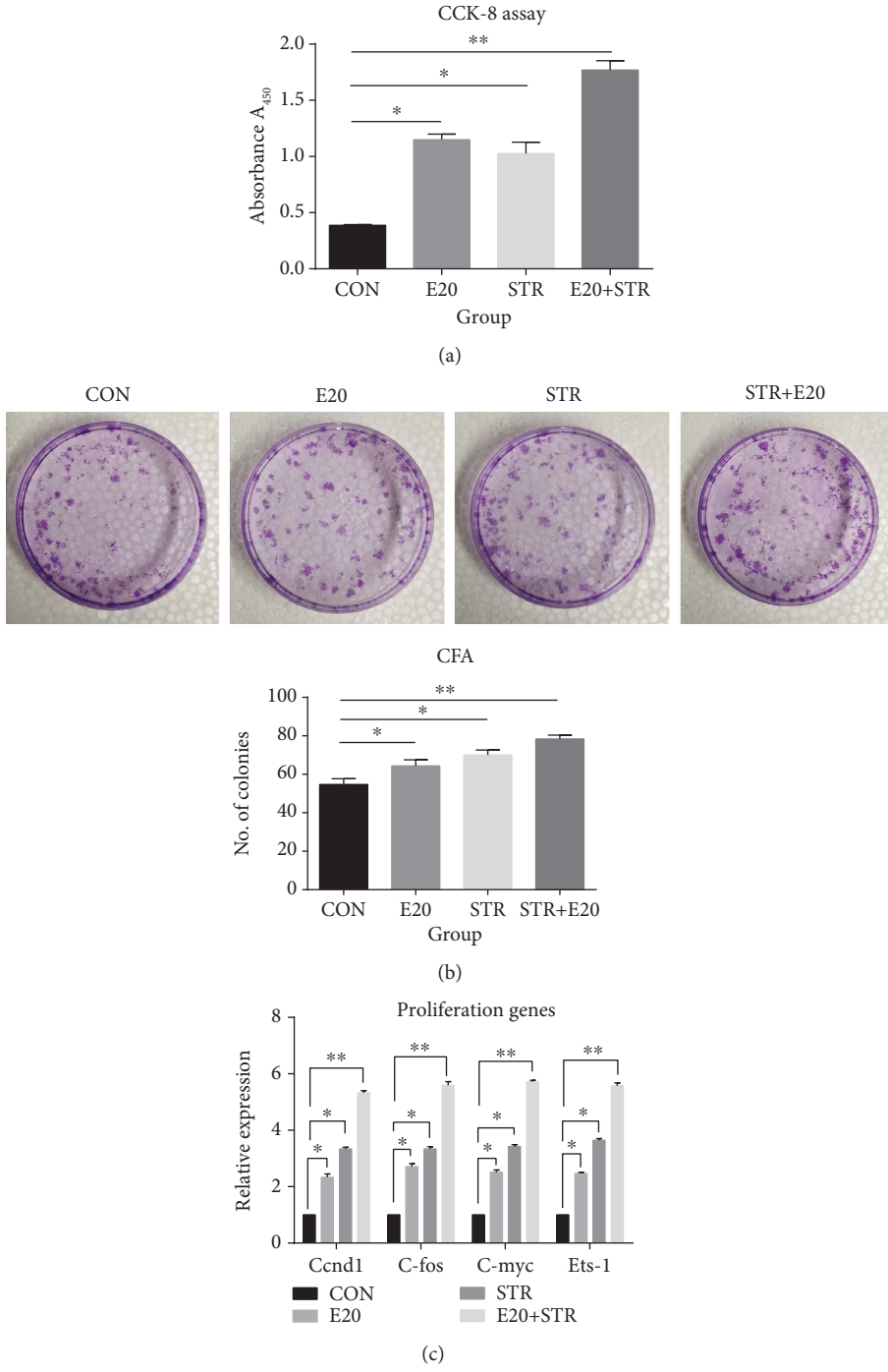

Figure 3: Effects of mechanical stretch combined with 20 IU/ml EPO on the cell proliferation, the distribution of the cell cycles, and the expression of proliferation genes. Under the stimulus of stretch with and without EPO, the cell proliferation increased significantly compared to the control. Among the experiment groups, the STR+EPO group showed the maximum value, with the cell proliferation significantly increased about 4.5-fold compared to the control (a). The number of cell colonies under the intervention of mechanical stretch with and without EPO. One representative well was presented for each group (b). Quantitative results for these assays are also presented as bar graphs. The number of cell colonies that developed was evidently higher under the intervention of mechanical stretch combined with 20 IU/ml EPO compared to the other groups (b). The results showed that mechanical stretch combined with 20 IU/ml EPO stimulated cell proliferation by promoting cell cycle progression from G1 to S-G2/M phases. Besides, qPCR was used to analyze the proliferation genes. BMSCs subjected to mechanical stretch with or without EPO clearly show a change in the mRNA expression levels of Ets-1, C-myc, Ccnd1, and C-fos compared to the control. The mRNA expression of Ets-1 in the group subjected to mechanical stretch combined with 20 IU/ml EPO showed the maximum value, with the expression significantly increased about 5.32-fold compared to the control. The mRNA expressions of C-myc, Ccnd1, and C-fos in the group subjected to mechanical stretch combined with 20 IU/ml EPO increased about 5.59-fold, 5.72-fold, and 5.58-fold, respectively, compared to the control (c). $^{*}p < 0.05$ and $^{**}p < 0.001$ compared with the control group.

20 IU/ml EPO increased about 5.59-fold, 5.72-fold, and 5.58-fold, respectively, compared to the control ($p < 0.001$). These results indicated that mechanical stretch combined with 20 IU/ml EPO promoted proliferation of BMSCs through upregulation of the mRNA expressions of Ets-1, C-myc, Ccnd1, and C-fos.

To understand the process of combining mechanical stretch with 20 IU/ml EPO to regulate the proliferation of BMSCs, flow cytometry was used to analyze the distribution of the cell cycles. As shown in Figure 4, there was a significantly high S-G2/M phase population with percentages of 27.0 ± 0.74 in the experimental cells (strains combined with 20 IU/ml EPO) compared to the other groups of cells with percentages of 10.7 ± 0.85, 17.9 ± 0.79, and 20.6 ± 0.68. The results showed that mechanical stretch combined with 20 IU/ml EPO stimulated cell proliferation by promoting cell cycle progression from G1 to S-G2/M phases.

3.5. Mechanical Stretch Combined with 20 IU/ml EPO Promoted the Osteogenic Differentiation of BMSCs. The osteogenic potential of BMSCs was detected using ALP activity and staining. As shown in Figures 5(a) and 5(b), the activity and staining of the cells subjected to mechanical stretch with or without EPO were more obvious than those in the control. The group subjected to mechanical stretch combined with 20 IU/ml EPO yielded the largest effect relative to the control. These results indicated that mechanical stretch combined with 20 IU/ml EPO promoted differentiation of BMSCs into osteoblasts.

ALP activity and staining is a marker not only of osteoblast differentiation but also of the genes ALP, OCN, COL, and Runx2. In Figure 5(c), we can clearly see that BMSCs subjected to mechanical stretch with or without EPO show a change in the mRNA expression levels of ALP, OCN, COL, and Runx2 compared to the control group ($p < 0.01$). The mRNA expression of ALP in the group of mechanical stretch combined with 20 IU/ml EPO showed the maximum value, with the expression significantly increased about 5.37-fold compared to that of the control ($p < 0.001$), as shown in Figure 5(c). The mRNA expressions of OCN, COL, and Runx2 in the group of mechanical stretch combined with 20 IU/ml EPO increased about 5.85-fold, 5.41-fold, and 5.42-fold, respectively, compared to those in the control ($p < 0.001$). These results indicated that mechanical stretch combined with 20 IU/ml EPO promoted osteogenic differentiation of BMSCs through upregulation of the mRNA expressions of ALP, OCN, COL, and Runx2.

3.6. Mechanical Stretch Combined with 20 IU/ml EPO Promoted the Osteogenic Differentiation of BMSCs via the Activation of the ERK1/2 Signaling Pathway. The ERK1/2 signal plays a vital role in the osteogenic differentiation of BMSCs; therefore, we analyzed the levels of p-ERK1/2. We found that the p-ERK1/2 expression of the cells subjected to mechanical stretch with or without EPO was more obvious than that of the control. The group subjected to mechanical stretch combined with 20 IU/ml EPO yielded the largest effect relative to the control, as shown in Figures 6(a) and 6(b). Furthermore, the U0126, an inhibitor of ERK1/2, inhibited the ALP activity induced by mechanical stretch combined with 20 IU/ml EPO, as shown in Figure 6(c). These results demonstrated that mechanical stretch combined with 20 IU/ml EPO promoted osteogenic differentiation of BMSCs via activating the ERK1/2 signaling pathway.

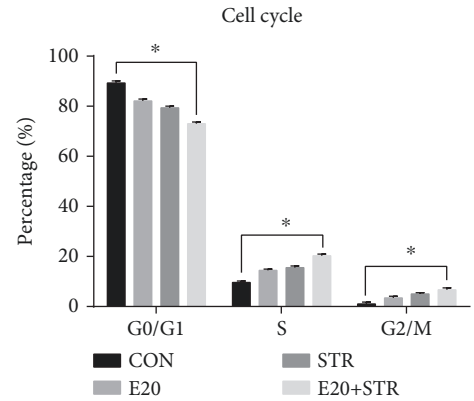

Figure 4: Flow cytometry was used to analyze the distribution of the cell cycles. There was a significantly high S-G2/M phase population with percentages of 27.0 ± 0.74 in the experimental cells (strains combined with 20 IU/ml EPO) compared to the other groups of cells with percentages of 10.7 ± 0.85, 17.9 ± 0.79, and 20.6 ± 0.68 (3B). $^{*}p < 0.05$ and $^{**}p < 0.001$ compared with the control group.

4. Discussion

It has been determined that EPO promoted the osteogenic differentiation of BMSCs [15–17]. Nevertheless, its effects on the behaviors of BMSCs subjected to mechanical stretch remain unclear. In this study, it was indicated that EPO promoted the proliferation and osteogenic differentiation of BMSCs in a dose-response relationship, with an optimal effect at the dosage of 20 IU/ml. Furthermore, synergistic effect on the proliferation and osteogenic differentiation of BMSCs was obtained from 10% mechanical stretch combined with 20 IU/ml EPO.

In this study, the effects of EPO on the proliferation and osteogenic differentiation of BMSCs were examined with a range of concentrations from 0 IU/ml to 40 IU/ml. Our findings indicated that EPO simultaneously enhanced the proliferation and osteogenic differentiation of BMSCs, with the optimal effects at the dosage of 20 IU/ml. It seems that the effects of EPO depend on not only its concentration but also the type and quantity of BMSCs, and the duration under the treatment as well. Dose-dependent effects of EPO were ever suggested on the osteogenic differentiation of human mesenchymal stromal cells with a range of concentrations from 0 IU/ml to 100 IU/ml, and 20 IU/ml EPO was the lowest effective dose that produced a consistent osteogenic effect on the cells [14]. Kim et al. demonstrated that 20 IU/ml EPO could directly induce the differentiation of human mesenchymal stromal cells into osteoblasts [23]. Nevertheless, in another study, the proliferation effect of EPO was most obvious when the time was 12 hours and the concentration was 5 U/ml [15]. As supposed, with the increase of its concentration, EPO would combine with more erythropoietin

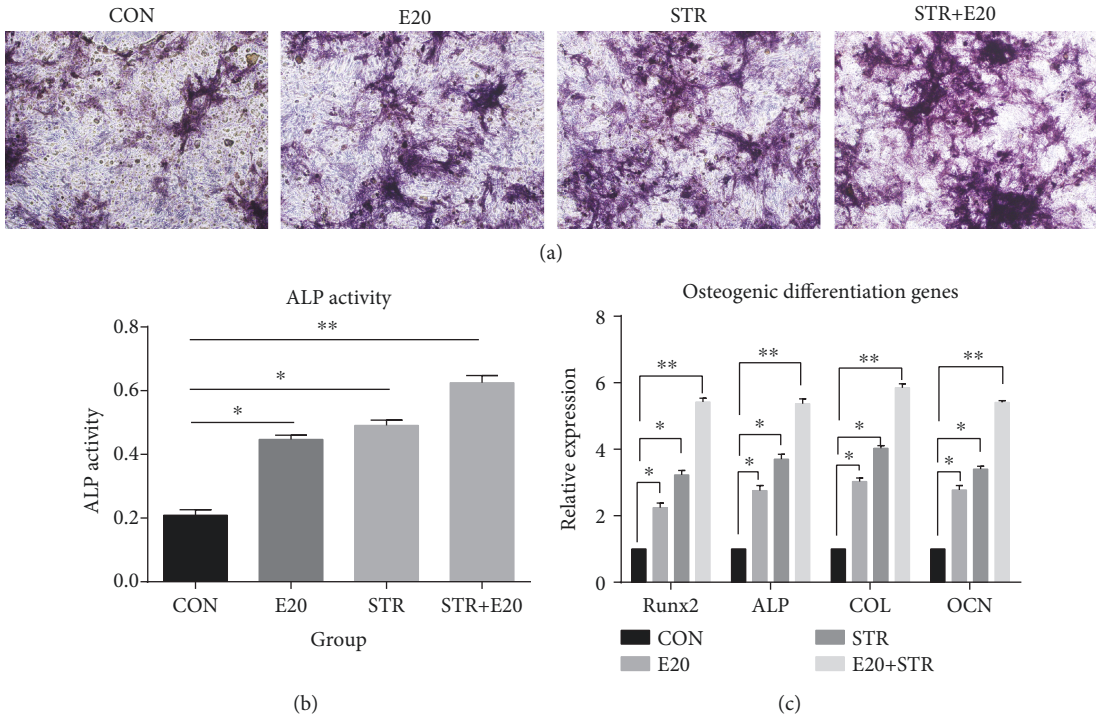

Figure 5: The ALP staining of the cells subjected to mechanical stretch with or without EPO was more obvious than that of the control (a). The group subjected to mechanical stretch combined with 20 IU/ml EPO yielded the largest ALP activity relative to the control (b). BMSCs subjected to mechanical stretch with or without EPO show a change in the mRNA expression levels of ALP, OCN, COL, and Runx2 compared to the control group. The mRNA expression of ALP in the group of mechanical stretch combined with 20 IU/ml EPO showed the maximum value, with the expression significantly increased about 5.37-fold compared to that of the control. The mRNA expressions of OCN, COL, and Runx2 in the group of mechanical stretch combined with 20 IU/ml EPO increased about 5.85-fold, 5.41-fold, and 5.42-fold, respectively, compared to those of the control (c). $^{*}p < 0.05$ and $^{**}p < 0.001$ compared with the control group.

receptors (EPORs), leading to a gradually increased effect on the proliferation and osteogenic differentiation of BMSCs. Nevertheless, the high concentration of 40 IU/ml has delayed effect on the proliferation and osteogenic differentiation. It was therefore assumed that there might exist a negative feedback mechanism for the regulation of EPO on the proliferation and osteogenic differentiation when the concentration of EPO amounts to a certain level. This requires further investigation.

The effect of mechanical stretch has been extensively investigated on cell behaviors using various magnitudes. For example, it was reported that mechanical stretch on the order of 1%–3% elongation is needed to obtain a cellular response in vitro [24]. Positive effects were also found using 6% elongation of cyclic mechanical stretch on the osteogenic differentiation of MSCs [25], 8% elongation of strain on the proliferation of rat BMSCs [26], 10% elongation of mechanical stretch on the differentiation of BMSCs [14, 27], and 12% elongation of cyclic stretch on the osteogenesis-related gene expression of osteoblast-like cells [28]. As such, 10% elongation of mechanical stretch was chosen in this study in order to enhance the proliferation and differentiation of BMSCs.

Bone formation following the DO technique is a complex process that involves a series of BMSC activities, including proliferation and osteogenic differentiation [29]. According to the literature, the effect of mechanical stretch on the proliferation of BMSCs is inconsistent. Some studies reported that appropriate mechanical stretch promotes the proliferation of BMSCs [25, 27, 30], whereas many others reported the opposite results [31, 32]. Such discrepancies may be attributable to different strain parameters selected in these studies, including type, magnitude, frequency, and duration. A body of evidence indicates that EPO enhances the proliferation of BMSCs *in vitro* [17, 18] and *in vivo* [19, 20]. In this study, the mRNA expressions of Ets-1, C-myc, Ccnd1, and C-fos of BMSCs, subjected to mechanical stretch with 20 IU/ml EPO, were quantified by qPCR. Ets-1 played a vital role mainly during the first proliferation phase and is also a critical transcription factor in regulating the expression of numerous genes involved in bone development [33]. C-myc is activated by Wnt/β-catenin signaling and then induces the proliferation of BMSCs [34]. Moreover, Ccnd1 and C-fos both play important roles in the proliferation of cells, and the activation of these genes could be used as an index of cell proliferation [35, 36]. Our results indicated that the mRNA expression of these genes increased significantly compared to the strain alone, the EPO dosage of 20 IU/ml alone, or the control. In addition, the results of the CCK-8 assay, CFA, and cell cycle assay also supported the aforementioned results. All these results showed that mechanical stretch incorporated with 20 IU/ml EPO significantly promoted the proliferation of BMSCs.

In addition to proliferation, our results indicated that mechanical stretch combined with 20 IU/ml EPO can also

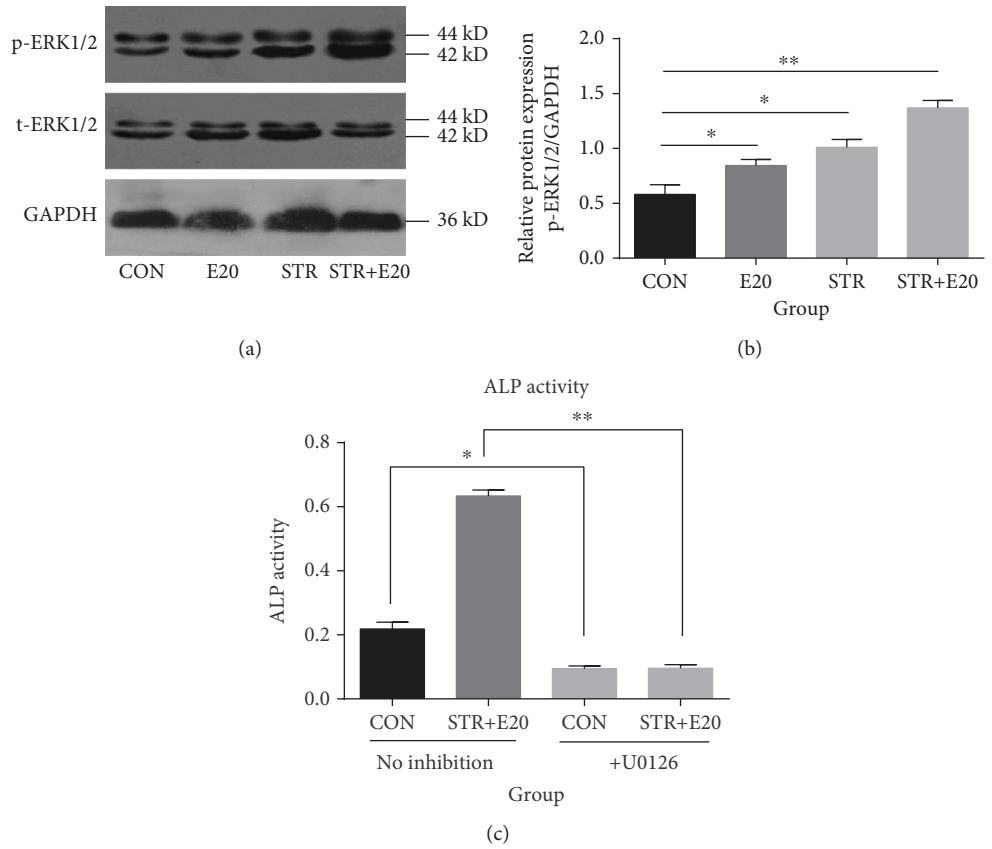

Figure 6: The levels of p-ERK1/2 under mechanical stretch combined with 20 IU/ml EPO. The p-ERK1/2 expression of the cells subjected to mechanical stretch with or without EPO was more obvious than the control. The group subjected to mechanical stretch combined with 20 IU/ml EPO yielded the largest effect relative to the control (a, b). Furthermore, the U0126, an inhibitor of ERK1/2, inhibited the ALP activity induced by mechanical stretch combined with 20 IU/ml EPO (c). $^{*}p < 0.05$ and $^{**}p < 0.001$ compared with the control group.

enhance the osteogenic differentiation of BMSCs. Osteogenic differentiation of BMSCs is the final and vital step in the process of bone formation. As shown, the Runx2 protein has the ability to bind to and regulate the expression of other genes, including those for collagen type I, osteocalcin, and osteopontin [37], and it is necessary for membranous bone formation [38]. Several studies have reported that Runx2 is a mechanical stretch target gene that increases osteoblastic activity [39, 40]. Meanwhile, Shiozawa et al. proved that when BMSCs were treated with EPO, the mRNA expression of Runx2, the mineral deposition, and the ALP activity were enhanced [41]. In addition to Runx2, ALP, OCN, and COL I are also typically used in the identification of osteogenic differentiation of cells [30, 42, 43]. Our result is consistent with those mentioned above; additionally, among the experiment groups, the group of mechanical stretch combined with 20 IU/ml EPO showed the maximum value.

However, the real mechanism of mechanical stretch combined with EPO affecting the osteogenic differentiation of BMSCs remains to be discovered. EPO, a hypoxia-regulated factor, combined with different kinds of cells through EPORs and elicited a variety of reactions in the cells [44–46]. There are EPORs in the surface of BMSCs, and the EPO can activate the ERK1/2 signaling pathway. Previous studies also confirmed that mechanical stretch can activate the ERK1/2 signaling pathway [39, 44], and the ERK1/2 signal plays a vital role in the osteogenic differentiation of BMSCs. One hypothesis is that when BMSCs are subjected to mechanical stretch, the stretch may induce the cells into a hypoxic state [41, 44]; as a result, cells may have a stronger ability to combine with EPO. Meanwhile, the application of EPO would activate the ERK1/2 signaling pathway, the same function of mechanical stretch on the cells; therefore, stretch and EPO may work synergistically, activating the ERK1/2 signaling pathway and finally promoting the osteogenic differentiation of BMSCs. Additionally, consistent with previous studies [30, 47], BMSCs in this study were observed to be oriented perpendicularly to the stretch axis after applied stretch (10% elongation). Cell function and cell fate are often determined by cell shape. Cells in different native tissues often show different specific morphologies, such as spindle tendon cells, dendritic neuronal cells, or flattened osteogenic cells. Cell fate is primarily determined by its morphology. For example, at the same occupying area, BMSCs with a sharp pentagon and high aspect ratio exhibit higher cell contractility, thus leading preferentially to osteogenic differentiation [48, 49]. Therefore, with an appropriate parameter of mechanical stretch, the F-actin filaments in BMSCs would become more arranged and oriented perpendicular to the axis of mechanical loading [47], then change cells' morphology, and finally lead preferentially to osteogenic differentiation.

Mechanical stretch on cells in vitro is somehow like the DO technique in vivo. This work demonstrated that an appropriate parameter of mechanical stretch (10%, 1 Hz, twice every day, for 4 h for each treatment, 7 days) enhances the proliferation, migration (data not shown), and differentiation of BMSCs. This combination may provide an effective therapeutic strategy for posttraumatic complex nonunion with shortening treatment duration, decreasing complications and reducing hospital costs. Nevertheless, we should acknowledge that there are some limitations to this study. First, the parameter of mechanical stretch used in this study needs to be optimized, although the positive effect was noted. Further investigations are needed to understand the best parameters for the osteogenesis of BMSCs. Second, this study found that 20 IU/ml EPO yielded the largest effect on BMSCs, but the concentration of EPO between 20 IU/ml and 40 IU/ml might yield a larger effect if combined with higher numbers of EPORs. Third, this study found that mechanical stretch promoted the osteogenic differentiation of BMSCs induced by erythropoietin via activating the ERK1/2 signaling pathway, but the upstream and downstream factors involved in the ERK1/2 signaling pathway remain unclear. Finally, the *in vivo* experiment is necessary to further determine the effects of mechanical stretch combined with EPO on bone formation.

5. Conclusion

In summary, our findings suggested that EPO was able to promote the proliferation and osteogenic differentiation of BMSCs, and these effects were enhanced when combined with mechanical stretch. The underlying mechanism may be related to the activation of the ERK1/2 signaling pathway.

Data Availability

The data used to support the findings of this study are included within the article.

Disclosure

None of the authors has any financial or personal interest in the products mentioned in this article.

Conflicts of Interest

The authors declare that there is no conflict of interest regarding the publication of this paper.

Authors' Contributions

Yong-Bin He and Sheng-Yao Liu contributed equally to this work.

Acknowledgments

This work was supported by the National Natural Science Foundation of China (81572219, 81871848) and Natural Science Foundation of Fujian (2016J01450).

References

[1] B. R. Singer, G. J. McLauchlan, C. M. Robinson, and J. Christie, "Epidemiology of fractures in 15,000 adults: the influence of age and gender," *Journal of Bone and Joint Surgery British Volume (London)*, vol. 80, no. 2, pp. 243–248, 1998.

[2] E. M. Curtis, R. van der Velde, R. J. Moon et al., "Epidemiology of fractures in the United Kingdom 1988–2012: variation with age, sex, geography, ethnicity and socioeconomic status," *Bone*, vol. 87, pp. 19–26, 2016.

[3] J. E. Mumford and A. H. R. W. Simpson, "Management of bone defects: a review of available techniques," *The Iowa Orthopaedic Journal*, vol. 12, pp. 42–49, 1990.

[4] M. M. Alzahrani, E. Anam, S. M. AlQahtani, A. M. Makhdom, and R. C. Hamdy, "Strategies of enhancing bone regenerate formation in distraction osteogenesis," *Connective Tissue Research*, vol. 59, no. 1, pp. 1–11, 2018.

[5] J. Xu, Y. C. Jia, Q. L. Kang, and Y. M. Chai, "Management of hypertrophic nonunion with failure of internal fixation by distraction osteogenesis," *Injury*, vol. 46, no. 10, pp. 2030–2035, 2015.

[6] I. L. ERALP, "Treatment of infected nonunion of the juxta-articular region of the distal tibia," *Acta Orthopaedica et Traumatologica Turcica*, vol. 50, no. 2, pp. 139–146, 2015.

[7] W. Azzam and M. El-Sayed, "Ilizarov distraction osteogenesis over the preexisting nail for treatment of nonunited femurs with significant shortening," *European Journal of Orthopaedic Surgery and Traumatology*, vol. 26, no. 3, pp. 319–328, 2016.

[8] H. Terheyden, H. Wang, P. H. Warnke et al., "Acceleration of callus maturation using rhOP-1 in mandibular distraction osteogenesis in a rat model," *International Journal of Oral and Maxillofacial Surgery*, vol. 32, no. 5, pp. 528–533, 2003.

[9] T. Haque, F. Hamade, N. Alam et al., "Characterizing the BMP pathway in a wild type mouse model of distraction osteogenesis," *Bone*, vol. 42, no. 6, pp. 1144–1153, 2008.

[10] X. Yang, P. Gong, Y. Lin et al., "Cyclic tensile stretch modulates osteogenic differentiation of adipose-derived stem cells via the BMP-2 pathway," *Archives of Medical Science*, vol. 6, no. 2, pp. 152–159, 2010.

[11] Y. Li, R. Li, J. Hu, D. Song, X. Jiang, and S. Zhu, "Recombinant human bone morphogenetic protein-2 suspended in fibrin glue enhances bone formation during distraction osteogenesis in rabbits," *Archives of Medical Science*, vol. 12, no. 3, pp. 494–501, 2016.

[12] F. Westhauser, M. Höllig, B. Reible, K. Xiao, G. Schmidmaier, and A. Moghaddam, "Bone formation of human mesenchymal stem cells harvested from reaming debris is stimulated by low-dose bone morphogenetic protein-7 application in vivo," *Journal of Orthopaedics*, vol. 13, no. 4, pp. 404–408, 2016.

[13] J. J. Minguell, A. Erices, and P. Conget, "Mesenchymal stem cells," *Experimental Biology and Medicine*, vol. 226, no. 6, pp. 507–520, 2001.

[14] J. H. D. Rölfing, A. Baatrup, M. Stiehler, J. Jensen, H. Lysdahl, and C. Bünger, "The osteogenic effect of erythropoietin on human mesenchymal stromal cells is dose-dependent and involves non-hematopoietic receptors and multiple intracellular signaling pathways," *Stem Cell Reviews*, vol. 10, no. 1, pp. 69–78, 2014.

[15] L. Ye, L. Chen, Q. Yu, and F. Cheng, "Effect of recombinant human erythropoietin on the stemness of bone marrow-derived mesenchymal stem cells in vitro," *International Journal of Stem Cells*, vol. 3, no. 2, pp. 175–182, 2010.

[16] J. H. Holstein, M. Orth, C. Scheuer et al., "Erythropoietin stimulates bone formation, cell proliferation, and angiogenesis in a femoral segmental defect model in mice," *Bone*, vol. 49, no. 5, pp. 1037–1045, 2011.

[17] H. Sun, Y. Jung, Y. Shiozawa, R. S. Taichman, and P. H. Krebsbach, "Erythropoietin modulates the structure of bone morphogenetic protein 2–engineered cranial bone," *Tissue Engineering. Part A*, vol. 18, no. 19-20, pp. 2095–2105, 2012.

[18] J. R. Mauney, S. Sjostorm, J. Blumberg et al., "Mechanical stimulation promotes osteogenic differentiation of human bone marrow stromal cells on 3-D partially demineralized bone scaffolds in vitro," *Calcified Tissue International*, vol. 74, no. 5, pp. 458–468, 2004.

[19] Y. Wu, X. Zhang, P. Zhang, B. Fang, and L. Jiang, "Intermittent traction stretch promotes the osteoblastic differentiation of bone mesenchymal stem cells by the ERK1/2-activated Cbfa1 pathway," *Connective Tissue Research*, vol. 53, no. 6, pp. 451–459, 2012.

[20] D. Pavlin, S. B. Dove, R. Zadro, and J. Gluhak-Heinrich, "Mechanical loading stimulates differentiation of periodontal osteoblasts in a mouse osteoinduction model: effect on type I collagen and alkaline phosphatase genes," *Calcified Tissue International*, vol. 67, no. 2, pp. 163–172, 2000.

[21] S. Y. Liu, Y. B. He, S. Y. Deng, W. T. Zhu, S. Y. Xu, and G. X. Ni, "Exercise affects biological characteristics of mesenchymal stromal cells derived from bone marrow and adipose tissue," *International Orthopaedics*, vol. 41, no. 6, pp. 1199–1209, 2017.

[22] N. Su, Q. Sun, C. Li et al., "Gain-of-function mutation in FGFR3 in mice leads to decreased bone mass by affecting both osteoblastogenesis and osteoclastogenesis," *Human Molecular Genetics*, vol. 19, no. 7, pp. 1199–1210, 2010.

[23] J. Kim, Y. Jung, H. Sun et al., "Erythropoietin mediated bone formation is regulated by mTOR signaling," *Journal of Cellular Biochemistry*, vol. 113, no. 1, pp. 220–228, 2012.

[24] M. Koike, H. Shimokawa, Z. Kanno, K. Ohya, and K. Soma, "Effects of mechanical strain on proliferation and differentiation of bone marrow stromal cell line ST2," *Journal of Bone and Mineral Metabolism*, vol. 23, no. 3, pp. 219–225, 2005.

[25] Y. Song, Y. Tang, J. Song et al., "Cyclic mechanical stretch enhances BMP9-induced osteogenic differentiation of mesenchymal stem cells," *International Orthopaedics*, vol. 42, no. 4, pp. 947–955, 2018.

[26] G. Song, Y. Ju, X. Shen, Q. Luo, Y. Shi, and J. Qin, "Mechanical stretch promotes proliferation of rat bone marrow mesenchymal stem cells," *Colloids and Surfaces B: Biointerfaces*, vol. 58, no. 2, pp. 271–277, 2007.

[27] Y. Wu, P. Zhang, Q. Dai et al., "Effect of mechanical stretch on the proliferation and differentiation of BMSCs from ovariectomized rats," *Molecular and Cellular Biochemistry*, vol. 382, no. 1-2, pp. 273–282, 2013.

[28] J. Gao, S. Fu, Z. Zeng et al., "Cyclic stretch promotes osteogenesis-related gene expression in osteoblast-like cells through a cofilin-associated mechanism," *Molecular Medicine Reports*, vol. 14, no. 1, pp. 218–224, 2016.

[29] G. Ma, J. L. Zhao, M. Mao, J. Chen, Z. W. Dong, and Y. P. Liu, "Scaffold-based delivery of bone marrow mesenchymal stem cell sheet fragments enhances new bone formation in vivo," *Journal of Oral and Maxillofacial Surgery*, vol. 75, no. 1, pp. 92–104, 2017.

[30] K. M. Choi, Y. K. Seo, H. H. Yoon et al., "Effects of mechanical stimulation on the proliferation of bone marrow-derived human mesenchymal stem cells," *Biotechnology and Bioprocess Engineering*, vol. 12, no. 6, pp. 601–609, 2007.

[31] A. Charoenpanich, M. E. Wall, C. J. Tucker et al., "Cyclic tensile strain enhances osteogenesis and angiogenesis in mesenchymal stem cells from osteoporotic donors," *Tissue Engineering. Part A*, vol. 20, no. 1-2, pp. 67–78, 2014.

[32] C. A. Simmons, S. Matlis, A. J. Thornton, S. Chen, C. Y. Wang, and D. J. Mooney, "Cyclic strain enhances matrix mineralization by adult human mesenchymal stem cells via the extracellular signal-regulated kinase (ERK1/2) signaling pathway," *Journal of Biomechanics*, vol. 36, no. 8, pp. 1087–1096, 2003.

[33] M. C. Qi, J. Hu, S. J. Zou, H. Q. Chen, H. X. Zhou, and L. C. Han, "Mechanical strain induces osteogenic differentiation: Cbfa1 and Ets-1 expression in stretched rat mesenchymal stem cells," *International Journal of Oral and Maxillofacial Surgery*, vol. 37, no. 5, pp. 453–458, 2008.

[34] Y. He, F. Lin, Y. Chen, Z. Tan, D. Bai, and Q. Zhao, "Overexpression of the circadian clock gene *Rev-erbα* affects murine bone mesenchymal stem cell proliferation and osteogenesis," *Stem Cells and Development*, vol. 24, no. 10, pp. 1194–1204, 2015.

[35] J. Yuan, F. Xin, and W. Jiang, "Underlying signaling pathways and therapeutic applications of pulsed electromagnetic fields in bone repair," *Cellular Physiology and Biochemistry*, vol. 46, no. 4, pp. 1581–1594, 2018.

[36] R. C. Riddle, K. R. Hippe, and H. J. Donahue, "Chemotransport contributes to the effect of oscillatory fluid flow on human bone marrow stromal cell proliferation," *Journal of Orthopaedic Research*, vol. 26, no. 7, pp. 918–924, 2008.

[37] P. Ducy, R. Zhang, V. Geoffroy, A. L. Ridall, and G. Karsenty, "Osf2/Cbfa1: a transcriptional activator of osteoblast differentiation," *Cell*, vol. 89, no. 5, pp. 747–754, 1997.

[38] F. Otto, A. P. Thornell, T. Crompton et al., "Cbfa1, a candidate gene for cleidocranial dysplasia syndrome, is essential for osteoblast differentiation and bone development," *Cell*, vol. 89, no. 5, pp. 765–771, 1997.

[39] P. Zhang, Y. Wu, Z. Jiang, L. Jiang, and B. Fang, "Osteogenic response of mesenchymal stem cells to continuous mechanical strain is dependent on ERK1/2-Runx2 signaling," *International Journal of Molecular Medicine*, vol. 29, no. 6, pp. 1083–1089, 2012.

[40] T. Kanno, T. Takahashi, T. Tsujisawa, W. Ariyoshi, and T. Nishihara, "Mechanical stress-mediated Runx2 activation is dependent on Ras/ERK1/2 MAPK signaling in osteoblasts," *Journal of Cellular Biochemistry*, vol. 101, no. 5, pp. 1266–1277, 2007.

[41] Y. Shiozawa, Y. Jung, A. M. Ziegler et al., "Erythropoietin couples hematopoiesis with bone formation," *PLoS One*, vol. 5, no. 5, article e10853, 2010.

[42] Q. Chen, W. Liu, K. M. Sinha, H. Yasuda, and B. de Crombrugghe, "Identification and characterization of microRNAs controlled by the osteoblast-specific transcription factor Osterix," *PLoS One*, vol. 8, no. 3, article e58104, 2013.

[43] W. L. Xiao, D. Z. Zhang, C. H. Fan, and B. J. Yu, "Intermittent stretching and osteogenic differentiation of bone marrow derived mesenchymal stem cells via the p38MAPK-Osterix signaling pathway," *Cellular Physiology and Biochemistry*, vol. 36, no. 3, pp. 1015–1025, 2015.

[44] M. Brines and A. Cerami, "Erythropoietin-mediated tissue protection: reducing collateral damage from the primary injury response," *Journal of Internal Medicine*, vol. 264, no. 5, pp. 405–432, 2008.

[45] K. J. Zwezdaryk, S. B. Coffelt, Y. G. Figueroa et al., "Erythropoietin, a hypoxia-regulated factor, elicits a pro-angiogenic program in human mesenchymal stem cells," *Experimental Hematology*, vol. 35, no. 4, pp. 640–652, 2007.

[46] J. Zhang, Y. Yang, T. He et al., "Expression profiles uncover the relationship between erythropoietin and cell proliferation in rat hepatocytes after a partial hepatectomy," *Cellular and Molecular Biology Letters*, vol. 19, no. 3, pp. 331–346, 2014.

[47] A. Parandakh, M. Tafazzoli-Shadpour, and M. M. Khani, "Stepwise morphological changes and cytoskeletal reorganization of human mesenchymal stem cells treated by short-time cyclic uniaxial stretch," *In Vitro Cellular & Developmental Biology. Animal*, vol. 53, no. 6, pp. 547–553, 2017.

[48] K. A. Kilian, B. Bugarija, B. T. Lahn, and M. Mrksich, "Geometric cues for directing the differentiation of mesenchymal stem cells," *Proceedings of the National Academy of Sciences of the United States of America*, vol. 107, no. 11, pp. 4872–4877, 2010.

[49] W. Wang, D. Deng, J. Li, and W. Liu, "Elongated cell morphology and uniaxial mechanical stretch contribute to physical attributes of niche environment for MSC tenogenic differentiation," *Cell Biology International*, vol. 37, no. 7, pp. 755–760, 2013.

Hindawi
Stem Cells International
Volume 2019, Article ID 1351860, 15 pages
https://doi.org/10.1155/2019/1351860

Research Article

Promoting Osteogenic Differentiation of Human Adipose-Derived Stem Cells by Altering the Expression of Exosomal miRNA

Shude Yang, Shu Guo, Shuang Tong, and Xu Sun

Department of Plastic Surgery, The First Hospital of China Medical University, No. 155, Nanjing North Street, Heping District, Shenyang, 110002 Liaoning Province, China

Correspondence should be addressed to Shu Guo; guoshu187@139.com

Received 7 March 2019; Revised 7 May 2019; Accepted 23 May 2019; Published 1 July 2019

Guest Editor: Yongcan Huang

Human adipose-derived stem cells (ADSCs) can release exosomes; however, their specific functions remain elusive. In this study, we verified that exosomes derived from osteogenically differentiated ADSCs can promote osteogenic differentiation of ADSCs. Furthermore, in order to investigate the importance of exosomal microRNAs (miRNAs) in osteogenic differentiation of ADSCs, we used microarray assays to analyze the expression profiles of exosomal miRNAs derived from undifferentiated as well as osteogenically differentiated ADSCs; 201 miRNAs were upregulated and 33 miRNAs were downregulated between the two types of exosomes. Additionally, bioinformatic analyses, which included gene ontology analyses, pathway analysis, and miRNA-mRNA-network investigations, were performed. The results of these analyses revealed that the differentially expressed exosomal miRNAs participate in multiple biological processes, such as gene expression, synthesis of biomolecules, cell development, differentiation, and signal transduction, among others. Moreover, we found that these differentially expressed exosomal miRNAs connect osteogenic differentiation to processes such as axon guidance, MAPK signaling, and Wnt signaling. To the best of our knowledge, this is the first study to identify and characterize exosomal miRNAs derived from osteogenically differentiated ADSCs. This study confirms that alterations in the expression of exosomal miRNAs can promote osteogenic differentiation of ADSCs, which also provides the foundation for further research on the regulatory functions of exosomal miRNAs in the context of ADSC osteogenesis.

1. Introduction

Effective reconstruction of craniomaxillofacial bone defects caused by trauma, tumor resection, or congenital malformation is a major problem in orthopedic surgery. In most cases, bones can regenerate and heal themselves [1]. However, this ability is lost when the area of the bone defect exceeds a critical size. In clinical practice, autologous and allogenic bone grafts can be a "gold standard" in bone defect treatment, even they have certain limitations such as chronic pain, poor cosmesis, nonunion, and infection [2, 3]. Over the last decades, mesenchymal stem cells (MSCs) have attracted extensive attention in the field of bone regeneration [4–7].

MSCs are a population of nonhematopoietic adult stem cells that have the property of self-renewal and can differentiate into multiple lineages [8–10]. They were initially found in the bone marrow [11] but can also be found in other tissues, such as adipose, periosteum, muscle, placenta, and trabecular bone [12]. Among these, adipose-derived stem cells (ADSCs) are a type of mesenchymal stem cell isolated from adipose tissue, which has the advantages of abundant storage *in vivo*, easy acquisition, and expansion [13–15]. Recently, a number of studies have confirmed that ADSCs possess the ability to differentiate into adipocytes, osteoblasts, and chondrocytes [16–18], suggesting that a broader source of stem cells is available for application in tissue engineering. ADSCs have already been used in bone regeneration [19, 20].

With the in-depth researches of MSCs, an increasing number of studies have indicated that the therapeutic effects of MSCs can be attributed not only to their differentiation capacity but also to their paracrine action [21]. Most of these paracrine secretions include soluble factors and exosomes, which regulate the repair and regeneration processes at sites of damage by affecting cell proliferation, migration, and

differentiation [22, 23]. Exosomes are a type of sphere- or dish-shaped extracellular vesicle whose diameter is between 30 and 150 nm. Exosomes are found in abundance in endosome-derived components, which are considered to play important roles in intercellular communication due to their ability to transfer "cargos" [24, 25]. By transporting "cargos" such as proteins, RNAs, DNAs, and lipids [26], exosomes regulate the eventual fate of recipient cells. Recently, several studies have shown that ADSC-derived exosomes can exert similar biological effects as ADSCs and enhance bone regeneration [27, 28].

However, how exosomes function in osteogenic differentiation of ADSCs still needs to be further explored. As exosome research techniques develop, researchers have discovered that exosomes can induce epigenetic changes and regulate the fate of receptor cells in the process of promoting bone tissue repair and regeneration, including promoting proliferation or inhibiting apoptosis. Proteins and RNAs play vital roles in such processes [29–31]. MicroRNAs (miRNAs) are endogenous non-protein-coding RNAs with a length of approximately 22 nt. They can act as quintessential post-transcriptional regulators and can regulate the expression of target genes, mainly through specific binding to the $3'$ untranslated regions (UTRs) of target genes [32]. Targeted binding of miRNAs to mRNAs leads to recruitment of the targeted mRNAs to the RNA-induced silencing complex (RISC), which then leads to translation stoppage and degradation of mRNA [32, 33]. Through this process, miRNAs can inhibit protein expression of targeted mRNAs. In recent years, an increasing number of studies have demonstrated that miRNAs play important roles in bone formation [34, 35]. Additionally, it has been found that exosomes contain miRNAs [36], which can regulate the process of bone regeneration by targeting multiple genes in recipient cells [34]. Nevertheless, there is a lack of data regarding the global expression profiles of miRNAs in exosomes derived from undifferentiated and osteogenic-differentiated ADSCs.

In this study, we verified that only exosomes derived from osteogenically differentiated ADSCs can promote osteogenic differentiation of ADSCs. Moreover, we compared the expression profiles of miRNAs in exosomes derived from undifferentiated ADSCs with those from osteogenically differentiated ADSCs using microarray assays and performed bioinformatic analyses to further explore the biological functions of these differentially expressed miRNAs, which will lay the foundation for further study regarding ADSCs' osteogenic regulatory functions of exosomal miRNAs.

2. Material and Methods

The study was approved by the Ethics Committee of the First Hospital of China Medical University, Shenyang, China.

2.1. Isolation, Culture, and Characterization of ADSCs

2.1.1. Isolation and Culture of ADSCs. Human adipose tissue was obtained from 6 female patients aged 26.67 ± 5.57 years undergoing liposuction and without metabolic disease, hepatitis, HIV, syphilis, and other systemic diseases, which might affect the ongoing study at the Department of Plastic Surgery, in the first hospital of China Medical University.

ADSCs were separated and expanded according to the methods previously reported [37, 38]. In brief, the obtained adipose tissue was added into 50 mL centrifuge tubes and washed with sterile phosphate-buffered saline (PBS (Gibco, USA)), then centrifuged at 1200 $\times g$ for 5 min to remove red blood cells (RBCs). The above procedure was repeated 3–4 times before enzymatic digestion with 0.2% collagenase type I (Sigma, USA) at 37°C. Dulbecco's Modified Eagle's Medium/Nutrient F-12 Ham (DME F12 (HyClone, USA)), containing 10% fetal bovine serum (FBS (Gibco, USA)), was added to the digested lipoaspirates for 5 min in order to neutralize enzyme activity; this was followed by centrifugation at 1200 $\times g$ for 5 min. The pellet was resuspended and filtered through a 100 μm mesh filter to remove cellular debris. Finally, cells were plated in 75 cm^2 culture flasks and incubated in culture medium (DME F12, 10% FBS, 1% Penicillin-Streptomycin Solution (Gibco, USA)) at 37°C in 5% CO_2 with saturated humidity. The culture flasks were washed thoroughly with PBS to remove RBCs, and the medium was changed every two days. ADSCs were passaged until they were 90% confluent; 0.25% trypsin: 0.2% EDTA at a ratio of 1 : 3 was used to dissociate the cells. ADSCs at passage three were used for subsequent experiments.

2.1.2. Characterization of ADSCs by Flow Cytometry. Cells at the third passage (P3) were digested with trypsin to form a single cell suspension solution, which was incubated with antibodies, including anti-CD34-PE, anti-CD31-APC, anti-CD45-PerCP-Cy5-5, anti-CD10-APC-Cy7 (BioLegend, USA), anti-CD13-PE, and anti-CD49d-PE-Cy7 (BD Biosciences, USA). All antibody incubations were performed at 37°C in the dark for 30 min. The cells were analyzed by flow cytometry (LSR II, BD Biosciences, USA) and Treestar FlowJo software.

2.1.3. Multilineage Potential Assay of ADSCs. Third passage ADSCs were used to demonstrate their ability to differentiate into adipocytes, osteoblasts, and chondrocytes. Briefly, cells were seeded in a 24-well plate at a density of 5×10^3 cells/cm^2 in standard growth medium. According to the manufacturer's instructions, when the cells reached 90–100% confluence, the basal medium was replaced with complete OriCell™ osteogenic differentiation medium (Cyagen, USA) and complete MesenCult™ Adipogenic Differentiation Medium (Stem Cell Technologies, Canada) for aiding osteogenesis and adipogenesis of ADSCs. The medium was changed every 3 days for 2–4 weeks. Adipogenic and osteogenic differentiations were detected by oil red O (Cyagen, USA) and alizarin red S (Solarbio, China) staining, respectively.

To verify the chondrogenic differentiation ability of ADSCs, MesenCult™ Chondrogenic Differentiation Medium was added based on the manufacturer's instructions. Briefly, 5×10^5 cells were resuspended in 0.5 mL of complete MesenCult™ Chondrogenic Differentiation Medium and added into 15 mL polypropylene tubes, followed by centrifugation at 300 $\times g$ for 10 min. The caps of the tubes were loosened prior to incubation at 37°C under 5% CO_2 for 3 days. Then,

0.5 mL complete MesenCult™ Chondrogenic Differentiation Medium was added to a final volume of 1 mL, and incubation was continued at 37°C under 5% CO_2 for 3 days. The medium was changed every three days until day 28. Subsequently, the cartilage mass was fixed with formalin and embedded in paraffin. Finally, alcian blue (Solarbio, China) staining was performed to detect chondrogenic differentiation.

2.2. Extraction and Identification of ADSC-Derived Exosomes. When the cells reached 80%–90% confluence, we replaced the standard growth medium with serum-free medium and collected conditioned medium after incubating for an additional 24 h. Similarly, the cells in the experimental group were induced by treating with complete OriCell™ osteogenic differentiation medium (Cyagen, USA) for 14 days, and the conditioned medium was collected after 24 h of continuous culture with serum-free medium instead of the original medium. Exosomes were harvested by centrifugation and ultracentrifugation of the conditioned medium containing undifferentiated ADSCs (Exos_D0) and osteogenically differentiated ADSCs after 14 days (Exos_D14), respectively.

2.2.1. Extraction of ADSC-Derived Exosomes. The conditioned medium was centrifuged at 300 ×*g* for 10 min at 4°C, and the supernatant was collected. Next, the supernatant was centrifuged at 2000 ×*g* for 20 min at 4°C, and the resulting supernatant was transferred to a new tube and centrifuged at 10000 ×*g* for 30 min in a 45TI rotor (Beckman, USA). Finally, the precipitates containing the exosomes and contaminating proteins were collected after centrifugation at 130000 ×*g* for 70 min and were resuspended in 50 mL PBS. The resuspension was recentrifuged under the same conditions as the previous step to obtain exosomes, which were resuspended in PBS and sterilized by filtration using a 0.45 μm filter.

2.2.2. Identification of ADSC-Derived Exosomes. The structure of exosomes was observed by transmission electron microscopy (TEM, (HITACHI, Japan)). Characteristic surface markers of exosomes such as TSG101, CD9, and calnexin were detected by western blotting, as described in Section 2.6.

2.2.3. Uptake Assay of ADSC-Derived Exosomes In Vitro. To identify uptake of exosomes by ADSCs, exosomes were labeled with Dil (Beyotime Biotechnology, China) at a concentration of 10 μM for 15 min, according to the manufacturer's instructions. Then, the exosomes were incubated with ADSCs for 6 h. Nuclei of ADSCs were stained with Hoechst33258 (Solarbio, China). Exosome uptake was observed by fluorescence microscopy (OLYMPUS, Japan).

2.3. Osteogenic Differentiation of ADSCs with Exosomes and Alizarin Red S (ARS) Assay. ADSCs (P3) were seeded in a 6-well plate at a density of 2×10^4 cells/cm^2 in standard growth medium until the cells reached 90% confluence. Subsequently, the standard growth medium was changed to complete OriCell™ osteogenic differentiation medium (Cyagen, USA) with the medium containing Exos_D0 or Exos_D14, whose concentration was 20 μg/mL, compared to negative controls without simulation. The medium was changed every two days until day 21. According to the manufacturer's instructions, the cells were washed with PBS once or twice and fixed for 30 min with 2 mL of 4% neutral formaldehyde solution in each well. After the formaldehyde solution was aspirated away and wells washed with PBS twice, 1 mL of alizarin red S solution was added for 5 min. The plate was washed with PBS twice, followed by placement under a light microscope to observe the stained cells.

2.4. Alkaline Phosphatase (ALP) Activity Assay. The detected ADSCs were lysed by cell lysis buffer for Western and IP without inhibitors (Beyotime Biotechnology, China). Then, the supernatant was collected by centrifugation for semiquantitative analyses of ALP using an Alkaline Phosphatase Assay Kit (Beyotime Biotechnology, China) according to the manufacturer's instructions. As a common chromogenic substrate of phosphatase activity, paranitrophenol (p-nitrophenol) yields a yellow product under alkaline conditions. Optical density (OD) values were determined using a spectrophotometer (SpectraMax Plus384, Molecular Devices, USA) at 405 nm. Finally, we normalized ALP expression levels to the total cell protein content to obtain an absorbance index.

2.5. Isolation of Exosomal RNA. Exosomal RNA was isolated by the SeraMir Exosome RNA Purification kit (System Biosciences, USA), according to the manufacturer's instructions. The exosome RNA isolation protocol was mainly divided into three parts: exosome isolation and lysis, exoRNA purification, and exoRNA elution. For the isolation and lysis steps, culture medium was combined with ExoQuick-TC before thorough mixing by inversion three times. Then, the mixture was placed at 4°C for 6 h overnight and centrifuged at 11200 ×*g* for 2 min. After that, supernatant was removed and lysis buffer was added to the exosome pellet. After vortexing for 15 s, the mixture was placed at room temperature (25°C) for 5 min to allow complete lysis. For exoRNA purification, 100% ethanol was added before vortexing for 10 s. After the assembly of spin column and collection tubes, the mixture was transferred to spin columns and centrifuged at 11200 ×*g* for 1 min. The flow-through was discarded, and the spin column was placed back into a collection tube. Then, wash buffer was added before centrifugation at 11200 ×*g* for 1 min, and this step was repeated twice. Lastly, the flow-through was discarded and the mixture was centrifuged at 11200 ×*g* for 2 min to dry. For elution, the collection tube was discarded, and the spin column was assembled with a fresh, RNase-free 1.5 mL elution tube. Elution buffer was added directly to the spin column membrane and centrifuged at 300 ×*g* for 2 min and then 11200 ×*g* for 1 min to elute exoRNAs. After that, exosome RNA was recovered.

2.6. Quantitative Real-Time PCR (qPCR). Extraction of cellular total RNAs and synthesis of cDNA were performed using TRIzol™ Reagent (Invitrogen, USA) and PrimeScript™ RT Master Mix (TAKARA, Japan), respectively, according to the manufacturer's instructions. Quantitative fluorescence detection was performed using TB Green™ Premix Ex

Table 1: List of gene primers.

Gene	Forward sequence	Reverse sequence
ALP	CAACGAGGTCATCTCCGTGATG	TACCAGTTGCGGTTCACCGTGT
RUNX2	CCCAGTATGAGAGTAGGTGTCC	GGGTAAGACTGGTCATAGGACC
GAPDH	GTCTCCTCTGACTTCAACAGCG	ACCACCCTGTTGCTGTAGCCAA
U6	CTCGCTTCGGCAGCACA	AACGCTTCACGAATTTGCGT
miR-130a-3p	GATGCTCTCAGTGCAATGTTA	
miR-34a-5p	AGCCGCTGGCAGTGTCTTA	
miR-30b-5p	GCTGCCGTTGTAAACATCCTAC	
miR-324-5p	CAGCCTAATCGCATCCCCTA	
miR-513b-5p	GCCGCTTCACAAGGAGGT	
miR-378f	GCTGGGACTGGACTTGGA	

Taq™ II (TAKARA, Japan) according to the manufacturer's instructions, under the PCR conditions of predenaturation at 95°C for 30 s, denaturation at 95°C for 5 s, and extension at 60°C for 30 s, for 40 cycles. The relative expression was calculated by the $2^{-\Delta\Delta CT}$ method, and each experiment was repeated 3 times. Sequences of PCR primers for Runt-related transcription factor 2 (*RUNX2*), alkaline phosphatase (*ALP*), glyceraldehyde-3-phosphate dehydrogenase (*GAPDH*), differentially expressed miRNAs (miR-130a-3p, miR-30b-5p, miR-34a-5p, miR-324-5p, miR-378f, and miR-513b-5p), and *U6* are given in Table 1. *GAPDH* was used for mRNA normalization. *U6* was used for miRNA normalization. We defined significant results according to p value threshold (<0.05) and FC (fold change) threshold (≥2).

2.7. Western Blotting. Proteins were separated by electrophoresis on 11% SDS-PAGE gels and transferred to PVDF membranes (Millipore, USA) and stained with Ponceau S staining solution (Beyotime Biotechnology, China) for 5-10 min. Membranes were then incubated with each primary antibody, including anti-ALP, anti-RUNX2, anti-TSG101, anti-CD9, and anti-calnexin (Abcam, USA, 1 : 1000 dilution) for 16 h, and the respective secondary antibody (Cell Signaling Technology, USA, 1 : 5000 dilution) after the membrane was blocked with 5% evaporated skimmed milk. After each incubation, the membrane was washed three times with TBST. Target bands were developed using an enhanced chemiluminescence (ECL) kit (Solarbio, China) according to the manufacturer's instructions. To quantify the results of western blots, we calculated mean Intden (integrated density) values using ImageJ 1.8.0 software. The relative intensity was measured by normalization using GAPDH.

2.8. Microarray Assays. Total RNAs of Exos_D0 and Exos_D14 were extracted from exosomes using TRIzol™ Reagent (Invitrogen, USA) according to the manufacturer's instructions. The quantity and quality of RNA were examined by NanoDrop 2000 and Agilent Bioanalyzer 2100. Expression profiles of miRNA were tested by GeneChip 4.0 (Affymetrix, USA) and verified using three parallel replicates.

2.9. Bioinformatics Analysis. Recognition of differentially expressed genes was performed using the limma package of the R program [39] with thresholds of p values < 0.05 and $\log_2 |FC| \geq 1 (|FC| \geq 2)$. Differentially expressed genes in two datasets were selected for further analysis. In order to avoid biasing of results from different analysis platforms, we use DAVID Bioinformatics Resources 6.8 (https://david.ncifcrf.gov/) [40] for pathway analysis and gene ontology (GO) analyses, in which pathway analyses included Kyoto Encyclopedia of Genes and Genomes (KEGG) pathway analysis and Biocarta pathway analysis. GO analysis included biological process (BP), cellular component (CC), and molecular function (MF) categories. For the analysis results, we considered p values < 0.05 as significant. In addition, we selected 10 miRNAs with the most obvious differential expression to predict downstream target genes using three online analysis platforms: TargetScan (http://www.targetscan.org), microRNA.ORG (http://www.microrna.org/microrna/), and miRDB (http://mirdb.org/). We regarded the intersection of the three platforms as the ultimate target genes. In order to depict pathway and GO analysis results intuitively, we constructed enrichment analysis maps using R. The miRNA-Gene-Network was visually presented through Cytoscape 3.60.

2.10. Statistical Analysis. In this study, each experiment was checked by three parallel replicates to ensure the repeatability of the experiments. Statistical analysis was performed using SPSS 17.0 software and GraphPad Prism 7.0. For all data, p values < 0.05 were considered statistically significant.

3. Results

3.1. Identification of Human ADSCs. ADSCs that we used in this study were obtained by a method involving collagenase digestion and adherent cell culture. We detected characteristic ADSC surface markers using flow cytometry and obtained the following results: CD10, CD13, and CD49d expression was positive, while the expression of CD34, CD31, and CD45 was negative, as shown in Figure 1(a). Importantly, ADSCs can differentiate into adipocytes, osteoblasts, and chondrocytes (Figures 1(b)–1(d)), confirming multilineage potential, in line with the recognized standard for identification of ADSCs [9, 41].

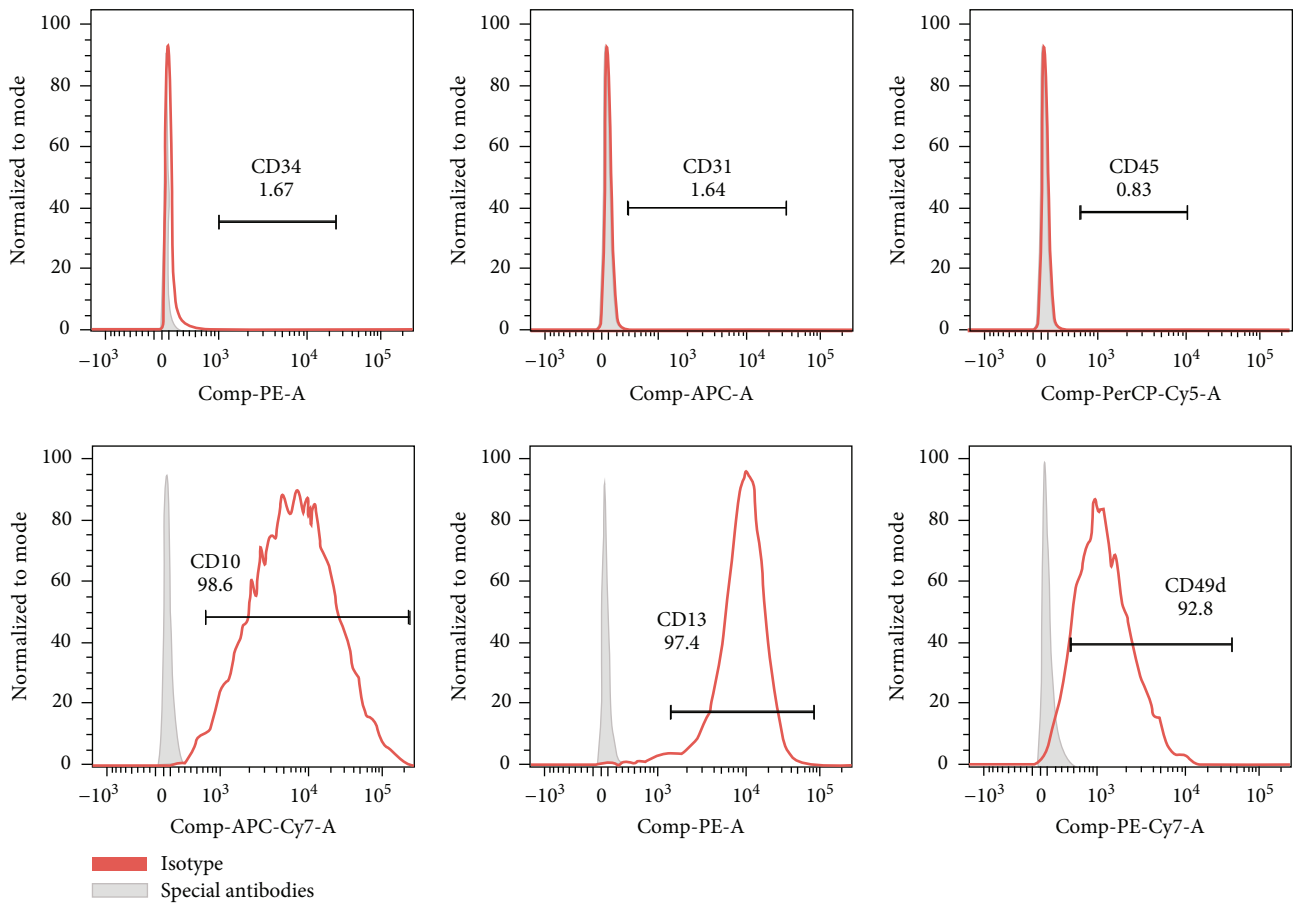

Figure 1: Characterization of ADSCs (P3). (a) The expression of the characteristic surface markers of ADSCs shown by flow cytometry. (b) Lipid droplets formed after 14 days of adipogenic induction, which is confirmed by oil red O staining. (c) Calcium nodules formed during osteogenic differentiation, which is identified by ARS after 28 days of osteogenic induction. (d) The chondrocytes stained by alcian blue after 28 days of chondrogenic induction. Notes: ADSCs: human adipose-derived stem cells; ARS: alizarin red S. Scale bar: 100 μm.

3.2. Exosomes Derived Only from Osteogenically Differentiated ADSCs Can Promote Osteogenic Differentiation

3.2.1. Identification of ADSC-Derived Exosomes. ADSC-derived exosomes were isolated by centrifugation and ultracentrifugation from conditioned medium. As shown in Figure 2(a), TEM revealed that vesicles with particle sizes between 30 nm and 150 nm exhibited spherical morphology, proving the presence of exosomes. In addition, the western blot results showed that the exosome-associated proteins TSG101 and CD9 were expressed while the endoplasmic reticulum protein calnexin was hardly expressed in exosomes (Figure 2(b)). The above results demonstrate that we successfully extracted ADSC-derived exosomes.

3.2.2. Exosome Uptake by ADSCs. To explore whether ADSCs can internalize exosomes, we incubated Dil-labeled exosomes with ADSCs for 6 h. As shown in Figure 3, exosomes labeled with Dil (red dots) were gradually internalized by ADSCs. Many exosomes were observed in the cytoplasm of their

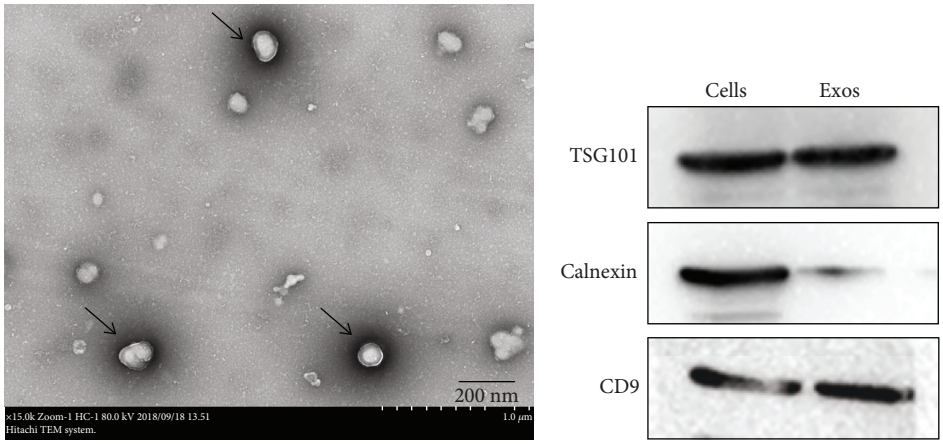

Figure 2: Identification of ADSCs-derived exosomes from the conditioned medium. (a) The image of TEM of ADSC-derived exosomes, scale bar: 200 nm. (b) Western blot analysis of the exosome-associated protein TSG101 and CD9 was expressed while endoplasmic reticulum proteins calnexin was hardly expressed. Notes: TEM: transmission electron microscopy.

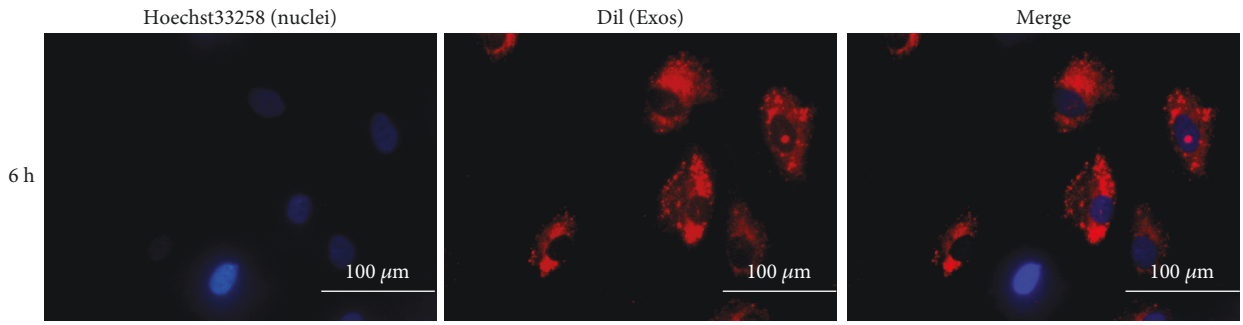

Figure 3: Internalization of exosomes by ADSCs. ADSCs can ingest a large number of exosomes at only 6 h postincubation. The results shown in Figure S1 further confirmed that exosomes can be internalized by ADSCs. Exosomes were labeled with Dil (red), and the nuclei were stained with Hoechst33258 (blue). Scale bar: 100 μm.

homotypic cells—ADSCs at only 6 h postincubation by fluorescence microscopy.

3.2.3. Exosomes Derived from Osteogenically Differentiated and Undifferentiated ADSCs Promote Osteogenic Differentiation of ADSCs. To investigate differences in exosome function, exosomes derived from undifferentiated ADSCs (Exos_D0) and osteogenically differentiated ADSCs at 14 days (Exos_D14) were extracted. Exos_D0 and Exos_D14 were used as stimuli to treat third passage ADSCs without other osteogenic interference factors. In order to establish more accurate results, we set-up 4 comparative groups: a negative control (NC) group, a positive control (PC) group, an Exos_D0 group, and an Exos_D14 group. ADSCs in the PC group were induced with osteogenic differentiation medium, while the NC group remained untreated.

qPCR and ALP activity assays were performed 7 days after treatment. Compared with NC and Exos_D0, the expression of osteogenesis-related genes such as *ALP* and *RUNX2* was significantly increased (FC > 2, $p < 0.05$) in the Exos_D14 and PC groups. Interestingly, there were no significant differences between the NC and Exos_D0 groups, but the difference between the Exos_D0 and Exos_D14 groups was obvious (Figure 4(a)). ALP semiquantitative analyses also showed similar results to those of qPCR. ALP activity was dramatically higher in the Exos_D14 and PC groups. In comparisons between NC and Exos_D0, Exos_D0 and Exos_D14 groups, the results exhibited no significant differences and notable differences (Figure 4(b)). Additionally, western blot analysis was corroborated by qPCR results in that protein expression of ALP, and RUNX2 was remarkably elevated in the Exos_D14 and PC groups, compared with NC and Exos_D0, as shown in Figures 4(c) and 4(d).

After 21 days of treatment, alizarin red staining revealed that there were significantly more calcium nodules formed in the Exos_D14 and PC groups (Figure 4(e)). These results confirmed that Exos_D14 rather than Exos_D0 can effectively promote osteogenic differentiation of ADSCs.

3.3. Distinct Levels of miRNA Expression in Exosomes Derived from Osteogenically Differentiated ADSCs and Undifferentiated ADSCs. In order to understand the underlying mechanisms of how exosomes promoted osteogenic differentiation of ADSCs, the miRNA expression profiles of exosomes derived from undifferentiated and osteogenically differentiated ADSCs were analyzed by microarray. We detected a total of 2170 mature miRNAs and 1868 pre-miRNAs expressed in ADSC-derived exosomes in which hierarchical clustering

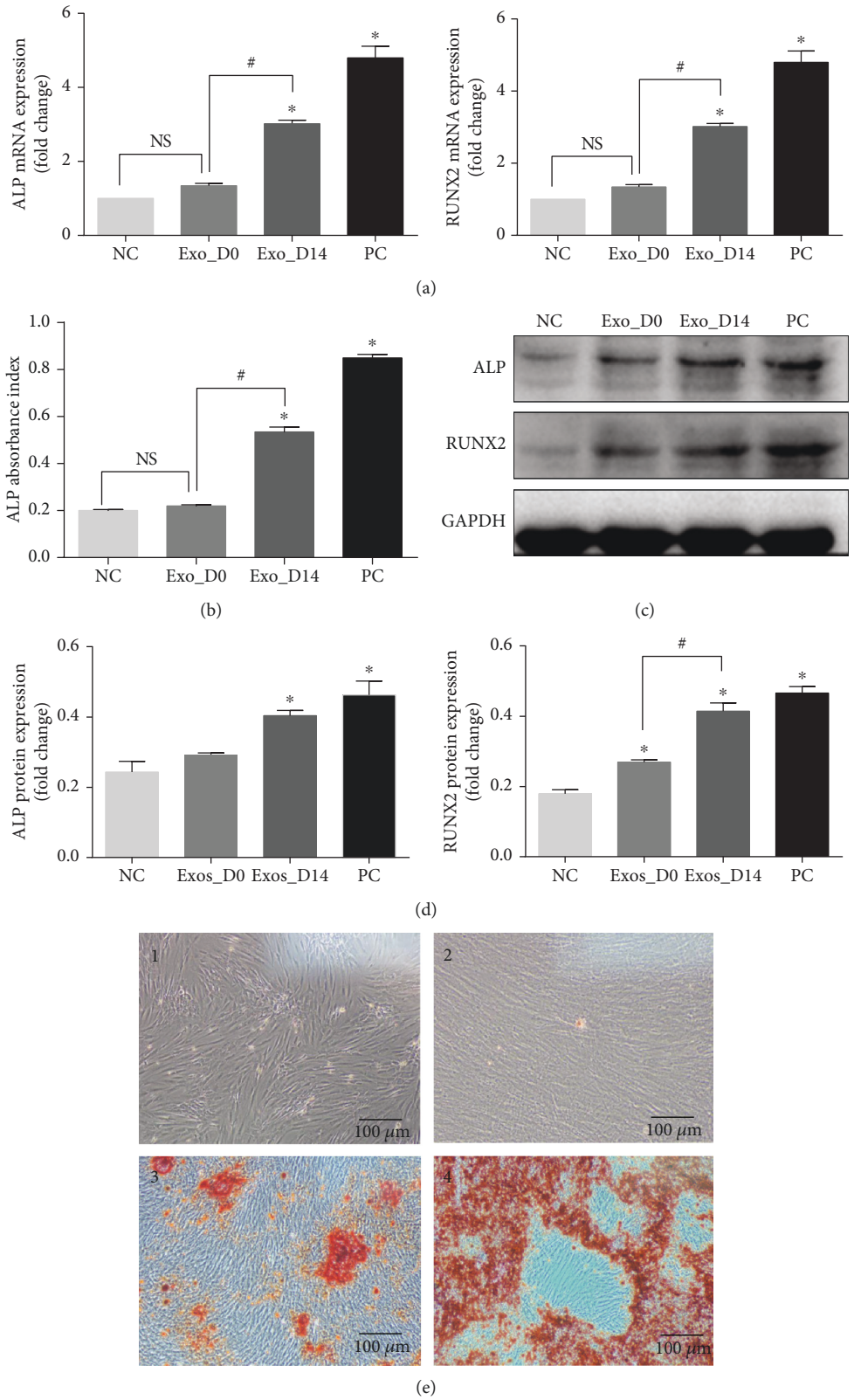

Figure 4: The Potential of exosomes' ability to promote osteogenic differentiation of ADSCs. (a) qPCR analysis expression of osteogenesis-related genes (ALP, RUNX2) in NC, Exos_D0, Exos_D14, and PC on 7th day. (b) Semiquantitative analyses of ALP activity on 7th day. (c) Western blot analyses of the protein expression of ALP and RUNX2 on 14th day. (d) Relative intensity analyses of western blot results of ALP and RUNX2. (e) ARS staining on 21st day (1 represents NC, 2 represents Exos_D0, 3 represents Exos_D14, and 4 represents PC), scale bar: 100 μm. Notes: *represents significant differences between NC and other groups; $^{\#}$represents significant differences between Exos_D14 and Exos_D0; NS represents no significant differences. $^{*}p < 0.05$; $^{\#}p < 0.05$.

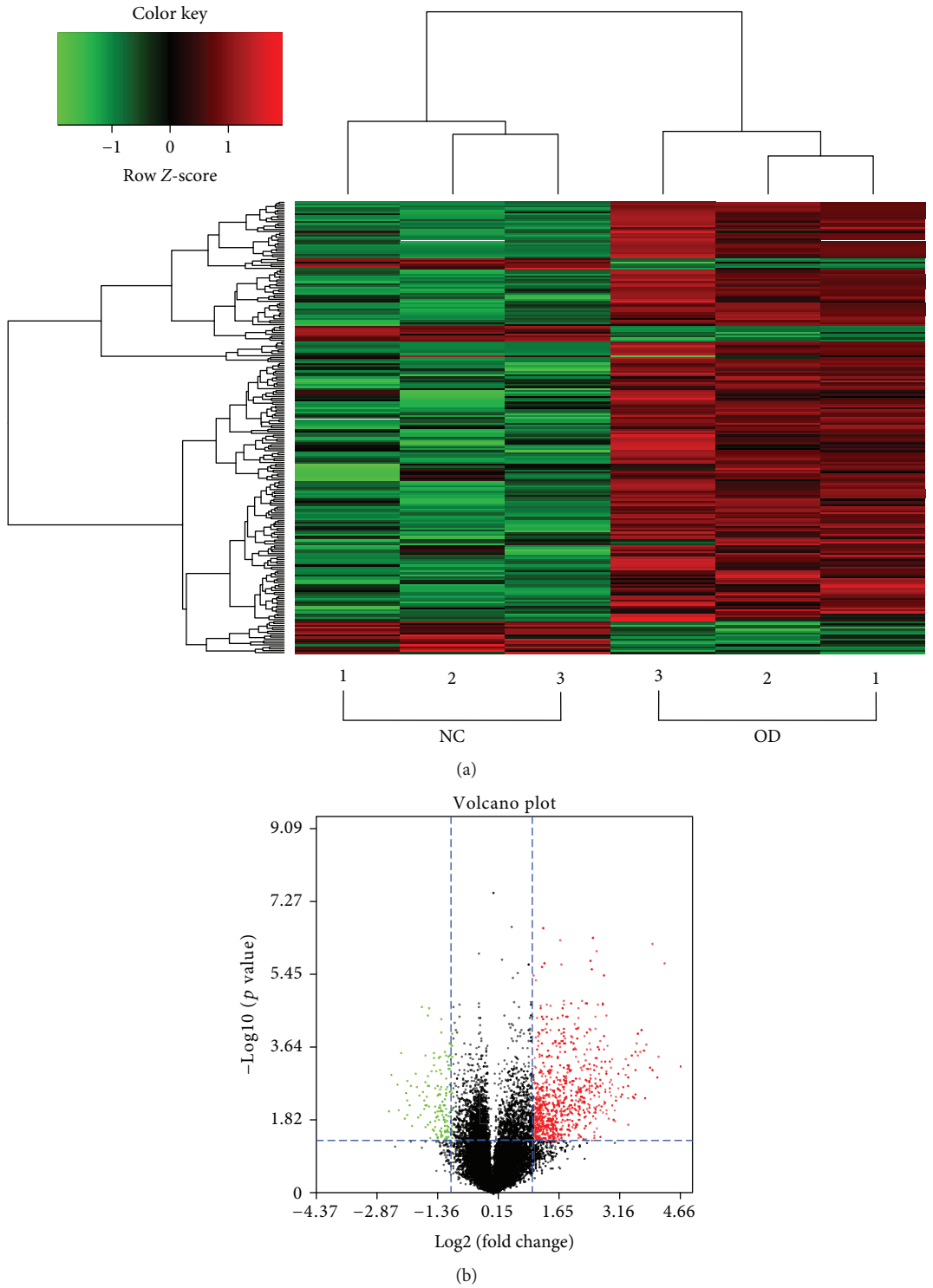

Figure 5: The miRNA differential expression profiles in exosomes. (a) The heat map of distinct miRNAs in exosomes derived from undifferentiated and osteogenically differentiated ADSCs based on microarray. (b) The volcano plot of miRNAs in exosomes derived from undifferentiated and osteogenically differentiated ADSCs. The red dots represent upregulation, and the green dots represent downregulation of expression with statistical significance (fold change ≥2, p value < 0.05). Notes: NC: normal control (exosomes derived from undifferentiated ADSCs); OD: osteogenic differentiation (exosomes derived from osteogenically differentiated ADSCs).

showed that miRNA expression profiles in the same group were consistent, while the expression profiles between the two groups were distinct. As shown in Figure 5(a), the abscissa represents sample clustering (the first three columns represent exosomes derived from undifferentiated ADSCs, and the last three columns represent exosomes derived from osteogenically differentiated ADSCs) and the ordinate represents gene clustering. The deeper the red, the more obvious

the upregulation of the gene, and the deeper the green, the more obvious the downregulation of the gene.

Compared with exosomes derived from undifferentiated ADSCs, 201 miRNAs were upregulated and 33 miRNAs were downregulated in exosomes derived from osteogenically differentiated ADSCs (FC $\geq$ 2, p value < 0.05), as represented by a volcano plot (Figure 5(b)).

3.4. Exosomal miRNAs Affect Osteogenic Differentiation via a Series of Biological Processes. Exosomal miRNAs can affect the osteogenic differentiation process through a series of biological processes in which they first target related genes such that they can regulate axon guidance, MAPK signaling, and Wnt signaling and modify gene expression, cell metabolism, and other biological functions.

3.4.1. Pathway Analysis and Functional Analysis of Exosomal miRNAs. To determine which signaling pathways were changed during osteogenic differentiation of ADSCs regulated by exogenous microRNAs, KEGG pathway analysis and Biocarta pathway analysis were performed. The results revealed that the target genes of the differentially expressed miRNAs are principally related to processes such as axon guidance (p value = 1.16E-18), MAPK signaling (p value = 2.31E-16), Wnt signaling (p value = 1.03E-15), endocytosis (p value = 7.1E-12), regulation of actin cytoskeleton (p value = 1.31E-11), and the TGF-β signaling pathway (p value = 5.26E-10) (Figure 6(a)). It suggested that these biologic pathways were involved in osteogenic differentiation of ADSCs.

To explore the potential biological functions of differentially expressed miRNAs, we performed GO enrichment analyses, including BP, CC, and MF by DAVID. According to statistically significant GO analysis results (p values < 0.05), we found that functions such as enzyme binding (p value = 7.7E-69), cell projection (p value = 1.29E-54), transcription factor activity (p value = 1.53E-45), regulation of gene expression (p value = 4.52E-74), and cell metabolism (p value = 5.92E-74) are mainly affected by differentially expressed miRNAs (Figures 6(b)–6(d)). Interestingly, these functions were closely related to osteogenic differentiation of ADSCs.

3.4.2. miRNA-mRNA Network Analysis. miRNAs can target single or multiple genes involved in the same or different signaling pathways in order to regulate the process of bone regeneration [30]. To explore the link between differentially expressed miRNAs and associated protein-encoding mRNAs, we chose 10 miRNAs (miR-130a-3p, miR-30b-5p, miR-34a-5p, miR-183-5p, miR-212-3p, miR-324-5p, miR-345-5p, miR-378f, miR-513a-5p, and miR-513b-5p) with the most obvious differential expression to predict downstream target genes using TargetScan, microRNA.ORG, miRDB, and constructed miRNA-mRNA networks using Cytoscape. As shown in Figure 7, we discovered that one miRNA may recognize multiple target mRNAs simultaneously, and one gene may also be regulated by multiple miRNAs. More importantly, a great quantity of miRNAs was predicted to be involved in a variety of pathways that promote osteogenic differentiation. For instance, mir-130a-3p was a miRNA with the highest differential expression and which was predicted to have a high probability of binding to *SIRT7*. Previous research has found that knockdown of SIRT7 enhances osteogenic differentiation of bone marrow mesenchymal stem cells (BMSCs) [42].

3.4.3. qPCR Validation of miRNA Expression. The 6 miRNAs (miR-130a-3p, miR-513b-5p, miR-30b-5p, miR-34a-5p, miR-324-5p, and miR-378f) with the most obvious differential expression were chosen to validate the results of microarray analyses using qPCR. In agreement with the preliminary conclusions obtained by microarray, compared with exosomes derived from undifferentiated ADSCs, the expression of 5 miRNAs (miR-130a-3p, miR-30b-5p, miR-34a-5p, miR-324-5p, and miR-378f) in exosomes derived from osteogenically differentiated ADSCs was significantly increased (FC > 2, $p < 0.05$) while the expression of miR-513b-5p was decreased (Figure 8). qPCR results confirmed the validity of differentially expressed miRNAs identified by microarray, which revealed that these miRNAs have functions in regulating ADSC osteogenesis.

4. Discussion

A major issue in the field of bone regeneration is inducing differentiation of stem cells into osteoblasts. In addition to osteogenic differentiation medium, genetic modification, and growth factors, MSC-derived exosomes have also drawn much attention in recent years because of their ability to induce osteogenic differentiation of stem cells [28, 43, 44]. However, ADSC-derived exosomes have rarely been examined in the field of bone regeneration. In our current study, we explored the differences between the effects of exosomes derived from osteogenically differentiated ADSCs and undifferentiated ADSCs separately on osteogenic differentiation of ADSCs *in vitro*. Our results indicated that osteogenically differentiated ADSC-derived exosomes can promote osteogenic differentiation of ADSCs, whereas undifferentiated ADSC-derived exosomes cannot (Figure 4). This finding provides evidence that ADSC-derived exosomes can be an ideal inducing factor with excellent osteogenic efficacy, safety, and widespread availability in bone regeneration and clinical applications. Li et al. have proven that the addition of ADSC-derived exosomes to osteogenic differentiation medium can promote osteogenic differentiation of bone marrow MSCs *in vitro* [28]. To our knowledge, in the absence of factors intervening in osteogenic differentiation, for the first time, we have demonstrated excellent osteogenic activity of osteogenically differentiated ADSC-derived exosomes. In addition, we found that it took only 6 h for ADSCs to ingest a large number of ADSC-derived exosomes (Figure 3), compared to 48 h for bone marrow-derived stem cells (BMSCs) [28]. We speculated that perhaps this may be because ADSC-derived exosomes are more easily ingested by homotypic cells, namely, ADSCs. This suggests that the combination of ADSC-derived exosomes and ADSCs in bone tissue engineering can reduce the loss of exosomes, which is due to a longer uptake time, thus promoting bone regeneration more efficiently.

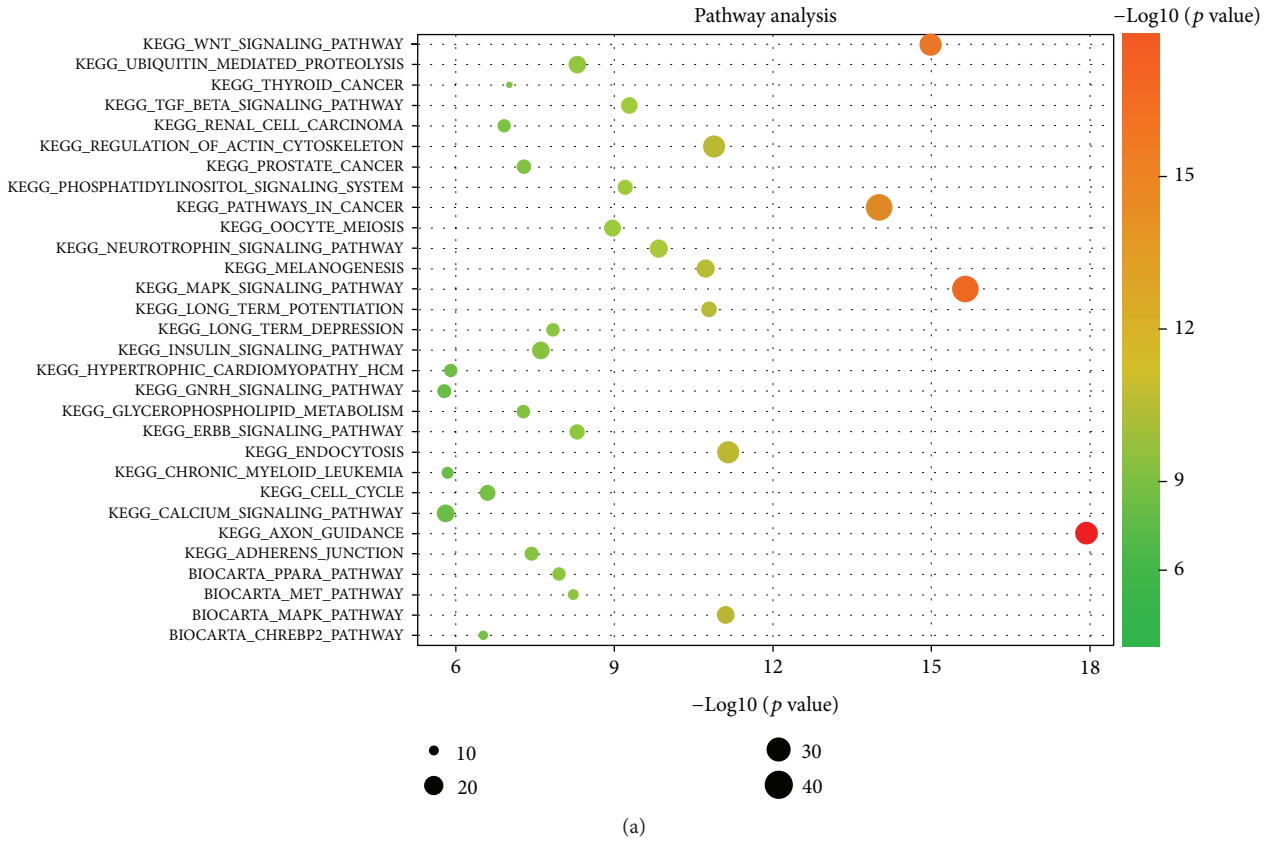

(a)

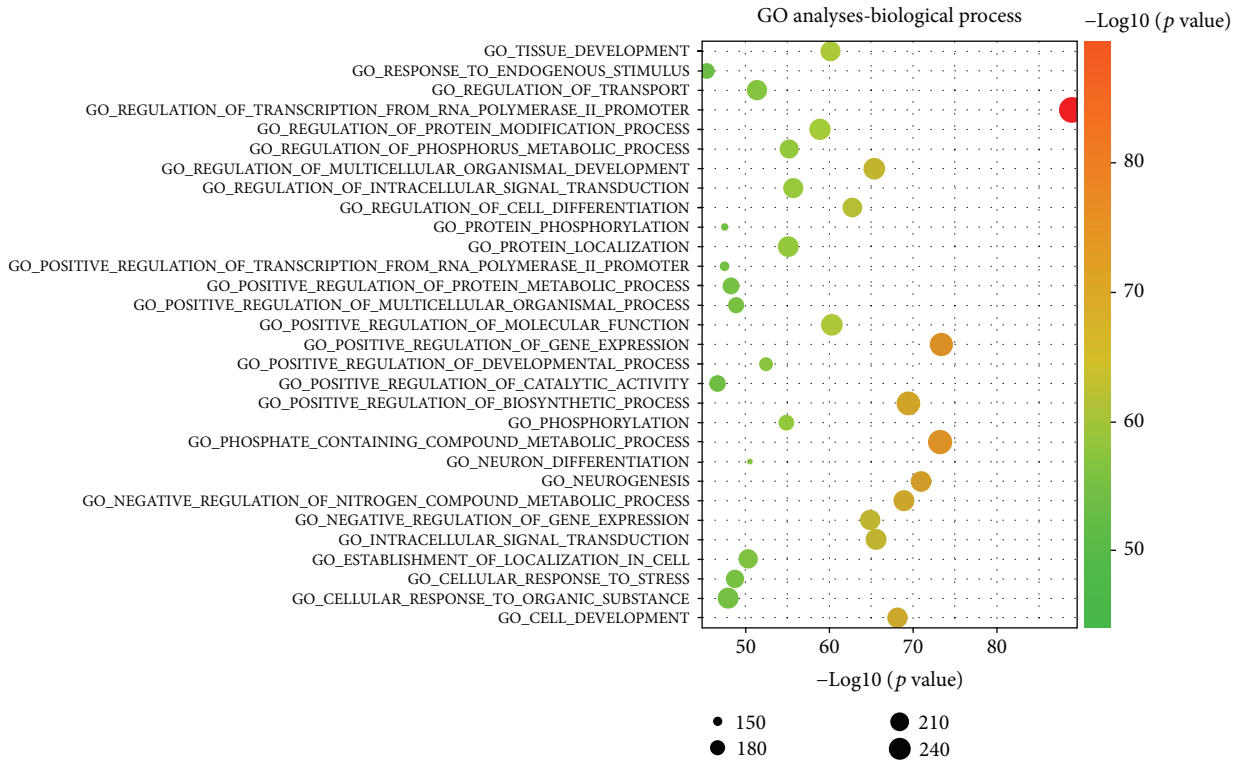

(b)

Figure 6: Continued.

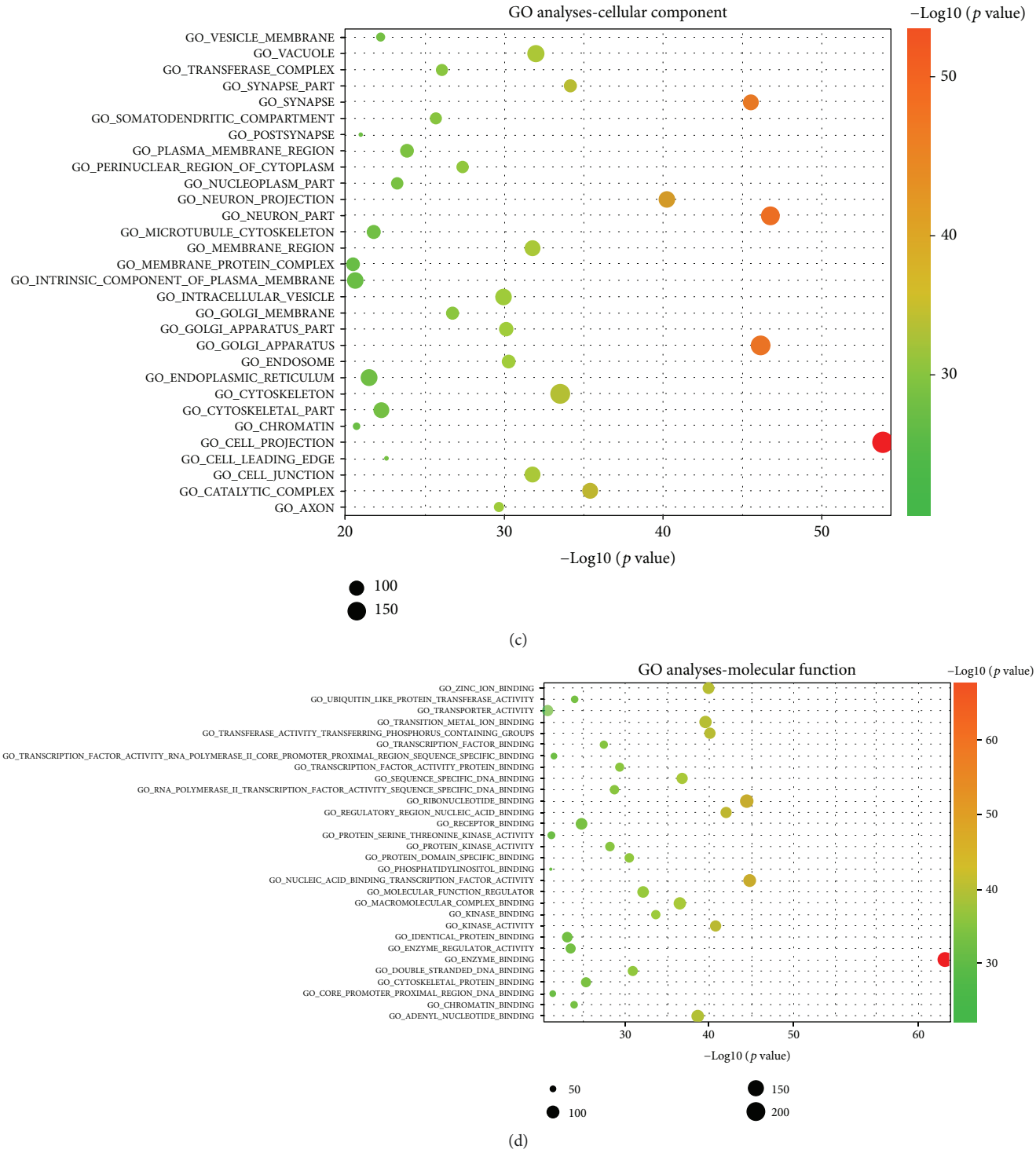

Figure 6: Pathway analysis and GO analyses. (a) Enrichment map of KEGG pathway analysis and Biocarta pathway analysis. (b) Enrichment map of GO analyses—biological process analysis. (c) Enrichment map of GO analyses—cellular component analysis. (d) Enrichment map of GO analyses—molecular function. Notes: KEGG: Kyoto Encyclopedia of Genes and Genomes pathway analysis; GO: gene ontology.

Understanding the precise molecular mechanisms of osteogenesis is of immense importance for promoting the osteogenic efficacy and clinical application of stem cells in bone regeneration. To date, most research has focused on the study of epigenetic and transcriptional factors involving stem cells themselves [45–47], whereas few studies have focused on the effects of exosome "cargo" on the osteogenic differentiation of stem cells. It has been noted that exosomes can regulate corresponding biological processes by affecting related pathways in receptor cells. For example, Yue et al.

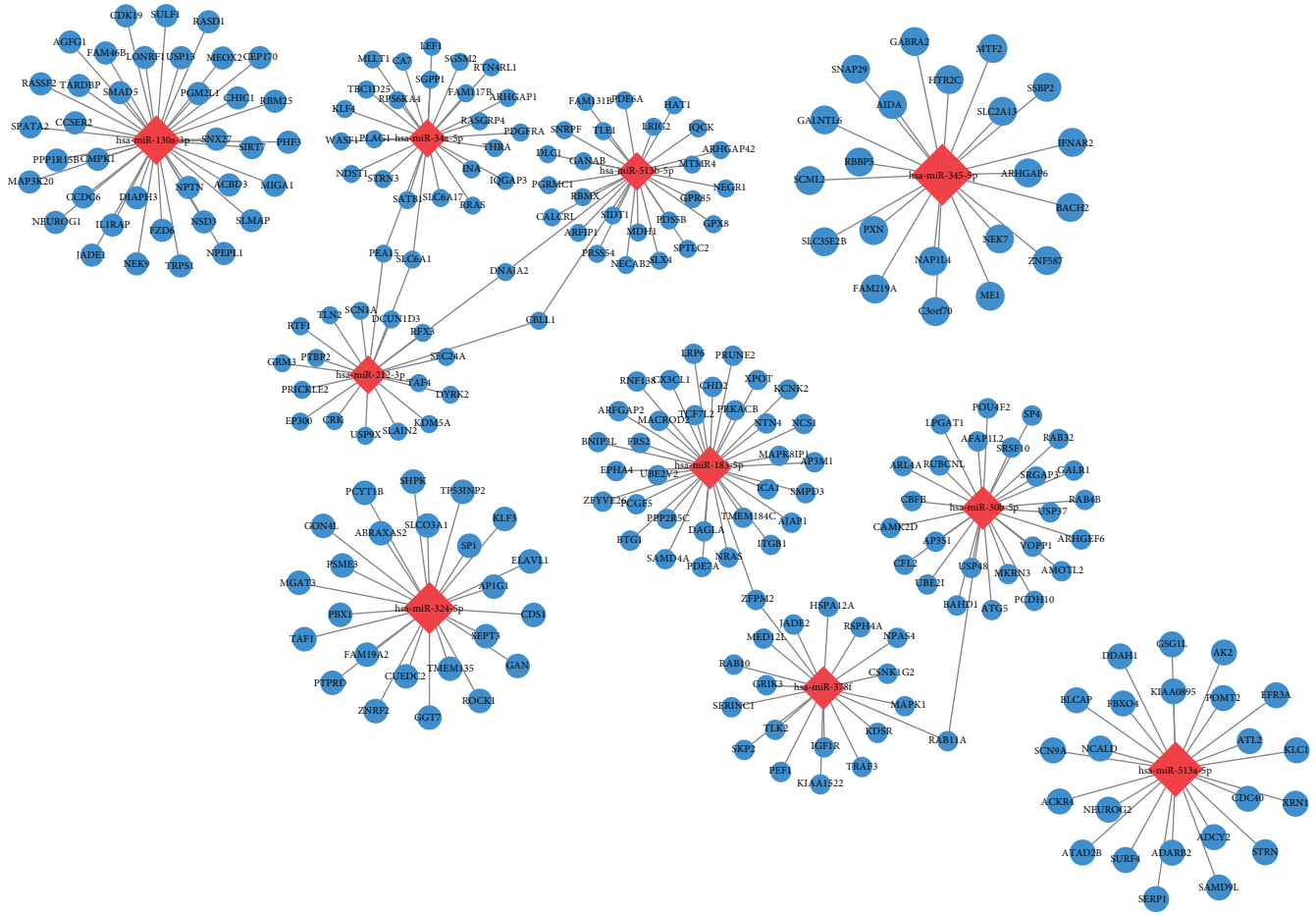

Figure 7: miRNA-mRNA network. The relationship between differentially expressed miRNAs and predicted downstream mRNA is clearly shown in the miRNA-mRNA network, which reveals that one miRNA may recognize multiple target mRNAs simultaneously, and one gene may also be regulated by multiple miRNAs. Notes: miRNA: microRNA; mRNA: messenger RNA.

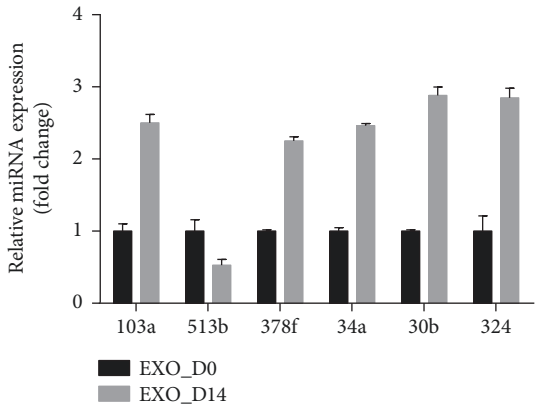

Figure 8: Comparison of the expression of chosen miRNA between Exos_D0 and Exos_D14 and qPCR results. For qPCR analyses, miRNA expression was normalized to U6 expression. Note: *represents significant differences between Exos_D0 and Exos_D14. $^{*}p < 0.05$.

showed that huc-MSC-derived exosomes promote cutaneous wound healing by influencing Wnt4 signaling [48]. Zhang et al. demonstrated that exosomes can enhance bone regeneration by activating the PI3K/Akt signaling pathway [49]. Interestingly, microRNAs can regulate the expression of mRNA by binding specifically to the 3′UTR of target genes, thus affecting the corresponding signaling pathways [32]. Based on previous studies, we have learned that there are proteins, DNAs, RNAs, lipids, and other biomolecules in exosomes, among which proteins and RNAs play important roles [25, 28]. miRNAs, an important class of RNA, are involved in a series of crucial processes, including cell growth, cell proliferation, differentiation, apoptosis, and cell death. Numerous reviews have mentioned that miRNAs play a critical role in bone biology [50–52]. Moreover, there are no reports concerning the genome-wide expression and function of miRNAs in ADSC-derived exosomes. We analyzed differences in the expression of miRNAs between undifferentiated ADSC-derived exosomes and osteogenically differentiated ADSC-derived exosomes by microarray assays.

Dysregulation of exosome-derived miRNA expression has been reported in schizophrenia and localized breast cancer [53, 54]. These studies suggested that the expression of miRNAs in exosomes changed significantly under different conditions. In this study, we detected 2170 mature miRNAs and 1868 pre-miRNAs in ADSC-derived exosomes. Compared with undifferentiated ADSC-derived exosomes, there

were 234 significantly differentially expressed miRNAs (201 upregulated and 33 downregulated) in osteogenically differentiated ADSC-derived exosomes. A heat map of distinct miRNAs in exosomes indicates that miRNAs may play an important regulatory role in the process of osteogenic differentiation of ADSCs, promoted by exosomes.

miRNAs act through base pairing with complementary sequences within mRNAs and silence expression of corresponding genes, thus interfering with signaling pathways [55]. Furthermore, 10 differentially expressed miRNAs showing a high fold change were selected to predict their target genes and to perform pathway analysis. We found that one miRNA can target multiple mRNAs and that one mRNA can be regulated by one or more miRNAs. This conclusion is consistent with previous reports [56]. In our study, a majority of predicted miRNAs involved in signaling pathways were related to osteogenic differentiation, including the MAPK signaling pathway, Wnt signaling pathway, and TGF-β signaling pathway, among others (Figure 6(a)). For example, *SIRT7* is predicted to be a highly likely target of miR-130a-3p, with the highest fold change. We also confirmed that the expression of miR-130a-3p was significantly increased in Exo_D14, compared with Exos_D0 (Figure 8). Previous studies have demonstrated that SIRT7 inhibits osteogenic differentiation of BMSCs by antagonizing the Wnt signaling pathway, while mir-130a-3p promotes it [42, 57], which is consistent with our prediction. It is a fact that the Wnt signaling pathway is a highly conserved pathway involved in the regulation of cell growth, differentiation, survival, and apoptosis and plays a key role in the self-renewal and maintenance of stem cells [58]. To date, many studies have confirmed the important regulatory role of the Wnt signaling pathway in the process of osteogenic differentiation of stem cells [59, 60]. Consequently, the mir-130a-3p/SIRT7/Wnt axis may be a novel molecular mechanism regulating osteogenic differentiation of ADSCs. To further clarify the biological function of target genes of differentially expressed microRNAs, GO analyses, including BP, CC, and MF, were carried out. The results of the GO analyses revealed that the affected target genes are mainly involved in enzyme binding, cell projection, transcription factor activity, regulation of gene expression, and cell metabolism (Figures 6(b)–6(d)). It is clear that certain differentially expressed miRNAs in exosomes are closely related to cellular and molecular responses in the osteogenic differentiation process of ADSCs.

Our results indicated that exosomal miRNAs may play a vital role in enhancing bone regeneration. Exosomes can be ingested more rapidly by homotypic cells, as opposed to other cells. We believe that the combination of ADSC-derived exosomes and ADSCs will serve as excellent "inducing factors" and "seed cells" during the creation of tissue engineered bone—a development that would aid the repair of clinical bone defects. Moreover, the detailed mechanisms of how ADSC-derived exosomes enhance osteogenic differentiation of ADSCs require further exploration, but these comprehensive analytical experiments will build a rich information base for understanding the mechanisms underlying exosome-mediated promotion of osteogenic differentiation of ADSCs.

We should indicate that there are some limitations to this study. We only compared exosomes derived from osteogenically differentiated ADSCs and undifferentiated ADSCs. This may lead us to lose information regarding the dynamic changes in exosomal miRNAs throughout the osteogenic differentiation process. In addition, the specific molecular mechanisms involving exosomes remain elusive. Therefore, these issues should be explored in future studies.

5. Conclusion

In summary, to the best of our knowledge, we demonstrated for the first time that osteogenically differentiated ADSC-derived exosomes can promote osteogenic differentiation of ADSCs. Importantly, we successfully identified miRNAs of exosomes and performed functional analyses involving coregulated networks. These will serve as a new foundation for basic research in bone regeneration and clinical bone regeneration therapy.

Data Availability

The data used to support the findings of this study are available from the corresponding author upon request.

Conflicts of Interest

No conflicts of interest exist.

Acknowledgments

We thank all the donors who participated in this program and all coworkers who contributed to collection of human adipose tissue sponsored by the Department of Plastic Surgery, in the first hospital of China Medical University. This work was supported by grants from the National Natural Science Foundation of China (no. 51872332), the National Natural Science Foundation of Liaoning province (no. 20170541040), and the Certificate of China Postdoctoral Science Foundation Grant (no. 2018M641741).

Supplementary Materials

(a) The result of real-time imaging by fluorescence confocal microscopy showed the process that ADSCs gradually internalized homologous exosomes labeled with Dil (the red dots) from 0 minute to 360 minute. (b) 9 time points (1 min, 30 min, 60 min, 90 min, 120 min, 180 min, 240 min, 300 min, and 360 min) in the same field of view were chosen to acquire images. *(Supplementary Materials)*

References

[1] G. G. Walmsley, R. C. Ransom, E. R. Zielins et al., "Stem cells in bone regeneration," *Stem Cell Reviews*, vol. 12, no. 5, pp. 524–529, 2016.

[2] C. E. Schwartz, J. F. Martha, P. Kowalski et al., "Prospective evaluation of chronic pain associated with posterior autologous iliac crest bone graft harvest and its effect on

postoperative outcome," *Health and Quality of Life Outcomes*, vol. 7, no. 1, p. 49, 2009.

[3] J. I. Sorger, F. J. Hornicek, M. Zavatta et al., "Allograft fractures revisited," *Clinical Orthopaedics and Related Research*, vol. 382, pp. 66–74, 2001.

[4] J. H. Hong, E. S. Hwang, M. T. McManus et al., "TAZ, a transcriptional modulator of mesenchymal stem cell differentiation," *Science*, vol. 309, no. 5737, pp. 1074–1078, 2005.

[5] M. Guan, W. Yao, R. Liu et al., "Directing mesenchymal stem cells to bone to augment bone formation and increase bone mass," *Nature Medicine*, vol. 18, no. 3, pp. 456–462, 2012.

[6] C. Liu, H. Zhang, X. Tang et al., "Mesenchymal stem cells promote the osteogenesis in collagen-induced arthritic mice through the inhibition of TNF-α," *Stem Cells International*, vol. 2018, Article ID 4069032, 10 pages, 2018.

[7] J. Li, Y. Huang, J. Song et al., "Cartilage regeneration using arthroscopic flushing fluid-derived mesenchymal stem cells encapsulated in a one-step rapid cross-linked hydrogel," *Acta Biomaterialia*, vol. 79, pp. 202–215, 2018.

[8] M. F. Pittenger, A. M. Mackay, S. C. Beck et al., "Multilineage potential of adult human mesenchymal stem cells," *Science*, vol. 284, no. 5411, pp. 143–147, 1999.

[9] M. Dominici, K. Le Blanc, I. Mueller et al., "Minimal criteria for defining multipotent mesenchymal stromal cells. The International Society for Cellular Therapy position statement," *Cytotherapy*, vol. 8, no. 4, pp. 315–317, 2006.

[10] A. G. Via, A. Frizziero, and F. Oliva, "Biological properties of mesenchymal stem cells from different sources," *Muscles, Ligaments and Tendons Journal*, vol. 2, no. 3, pp. 154–162, 2012.

[11] F. G. Teixeira, M. M. Carvalho, N. Sousa, and A. J. Salgado, "Mesenchymal stem cells secretome: a new paradigm for central nervous system regeneration?," *Cellular and Molecular Life Sciences*, vol. 70, no. 20, pp. 3871–3882, 2013.

[12] H. Wang, F. Cao, A. De et al., "Trafficking mesenchymal stem cell engraftment and differentiation in tumor-bearing mice by bioluminescence imaging," *Stem Cells*, vol. 27, no. 7, pp. 1548–1558, 2009.

[13] H. Tapp, E. N. Hanley, J. C. Patt, and H. E. Gruber, "Adipose-derived stem cells: characterization and current application in orthopaedic tissue repair," *Experimental Biology and Medicine*, vol. 234, no. 1, pp. 1–9, 2015.

[14] T. Rada, R. L. Reis, and M. E. Gomes, "Adipose tissue-derived stem cells and their application in bone and cartilage tissue engineering," *Tissue Engineering Part B: Reviews*, vol. 15, no. 2, pp. 113–125, 2009.

[15] X. Zhang, J. Guo, G. Wu, and Y. Zhou, "Effects of heterodimeric bone morphogenetic protein-2/7 on osteogenesis of human adipose-derived stem cells," *Cell Proliferation*, vol. 48, no. 6, pp. 650–660, 2015.

[16] A. Dicker, K. Le Blanc, G. Aström et al., "Functional studies of mesenchymal stem cells derived from adult human adipose tissue," *Experimental Cell Research*, vol. 308, no. 2, pp. 283–290, 2005.

[17] H. Chen, Y. Qian, Y. Xia et al., "Enhanced osteogenesis of ADSCs by the synergistic effect of aligned fibers containing collagen I," *ACS Applied Materials & Interfaces*, vol. 8, no. 43, pp. 29289–29297, 2016.

[18] X. Ding, M. Zhu, B. Xu et al., "Integrated trilayered silk fibroin scaffold for osteochondral differentiation of adipose-derived stem cells," *ACS Applied Materials & Interfaces*, vol. 6, no. 19, pp. 16696–16705, 2014.

[19] Q. Xie, Z. Wang, H. Zhou et al., "The role of miR-135-modified adipose-derived mesenchymal stem cells in bone regeneration," *Biomaterials*, vol. 75, pp. 279–294, 2016.

[20] J. Du, P. Xie, S. Lin et al., "Time-phase sequential utilization of adipose-derived mesenchymal stem cells on mesoporous bioactive glass for restoration of critical size bone defects," *ACS Applied Materials & Interfaces*, vol. 10, no. 34, pp. 28340–28350, 2018.

[21] M. Madrigal, K. S. Rao, and N. H. Riordan, "A review of therapeutic effects of mesenchymal stem cell secretions and induction of secretory modification by different culture methods," *Journal of Translational Medicine*, vol. 12, no. 1, p. 260, 2014.

[22] A. I. Caplan and D. Correa, "The MSC: an injury drugstore," *Cell Stem Cell*, vol. 9, no. 1, pp. 11–15, 2011.

[23] L. da Silva Meirelles, A. M. Fontes, D. T. Covas, and A. I. Caplan, "Mechanisms involved in the therapeutic properties of mesenchymal stem cells," *Cytokine & Growth Factor Reviews*, vol. 20, no. 5-6, pp. 419–427, 2009.

[24] M. Tkach and C. Théry, "Communication by extracellular vesicles: where we are and where we need to go," *Cell*, vol. 164, no. 6, pp. 1226–1232, 2016.

[25] G. Raposo and W. Stoorvogel, "Extracellular vesicles: exosomes, microvesicles, and friends," *The Journal of Cell Biology*, vol. 200, no. 4, pp. 373–383, 2013.

[26] M. Yáñez-Mó, P. R. M. Siljander, Z. Andreu et al., "Biological properties of extracellular vesicles and their physiological functions," *Journal of Extracellular Vesicles*, vol. 4, no. 1, 2015.

[27] G. Togliatto, P. Dentelli, M. Gili et al., "Obesity reduces the pro-angiogenic potential of adipose tissue stem cell-derived extracellular vesicles (EVs) by impairing miR-126 content: impact on clinical applications," *International Journal of Obesity*, vol. 40, no. 1, pp. 102–111, 2016.

[28] W. Li, Y. Liu, P. Zhang et al., "Tissue-engineered bone immobilized with human adipose stem cells-derived exosomes promotes bone regeneration," *ACS Applied Materials & Interfaces*, vol. 10, no. 6, pp. 5240–5254, 2018.

[29] D. Koppers-Lalic, M. M. Hogenboom, J. M. Middeldorp, and D. M. Pegtel, "Virus-modified exosomes for targeted RNA delivery; a new approach in nanomedicine," *Advanced Drug Delivery Reviews*, vol. 65, no. 3, pp. 348–356, 2013.

[30] S. Zhang, W. C. Chu, R. C. Lai, S. K. Lim, J. H. P. Hui, and W. S. Toh, "Exosomes derived from human embryonic mesenchymal stem cells promote osteochondral regeneration," *Osteoarthritis and Cartilage*, vol. 24, no. 12, pp. 2135–2140, 2016.

[31] K. Nong, W. Wang, X. Niu et al., "Hepatoprotective effect of exosomes from human-induced pluripotent stem cell-derived mesenchymal stromal cells against hepatic ischemia-reperfusion injury in rats," *Cytotherapy*, vol. 18, no. 12, pp. 1548–1559, 2016.

[32] D. P. Bartel, "MicroRNAs: genomics, biogenesis, mechanism, and function," *Cell*, vol. 116, no. 2, pp. 281–297, 2004.

[33] S. L. Ameres, J. Martinez, and R. Schroeder, "Molecular basis for target RNA recognition and cleavage by human RISC," *Cell*, vol. 130, no. 1, pp. 101–112, 2007.

[34] N. S. Dole and A. M. Delany, "MicroRNA variants as genetic determinants of bone mass," *Bone*, vol. 84, pp. 57–68, 2016.

[35] T. Gaur, S. Hussain, R. Mudhasani et al., "Dicer inactivation in osteoprogenitor cells compromises fetal survival and bone formation, while excision in differentiated osteoblasts increases bone mass in the adult mouse," *Developmental Biology*, vol. 340, no. 1, pp. 10–21, 2010.

[36] H. Valadi, K. Ekström, A. Bossios, M. Sjöstrand, J. J. Lee, and J. O. Lötvall, "Exosome-mediated transfer of mRNAs and microRNAs is a novel mechanism of genetic exchange between cells," *Nature Cell Biology*, vol. 9, no. 6, pp. 654–659, 2007.

[37] P. A. Zuk, M. Zhu, H. Mizuno et al., "Multilineage cells from human adipose tissue: implications for cell-based therapies," *Tissue Engineering*, vol. 7, no. 2, pp. 211–228, 2001.

[38] B. A. Bunnell, M. Flaat, C. Gagliardi, B. Patel, and C. Ripoll, "Adipose-derived stem cells: isolation, expansion and differentiation," *Methods*, vol. 45, no. 2, pp. 115–120, 2008.

[39] I. Diboun, L. Wernisch, C. A. Orengo, and M. Koltzenburg, "Microarray analysis after RNA amplification can detect pronounced differences in gene expression using limma," *BMC Genomics*, vol. 7, no. 1, p. 252, 2006.

[40] D. W. Huang, B. T. Sherman, and R. A. Lempicki, "Systematic and integrative analysis of large gene lists using DAVID bioinformatics resources," *Nature Protocols*, vol. 4, no. 1, pp. 44–57, 2009.

[41] P. Bourin, B. A. Bunnell, L. Casteilla et al., "Stromal cells from the adipose tissue-derived stromal vascular fraction and culture expanded adipose tissue-derived stromal/stem cells: a joint statement of the International Federation for Adipose Therapeutics and Science (IFATS) and the International Society for Cellular Therapy (ISCT)," *Cytotherapy*, vol. 15, no. 6, pp. 641–648, 2013.

[42] E. E. M. Chen, W. Zhang, C. C. Y. Ye et al., "Knockdown of SIRT7 enhances the osteogenic differentiation of human bone marrow mesenchymal stem cells partly via activation of the Wnt/β-catenin signaling pathway," *Cell Death & Disease*, vol. 8, no. 9, article e3042, 2017.

[43] M. Martins, D. Ribeiro, A. Martins, R. L. Reis, and N. M. Neves, "Extracellular vesicles derived from osteogenically induced human bone marrow mesenchymal stem cells can modulate lineage commitment," *Stem Cell Reports*, vol. 6, no. 3, pp. 284–291, 2016.

[44] Y. Qin, L. Wang, Z. Gao, G. Chen, and C. Zhang, "Bone marrow stromal/stem cell-derived extracellular vesicles regulate osteoblast activity and differentiation *in vitro* and promote bone regeneration *in vivo*," *Scientific Reports*, vol. 6, no. 1, article 21961, 2016.

[45] Y. Wang, Y. Liu, M. Zhang et al., "Inhibition of PTGS1 promotes osteogenic differentiation of adipose-derived stem cells by suppressing NF-kB signaling," *Stem Cell Research & Therapy*, vol. 10, no. 1, p. 57, 2019.

[46] Y. Shin, Y. Won, J. I. Yang, and J. S. Chun, "CYTL1 regulates bone homeostasis in mice by modulating osteogenesis of mesenchymal stem cells and osteoclastogenesis of bone marrow-derived macrophages," *Cell Death & Disease*, vol. 10, no. 2, p. 47, 2019.

[47] S. Agrawal Singh, M. Lerdrup, A. L. R. Gomes et al., "PLZF targets developmental enhancers for activation during osteogenic differentiation of human mesenchymal stem cells," *eLife*, vol. 8, article e40364, 2019.

[48] R. Yue, B. O. Zhou, I. S. Shimada, Z. Zhao, and S. J. Morrison, "Leptin receptor promotes adipogenesis and reduces osteogenesis by regulating mesenchymal stromal cells in adult bone marrow," *Cell Stem Cell*, vol. 18, no. 6, pp. 782–796, 2016.

[49] B. Zhang, M. Wang, A. Gong et al., "HucMSC-exosome mediated-Wnt4 signaling is required for cutaneous wound healing," *Stem Cells*, vol. 33, no. 7, pp. 2158–2168, 2015.

[50] V. K.-F. Cheng, P. C.-M. Au, K. C. B. Tan, and C.-L. Cheung, "MicroRNA and human bone health," *JBMR Plus*, vol. 3, no. 1, pp. 2–13, 2019.

[51] R. Rupaimoole and F. J. Slack, "MicroRNA therapeutics: towards a new era for the management of cancer and other diseases," *Nature Reviews Drug Discovery*, vol. 16, no. 3, pp. 203–222, 2017.

[52] M. T. Valenti, L. Dalle Carbonare, and M. Mottes, "Role of microRNAs in progenitor cell commitment and osteogenic differentiation in health and disease (review)," *International Journal of Molecular Medicine*, vol. 41, no. 5, pp. 2441–2449, 2018.

[53] Y. Du, Y. Yu, Y. Hu et al., "Genome-wide, integrative analysis implicates exosome-derived microRNA dysregulation in schizophrenia," *Schizophrenia Bulletin*, 2019.

[54] A. Rodríguez-Martínez, D. de Miguel-Pérez, F. G. Ortega et al., "Exosomal miRNA profile as complementary tool in the diagnostic and prediction of treatment response in localized breast cancer under neoadjuvant chemotherapy," *Breast Cancer Research*, vol. 21, no. 1, pp. 21–29, 2019.

[55] D. P. Bartel, "MicroRNAs: target recognition and regulatory functions," *Cell*, vol. 136, no. 2, pp. 215–233, 2009.

[56] X. J. Wang, J. L. Reyes, N. H. Chua, and T. Gaasterland, "Prediction and identification of *Arabidopsis thaliana* microRNAs and their mRNA targets," *Genome Biology*, vol. 6, no. 9, article R65, 2004.

[57] K. Seenprachawong, T. Tawornsawutruk, C. Nantasenamat, P. Nuchnoi, S. Hongeng, and A. Supokawej, "miR-130a and miR-27b enhance osteogenesis in human bone marrow mesenchymal stem cells via specific down-regulation of peroxisome proliferator-activated receptor γ," *Frontiers in Genetics*, vol. 9, 2018.

[58] Y. Atlasi, L. Looijenga, and R. Fodde, "Cancer stem cells, pluripotency, and cellular heterogeneity: a WNTer perspective," *Current Topics in Developmental Biology*, vol. 107, pp. 373–404, 2014.

[59] Z. Yuan, Q. Li, S. Luo et al., "PPARγ and Wnt signaling in adipogenic and osteogenic differentiation of mesenchymal stem cells," *Current Stem Cell Research & Therapy*, vol. 11, no. 3, pp. 216–225, 2016.

[60] Y. Zhu, Y. Wang, Y. Jia, J. Xu, and Y. Chai, "Catalpol promotes the osteogenic differentiation of bone marrow mesenchymal stem cells via the Wnt/β-catenin pathway," *Stem Cell Research & Therapy*, vol. 10, no. 1, p. 37, 2019.

Hindawi
Stem Cells International
Volume 2019, Article ID 8150123, 14 pages
https://doi.org/10.1155/2019/8150123

Research Article

Activated B Lymphocyte Inhibited the Osteoblastogenesis of Bone Mesenchymal Stem Cells by Notch Signaling

Mengxue Pan,[1] Wei Hong,[2,3] Ye Yao,[4] Xiaoxue Gao,[1] Yi Zhou,[1] Guoxiang Fu,[1] Yuanchuang Li,[1] Qiang Guo,[1] Xinxin Rao,[1] Peiyuan Tang,[1] Shengzhi Chen,[1] Weifang Jin,[1] Guoqiang Hua,[1] Jianjun Gao,[1] and Xiaoya Xu[1]

[1]*Department of Radiation Biology, Institute of Radiation Medicine, Fudan University, No. 2094 Xie-Tu Rd. Building 1, Shanghai 200032, China*
[2]*Department of Geriatrics, Huadong Hospital, Research Center on Aging and Medicine, Fudan University, Shanghai 200040, China*
[3]*Department of Bone Metabolism, Shanghai Key Laboratory of Clinical Geriatric Medicine, Shanghai 200040, China*
[4]*Department of Radiation Oncology, Fudan University Shanghai Cancer Center, Fudan University, Shanghai 200032, China*

Correspondence should be addressed to Guoqiang Hua; guoqianghua@fudan.edu.cn, Jianjun Gao; jjgao@shmu.edu.cn, and Xiaoya Xu; xiaoyaxu@fudan.edu.cn

Received 22 January 2019; Revised 17 April 2019; Accepted 6 May 2019; Published 2 June 2019

Guest Editor: Fengjuan Lv

Estrogen is very important to the differentiation of B lymphocytes; B lymphopoiesis induced by OVX was supposedly involved in osteoporosis. But the effects of B lymphocytes on the osteogenic differentiation of bone mesenchymal stem cells (BMSCs) are not clear. In this study, we detected bone quality and bone loss in a trabecular bone by electronic universal material testing machine and microcomputed tomography (micro-CT) in OVX and splenectomized-ovariectomy (SPX-OVX) rats. Additionally, changes in lymphocytes (B lymphocyte, $CD4^+$ and $CD8^+$ T lymphocytes, and macrophages) in the bone marrow were analyzed by flow cytometry. The osteogenesis of BMSCs cocultured with normal and LPS-pretreated B lymphocytes was detected by BCIP/NBT and Alizarin red S staining. Measurement of the Notch2, Notch4, Hey1, Hey2, Hes1, and runt-related transcription factor 2 (Runx2) expression in BMSCs cocultured with B lymphocytes was done using real-time PCR. The effects of dexamethasone and DAPT (inhibitor of Notch signaling) on osteogenesis of BMSCs were detected by BCIP/NBT, Alizarin red S staining, and real-time PCR. Osteoporosis happened in OVX rats, more serious in SPX-OVX rats, B lymphocytes increased in OVX rats, and sharply higher in SPX-OVX rats. Osteoporosis did not happen in SPX rats which is still companied with a high increase of B lymphocytes. LPS-pretreated B lymphocytes suppressed the osteogenesis of BMSCs, but the normal B lymphocytes could not. The LPS-pretreated B lymphocytes upregulated the expression of Notch4, Hes1, and Hey2 and downregulated the expression of Runx2 in BMSCs. Dexamethasone and DAPT could downregulate the high expression of Notch4, Hes1, Hey2 and upregulate the low expression of Runx2 in BMSCs which cocultured with LPS treated B lymphocytes, the inhibited ALP and Alizarin red staining in BMSCs which cocultured with LPS treated B lymphocytes also partly restored.

1. Introduction

It has become clear that complex interactions underlie the relationship between the skeletal and immune systems. This is particularly true for the development of immune cells in the bone marrow as well as the functions of bone cells in skeletal homeostasis and pathologies. Estrogen deficiency caused by ovariectomy (OVX) results in a marked bone loss due to exceeded bone resorption by increased osteoclasts (OC), which are partly stimulated by the immune system [1]. Increase of T lymphopoiesis by OVX is detected in OVX mice [2, 3]; expanded T cells stimulate osteoclastogenesis by more cytokine production such as RANKL, TNFa, and IFN-gamma in OVX mice, which half of bone loss was attenuated by thymectomy [2]. The number of B lymphocytes in bone marrow increased after OVX, and these activated B

lymphocytes expressed RANKL contributing to bone resorption [4, 5]. Changes in B lymphocyte populations in the blood of postmenopausal osteoporosis patients have been shown [6]. However, as one of the important lymphocytes in the immune system, the role of B lymphocytes in bone mesenchymal stem cells of bone loss induced by estrogen deficiency remains unknown. These experiments were designed to investigate the skeleton phenotypes in splenectomized OVX female rats and the effects of B lymphocytes on OVX-induced bone loss. Meanwhile, we detected the differentiation of BMSCs cocultured with B lymphocytes which were pretreated with LPS. We also investigated the effects of dexamethasone in the differentiation of BMSCs which were cocultured with B lymphocytes and the changes of the Notch signaling in BMSCs; then, we used the inhibitor of Notch signaling to investigate the differentiation and the expression of Notch signaling in BMSCs.

2. Materials and Methods

2.1. Animal Studies. Female Sprague-Dawley rats (Shanghai Lab Animal Resource Center, STCSM, Shanghai, China) were bilateral splenectomized (SPX), ovariectomized (OVX), splenectomized OVX (SPX-OVX), and sham-operated (Sham), respectively, at 6 months of age under anesthesia. The animals were treated with benzylpenicillin sodium (D1110226, NCPC, China) for three days. All rats were maintained in a virus- and parasite-free barrier facility and exposed to a 12 h/12 h light/dark cycle and allowed free access to water and commercial standard rodent chow (containing: calcium: 1.8%, phosphorus: 0.6-1.2%). Tissues were collected at 3 months after surgery for densitometry, histomorphometry, and flow cytometry studies, respectively. This study was approved by the ethical committee for animal experiments in Fudan University, and all efforts were made to minimize suffering.

2.2. Histological Analyses of Bone. Bone mineral density (BMD) of either the femur or the lumbar (L1-5) was determined by dual-energy X-ray absorptiometry (DXA, Discovery A, Hologic Inc., Bedford, MA, USA) using an animal model at 3 months after surgery. The biomechanical quality was evaluated by the three-point bending test (femur) and compress test (L2), respectively, performed on an electronic universal material testing machine (INSTRON-5543, USA). For histomorphometry, the tissues were removed and fixed in PLP fixative (2% paraformaldehyde containing 0.075 M lysine and 0.01 M sodium periodate solution) 2 days at 5°C and processed histologically. Briefly, the distal end of the femurs was decalcified in EDTA glycerol solution for 28–30 days at 5°C. After paraffin embedding, 5 μm sections were cut on a rotary microtome. The sections were stained with H&E, and the changes of bone trabecula were measured with bone volume over total volume (BV/TV, %).

2.3. Micro-CT Analysis. The tibiae and lumbar (L3) obtained from rats were dissected free of soft tissue, fixed overnight in 70% ethanol, and analyzed by micro-CT with a SkyScan-1176 scanner (Bruker microCT, Belgium) [7]. The trabecular bone region of interest (ROI) was drawn to include all cancellous bone in the whole area of 0.2 mm below the growth plate for trabecular bone mineral density (tBMD) analysis. The trabecular bone volume fraction (BV/TV), trabecular thickness (Tb.Th), number (Tb.N), and separation (Tb.Sp) were calculated on a 2 mm region of metaphysical spongiosa 0.2 mm below the growth plate.

2.4. Flow Cytometry. Bone marrow was collected 3 months after surgery. B lymphocytes, macrophages, and $CD4^+$ and $CD8^+$ T lymphocytes were detected by flow cytometry. The antibodies and protocol were previously described [7, 8].

2.5. Cell Culture and Coculture. BMSCs and B lymphocytes of the spleen from normal rats were collected according to the previous protocol [7]: (1) normal BMSCs cocultured for 3 days with different B lymphocytes density (0, 10^4, 2×10^4, 4×10^4) for 3 days; (2) B lymphocytes treated with LPS (0, 1, 10, 100 μmol/L) for 3 days, then collected cells and immediately cocultured with normal BMSCs for 3 days in the same B lymphocytes density (2×10^4). ALP staining and Alizarin red staining were performed at 14 and 28 days.

LPS- (10 μmol/L) treated B lymphocytes above were cocultured with normal BMSCs for 3 days and grouped into (1) control (BMSCs+without lymphocyte), lymphocyte (BMSCs+lymphocyte), DXM (BMSCs+dexamethasone (DXM, 10^{-8} M)), and DXM+lymphocyte (BMSCs+lymphocyte+DXM, 10^{-8} M); (2) control (BMSCs+without lymphocyte), DAPT (BMSCs+DAPT, 5 μM), lymphocyte (BMSCs +lymphocyte), and lymphocyte+DAPT (BMSCs+lymphocyte+DAPT, 5 μM). Some samples were used for real-time PCR; others were replaced with osteogenic differentiation medium; ALP staining and Alizarin red staining were performed at 14 and 28 days.

2.6. Quantitative Real-Time PCR. The real-time PCR was performed according to the previous protocol [7]. Primers with the following sequences were obtained from SBSgene (http://www.sbsgene.com) using a previously described protocol: Runx2, 5′-AGCCTCTTCAGCGCAGTGAC-3′ and 5′-CTGGTGCTCGGATCCCAA-3′ (132 bp, AF187319); Hey1, 5′-AGTGAGCTGGACGAGACCAT-3′ and 5′-CTGG GTACCAGCCTTCTCAG-3′ (197 bp, XM_017590595.1); Hey2, 5′-GATCTGCCAAGTTGGAAAAGG-3′ and 5′-TGTTGCCTGGAGCATCTTC-3′ (71 bp, NM_130417.1); Hes1, 5′-CAGAAAGTCATCAAAGCCTATCATG-3′ and 5′-TCAGTGTTTTCAGTTGGCTCAAA-3′ (80 bp, NM_ 024360.3); Notch4: 5′-CCTGGACAG CAATGCCAAGA-3′ and 5′-AGTCCAGCCCTCGTTACACACAC-3′ (147 bp, XM_017601710.1); Notch2: 5′-GACTGCCAATACTCGACCT C-3′ and 5′-TTCAGAAGTGAAGTCTCCAG-3′ (438 bp, NM_024358.1); and GAPDH, 5′-AAACCCATCACCATCT TCCA-3′ and 5′-GTGGTTCACACCCATCACAA-3′ (198 bp, DQ403053). The cDNA content was normalized by subtracting the cycle numbers of GAPDH from those of the target gene (ΔCt = Ct of target gene–Ct of GAPDH), and gene expression levels were calculated using the $2^{-(\Delta Ct)}$ method [9].

2.7. Statistical Analysis. Differences were determined by one-way ANOVA with Bonferroni post hoc testing or by paired or unpaired Student's t-test, as appropriate (GraphPad, Prism 6, version 6.0c). The results were expressed as the means ± standard derivations, and $p < 0.05$ was considered significant.

3. Results

3.1. The Bone Mass and Biomechanical Quality Changed in OVX and SPX-OVX Rats. Uterus weight from OVX and SPX-OVX rats decreased obviously while the spleen weight increased 3 months after surgery (Figures 1(a) and 1(b)). The max loading of the femur, as determined by the three-point bending test, was slight but not significant. The max loading of the lumbar as determined by the compress test was reduced by 13% ($p < 0.05$) and 15% ($p < 0.05$) in OVX and OVX-SPX, respectively, compared with Sham (Figure 1(c)). BMD of the femur and lumbar, as determined by dual-energy X-ray absorptiometry (DXA), was decreased by 6% ($p < 0.05$) and 19% ($p < 0.001$), respectively, in OVX rats compared with Sham but was decreased by 6.5% ($p < 0.01$) and by 19.8% ($p < 0.001$) in OVX-SPX rats compared with Sham (Figure 1(d)). After 3 months of surgery, the structure of trabecular bone was significantly altered in the OVX and OVX-SPX compared with Sham. The diminished trabecular bone volume decreased by 29% ($p < 0.001$) and 42% ($p < 0.001$), respectively, in OVX and OVX-SPX rats compared with Sham (Figures 1(e) and 1(f)).

3.2. Bone Microarchitecture Is Changed in OVX and SPX-OVX Rats. We used μCT to delineate a purely trabecular region of interest that showed changes in bone volume and microarchitectural structure. Three months after surgery, trabecula bone mineral density (tBMD) was reduced by 49.3% ($p < 0.001$) in the OVX tibia and by 58.5% ($p < 0.001$) in the SPX-OVX tibia relative to Sham, while further decreased by 18.1% ($p < 0.05$) in the SPX-OVX tibia relative to OVX (Figures 2(a) and 2(b)). The trabecular bone volume (BV/TV) was reduced by 46.1% ($p < 0.01$) in the OVX tibia and by 49.5% ($p < 0.01$) in the SPX-OVX tibia relative to Sham (Figure 2(c)). The Tb.Th of the tibia only changed slightly, and no significant differences were observed (Figure 2(d)). The Tb.N was reduced by 44.8% ($p < 0.01$) in the OVX tibia and by 56.0% ($p < 0.01$) in the SPX-OVX tibia relative to Sham (Figure 2(e)). The Tb.Sp increased by 69.5% ($p < 0.01$) in the OVX tibia and by 95.6% ($p < 0.01$) in the SPX-OVX tibia relative to Sham (Figure 2(f)).

The microarchitecture of the lumbar showed the same trend with the tibia after surgery. The tBMD was reduced by 32.5% ($p < 0.001$) in the OVX lumbar and by 42.3% ($p < 0.001$) in the SPX-OVX lumbar relative to Sham, while further decreased by 14.5% ($p < 0.05$) in the SPX-OVX lumbar relative to OVX (Figures 2(g) and 2(h)). The trabecular bone volume (BV/TV) was reduced by 15.3% ($p < 0.05$) in the OVX lumbar and by 32.9% ($p < 0.01$) in the SPX-OVX lumbar relative to Sham, while further decreased by 20.8% ($p < 0.05$) in the SPX-OVX lumbar relative to OVX (Figure 2(i)). The Tb.Th of the lumbar was reduced by12.2% ($p < 0.05$) in the OVX lumbar and by 15.9% ($p < 0.05$) in the SPX-OVX lumbar relative to Sham (Figure 2(j)). The Tb.N was reduced by 20.1% ($p < 0.05$) in the OVX lumbar and by 24.2% ($p < 0.05$) in the SPX-OVX lumbar relative to Sham (Figure 2(k)). The Tb.Sp increased by 21.8% ($p < 0.05$) in the OVX lumbar and by 49.6% ($p < 0.01$) in the SPX-OVX lumbar relative to Sham (Figure 2(l)).

3.3. Numbers of Lymphocytes in Bone Marrow Were Altered in OVX and SPX-OVX Rats. The numbers of lymphocytes in bone marrow changed significantly in OVX and SPX-OVX rats. The B lymphocyte (CD3-CD45RA$^+$) in bone marrow increased by 158.6% ($p < 0.001$) in OVX, by 210.3% ($p < 0.001$) in SPX rats, and by 224.1% ($p < 0.001$) in SPX-OVX rats (Figures 3(a) and 3(e)). The CD4$^+$ T lymphocytes (CD3-CD4$^+$) decreased by 40% ($p < 0.05$) in OVX and by 35% ($p < 0.05$) in OVX-SPX (Figures 3(b) and 3(f)). The CD8$^+$ T lymphocytes (CD3-CD8$^+$) decreased by 18.9% ($p < 0.05$) in OVX and by 37.8% ($p < 0.05$) in OVX-SPX (Figures 3(c) and 3(g)), while macrophages decreased by 41.7% ($p < 0.05$) in OVX and by 38.9% ($p < 0.05$) in OVX-SPX (Figures 3(d) and 3(h)).

3.4. Effect of B Lymphocytes on the Differentiation of BMSCs into Osteoblasts In Vitro. After being cocultured with normal B lymphocytes, the potential differentiation of BMSCs into osteoblasts did not change obviously (Figure 4(a)). While being cocultured with LPS-pretreated B lymphocytes, the differentiation of BMSCs into osteoblasts decreased. ALP staining showed markedly decreased ALP-positive osteoblasts in cocultures with B lymphocytes from LPS (10, 100) relative to LPS0, and Alizarin red staining showed the same trend (Figure 4(b)).

3.5. Effect of DXM on the Differentiation of Cocultured BMSCs into Osteoblasts In Vitro. The potential of BMSCs to differentiate into osteoblasts showed no obvious changes in the control and the DXM group. After being cocultured with LPS-pretreated B lymphocytes, the potential of BMSCs to differentiate into osteoblasts clearly decreased, and this would be partly recovered when DXM was used in coculture medium. ALP staining showed markedly decreased ALP-positive osteoblasts in cocultured with LPS-pretreated B lymphocytes relative to control, but the potential of BMSCs to differentiate into osteoblasts clearly was partly recovered if DXM was used in the coculture medium, and Alizarin red staining showed the same trend (Figure 4(c)). The RNA expression of Runx2 decreased significantly in BMSCs after being cocultured with LPS-pretreated B lymphocytes, showing a 51.7% ($p < 0.01$) reduction relative to control and increased by 48.9% ($p < 0.05$) when DXM was used in coculture medium compared to the lymphocyte group (Figure 4(d)). The RNA expression of Hey1, Hey2, Hes1, Notch2, and Notch4 increased in BMSCs after being cocultured with lymphocyte, showing 106.4% ($p < 0.05$), 1299.2% ($p < 0.001$), 391.7% ($p < 0.001$), 67.2%($p < 0.05$), and 411.1% ($p < 0.001$) relative to control, and all decreased when DXM was used, showing a 23.5% ($p < 0.05$), 76.5%

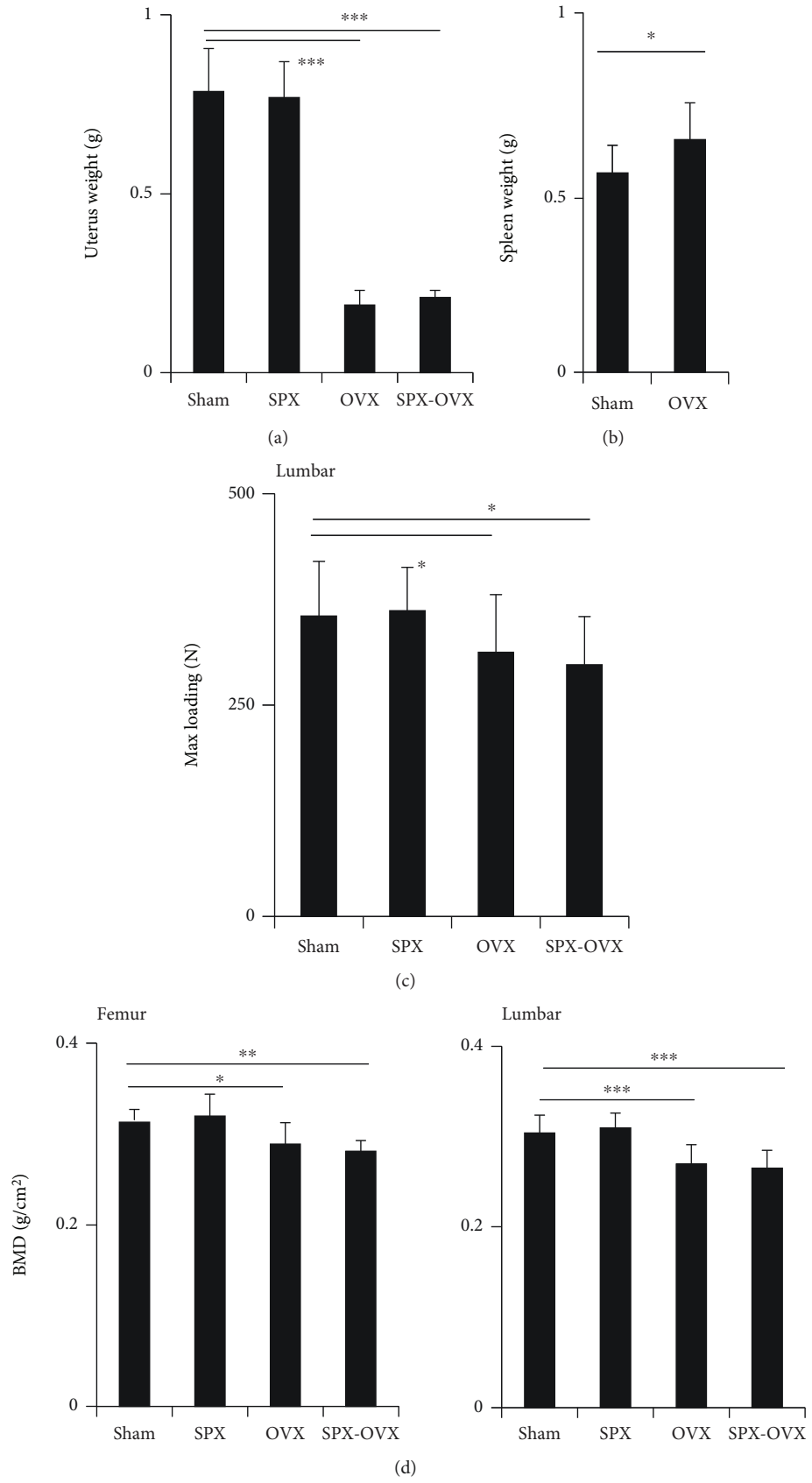

Figure 1: Continued.

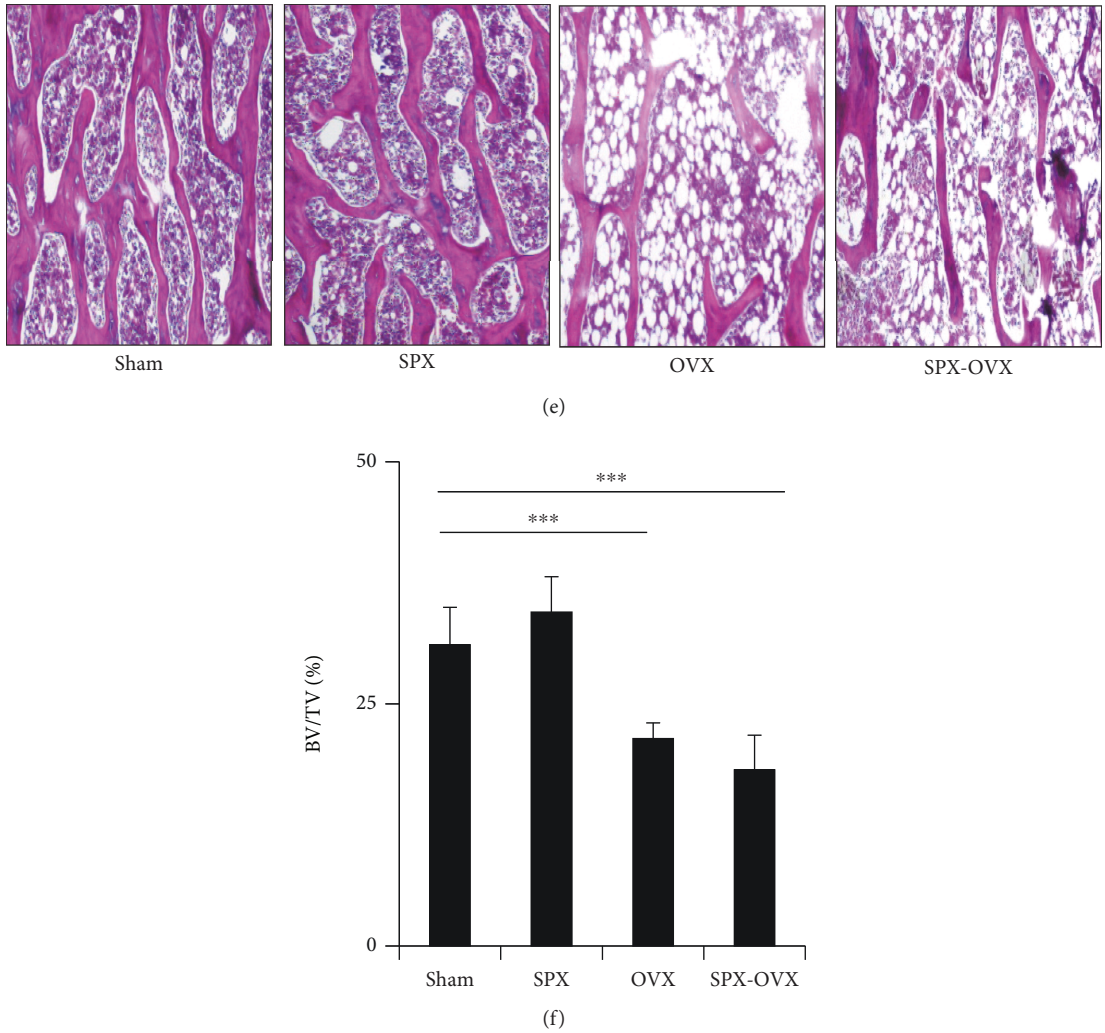

Figure 1: Effects on bone in OVX and SPX-OVX rats. (a) Uterus weight. (b) Spleen weight. (c) Max loading of the lumbar reduced in SPX and SPX-OVX. (d) BMD of the femur and lumbar decreased in SPX and SPX-OVX. (e) The HE staining showed decreased bone trabecula of the femur. (f) Bone volume of the femur decreased in SPX and SPX-OVX. Data are presented as the means ± standard deviations; $^{*}p < 0.05$, $^{**}p < 0.01$, and $^{***}p < 0.001$ ($n = 10$/group).

($p < 0.01$), 69.7% ($p < 0.01$), 36.8% ($p < 0.05$), and 69.3% ($p < 0.01$) reduction compared to the lymphocyte group (Figure 4(d)). The RNA expression showed no obvious changes between control and DXM.

3.6. Effect of Notch Inhibitor (DAPT) on the Differentiation of Cocultured BMSCs into Osteoblasts In Vitro. The potential of BMSCs to differentiate into osteoblasts increased in the DAPT group and decreased in the lymphocyte group. The potential of BMSCs to differentiate into osteoblasts would be partly recovered when DAPT was used in the lymphocyte group. ALP staining showed markedly decreased ALP-positive osteoblasts in cocultures with pretreated B lymphocytes and increased ALP-positive osteoblasts in the DAPT group relative to control. The potential of BMSCs to differentiate into osteoblasts clearly was partly recovered if DAPT was used in the coculture medium, and Alizarin red staining showed the same trend (Figure 5(a)). Runx2 still decreased in BMSCs after being cocultured with B lymphocyte and by 51.7% ($p < 0.01$) in the lymphocyte group compared to control. The Runx2 expression sharply increased by 285.8% ($p < 0.01$) in the lymphocyte+DAPT group compared to the lymphocyte group (Figure 5(b)). The RNA expression of Hey1, Hey2, Hes1, Notch2, and Notch4 increased in BMSCs after being cocultured with B lymphocyte, and the Hes1, Hey2, and Notch4 expression decreased when DAPT was used, showing a 83.1% ($p < 0.01$), 83.5% ($p < 0.001$), and 78.3% ($p < 0.01$) reduction compared to the lymphocyte group (Figure 5(b)). The RNA expression of Runx2 increased by 62.3% ($p < 0.05$) in DAPT relative to control, while the expression of Hes1 and Hey2 decreased by 52.8% ($p < 0.05$) and 46.9% ($p < 0.05$) in DAPT relative to control (Figure 5(b)).

4. Discussion

In our study, the osteoporotic phenotypes in OVX rats showed the marked decrease of bone mineral density in the

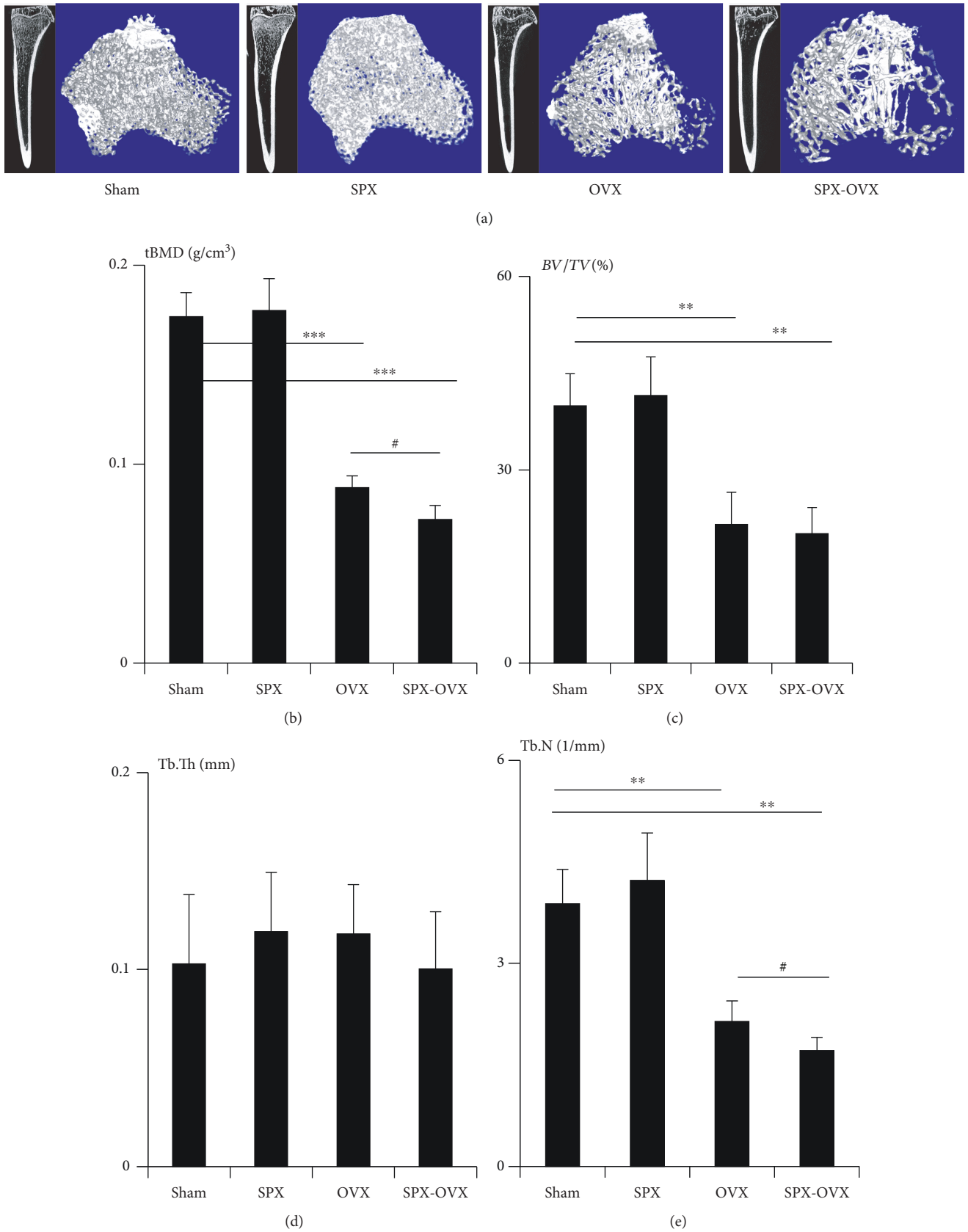

Figure 2: Continued.

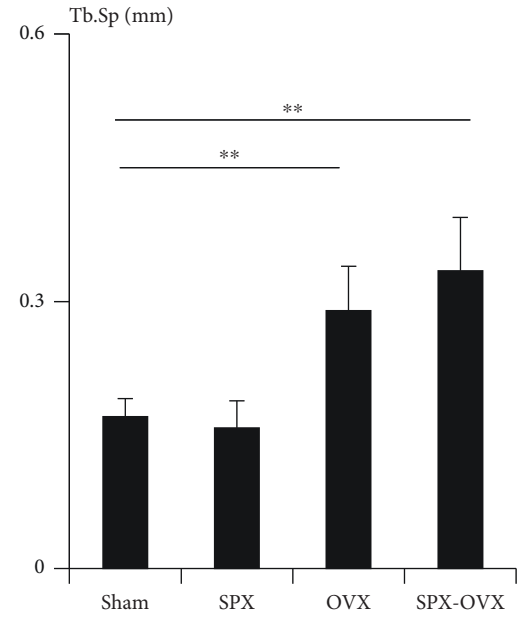

(f)

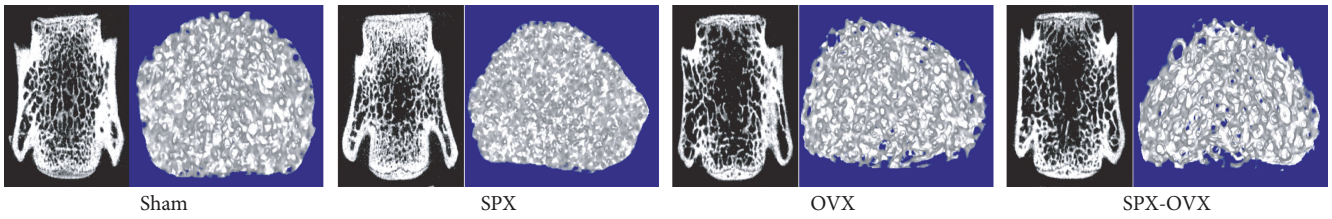

(g)

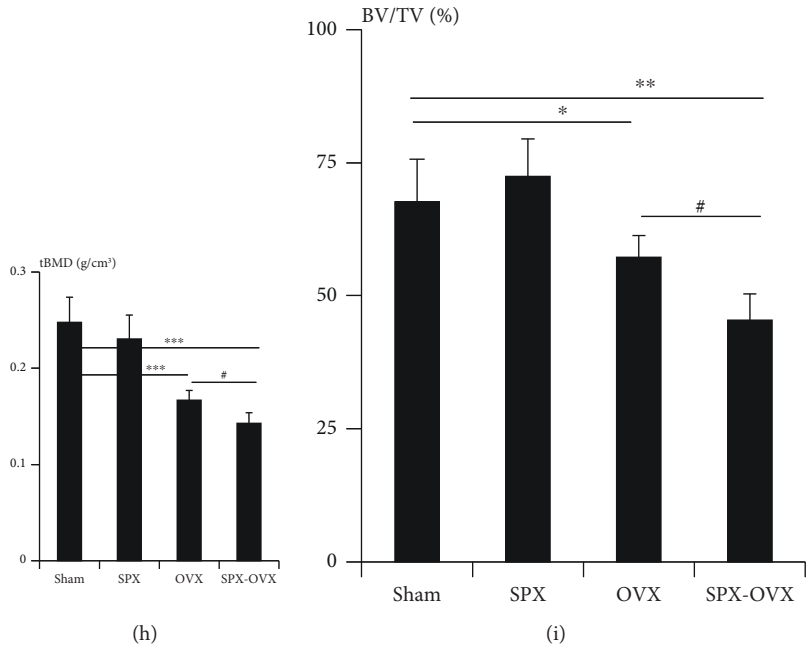

(h) (i)

Figure 2: Continued.

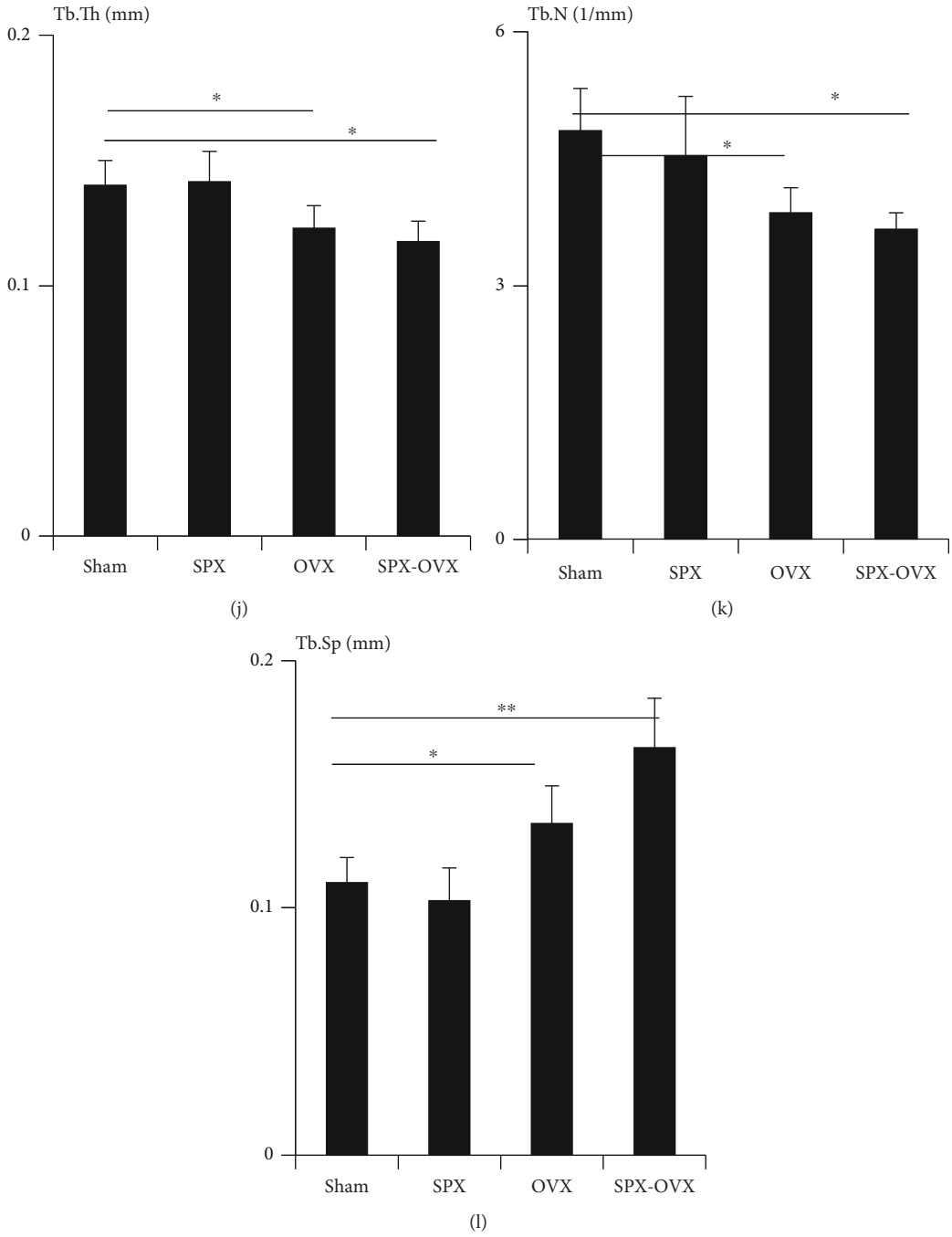

Figure 2: Effects on trabecular of the tibia and lumbar of OVX and SPX-OVX rats. (a, g) Representative reconstructed images of μCT scans showing trabecular in the tibia and lumbar. (b) tBMD changed in the tibia. Differences in (c) BV/TV, (d) Tb.Th, (e) Tb.N, and (f) Tb.Sp in the tibia. (h) tBMD changed in the lumbar. Differences in (i) BV/TV, (j) Tb.Th, (k) Tb.N, and (l) Tb.Sp in the lumbar. Data are presented as the means ± standard deviations; *compared with Sham, $^{*}p < 0.05$, $^{**}p < 0.01$, and $^{***}p < 0.001$; $^{\#}$compared with OVX, $^{\#}p < 0.05$ ($n = 10$/group).

femur, tibia, and lumbar and the significant decrease of the trabecular bone volume, which were worse after spleen removal. All that were not in our expectation of bone loss would be attenuated by splenectomy as like thymectomy. In the research, we found obvious myeloproliferation after surgeries; the medullary cavity of bones was full of lymphocytes. We know that estrogens are potent regulators of B lymphopoiesis at a very early stage [10]; estrogen deficiency may delay the differentiation of B lymphocytes and make them stay at a very early stage. Some studies also show in mice the absolute number of B lymphocyte (defined by the expression of the antigen CD45R/B200) in bone marrow roughly doubles after ovariectomy [4]. In our experiments, we detected the obvious changes in lymphocytes in OVX and SPX-OVX rats, especially in the sharply increased B lymphocytes. The question then arises: why so many B lymphocytes in bone marrow by OVX, even much more by SPX-OVX. Lymphocytes could increase osteoclasts and decrease

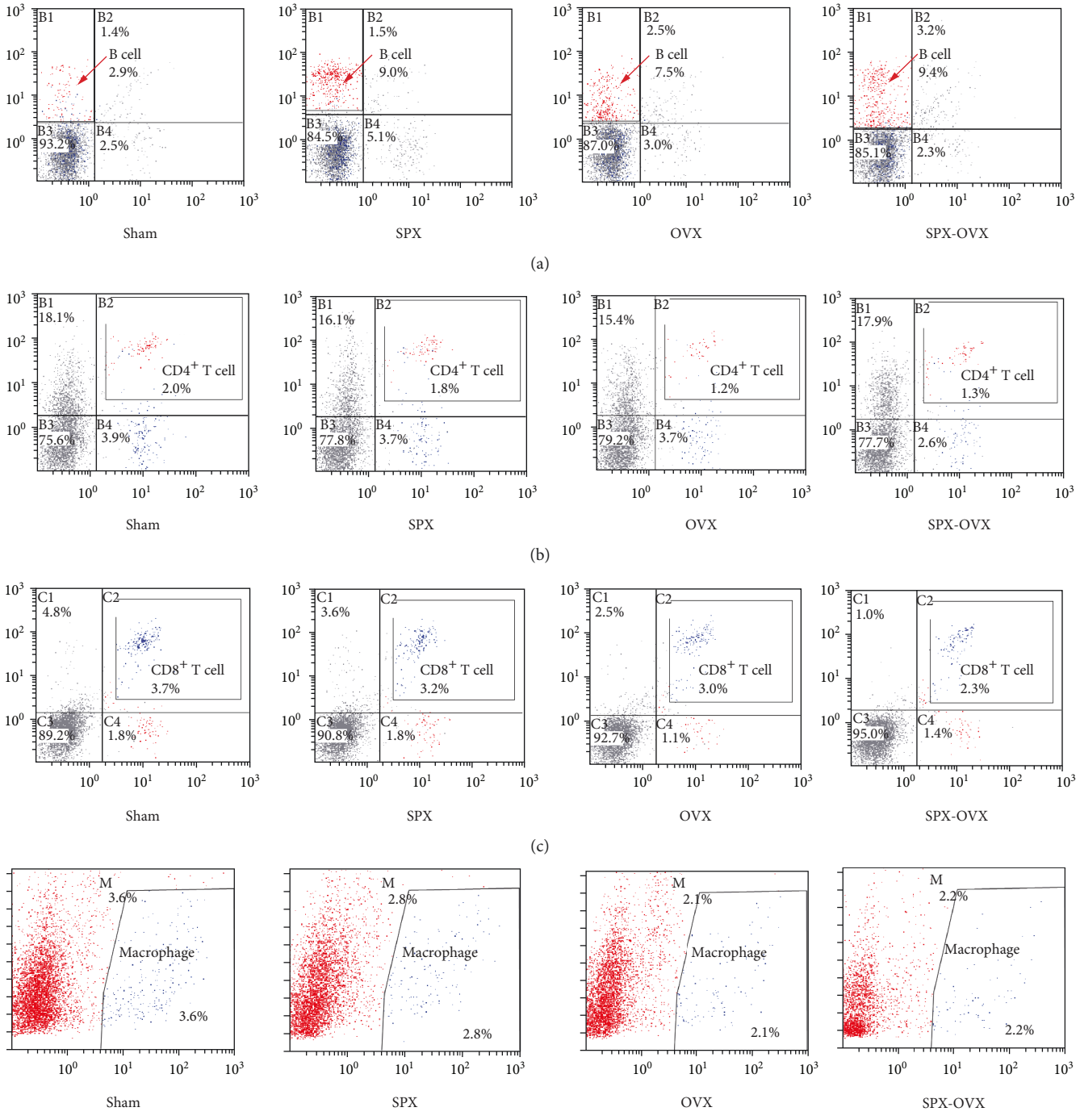

Figure 3: Continued.

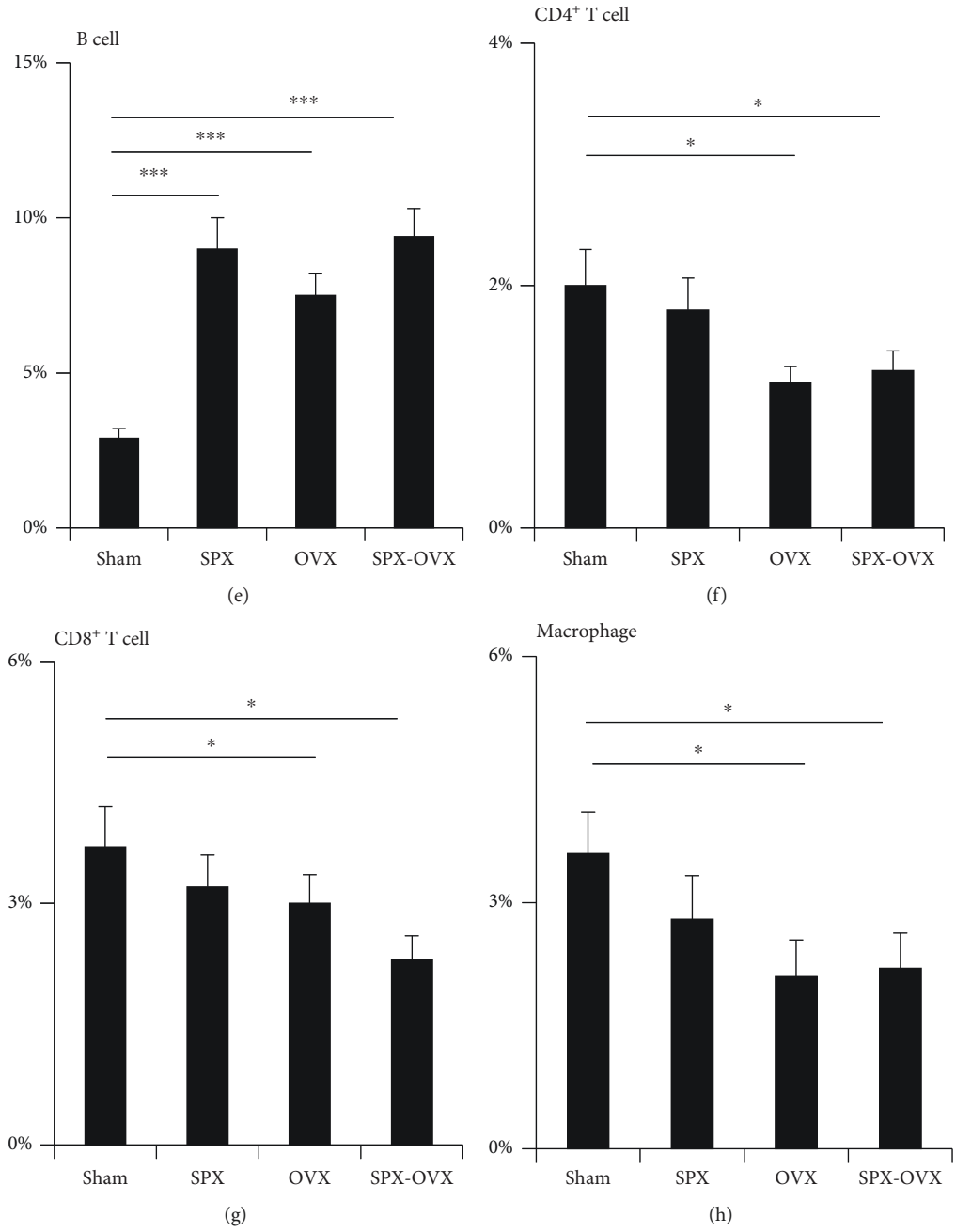

Figure 3: Lymphocytes and macrophages from bone marrow in OVX and SPX-OVX detected by flow cytometry. (a) Flow cytometry of B lymphocytes; (e) B lymphocyte numbers increased in SPX, OVX, and SPX-OVX. (b) Flow cytometry of $CD4^+$ T lymphocytes; (f) $CD4^+$ T lymphocyte numbers decreased in OVX and SPX-OVX. (c) Flow cytometry of $CD8^+$ T lymphocytes; (g) $CD8^+$ T lymphocyte numbers decreased in OVX and SPX-OVX. (d) Flow cytometry of macrophages; (h) macrophage numbers decreased in OVX and SPX-OVX. Data are presented as the means ± standard deviations; $^*p < 0.05$ and $^{***}p < 0.001$ ($n = 6$/group).

osteoblasts by producing proinflammatory cytokines in pathological osteoporosis [11–13]. Many researches have illustrated that normal and activated B lymphocytes play different roles in the bone [7, 14]. Normal B lymphocytes could produce osteoprotegerin to increase osteoblastogenesis, and the mice would have osteoporotic phenotype if normal B lymphocytes were knockout [15]. In contrast, the activated B lymphocytes suppressed bone turnover and osteoblastogenesis [7, 16–21]. However, there were few researches on the effects of B lymphocyte on the osteoblastogenesis of BMSCs. Only two studies showed that abnormal lymphocytes inhibited the differentiation of BMSCs into osteoblasts [7, 22]. In our study, we found that LPS-pretreated B lymphocytes inhibited the osteoblastogenesis of BMSCs by coculture, but the normal B lymphocytes did not. It means that only the activated B lymphocytes could induce bone loss, which may be the reason why osteoporosis happened in OVX rats, not in SPX rats, but even much more

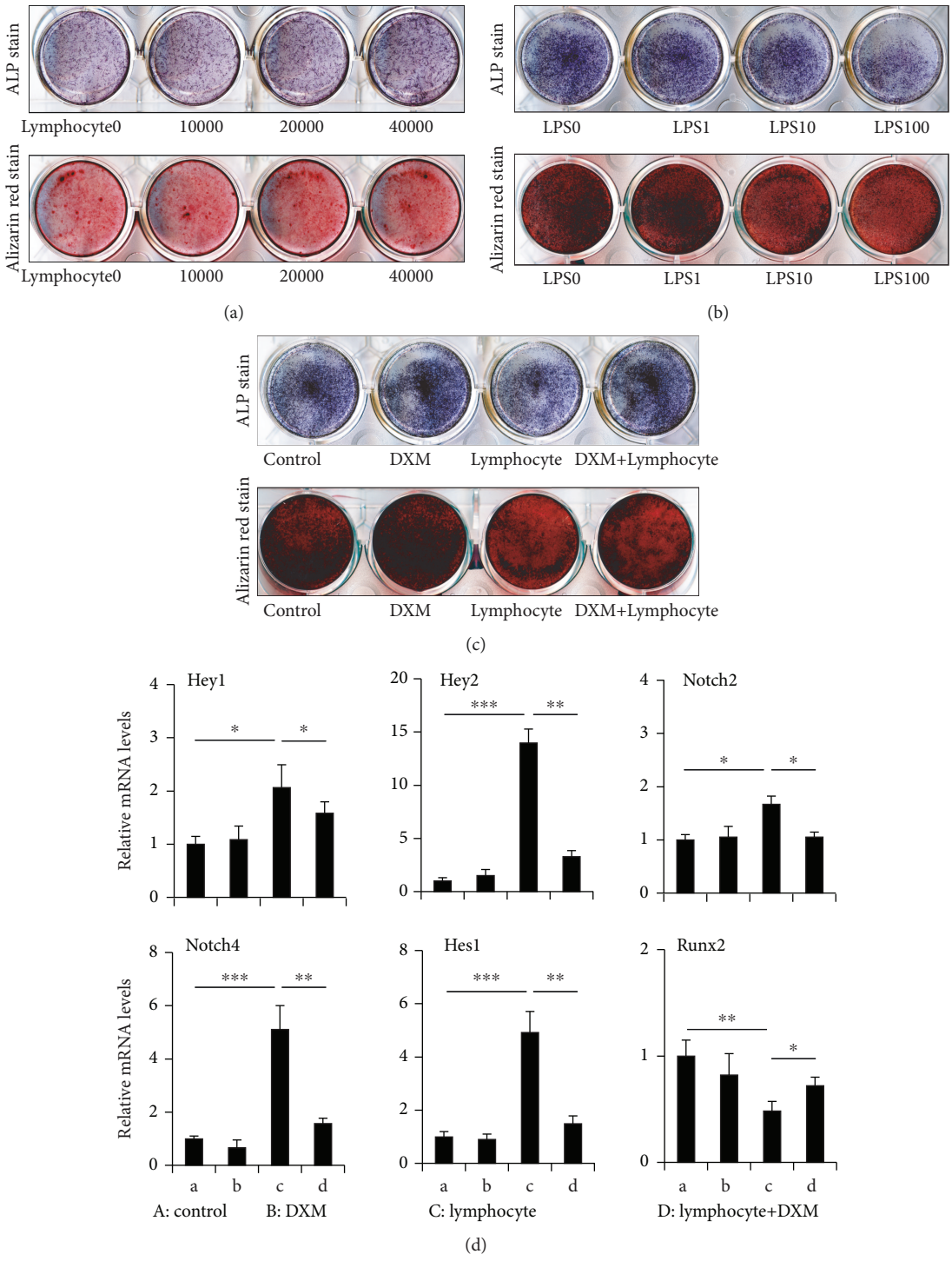

Figure 4: The osteoblastogenesis of BMSCs cocultured with normal B lymphocytes and LPS-pretreated B lymphocytes. (a) ALP and Alizarin red staining of BMSCs cocultured with normal B lymphocytes. (b) ALP and Alizarin red staining of BMSCs cocultured with LPS-pretreated B lymphocytes. (c) ALP and Alizarin red staining of BMSCs cocultured with LPS-pretreated B lymphocytes and dexamethasone. Alizarin red staining: calcified matrix in red and mineralization nodules in the dark. (d) mRNA expression of Hey1, Hey2, Notch2, Notch4, Hes1, and Runx2 in BMSCs. Data are presented as the means ± standard deviations; $^{*}p < 0.05$, $^{**}p < 0.01$, and $^{***}p < 0.001$ ($n = 6$/group).

worse in SPX-OVX rats. Our research showed the activated B lymphocytes will disrupt the bone homeostasis by suppressing the osteoblastogenesis of BMSCs. According to the important relation of bone loss and activated B lymphocytes, it should be given special attention to the therapy of osteoporosis companied with increasing abnormal B lymphocytes.

Dexamethasone, a steroidal anti-inflammatory drug which suppresses lymphocytes, was reported to increase

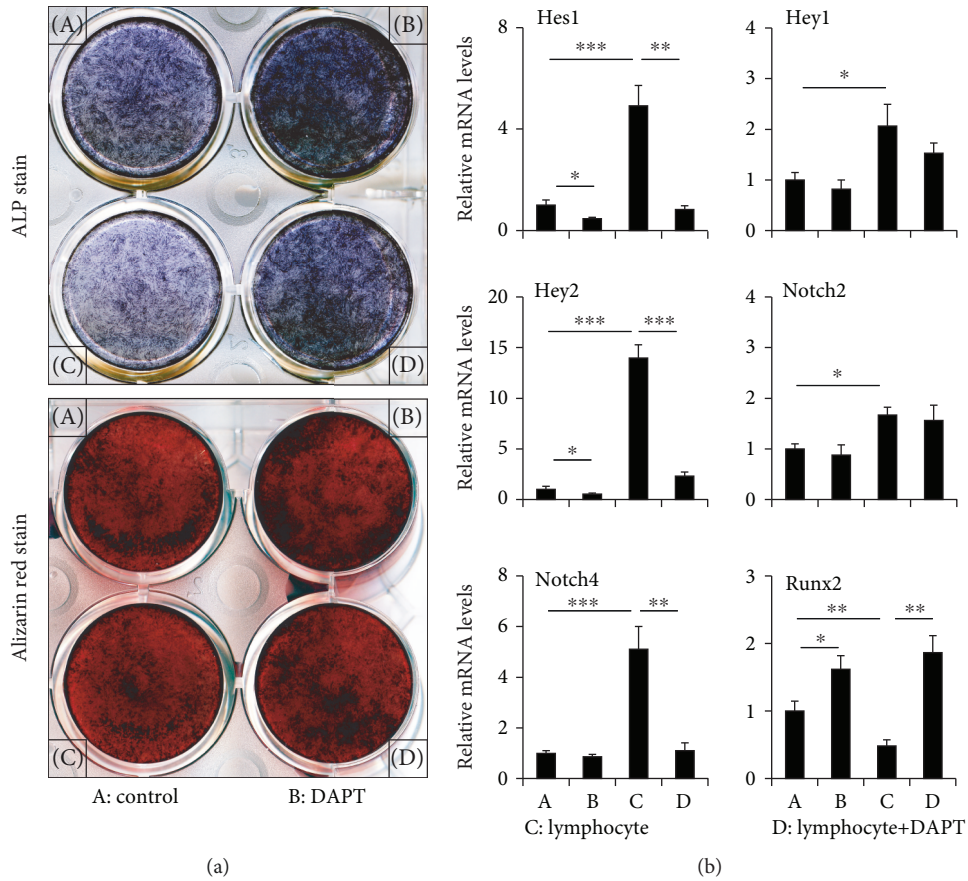

Figure 5: The osteoblastogenesis of BMSCs cocultured with LPS-pretreated B lymphocytes and DAPT. (a) ALP and Alizarin red staining of BMSCs cocultured with LPS-pretreated B lymphocytes and DAPT. Alizarin red staining: calcified matrix in red and mineralization nodules in the dark. (b) mRNA expression of Hey1, Hey2, Notch2, Notch4, Hes1, and Runx2 in BMSCs cocultured with LPS-pretreated B lymphocytes and DAPT. Data are presented as the means ± standard deviations; $^{*}p < 0.05$, $^{**}p < 0.01$, and $^{***}p < 0.001$ ($n = 6$/group).

trabecular bone tissue in OVX mice, but nonsteroidal anti-inflammatory drugs which does not suppress lymphocytes did not [7, 23], and the mechanism was not clear. In our study, ALP staining-positive cells increased in the DXM+ lymphocyte group relative to the lymphocyte group; a similar trend occurred in Alizarin red staining. It means the potency of differentiation of BMSCs into osteoblasts recovered when activated B lymphocytes were suppressed by dexamethasone. The Notch signaling pathway is conserved and regulates the development of any cells or organisms, of course, which is also deeply involved in the development of B lymphocytes and bone [24, 25]. Recent studies showed that Notch signaling enhanced B lymphocyte differentiation, proliferation, and T-dependent immune response [26]. Researches about bone showed that activation of Notch signaling arrested pluripotent precursors to the osteoblastic lineage, but inactivation of Csl/Rbpjκ restores normal osteoblastic differentiation [24, 27, 28]. Studies from different fields seem to demonstrate that the activated Notch signaling would play entirely different roles on different cell developments. As we all know, the Hes family and the Hey family are target genes of notch intracellular domain in the nucleus. Overexpression of Hes1 causes osteopenia in female mice, and inactivation of Hes1 in osteoblasts increases trabecular bone volume in male mice [29]. Taken together, these researches highlight that activated Notch signaling is essential in regulating B lymphocyte survival, activation, proliferation, and differentiation. Meanwhile, the osteoblastogenesis of BMSCs will be suppressed when Notch signaling is activated. Notch signaling play an unexpected role in the balance of homeostasis between the development of B lymphocytes and osteoblasts differentiated from BMSCs. In our study, we found that the mRNA expression of Notch2, Notch4, Hes1, Hey1, and Hey2 increased in BMSCs cocultured with pretreated B lymphocytes, especially Notch4, Hes1, and Hey2, while the high expression will turn down when dexamethasone was used in the coculture system. This study showed that activated B lymphocytes would activate Notch signaling in BMSCs, while dexamethasone can weaken this effect by suppressing the activated B lymphocytes. As we all know, the transactivation of Runx2 is necessary for osteoblast differentiation of BMSCs, and it is also a target gene of notch intracellular domain [27]. So we also detected that the expression of Runx2 decreased in BMSCs cocultured with activated B lymphocytes, and this effect would partly restore when dexamethasone was used. Meanwhile, DAPT (an inhibitor of Notch signaling) was used in the coculture system; the suppression of osteoblastogenesis of BMSCs was also restored by inhibiting the activated Notch signaling of BMSCs. The expression of Notch4, Hes1, and Hey2 was

sharply decreased, and the expression of Runx2 increased when DAPT was used in the coculture system.

5. Conclusions

This study revealed a role of B lymphocytes in the osteoblastogenesis of BMSCs in ovariectomized and splenectomized-ovariectomy rats. The much more serious osteoporosis accompanied with increasing B lymphocytes in bone marrow by splenectomy which was opposite to the outcomes of thymectomy and which suggested the balance of the immune system, especially among immune organs, contributes to the maintenance of skeletal homeostasis in estrogen deficiency. Meanwhile, Notch signaling is activated in BMSCs when cocultured with LPS-pretreated B lymphocytes. The expression of Notch2, Notch4, Hes1, Hey1, and Hey2 increased in cocultured BMSCs and decreased when dexamethasone (suppress the lymphocytes) or DAPT (inhibitor of Notch signaling) was in the coculture system. It means that the activated B lymphocytes would suppress the osteoblastogenesis of BMSCs by activating the Notch signaling, and the osteoblastogenesis of BMSCs would partly restore when B lymphocytes were suppressed or Notch signaling was inactivated. It should be taken into attention that inhibitors of Notch signaling may play a promising role in osteoporosis accompanied with abnormal B lymphocyte differentiation.

Abbreviations

BMSCs: Bone mesenchymal stem cells
Runx2: Runt-related transcription factor 2
ALP: Alkaline phosphatase
tBMD: Trabecular bone mineral density
BV/TV: Bone volume fraction, ratio of the segmented bone volume to the total volume of the region of the region of interest
Tb/Th: Trabecular thickness, mean thickness of trabeculae
Tb.Sp: Trabecular separation, mean distance between trabeculae
Tb.N: Trabecular number, measure of the average number of trabeculae per unit length.

Data Availability

The data used to support the findings of this study are available from the corresponding authors upon request.

Ethical Approval

The experiment procedure and isolation of primary rat BMSCs were performed according to the protocol approved by the Fudan University Animal Care and Use Committee. The protocol was approved by the Fudan University Animal Care and Use Committee (No. 2012-03-FYS-GJJ-01). All surgeries were performed under anesthesia, and all efforts were made to minimize suffering.

Conflicts of Interest

The authors declare that they have no competing interests.

Authors' Contributions

The manuscript was written by Xiaoya Xu, Mengxue Pan, and Wei Hong and revised by all authors. The design of the study was discussed by Xiaoya Xu, Jianjun Gao, Wei Hong, and Guoqiang Hua. The animal model was carried out by Mengxue Pan, Ye Yao, and Guoxiang Fu. The analysis of micro-CT was done by Xiaoxue Gao, Xinxin Rao, and Weifang Jin. Histology was carried out by Yi Zhou and Qiang Guo. Cell culture and PCR were carried out by Yuanchuang Li, Peiyuan Tang, and Shengzhi Chen. The final data was interpreted by all authors. All authors read and approved the final manuscript. Mengxue Pan and Wei Hong contributed equally to this work.

Acknowledgments

The authors are grateful to Prof. Chunlin Shao and MD. Zhanying Wei for providing the facilities in analysis and for scientific discussions. This work was supported by funds from the National Natural Science Foundation of China (No. 81102071, Xiaoya Xu) and the Shanghai Municipal Planning Commission of Science and Research Fund (No. 201740028, Wei Hong).

References

[1] J. Lorenzo and Y. Choi, "Osteoimmunology," *Immunological Reviews*, vol. 208, no. 1, pp. 5-6, 2005.

[2] M. R. Ryan, R. Shepherd, J. K. Leavey et al., "An IL-7-dependent rebound in thymic T cell output contributes to the bone loss induced by estrogen deficiency," *Proceedings of the National Academy of Sciences*, vol. 102, no. 46, pp. 16735–16740, 2005.

[3] C. Miyaura, Y. Onoe, M. Inada et al., "Increased B-lymphopoiesis by interleukin 7 induces bone loss in mice with intact ovarian function: similarity to estrogen deficiency," *Proceedings of the National Academy of Sciences*, vol. 94, no. 17, pp. 9360–9365, 1997.

[4] T. Masuzawa, C. Miyaura, Y. Onoe et al., "Estrogen deficiency stimulates B lymphopoiesis in mouse bone marrow," *Journal of Clinical Investigation*, vol. 94, no. 3, pp. 1090–1097, 1994.

[5] M. Kanematsu, T. Sato, H. Takai, K. Watanabe, K. Ikeda, and Y. Yamada, "Prostaglandin E_2 induces expression of receptor activator of nuclear factor–κB ligand/osteoprotegrin ligand on pre-B cells: implications for accelerated osteoclastogenesis in estrogen deficiency," *Journal of Bone and Mineral Research*, vol. 15, no. 7, pp. 1321–1329, 2000.

[6] V. Breuil, M. Ticchioni, J. Testa et al., "Immune changes in post-menopausal osteoporosis: the Immunos study," *Osteoporosis International*, vol. 21, no. 5, pp. 805–814, 2010.

[7] X. Xu, R. Li, Y. Zhou et al., "Dysregulated systemic lymphocytes affect the balance of osteogenic/adipogenic differentiation of bone mesenchymal stem cells after local irradiation," *Stem Cell Research & Therapy*, vol. 8, no. 1, p. 71, 2017.

[8] B. Ignatowska-Jankowska, M. Jankowski, W. Glac, and A. H. Swiergel, "Cannabidiol-induced lymphopenia does not involve

NKT and NK cells," *Journal of Physiology and Pharmacology*, vol. 60, Supplement 3, pp. 99–103, 2009.

[9] W. J. Tang, L. F. Wang, X. Y. Xu et al., "Autocrine/paracrine action of vitamin D on fgf23 expression in cultured rat osteoblasts," *Calcified Tissue International*, vol. 86, no. 5, pp. 404–410, 2010.

[10] P. W. Kincade, K. L. Medina, K. J. Payne et al., "Early B lymphocyte precursors and their regulation by sex steroids," *Immunological Reviews*, vol. 175, no. 1, pp. 128–137, 2000.

[11] S. Cenci, M. N. Weitzmann, C. Roggia et al., "Estrogen deficiency induces bone loss by enhancing T-cell production of TNF-α," *Journal of Clinical Investigation*, vol. 106, no. 10, pp. 1229–1237, 2000.

[12] R. Pacifici, "Estrogen deficiency, T cells and bone loss," *Cellular Immunology*, vol. 252, no. 1-2, pp. 68–80, 2008.

[13] U. Islander, C. Jochems, M. K. Lagerquist, H. Forsblad-d'Elia, and H. Carlsten, "Estrogens in rheumatoid arthritis; the immune system and bone," *Molecular and Cellular Endocrinology*, vol. 335, no. 1, pp. 14–29, 2011.

[14] G. Wheater, V. E. Hogan, Y. K. O. Teng et al., "Suppression of bone turnover by B-cell depletion in patients with rheumatoid arthritis," *Osteoporosis International*, vol. 22, no. 12, pp. 3067–3072, 2011.

[15] Y. Li, G. Toraldo, A. Li et al., "B cells and T cells are critical for the preservation of bone homeostasis and attainment of peak bone mass in vivo," *Blood*, vol. 109, no. 9, pp. 3839–3848, 2007.

[16] A. M. Tyagi, K. Srivastava, M. N. Mansoori, R. Trivedi, N. Chattopadhyay, and D. Singh, "Estrogen deficiency induces the differentiation of IL-17 secreting Th17 cells: a new candidate in the pathogenesis of osteoporosis," *PLoS One*, vol. 7, no. 9, article e44552, 2012.

[17] N. Giuliani, S. Colla, R. Sala et al., "Human myeloma cells stimulate the receptor activator of nuclear factor-κB ligand (RANKL) in T lymphocytes: a potential role in multiple myeloma bone disease," *Blood*, vol. 100, no. 13, pp. 4615–4621, 2002.

[18] X. Han, X. Lin, X. Yu et al., "*Porphyromonas gingivalis* infection-associated periodontal bone resorption is dependent on receptor activator of NF-κB ligand," *Infection and Immunity*, vol. 81, no. 5, pp. 1502–1509, 2013.

[19] L. Yeo, K. M. Toellner, M. Salmon et al., "Cytokine mRNA profiling identifies B cells as a major source of RANKL in rheumatoid arthritis," *Annals of the Rheumatic Diseases*, vol. 70, no. 11, pp. 2022–2028, 2011.

[20] C. Guo, C. Li, K. Yang et al., "Increased EZH2 and decreased osteoblastogenesis during local irradiation-induced bone loss in rats," *Scientific Reports*, vol. 6, no. 1, article 31318, 2016.

[21] M. Onal, J. Xiong, X. Chen et al., "Receptor activator of nuclear factor κB ligand (RANKL) protein expression by B lymphocytes contributes to ovariectomy-induced bone loss," *Journal of Biological Chemistry*, vol. 287, no. 35, pp. 29851–29860, 2012.

[22] G. C. Yang, Y. H. Xu, H. X. Chen, and X. J. Wang, "Acute lymphoblastic leukemia cells inhibit the differentiation of bone mesenchymal stem cells into osteoblasts in vitro by activating notch signaling," *Stem Cells International*, vol. 2015, Article ID 162410, 11 pages, 2015.

[23] L. Grahnemo, C. Jochems, A. Andersson et al., "Possible role of lymphocytes in glucocorticoid-induced increase in trabecular bone mineral density," *Journal of Endocrinology*, vol. 224, no. 1, pp. 97–108, 2015.

[24] S. Zanotti and E. Canalis, "Notch and the skeleton," *Molecular and Cellular Biology*, vol. 30, no. 4, pp. 886–896, 2010.

[25] M. N. Cruickshank and D. Ulgiati, "The role of Notch signaling in the development of a normal B-cell repertoire," *Immunology and Cell Biology*, vol. 88, no. 2, pp. 117–124, 2010.

[26] M. Thomas, M. Calamito, B. Srivastava, I. Maillard, W. S. Pear, and D. Allman, "Notch activity synergizes with B-cell–receptor and CD40 signaling to enhance B-cell activation," *Blood*, vol. 109, no. 8, pp. 3342–3350, 2007.

[27] M. J. Hilton, X. Tu, X. Wu et al., "Notch signaling maintains bone marrow mesenchymal progenitors by suppressing osteoblast differentiation," *Nature Medicine*, vol. 14, no. 3, pp. 306–314, 2008.

[28] Y. Dong, A. M. Jesse, A. Kohn et al., "RBPjκ-dependent Notch signaling regulates mesenchymal progenitor cell proliferation and differentiation during skeletal development," *Development*, vol. 137, no. 9, pp. 1461–1471, 2010.

[29] S. Zanotti, A. Smerdel-Ramoya, and E. Canalis, "HES1 (hairy and enhancer of split 1) is a determinant of bone mass," *Journal of Biological Chemistry*, vol. 286, no. 4, pp. 2648–2657, 2011.

Hindawi
Stem Cells International
Volume 2019, Article ID 7213854, 11 pages
https://doi.org/10.1155/2019/7213854

Research Article

Influence of Lineage-Negative Stem Cell Therapy on Articulatory Functions in ALS Patients

Wioletta Pawlukowska,[1,2] **Bartłomiej Baumert**,[3] **Monika Gołąb-Janowska**,[2] **Anna Sobuś**,[3] **Agnieszka Wełnicka**,[2] **Agnieszka Meller**,[2] **Karolina Machowska-Sempruch**,[2] **Alicja Zawiślak**,[3] **Karolina Łuczkowska**,[3] **Sławomir Milczarek**,[3] **Bogumiła Osękowska**,[3] **Edyta Paczkowska**,[3] **Iwona Rotter**,[1] **Przemysław Nowacki**,[2] **and Bogusław Machaliński**[3]

[1]*Department of Medical Rehabilitation and Clinical Physiotherapy, Pomeranian Medical University, Szczecin, Poland*
[2]*Department of Neurology, Pomeranian Medical University, Szczecin, Poland*
[3]*Department of General Pathology, Pomeranian Medical University, Szczecin, Poland*

Correspondence should be addressed to Wioletta Pawlukowska; wsna@o2.pl

Received 26 February 2019; Revised 17 April 2019; Accepted 8 May 2019; Published 2 June 2019

Guest Editor: Jun Li

Introduction. Amyotrophic lateral sclerosis (ALS) is a fatal, neurodegenerative disease, leading to loss of muscle strength and motor control. Impaired speech and swallowing lower the quality of life and consequently may induce acute respiratory failure. Bone marrow-derived stem and progenitor cells (SPCs) may be a valuable source of trophic factors. In this study, we assessed whether adjuvant cellular therapy could affect the levels of selected neurotrophins and proinflammatory factors in the cerebrospinal fluid (CSF) and subsequently prevent the deterioration of articulation. *Materials and Methods*. The study group consisted of 32 patients with sporadic ALS who underwent autologous lineage-negative (Lin^-) stem cell intrathecal administration to the spinal canal. Lin^- cells were aspirated from the bone marrow and isolated using immunomagnetic beads and a lineage cell depletion kit. Patients were examined for articulatory functions by means of the Voice Handicap Index (VHI) questionnaire and Frenchay Dysarthria Assessment (FDA). In parallel, we carried out the analysis of selected trophic and proinflammatory factors in CSF utilizing multiplex fluorescent bead-based immunoassays. *Results*. Of the 32 patients who received the Lin^- progenitor cell therapy, 6 (group I) showed improvement in articulatory functions, 23 remained stable (group II), and 3 deteriorated (group III) on the 28^{th} day. The improvement was particularly noticeable in a better cough reflex, laryngeal time, and dribble reflex. A statistically significant lower level of brain-derived neurotrophic factor (BDNF) was observed on day 0 in group I compared to group II. The CSF concentrations of C-reactive protein (CRP) in group I significantly decreased 7 days after Lin^- SPC transplantation. On the contrary, a significant increase in the tumor necrosis factor receptor (TNF-R) level was confirmed among patients from group I with improvement of dribble and coughing reflex, tongue movements, and respiration on the 7^{th} day, as well as on day 28 including dribble reflex solely. *Conclusions*. An application of Lin^- stem cells could potentate the beneficial humoral effect. The prevention of deterioration of articulatory functions in ALS patients after applying adjuvant Lin^- stem cell therapy seems to be promising. Although the procedure is safe and feasible, it requires further in-depth studies.

1. Introduction

Amyotrophic lateral sclerosis is a neurodegenerative disease which causes progressive muscle weakness and loss of motor control [1]. Speech deterioration occurs as a prodromal symptom in about 25-30% of ALS sufferers, who display lower speech volume, imprecise articulation, or difficulties in raising the voice, screaming, or singing. Repetitive movements of the lips, tongue, and pharynx become slower due to a decline in the range of motion within those organs [2]. The time between the occurrence of the first signs of speech deterioration and a definitive diagnosis of ALS varies

between 33 and 60 months [3]. Speech impairments in ALS manifest themselves in the form of flaccid, spastic, or mixed flaccid-spastic dysarthria [4]. Dysarthric disorders in ALS affect articulation, phonation, breathing, prosody, and resonance [5, 6]. Bulbar dysarthria is characterized by the most rapid progressive changes which first affect the tongue muscles and the orbicularis oris to subsequently impair the musculature of the soft palate, mandible, and pharynx. The facial and laryngeal muscles become dysfunctional last [7, 8]. Spastic and mixed flaccid-spastic dysarthria in ALS manifest themselves in distorted articulation, disturbed prosody, spastic dysphonia, and decreased respiratory capacity while speaking [9]. Other symptoms include monopitch voice, short phrases, distorted vowels, monoloudness, and "breathy" voice quality [10].

There is no effective treatment for dysarthria in ALS. Some symptomatic and compensatory therapies used today bring only temporary improvement in communication and raise quality of life in ALS patients [11–13]. Pharmacological treatment is limited with only class IV evidence. Sometimes patients with spastic dysarthria are temporarily helped by sucking ice, having it placed over the larynx, or taking antispastic drugs such as baclofen [14]. Botulinum toxin type A has been reported as effective in spastic dysarthria [15] and spasmodic dysphonia [16, 17]. Pyridostigmine may bring a temporary effect in some patients [18]. Another method of therapy is a palatal lift. The procedure may temporarily improve resonance by raising the weak soft palate to the level of normal palatal elevation and thus reduce hypernasality and hypophonia [19, 20]. A palatal augmentation prosthesis may also temporarily enhance articulation by lowering the palate, which improves the production of the lingual consonant sounds [20, 21]. There is no solid evidence as to how effective these prostheses are or how long they remain effective [22, 23].

The autologous bone marrow stem cell application might prove an effective alternative to classic ALS treatments. Stem cells seem to be a reasonable and promising option, all the more so since the intrathecal administration of neurotrophic factors alone failed to bring expected results in clinical trials [24] mainly due to their low bioavailability and very short half-life in the spinal canal. The administration of autologous stem/progenitor cells (SPCs) to individuals with neurodegenerative diseases is expected to result in trophic support for the host's neurons; slowdown in the progression of the disease, stimulating the secretion of deficient neurotransmitters; and differentiation into oligodendrocyte progenitor cells or neurons [25]. Since the 1960s, when the first neurotrophic factors were discovered and defined, there has been a steady increase in the research dedicated to neurotrophic protective factors, with a particular focus on "classical" brain-derived neurotrophins (NTs): nerve growth factor-beta (NGF-β), brain-derived neurotrophic factor (BDNF), and neurotrophin-3 (NT-3) [26, 27].

Apart from having a crucial neuroprotective effect, BDNF was also found to play an important role in neuronal survival and growth. It also serves as a neurotransmitter modulator [28, 29]. As most NTs present in body fluids have a very short half-life, any attempted treatments with recombined factors would be costly and the effects short-lived. Repeated cell injections performed at short intervals or administration of genetically modified stem cells would ensure prolonged and steady secretion of the desired soluble neurotrophic agents and create an appropriate microenvironment for the neuroregenerative processes [30]. First reports regarding the effects of such a pathophysiological compilation following the delivery of BDNF from genetically modified mesenchymal stem cells with overexpressed NTs are promising [31]. It has been recently shown that neuroinflammation mediated by glial cells and systemic immune activation may be a key factor contributing to the progression of ALS through mechanisms that can be either neuroprotective or neurodegenerating, depending on the type of cells and the motor neuron compartment involved [32, 33]. It has also been declared that ALS patients present signs of systemic inflammation, reflected in increased levels of CRP, tumor necrosis factor-alpha (TNF-α), interleukins (IL-6, IL-8), interferon-beta (IFN-β), and complement components such as C3 and C4 [34–36]. In ALS patients, CRP could be produced not only by the liver but also locally in the brain [37]. Moreover, the CRP level correlates with neurologic functional impairment and survival [38]. A meta-analysis by Hu et al. [39] provided a systematic review of 25 publications regarding blood inflammatory cytokines in ALS patients vs. control subjects. Results showed that the levels of TNF-α, TNF receptor 1, IL-6, IL-1β, IL-8, and vascular endothelial growth factor (VEGF) were significantly higher in ALS patients compared to controls, suggesting that these peripheral inflammatory cytokines might be biomarkers for ALS.

Lineage-negative cells are a very rare population of cells compared to mononuclear cells (MNCs) or mesenchymal stem cells. However, they are highly enriched by immature SPCs, including $CD34^+$ cells, $CD133^+$ cells, and expressing markers involved in migration, adhesion, and homing to the bone marrow and sites of tissue injury [27]. We have previously shown that umbilical cord blood- (UCB-) derived Lin^- cells strongly and specifically express classical NTs like BDNF, NGF, NT-3, NT-4, and the novel neurotrophic cytokines, as well as VEGF [27]. NT expression in the Lin^- population was much higher than in unsorted nucleated cells (NCs) [27]. We have also shown that these secreted factors support neuronal proliferation and *in vitro* survival in a conditioned medium from Lin^- SPCs [27]. The influence of intrathecal administration of Lin^- cells on trophic factors and proinflammatory factors in patients with ALS has been the subject of our previous published study [26].

In this consecutive study, we aimed to investigate whether intrathecal administration of autologous bone marrow-derived Lin^- cells can lead to the prevention of deterioration of articulatory functions. Additionally, we used functional scales (Norris and ALS Functional Rating Scale) to assess the overall neurological condition of ALS patients and confront it with the objective evaluation of articulation. Because growth factors play a pivotal role in the regeneration and SPCs can release a number of growth factors, we hypothesized that adjuvant stem cell-based therapy could also bring specific changes in various neurotrophins and proinflammatory factors profiles in the CSF of ALS patients.

2. Material and Methods

2.1. Subjects. The study was designed as a prospective, open-label, nonrandomized clinical trial in a single center for subjects with ALS. The trial (international number: NCT02193893) was approved by the Ethics Committee of the Pomeranian Medical University in Szczecin and conducted in accordance with the Declaration of Helsinki [26]. Prior written informed consent was obtained from all of the subjects. Patients enrolled in the study met the following criteria:

(a) Under 65 years of age

(b) The diagnosis of a probable or certain sporadic ALS form based on the El Escorial Revised Criteria

(c) Ability to express informed consent

(d) Observation of the course of riluzole-controlled disease for 3 months preceding the use of cell therapy

(e) Mild to moderate disability documented by satisfactory bulbar and spinal motor functions (minimum score 3 on the ALS-FRSr scale for swallowing and 2 points for food preparation and walking)

(f) Forced vital capacity (FVC) result greater than or equal to 50%

(g) Without cancer, signs of inflammation, diabetes, cardiovascular disease, chronic kidney, and liver disease, in euthyreosis, not receiving drugs that could affect stem cell activity

The study enrolled 32 patients—sixteen females and sixteen males—aged between 27 and 65 years (mean: 53.8 ± 8.17) with sporadic ALS [26] according to the El Escorial Revised Criteria [40]. The patients with predicted survival time of over 12 months established on the basis of the general and neurological condition were administered Lin^- SPCs during their stay in the Department of Neurology of the Pomeranian Medical University in Szczecin.

The outcome measures were as follows:

(a) *Primary outcome measures:* safety of autologous bone marrow Lin^- stem/progenitor cell infusion in enrolled patients

(b) *Secondary outcome measures:* efficacy of autologous bone marrow Lin^- stem/progenitor cell infusion in enrolled patients

A 3-month period following the enrollment was dedicated to natural history observation, during which controlled administration of riluzole was continued. Patients over 65 were excluded from the study, as it had been previously demonstrated that cell growth of expanded *in vitro* stem cells is strictly related to the donor's age [41]. Patients with evidence of any concurrent illness or receiving any medications (including potentially other previously applied stem cell-based therapies) which might affect bone marrow were also excluded.

2.1.1. Speech Test: VHI Questionnaire. International research projects have demonstrated that the Voice Handicap Index (VHI) questionnaire is a reliable tool for the subjective evaluation of voice in ALS patients and that the scores it provides are consistent. The 30-item VHI questionnaire comprising 3 subscales of 10 items each—the physical (P) items, functional (F) items, and emotional (E) items—is a recommended method of subjective assessment of the severity of speech disorders by ALS patients themselves. Cronbach's alpha for the entire cohort was 0.95, indicating high internal consistency of the 30 items. The VHI is a reliable and valid tool that can be recommended for ALS. The questionnaire is widely used throughout the world in a number of language versions including Persian, Croatian, Italian, Brazil, Latvian, Greek, and Polish [42–47]. The subjects underwent the assessment on days 0, 7, and 28 following the Lin^- cell administration.

2.1.2. Speech Test: FDA. One of the most important objective tests for evaluating articulation organs is the Frenchay Dysarthria Assessment (FDA). The FDA is a standardized test which relies on a 9-point rating scale applied to a patient. It provides information based on the observation of oral structures, functions, and speech. The test evaluates the following functions: reflexes, respiration, tongue, lips, the soft palate, laryngeal, and intelligibility. A 5-point rating scale (a–e) is used for the assessment, where letter "a" represents norm, "b" mild severity, "c" moderate, "d" considerable severity, and "e" profound severity. FDA is also used to assess the severity of the articulatory organ disorders and to monitor the effects of treatment [48]. The test was conducted by a clinical speech therapist with 12 years' experience of treating neurological conditions, predominantly Parkinson's disease. The second edition of FDA utilizes the latest findings concerning motor speech disorders and their contribution to neurological diagnosis. It has good feasibility (missing data < 5%), a high reliability of the total score (0.94), an excellent interrater agreement for the total score (0.96), and moderate to large construct validity for 81% of its items [48]. The subjects underwent the assessment on days 0, 7, and 28 following the Lin^- cell administration. Based on a detailed analysis of the FDA scores, the patients were divided into 3 groups: group I—comprising patients who demonstrated improvement of the articulation organs, group II—patients whose articulation remained stable, and group III—patients with deterioration.

2.1.3. Neurological Assessment. Assessment of disease progression was performed using two functional ALS scales—the Norris scale and the revised ALS Functional Rating Scale—on 0 (on the day of bone marrow collection and Lin^- cell administration), 7, and 28 days after cell application. The Norris scale describes limb and bulbar functions. The limb scale evaluates 21 items and the bulbar scale 13. Each item is rated in four ordinal categories [49]. Revised ALS-FRS is based on a questionnaire which allows the assessment

of physical functions in activities of daily living, and it is the most widely used system for the functional rating of ALS patients. It is divided into four clinical domains: (1) bulbar function, (2) fine motor function, (3) gross motor function, and (4) respiratory function. Each section includes 3 questions scored from 0—loss of function, to 4—normal function. Total score ranges from 0 to 48 [50].

2.2. Cells. Bone marrow (BM) was harvested from the patients after we had obtained their written informed consent. BM samples (100-120 ml) were aspirated in local anesthesia from the posterior iliac crest of the recruited patients and subsequently resuspended in collecting the medium (phosphate-buffered saline, pH 7.2) and heparin (20 U/ml; Gibco, USA). Bone marrow samples were lysed in BD Pharm Lyse lysing solution (BD Biosciences, San Jose, CA, USA) for 15 min at room temperature in the dark and washed twice in phosphate-buffered saline (PBS). The obtained suspension of BM nucleated cells (NCs) was subjected to immunomagnetic separation procedures. Isolation procedures were performed according to the manufacturer's instructions, according to the GMP conditions. Briefly, lineage-negative cells were isolated through negative selection using a MidiMACS separator (Miltenyi Biotec, Auburn, CA, USA). To isolate a lineage-negative cell population, a Lineage Cell Depletion Kit (Miltenyi Biotec, Auburn, CA, USA) was used. One hundred microliters of biotin-antibody cocktail recognizing the lineage-specific cell antigens was added per 10^8 cells according to the manufacturer's recommendations. After washing in PBS, 100 μl of Anti-Biotin MicroBeads for magnetic cell labeling was added. Labeled cell suspension was loaded onto a MACS LS column (Miltenyi Biotec), and unlabeled cells passing through the column were collected (Lin^-) [27]. Before administration, the cells were maintained in 2 ml of sterile PBS.

After isolation, lineage-negative cells were resuspended in 100 μl PBS and stained with mouse anti-human monoclonal antibodies for the following SPC markers: CD34 conjugated with allophycocyanin (APC) (BD Biosciences, San Jose, CA, USA), CD133 conjugated with phycoerythrin (PE) (Miltenyi Biotec, Auburn, CA, USA), and CD144 (FITC) (BD Biosciences, San Jose, CA, USA). After incubation for 20 min at 4°C, the cells were washed twice in PBS. Cell fluorescence was measured, and the data were analyzed using a fluorescence-activated cell analyzer (LSRII, BD Biosciences, San Jose, CA, USA) and BD FACSDiva software. Typically, 10,000 events were acquired to determine the percentage of a subpopulation within the lineage-negative SPCs. Populations of hematopoietic SPCs based on $CD34^+$ and $CD133^+$ expressions, early $CD34^+/CD133^+/CD144^+$ endothelial progenitor cells (EPCs), and endothelial $CD144^+$ cells were analyzed [27].

2.3. Administration Procedure. The total isolated Lin^- SPCs were slowly administered into the subarachnoid space via lumbar puncture (between vertebrae L3-L4 or L4-L5). The number of administered Lin^- cells varied among patients (mean: $6.26 \times 10^6 \pm 5.84$). After the injection, the patients were advised to maintain the supine position for at least 24 hours.

2.4. Molecular Analysis: Multiplex Assay. Concentrations of selected factors (TNF-α, TNF-R, CRP, BDNF, NT-3, and NGF-β) were assessed in CSF using multiplex fluorescent bead-based immunoassays (Luminex Corporation, Austin, TX, USA). Analyzed CSF samples were collected on the day of the cell injection (day 0) and on the 7^{th} day. Assays were performed according to the manufacturer's protocol, as described previously [51].

2.5. Statistical Analysis. The statistical null hypothesis we tested was that the intrathecal administration of autologous BM-derived Lin^- cells cannot lead to the prevention of deterioration of articulation. The primary objective of this investigation was to analyze the alternative hypothesis that intrathecal administration of autologous BM-derived Lin^- cells can lead to the prevention of deterioration of articulation. We also hypothesized that adjuvant cell therapy could also bring specific changes in various neurotrophins and proinflammatory factor profiles in CSF of ALS patients. To assess the equality of variances for variables, Levene's test was used before a comparison of means. The test has shown significance ($p < 0.05$). For this reason and because of the nonnormality of the distributions between variables (Shapiro–Wilk test), the numerical data were compared between groups using the nonparametric Friedman analysis of variance by ranks for more than two groups of repeated variables. The occurrence of nominative clinical data was compared between groups by means of the chi-squared test or Yates' chi-squared test if needed. $p < 0.05$ was considered to indicate statistical significance. All statistical analyses were performed with STATISTICA 12.5 PL.

3. Results

32 patients suffering from sporadic ALS (sixteen females and sixteen males) were included in the study. All of them were administered autologous bone marrow-derived Lin^- cells injected intrathecally. A thorough analysis of a fraction of Lin^- cells in our earlier studies revealed its composition as a heterogenic population of cells consisting of precursor cells, progenitor cells, and stem cells [27]. By employing flow cytometry, we had previously shown that Lin^- cells contain populations of $CD34^+$ cells ($12.1\% \pm 7.2$), $CD133^+$ cells ($12.3\% \pm 8.2$), endothelial progenitor cells ($CD34^+$, $CD133^+$, and $CD144^+$ cells, $1.7\% \pm 1.1$), and cells with the mesenchymal stem cell phenotype ($CD105^+$, $CD73^+$, $CD90^+$, $CD45^-$, $CD34^-$, $CD11b^-$, $CD19^-$, and HLA-DR^- cells, $0.0084\% \pm 0.0108$) [27]. FDA and VHI scales were used for the objective and subjective evaluations of the patients' articulation functions, respectively, performed at baseline, 7 days, and 28 days following the cell administration. The Norris scale and revised ALS Functional Rating Scale were used for the functional evaluation of enrolled patients, performed similarly at baseline, 7 days, and 28 days following the cell infusion.

3.1. Speech Tests and Neurological Evaluation. Of the 32 patients who received the Lin^- stem/progenitor cell therapy, 6 (group I) showed improvement in articulatory functions,

Table 1: Characteristic of the groups with ALS-FRSr and Norris scale results.

Characteristic	Group I ($n = 6$)	Group II ($n = 23$)	Group III ($n = 3$)	p value		
				I vs. II	I vs. III	II vs. III
Age (mean ± SD, years)	60.3 ± 3.82	51.8 ± 8.55	56.3 ± 3.05	0.021[a]	0.97[a]	0.89[a]
Sex (male/female)	4/2	11/12	1/2	0.72[b]	0.81[b]	0.89[b]
Time from symptom to diagnosis (mean ± SD, months)	40.8 ± 31.03	31.13 ± 27.62	26 ± 19.28	0.87[a]	0.92[a]	0.41[a]
Number of Lin^- cells administered (mean ± SD)	$(6.47 \pm 6.74) \times 10^6$	$(6.44 \pm 6.11) \times 10^6$	$(4.5 \pm 0.89) \times 10^6$	0.51[a]	0.15[a]	0.21[a]
ALS-FRSr score (mean ± SD)						
Before Lin^- infusion	30 ± 5.4	26.9 ± 4.3	33 ± 5.6	0.63[c]	1.0[c]	0.17[c]
7 days after Lin^- infusion	30 ± 5.4	26.9 ± 4.3	33 ± 5.6	0.63[c]	1.0[c]	0.17[c]
28 days after Lin^- infusion	31.5 ± 6.4	27.7 ± 4.6	30.7 ± 7.4	0.58[c]	1.0[c]	0.28[c]
Norris scale score (mean ± SD)						
Before Lin^- infusion	84.5 ± 16.9	81.2 ± 15.6	97 ± 14.1	1.0[c]	0.47[c]	0.25[c]
7 days after Lin^- infusion	87.6 ± 14.1	81.2 ± 15.6	97 ± 14.1	1.0[c]	0.77[c]	0.19[c]
28 days after Lin^- infusion	92.5 ± 14.8	82.8 ± 15.5	97 ± 14.1	0.64[c]	1.0[c]	0.65[c]

[a]Friedman analysis of variance by ranks for more than two groups. [b]Chi-squared test or Yates' chi-squared test. [c]ANOVA Kruskal-Wallis test.

23 remained stable (group II), and 3 deteriorated (group III) on the 28th day according to the objective FDA scale. Table 1 shows the comparison of the initial anthropometric parameters of the groups. Group I subjects were older than their group II counterparts, and the difference in age was statistically significant ($p = 0.021$). No notable differences were recorded between the three groups regarding the quantities of administered Lin^- cells and sex of the patients. The patients from group I had a tendency towards a longer interval from symptom onset to diagnosis, although statistically insignificant. However, this factor is considered as a marker of favorable prognosis [52].

Additionally, we confronted articulation according to the FDA scale with functional condition based on two scales—Norris and ALS-FRSr. Assessment was performed on 0, 7, and 28 days after infusion of Lin^- cells. The results, although not statistically significant, were consistent with those obtained from the evaluation of the articulation. The ALS-FRSr and Norris scale scores increased slightly on the 28th day among patients from groups I and II. Group III patients deteriorated according to ALS-FRSr and remained unaffected according to the Norris scale. It is interesting to note that the patients from group III with the deterioration of articulation initially had the highest score in Norris scales and ALS-FRSr scales. The described changes are presented in Table 1.

Table 2 shows the efficiency of the articulation organ functions in 32 ALS patients divided into 3 groups evaluated at different time points (0, 7, and 28 days). The most significant improvement was noticed on the 7th day following the cell administration in respect of cough reflex (34%), laryngeal time (32%), and dribble/drool reflex (28%). The improvement, though, was short-lasting and was no longer observed on the 28th day after the cell infusion.

Table 3 illustrates the subjective assessment of articulation based on the VHI questionnaire carried out by 32 ALS patients divided into 3 groups at different time intervals following the Lin^- cell administration. On the 7th day, 53% of the subjects reported improvement in articulation. On the 28th day, the figure grew to 62.5% and 9.3% did not feel any change in their speech, whereas 28% of the patients claimed that in their case, speech/articulation had actually deteriorated. Statistically, significant correlation was observed between the baseline FDA and VHI scores and those obtained on day 7 following the application of Lin^- cells ($p = 0.0128$).

3.2. Molecular Analysis. Using Luminex multiplex assay, we have investigated concentrations of CRP, TNF-α, TNF-R, BDNF, NGF-β, and NT-3 in CSF on day 0 and the 7th day post-cell infusion. The subjects with improved articulation objectively established by means of FDA (group I) demonstrated a statistically significant decrease in CRP levels during the first seven days after transplantation ($p = 0.043$). The analysis of FDA scores recorded in groups I and II (improvement vs. no improvement) on day 0 revealed a significantly lower BDNF level in group I compared to group II ($p = 0.028$). Besides, we noticed a tendency to increase the level of BDNF ($p = 0.14$) and TNF-α ($p = 0.068$) on the 7th day from the application of the Lin^- cells in group I. A statistically significant correlation was also found in groups I and II between the patients' age and their FDA scores obtained on days 0–7 ($p = 0.043$)—improved articulation was recorded in statistically older subjects. Changes in concentrations of proinflammatory factors and neurotrophins in CSF are presented in Table 4 and Figure 1 (selected factors).

Analysis of particular functions and efficiency of the articulation organs using the FDA scale revealed a statistically significant increase in the concentration of TNF-R in group I on the 7th day following the Lin^- administration and improvement in the following: dribble reflex ($p = 0.018$), cough reflex ($p = 0.015$), tongue movements ($p = 0.015$), and respiration ($p = 0.046$). Moreover, group I subjects with

Table 2: Evaluation of articulation organ functions by FDA in 32 ALS patients divided into 3 groups (I—improved articulation, II—lack of improvement, and III—deteriorated articulation), measured 7 and 28 days after Lin$^-$ cell administration compared to the baseline values (day 0).

	0 day vs. 7th day			7th day vs. 28th day			0 day vs. 28th day		
	Group I	Group II	Group III	Group I	Group II	Group III	Group I	Group II	Group III
Cough reflex	11	16	5	5	17	10	7	18	7
Swallow reflex	6	23	3	2	25	5	6	19	7
Dribble/drool reflex	9	20	3	6	20	6	10	19	3
Respiration	8	18	6	3	23	6	9	14	9
Lips	6	24	2	2	26	4	9	17	6
Soft palate	7	22	3	2	26	4	6	22	4
Laryngeal time	10	21	1	4	17	11	9	17	6
Laryngeal pitch	6	23	3	4	20	8	8	18	6
Laryngeal volume	8	20	4	3	23	6	9	18	5
Laryngeal in speech	7	21	4	4	22	6	8	19	5
Tongue	7	17	8	4	21	7	10	12	10
Intelligibility words	4	24	4	3	25	4	3	28	1
Intelligibility sentences	4	24	4	5	24	3	7	24	1
Intelligibility conversation	6	20	6	6	23	3	8	19	5

Table 3: Subjective evaluation of articulation improvement carried out by means of the VHI scale at different time intervals following Lin$^-$ cell administration in 32 ALS patients divided into 3 groups according to FDA (I—improved articulation; II—lack of improvement; III—deteriorated articulation).

	0 day vs. 7th day	7th day vs. 28th day	0 day vs. 28th day
Group I	17	9	20
Group II	6	16	3
Group III	9	7	9

improved dribble reflex demonstrated a significantly higher TNF-R concentration ($p = 0.036$) on day 28, while on the same day, group III patients with declined postinfusion laryngeal time showed a statistically significant increase in the concentration of TNF-α in CSF ($p = 0.043$).

4. Discussion

ALS is classified as sporadic (90 to 95% of the diagnosed cases), of unknown etiology, and familiar [53]. It is believed that there are several factors that may contribute to the onset of the disease, such as excitotoxicity by neurotransmitter glutamate, accumulation of neurofilaments, deficiency of neurotrophic factors, immunity changes, physical trauma, and persistent viral infections, as well as chemical and physical environmental factors [54]. With the progress of the disease, communication difficulties increase while sentences become simpler and shorter, culminating, in advanced phases, to answering questions through the use of keywords or "yes/no" answers [55]. These changes, together with the loss of functional independence caused by ALS, lead to an extremely discouraging situation for the individual.

The assumed effectiveness of Lin$^-$ stem cell therapy for ALS is based on SPCs' ability to produce growth factors and cytokines that exert neuroprotective activity, thus providing supportive environment and protection for neurons [56]. In our earlier study, we demonstrated that the therapy is safe and feasible [26]. An autologous population of bone marrow-derived lineage-negative SPCs demonstrates higher long-term self-regeneration potential and capacity to produce neurotrophic and angiopoietic factors than other nucleated cells [48].

The potential of stem cell-based therapy has not yet been explored in the context of its employment for treatments aimed at ameliorating articulation in ALS patients. In the course of our study, we carried out the assessment of articulation disorders in ALS patients utilizing the subjective VHI questionnaire and the objective FDA scale. We also analyzed the effect of the adjuvant Lin$^-$ stem cell administration on the articulatory functions and the CSF levels of neurotrophic and inflammatory factors. Our methodology was based on previous findings which demonstrated that the half-time of trophic factors, and thus the clinical effect, is limited to a few days following the cell infusion [26]. At the same time, we used functional scales (Norris and ALS-FRSr) to assess the overall neurological condition and confront it with the objective evaluation of articulation.

According to the FDA scale applied on the 28th day, 6 of the 32 patients who had received the Lin$^-$ SPCs showed slight improvement in articulatory functions, 23 remained stable, and in 3 others the functions deteriorated. However, the effects were transient and the observation time was short. The results, although not statistically significant between groups, were consistent with those obtained from the evaluation of the functional condition based on the ALS-FRSr and Norris scales. Patients with stabilization or with an inconsiderable improvement in articulation also showed a tendency

Table 4: The CSF concentrations of TNF-α, BDNF, NGF-β, CRP, NT-3, and TNF-R in groups I, II, and III (0 and 7th days).

Concentration in CSF	Group I ($n = 6$)			Group II ($n = 23$)			Group III ($n = 3$)		
	Median (pg/ml)	Interquartile range	p value	Median (pg/ml)	Interquartile range	p value	Median (pg/ml)	Interquartile range	p value
TNF-α 0 d	2.88	0.29	0.068	3.31	0.58	0.409	3.026	0.58	0.180
TNF-α 7 d	3.31	0.29		3.17	0.29		3.32	0.00	
BDNF 0 d	2.45*	0.45	0.144	3.75*	2.17	0.262	3.27	1.71	0.990
BDNF 7 d	3.35	0.30		3.64	1.48		3.27	1.63	
NGF-β 0 d	0.74	0.20	0.500	0.84	0.20	0.948	0.95	0.16	0.109
NGF-β 7 d	0.84	0.20		0.84	0.20		0.74	0.00	
CRP 0 d	31104	30462	0.043	11667	24463	0.807	6472	40628	0.593
CRP 7 d	6680	16966		5144	34944		9862	36053	
NT-3 0 d	352.73	0.00	1.000	352.73	113.79	0.675	352.73	168.26	0.180
NT-3 7 d	352.73	54.47		352.73	107.39		352.73	233.68	
TNF-R 0 d	918.28	144.34	0.138	1006.18	190.83	0.115	1086.91	277.03	0.285
TNF-R 7 d	1176.05	335.68		1073.01	364.67		1070.30	318.57	

Data are expressed as median (interquartile range); p value—0 day vs. 7th day; $^*p < 0.05$ for difference between group I and II patients; Mann-Whitney U test.

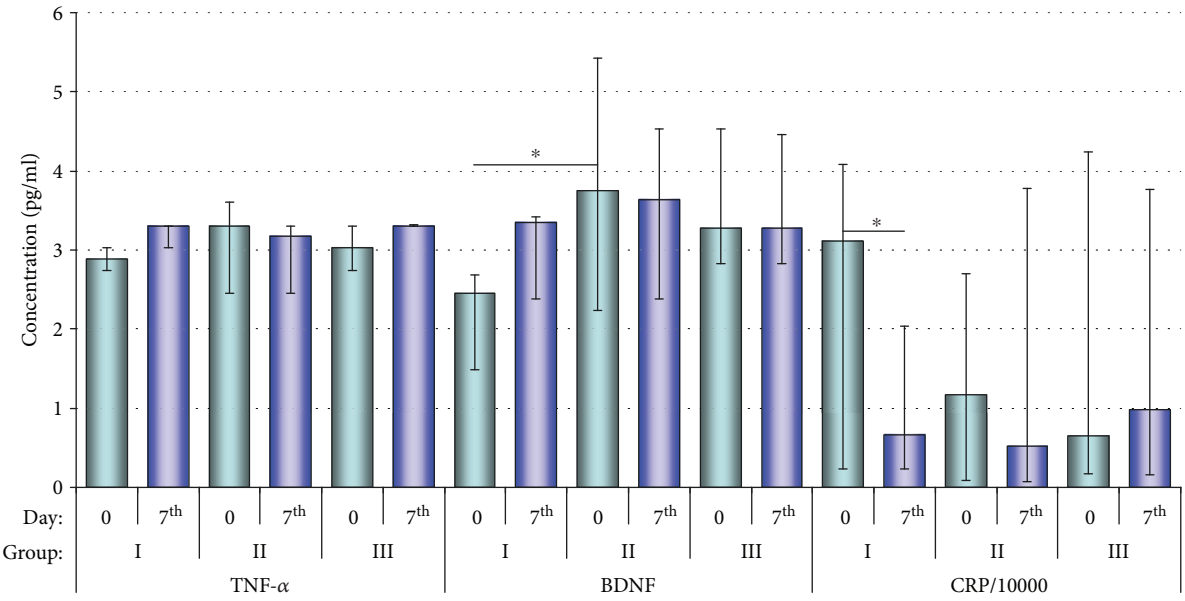

Figure 1: The CSF levels of TNF-α, BDNF, and CRP in different groups (0 and 7th days). Data are presented as median (interquartile range); $^*p < 0.05$.

to the improvement in the functional scales. Similarly, in the group of patients with progression of articulatory dysfunction, a slight deterioration according to the functional scales was also observed.

The noticeable improvement observed on the 7th day after the cell infusion was seen in regard to cough reflex (34% of the subjects), laryngeal time (32%), and dribble/drool reflex (28%). Correlation between the objective FDA scores and the results of subjective VHI questionnaire could only be observed until the 7th day following the procedure. Between days 7 and 28, the patients subjectively reported a deterioration of their articulatory functions, which did not reflect the positive FDA scores. Improved articulation based on the FDA scale was demonstrated in statistically older patients ($p = 0.043$).

Analysis of factors in CSF on the 7th day following the Lin$^-$ cell administration revealed a statistically significant correlation of the decrease in CRP concentration in patients with improved articulatory function. Interestingly, patients with the highest baseline CRP levels demonstrated the best response, whereas those with low baseline CRP concentration with a growing tendency showed clinical deterioration in their condition on the 7th day.

The important role of neuroinflammation mediated by glial and immune cells in the pathogenesis of ALS is widely accepted [57]. Numerous inflammatory proteins have been

previously shown to be altered by this disease [58, 59]. CRP has been described as a biomarker of the inflammatory response with significant prognostic value in a vast number of tumors and rheumatic and cardiovascular diseases [60]. CRP could be produced not only by the liver but also locally in the brain [37]. Keizman et al. have previously correlated CRP levels with neurological disability in ALS [61]. Lu et al. established that IL-6 associated with CRP levels is the only marker, which shows an increase in the expression toward the end-stage ALS [62]. A study by Nagel et al. on 289 ALS patients and 506 controls showed a moderate inverse correlation of CRP with the revised ALS Functional Rating Scale (ALS-FRSr) [63]. Our previous and current observation might lead to the conclusion that humoral therapy has a suppressive effect on inflammation [26]. However, as ALS is a disease of complex etiopathogenesis, the therapy does not always bring substantial clinical improvement. High baseline levels of proinflammatory factors may appear to be a positive prognostic indicator related to the ability to control its course.

Baseline BDNF concentration in CSF was significantly lower in patients who demonstrated improved articulation compared to those whose articulation had remained unchanged. The improvement in articulation was accompanied by a tendency toward higher levels of BDNF on the 7^{th} day after the cell infusion ($p = 0.14$).

Analysis of individual functions and efficiency of the articulatory organs carried out using the FDA scale on the 7^{th} day following the Lin^- cell administration showed a statistically significant increase in TNF-R concentration in the group I subjects who demonstrated improvement in dribble/drool reflex ($p = 0.018$), cough reflex ($p = 0.015$), tongue movements ($p = 0.015$), and respiration ($p = 0.046$). On top of that, on the 28^{th} day following the Lin^- application, we observed a considerable increase in the concentration of TNF-R in group I patients with improved dribble/drool reflex ($p = 0.036$). However, on the same day, group III subjects, with declined laryngeal time, showed a statistically significant increase in the levels of TNF-α in CSF ($p = 0.043$).

TNF-α can be synthesized and released in the brain by astrocytes and some populations of neurons. There is a robust and rapid increase in TNF-α expression levels in the CNS both after acute insults and in a number of chronic neurodegenerative disorders [64, 65]. Hattori et al. reported that TNF-α is involved in modulating neuronal cell function through an indirect mechanism by which it stimulates the synthesis and secretion of the nerve growth factor (NGF) in fibroblasts and glial cells [66]. TNF-α induces BDNF expression in astrocytes not only through the activation of NF-κB but also via the activation of the C/EBPβ transcription factor connected with the ERK MAP kinase pathway [67]. Based on various studies focused on the role of proinflammatory cytokines in the brain, TNF-α is usually regarded as an agent playing an important role in sustaining and modulating neurodegenerative events or sometimes promoting cell survival [68, 69]. Brambilla et al. identified TNF receptor 1 (TNFR1) signaling as a major promoter of glial cell line-derived neurotrophic factor (GDNF) synthesis/release from human and mouse spinal cord astrocytes *in vitro* and *in vivo* [70]. They also demonstrated that motor neuron loss is more pronounced in $SOD1^{G93A}$ mice lacking the TNFR1 at the late phase of the disease, i.e., when ALS progression is significantly accelerated [70].

Of the 32 ALS patients subjected to the Lin^- cell infusion, 11 demonstrated improved articulatory functions on the 7^{th} day, particularly noticeable in the cough reflex and laryngeal time (10 patients) and dribble/drool reflex (9 patients). Reduced or absent cough reflex in ALS sufferers is a serious abnormality inevitably leading to the accumulation of excessive saliva in the airways, which adversely affects respiration [71]. Secretions that obstruct the airways can result in a partial or complete collapse of the lung, contributing to acute or acute-on-chronic respiratory failure, which remains the most common cause of death in ALS [72, 73]. Maintaining an effective cough reflex could significantly contribute to the reduction of mortality and many serious infectious complications in patients with ALS.

In conclusion, our experimental adjuvant therapy with the application of autologous bone marrow-derived lineage-negative cells injected intrathecally proved entirely safe for ALS patients. No immediate or delayed, topical or systemic adverse events following the treatment were observed. During this short observation, some patients from the study deteriorated while others remained stable. The postapplication, short-termed improvement of articulatory functions, particularly the cough reflex, laryngeal time, and dribble reflex, observed in one third of the subjects, may provide valuable incentives for further comprehensive investigations. Establishing whether local neuroinflammation and CRP production could be direct prognostic factors or targets for therapy requires further studies, but our results seem to be promising.

5. Potential Study Limitations

Although our study provides valuable findings, there are a few limitations that need to be taken into account. The first one is a relatively small number of patients enrolled in the study, mainly limited by strict inclusion criteria. The second one refers to a considerable heterogeneity of the studied sample in respect of the age of onset of the symptoms, their duration, and the number of cells harvested and administered (mostly statistically insignificant). This heterogeneity, however, corresponds with typical key features of ALS. Another limitation concerns the fact that the study was carried out without the control group, which limits the possibility of drawing a direct conclusion regarding the effects of Lin^- cell application. In the case of a fatal, neurodegenerative disease such as ALS, it seems rather unethical to enroll patients without offering them a chance for potentially beneficial intervention.

Since this is still a preliminary study of such cell application, we must be cautious when interpreting the obtained data. Taking into consideration the complexity of ALS pathophysiology, it is still unclear whether the described correlations favor Lin^- cell administration as a beneficial treatment strategy for ALS or reflect other, unknown factors. Additionally, we can expect that the potential beneficial

effects of humoral therapy in ALS patients may possibly be prolonged with repeated cell injections. The last drawback of the study is a short observation period. It is due to the fact that the study is being continued on a larger cohort of ALS subjects who undergo a cyclical Lin^- cell infusion during which they receive in total three injections and the levels of trophic and proinflammatory factors are measured at different time intervals.

Data Availability

The data used to support the findings of this study are available from the corresponding author upon request.

Conflicts of Interest

The authors declare no conflict of interest.

Authors' Contributions

Wioletta Pawlukowska, Bartłomiej Baumert, Przemysław Nowacki, and Bogusław Machaliński designed the study; Wioletta Pawlukowska, Bartłomiej Baumert, Monika Gołąb-Janowska, Anna Sobuś, Agnieszka Wełnicka, Agnieszka Meller, Karolina Machowska-Sempruch, Alicja Zawiślak, Karolina Łuczkowska, Sławomir Milczarek, and Bogumiła Osękowska performed the experiments and analysis; Wioletta Pawlukowska, Monika Gołąb-Janowska, Agnieszka Wełnicka, Agnieszka Meller, and Karolina Machowska-Sempruch provided and cared for the study patients; Edyta Paczkowska, Iwona Rotter, Przemysław Nowacki, and Bogusław Machaliński analyzed the data and supervised the study; Wioletta Pawlukowska wrote the manuscript; and Bogusław Machaliński, Przemysław Nowacki, and Bartłomiej Baumert edited the manuscript. Wioletta Pawlukowska and Bartłomiej Baumert contributed equally to this work.

Acknowledgments

This work was supported by the National Center for Research and Development (grant number STRATEGMED1/234261/2NCBR/2014).

References

[1] J. M. Hausdorff, A. Lertratanakul, M. E. Cudkowicz, A. L. Peterson, D. Kaliton, and A. L. Goldberger, "Dynamic markers of altered gait rhythm in amyotrophic lateral sclerosis," *Journal of Applied Physiology*, vol. 88, no. 6, pp. 2045–2053, 2000.

[2] J. R. Bach, "Amyotrophic lateral sclerosis: communication status and survival with ventilatory support," *American Journal of Physical Medicine & Rehabilitation*, vol. 72, no. 6, pp. 343–349, 1993.

[3] K. M. Yorkston, E. Strand, R. Miller, A. Hillel, and K. Smith, "Speech deterioration in amyotrophic lateral sclerosis: implications for the timing of intervention," *Journal of Medical Speech-Language Pathology*, vol. 1, pp. 35–46, 1993.

[4] B. J. Traynor, M. B. Codd, B. Corr, C. Forde, E. Frost, and O. M. Hardiman, "Clinical features of amyotrophic lateral sclerosis according to the El Escorial and Airlie House diagnostic criteria: a population-based study," *Archives of Neurology*, vol. 57, no. 8, pp. 1171–1176, 2000.

[5] M. Mulligan, J. Carpenter, J. Riddel et al., "Intelligibility and the acoustic characteristics of speech in amyotrophic lateral sclerosis (ALS)," *Journal of Speech and Hearing Research*, vol. 37, no. 3, pp. 496–503, 1994.

[6] C. R. Watts and M. Vanryckeghem, "Laryngeal dysfunction in amyotrophic lateral sclerosis: a review and case report," *Ear, Nose and Throat Disorders*, vol. 1, no. 1, p. 1, 2001.

[7] A. D. Hillel and R. Miller, "Bulbar amyotrophic lateral sclerosis: patterns of progression and clinical management," *Head and Neck*, vol. 11, no. 1, pp. 51–59, 1989.

[8] M. J. Strong, G. M. Grace, J. B. Orange, and H. A. Leeper, "Cognition, language, and speech in amyotrophic lateral sclerosis: a review," *Journal of Clinical and Experimental Neuropsychology*, vol. 18, no. 2, pp. 291–303, 1996.

[9] C. R. Roth, L. E. Glaze, G. S. Goding Jr., and W. S. David, "Spasmodic dysphonia symptoms as initial presentation of amyotrophic lateral sclerosis," *Journal of Voice*, vol. 10, no. 4, pp. 362–367, 1996.

[10] B. Okuda, N. Kodama, K. Kawabata, H. Tachibana, and M. Sugita, "Corneomandibular reflex in ALS," *Neurology*, vol. 52, no. 8, pp. 1699–1701, 1999.

[11] S. E. Langmore and M. E. Lehman, "Physiologic deficits in the orofacial system underlying dysarthria in amyotrophic lateral sclerosis," *Journal of Speech, Language, and Hearing Research*, vol. 37, no. 1, pp. 28–37, 1994.

[12] R. J. Carpenter III, T. J. McDonald, and F. M. Howard Jr., "The otolaryngologic presentation of amyotrophic lateral sclerosis," *Otolaryngology–Head and Neck Surgery*, vol. 86, no. 3, pp. 479–484, 1978.

[13] B. Tomik, J. Krupinski, L. Glodzik-Sobanska et al., "Acoustic analysis of dysarthria profile in ALS patients," *Journal of the Neurological Sciences*, vol. 169, no. 1-2, pp. 35–42, 1999.

[14] J. Murphy, "Communication strategies of people with ALS and their partners," *Amyotrophic Lateral Sclerosis and Other Motor Neuron Disorders*, vol. 5, no. 2, pp. 121–126, 2004.

[15] R. Langton-Hewer, "The management of motor neuron disease," in *Motor Neuron Disease Biology and Management*, P. N. Leigh and M. Swash, Eds., pp. 375–406, SpringerVerlag, London, 1995.

[16] M. McHenry, J. Whatman, and A. Pou, "The effect of botulinum toxin A on the vocal symptoms of spastic dysarthria: a case study," *Journal of Voice*, vol. 16, no. 1, pp. 124–131, 2002.

[17] P. K. Holden, D. E. Vokes, M. B. Taylor, J. A. Till, and R. L. Crumley, "Long-term botulinum toxin dose consistency for treatment of adductor spasmodic dysphonia," *Annals of Otology, Rhinology & Laryngology*, vol. 116, no. 12, pp. 891–896, 2007.

[18] C. Watts, C. Nye, and R. Whurr, "Botulinum toxin for treating spasmodic dysphonia (laryngeal dystonia): a systematic Cochrane review," *Clinical Rehabilitation*, vol. 20, no. 2, pp. 112–122, 2006.

[19] L. Y. Cui, M. S. Liu, and X. F. Tang, "Single fiber electromyography in 78 patients with amyotrophic lateral sclerosis," *Chinese Medical Journal*, vol. 117, no. 12, pp. 1830–1833, 2004.

[20] H. Mitsumoto, D. A. Chad, and E. K. Pioro, "Speech and communication management," in *Amyotrophic Lateral Sclerosis*, H. Mitsumoto, D. A. Chad, and E. K. Pioro, Eds., pp. 405–420, FA Davis Co, New York, NY, USA, 1998.

[21] S. J. Esposito, H. Mitsumoto, and M. Shanks, "Use of palatal lift and palatal augmentation prostheses to improve dysarthria in patients with amyotrophic lateral sclerosis: a case series," *The Journal of Prosthetic Dentistry*, vol. 83, no. 1, pp. 90–98, 2000.

[22] T. Ono, M. Hamamura, K. Honda, and T. Nokubi, "Collaboration of a dentist and speech-language pathologist in the rehabilitation of a stroke patient with dysarthria: a case study," *Gerodontology*, vol. 22, no. 2, pp. 116–119, 2005.

[23] M. Suwaki, K. Nanba, E. Ito, I. Kumakura, and S. Minagi, "Nasal speaking valve: a device for managing velopharyngeal incompetence," *Journal of Oral Rehabilitation*, vol. 35, no. 1, pp. 73–78, 2008.

[24] M. S. Nayak, Y. S. Kim, M. Goldman, H. S. Keirstead, and D. A. Kerr, "Cellular therapies in motor neuron diseases," *Biochimica et Biophysica Acta (BBA) - Molecular Basis of Disease*, vol. 1762, no. 11-12, pp. 1128–1138, 2006.

[25] B. Machaliński, P. Lażewski-Banaszak, E. Dąbkowska, E. Paczkowska, M. Gołąb-Janowska, and P. Nowacki, "The role of neurotrophic factors in regeneration of the nervous system," *Neurologia i Neurochirurgia Polska*, vol. 46, no. 6, pp. 579–590, 2012.

[26] A. Sobuś, B. Baumert, Z. Litwińska et al., "Safety and feasibility of Lin^- cells administration to ALS patients: a novel view on humoral factors and miRNA profiles," *International Journal of Molecular Sciences*, vol. 19, no. 5, article 1312, 2018.

[27] E. Paczkowska, K. Kaczyńska, E. Pius-Sadowska et al., "Humoral activity of cord blood-derived stem/progenitor cells: implications for stem cell-based adjuvant therapy of neurodegenerative disorders," *PLoS One*, vol. 8, no. 12, article e83833, 2013.

[28] V. Silani, C. Calzarossa, L. Cova, and N. Ticozzi, "Stem cells in amyotrophic lateral sclerosis: motor neuron protection or replacement?," *CNS & Neurological Disorders - Drug Targets*, vol. 9, no. 3, pp. 314–324, 2010.

[29] M. Hajivalili, F. Pourgholi, H. Samadi Kafil, F. Jadidi-Niaragh, and M. Yousefi, "Mesenchymal stem cells in the treatment of amyotrophic lateral sclerosis," *Current Stem Cell Research & Therapy*, vol. 11, no. 1, pp. 41–50, 2016.

[30] D. H. Hwang, H. J. Lee, I. H. Park et al., "Intrathecal transplantation of human neural stem cells overexpressing VEGF provide behavioral improvement, disease onset delay and survival extension in transgenic ALS mice," *Gene Therapy*, vol. 16, no. 10, pp. 1234–1244, 2009.

[31] M. M. Harper, S. D. Grozdanic, B. Blits et al., "Transplantation of BDNF-secreting mesenchymal stem cells provides neuroprotection in chronically hypertensive rat eyes," *Investigative Opthalmology & Visual Science*, vol. 52, no. 7, pp. 4506–4515, 2011.

[32] J. Liu and F. Wang, "Role of neuroinflammation in amyotrophic lateral sclerosis: cellular mechanisms and therapeutic implications," *Frontiers in Immunology*, vol. 78, article 1005, 2017.

[33] G. P. Diniz and D. Z. Wang, "Regulation of skeletal muscle by microRNAs," *Comprehensive Physiology*, vol. 6, pp. 1279–1294, 2016.

[34] J. Ganesalingam, J. An, C. E. Shaw, G. Shaw, D. Lacomis, and R. Bowser, "Combination of neurofilament heavy chain and complement C3 as CSF biomarkers for ALS," *Journal of Neurochemistry*, vol. 117, no. 3, pp. 528–537, 2011.

[35] M. C. O. Rodrigues, D. G. Hernandez-Ontiveros, M. K. Louis et al., "Neurovascular aspects of amyotrophic lateral sclerosis," *International Review of Neurobiology*, vol. 102, pp. 91–106, 2012.

[36] J. Ehrhart, A. J. Smith, N. Kuzmin-Nichols et al., "Humoral factors in ALS patients during disease progression," *Journal of Neuroinflammation*, vol. 12, no. 1, p. 127, 2015.

[37] K. Yasojima, C. Schwab, E. G. McGeer, and P. L. McGeer, "Human neurons generate C-reactive protein and amyloid P: upregulation in Alzheimer's disease," *Brain Research*, vol. 887, no. 1, pp. 80–89, 2000.

[38] K. Lunnon, J. L. Teeling, A. L. Tutt, M. S. Cragg, M. J. Glennie, and V. H. Perry, "Systemic inflammation modulates Fc receptor expression on microglia during chronic neurodegeneration," *The Journal of Immunology*, vol. 186, no. 12, pp. 7215–7224, 2011.

[39] Y. Hu, C. Cao, X.-Y. Qin et al., "Increased peripheral blood inflammatory cytokine levels in amyotrophic lateral sclerosis: a meta-analysis study," *Scientific Reports*, vol. 7, no. 1, p. 9094, 2017.

[40] B. R. Brooks, R. G. Miller, M. Swash, and T. L. Munsat, "El escorial revisited: revised criteria for the diagnosis of amyotrophic lateral sclerosis," *Amyotrophic Lateral Sclerosis and Other Motor Neuron Disorders*, vol. 1, no. 5, pp. 293–299, 2000.

[41] K. Mareschi, I. Ferrero, D. Rustichelli et al., "Expansion of mesenchymal stem cells isolated from pediatric and adult donor bone marrow," *Journal of Cellular Biochemistry*, vol. 97, no. 4, pp. 744–754, 2006.

[42] M. Behlau, L. . M. Alves dos Santos, and G. Oliveira, "Cross-cultural adaptation and validation of the voice handicap index into Brazilian Portuguese," *Journal of Voice*, vol. 25, no. 3, pp. 354–359, 2011.

[43] A. Bonetti and L. Bonetti, "Cross-cultural adaptation and validation of the Voice Handicap Index into Croatian," *Journal of Voice*, vol. 27, no. 1, pp. 130.e7–130.e14, 2013.

[44] M. E. Helidoni, T. Murry, J. Moschandreas, C. Lionis, A. Printza, and G. A. Velegrakis, "Cross-cultural adaptation and validation of the voice handicap index into Greek," *Journal of Voice*, vol. 24, no. 2, pp. 221–227, 2010.

[45] A. Schindler, F. Ottaviani, F. Mozzanica et al., "Cross-cultural adaptation and validation of the Voice Handicap Index into Italian," *Journal of Voice*, vol. 24, no. 6, pp. 708–714, 2010.

[46] B. Trinite and J. Sokolovs, "Adaptation and validation of the Voice Handicap Index in Latvian," *Journal of Voice*, vol. 28, no. 4, pp. 452–457, 2014.

[47] A. Pruszewicz, A. Obrębowski, B. Wiskirska-Woźnica, and W. W. Wojnowski, "Sprawie kompleksowej oceny głosu – własna modyfikacja testu samooceny niesprawności głosu (Voice Handicap Idex)," *Otolaryngologia Polska*, vol. 58, pp. 547–549, 2004.

[48] P. Enderby and R. Palmer, *Frenchay Dysarthria Assessment 2 edition (FDA-2)*, English, 2008.

[49] E. Oda, Y. Ohashi, K. Tashiro, Y. Mizuno, H. Kowa, and N. Yanagisawa, "Reliability and factorial structure of a rating scale for amyotrophic lateral sclerosis," *No To Shinkei*, vol. 48, no. 11, pp. 999–1007, 1996.

[50] P. Kaufmann, G. Levy, J. L. P. Thompson et al., "The ALSFRSr predicts survival time in an ALS clinic population," *Neurology*, vol. 64, no. 1, pp. 38–43, 2005.

[51] A. Cymbaluk-Płoska, A. Chudecka-Głaz, E. Pius-Sadowska et al., "Clinical relevance of NGAL/MMP-9 pathway in patients with endometrial cancer," *Disease Markers*, vol. 2017, Article ID 6589262, 8 pages, 2017.

[52] J. A. Knibb, N. Keren, A. Kulka et al., "A clinical tool for predicting survival in ALS," *Journal of Neurology, Neurosurgery & Psychiatry*, vol. 87, no. 12, pp. 1361–1367, 2016.

[53] S. Byrne, C. Walsh, C. Lynch et al., "Rate of familial amyotrophic lateral sclerosis: a systematic review and meta-analysis," *Journal of Neurology, Neurosurgery & Psychiatry*, vol. 82, no. 6, pp. 623–627, 2011.

[54] J. R. Cannon and J. T. Greenamyre, "The role of environmental exposures in neurodegeneration and neurodegenerative diseases," *Toxicological Sciences*, vol. 124, no. 2, pp. 225–250, 2011.

[55] L. L. Neto and A. C. Constantini, "Dysarthria and quality of life in patients with amyotrophic lateral sclerosis," *Revista CEFAC*, vol. 19, no. 5, pp. 664–673, 2017.

[56] J. Czarzasta, A. Habich, T. Siwek, A. Czapliński, W. Maksymowicz, and J. Wojtkiewicz, "Stem cells for ALS: an overview of possible therapeutic approaches," *International Journal of Developmental Neuroscience*, vol. 57, pp. 46–55, 2017.

[57] J. Kuhle, R. L. P. Lindberg, A. Regeniter et al., "Increased levels of inflammatory chemokines in amyotrophic lateral sclerosis," *European Journal of Neurology*, vol. 16, no. 6, pp. 771–774, 2009.

[58] P. Petrou, Y. Gothelf, Z. Argov et al., "Safety and clinical effects of mesenchymal stem cells secreting neurotrophic factor transplantation in patients with amyotrophic lateral sclerosis: results of phase 1/2 and 2a clinical trials," *JAMA Neurology*, vol. 73, no. 3, pp. 337–344, 2016.

[59] R. T. Bartus and E. M. Johnson Jr., "Clinical tests of neurotrophic factors for human neurodegenerative diseases, part 1: where have we been and what have we learned?," *Neurobiology of Disease*, vol. 97, Part B, pp. 156–168, 2017.

[60] B. P. Prins, A. Abbasi, A. Wong et al., "Investigating the causal relationship of C-reactive protein with 32 complex somatic and psychiatric outcomes: a large-scale cross-consortium Mendelian randomization study," *PLOS Medicine*, vol. 13, no. 6, article e1001976, 2016.

[61] D. Keizman, O. Rogowski, S. Berliner et al., "Low-grade systemic inflammation in patients with amyotrophic lateral sclerosis," *Acta Neurologica Scandinavica*, vol. 119, no. 6, pp. 383–389, 2009.

[62] C. H. Lu, K. Allen, F. Oei et al., "Systemic inflammatory response and neuromuscular involvement in amyotrophic lateral sclerosis," *Neurology - Neuroimmunology Neuroinflammation*, vol. 3, no. 4, article e244, 2016.

[63] G. Nagel, R. S. Peter, A. Rosenbohm et al., "Adipokines, C-reactive protein and amyotrophic lateral sclerosis - results from a population- based ALS registry in Germany," *Scientific Reports*, vol. 7, no. 1, article 4374, 2017.

[64] S. M. Allan and N. J. Rothwell, "Cytokines and acute neurodegeneration," *Nature Reviews Neuroscience*, vol. 2, no. 10, pp. 734–744, 2001.

[65] B. Viviani, S. Bartesaghi, E. Corsini, C. L. Galli, and M. Marinovich, "Cytokines role in neurodegenerative events," *Toxicology Letters*, vol. 149, no. 1-3, pp. 85–89, 2004.

[66] A. Hattori, E. Tanaka, K. Murase et al., "Tumor necrosis factor stimulates the synthesis and secretion of biologically active nerve growth factor in non-neuronal cells," *Journal of Biological Chemistry*, vol. 268, no. 4, pp. 2577–2582, 1993.

[67] R. N. Saha, X. Liu, and K. Pahan, "Up-regulation of BDNF in astrocytes by TNF-α: a case for the neuroprotective role of cytokine," *Journal of Neuroimmune Pharmacology*, vol. 1, no. 3, pp. 212–222, 2006.

[68] K. Sriram and J. P. O'Callaghan, "Divergent roles for tumor necrosis factor-α in the brain," *Journal of Neuroimmune Pharmacology*, vol. 2, no. 2, pp. 140–153, 2007.

[69] M. K. McCoy and M. G. Tansey, "TNF signaling inhibition in the CNS: implications for normal brain function and neurodegenerative disease," *Journal of Neuroinflammation*, vol. 5, no. 1, p. 45, 2008.

[70] L. Brambilla, G. Guidotti, F. Martorana et al., "Disruption of the astrocytic TNFR1-GDNF axis accelerates motor neuron degeneration and disease progression in amyotrophic lateral sclerosis," *Human Molecular Genetics*, vol. 25, no. 14, pp. 3080–3095, 2016.

[71] M. Toussaint, L. J. Boitano, V. Gathot, M. Steens, and P. Soudon, "Limits of effective cough-augmentation techniques in patients with neuromuscular disease," *Respiratory Care*, vol. 54, pp. 359–366, 2009.

[72] P. Corcia, P. F. Pradat, F. Salachas et al., "Causes of death in a post-mortem series of ALS patients," *Amyotrophic Lateral Sclerosis*, vol. 9, no. 1, pp. 59–62, 2008.

[73] M. C. Kiernan, S. Vucic, B. C. Cheah et al., "Amyotrophic lateral sclerosis," *The Lancet*, vol. 377, no. 9769, pp. 942–955, 2011.